tained about one C^{14}-labeled ethyl group per molecule.[13] The C^{14} specific activity in these polymers gave $\bar{M}_n$ values directly, with appropriate calibration converting counts per minute to moles of C^{14}-labeled alkyl groups.

This method cannot be used directly on systems in which chain transfers with monomer or solvent, or via hydride formations give nonlabeled new chains or in which chain termination is by bimolecular combination. However, when properly used with other methods of molecular weight determination, it yields a wealth of information.

Viscometric Determination of $\bar{M}_n$

By refractionation of fractions of 50 g. samples of Hi-fax polyethylene, Henry[15] obtained

$$[\eta] = 4.60 \times 10^{-4} \bar{M}_\eta^{0.73} \tag{1}$$

for fractions of very narrow distribution. To obtain $\bar{M}_w$, it is assumed that the Wesslau distribution function adequately describes the polymers,

$$\bar{M}_w = M_0 \exp \{\beta^2/4\} \tag{2}$$

$$\bar{M}_n = M_0 \exp \{-\beta^2/4\} \tag{3}$$

and

$$\bar{M}_\eta = M_0 \exp \{\alpha\beta^2/4\} \tag{4}$$

The definitions of M_0 and β can be found elsewhere.[6] Combination of eqs. (1), (2), and (4) gives

$$[\eta] = 4.60 \times 10^{-4} \bar{M}_w^{0.73} \exp \{(\alpha\beta^2/4)(\alpha-1)\} \tag{5}$$

Values of β were determined by polymer fractionations.

Sometimes, the value of β is not known. Then $\bar{M}_w$ may be calculated from viscometric data by using Chiang's equation,[3]

$$[\eta] = 6.77 \times 10^{-4} \bar{M}_w^{0.67} \tag{6}$$

This equation gives the correct $\bar{M}_w$ if the unknown polymers and the polymers used originally to derive the equation have the same values of α and β. Otherwise, the error involved in the use of eq. (6) to calculate values of $\bar{M}_w$ is estimated as follows.

Intrinsic viscosity is related directly only to $\bar{M}_\eta$ by

$$[\eta] = k\bar{M}_\eta^\alpha \tag{7}$$

Assuming that the polymers have a Wesslau type of distribution, it can be shown that

$$\bar{M}_w = ([\eta]/k)^{1/\alpha} \exp \{(\beta^2/4)(1 - \alpha)\} \tag{8}$$

The error is then simply

$$\text{Error, } \% = [\exp\{(1 - \alpha)/4\} \ (\beta_1^2 - \beta_2^2) - 1]100 \tag{9}$$

where β_1 is that of the polymer used to obtain eq. (6) ($\beta_1 = 2.18$) and β_2 is that of the polymer under investigation.

Calculation of $\bar{M}_w$ and $\bar{M}_n$ from Kinetic Data

In ethylene polymerizations initiated by the $(C_5H_5)_2TiCl_2$–$(CH_3)_2AlCl$ system, the individual processes may be represented by the equation:[12]

$$(C_5H_5)_2TiCl_2 + (CH_3)_2AlCl \xrightarrow{\text{fast}} (C_5H_5)_2TiCl_2 \cdot (CH_3)_2AlCl \qquad (10)$$

$$(C_5H_5)_2TiCl_2 \cdot (CH_3)_2AlCl \xrightarrow{k_i} [AT]\,(CH_3) \qquad (11)$$

$$[AT]\,(CH_3) + n C_2H_4 \xrightarrow{k_p} [AT]\,(C_2H_4)_n(CH_3) \qquad (12)$$

$$2\,[AT]\,(C_2H_4)_n(CH_3) \xrightarrow{k_t} \text{polymers} \qquad (13)$$

$$\bar{M}_n = \frac{k_p[m]28}{k_t\,[T]_0\,(1 - x^2)f} \ln\left[\frac{K_0(a_0x) + A'I_0(a_0x)}{K_0(a_0) + A'I_0(a_0)}\right] \qquad (14)$$

$$\bar{M}_w = \left\{[T]_0\,(1 - x^2)f + \frac{3k_p[m]}{k_t} \ln\left[\frac{K_0(a_0x) + A'I_0(a_0x)}{K_0(a_0) + A'I_0(a_0)}\right] - \frac{4k_p^2[m]^2}{k_tk_t}\left(\ln x - [K_0(a_0) + A'I_0(a_0)]\int_1^x \frac{dw}{w[K_0(a_0w) + A'I_0(a_0w)]}\right)\right\}$$
$$\left\{[T]_0(1 - x^2)f + \frac{k_p[m]}{k_t} \ln\left[\frac{K_0(a_0x) + A'I_0(a_0x)}{K_0(a_0) + A'I_0(a_0)}\right]\right\}^{-1} \qquad (15)$$

where [m] is the monomer concentration; $[T]_0$ is the initial concentration of $(C_5H_5)_2TiCl_2$; f = catalyst efficiency; $x = \exp\{-k_t t/2\}$; $a_0 = 2(k_t[T]_0/k_i)^{1/2}$; $A' = K_1(a_0)/I_1(a_0)$; and I_0, K_0, and I_1, K_1 are hyperbolic Bessel functions of zero and first order, respectively.

For propylene polymerizations initiated by α-$TiCl_3$–$(C_2H_5)_2AlCl$, time-dependent expressions were similarly derived for $\bar{M}_n$ and $\bar{M}_w$.[13]

EXPERIMENTAL

The preparation of the catalyst systems, the purification of the solvents, the polymerization technique, the sampling procedures, the polymer work-up methods, the radioactivity determinations, and the viscometric measurements with the appropriate shear corrections have been given in detail.[12,13,16] Shyluk fractionated the polymers, using the method of Francis, Cooke, and Elliott[16] for polyethylenes and the method of Shyluk[7] for polypropylenes.

RESULTS

Comparison of $\bar{M}_w$ Obtained by Fractionation and by Viscometry for Linear Polyethylene

In Table I, the values of $\bar{M}_w$ for eleven samples of linear polyethylenes obtained by various methods are compared. The fractionation data were

treated by the method of summation[15] (method A) to give the values of $\bar{M}_w$ listed in Column 2. The values of $\bar{M}_w$ calculated from viscometric data by using eqs. (5) and (6) are found in columns 3 and 4, respectively. In the calculations employing eq. (5), values of β obtained from fractionation experiments were used. Column 5 gives the errors for the results in column 4 as estimated according to eq. (9).

TABLE I
Comparison of $\bar{M}_w$ Calculated from Viscometric Data

	$\bar{M}_w \times 10^{-4}$			
No.	Determined by fractionation method A	Calculated from eq. (5)	Calculated from eq. (6)	Error estimated for the use of eq. (6), %
1	3.9	4.1	4.1	+8.5
2	8.6	9.4	10.6	+7.6
3	10.5	10.2	11.8	+7.6
4	17.5	14.1	16.4	+9.8
5	40.3	—	24.8	—
6	1.6	1.7	2.1	+30
7	5.5	5.7	6.6	+13
8	4.8	5.7	7.1	+23
9	57.6	36.3	37.0	−14
10	6.6	6.4	8.1	+22
11	60.6	37.1	47.1	+9.0
Avg.				+11.6

Comparison of the Results of $\bar{M}_w/\bar{M}_n$ Determinations

Fractionation data were also treated by the use of a Wesslau distribution function (method B). Table II summarizes and compares the results of $\bar{M}_w$, $\bar{M}_n$, and $\bar{M}_w/\bar{M}_n$ as obtained by fractionation methods A and B, viscometry, and the ratioactive tracer method.

A similar comparison of the results of $\bar{M}_w$, $\bar{M}_n$, and $\bar{M}_w/\bar{M}_n$ for three samples of crystalline polypropylenes was made in Table III.

$\bar{M}_w/\bar{M}_n$ Variation During Ethylene Polymerization

In most psuedosteady-state polymerizations, the molecular weight distributions of the products do not vary with the polymerization time. Whereas it is the general belief that olefin polymerization initiated by Zeigler-type catalysts gives products with time-dependent molecular weight distributions, no definitive results have been reported to date. The methods described here for the determination of $\bar{M}_w/\bar{M}_n$ and their ratio made possible measurements on small samples taken during a polymerization. The variation of $\bar{M}_w/\bar{M}_n$ during polymerizations is illustrated in Figures 1 and 2. Also included were the results calculated with eqs. (14) and (15). Also shown are the amounts of I^{131} introduced into the

TABLE II
$\bar{M}_n$, $\bar{M}_w$ and $\bar{M}_w/\bar{M}_n$ for Linear Polyethylenes

No.	η_{sp}/c	$\bar{M}_n \times 10^{-3}$ Method A	$\bar{M}_n \times 10^{-3}$ Method B	$\bar{M}_n \times 10^{-3}$ C^{14}	$\bar{M}_n$ deviation, % Method A	$\bar{M}_n$ deviation, % Method B	$\bar{M}_w \times 10^{-4}$ Method A	$\bar{M}_w \times 10^{-4}$ Method B	$\bar{M}_w \times 10^{-4}$ $[\eta]$	$\bar{M}_w$ deviation, % Method A	$\bar{M}_w$ deviation, % Method B	$\bar{M}_w/\bar{M}_n$ Method A	$\bar{M}_w/\bar{M}_n$ Method B	$\bar{M}_w/\bar{M}_n$ C^{14} and $[\eta]$	$\bar{M}_w/\bar{M}_n$ deviation, % Method A	$\bar{M}_w/\bar{M}_n$ deviation, % Method B
1	0.94	8.9	8.3	8.4	6.0	1.2	3.9	5.4	3.1	22.7	74.0	4.3	6.5	3.7	13.5	76.6
2	1.66	15.8	20.0	20.4	22.5	2.0	8.6	13.4	10.6	19.0	26.4	5.5	6.7	5.2	5.8	28.8
3	1.82	21.9	22.3	22.3	1.8	0	10.5	15.7	11.8	11.0	33.0	4.8	7.0	5.3	9.5	32.0
4	2.36	37.6	43.3	35.1	7.1	23.4	17.5	26.3	16.4	6.4	61.0	4.6	6.1	4.7	2.1	29.8
5	3.28	15.9	14.4	21.7	26.7	33.7	40.3	47.8	24.8	62.5	92.7	25.0	33.0	11.5		
6	0.5	8.4	10.0	10.6	20.7	5.6	1.6	2.0	2.1	23.1	2.4	1.9	2.0	2.0	5.0	0
7	1.17	12.8	15.8	15.6	18.0	1.3	5.5	7.9	6.6	16.7	19.7	4.3	5.0	4.2	2.4	19.1
8	1.09	17.6	23.7	21.6	18.5	9.7	4.8	7.1	7.1	32.1	0	2.8	3.0	3.3	15.1	9.1
9	3.80	24.1	24.3	29.9	39.6	39.1	57.6	69.4	37	55.7	87.6	23.9	28.6	9.3		
10	1.32	23.8	30.5	35.7	33.3	14.5	6.6	9.6	8.1	19.0	17.6	2.8	3.1	2.3	21.7	34.8
11	5.76	79.7	111	149	16.5	25.5	60.6	68.5	47.1	28.7	45.5	7.6	6.2	3.2		
Avg.					21.9	14.2				27.9	45.5				8.3	25.5

TABLE III
$\bar{M}_n$, $\bar{M}_w$ and $\bar{M}_w/\bar{M}_n$ for Crystalline Polypropylenes

No.	η_{sp}/c	$\bar{M}_n \times 10^{-4}$ Method A	$\bar{M}_n \times 10^{-4}$ Method B	$\bar{M}_n \times 10^{-4}$ C^{14}	$\bar{M}_n$ deviation, % Method A	$\bar{M}_n$ deviation, % Method B	$\bar{M}_w \times 10^{-5}$ Method A	$\bar{M}_w \times 10^{-5}$ Method B	$\bar{M}_w \times 10^{-5}$ $[\eta]$	$\bar{M}_w$ deviation, % Method A	$\bar{M}_w$ deviation, % Method B	$\bar{M}_w/\bar{M}_n$ Method A	$\bar{M}_w/\bar{M}_n$ Method B	$\bar{M}_w/\bar{M}_n$ C^{14} and $[\eta]$	$\bar{M}_w/\bar{M}_n$ deviation, % Method A	$\bar{M}_w/\bar{M}_n$ deviation, % Method B
1	4.79	6.8	4.8	10.3	34	53	6.0	7.2	5.7	5.2	23	8.8	15.0	5.5	60	173
2	2.09	3.2	2.2	3.4	5.9	35	2.3	2.4	2.3	0	4.3	7.1	11.2	6.8	4.4	65
3	9.14	18.0	—	22.3	18	—	11.2	—	11.4	1.8	—	6.2	—	5.1	18	—

polymer by quenching a polymerization sample with I^{131}-labeled iodine. These values are used as a measurement for the number of active growing chains in the system.[12] Both the observed and the calculated values of $\bar{M}_w/\bar{M}_n$ for the early samples were less reliable than the samples taken at later stages of polymerizations. The observed values were less certain because the very low molecular weight portion of the sample is not retained by precipitation. The calculated results were less valid because of the small values of t used in the calculations.

Dependence of $\bar{M}_w/\bar{M}_n$ upon Experimental Variables in Ethylene Polymerizations

A study was made on the effect of the temperature of polymerization upon the nonuniformity of the polymers. The results are summarized in Table IV. The dependence of $\bar{M}_w/\bar{M}_n$ upon catalyst concentrations are shown in Table V.

TABLE IV
$\bar{M}_w/\bar{M}_n$ of Polyethylenes Obtained at Various Temperatures[a]

Temp., °C.	$(\bar{M}_w/\bar{M}_n)_f$[b]
60	2.4
45	3.6
30	4.5
15	5.4
0	6.1

[a] Conditions of polymerization: $[(C_5H_5)_2TiCl_2]_0$ = 2 mmole/l.; $[(CH_3)_2AlCl]_0$ = 5 mmole/l.; $p_{C_2H_4}$ = 100 cm.

[b] Values of $\bar{M}_w/\bar{M}_n$ at the end of polymerization.

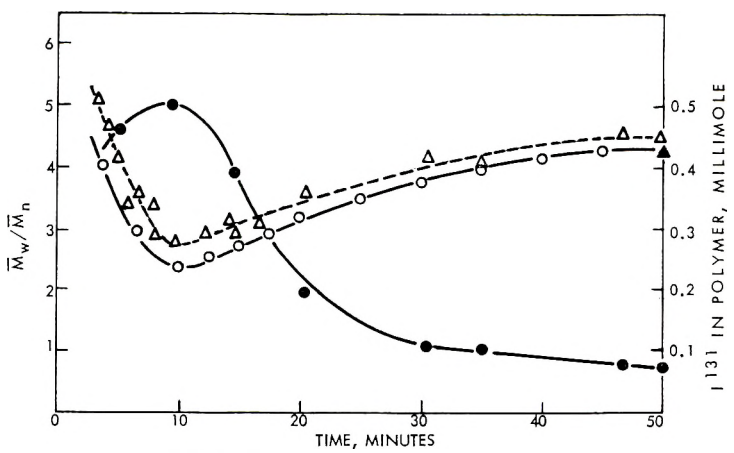

Fig. 1. Variation of $\bar{M}_w/\bar{M}_n$ during an ethylene polymerization: (△) observed; (○) calculated; (▲) fractionation value. Experimental conditions: $[(C_5H_5)_2TiCl_2]_0$ = $2mM$; $[(CH_3)_2AlCl]_0$ = $5mM$; t = 30°; $p_{C_2H_4}$ = 100 cm. Also shown (●) is ^{131}I in polymer, mmoles.

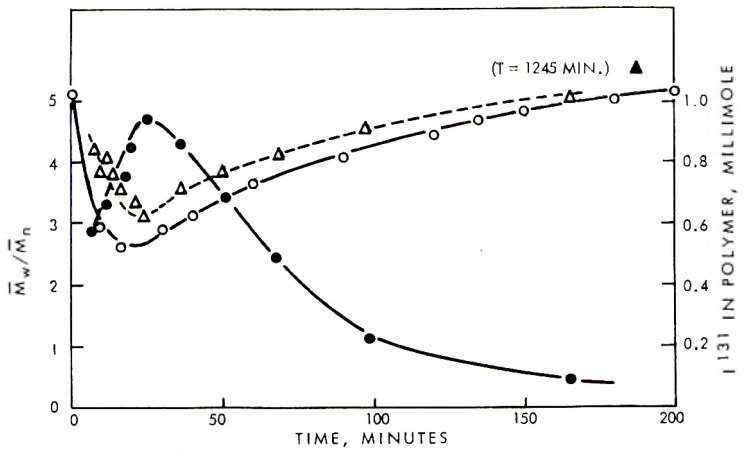

Fig. 2. Variation of $\bar{M}_w/\bar{M}_n$ during an ethylene polymerization: (△) observed; (○) calculated; (▲) fractionation value. Experimental conditions: $[(C_5H_5)_2TiCl_2]_0 = 2mM$; $[(CH_3)_2AlCl]_0 = 5mM$; $t = 15°$; $p_{C_2H_4} = 100$ cm. Also shown (●) is ^{131}I in polymer, mmoles.

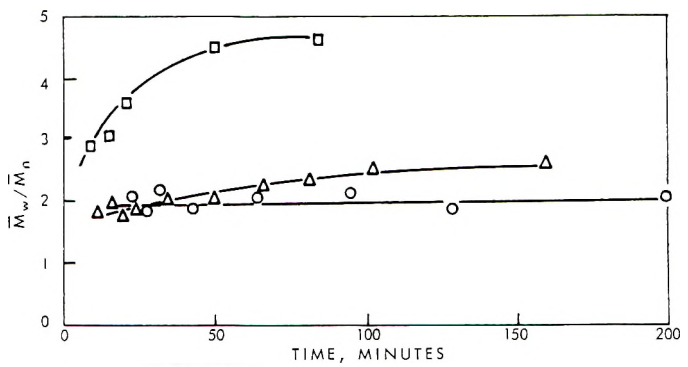

Fig. 3. Dependence of $\bar{M}_w/\bar{M}_n$ on Al/Ti ratios in ethylene polymerizations: Experimental conditions: $[(CH_3)_2AlCl]_0 = 5mM$; $t = 30°$; $p_{C_2H_4} = 100$ cm. Al/Ti ratios: (□) 2.5; (△) 5; (○) 10.

TABLE V

Dependence of $\bar{M}_w/\bar{M}_n$ on Catalyst Concentration in Ethylene Polymerizations[a]

[Ti],[b] mmole/l.	$[Al]_0$,[c] mmole/l.	Temp., °C.	$(\bar{M}_w/\bar{M}_n)_f$
2	5	30	4.5
1	2.5	30	3.3
4	10	15	7.4
2	5	15	5.4
1	2.5	15	3.6
4	10	0	8.2
2	5	0	6.1
1	2.5	0	4.6

[a] Polymerizations at a monomer pressure of 100 cm.
[b] As $(C_5H_5)_2TiCl_2$.
[c] As $(CH_3)_2AlCl$.

The influence of the Al/Ti ratio on the uniformity of the polyethylenes is illustrated in Figure 3.

$\bar{M}_w/\bar{M}_n$ Variation During Propylene Polymerizations

The variations of $\bar{M}_w/\bar{M}_n$ during propylene polymerization was insensitive to experimental variables such as the catalyst concentration, the

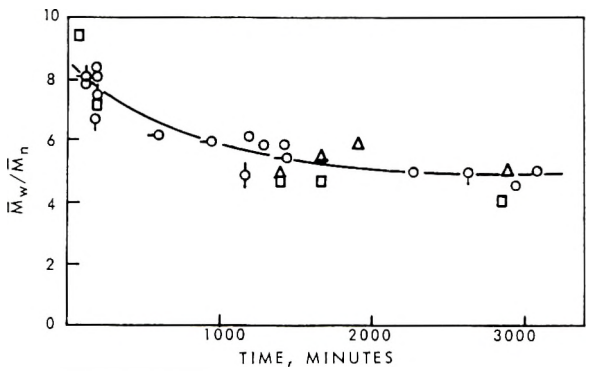

Fig. 4. Variation of $\bar{M}_w/\bar{M}_n$ of crystalline polypropylene with polymerization time. Experimental conditions: t = 50°; $p_{C_3H_6}$ = 100 cm. Concentrations of α-$TiCl_3$ and $(C_2H_5)_2AlCl$, millimolar, respectively: (O) 5, 1.3; (△) 2.5, 5; (□) 1.25, 10; (⊙) 10, 20; (-⊙) 5, 40; (-⊙) 10, 5.

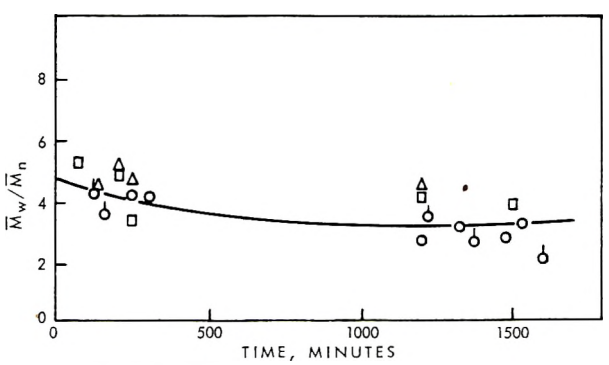

Fig. 5. Variation of $\bar{M}_w/\bar{M}_n$ of crystalline polypropylene with polymerization time. Experimental conditions: t = 90°; $p_{C_3H_6}$ = 100 cm. Concentrations of α-$TiCl_3$ and $(C_2H_5)_2AlCl$, millimolar, respectively: (O) 2.5, 5; (△) 2.5, 10; (□) 2.5, 20; (⊙) 2.5, 2.5.

Al/Ti ratios and the monomer pressures and sensitive only to polymerization temperatures. These are shown in Figures 4 and 5.

The variation of $\bar{M}_w/\bar{M}_n$ of atactic polypropylene as a function of the polymerization time is summarized in Figure 6. The uncertainty of these results is discussed below.

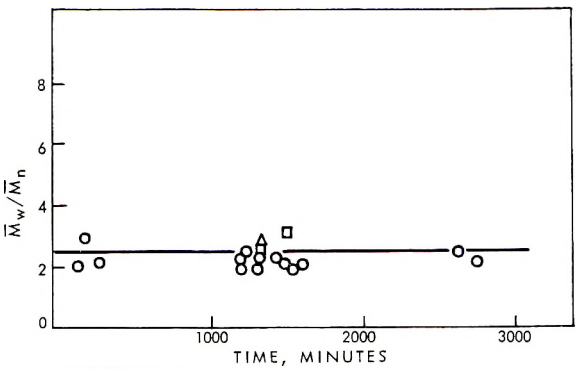

Fig. 6. Variation of $\bar{M}_w/\bar{M}_n$ of amorphous polypropylene with polymerization time. Experimental conditions: t = 90° (one exception); $p_{C_3H_6}$ = 100 cm. Concentrations of α-$TiCl_3$ and $(C_2H_5)_2AlCl$, millimolar, respectively: (O) 2.5, 5; (△) 2.5, 10; (□) 2.5, 20; (⊙) 5, 15 (95°).

DISCUSSION OF RESULTS

Comparison of $\bar{M}_w$, $\bar{M}_n$, and $\bar{M}_w/\bar{M}_n$ Obtained by Various Methods

The values of $\bar{M}_w$ calculated from viscometric data by use of eqs. (5) and (6) were in good agreement (Table I). The average deviation was +11.6%. Furthermore, these values were also in good agreement with those obtained by the summation fractionation method A. For the purpose of calculating the nonuniformity coefficient, the values of $\bar{M}_w$ derived from the approximate relationship (6) are adequate. These values will be used in subsequent discussions.

For polyethylenes with viscosities ranging from 0.5 to 2.36, there was substantial agreement in the values of $\bar{M}_n$ obtained by fractionation (both methods A and B) and by the tracer method. The values of $\bar{M}_w$ obtained by viscometry and by fractionation method A were also in good agreement. However, higher values of $\bar{M}_w$ were obtained when the fractionation data were treated according to method B. The reason is that the Wesslau distribution function is a definite integral with limits of zero to infinite degree of polymerization. Calculations based on this distribution function would be expected to give values of $\bar{M}_w$ that are too high (see discussion below). The values of $\bar{M}_n$ are relatively insensitive to the overestimation of a small number of polymer molecules of very high molecular weight. Therefore, the values of $\bar{M}_n$ obtained by the fractionation method B are in better agreement with the others except for extreme cases.

There are three samples of polyethylene, sample nos. 5, 9, and 11 in Table I, whose fractionation gave values of $\bar{M}_n$ much lower than those obtained by the tracer method and values of $\bar{M}_w$ much higher than those obtained by the viscometric method. All three samples have high viscosities.

The results on crystalline polypropylene obtained by all methods compare favorably. Again, higher values of $\bar{M}_w$ were obtained by the frac-

tionation method B. However, data on more samples are required to make a valid comparison of the various methods. In fact, there were many samples of high viscosity polypropylene of which the values of $\bar{M}_w$, $\bar{M}_n$, and $\bar{M}_w/\bar{M}_n$ were readily determined by the present method. These results are not included here because the available technique does not allow the fractionation of these polymers. The polymerization conditions used to obtain polymers 5, 9, and 11 were not very different from the conditions used to prepare the other polymers. The values of $\bar{M}_w/\bar{M}_n$ determined by the present method are in line with the expected, whereas those calculated from fractionation data appeared high. The integral distribution curves and the probability distribution curves of these samples indicated that the fractionation technique used was not able to resolve the high molecular weight portion of the samples. These samples will be fractionated again by use of improved techniques and solvent systems.

$\bar{M}_w/\bar{M}_n$ and Ethylene Polymerizations

In ethylene polymerizations initiated by the soluble $(C_5H_5)_2TiCl_3$–$(CH_3)_2AlCl$ system the initiation is first-order and the termination is bimolecular disproportionation. It was expected that the $\bar{M}_w/\bar{M}_n$ of the polymers would first decrease to a minimum and then increase asymptotically to a final value. The results shown in Figures 1 and 2 realized the expectation, in that they agreed with the calculated values. Polymers of narrowest distributions should be formed when the number of growing chains is at the maximum. The number of growing chains could be determined by reacting a polymerization sample with I^{131}-labeled iodine and counting of the I^{131} activity in the polymers. Figures 1 and 2 showed that the time when polyethylenes with lowest $\bar{M}_w/\bar{M}_n$ were formed corresponded approximately to the time when the concentration of the growing chains is at the maximum.

The above results suggested that it is feasible to prepare polymers of high uniformity under a pseudosteady-state condition by replenishing catalysts during a polymerization. Under carefully controlled conditions, the polymers would have $\bar{M}_w/\bar{M}_n \rightarrow 2$ as anticipated for systems terminating by bimolecular disproportionation.[18]

The dependence of $\bar{M}_w/\bar{M}_n$ upon the temperatures of polymerizations shown in Table IV can be easily understood. Polymers with a narrow distribution were obtained at 60°C.; at this temperature, the initiation and the termination processes were very fast. Values of $\bar{M}_w/\bar{M}_n$ increased with the decrease of polymerization temperature. The decrease of initiation rates with temperature was accompanied by a larger decrease of the termination rates, giving polymers with increasing width of distribution. The activation energy for the termination process is 16.4 kcal./mole; the activation energy for the initiation process is 15.5 kcal./mole.[12]

The kinetics of the second-order termination process required the termination of many short growing chains when the concentration of growing chains is large. Consequently, polymers formed at high catalyst concen-

tration will have a broader distribution than those prepared at low catalyst concentrations. The results in Table V support this prediction.

In Figure 3 the values of $\bar{M}_w/\bar{M}_n$ of polymers for three polymerizations carried out at different Al/Ti ratios but constant $[(CH_3)_2AlCl]$ are summarized. In these experiments, two variables need to be taken into consideration, the concentration of $[(C_5H_5)_2TiCl_2]$ and the Al/Ti ratios. At the lowest [Ti] and the largest Al/Ti ratio, the values of $\bar{M}_w/\bar{M}_n$ is low, about 2, and is independent of the polymerization time. The low catalyst concentration and the fact that chain transfer processes are important at this Al/Ti ratio are responsible for the observation. In average, each Ti initiated about seven polymer chains.[3] At a somewhat higher $(C_5H_5)_2TiCl_2$ concentration (1 mmole/l.) and Al/Ti ratio (5), the distribution is slightly broader; the distribution increases gradually with polymerization time. Each Ti initiated about three polymer chains in this experiment. At a $(C_5H_5)_2TiCl_2$ concentration of 2 mmole/l. and an Al/Ti ratio of 2.5, where each Ti initiated about one polymer chain, $\bar{M}_w/\bar{M}_n$ increases rapidly to 4.5.

$\bar{M}_w/\bar{M}_n$ and Polymerizations to Crystalline Polypropylenes

The crystalline polymer samples taken during a propylene polymerization initiated by α-$TiCl_3$–$(C_2H_5)_2AlCl$[13] have different distributions. The values of $\bar{M}_w/\bar{M}_n$ were high at the beginning and decreased to a low constant value with the polymerization time. This variation is especially noticeable at lower polymerization temperatures.

At 50°C. (Fig. 4), the initial values of $\bar{M}_w/\bar{M}_n$ were between 8 and 10, and the final values were between 4 and 5. The dependence of $\bar{M}_w/\bar{M}_n$ upon catalyst concentration and the Al/Ti ratio is not marked. Somewhat narrower distribution polymers were obtained at large Al/Ti ratios.

According to the kinetics of the propylene polymerization there are no important termination reactions. Therefore, variation of catalyst concentration should have no effect on the molecular weight distribution of the polymers formed. Furthermore, in these heterogeneous systems, the concentration of $(C_2H_5)_2AlCl$ is in large excess over the concentration of surface sites on α-$TiCl_3$. Consequently, there should be no significant dependence of $\bar{M}_w/\bar{M}_n$ upon the Al/Ti ratios. The time dependence of $\bar{M}_w/\bar{M}_n$ is interpreted as follows. It was postulated[13] that the sites initially on α-$TiCl_3$ were mostly $(C_2H_5)TiCl_2 \cdot (C_2H_5)AlCl_2$. When $TiCl_3$ catalyst was added to a solution of $(C_2H_5)_2AlCl$, $(C_2H_5)TiCl_2 \cdot (C_2H_5)_2AlCl$ sites were also formed. The latter is the more reactive species. The polymers formed at the beginning of the polymerization should have broad molecular weight distribution. $\bar{M}_w/\bar{M}_n$ decreases to a final low value when a state of pseudoequilibrium is established for the active sites. Chain transfers also contribute to the lowering of $\bar{M}_w/\bar{M}_n$.

Another mechanism must also be considered in any explanation for the time dependence of $\bar{M}_w/\bar{M}_n$. The catalyst particles may be considered as polymer-coated permeable spheres containing inner active sites. The

concentration of monomer within the sphere is determined by diffusion processes and by the rate of monomer consumption. A gradient of monomer concentrations results. Combining the second law of Fick and the rate equation of polymerization gives the expression

$$(d^2[\mathrm{m}]/dr^2) - (k_p[\mathrm{Ti}]_i/D)[\mathrm{m}] = 0$$

which describes the situation under pseudosteady-state conditions, where r is the distance from the center of the particle, [m] is the monomer concentration, D is the diffusion coefficient, and $[\mathrm{Ti}]_i$ is the concentration of active sites inside the sphere. The solution is simply

$$[\mathrm{m}] = A\cos(k_p[\mathrm{Ti}]_i/D)^{1/2}r + B\sin(k_p[\mathrm{Ti}]_i/D)^{1/2}r$$

The constants A and B can be determined from the initial conditions. It is not possible to estimate the contribution of the polymerization without the knowledge of $[\mathrm{Ti}]_i$ and of the diffusion coefficient of propylene in $TiCl_3$ coated with solvent swollen polypropylene. Furthermore, the real system is more complicated because the particles grow and change in porosity with polymerization. Qualitatively, the diffusion controlled polymerization could give rise to products of large $\bar{M}_w/\bar{M}_n$ but it is not possible to predict whether the value would increase or decrease with polymerization time. This process may not be of importance here since the catalyst system is relatively inactive and the monomer concentration gradient discussed above is probably small. It is conceivable that the process may become one of great significance for very active catalyst systems.

At elevated temperatures, the dependence of the $\bar{M}_w/\bar{M}_n$ of the polymers upon polymerization time was less pronounced than at 50°C. (compare Figs. 4 and 5). Furthermore, lower values of $\bar{M}_w/\bar{M}_n$ were obtained at higher temperatures. Probably the equilibration of the two types of active sites was achieved more rapidly at higher temperatures. In addition, one of the transfer processes in this system[13] has a high activation energy (18.6 kcal./mole). At these temperatures more frequent chain transfers would lead to narrower polymer distributions. However, it is not possible to rule out the effect of diffusion-controlled polymerizations at less accessible sites under the catalyst particle surface. Increase of temperature would increase the monomer diffusion velocity constant and increase swelling of the polymer coatings on these particles. Both factors could contribute toward yielding polymers of narrower distributions.

$\bar{M}_w/\bar{M}_n$ and Polymerizations to Amorphous Polypropylenes

The values of $\bar{M}_n$ for amorphous polypropylenes were calculated from the C^{14} specific activity. However, corresponding polymers have not been fractionated to check these values. The values of $\bar{M}_w$ were calculated from the intrinsic viscosity by use of the relationship[5] developed for crystalline polypropylene, with the assumption that the same relationship describes the amorphous polypropylene. The numerical values for K and α in the relationship $[\eta] = K\bar{M}_n^{\alpha}$ between isotactic and atactic poly-

styrenes are the same within the limits of experimental error.[19] In view of these uncertainties, the validity of the $\bar{M}_w/\bar{M}_n$ values obtained here is unknown. However, the relative values are believed to be correct.

Conclusions in the kinetic study of propylene polymerization to amorphous products were that the active sites were formed at the expense of those sites which yield crystalline polymers and that the former were also heterogeneous sites which differ from the others in the great ease of chain transfers. Figure 6 shows that the $\bar{M}_w/\bar{M}_n$ of amorphous polypropylenes is independent of polymerization time, catalyst concentrations, Al/Ti ratios and other variables. The values of $\bar{M}_w/\bar{M}_n$ remained consistently at about 2. These observations are consistent with the conclusions of the kinetic study summarized above.

The author is grateful to Dr. H. M. Spurlin for critical comments on the treatment of the data, to Dr. W. E. Davis for derivations of eqs. (14) and (15), to Mrs. S. K. Shyluk for fractionation of polymer samples, and to Mr. C. E. Green for programming and computation of $\bar{M}_w$ and $\bar{M}_n$.

APPENDIX

From the reactions (10) to (13), we can write the rate equations for $[(CH_3)_2AlCl)] > [(C_5H_5)_2TiCl_2]$ as

$$d[[AT](CH_3)]/dt = k_t[T]_0 \tag{16}$$

$$d[R_1]/dt = k_t[T]_0 e^{-k_i t} - k_p\,[m]\,[R_1] - k_t\,[R_1]\,[R] \tag{18}$$

$$d[R_2]/dt = k_p\,[m]\,[R_1] - k_p\,[m]\,[R_2] - k_t\,[R_2]\,[R] \tag{19}$$

$$\vdots$$

$$d[R_i]/dt = k_p\,[m]\,[R_{i-1}] - k_p[m]\,[R_i] - k_t\,[R_i]\,[R] \tag{20}$$

where

$$[R_1] = [[AT]\,(C_2H_4)(CH_3)]$$

$$[R_2] = [[AT]\,(C_2H_4)_2\,(CH_3)]$$

$$[R]_t = [[AT]\,(C_2H_4)_i(CH_3)]$$

and

$$R \equiv \sum_{i=1}^{\infty} R_i$$

Additions of equations over all values of i yields

$$d[R]/dt = k_i\,[(C_2H_5)_2TiCl]_0 e^{-k_i t} - k_t[R]^2$$

the solution of which is

$$[R] = x\,(k_t[T]_0/k_t)^{1/2} \begin{Bmatrix} K_1(a_0x) - A'I_1(a_0x) \\ K_0(a_0x) + A'I_0(a_0x) \end{Bmatrix} \tag{22}$$

where

$$x = \exp\left\{-k_t t/2\right\}$$

$$a_0 = 2\,(k_t[\mathrm{T}]_0/k_i)^{1/2}$$

$$A' = K_1(a_0)/I_1(a_0)$$

and I_0, K_0 and I_1, K_1 are hyperbolic Bessel functions of zero and first order, respectively. Using the usual definitions for the first and the second moment of the DP (degree of polymerization) distribution,

$$Z = \sum_{i=1}^{\infty} i[\mathrm{R}_i] \tag{23}$$

and

$$y = \sum_{i=1}^{\infty} i^2[\mathrm{R}_i] \tag{24}$$

the following results were obtained.

$$Z = [\mathrm{R}] + \frac{k_p[\mathrm{m}]}{k_t}\left\{1 - \frac{K_0(a_0) + A'I_0(a_0)}{K_0(a_0x) + A'I_0(a_0x)}\right\} \tag{25}$$

$$y = 3Z - 2[\mathrm{R}] + \frac{4k_p^2[m^2]}{k_ik_t} \times$$

$$\left\{\frac{[K_0(a_0) + A'I_0(a_0)]\ln x - \int_1^x [K_0(a_0w) + A'T_0(a_0w)]\,dw/w}{K_0(a_0x) + A'I_0(a_0x)}\right\} \tag{26}$$

The results for [R], Z, and y are those of the active polymers. Differential eqs. (16) to (20) neglected the fact that when R_i reacts with R_i, both disappear. The correct equations are

$$d[\mathrm{R}_1]/dt = k_i[\mathrm{T}]_0e^{-k_it} - k_p[\mathrm{m}][\mathrm{R}_1] - k_t[\mathrm{R}_1]\,[\mathrm{R}] - k_t[\mathrm{R}_1]^2 \tag{22}$$

$$d[\mathrm{R}_2]/dt = k_p[\mathrm{m}][\mathrm{R}_1] - k_p[\mathrm{m}]\,[\mathrm{R}_2] - k_t[\mathrm{R}_2]\,[\mathrm{R}] - k_t[\mathrm{R}_2]^2 \tag{23}$$

$$d[\mathrm{R}_i]/dt = k_p[\mathrm{m}]\,[\mathrm{R}_{i-1}] - k_p[\mathrm{m}][\mathrm{R}_i] - k_t[\mathrm{R}_i][\mathrm{R}] - k_t[\mathrm{R}_1]^2 \tag{24}$$

These equations do not appear to be soluble in closed forms. However, the approximate expressions for [R], Z, and y above are reasonably accurate when i does not approach infinity for any R_i.

To derive the expressions for the moments of the DP distribution of the total polymers, let

$$[\mathrm{P}_i] = [\mathrm{R}_i] + [\mathrm{Q}_i] \tag{25}$$

where $[\mathrm{P}_i]$ is total concentration of i-mer and $[\mathrm{R}_i]$ and $[\mathrm{Q}_i]$ are concentrations of active i-mer and of inactive i-mer, respectively. Since the system under consideration terminates predominantly by disproportionation, that is,

$$d[\mathrm{Q}_i]/dt = k_t\left\{[\mathrm{R}_i]\,[\mathrm{R}] + [\mathrm{R}_i]^2\right\} \tag{26}$$

Then,

$$d[P_i]/dt = k_i[T]_0 e^{-k_i t} - k_p[m]\,[R_1] \tag{27}$$

$$d[P_2]/dt = k_p[m]\,[R_1] - k_p\,[m]\,[R_2] \tag{28}$$

$$\vdots$$

$$d[P_i]/dt = k_p[m]\,[R_{i-1}] - k_p[m]\,[R_i] \tag{29}$$

Define the zeroth, first, and second moments of DP distribution as

$$M_0 = \sum_{i=1}^{\infty} [P_i] \tag{30}$$

$$M_1 = \sum_{i=1}^{\infty} i[P_i] \tag{31}$$

and

$$M_2 = \sum_{i=1}^{\infty} i^2[P_i] \tag{32}$$

Then,

$$dM_0/dt = k_i\,[T]_0 e^{-k_i t} \tag{33}$$

$$dM_1/dt = k_i[T]_0 e^{-k_i t} + k_p[m]\,([R] + 2Z) \tag{34}$$

$$dM_2/dt = k_i[T]_0 e^{-k_i t} + k_p[m]\,([R] + 2Z) \tag{35}$$

The solutions of eqs. (34) and (35) are

$$M_0 = [T]_0\,(1 - x^2)^* \tag{36}$$

$$M_1 = [T]_0(1 - x^2) + \frac{k_p[m]}{k_t} \ln\left[\frac{K_0(a_0x) + A'I_0(a_0x)}{K_0(a_0) + A'I_0(a_0)}\right] \tag{37}$$

$$M_2 = [T]_0\,(1 - x^2) + \frac{3k_p[m]}{k_t} \ln\left[\frac{K(a_0x_0) + A'I_0(a_0x)}{K_0(a_0) + A'I_0(a_0)}\right]$$

$$- \frac{4k_p^2[m]^2}{k_ik_t}\left\{\ln x - [K_0(a_0) + A'I_0(a_0)]\int_1^x \frac{dw}{w[K_0(a_0w) + A'I_0(a_0w)]}\right\} \tag{38}$$

Depending upon the ratios of $(CH_3)_2AlCl$ to $(C_5H_5)_2TiCl_2$ used in the catalyst system, each Ti initiates f polymer chains. On incorporating the catalyst efficiency and eqs. (37) and (38) into the relationships between $\bar{M}_w$ and $\bar{M}_n$, and $\bar{M}_0$, $\bar{M}_1$, and $\bar{M}_2$, one obtains the eqs. (14) and (15) for $\bar{M}_n$ and $\bar{M}_w$, respectively.

References

1. Tung, L. H., *J. Polymer Sci.*, **24**, 333 (1957).
2. Kaufman, H. S., and E. K. Walsh, *J. Polymer Sci.*, **26**, 124 (1957).
3. Chiang, R., *J. Polymer Sci.*, **36**, 91 (1959).

4. Ciampa, G., *Chim. e ind.* (*Milan*), **38**, 298 (1956).
5. Chiang, R., *J. Polymer Sci.*, **28**, 235 (1958).
6. Wesslau, H., *Makromol Chem.*, **20**, 111 (1956).
7. Shyluk, S. K., *J. Polymer Sci.*, in press.
8. Taylor, W. C., and L. H. Tung, paper presented at 140th Natl. Meeting, American Chemical Society, Chicago, September 1961, *Abstracts of Papers*, p. 204.
9. Blackmore, W. R., and W. Alexander, *Can. J. Chem.*, **39**, 1888 (1961).
10. Gold, L., *J. Chem. Phys.*, **28**, 91 (1958).
11. Kyner, W. T., J. R. M. Radock, and M. Wales, *J. Chem. Phys.*, **30**, 363 (1959).
12. Chien, J. C. W., *J. Am. Chem. Soc.*, **81**, 86 (1959).
13. Chien, J. C. W., *J. Polymer Sci.*, in press.
14. Arnett, L. M., *J. Am. Chem. Soc.*, **74**, 2027 (1952); L. M. Arnett and J. H. Peterson, *ibid.*, **74**, 2031 (1952).
15. Henry, P. M., *J. Polymer Sci.*, **36**, 3 (1959).
16. Francis, P. S., R. C. Cooke, Jr., and J. H. Elliott, *J. Polymer Sci.*, **31**, 453 (1958).
17. Irani, R. R., *J. Phys. Chem.*, **63**, 1603 (1959).
18. Flory, P. J., *Principles of Polymer Chemistry*, Cornell Univ. Press, Ithaca, N.Y., 1953.
19. Gaylord, N. G., and H. F. Mark, *Linear and Stereoregular Addition Polymers*, Interscience, New York, 1959.

Résumé

On a décrit une méthode pour la détermination rapide du coefficient de nonuniformité (M_w/M_n) de polyéthylènes linéaires et de polypropylènes cristallins. Le poids moléculaire moyen en nombre, M_n, était déterminé en comptant le nombre des groupes alcoyles maqués au C^{14}, introduits pendant l'initiation. Le poids moléculaire moyen en poids, M_w, était calculé à partir de données viscosimétriques. On a évalué les erreurs de ces calculs. Pour zone échantillons de polyéthylènes linéaires et pour trois échantillons de polypropylènes cristallins, on a comparé les valeurs ainsi obtenues aux résultats correspondants obtenus par fractionnement des polymères. Il y avait une bonne concordance pour tous les échantillons de polyéthylène de haute viscosité avec des valeurs élevées de M_w et des valeurs basses de M_n, trouvées par fractionnement. Les valeurs M_w/M_n on été déterminées pour des échantillons de polymères, prises durant les polymérisations de l'éthylène initiées par le système $(C_5H_5)_2TiCl_2$–$(CH_3)_2AlCl$. Ce rapport diminuait au début avec la durée de polymérisation, puis atteignait un minimum quand la concentration de chaînes croissantes atteignit un maximum. La comparaison de polyéthylènes, produits à différentes températures, montre que la largeur de distribution des polymères diminue pour des températures de polymérisation croissantes. Cette décroissance est attribuée à une augmentation de vitesses d'initiation et de terminaison et à une valeur plus élevée de l'énergie d'activation des processus de terminaison. Des concentrations élevées en catalyseur produisent des polyéthylènes de large distribution. Pour des concentrations élevées en catalyseur, les concentrations en chaînes en croissance sont également élevées. De ce fait, un nombre plus élevé de chaînes de poids moléculaire bas termine rapidement en donnant des produits de M_w/M_n élevé. D'autre part, l'augmentation du rapport Al/Ti dait augmenter le transfert de chaînes donnant du polyéthylène qui ont un M_w/M_n bas. Un effet additionnel de l'augmentation du rapport Al/Ti est une variation plus faible de M_w/M_n en fonction de t. On présente également les valeurs M_w/M_n d'échantillons de polypropylène prélévés au cours de polymérisation initiées par α-$TiCl_3$–$(C_2H_5)_2AlCl$. Elles étaient élevées au début des polymérisations et décroissent graduellement jusqu'à une valeur constante plus faible. A températures plus élevées, cette variation était moins prononcée et les valeurs de M_w/M_n étaient plus faibles que celles des polymères obtenus à plus basses temperatures. En accord avec les résultats cinétiques, les valeurs de M_w/M_n étaient insensibles aux variables expérimentales telles que concentration en catalyseur, rapport Al/Ti et pression en

monomère. Les valeurs M_w/M_n d'échantillons de polypropylènes amorphes pris au cours de polymérisation de propylène ne varient ni avec t ni avec les autres conditions de polymérisation. Ces résultats appuyent l'interprétation cinétique antérieure selon laquelle des transferts de chaînes importants auraient lieu au cours de la formation de polypropylènes amorphes.

Zusammenfassung

Eine Methode zur raschen Bestimmung des Uneinheitlichkeitskoeffizienten $\bar{M}_w/\bar{M}_n$ von linearem Polyäthylen und kristallinem Polypropylen wird beschrieben. Das Zahlenmittel des Molekulargewichts, $\bar{M}_n$, wurde durch Zählung der beim Startschritt in das Polymere eigenführten C^{14}-markierten Alkylgruppen bestimmt. Das Gewichtsmittel des Molekulargewichts, $\bar{M}_w$, wurde aus Viskositätsdaten berechnet. Die bei diesen Berechnungen auftretenden Fehler wurden bestimmt. Die so für elf Proben von linearem Polyäthylen und drei Proben von kristallinem Polypropylen erhaltenen $\bar{M}_w/\bar{M}_n$-Werte werden mit den entsprechenden Fraktionierungsergebnissen verglichen. Die Übereinstimmung war für alle untersuchten Polyäthylen- und Polypropylenproben gut, mit Ausnahme von drei Polyäthylenproben hoher Viskosität mit hohen $\bar{M}_w$-Werten und niedrigen $\bar{M}_n$-Werten aus der Fraktionierung. Die $\bar{M}_w/\bar{M}_n$-Werte wurden an Polymerproben bestimmt, die während der durch $(C_5H_5)_2TiCl_2$–$(CH_3)_2AlCl$ gestarteten Äthylenpolymerisation entnommen worden waren. Dieser Wert nahm zuerst mit der Reaktionsdauer ab und erreichte bei der maximalen Konzentration der wachsenden Ketten ein Maximum. Ein Vergleich des bei verschiedenen Temperaturen gebildeten Polyäthylens zeigt, dass die Verteilungsbreite mit steigender Polymerisationstemperatur abnimmt. Diese Abnahme wird einer Erhöhung der Start- und Abbruchsgeschwindigkeit und der höheren Aktivierungsenergie für den Abbruchsprozess zugeschrieben. Bei hoher Katalysatorkonzentration wurde Polyäthylen mit breiter Verteilung erhalten. Folglich werden mehr niedermolekulare Ketten unter Bildung von Produkten mit hohem $\bar{M}_w/\bar{M}_n$ frühzeitig abgebrochen. Andererseits erhöht eine Zunahme des Verhältnisses Al/Ti die Kettenübertragung und liefert Polyäthylen mit niedrigem $\bar{M}_w/\bar{M}_n$. Eine zusätzliche Wirkung der Erhöhung des Verhältnisses Al/Ti ist die Abnahme der Abhängigkeit von $\bar{M}_w/\bar{M}_n$ von t. Weiters werden $\bar{M}_w/\bar{M}_n$-Werte für kristalline Polypropylenproben mitgeteilt, die während der α-$TiCl_3$-$(C_2H_5)_2AlCl$-gestarteten Polymerisation entnommen wurden. Diese waren am Beginn der Polymerisation hoch und fielen mit fortschreitender Polymerisation zu einem niedrigeren konstanten Wert ab. Bei höherer Temperatur war diese Abhängigkeit weniger ausgeprägt und die $\bar{M}_w/\bar{M}_n$-Werte lagen niedriger als bei den bei niedrigeren Temperaturen erhaltenen Polymeren. Die $\bar{M}_w/\bar{M}_n$-Werte waren in Übereinstimmung mit den kinetischen Ergebnissen gegen Variation von Katalysatorkonzentration, Al/Ti-Verhältnis und Monomerdruck unempfindlich. Die $\bar{M}_w/\bar{M}_n$-Werte von amorphen Polypropylenproben, die während der Propylenpolymerisation entnommen wurden, zeigten weder eine Abhängigkeit von t, noch von den anderen Polymerisationsbedingungen. Diese Ergebnisse bilden eine Stütze für den früheren kinetischen Befund, dass nämlich bei der Bildung von amorphen Polypropylen die Kettenübertragung eine bedeutende Rolle spielt.

Received February 26, 1962

JOURNAL OF POLYMER SCIENCE: PART A VOL. 1, PP. 1857–1863 (1963)

The Reference Point for Liquid Relaxation Processes. I. Melt Viscosity of Polystyrene

A. A. MILLER, *General Electric Company Research Laboratory, Schenectady, New York*

Synopsis

Recent theories have suggested or implied that below the experimental glass temperature, T_g, there exists a temperature, T_0, which governs the temperature dependence of relaxation processes in a liquid. In the "free-volume" approach, T_0 should be associated with an "occupied" volume, v_o. In the present paper, published melt viscosity–temperature data for a series of polystyrene fractions (M = 1675–134,000) are shown to conform to a "modified" Arrhenius equation: $\eta = A \exp\{B/(T - T_0)\}$. From this and from a previous free-volume treatment of the same data, the reference point (T_0, v_o) is derived. Either or both of these approaches indicate that this reference point is situated on the liquid specific volume–temperature curve, extrapolated linearly into the glass region. In the series of polystyrene fractions for which T_g increases from 40 to 100°C., the corresponding T_0 values increase from 5 to 50°C. Further relationships between the parameters in the modified Arrhenius, the Doolittle free-volume, and the Williams-Landel-Ferry (WLF) equations, are expressed.

Introduction

It is well known that the simple Arrhenius equation, $\tau = A \exp\{E/RT\}$, does not adequately describe the temperature dependence, at constant pressure, of relaxation processes in liquids, particularly at temperatures approaching the glass transition region. For this region, the relaxation behavior usually requires an empirical equation (which hereinafter will be referred to as the "modified" Arrhenius equation) of the form $\tau = A \exp\{B'/(T - T_0)\}$, where T_0 may be well below the experimental glass transition temperature, T_g.[1]

On the basis of the viscosity behavior of n-alkanes, Doolittle developed the "free-volume" concept with the relation $\eta = A \exp\{Bv_o/v_f\}$, where A and B are temperature-independent constants, v_f is a "free" volume, and v_o is an "occupied" volume.[2a] Guttmann and Simmons[3] reported that the n-alkane viscosity data could be represented equally well by the "modified" Arrhenius equation.

More recently, in a discussion of molecular transport in liquids and glasses, Cohen and Turnbull demonstrated that, at least with respect to the exponential terms, the free-volume and the "modified" Arrhenius equations are equivalent.[4] For the present discussion, the essential features of the Cohen-Turnbull theory are that $v_f = 0$ at T_0 and that v_f increases linearly with temperature above T_0. In the present paper,

these ideas will be applied to published viscosity–temperature data for polystyrene and related to previous treatments of these data.

Williams' Free Volume Approach[5]

Using the glass temperature, T_g, as a reference point, Williams expressed the specific volume of the liquid above T_g as: $v = v_g + (dv/dT)(T - T_g)$, where dv/dT is the thermal expansion coefficient of the liquid and v_g is the specific volume at T_g. Substituting in the Doolittle free-volume equation he derived a relation for viscosity containing the experimentally measurable quantities η, T_g, v_g, dv/dT, and the three Doolittle parameters A, B, and v_o. This relation was applied to the Fox and Flory viscosity–temperature data for twelve fractions of polystyrene[6] and the best values of A, B, and v_o were determined on a programmed (least-squares) computer. Williams found $B = 0.91$, essentially independent of molecular weight, and $v_o = 0.934$–0.940 cc./gm. He also showed that the parameter A was governed only by the molecular weight, with an approximately first-order dependency below $M = 35{,}000$.

An important consequence, not explicitly stated by Williams but implied in his treatment, is that v_o should lie on the *liquid* specific volume–temperature curve, extrapolated linearly into the glass region. This feature, together with the Cohen-Turnbull concepts, leads directly to the alternative method of treating the viscosity data.

Approach Based on Temperature Dependency

If we use a reference temperature T_0 rather than T_g we have $v = v_o + (dv/dT)(T - T_0)$, where dv/dT is the liquid expansion coefficient which, in principle, also applies in the glass below T_g, down to T_0. Since $v_f = v - v_2 = (dv/dT)(T - T^0)$ and $v_f/v_o = \alpha(T - T_0)$, where $\alpha = (dv/dT)/v_o$, the Doolittle equation becomes:

$$\eta = A \exp\{B/\alpha(T - T_0)\} \tag{1}$$

which is the modified Arrhenius equation.

The Fox and Flory viscosity–temperature data for polystyrene fraction C8 ($M = 1675$) were plotted as log η against $1/(T - T_0)$, with the use of trial values of T_0 until a straight line was obtained. As shown in Figure 1, the plot is linear for $T_0 = 5$°C., but has detectable upward and downward curvatures for $T_0 = 0$ and 10°C., respectively. Also shown for comparison are the curves for $T_0 = 0$°K. (the normal Arrhenius plot) and for $T_0 = T_g = 40$°C. The slope of the linear plot is 620° and the intercept is log $A = -3.45$.

From eq. (1) the slope of the linear log η versus $1/(T - T_0)$ plot equals $B/2.3\alpha$. Using Williams' values, $B = 0.91$ and $\alpha = 6.3 \times 10^{-4}$ for $M = 1675$, we obtain a calculated slope of 628°, in good agreement with the observed value. Similarly, for $M = 1675$ Williams' relationship* gives log $A = -3.47$, to be compared with the observed intercept, log $A = -3.45$.

* Equation (14), ref. 5.

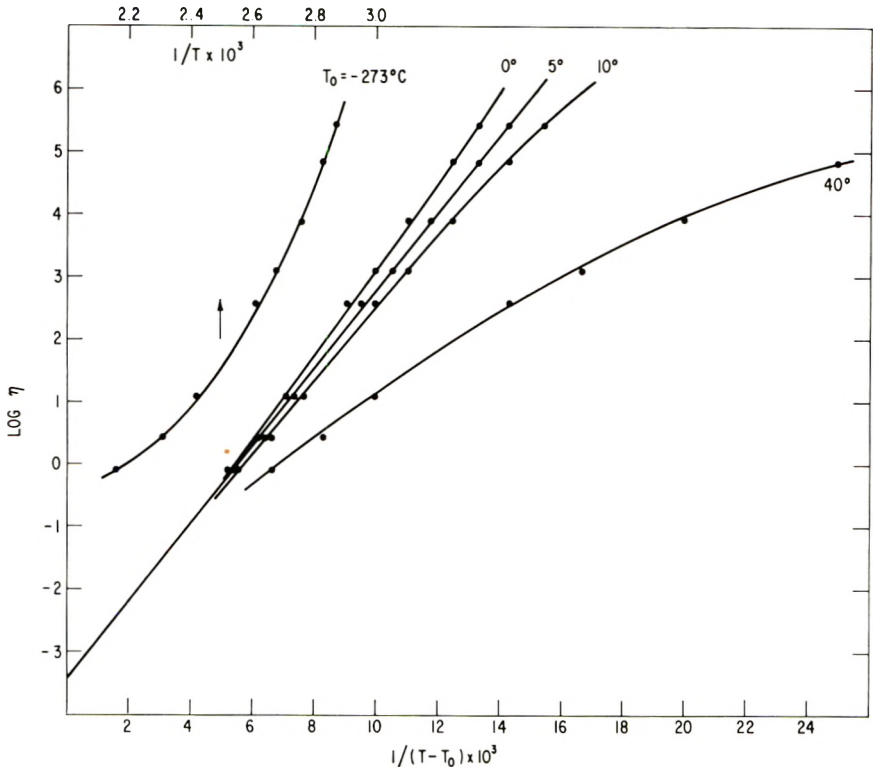

Fig. 1. Normal and modified Arrhenius plots of viscosity for polystyrene fraction: $M = 1675$ ($T_g = 40$°C.).

From the definitions of v in the Williams method and the present method, we have the simple relationship:

$$T_g - T_0 = (v_g - v_o)/(dv/dT) = (v_g - v_o)/\alpha v_o \qquad (2)$$

Using measured values for T_g, v_g, dv/dT, and Williams' derived value for v_o, we can calculate T_0 for any of the polystyrene fractions. Similarly, the slopes and intercepts for eq. (1) can be calculated from Williams' results, as indicated earlier. These derived parameters are shown in Table I for three polystyrene fractions.

In Figure 2 the straight lines are drawn by using the derived parameters log A and the slopes in Table I. The points are the Fox and Flory viscosity–temperature data for these fractions, and it is apparent that these conform satisfactorily to the modified Arrhenius equation.

TABLE I
Derived Parameters for $\log \eta = \log A + B/2.3\alpha(T - T_0)$

Fraction	M	T_g, °C.	T_0, °C.	log A	$B/2.3\alpha$
C8	1675	40	4	−3.47	628
C6	3041	64	22	−3.18	650
B4	6650	77	38	−2.80	665

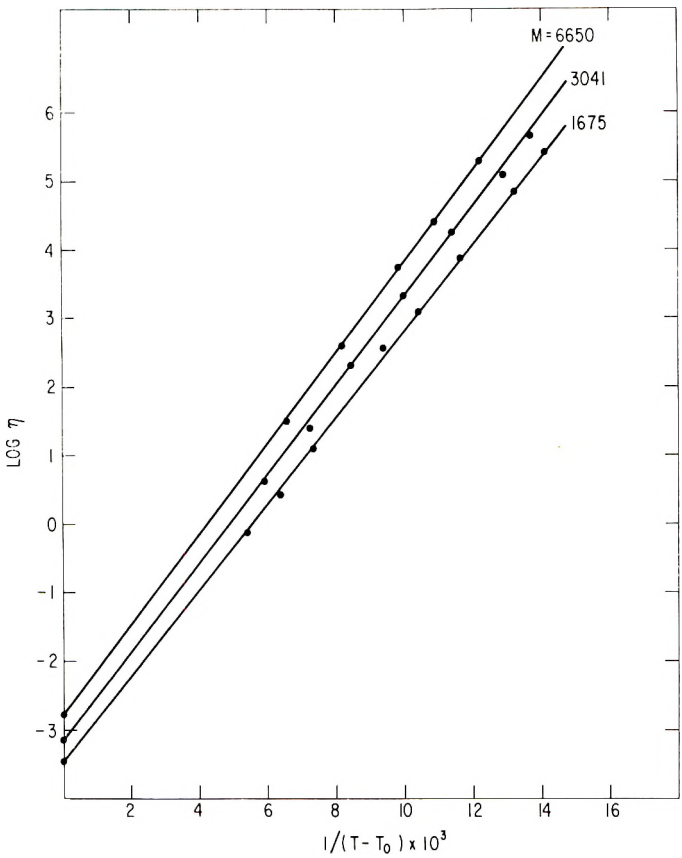

Fig. 2. Modified Arrhenius plots for three polystyrene fractions. Lines are drawn according to derived parameters: log A and slope. Points are Fox and Flory[6] viscosity data.

Viscosity–Temperature–Molecular Weight Relations

The complete viscosity–temperature–molecular weight relation for polystyrene will involve the molecular weight dependence of the several parameters in eq. (1). Thus, A is determined directly from the molecular weight, with a different dependency below and above $M = 35{,}000$.[5] The slope, $B/2.3\alpha$, contains the expansion coefficient which also varies with M: $dv/dT = (5.5 + 643/M)10^{-4}$.[7] Finally, T_0, through its relationship to T_g, is dependent on M (see, for example, Table I). If all of these factors were included, eq. (1) would lead to a complete η-T-M relationship as complex, though not necessarily of the same form, as the empirical equation found by Fox and Flory.[6]

Activation Energies

The slope of the modified Arrhenius plot gives the true activation energy for viscous flow: slope $= B/2.3\alpha = E/2.3R$. On the basis of Williams' values for B and α for polystyrene, the activation energies change only

slightly, from $E = 2.9$ kcal./mole for $M = 1675$ to $E = 3.1$ kcal./mole for $M = 134{,}000$.

The *apparent* activation energy, E_T, is obtained by differentiating the modified Arrhenius form:

$$2.3R[d \log \eta/d(1/T)] = E_T = E[T/(T - T_0)]^2$$

At high temperatures E_T approaches E, the true activation energy, as a limiting value. With decreasing temperature, E_T increases exponentially, attaining extremely high values at T_g.

Comparison with Williams-Landel-Ferry Equation[8]

Equation (1) can be readily converted into the WLF form, based on T_g, for example:

$$\log a_{Tg} = \log \eta/\eta_g = (B/2.3\alpha)[1/(T - T_0) - 1/(T_g - T_0)]$$

Substituting $T_0 = T_g - C_2^g$, we obtain:

$$\log a_{Tg} = (B/2.3\alpha C_2^g)[(T_g - T)/(C_2^g + T - T_g)]$$

$$= -C_1^g(T - T_g)/(C_2^g + T - T_g) \qquad \text{(WLF)}$$

where $C_1^g C_2^g = B/2.3\alpha$.

For the polystyrene fractions in the range $M = 1675$–$134{,}000$ the $C_1^g C_2^g$ values will change from 630 to 675, compared with the "universal" value of $C_1^g C_2^g = C_1 C_2 = 900$.[8] Since the viscosity data for the polystyrene fraction C8 ($M = 1675$, $T_g = 40°$C.) cover the temperature range 75–190°C. and are governed by eq. (1), which in turn can be expressed in the WLF form, it appears that the WLF equation should be applicable even for $T > T_g + 100$, provided the proper values of the constants, C_1 and C_2, are used for the specific material.

Discussion

The major conclusions derived in this paper are summarized in Figure 3, which shows specific volume–temperature plots for the three polystyrene fractions being considered. The lines are drawn so as to converge at absolute zero temperature, according to the relation[7] $v = 0.767 + (5.5 + 643/M)10^{-4}T$, and include the measured T_g and v_g values.[6] The v_g values are those derived by Williams[5] and the T_0 values are from the present work, derived directly (Fig. 1, $M = 1675$) or indirectly by eq (2) ($M = 3041$, 6650). The specific volume of the glass below T_g shown for $M = 1675$, is drawn according to $(dv/dT)_g = 2.5 \times 10^{-4}$.[6]

Definitions and theoretical interpretations of "free" and "occupied" volume have been discussed by others[4,7,9–11] and are beyond the scope of the present paper. It may be pointed out that above (v_0, T_0) the present treatment does not specify whether v_f depends on α, the liquid expansion coefficient alone, or on $\Delta\alpha$, the difference between the liquid and "solid" expansion coefficients. In either case, v_f should be directly proportional to $T - T_0$. Also, it may be mentioned that the locus of the (v_0, T_0) points

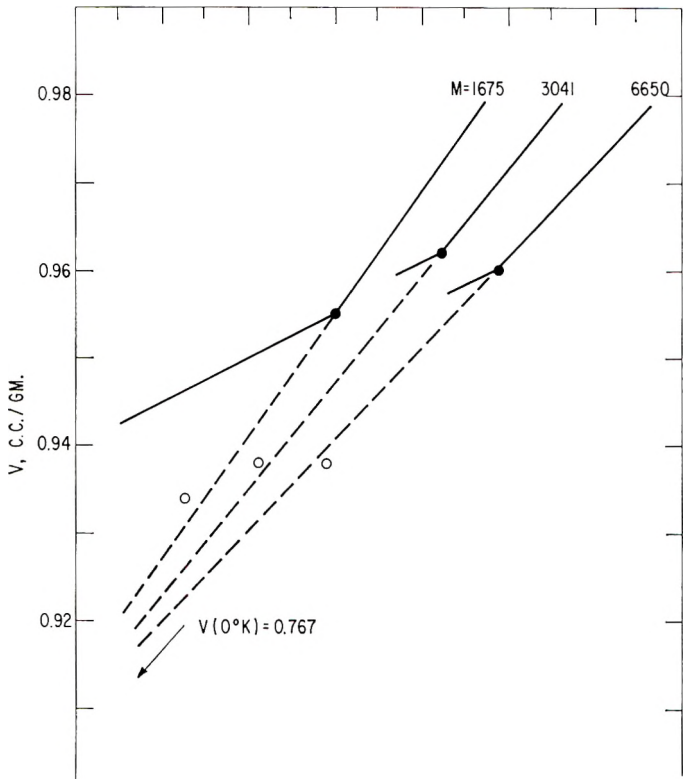

cc./gm./°C. This value, derived from a series of polystyrene samples, may be related to the true "solid" expansion coefficient for a single sample.

Conclusion

The treatment of the polystyrene viscosity data described here, together with Williams' approach, supports the idea that there exists a unique zero point, T_0,v_0, situated below and quantitatively related to (T_g,v_g), which is the true reference point for kinetic relaxation processes occurring in the liquid above T_g. As implied by others,[12] this may be a thermodynamic transition point and the theoretical lower limit for experimental T_g and v_g values at "infinite" equilibration times. Although not *directly* accessible by practical measurements because of the kinetic barrier in the glass, this reference point, together with the directly measurable glass transition point (T_g,v_g), should provide a basis for the further understanding of glass transition phenomena and liquid state theory.

Stimulating and informative discussions with J. M. O'Reilly are acknowledged.

References

1. Cole, R. H., *Ann. Rev. Phys. Chem.*, **11**, 161 (1960).
2. Doolittle, A. K., *J. Appl. Phys.*, **22**, 1031, 1471 (1951); *J. Appl. Phys.*, **23**, 418 (1952).
3. Guttmann, F., and L. M. Simmons, *J. Appl. Phys.*, **23**, 977 (1952).
4. Cohen, M. H., and D. Turnbull, *J. Chem. Phys.*, **31**, 1164 (1959).
5. Williams, M. L., *J. Appl. Phys.*, **29**, 1395 (1958).
6. Fox, T. G, and P. J. Flory, *J. Appl. Phys.*, **21**, 581 (1950); *J. Polymer Sci.*, **14**, 315 (1954).
7. Fox, T. G, and S. Loshaek, *J. Polymer Sci.*, **15**, 371 (1955).
8. Ferry, J. D., *Viscoelastic Properties of Polymers*, Wiley, New York, 1961, Ch. 11.
9. Bondi, A., *J. Phys. Chem.*, **58**, 929 (1954).
10. Turnbull, D., and M. H. Cohen, *J. Chem. Phys.*, **34**, 120 (1961).
11. Hildebrand, J. H., *J. Chem. Phys.*, **31**, 1423 (1959).
12. Gibbs, J. H., and E. A. DiMarzio, *J. Chem. Phys.*, **28**, 373 (1958).

Résumé

Des théories récentes ont suggéré ou impliqué qu'en dessous de la température vitreuse expérimentale, T_g, il existe une température T_0 qui détermine la dépendance de la température du processus de rélaxation dans un liquide. Dans l'approximation du "volume libre" T_0 doit être associé à un volume "occupé" v_o. Dans le présent article, on montre que les données publiées sur la viscosité à l'état fondu et la température pour une série de fractions de polystyrène (M = 1675 à 134.000) sont conformes à une équation d'-Arrhénius "modifiée": $\eta = A \exp\{B'/(T - T_0)\}$. À partir de cette équation et à partir du traitement antérieur du volume libre des mêmes données, on dérive le point de référence (T_0, v_o). L'une ou l'autre de ces approximations indique que ce point de référence est situé sur la courbe du volume spécifique-température du liquide, extrapolée linéairement dans la région de vitrification. Dans les séries des fractions de polystyrène pour lesquelles T_g augmente de 40 à 100°C, les valeurs correspondantes T_0 augmentent de 5 à 50°C. On exprime en plus des relations entre les paramètres dans l'équation d'-Arrhénius "modifiée", l'équation du volume libre de Doolittle et l'équation de Williams-Landel-Perry (WLF).

Zusammenfassung

Neuere Theorien bedienen sich der Annahme, dass unterhalb der experimentellen Glastemperatur, T_g, eine Temperatur, T_0, besteht, welche die Temperaturabhängigkeit der Relaxationsprozesse in einer Flüssigkeit beherrscht. Bei der Methode des "freien Volumens" sollte T_0 mit einem "besetzten" Volumen zusammenhängen. In der vorliegenden Mitteilung wird gezeigt, dass in der Literatur vorhandene Daten für die Schmelzviskositäts–Temperaturabhängigkeit einer Reihe von Polystyrolfraktionen (M = 1675 bis 134000) einer "modifizierten" Arrheniusgleichung entsprechen: $\eta = A \exp\{B'/(T - T_0)\}$. Daraus und aus einer früher durchgeführten Behandlung der gleichen Daten nach der Methode des "freien Volumens" wird der Bezugspunkt (T_0, v_o) abgeleitet. Jede der beiden Methoden zeigt, dass dieser Bezugspunkt auf der linearen Extrapolation der Kurve spezifisches Volumen der Flüssigkeit gegen Temperatur in den Glasbereich liegt. In der Reihe der Polystyrolfraktionen, bei welchem T_g von 40 auf 100°C ansteigt, nehmen die entsprechenden T_0-Werte von 5 auf 50°C zu. Weitere Beziehungen zwischen den Parametern der "modifizierten" Arrhenius-Beziehung, der Freien-Volums-Gleichung von Doolittle und der Williams-Landel-Ferry-(WLF)-Gleichung werden angegeben.

Received June 27, 1962

JOURNAL OF POLYMER SCIENCE: PART A VOL. 1, PP. 1865–1874 (1963)

The Reference Point for Liquid Relaxation Processes. II. Melt Viscosity of Polyisobutylene

A. A. MILLER, *General Electric Research Laboratory, Schenectady, New York*

Synopsis

Published (Fox and Flory) viscosity–temperature data for polyisobutylene are expressed by a modified Arrhenius equation: $\log \eta = \log A + B'/(T - T_0)$. For higher molecular weight fractions ($M > 2000$) with estimated glass temperatures in the range $T_g = -64$ to -79°C., the derived reference temperature T_0 is -150 (± 10)°C., and $B' = 1240$°. By comparison with Fox and Flory's empirical equations, the molecular weight dependency of the A parameter, below and above the "chain-entanglement" point ($M = 17000$), is derived. The modified Arrhenius equation can also be expressed with WLF (Williams-Landel-Ferry) constants, where $T_0 = T_g - C_2^g$ and $B' = C_1^g C_2^g$. The melt viscosity–temperature behavior is consistent with free-volume concepts if $v_f \simeq (T - T_0)$, as suggested by the Cohen-Turnbull theory.

INTRODUCTION

In the previous paper[1] it was shown that the temperature dependence of melt viscosity for polystyrene fractions could be expressed by a modified Arrhenius equation of the form:

$$\log \eta = \log A + B'/(T - T_0) \tag{1}$$

which could be related to the Doolittle free volume and the Williams-Landel-Ferry (WLF) equations. The merits of this approach, as a basis for viscosity–temperature–molecular weight (η–T–M) relationships in polymers and as a method of deriving some fundamental parameters for viscosity theory, are further demonstrated in the present paper, which deals with polyisobutylene (PIB).

VISCOSITY RELATIONS FOR POLYISOBUTYLENE

Fox and Flory[2] measured melt viscosities up to 217°C. for a series of PIB fractions ranging from $M = 520$ to 1,480,000. The following are some of the empirical η–T–M relationships which were derived:

$$\log \eta_T/\eta_{217} = 5.6 \times 10^5[(1/T^2) - (1/490^2)]e^{-163/M} \tag{2}$$

$$E_T = (5.1 \times 10^6/T)e^{-163/M} \tag{2a}$$

$$\log \eta_{217} = 3.4 \log M - 13.56 \quad (M > 17000) \tag{3}$$

$$\log \eta_{217} \simeq 1.75 \log M - 6.55 \quad (M < 17000) \tag{4}$$

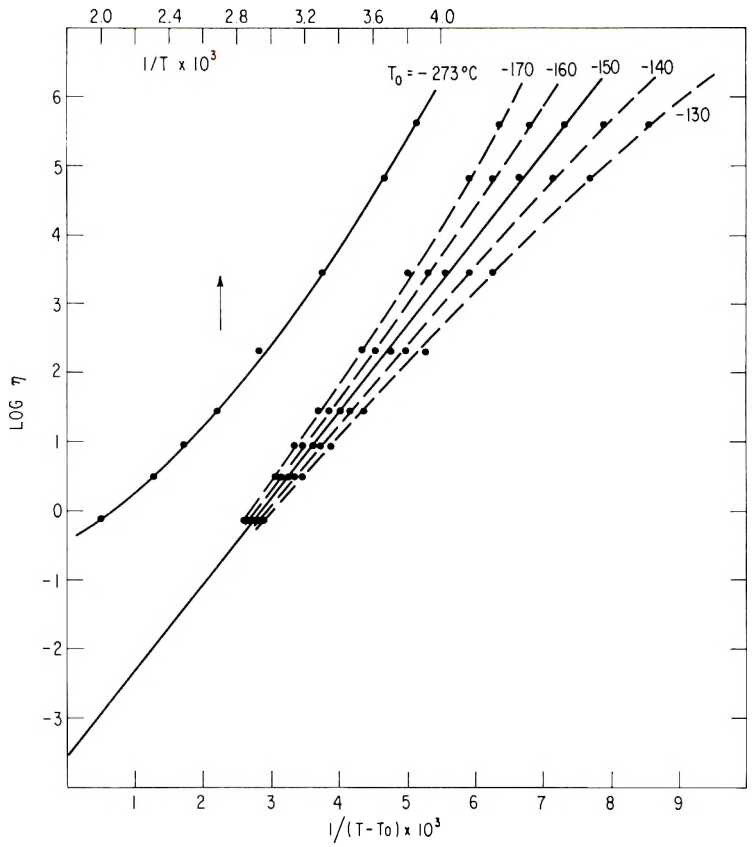

Fig. 1. Normal and modified Arrhenius plots of viscosity for polyisobutylene (M = 5380).

Fox and Flory found that the log η_T/η_{217} versus $1/T$ curves coincided for all fractions with $M > 2000$, where the $e^{-163/M}$ term in eq. (2) approaches unity. In eqs. (3) and (4), the value M = 17,000 is the chain-entanglement transition point for PIB.[3]

In the present paper, only the range $M > 2000$ will be considered in detail. The Fox and Flory data for M = 5380 are shown in Figure 1, plotted according to eq. (1), with trial values of T_0 in increments of 10° between −130 and −170°C. The best straight line is obtained for T_0 = −150°C. (±10) or 123°K., giving a slope of B' = 1240° and an intercept log A = −3.50. Trial plots for several other fractions with $M > 2000$ showed that the same values of T_0 and B' were applicable and this will be confirmed shortly. Thus, for $M > 2000$, we obtain:

$$\log \eta = \log A + 1240/(T - 123)$$

and at 217°C.:

$$\log \eta_{217} = \log A + 3.38$$

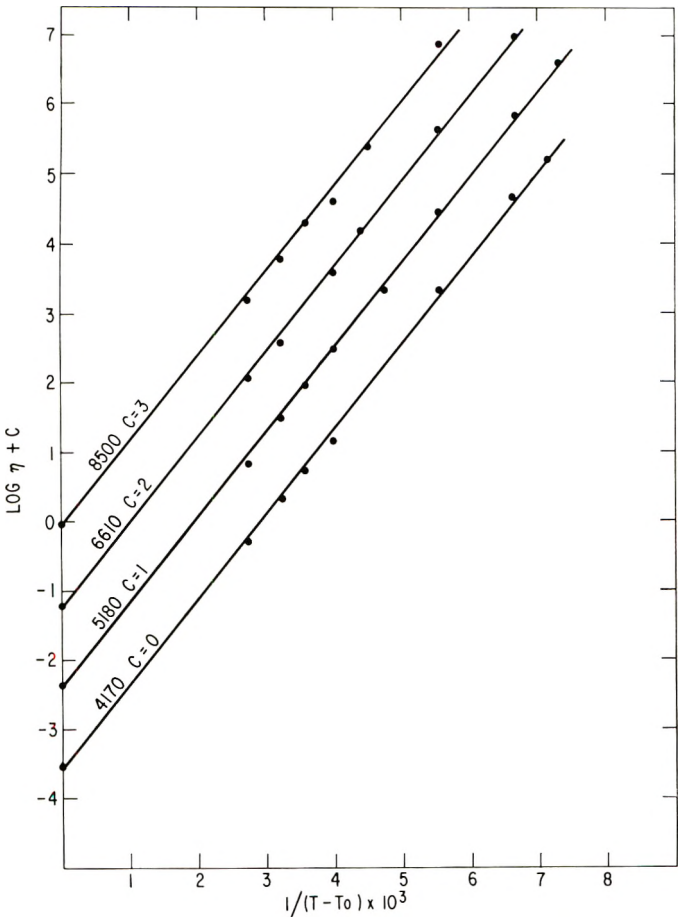

Fig. 2. Modified Arrhenius plots of viscosity for polyisobutylene fractions with $M < 17000$. Lines are drawn according to derived parameters: $B' = 1240°$ and log A from Table I. Points are Fox and Flory[2] data with $T_0 = -150°C$. Log η displacements indicated by C values.

Comparing this with the Fox and Flory eqs. (3) and (4) we find:

$$\log A = 3.4 \log M - 16.94 \quad (M > 17000) \tag{5}$$

$$\log A \simeq 1.75 \log M - 9.93 \quad (M < 17000) \tag{6}$$

The values of log A calculated by these two equations are listed in Table I.

In Figures 2 and 3, the straight lines are drawn according to the parameters: log A from Table I and slope $B' = 1240°$. An additive constant c was used where indicated on the log η axis to disperse the curves. The points are the Fox and Flory viscosity data, all plotted with $T_0 = -150°C$. The experimental values conform very well to the modified Arrhenius eq. (1), particularly for the higher fractions (Fig. 3).

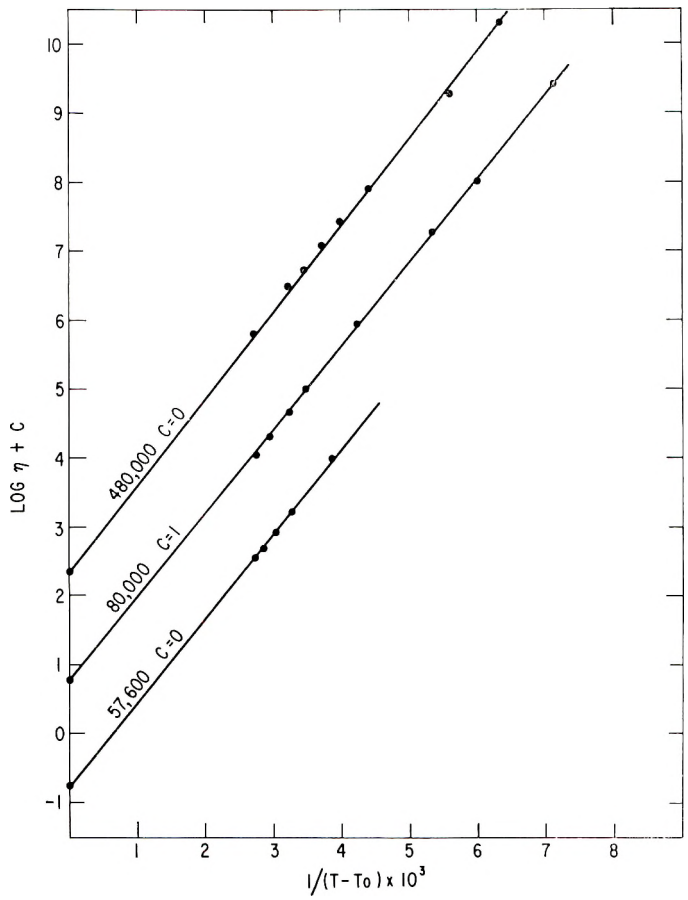

Fig. 3. Modified Arrhenius plots of viscosity for polyisobutylene fractions with $M >$ 17000.

The true, temperature-independent activation energy for viscous flow is given by $E = 2.3\ RB'$, and for PIB the value thus obtained is $E = 5.7$ kcal./mole, compared to 3.0 kcal./mole for polystyrene.[1] The apparent activation energy is given by $E_T = E(T/T - T_0)$.[2] For $T_0 = -150$°C. calculated values are 18.8 kcal. at 0°C., decreasing to 10.3 kcal. at 200°C. The Fox and Flory eq. (2a) for this range of M, where $e^{-163/M} \simeq 1$, gives $E_T = 18.7$ and 10.8 kcal. at these two temperatures. It should be noted

TABLE I
Log A Parameters for PIB

M (<17000)	Log A	M(>17000)	Log A
4170	−3.58	57,600	−0.74
5380	−3.40	80,000	−0.24
6610	−3.24	480,000	+2.36
8500	−3.05		

that the limiting, high temperature value for E_T is $E = 5.7$ by the modified Arrhenius form, but reduces to zero by the Fox and Flory equation. The former is probably more reasonable.

FREE VOLUME REPRESENTATION

Fox and Loshaek[4] have reported the following relationships for PIB. For the glass temperature, $T_g = T_g(\infty) - 0.7 \times 10^5/M$, where $T_g(\infty) = 210°K.$ (−63°C.); and for specific volumes of the liquid: $dv/dT = (6 + 1020/M)\ 10^{-4}$ and $v_{30°C.} = 1.131 + 31/M$.

As a basis for further discussion, the calculated values are shown in Table II over a broad range of M.

TABLE II
Calculated Parameters for PIB

M	T_g, °C.	$v_{30°C.}$, cc./g.	$dv/dT \times 10^4$, cc./g./°K.
≧57600	−64	1.131	6.0
8500	−71	1.134	6.12
4170	−79	1.138	6.25
2000	−98	1.147	6.5
1000	−133	1.162	7.0

It can be seen that these parameters approach constant, limiting values at high M but become increasingly sensitive to M at lower molecular weights.

Figure 4 shows the specific volume as a function of temperature for high molecular weight fractions of PIB. The line, $\alpha\ell$, is drawn according to the parameters: $v = 0.95$ cc./g. at 0°K.;[4] $v_{30°C.} = 1.131$ cc./g., and $dv/dT = 6 \times 10^{-4}$ (Table II). The limiting value of $T_g(\infty) = 210°K.$, with the corresponding volume, $v_g = 1.075$ cc./g., are also shown. The derived value of $T_0 = 123\ (\pm 10)°K.$, placed on the linear v–T plot,[1] gives $v_0 = 1.023\ (\pm 0.005)$ cc./g. Ferry and co-workers[5,6] found that for the liquid and glass expansion coefficients of PIB ($M_n \sim 4900$), $\alpha\ell - \alpha_g = 4.5 \times 10^{-4}$ which, for $\alpha\ell = 6 \times 10^{-4}$, gives $\alpha_g = 1.5 \times 10^{-4}$. In Figure 4, this value is used for the v–T line of the glass.

In discussions of free volume, two limiting cases have been mentioned.[4] (1) The "occupied" volume v_0 does not change with temperature; in the present treatment, this leads to

$$v_f = \alpha\ell(T - T_0)$$

where the temperature coefficient of v_f is equal to the liquid expansion coefficient alone. (2) The occupied volume v_0 also increases with temperature, corresponding to a "solid-lattice" expansion coefficient α_s and the change in v_f is governed by the difference:

$$v_f = (\alpha\ell - \alpha_s)\ (T - T_0)$$

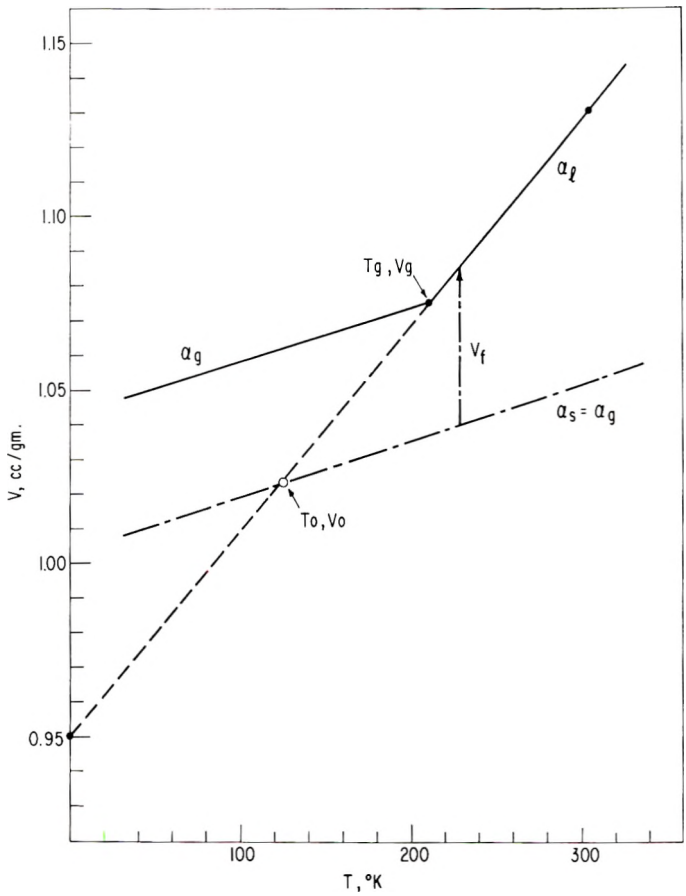

Fig. 4. Specific volumes and suggested free volume representation, typical for high molecular weight PIB ($M \gg 2000$).

Since in either case, v_f is directly proportional to $(T - T_0)$, the present method in itself cannot distinguish between the two. For PIB, if case (1) obtains, the volume fraction of free volume at the glass point is

$$f_g = (v_g - v_0)/v_g = 0.048$$

For case (2), if we assume $\alpha_s \leqq \alpha_g$, we obtain as a minimum, $v_g = (4.5 \times 10^{-4})\ 87 = 0.039$ cc., leading to $f_g \geqq 0.036$. For either case, these values are greater than the "universal" WLF value, $f_g \simeq 0.025$.[9a]

In relation to the Doolittle free volume equation: $\log \eta = \log A + Bv_0/2.3v_f$, previous papers derived $B = 0.91$ for polystyrene[1,7] on the basis that $\alpha_s = 0$ in the more general expression:

$$v_f = (\alpha\ell - \alpha_s)\ (T - T_0)$$

It is now evident that the value of the Doolittle B constant derived from B′, the slope of the linear $\log \eta$ versus $1/(T - T_0)$ plot, will depend on the

assumption regarding α. For polyisobutylene, case (1) with $\alpha_s = 0$, gives $B = 2.3(1240)\ 6 \times 10^{-4}/1.023 = 1.67$. For case (2), with $\alpha_s = \alpha_g = 1.5 \times 10^{-4}$ and $\alpha\ell - \alpha_s = 4.5 \times 10^{-4}$, we obtain $B = 1.25$.

In a theoretical approach to the WLF equation, Bueche suggested that the Doolittle B constant can be identified with a minimum critical volume required for the "jump" of a group of polymer segments.[8] On this basis it would appear reasonable that within a homologous polymer series B should remain constant, independent of molecular weight, but it may still vary significantly between different polymers, presumably according to chemical structure. Indeed, on the basis of WLF parameters, if $B = 2.3\Delta\alpha C_1^g C_2^g$,[1] several-fold variations in B between different polymer systems are already indicated by reported values of the WLF constants.[9b] It may be recalled that the calculated WLF free-volume values, i.e., f_g, have assumed that $B \simeq 1$ for all materials.[9a]

Although the present approach does not eliminate the uncertainties regarding the quantitative values of f_g and B, it is still completely consistent with the free-volume concepts, if $v_f \sim (T - T_0)$, as suggested by the Cohen-Turnbull theory.[11] For the higher molecular weight fractions of PIB, since the specific volumes and expansion coefficients are not very sensitive to M (Table II), the slope B' in eq. (1) remains relatively constant. Similarly, the calculated T_g in Table II shows only a 15° decrease down to $M = 4170$. Since T_0 is related to T_g,[1] the decrease in the true value of T_0 in this molecular weight range should be of the same order. Apparently, this change in T_0 is not great enough to be readily detected by the log η versus $1/(T - T_0)$ plot, particularly since T_0 is so far removed from the temperature range of the viscosity measurements (−13 to 217°C.).

COMPARISON WITH WLF CONSTANTS

The WLF equation with T_g as the reference temperature is:

$$\log a_T = \log \eta_T/\eta_g = -C_1^g(T - T_g)/(C_2^g + T - T_g).$$

For high molecular weight ($M_v \sim 10^6$) PIB, the WLF constants have been reported as $C_1^g = 16.56$, $C_2^g = 104.4°$, and $C_1^g C_2^g = 1731$.[9b] In relation to the modified Arrhenius equation, it was shown in the previous paper[1] that $C_2^g = T_g - T_0$ and $C_1^g C_2^g = B'$. Thus, from the present results, for $T_g = 210$°K. we find $C_2^g = 87\ (\pm 10)°$, $C_1^g C_2^g = 1240$, giving $C_1^g = 14.3$. (The Fox and Loshaek limiting value (Table II) is used, which is higher than the value 202°K. cited by Ferry.[9b])

The two sets of constants are compared in Figure 5 on the basis of the Fox and Flory viscosity data for $M = 80{,}000$, a molecular weight high enough to attain the limiting values in Table II. The solid straight line is based on $T_0 = -150$°C. and $B' = 1240$. The broken straight line is for the WLF value, $C_1^g C_2^g = B' = 1731$. The intercepts of both of these lines were fixed at $\log A = -0.24$ (Table I). For $T_g = 206$°K. (the mean of the two reported values) and the WLF value $C_2^g = 104$, we have T_0

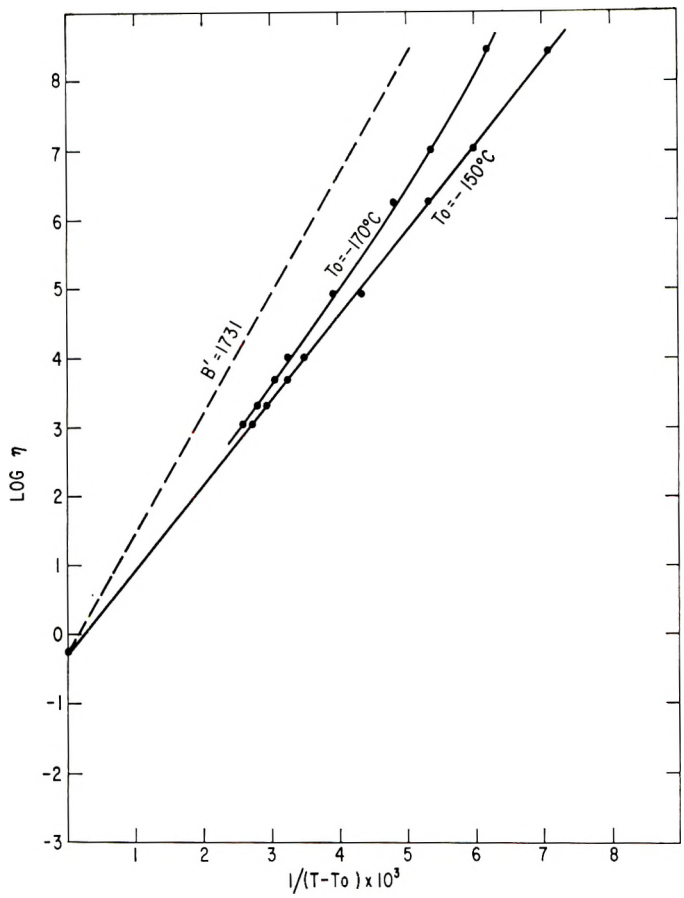

Fig. 5. Comparison of present parameters with reported WLF constants[9a] for high molecular weight PIB ($M \gg 2000$).

$\simeq -170$°C. In Figure 5, not only does this value of T_0 show an upward curvature but also its slopes do not conform to the value given by $C_1^g C_2^g = 1731$. This suggests that, at least for viscosities of high molecular weight PIB, the revised WLF constants may be more appropriate.

CONCLUSIONS

For polystyrene[1] and for polyisobutylene the η–T–M data can be expressed by a modified Arrhenius equation. Only one adjustable parameter T_0 is used for viscosity–temperature data referring to a single material or polymer fraction. The proper T_0 immediately defines the intercept A and the slope B'. For a given polymer system, the parameter A is apparently governed only by the molecular weight, with different dependencies below and above the chain-entanglement point. For a given polymer, B' and T_0 are essentially constant in the high M range, becoming increasingly sensitive to M for lower molecular weights. This behavior is the

result of parallel changes in specific volumes, expansion coefficients, and T_g, with decreasing M.

Empirical equations have been reported which show log η as linear functions of $1/T^n$, with n ranging from 1 to 6.[10] The present work suggests that all such empirical equations should be equivalent to the modified Arrhenius equation. Even for measurements of highest accuracy, the choice of the best empirical equation will be determined by such factors as the number of η–T points measured, the temperature range, and especially the temperature *region* with respect to T_0. For example, by inspection of eq. (1), the further the experimental temperature range is from T_0, the more nearly will the viscosity data appear to conform to the ordinary Arrhenius relationship ($n = 1$).

Equation (1) can also be expressed with WLF parameters with T_g as the reference. Since $C_2^g = T_g - T_0$, and $B' = C_1^g C_2^g$,[1] we have:

$$\log \eta = \log A + C_1^g C_2^g/(C_2^g + T - T_g).$$

This equation retains the important log A term which has been cancelled out in the log a_T form of the original WLF equation. It becomes evident that although the two approaches are essentially equivalent, the emphasis is quite different. The WLF method emphasizes T_g, v_g as the reference, while the present method, based on the modified Arrhenius equation, bypasses the experimental glass point and leads directly to T_0, v_0, which seems to be the ultimate reference point for liquid relaxation processes.

Note Added in Proof. With regard to the free volume interpretation of polyisobutylene and polystyrene[1] viscosities, a more recent analysis suggests that the occupied volume, v_s, is determined by the liquid structure and that the temperature coefficient, α_s, is neither zero nor related to α_v.

References

1. Miller, A. A., *J. Polymer Sci.*, **A1**, 1857 (1963).
2. Fox, T. G, and P. J. Flory, *J. Phys. Chem.*, **55**, 221 (1951).
3. Bueche, F., *J. Chem. Phys.*, **20**, 1959 (1952).
4. Fox, T. G, and S. Loshaek, *J. Polymer Sci.*, **15**, 371 (1955).
5. Ferry, J. D., and G. S. Parks, *J. Chem. Phys.*, **4**, 70 (1936).
6. Williams, M. L., R. F. Landel, and J. D. Ferry, *J. Am. Chem. Soc.*, **77**, 3701 (1955).
7. Williams, M. L., *J. Appl. Phys.*, **29**, 1395 (1958).
8. Bueche, F., *J. Chem. Phys.*, **24**, 418 (1956).
9. Ferry, J. D., *Viscoelastic Properties of Polymers*, Wiley, New York, 1961, (a) Chap. 11; (b) Table 11-II.
10. Fox, T. G, S. Gratch, and S. Loshaek, in *Rheology*, F. R. Eirich, Ed., Academic Press, New York, 1956, Vol. I, Chap. 12.
11. Cohen, M. H., and D. Turnbull, *J. Chem. Phys.*, **31**, 1164 (1959).

Résumé

Des données viscosité–température publiées (Fox et Flory) pour le polyisobutylène ont été exprimées à l'aide d'une équation d'Arrhénius modifiée: log η = log $A + B'/(T - T_0)$. Pour les fractions de poids moléculaires plus élevés ($M > 2000$) avec estimation des températures de transition vitreuse dans le domaine $T_g = -64$ à -79°C, la température

de référence dérivée, T_0, est de -150 (± 10°C), et $B' = 1240$°. Par comparison avec les équations empiriques de Fox et Flory, on a déduit la dépendance du poids moléculaire en fonction du paramètre A, en-dessous et au-dessus du point d'enchevêtrement des chaînes (M = 17.000). L'équation modifiée d'Arrhénius peut aussi être exprimée à l'aide des constantes WLF (Williams-Landel-Ferry), où $T_0 = T_g - C_2^g$ et $B' = C_1^g C_2^g$. Le comportement température–viscosité à l'état fondu est compatible avec les concepts "volume libre" si $V_f \simeq (T - T_0)$, comme il l'a été suggéré par la théorie Cohen-Turnbull.

Zusammenfassung

Literaturdaten (Fox und Flory) über die Viskosität von Polyisobutylen in Abhängigkeit von der Temperatur werden durch eine modifizierte Arrhenius-Gleichung dargestellt: $\log \eta = \log A + B'/(T - T_0)$. Für höhermolekulare Fraktionen ($M > 2000$) mit Glastemperaturen im Bereich $T_g = -64$ bis -79°C beträgt die abgeleitete Bezugstemperatur, $T_0 = -150$ (± 10)°C und $B' = 1240$°. Durch Vergleich mit der empirischen Gleichung von Fox und Flory wird die Molekulargewichtsabhängigkeit des Parameters A unterhalb und oberhalb des "Kettenverschlingungspunktes" ($M = 17000$) erhalten. Die modifizierte Arrhenius-Gleichung kann auch mit WLF (Williams-Landel-Ferry) Konstanten dargestellt werden; es ist dann $T_0 = T_g - C_2^g$ und $B' = C_1^g C_2^g$. Die Schmelzviskositäts-Temperaturabhängigkeit stimmt mit $v_f \sim (T - T_0)$, wie es von der Cohen-Turnbull-Theorie angenommen wird, mit dem Konzept des "freien Volumens" überein.

Received July 17, 1962

JOURNAL OF POLYMER SCIENCE: PART A VOL. 1, PP. 1875–1892 (1963)

Growth and Morphology of Single Crystals of Cellulose Triacetate

R. ST. JOHN MANLEY, *Physical Chemistry Division, Pulp and Paper Research Institute of Canada, and Department of Chemistry, McGill University, Montreal, Canada*

Synopsis

Single crystals of cellulose triacetate were prepared by supercooling dilute solutions in mixtures of nitromethane and *n*-butanol. The crystals are approximately square in shape and thicken by spiral growths centered on screw dislocations. The chain molecules are perpendicular to the lamellae which are about 180 A. thick. In spite of their stiffness the molecules appear to assume folded configurations in the lamellae. Various morphological features of the crystals are described and discussed.

INTRODUCTION

In recent years a number of investigators[1–6] have described the growth of single crystals of several linear synthetic high polymers by precipitation from dilute solution through supercooling. The crystals thicken by a screw dislocation mechanism and consist of layers about 100 A. in thickness. Electron diffraction patterns show that the long chain molecules are oriented normal to the plane of the layers, and since the chain length greatly exceeds the layer thickness, it has been proposed by Keller[2] that the chain molecules must be sharply folded in order to fit into the layers. Thus the crystal is built up of sharply folded polymer chains packed in an ordered arrangement. This hypothesis is now considered to be well established.

In comparison with the synthetic polymers on which these observations have been made, it is well known that molecules of cellulose and its derivatives are relatively inflexible. Consequently, the question arises whether the phenomenon of chain folding can also exist in these polymers. The long-range interest of the present work lies in the possible role of chain folding in the fine structure of fibers of native and regenerated cellulose. As a starting point we have chosen the study of single crystals and their aggregates in cellulose and its derivatives. The present paper deals with a study of the growth and morphology of single crystals of cellulose triacetate.

Cellulose triacetate is a linear macromolecule composed of glucose triacetate residues connected by 1 → 4 β-glycosidic bonds. The chains possess sterical as well as chemical regularity and as such are able to

crystallize. There are two stable polymorphic modifications; cellulose triacetate I and cellulose triacetate II. The first form can be obtained by the heterogeneous acetylation of cellulose I, while cellulose triacetate II is formed during the acetylation of cellulose II or by the precipitation of homogeneously acetylated triacetate I from solution. The material of the present investigation was the triacetate II modification. Interplanar spacings for cellulose triacetates have been published by a number of authors,[7-14] and Dulmadge[13] has determined the crystal structure of cellulose triacetate II. The unit cell is orthorhombic and contains four cellobiose octaacetate residues, pairs of which are related by a twofold screw axis in the direction of the fiber axis. The glucose residues of such a pair are parallel and inclined at about 45° with respect to the a axis.

In this paper it will be shown that under suitable conditions cellulose triacetate can be made to form well-defined single crystals having a morphology quite analogous to that of crystals of the linear synthetic polymers.

EXPERIMENTAL

a. Materials and Experimental Technique

The material used was a highly substituted acetate obtained through the courtesy of Eastman Kodak, Rochester. The acetyl value of 44.7% corresponds to virtually maximum substitution. The intrinsic viscosity in methylene chloride/methanol (90/10) was 2.12, corresponding to an estimated degree of polymerization of 300. Several fractions ranging in molecular weight from 36,000 to 135,000 were prepared by the fractional solution process using mixtures of methylene chloride and ethanol.

In preliminary experiments crystallization was effected by dissolving the polymer in hot nitromethane and cooling the solution to room temperature. Under these conditions the polymer precipitates from solution as spherulites at higher concentrations (above about 0.5%) and as small thick crystals at lower concentrations.[15] However, as these crystals were unsuitable for electron microscope studies, attempts were made to grow them wider and thinner. It was found that this could not be achieved from pure nitromethane, and it was necessary to add a nonsolvent in suitable quantities in order to facilitate growth. Although many other solvents were tried, none were found to give crystals. The crystals used in the present investigation were grown as follows. The polymer was dissolved in hot nitromethane at concentrations varying from 0.002 to 0.05%. To this solution was added an appropriate amount of hot n-butanol. The solution was then either cooled slowly to room temperature, or else placed in a thermostat at the desired crystallization temperature (usually in the range 20–50°C.). The amount of butanol used depends on the molecular weight of the polymer; the higher the molecular weight, the lower the volume ratio of butanol/nitromethane.

For examination in the optical microscope, drops of the crystal suspension were placed on a glass slide and the solvent allowed to evaporate at room

temperature. For electron microscopy the suspension was placed on a slide precoated with carbon. After drying, the specimen was shadowed with Au–Pd; the film was subsequently floated off on water and then transferred to electron microscope grids.

In the optical microscope the crystals were best viewed with incident illumination. Electron optical investigations were made in a Siemens Elmiskop I instrument. Electron diffraction experiments were carried out in the electron microscope with the lenses set in the diffraction condition.

b. Observations

It was found that the habit of the crystals is rather strongly dependent on the crystallization conditions, in particular on the polymer concentration and the proportion of butanol used. If an excessive amount of butanol was used the polymer precipitated exclusively in a compact globular form,

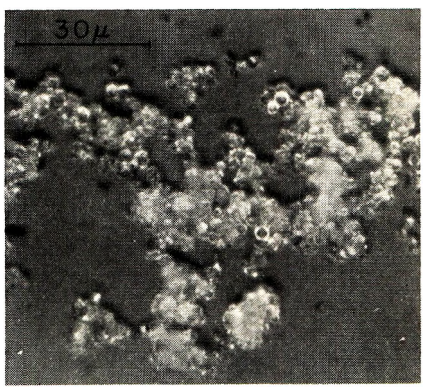

Fig. 1. Globular particles of cellulose triacetate. Optical micrograph with incident steep oblique illumination. 570×.

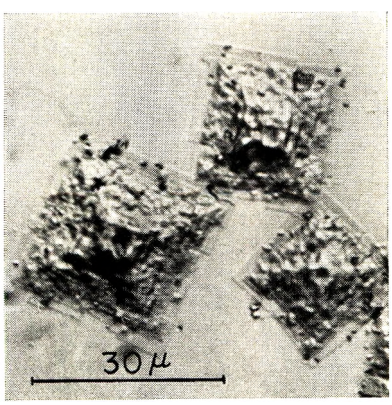

Fig. 2. Optical micrograph of thick pyramidal crystals of cellulose triacetate. Thin square shaped basal lamellae can be recognized. Incident steep oblique illumination. 855×.

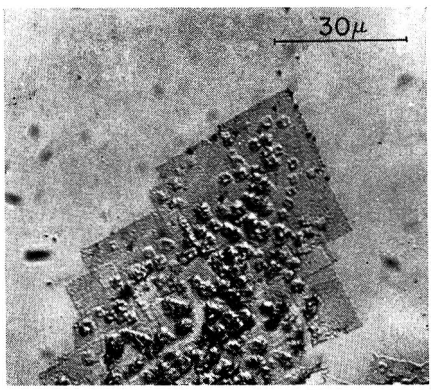

(*a*)

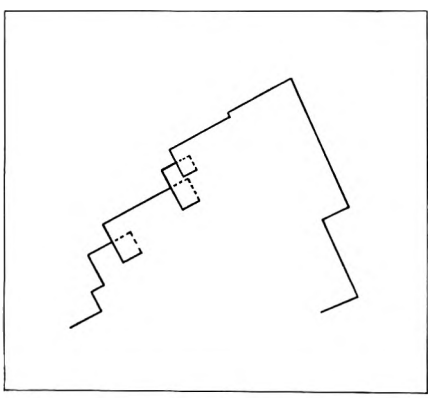

(*b*)

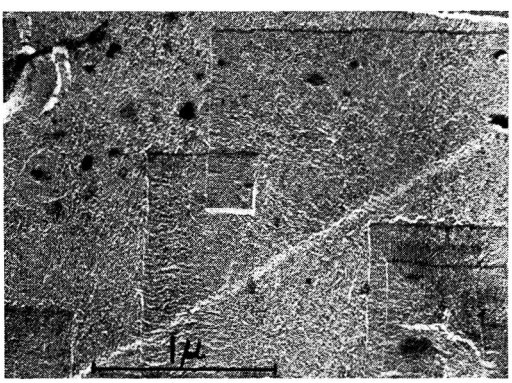

(*c*)

Fig. 3. (*a*) Optical micrograph with incident steep oblique illumination showing a cellulose triacetate crystal with overlapping lamellae (the wartlike protrusions are dislocation overgrowths), 585×; (*b*) tracing of the crystal in Fig. 3(*a*) illustrating the closed loops by which each lamella grows into the next; (*c*) electron micrograph showing an example of a closed dislocation loop. Shadowed with gold-palladium, 13,200×.

as shown in Figure 1. Although no detailed investigation of these structures has been made, it is believed that they are spherulitic in nature. As already stated, cellulose triacetate can be crystallized from solution as spherulites.

On the other hand, if the ratio of butanol to nitromethane was too low, the crystals obtained tended to be rather thick and were in the form of a pyramid with a craterlike depression at the apex (Fig. 2). The origin of this depression is not known at present. In many cases the thin, square-shaped basal lamella could be seen protruding around the edge of the crystals.

Under optimal conditions of growth the crystals attained widths up to about 200 μ without excessive thickening. Figure 3*a* is an optical micrograph showing a characteristic mode of development in which the square-shaped basal lamellae overlap one another in such a manner as to produce re-entrant faces. This type of growth is very similar to that found in some polyethylene crystals[19] which consist of twins repeating in a regular sequence. Actually, it appears that the various lamellae form a single continuous sheet. As seen in the line drawing of Figure 3*b*, overlapping occurs only at those positions, adjacent to the re-entrant angles, where the lamellae merge into one another. The agency through which the lamellae grow into one another is an apparent closed dislocation loop, an example of which is shown in Figure 3*c*. The appearance of these loops, with the shadow ending halfway along one face (Fig. 3*c*), strongly suggests that they actually consist of two spirals at the top and bottom of the lamella. It may be presumed that during solvent removal the shearing of the layers produces the closed loops seen.

An increase in the concentration of the polymer solution (0.05%) favored the growth of large thick dendritic crystals as illustrated in the optical micrographs of Figure 4. At lower concentrations the tendency towards dendritic growth was also found to increase for higher molecular weight fractions. The central portion of a large dendritic crystal is shown in Figure 4*a*. The crystal is thickest in the middle due to a broad ridge running lengthwise. Fracture has occurred at several points along the ridge, probably on drying down. Figure 4*b* shows an area near the tip of another dendritic crystal. The crystal of Figure 4*a* tapered off in a similar manner. The dendritic crystals so far described had only a simple elongated habit. In some other preparations (Fig. 4*c*) the crystals had an overall starlike habit. The diagonals consisted of pronounced ridges intersecting at right angles, and there was a depression at the point of intersection similar to that seen in the square crystals of Figure 2.

In some preparations, "picture frame" type crystals were observed (Fig. 5) similar to those reported by Keller for polyethylene[16] and poly-4-methylpentene-1.[17] Even in the optical micrographs it could be clearly seen that the frame formed a border around a thin plate. These crystals formed whenever a suspension of the crystals in their growth medium was heated close to the solution temperature and then allowed to cool. Keller[16]

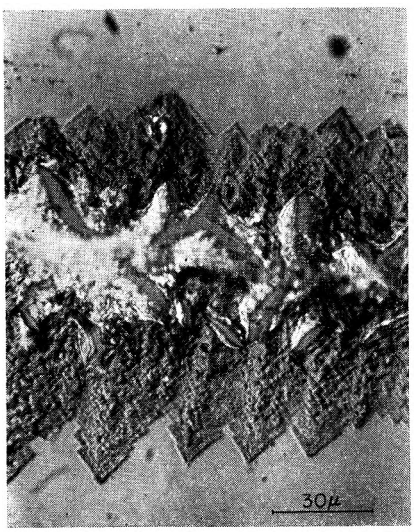

(a)

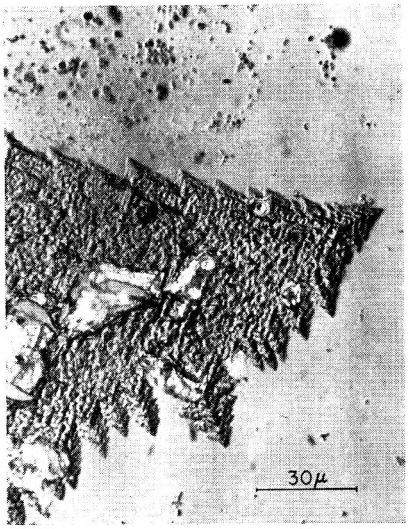

(b)

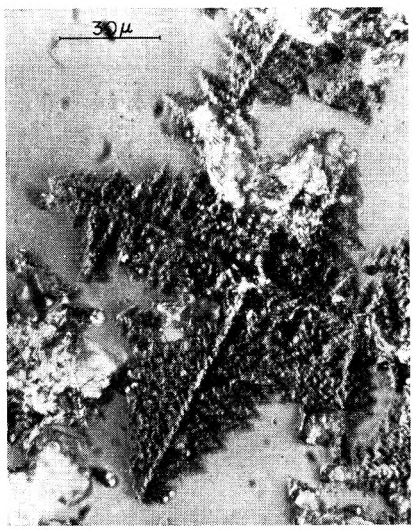

(c)

Fig. 4. Optical micrographs with steep incident oblique illumination showing thick dendritic crystals of cellulose triacetate: (*a*) central portion of a crystal 450×; (*b*) region near the tip of a crystal 450×; (*c*) crystal with heavy ridges along the principal diagonals. There is a craterlike depression at the intersection of the diagonals. 450×.

has shown that the picture-frame phenomenon is due to reprecipitation of dissolved polymer.

Electron micrographs (Fig. 6–8) confirmed that the crystals consist of approximately square-shaped lamellae, and indicated further that thickening takes place by spiral growth centered on screw dislocations in accordance with Frank's theory of crystal growth.[18] For all the fractions

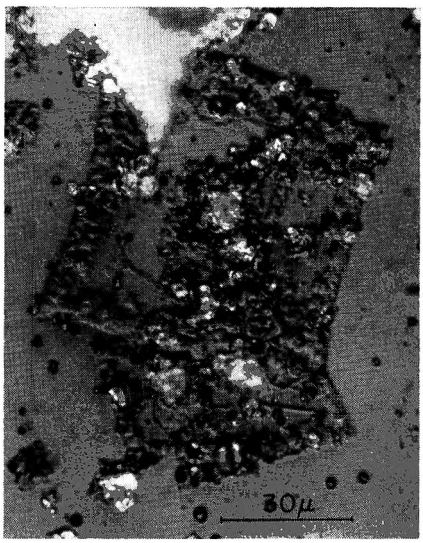

Fig. 5. Optical micrograph of "picture-frame" type crystals. Incident steep oblique illumination. 580×.

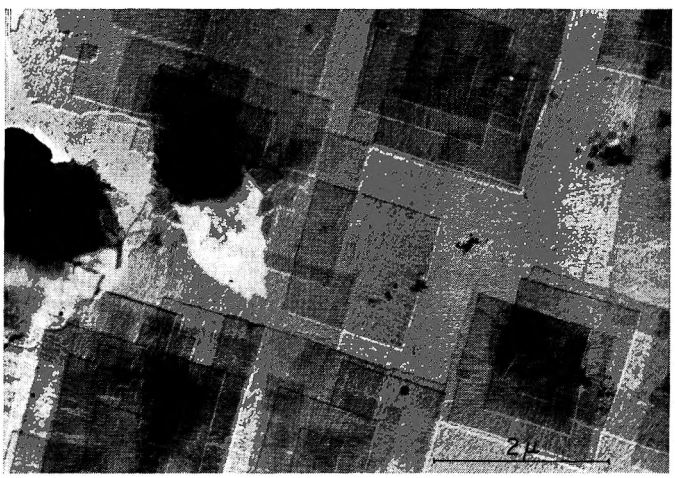

Fig. 6. Electron micrograph of a cellulose triacetate crystal showing (at the center of the photograph) the development of a closed sheet from two dislocations of opposite hand. Shadowed with gold–palladium. 11,400×.

investigated the layer thickness was of the order of 180–200 A. as determined by the shadow length method.

In Figure 6 there are two screw dislocations of opposite hand close to each other and equally developed. The resultant growth pattern leads to a closed sheet. Figure 7 shows a further example of the interaction of dislocations of opposite sign leading to an interleaving of the growth layers. The more complex growth which arises from the development and interaction of large numbers of dislocations is shown in Figure 8.

A characteristic feature of the crystals is a pronounced system of coarse striations running perpendicular to the edges of each layer. This is particularly well revealed in Figure 7. The striations change direction along the layer diagonals. Accordingly, each layer of the crystal appears

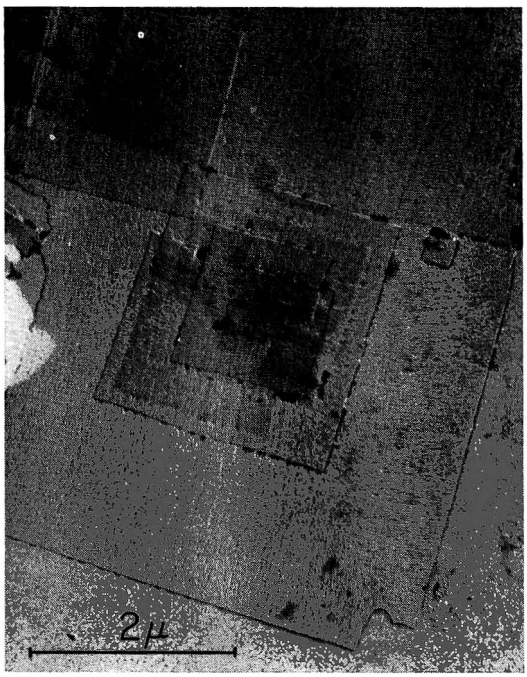

Fig. 7. Electron micrograph of a cellulose triacetate crystal showing interleaving from dislocations of opposite hand. Note particularly the surface striations changing direction at the layer diagonals. Shadowed with gold–palladium. 13,440×.

Fig. 8. Electron micrograph of a crystal showing complex growth from multiple dislocation centers. Shadowed with gold-palladium. 11,400×.

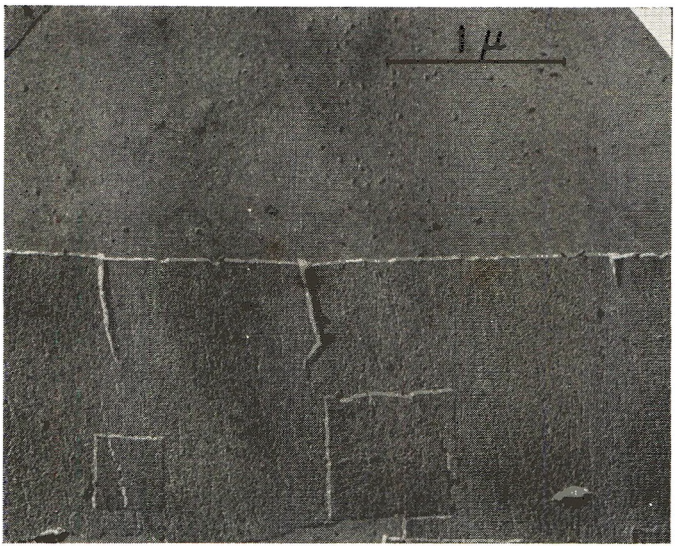

Fig. 9. Electron micrograph showing pleats along the edge of a crystal. Shadowed with gold–palladium. 24,000×.

to be divided into four sectors which differ from one another in the direction of the striations. In some photographs crystals were observed which had folded back on themselves near a corner on drying down; the lower surfaces could then also be seen. When allowance is made for the fold, the striations are in the same direction as those on the top surface of the crystal. The striations must therefore either be restricted to the upper and lower surfaces of the layers or else pass right through them, giving a lamellalike structure perpendicular to the face of the crystals. On the face of it neither alternate can be dismissed as *a priori* improbable. However, were the latter true, it might be expected that the crystals should show a tendency to fracture preferentially along the striations under suitable stress. In Figure 7 the crystal is broken at one corner. The fracture obviously occurred subsequent to the completion of growth, presumably on drying down, and is along the striations. Other photographs show similar effects. This suggests that the striations are points of weakness in the crystal, and offers some support to the view that the striations are not merely a surface feature, but constitute a structural discontinuity running through the layers.

Figure 9 shows a further interesting morphological feature frequently observed. These are short pleats running parallel to the striations and invariably terminating on a bounding face of a lamella. Pleats have been observed previously[26,27] in lozenge-shaped polyethylene crystals, their direction being most frequently along the short diagonal. These have been explained on the basis that the crystals grow as hollow pyramids which collapse and flatten on drying down, the excess material being pushed into a pleat. In the present case the appearance of the pleats indicates

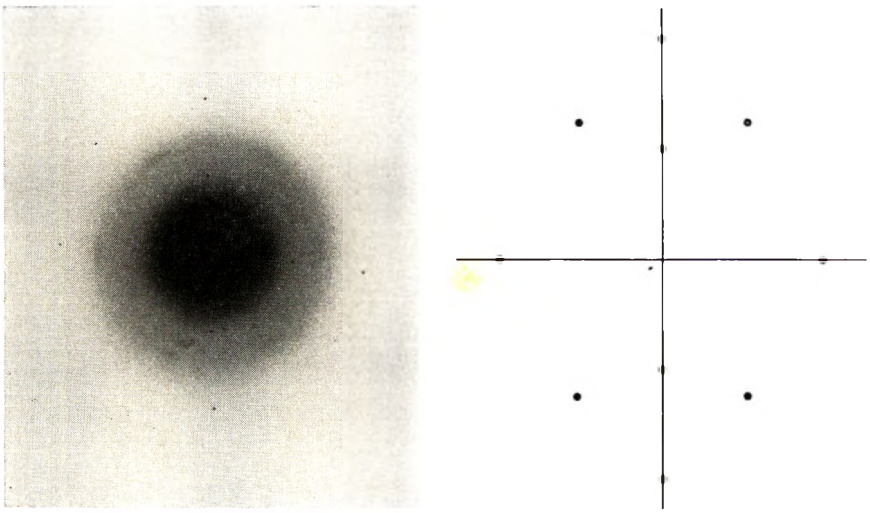

(*a*) (*b*)

Fig. 10. (*a*) Electron diffraction pattern of cellulose triacetate crystals; (*b*) scale drawing showing the position of the principal spots in Fig. 10 *a*.

that they are not formed during the growth of the crystal but are the result of compression forces acting parallel to the plane of the layers during the removal of the solvent when the crystals are dried down on the specimen support. The location of the pleats at the crystal edges suggests that the crystals grow flat. If growth was nonplanar, the pleats would be expected near the center as in the case of polyethylene. It is interesting to note that the pleats always occur in the same direction as the striations. This does not seem fortuitous. It is suggested that this observation may lend further support to the previously mentioned hypothesis that the striations as structural discontinuities within the lamellae are points of weakness.

A considerable amount of attention was devoted to electron diffraction experiments in an effort to obtain unequivocal proof that the objects being investigated were single crystals, and to determine the orientation of the chain molecules with respect to the layers. The experiments proved to be very difficult. It is now well known that an electron beam destroys the diffracting power of polymer crystals without altering their shape.[19] Diffraction patterns can, however, be obtained by using low beam intensities and working rapidly. The triacetate crystals appear to be particularly sensitive to the electron beam, even at very low intensities. The few patterns obtained were very weak, poorly defined and difficult to reproduce.

Attempts were also made to photograph the crystals at very low magnification and intensity in an effort to detect any structures which might be beam sensitive. The technique employed was that found successful in photographing single crystals of polyethylene as described by Agar et al.[19] In no case was any diffraction contrast observed.

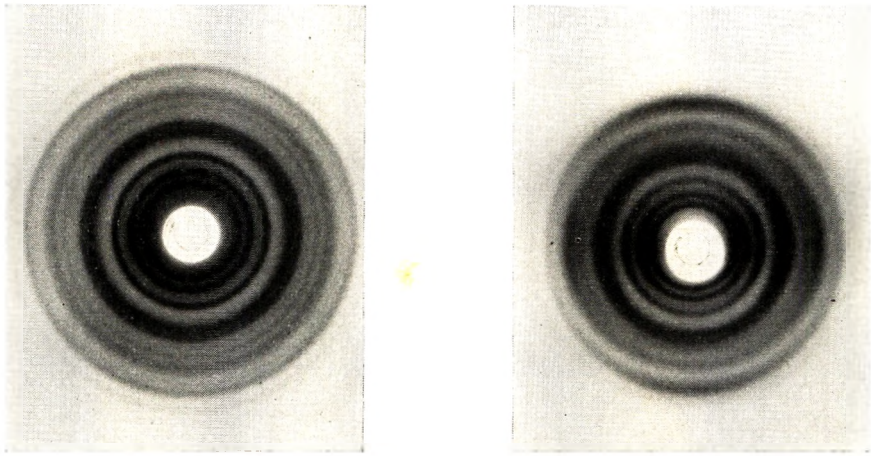

(*a*) (*b*)

Fig. 11. X-ray diffraction patterns of a tablet formed by filtering crystals from solution: (*a*) x-ray beam perpendicular to the plane of the tablet; (*b*) x-ray beam parallel to the plane of the tablet.

Figure 10*a* shows an electron diffraction pattern of the crystals. Because of the weakness of the spots, their positions are defined in the scale drawing of Figure 10*b*. The pattern corresponds to an orthogonal network in the basal plane of the reciprocal lattice. There are three principal reflections which have been indexed as (020), (040), and (600), the corresponding spacings being 5.92, 2.96, and 4.1 A., respectively. The dimensions of the unit cell in the plane normal to the electron beam are then 24.6 A. and 11.8 A. These values are in good agreement with the dimensions of the *ab* projection reported by Dulmadge,[13] who has proposed an orthorhombic unit cell with $a = 24.5$ A., $b = 11.56$ A., and c (the chain axis) $= 10.43$ A. From these observations we conclude that the chain molecules are oriented perpendicular to the plane of the lamellae.

According to x-ray evidence to be presented shortly, the strongest reflections are the (110), (210), and (310). These were not observed in any of the electron diffraction patterns, but at least two of them, (110) and (210), could be masked by the halo due to the main beam at the center. It can be clearly seen that there are three pairs of (600) reflections, and there are indications that there may be more than one pair of (020) and (040) reflections. None of the patterns were sufficiently well defined to allow more definite conclusions. It is, however, at least clear that this type of pattern cannot be due to a single triacetate crystal but must arise from the superposition of a number of the orthorhombic lattices in some form of twin orientation.

Corroborative evidence on the orientation of the molecules was obtained from a study of wide-angle x-ray diffraction patterns. The crystals were recovered from suspension by slow filtration. Diffraction patterns were obtained in a flat film camera with the use of nickel-filtered CuKα radia-

TABLE I
Observed X-Ray Spacings

Index	Observed spacing, A.	Intensity
110	10.32	vs
210	8.44	vs
111	7.47	vw
310	6.67	vs
(410)(220)	5.12	vs
320	4.70	s
212	4.43	w
600	4.16	m
(520)(430)	3.81	m
322	3.49	w
(422)(032)	3.31	m
(522)(232)	3.06	w
340	2.72	vw
004	2.60	vw

tion. When the x-ray beam was oriented perpendicular to the horizontal plane of the cake, a powder pattern showing several well defined reflections was obtained (Fig. 11*a*). With the beam parallel to the plane of the cake, which was oriented along the equator, the pattern showed preferred orientation (Fig. 11*b*), the intensity maxima for all (*hko*) reflections being on the equator and for (*hkl*) on the meridian. The positions of the intensity maxima are consistent with the assumption that the *ab* plane of the unit cells lie in the plane of the crystal and that within the cake the crystals are preferentially stacked on top of one another in the direction of their *c* axes.

In Table I the observed x-ray spacings are listed, together with the indices as obtained by reciprocal lattice methods. The data are in excellent agreement with the results of others[12,13] on oriented fibers and films and serve to identify the crystals as those of cellulose triacetate II as distinct from triacetate I.

We endeavored to obtain low-angle x-ray diffraction patterns in an attempt to uncover long spacings which might be identified with the thickness of the layers.[31] A Kiessig vacuum camera was used.[20] The pinholes were 0.3 mm. in diameter, the specimen film distance was 400 mm., and the resolution was about 300 A. The specimens were prepared as described above for wide-angle studies and the horizontal plane of the cake was oriented parallel to the beam. It was found that the crystal aggregates do not give discrete low-angle reflections but only a strong continuous scattering. In some experiments thick crystals were used. These contain many hundreds of layers stacked regularly on top of one another and would be expected to give at least a powder pattern with continuous rings. The absence of discrete reflections may indicate that within the filtered aggregate the mode of packing of the lamellae is not sufficiently uniform to fulfill the diffraction conditions. It may also be due to lack of uniformity in the thickness of the individual lamellae on the molecular scale.

DISCUSSION

In the preceding sections it has been shown that cellulose triacetate crystallizes from solution as square-shaped, lamellar crystals in which the chain molecules are oriented perpendicular to the layers. The observed layer thickness corresponds to about 18 unit cell lengths in the direction of the *c* axis. We wish now to consider the evidence for chain folding.

The molecular weights of the fractions were estimated by using Cumberbirch and Harland's relationship[21] connecting the molecular weight of this polymer and the limiting viscosity. In Table II the D.P. values for the various fractions are shown. The length of a glucose acetate residue is 5.15 A., and the identity period of 10.3 A. along the *c* axis indicates that the molecules must assume a highly extended configuration in the lattice. The length of the molecules may therefore be taken as the degree of polymerization multiplied by 5.15. The values thus obtained are given in Table II. It is seen that with the exception of fraction F1L the length of the molecules exceeds the measured layer thickness. Accordingly, as the molecules evidently cannot be simultaneously straight and perpendicular to the layers, it would appear the phenomena of folding also occurs in these crystals. A study of a Stuart-Briegleb atomic model indicates that provided the successive residues in the fold are permitted to rotate around the glycosidic linkages, only about four residues are required for the chain to fold back on itself.

It is seen from the foregoing that the inflexibility of the triacetate chains is really no hindrance to folding. However, having regard to the apparent ease with which it occurs, one is led to wonder whether the molecules may not already be folded in the solution. It is not proposed to enter here into considerations of the theory of the formation of polymer crystals with folded chains. This has been treated in detail by Lauritzen and Hoffman[24] and others.[28,29] Nevertheless, it may be of interest to give passing mention to an attempt to detect a possible one-dimensional ordering in the supercooled solutions due to intramolecular interactions. Viscosities of solutions of cellulose triacetate in nitromethane were measured over a wide temperature range (25–90°C.). Plots of viscosity against temperature gave smooth curves with no indication of a discontinuity which might be attributed to the onset of folding. This could mean either that the change in molecular configuration from the coiled to the folded state is not reflected in

TABLE II
Degrees of Polymerization and Molecular Lengths *L*

Fraction No.	$[\eta]$ dl./g.	Mol. wt.	D.P.	*L*, A.
F1L	0.30	10,000	35	180
F2L	0.42	15,000	50	270
F1H	0.90	36,000	125	640
F2H	1.55	85,000	300	1520
F5H	2.60	130,000	450	2300

the viscosity measurements or that folding does not occur in solution; the latter would imply that the molecules only fold when they are being laid down in the crystal lattice.

For one of the fractions (F1L, Table II) the chain length is of the same order of magnitude as the observed layer thickness. This suggests that in these crystals the step height is determined by the length of the fully extended chain. It would then follow that before folding can occur the chains must attain a certain critical length, which would appear to be about 180 A. In the case of polyethylene, Keller[22] has shown that when the hydrocarbon chains are shorter than 90 A., folding does not occur. The greater critical fold length in cellulose triacetate very likely results from the inflexibility of the molecular chains.

We consider next the question of the symmetry of the crystals. The observed apparent square habit suggests that the crystals have fourfold symmetry, yet the dimensions of the unit cell in the basal plane would lead one to expect twofold symmetry. This apparent inconsistency is, however, removed on closer examination. Indeed, measurement of the length of the diagonals and of the angles between adjacent bounding faces shows that the crystals are not square. The ratio of the lengths of the diagonals is about 1.04, and the angles between the bounding faces at the end of the long and short diagonals are approximately 87° and 93°. Thus, in reality the crystals have twofold symmetry as expected, and the apparent fourfold symmetry only results from the very close approach to a square habit. It is of interest then to enquire how this particular habit is developed.

Figure 12 shows a *c*-axis projection of the *ab* plane of the lattice. A monolayer crystal is drawn on the lattice with edges parallel to the [210]

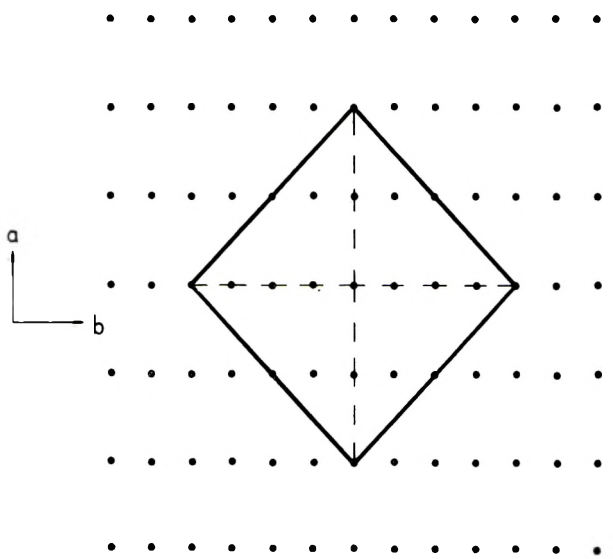

Fig. 12. Diagram showing a projection of a monolayer crystal of cellulose triacetate onto the {001} plane of the lattice.

directions. This is the only construction which satisfies the observed shape of the crystal. The angles of intersection of the {210} faces calculated on the basis of the unit cell dimensions given by Dulmadge[13] are 93.1° and 86.9°, in excellent agreement with the observed values given above. We infer from these considerations that the a and b axes are, respectively, along the long and short diagonals of the plates. Consequently, growth takes place along the {210} faces, and it is then reasonable to assume that the plane of the folded molecules lie in the {210} planes, i.e., parallel to the growth faces. The diagonals are in the [010] and [100] directions.

In the case of the crystals shown in Figure 3 each basal layer grows into the next through the development of an apparent closed dislocation loop situated adjacent to the re-entrant angles. Dislocations therefore appear to provide a mechanism not only for the thickening of the crystals but also for their lateral extension. The diffraction pattern of Figure 10 was obtained from crystals of the same type as those considered here. As discussed earlier this pattern is not that of a single triacetate crystal but arises from a superposition of lattices. It therefore seems reasonable to suggest that the type of growth in Figure 3 may be due to repeated twinning. Proof of this is, however, a matter for further investigation.

It was mentioned earlier that the diagonals divide each crystal layer into four distinct sectors. This is consistent with our interpretation of the folded chains being in the {210}, {$\bar{2}$10}, {2$\bar{1}$0}, and {$\bar{2}\bar{1}$0} planes. The striations and concomitant sectorization described here are not new. Similar observations have been made in polyethylene,[19] polyoxymethylene,[25] and nylon.[6] However, in contrast to the other polymers, the striations in cellulose triacetate do not appear to be sensitive to ageing on drying down or to destruction by the electron beam in the microscope.

In the terminology of Reneker and Geil[23] the sectors are defined as fold domains and the diagonals as fold domain boundaries. The latter are lines of demarcation between those sections of the crystal in which the fold planes have a common orientation. The lattice is however, continuous across the domain boundaries.

One of the most puzzling features of the striations is their direction. As the folded chains lie in the {210} planes, it would intuitively be expected that the striations should be parallel to the bounding faces and not perpendicular as observed. It may be noteworthy to point out here that the striations have also been observed in crystals for which, as shown earlier (fraction F1L, Table II) there is no folding, the layer thickness being equal to the length of the extended molecules. Accordingly the striations are not a feature related to chain folding, unless the terminal acetyl groups are able to act in the capacity of folds. The origin and significance of these striations is not understood at present, but it seems possible that they may be purely crystallographic in origin, being due to the manner in which the chain molecules are constrained to pack together in the chain direction. Keller[25] has accounted for striations in polyethylene on a similar basis.

It remains to consider briefly some possible modes of chain packing.

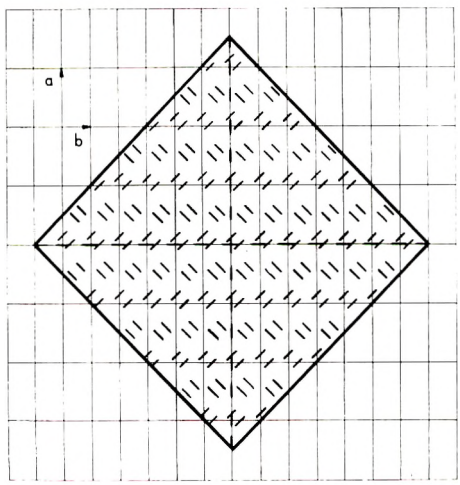

(*a*)

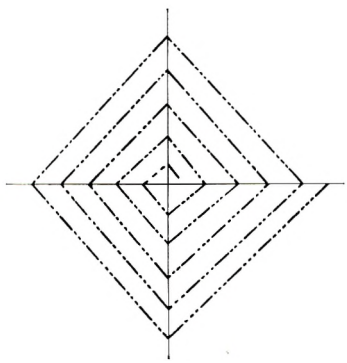

(*b*)

Fig. 13. (*a*) A *c*-axis projection of a crystal showing the positions of the chain molecules in the unit cells (The median plane of the chain segments is indicated by the short lines inclined to the *a* axis); (*b*) diagram showing one possible way in which a single molecule might fold to form a nucleus. View along the *c* axis. Solid lines indicate folds on upper surface of lamella; dashed lines indicate folds on lower surfaces.

According to the work of Dulmadge,[13] the unit cell of cellulose triacetate II contains two sets of cellulose acetate chains, each paired about a twofold screw axis in the direction of the chain molecules and with their median planes roughly perpendicular to each other. On the basis of this model two possible modes of chain packing are here discussed.

Consider the projection of a crystal on the {001} planes illustrated in Figure 13. The molecular chains are normal to the plane of the figure and the median plane of each chain is indicated by a line inclined at about 45° to the *a* axis. The pair of chains in the lower left-hand corner of each cell generates through the agency of the screw operations a new pair of chains in the center of each cell. Assuming, as before, that the folds lie in the {210} planes, we have the following possibilities.

The plane of adjacent segments of chains bridged by folds are turned at right angles or nearly so, to each other. This would require successive glucose triacetate residues within the fold to rotate around the glycosidic bonds, so as to permit the median plane of the chain segments to change direction. Following Lauritzen and Hoffman,[24] a single molecule might be considered to form the nucleus by folding in a spiral manner as indicated in Figure 13*b*. Folds on the upper 001 surface are indicated by the solid lines in the {210} planes while the dashed lines similarly indicate folds on the lower 001 surface. The plane of the folded molecules changes orientation at the domain boundaries but the planes are continuous across the boundaries.

The alternative structure is one in which the median planes of adjacent segments of chains connected by folds are parallel to each other. This would imply that the crystal contains two sets of folded chains, one running approximately parallel and the other perpendicular to each growth face. The fold length of each set of chains must differ so as to allow one set of chains to be caged within the other. This inclusion effect arises from the fact that the chains folded in one direction would have to cross over or under those folded in the other direction. Enough has been said to indicate the general properties of this type of fold packing. It must now be pointed out this arrangement is considered inadmissable, since in the first place segments of the folded molecules would protrude from the growth faces. Secondly, it is difficult to imagine the characteristics of the folded nucleus which would allow the development of a crystal with this disposition of the folds. On the basis of the above, it may be tentatively concluded that the chain segments joined by folds are those at the corner and center of each unit cell.

The success in growing lamellar crystals of cellulose triacetate raises the question of the possibility of saponifying them without destroying the lattice. A preliminary report of such an investigation has already been made.[30] The details will appear in a forthcoming paper.[32]

The author is indebted to Dr. S. T. Bayley, Division of Applied Biology, National Research Council, Ottawa, for his generous assistance in obtaining the electron micrographs. Thanks are also due to Mr. C. P. Henry for assistance with the experimental work and Dr. P. H. Geil of the Research Triangle Institute for his comments on the manuscript.

The work was supported under the Pioneering Research Program administered by the Institute of Paper Chemistry, Appleton, Wisconsin, to whom grateful acknowledgment is hereby made.

References

1. Till, P. H., *J. Polymer Sci.*, **24**, 301 (1957).
2. Keller, A., *Phil. Mag.* [8], **2**, 1171 (1957).
3. Fischer, E. W., *Z. Naturforsch.*, **12a**, 753 (1957).
4. Keller, A., and A. O'Connor, *Discussions Faraday Soc.*, **25**, 114 (1958).
5. Geil, P. H., N. K. J. Symons, and R. G. Scott, *J. Appl. Phys.*, **30**, 1516 (1959).
6. Geil, P. H., *J. Polymer Sci.*, **44**, 449 (1960).
7. Hess, K., and C. Trogus, *Z. Physik. Chem.* (*Leipzig*) **B5**, 161 (1929).
8. Hess, K., and C. Trogus, *Z. Physik. Chem.* (*Leipzig*), **B9**, 160 (1930).

9. Naray-Szabo, S., and G. Susich, *Z. Physik. Chem. (Leipzig)*, **B4**, 268 (1928).
10. Baker, W. O., C. S. Fuller, and N. R. Pape, *J. Am. Chem. Soc.*, **64**, 776 (1942).
11. Happey, F., *J. Textile Inst., Trans.*, **41**, 381 (1950).
12. Sprague, B. S., J. L. Riley, and H. D. Noether, *Textile Res. J.*, **28**, 275 (1958).
13. Dulmadge, W. J., *J. Polymer Sci.*, **26**, 277 (1957).
14. Passagez, B., and J. Tonssaint, *Bull. Classe Sci., Acad. Roy. Belg.*, **44**, 863 (1958).
15. Manley, R. St. J., *J. Polymer Sci.*, **47**, 509 (1960).
16. Keller, A., and D. C. Bassett, *J. Roy. Microscop. Soc.*, **79**, 243 (1960).
17. Frank, F. C., A. Keller, and A. O'Connor, *Phil. Mag.*, **4**, 200 (1959).
18. Frank, F. C., *Discussions Faraday Soc.*, **5**, 48, 186 (1949).
19. Agar, A. W., F. C. Frank, and A. Keller, *Phil. Mag.* [8], **4**, 32 (1959).
20. Kiessig, H., *Kolloid-Z.*, **152**, 62 (1957).
21. Cumberbirch, R. J., and W. G. Harland, *J. Textile Inst., Trans.*, **49**, 679 (1958).
22. Keller, A., and A. O'Connor, *Polymer*, **1**, 163 (1960).
23. Reneker, D. H., and P. H. Geil, *J. Appl. Phys.*, **31**, 1916 (1960).
24. Lauritzen, J. I., Jr., and J. D. Hoffman, *J. Res. Natl. Bur. Std.*, **64A**, 73 (1960).
25. Bassett, D. C., and A. Keller, *Phil. Mag.* [8], **6**, 345 (1961).
26. Niegisch, W. D., *J. Polymer Sci.*, **40**, 263 (1959).
27. Bassett, D. C., F. C. Frank, and A. Keller, *Nature*, **184**, 810 (1959).
28. Fischer, E. W., *Z. Naturforsch.*, **12a**, 753 (1957); *ibid.*, **14a**, 584 (1959).
29. Frank, F. C., and M. Tosi, *Proc. Roy. Soc. London*, **A263**, 323 (1961).
30. Manley, R. St. J., *Nature*, **189**, 390 (1961).
31. Keller, A., *Nature*, **180**, 1289 (1957).
32. Manley, R. St. J., *J. Polymer Sci.*, **A1**, 1893 (1963).

Résumé

On a préparé des monocristaux du triacétate de cellulose par surfusion dans des mélanges de nitrométhane et de *n*-butanol. Les cristaux ont environ une forme carrée et ils épaississent par croissance en spirale ecentrée par dislocations en hélice. Les chaînes moléculaires sont perpendiculaires avec lamelles qui ont une largeur d'environ 180 A. Malgré leur rigidité les molécules semblent avoir des configurations pliées dans les lamelles. Plusieurs données morphologiques des cristaux sont décrites et discutées.

Zusammenfassung

Cellulosetriacetat-Einkristalle wurden durch Unterkühlung verdünnter Lösungen in Nitromethan-*n*-Butanolgemischen dargestellt. Die Kristalle besitzen annähernd quadratische Gestalt und ihre Dickenzunahme erfolgt durch Spiralwachstum über Schraubenversetzungen. Die Kettenmoleküle stehen senkrecht zu den etwa 180 A. dicken Lamellen. Trotz ihrer Steifigkeit scheinen die Moleküle in den Lamellen gefaltete Konfigurationen anzunehmen. Verschiedene morphologische Eigenschaften der Kristalle werden beschrieben und diskutiert.

Received June 2, 1962

JOURNAL OF POLYMER SCIENCE: PART A VOL. 1, PP. 1893–1899 (1963)

Hydrolysis of Cellulose Triacetate Crystals

R. ST. JOHN MANLEY, *Physical Chemistry Division, Pulp and Paper Research Institute of Canada, and Department of Chemistry, McGill University Montreal, Canada*

Synopsis

Crystals of cellulose triacetate were hydrolyzed in an attempt to obtain single crystals of cellulose. The hydrolyzed material retains the morphology of the triacetate crystals, but its crystalline state depends upon the method of hydrolysis. In an aqueous medium, polycrystalline cellulose is formed, while a nonaqueous medium gives an amorphous cellulose. The results suggest that the hydrolysis is accompanied by a disruption of the lattice and that recrystallization of the resulting amorphous cellulose is caused by the water.

INTRODUCTION

In the first paper of this series the growth and morphology of crystals of cellulose triacetate was described.[1] It was shown that the crystals are lamellar in structure and thicken by spiral growths centered on screw dislocations. The chain molecules are oriented normal to the crystal layers and, since the length of the molecules exceeds the layer thickness, it was concluded that in spite of their inflexibility the molecules must assume folded configurations within the lamellae.

As an extension of this work it was of interest to investigate the possibility of saponifying the triacetate crystals without destroying the lattice. Crystals of cellulose would be thus obtained. A preliminary account of this work has already been given.[2] In the present paper further details are presented.

EXPERIMENTAL

The crystals of cellulose triacetate were grown, as described previously,[1] by supercooling dilute solutions in mixtures of nitromethane and butanol. The crystals so obtained were washed with absolute methanol and then saponified by two methods as follows.

a. Hydrolysis in Aqueous Media. Deacetylation was carried out in 2% potassium hydroxide solution in aqueous methanol (50:50 v/v) at room temperature for about 10 hr.[3] After saponification the crystals were separated from the saponification medium and washed thoroughly with water.

b. Hydrolysis in Nonaqueous Media. Deacetylation was performed in

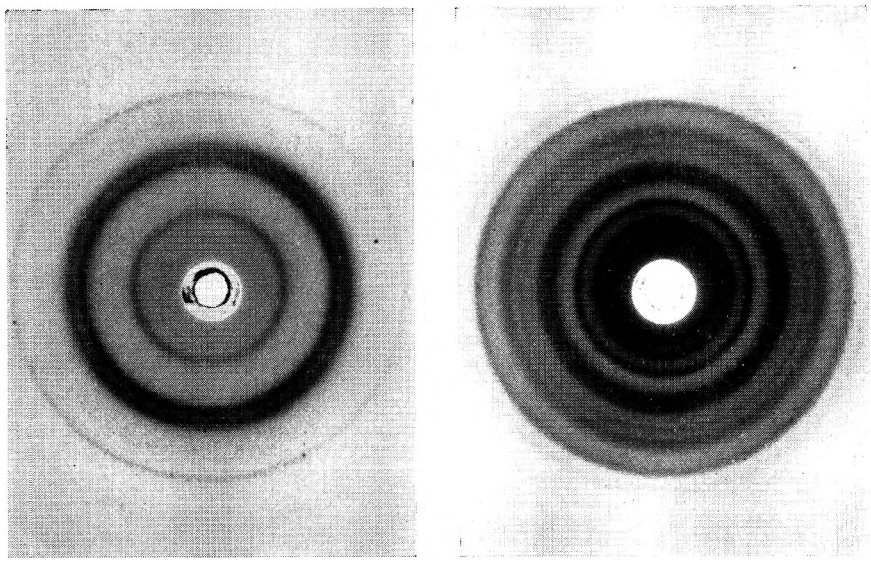

(*a*) (*b*)

Fig. 1. X-ray powder pattern of (*a*) cellulose II obtained when crystals of cellulose triacetate are saponified with potassium hydroxide in aqueous methanol; (*b*) cellulose triacetate crystals.

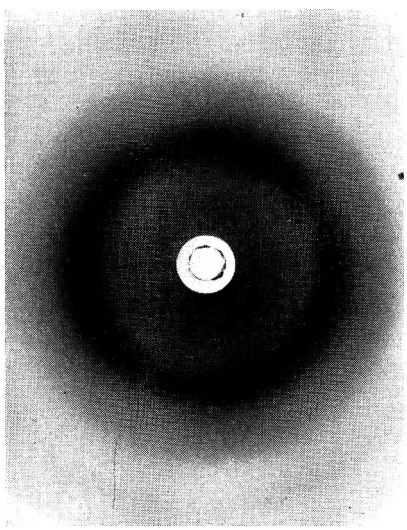

Fig. 2. X-ray diagram of cellulose triacetate crystals saponified with sodium methylate in absolute methanol.

0.5*N* sodium methylate in anhydrous methanol at room temperature for about 10 hr. The saponified crystals were separated from the reaction medium and washed with absolute methanol.

In both cases the suspension was agitated gently during the reaction.

Observations were made in the optical microscope after drying down the crystals on glass slides. It was found, as mentioned in an earlier paper,[2]

(*a*)

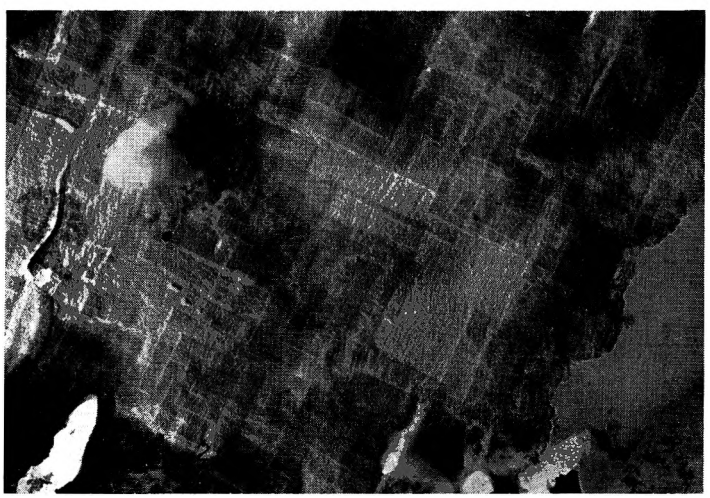

(*b*)

Fig. 3. Electron micrographs of (*a*) a cellulose triacetate crystal before hydrolysis; (*b*) a cellulose triacetate crystal after hydrolysis. 16,750×.

that the crystals remained intact following hydrolysis. The only conspicuous change was a lateral contraction of about 30%, which could be accounted for as due to the replacement of the bulky acetyl groups by hydrogen.

For x-ray examination the crystals were dried from their respective wash liquids, and powder patterns were obtained in a flat film camera with the use of nickel-filtered CuKα radiation. The results obtained in the two cases were quite different. Figure 1*a* shows the x-ray diagram of the crystals hydrolyzed in the aqueous medium. For comparison a powder pattern of the cellulose triacetate crystals is shown in Figure 1*b*. The

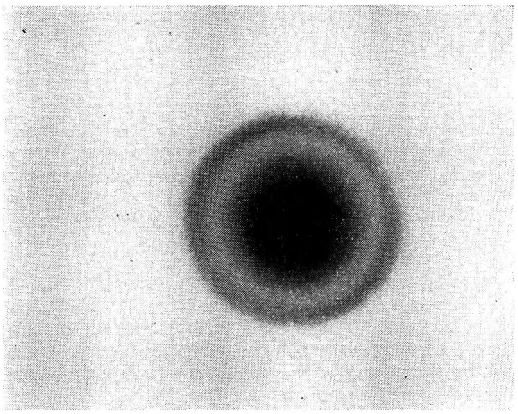

Fig. 4. Selected area electron diffraction pattern of a cellulose triacetate crystal hydrolyzed with potassium hydroxide in aqueous methanol.

pattern of the hydrolyzed specimen is well defined and corresponds to the structure of cellulose II. Furthermore, there are no residual reflections from the acetate, indicating that the reaction had proceeded throughout the lattice and not merely on the surfaces of the crystals.

This evidence for the completeness of reaction is, however, not conclusive as small amounts of acetyl groups could remain undetected by the x-ray method. However, the infrared diagram of the product showed no absorption for carbonyl groups, and an analysis for acetyl groups by the Eberstadt method[4] gave negative results. It can therefore be safely concluded that the hydrolysis was complete.

In sharp contrast is the diagram for crystals hydrolyzed in the non-aqueous medium (Fig. 2). A single, broad, diffuse maximum dominates the pattern, but weak traces of the strongest triacetate reflections could also be detected. The position of the diffuse halo corresponds to that of the $(10\bar{1})$ and (002) reflections in the cellulose II pattern. Thus this method of hydrolysis produces a two-phase system comprised chiefly of amorphous cellulose but also containing smaller amounts of unhydrolyzed triacetate. Accordingly, in this reaction the lattice is not completely penetrated.

For examination in the electron microscope the crystals were deposited on a carbon substrate, mounted on standard specimen screens and shadowed with gold–palladium. A Siemens Elmiscope I instrument was used. In Figure 3 electron micrographs of unhydrolyzed and hydrolyzed acetate crystals are shown. It is evident that there is not much difference in the surface morphology of the two specimens. The square-shaped lamellae, spiral growths, and striations are evident in both pictures. The hydrolyzed samples, however, usually showed a slight increase in surface irregularity, and the sharpness of the lamellar boundaries was reduced, as if a partial melting of the crystal had occurred. Similar pictures were obtained for both methods of hydrolysis.

Electron diffraction experiments were carried out on the hydrolyzed specimens in order to establish their crystalline nature. Patterns of

selected individual crystals were obtained in the electron microscope with the lenses set for diffraction. The hydrolyzed crystals proved to be rather less sensitive to destruction by the electron beam than were the acetate crystals.[1] Figure 4 shows a selected area electron diffraction pattern of the material hydrolyzed in the aqueous medium. In agreement with the x-ray evidence, the pattern is that of cellulose II. The appearance of rings as distinct from spots indicates that the specimen is polycrystalline. The innermost interference (101), is discontinuous and points to preferred orientation of the corresponding planes within the specimen.

DISCUSSION

The observations described above indicate that the hydrolysis of single crystals of cellulose triacetate takes place without a change in morphology. While at first sight this might seem somewhat surprising, it should be noted that a similar phenomenon is well known in mineralogy as pseudomorphism.[5] A change in the internal structure of a crystal need not necessarily be reflected in a change of external form. The hydrolyzed acetate crystal is, however, not a single crystal but is polycrystalline in nature, and may be referred to as a pseudomorph. Accordingly, in the hydrolyzed acetate pseudocrystals, the external morphology represents only a matrix or shell, the interior being fragmented into crystallites.

An estimate of the average size of the crystallites can be obtained by measuring the radial broadness of the x-ray reflections.[6] The dimensions can be calculated from the well-known Scherrer equation for line broadening.

$$D = (K \lambda / \beta_{1/2}) \sec \theta$$

where D is the mean crystallite dimension in angstroms, λ is the wavelength, K is a constant (here taken as unity), θ is the Bragg angle, and $\beta_{1/2}$ is the breadth of the diffraction defined as the angular width in radians at half maximum intensity. The D values thus obtained are 42 A., 36 A., and 32 A. corresponding to the (101), (10$\bar{1}$), and (002) reflections, respectively. These dimensions are of the same order of magnitude as those normally obtained for ordinary regenerated cellulose and suggest a comparable degree of molecular order. This conclusion is borne out by accessibility measurements by a gravimetric deuterium oxide exchange method.[7] Both bulk regenerated cellulose (e.g., cellophane) and triacetate crystals hydrolyzed by the aqueous method show accessibilities of about 78 per cent. On the other hand, the accessibility of crystals hydrolyzed in the nonaqueous medium was about 90%, in accord with the amorphous character as shown by the x-ray diagrams.

For the material hydrolyzed in the aqueous medium the electron diffraction patterns show that the (10$\bar{1}$) and (002) reflections are isotropic, while the (101) appears as arcs indicating preferred orientation. Accordingly, the crystallites are randomly arranged with the b axes (chain direction) roughly perpendicular to the plane of the pseudocrystal. This type of

diffraction pattern is typical of a selective uniplanar orientation,[8] which probably originated during the shrinkage of the crystal as described earlier. The presence of preferred orientation in the pseudocrystals clearly indicates that shrinkage does not occur along all three axes, as in that case all the interferences would have been isotropic. It can thus be reasonably anticipated that shrinkage occurs only in directions perpendicular to the chain direction of the original acetate crystals.

The marked difference between the results obtained in the two methods of hydrolysis (i.e., in aqueous and nonaqueous media) came as somewhat of a surprise. The potassium hydroxide method (aqueous medium) is a simple double decomposition reaction, while the sodium methylate method (nonaqueous medium) is a catalytic transesterification catalyzed by the sodium. From the chemical point of view, both reactions should give the same product. It is therefore of particular interest that crystalline cellulose is formed in one case and amorphous cellulose in the other. In an effort to further elucidate the significance of this observation a number of additional experiments were made.

Triacetate crystals were hydrolyzed with sodium methylate in absolute methanol, washed with methanol, followed by water and dried. The resulting material was crystalline, giving an x-ray diagram similar to that of Figure 1*a*. On the other hand, as shown earlier, when the hydrolysis is carried out in the same way and the drying done from methanol, an amorphous product is obtained. These observations indicate that the recrystallization is caused by water. It may be assumed that the water acting as a plasticizer promotes molecular motion so that interchain and intrachain hydrogen bonds may form and thereby lead to the development of lateral order.

The question now arises whether the hydrogen bonding takes place in the presence of water or whether it occurs only during the removal of water on drying. An effort was made to answer this question in the following manner. Crystals were saponified with potassium hydroxide in aqueous methanol, washed with water, and the x-ray diagram of the water wet crystals was taken. If the cellulose is already crystalline at this stage, the x-ray diagram should show the characteristic cellulose interferences superimposed on the water scattering. Although there were indications that this was so, the experiment was not entirely satisfactory as the cellulose reflections were largely masked by the strong scattering due to the water. In an alternative experiment, crystals saponified with potassium hydroxide in aqueous methanol were washed with water, followed by methanol, benzene and dried from hexane. The x-ray diagram was crystalline as in Figure 1*a*. It has already been shown above that amorphous cellulose does not crystallize when dried from nonaqueous media; it therefore appears that the cellulose was already crystalline in the presence of the water. Crystallization does not, therefore, appear to require the process of water removal by drying.

From the foregoing the following general picture emerges. The transformation of triacetyl cellulose to cellulose is not simply a question of replacement of acetyl groups by hydrogen in the crystal lattice. The hydrolysis is accompanied by a disruption of the lattice and recrystallization of the amorphous cellulose is induced by water. These results suggest that water plays an important role in the crystallization of cellulose.

The original purpose of this investigation was to attempt to produce single crystals of cellulose by the hydrolysis of triacetate crystals, and thereby to ascertain whether the cellulose molecules are folded in the lattice. In view of the polycrystalline nature of the hydrolyzed crystals, no deductions about chain folding are possible. Efforts to obtain single crystals of cellulose by more direct methods are in progress.

The author is indebted to Dr. S. T. Bayley, Division of Applied Biology, National Research Council, Ottawa, for his generous assistance in obtaining the electron micrographs. Thanks are also due to Mr. C. P. Henry for assistance with the experimental work.

The work was supported under the Pioneering Research Program administered by the Institute of Paper Chemistry, Appleton, Wisconsin, to whom grateful acknowledgement is hereby made.

References

1 Manley, R. St. J., *J. Polymer Sci.*, **A1**, 1875 (1963).
2. Manley, R. St. J., *Nature*, **189**, 390 (1961).
3. Howlett, F., and E. Martin, *J. Textile Inst., Trans.*, **35**, 1 (1944).
4. Genung, L. B., and R. C. Mallat, *Ind. Eng. Chem., Anal. Ed.*, **15**, 319 (1943).
5. Dana, E. S., *Manual of Mineralogy*, Wiley, New York, 1952, p. 132.
6. Klug, H. P., and L. E. Alexander, *X-Ray Diffraction Procedures*, Wiley, New York, 1954, Chap. 9.
7. Sepall, O., and S. G. Mason, *Can. J. Chem.*, **39**, 1934 (1961).
8. Sisson, W., *J. Phys. Chem.*, **44**, 513 (1940).

Résumé

On hydrolyse les cristaux de triacétate de cellulose afin d'obtenir des mono-cristaux de cellulose. Le produit hydrolysé conserve la morphologue des cristaux de triacétate mais son état cristallin dépend de la méthode d'hydrolyse. Dans un milieu aqueux on forme la cellulose polycristalline tandis qu'un milieu non-aqueux une cellulose amorphe. Les résultats supposent que l'hyrolyse est accompagnée d'une cassure du réseau et que la recristallisation de la cellulose amorphe résultante est due à l'eau.

Zusammenfassung

Um Einkristalle von Cellulose zu erhalten wurden Cellulosetriacetatkristalle hydrolysiert. Das hydrolysierte Material behält die Morphologie der Triacetatkristalle bei, sein Kristallinitätszustand hängt aber von der Hydrolysenmethode ab. In wässrigem Medium wird polykristalline Cellulose gebildet, während ein nichtwässriges Medium amorphe Cellulose liefert. Die Ergebnisse zeigen, dass die Hydrolyse von einer Zerstörung des Gitters begleitet und die Rekristallisation der entstehenden amorphen Cellulose durch das Wasser verursacht wird.

Received June 12, 1962

JOURNAL OF POLYMER SCIENCE: PART A VOL. 1, PP. 1901–1908 (1963)

Morphology of Polyethylene Single Crystals

P. GIORDANO ORSINI, B. MARCHESE, and L. MAZZARELLA,
Centro Nazionale di Chimica delle Macromolecole, Sez. III, Istituto Chimico University of Naples, Italy

Synopsis

An electron microscope study of polyethylene single crystals is reported. The following points have been investigated: (*1*) influence of crystallization temperature on crystal shape; (*2*) effect of solvent etching on already formed crystals. Crystals were deposited from very dilute solutions at temperature ranging between 80 and 120°C. Solvents like xylene, butyl acetate, isoamyl acetate, and diphenyl ether were used. Besides the already reported true and truncated lozenges, hexagonal crystals have been obtained with tendency to regularity as the temperature of crystallization increases. The melting point of hexagonal crystals is somewhat lower than that of lozenges. Their structure, as revealed by electron diffraction, is orthorhombic, similar to that of lozenges. Diamond-shaped crystals etched with solvent under strictly controlled conditions display unexpected morphology. The peripheral region of the crystal of the sectors composing the crystals is characterized by a lower solubility and a lower density.

Introduction

Polyethylene single crystals may be prepared by cooling solutions in several solvents at various temperatures.[1–3] The habit of these crystals appears to depend on the conditions of crystallization. Keller,[4] using xylene as solvent, at temperatures around 80°C. has prepared diamond-shaped crystals, while at temperature slightly above 85°C. truncated lozenges are deposited. Whatever the habit, these crystals have an orthorhombic symmetry and display a lamellar shape (thickness around 100 A.) implying a repeated folding of the molecules, their chain axis being perpendicular to the lamellar plane. A number of observations have led several authors[5–8] to propose a hollow pyramidal model for the lozenge-shaped crystals which tend to accommodate themselves on the specimen support with characteristic modifications of their morphology.[9] The present investigation was undertaken with the aim of studying the morphology of polyethylene single crystals obtained at higher crystallization temperatures and to obtain some information on the mechanism of their dissolution.

Experimental

a. Material. A commercial sample of unfractionated Marlex-50 was investigated. The density of the bulk polymer determined on a homogeneous thin film with the gradient tube method was 0.965 g./ml. The melt-

ing point measured with the procedure described below was 135°C., and the x-ray crystallinity, as evaluated according to Aggarwall and Tilley,[10] was 0.87.

b. Crystallization from Various Solvents. Polyethylene was crystallized from very dilute solutions (0.1 g./l.). Solvents like xylene, butyl acetate, isoamyl acetate, and diphenyl ether were used.[11] The bulk polymer was dissolved by heating in a thermostatted oven to a temperature well above the cloud points. The temperature of the oven was slowly lowered at a rate of 10°C./hr. When the cloud point was reached, the temperature was held constant overnight, and then lowered at a very slow rate down to 60°C. After reaching room temperature, the crystalline precipitate was dried in air on a glass slide, metal shadowed at 15° with Au-Pd alloy, and then reinforced with a carbon film. After detachment by floating on water, the specimen was transferred to the electron microscope grid with a supporting membrane of cellulose nitrate (Parlodion).

c. Melting Point. Crystals obtained from different solvents were kept several days in a dry state and successively 48 hr. under high vacuum, to remove solvent vapors completely. Melting points of crystallized samples as well as bulk polyethylene were measured by placing them on the heating stage of a Leitz microscope, model 350. Measurements were repeated many times, the position of the sample being changed each time in order to check the uniformity of temperature through the stage.

d. Electron Diffraction. Experiments were performed with a Philips electron microscope 11980. Unshadowed specimens were used. Suitable areas were selected by observation with a very low intensity beam in order to prevent excessive electron radiation damage.[12] However, since this effect could not be completely eliminated, no attempts were made to interpret either the degree of sharpness or the intensity of the diffraction spots on the photographs.

e. Controlled Solvent Etching. Etching of single crystal was achieved in two different ways. (*1*) Soon after the cloud point (85°C.) was reached, the xylene solution was reheated up to 90°C. and then cooled down to 86°C. in order to stop a further growth of crystals and partially dissolve them. The temperature was kept constant at 87°C. overnight and then lowered slowly down to 60°C. (*2*) A glass slide, on the surface of which single crystals had been deposited from xylene, was exposed for 10 min. to hot xylene vapors which, by condensing onto the slide, partly dissolved the crystals.

f. Density. Density differences between etched and intact crystals were evidenced by ultracentrifugation in a density gradient. The specimen obtained according to (*e*), method (*1*), was suspended in a xylene–carbon tetrachloride mixture and then centrifuged at 47,000 rpm at room temperature in the analytical cell of a Phywe ultracentrifuge. After 7 hr. of running a concentration gradient was set up along the cell. Suspended particles banded according to their own density. Light scattering by the particles allowed the observation and recording on a photographic plate of the formation of two sharp bands with different density. The particles

forming each band were withdrawn with a syringe and observed with the electron microscope.

Results and Discussion

Polyethylene crystallizes from isoamyl acetate at 144°C. as planar, irregular, hexagonal crystals (Fig. 1). Similar crystals deposit from butyl acetate at 108°C. Crystallization from diphenyl ether may be effected at temperatures as high as 120°C. Less irregular hexagonal crystals are obtained (Fig. 2).

The structure of these crystals, as revealed by the electron diffraction photographs, is orthorhombic. The two long prism faces in the crystals shown in Figure 1 have {100} indices, while the remaining four have {110} indices. The {100} faces form an average angle of 110°, whereas in lozenge-shaped crystals this angle is, with good constancy, 114°. According to

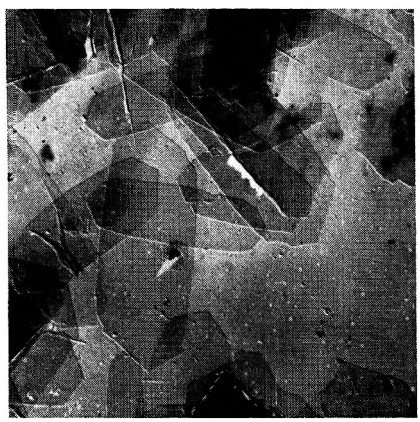

Fig. 1. Electron micrograph of polyethylene single crystals obtained from isoamyl acetate at 114°C. Magnification 3,900×.

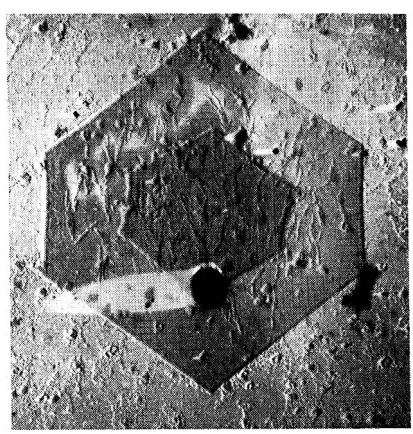

Fig. 2. Electron micrograph of polyethylene single crystal obtained from diphenyl ether at 120°C. Magnification 5,200×.

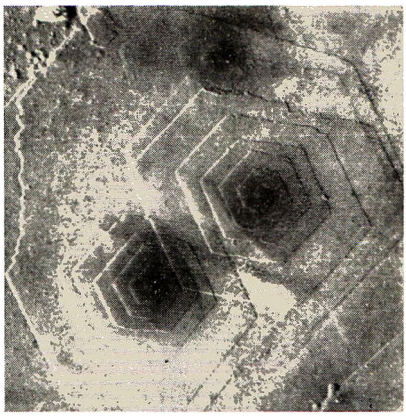

Fig. 3. Screw dislocation growth steps on crystal obtained from isoamyl acetate. Magnification 9,750×.

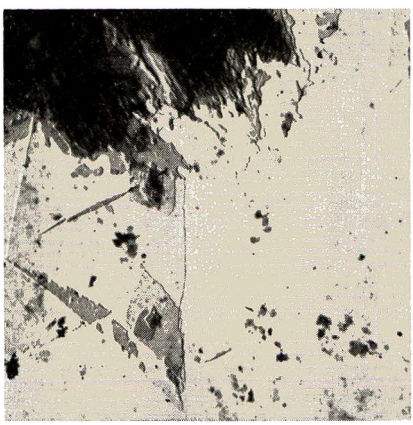

Fig. 4. Unmelted diamond-shaped crystals near melting six-faced prism-shaped crystals. Magnification 2,440×.

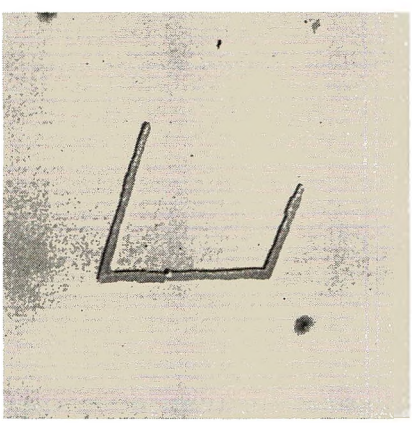

Fig. 5. Polyethylene single crystal partially dissolved. Magnification 7,150×.

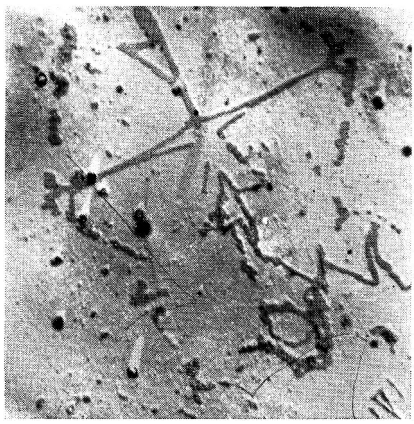

Fig. 6. Etched hollow pyramidal polyethylene single crystal. Magnification 4,550×.

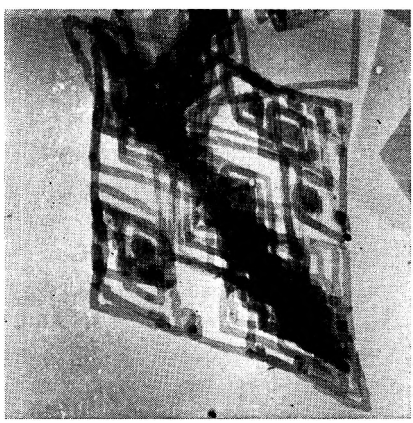

Fig. 7. Etched step-grown polyethylene single crystal. Magnification 2,600×.

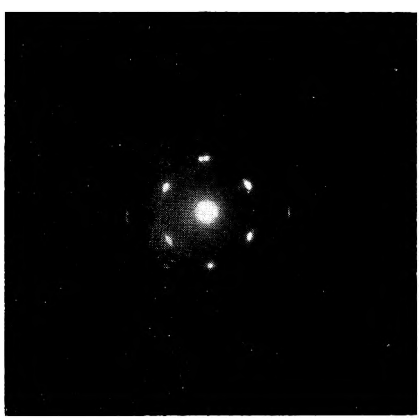

Fig. 8. Electron diffraction pattern from ribbonlike unextracted fraction.

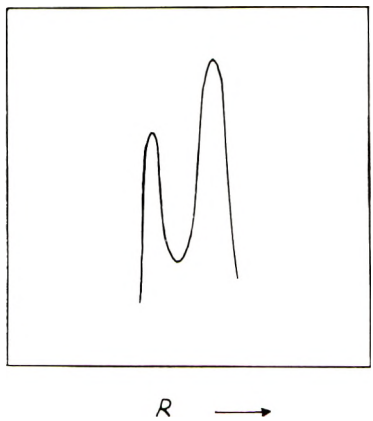

Fig. 9. Microphotometer scanning of the plate obtained in the ultracentrifugation.

Bunn's unit cell parameters,[13] this value should be 113°. X-ray diffraction studies on the polyethylene crystals showing the irregular hexagonal habit are in progress in our laboratories.

It is of interest that the six-faced, prism-shaped crystals show, like diamond-shaped ones,[14] screw dislocation growth steps as in Figure 3.

The melting point of six-faced prism-shaped crystals, whatever the solvent used, is 129.5°C., while the melting point of lozenges from xylene is 133°C. A record of this melting point difference has been obtained by placing a glass slide, with both types of crystals on it, on a temperature gradient bar in the region between the two melting points. In these conditions a selective melting of the six-faced prism-shaped crystals only was achieved (Fig. 4). A small but detectable difference in melting point between lozenge-shaped and six-faced prism-shaped crystals must therefore be correlated to the morphological differences. In future work it is intended to investigate possibly small structural differences by proper x-ray techniques.

As to the solvent etching of the diamond shaped crystals, as may be observed in Figures 5–7, it is of interest that the etched crystals display unexpectedly new morphology. In fact, ribbons are left after controlled solvent attack of the initial crystals, which are often reminiscent of an empty frame either of a lozenge-shaped crystal (Fig. 5), or of a collapsed hollow pyramidal crystal (Fig. 6) (which may incidentally be taken as a further proof of their existence). Segmented spiral ribbons are also observed mainly when the etched material contained a large amount of spiral grown steps (Fig. 7). As shown by electron diffraction (Fig. 8) the ribbons have in all cases the typical orthorhombic crystal structure, the chain axis of the molecules being perpendicular to the ribbon plane.

The density of these ribbonlike aggregates, as revealed by ultracentrifugation, is slightly smaller than the density of unetched crystals. Microphotometer scanning of the plate obtained in the ultracentrifugation in a density gradient described above, as shown in Figure 9 reveals two distinct

bands, whose separation corresponds approximately to 0.002 g./ml. difference in density, the average density being 0.9690 g./ml.

Electron microscope observations of the banded material show that ribbons are contained in the lighter fraction whereas the heavier layer consists of unetched crystals. From the above results it may be concluded that polyethylene single crystals do not have a strictly uniform structure. The peripheral region of the crystals or of the sectors composing the crystals as in the hollow pyramids is characterized by a higher stability toward solvent attack and a lower density than the core. However this well detectable distinction in behavior probably reflects only a subtle difference in structure, since no gross changes can be observed in the diffraction photographs.

It is hoped to grasp this aspect by a suitable x-ray technique.

It is a pleasant duty to acknowledge the kindness of Prof. A. M. Liquori for stimulating the authors' interest in the field of polymer single crystals and for continuous encouragement and suggestions. Thanks are due to the Consiglio Nazionale delle Ricerche for support given to this work, and to Dr. A. Keller for a critical reading of the manuscript.

References

1. Till, P. M., *J. Polymer Sci.*, **17**, 447 (1957).
2. Keller, A., *Phil. Mag.*, **2**, 21 (1957).
3. Fischer, E. W., *Z. Naturforsch.*, **12a**, 753 (1957).
4. Bassett, D. C., and A. Keller, *Phil. Mag.*, **6**, 345 (1961).
5. Bassett, D. C., F. C. Frank, and A. Keller, *Nature*, **184**, 810 (1959).
6. Niegisch, W. D., *J. Polymer Sci.*, **40**, 263 (1959).
7. Reneker, D. H., and Geil P. H., *J. Appl. Phys.*, **31**, 1916 (1960).
8. Niegisch, W. D., and P. R. Swann, *J. Appl. Phys.*, **31**, 1907 (1960).
9. Keller, A., lecture held in Varenna (Italy) during summer courses on advanced macromolecular chemistry, sponsored by the Consiglio Nazionale delle Ricerche.
10. Aggarwall, S. L., and G. P. Tilley, *J. Polymer Sci.*, **18**, 17 (1955).
11. Rånby, B. G., F. F. Morehead, and N. M. Walter, *J. Polymer Sci.*, **44**, 349 (1960).
12. Keller, A., and A. O'Connor, *Discussions Faraday Soc.*, **25**, 114 (1958).
13. Bunn, C. W., *Trans. Faraday Soc.*, **35**, 483 (1939).
14. Frank, F. C., *Discussions Faraday Soc.*. **5**, 48 (1949).

Résumé

On décrit l'étude au microscope électronique de monocristaux de polyéthylène. Les aspects suivants sont examinés: (*1*) l'influence de la température de cristallisation sur la forme du cristal; (*2*) l'effet du solvant sur des cristaux déjà formés. Des cristaux ont été déposés de solutions très diluées, à des températures entre 80 et 120°C. On employait des solvants comme le xylène l'acétate de butyle, l'acétate d'isoamyle et l'éther diphénylique. A côté de vraôs losanges et de losanges tronqués, on a obtenu des cristaux hexagonaux dont la régulairté augmente avec la température de cristallisation. Le point de fusion des cristaux hexagonaux est un peu plus bas que celui des losanges. La diffraction électronique montre qu'ils ont une structure orthorhombique semiblable à celle des losanges. Les cristaux de forme analogue au diamant présentent une morphologie inattendue quand ils sont attaqués par un solvant dans des conditions strictement contrôlées. La région superficielle des secteurs cristallins composant le cristal est caractérisée par une solubilité plus basse.

Zusammenfassung

Über die elektronenmikroskopische Untersuchung von Polyäthyleneinkristallen wird berichtet. Folgende Punkte wurden untersucht: (*1*) Einfluss der Kristallisationstemperatur auf die Kristallgestalt. (*2*) Einfluss von Lösungsmittelätzung auf schon gebildete Kristalle. Kristalle wurden aus sehr verdünnter Lösung bei Temperaturen zwischen 80 und 120°C. erhalten. Als Lösungsmittel wurden Xylol, Butylacetat, Isoamylacetat und Diphenyläther verwendet. Neben den schon beschriebenen vollständigen und verkürzten Rauten wurden sechseckige Kristalle mit grösserer Regelmässigkeit bei höherer Kristallisationstemperatur erhalten. Der Schmelzpunkt der sechseckigen Kristalle liegt etwas niedriger als der der rautenförmigen. Durch Elektronenbeugung ergibt sich ihre Struktur, ähnlich wie die der Rauten, als orthorhombisch. Rhombenförmige Kristalle zeigen bei der Ätzung mit Lösungsmittel unter streng definierten Bedingungen eine unerwartete Morphologie. Der periphere Kristallbereich in den Sektoren, die die Kristalle aufbauen, wird durch eine geringere Löslichkeit und geringere Dichte charakterisiert.

Received April 23, 1962

JOURNAL OF POLYMER SCIENCE: PART A VOL. 1, PP. 1909–1917 (1963)

Solid State Polymerization of Methacrylamide and *N*-Arylmethacrylamides

P. JÄGER* and E. S. WAIGHT, *Imperial College of Science and Technology, London, S.W. 7, England*

Synopsis

The γ-ray initiated solid state polymerization of methacrylamide at room temperature has been described and discussed in terms of reaction mechanisms previously applied to the radiation-induced polymerization of acrylamide. Log (M_0/M) increased, after a short initiation period, linearly with (time)^2 up to conversions of about 20%. This was followed at higher conversions by a second linear region with a higher slope. The conversion rate (%/Mrad.) increased for intensities between 0.3 and 0.075 Mrad./hr., but it dropped unexpectedly at the lowest dose rates. Irradiated methacrylamide showed a post-irradiation polymerization, the rate of which was influenced by the presence of air for reaction times longer than 200 hr. Among the solid *N*-arylmethacrylamides, which were all less reactive than methacrylamide, some *ortho*-substituted compounds (*o*-Cl, *o*-Br, *o*-ethoxy) showed a relatively high reactivity. These results are discussed in connection with differences in hydrogen bonding found in the infrared spectra.

Introduction

Following the first paper by Henglein and Schultz[1] a number of publications have dealt with the radiation-induced solid state polymerization of acrylamide.[2–11] Restaino et al.[5] found that the polymerization rate of methacrylamide was considerably less than that of acrylamide. Detailed results are presented on the course of the solid state polymerization of methacrylamide. An attempt has also been made to obtain polymers by irradiation of a number of solid *N*-arylmethacrylamides, some of which have been reported before.[12–16] For comparison, these substances have also been polymerized in solution using benzoyl peroxide as an initiator.

Experimental

Methacrylamide

A commercial product was dried and sublimed (at 10^{-3} mm.). The pure white material had a m.p. of 108–109°C.

* Present address: Forschungsabteilung, Emser Werke AG, Domat-Ems, Switzerland.

N-Arylmethacrylamides

These compounds were prepared as described in the literature[12–16]; their melting points are given in Table II.

Preparation and Irradiation of Samples

Weighed samples of monomer were evacuated (at 10^{-3} mm.) overnight in Pyrex tubes (6 or 12 mm. diam.), which were then sealed. In some experiments, samples were sealed after the admission of dry air. Irradiations were carried out at room temperature (20 ± 3°C.) with Co^{60} γ-ray sources of 80 and 1000 C. The field intensities at varying distances from the source were determined by ferrous sulfate dosimetry. The rate of energy input was corrected to current dates in accordance with the known decay rate of Co^{60}. The small difference between the electron densities of ferrous sulfate solution and monomer was neglected.

Determination of Monomer Conversion

The tubes used for "in-source" experiments were opened immediately after irradiation; those used for post-irradiation experiments were stored sealed at room temperature, or opened and kept in a desiccator. The monomer conversion was determined by one (or both) of the following methods:

Gravimetric Determination of Polymer

A weighed amount of irradiated monomer was poured with stirring into a large volume of methanol or chloroform. The precipitate was crushed, separated by centrifuging, washed with methanol, and dried at room temperature *in vacuo* (at 10^{-3} mm.).

Titrimetric Determination of Residual Methacrylamide

A weighed amount (60–80 mg.) of irradiated methacrylamide was shaken for 20 min. with a measured amount of standardized aqueous bromine-potassium bromide solution[17] and ice. Potassium iodide solution was added and the iodine formed titrated with 0.1*N* sodium thiosulfate. With samples of at least 45 mg. and a reagent excess of 60–80%, results were found to be reproducible within 1%. The contribution of terminal double bonds to the result was small, e.g., 0.75% with respect to polymer, for a monomer conversion of 18%. By combination of the gravimetric and titrimetric methods, 98% of the methacrylamide could be accounted for. For determination of the post-irradiation effect in air, the amount of polymer formed during the irradiation was determined on an aliquot of the sample. These polymer yields do not include the polymer formed during irradiation and are based on the experimentally determined concentration of monomer at the end of irradiation, M_0*, as 100%.

Results and Discussion

For the sake of convenience, the example of Baysal et al.[8] will be followed, and the in-source reaction and the post-irradiation effect will be discussed separately.

In-Source Reaction

Some data on conversion versus time for the in-source polymerization of methacrylamide are given in Figure 1. The results obtained showed only a slight difference in the reactions of samples which had been irradiated with or without the presence of air. It is suggested that the oxygen originally sealed into the tubes together with the monomer is exhausted after a short period by reaction with radicals formed during irradiation. As the samples received relatively high doses the difference between deaerated and aerated samples disappears. As will be shown later on, the polymerization rate of individual methacrylamide chains decays with time.

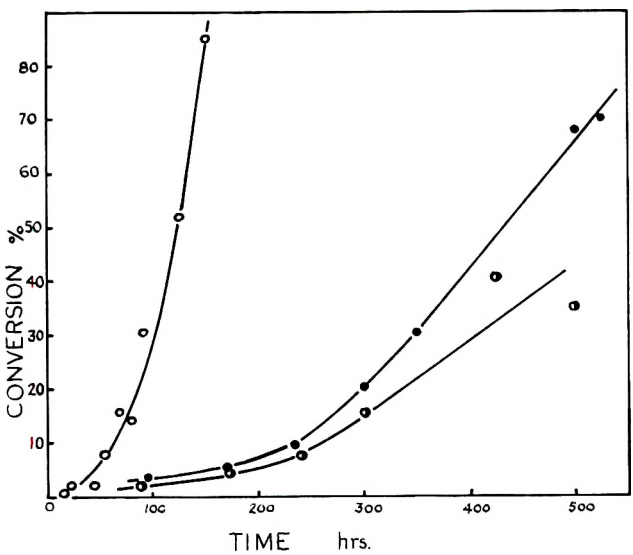

Fig. 1. In-source polymerization of methacrylamide. Dose rate: (○) 0.2 Mrad./hr., *in vacuo*; (●) 0.038 Mrad./hr., *in vacuo*; (◑) 0.038 Mrad./hr., sealed with air.

Over the long irradiation periods used, up to 320 hr., this decay in individual chain growth is expected to occur parallel with the initiation of new chains due to irradiation. The presence of chains at different stages of growth and with different growth rates leads to the exclusion of steady state kinetics at later stages of the irradiation.

Treating the data of Figure 1 in a way comparable to that used for acrylamide[8] using eq. (1) gave curves of similar character (Fig. 2):

$$\log(M_0/M) = k_p k_i f I t^2/4.606 \qquad (1)$$

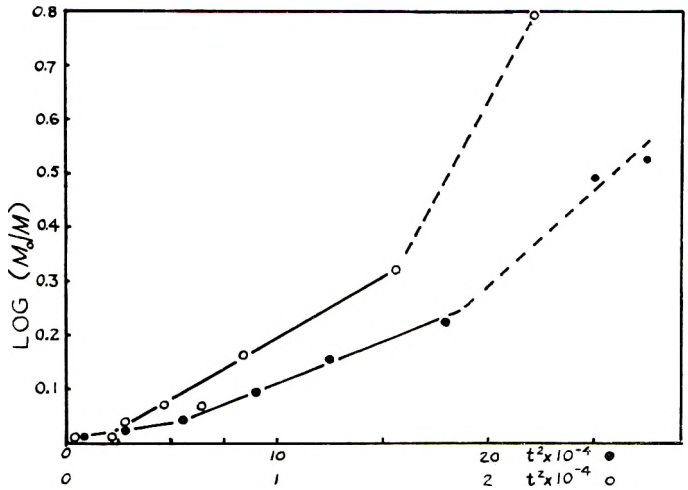

Fig. 2. Time dependence of the in-source polymerization of methacrylamide. Dose rate: (O) 0.2 Mrad./hr., (●) 0.038 Mrad./hr.

where k_i is the initiation rate constant, f is a frequency factor, and I is the radiation intensity. It is assumed that no radical termination step involving the growing chains R· occurs. As shown in Figure 2, $\log(M_0/M)$, after a short initiation period, increases linearly with t^2 up to conversions of about 20%, depending somewhat on the dose rate. This is followed, at higher conversions, by a second linear region with a higher slope. A similar effect has been reported previously by Baysal et al.[8] for acrylamide, where the break in the curve occurs at about 20% conversion for comparable dose rates, but at a much lower total dose. These workers concluded that the increasing rate can only be explained by an increase in f with higher conversions, due to the release of trapped radicals.

The influence of dose rate on conversion is shown in Figure 3 for intensities between 0.04 and 0.42 Mrad./hr. and for a constant dose of 12

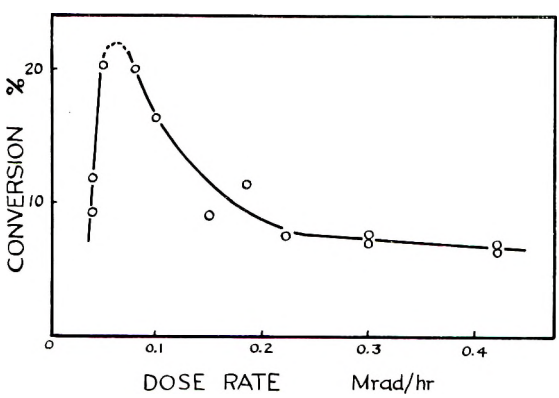

Fig. 3. In-source polymerization of methacrylamide *in vacuo*. Variation of conversion with dose rate. Total dose, 12 Mrad.

Mrad. At high dose rates, the conversion has a constant value of about 6%, increasing to a maximum conversion at an intensity of 0.06 Mrad./hr. This behavior is as expected since it follows from eq. (1) that

$$\log(M_0/M) = \text{const.} \times (\text{dose})^2/I \quad (2)$$

The sharp decrease at dose rates less than 0.06 Mrad./hr. cannot readily be explained.*

TABLE I
Post-Irradiation Effect[a]

Expt.	Post-irradiation treatment	Polymer formed, %
25*a*	Worked up immediately	0.05
25*b*	Kept open in desiccator for 19 hr. at 20°C.	2.1
27*a*	Kept sealed for 19 hr. at 20°C.	3.2
27*b*	As 27*a*, then kept open for 187 hr.	5.8
26	Kept sealed for 187 hr. at 20°C.	9.7
28	Kept sealed for 187 hr. at −78°C.	0.7

[a] Irradiation of methacrylamide at −78°C. Formation of polymer in the post-irradiation period (dose rate, 1 Mrad./hr.; total dose, 24 Mrad.).

The results in Table I indicate that methacrylamide shows a weak post-irradiation effect even at −78°C. At room temperature atmospheric oxygen acts as an inhibitor. The course of the post-irradiation effect in air

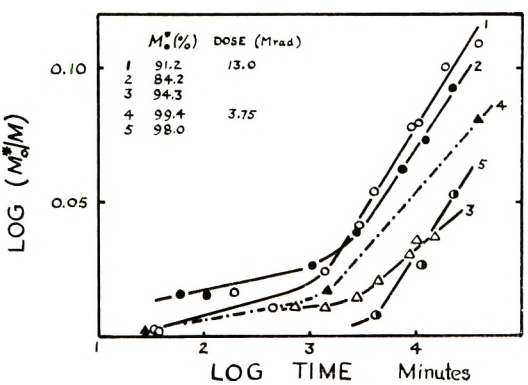

Fig. 4. Time dependence of the post-irradiation effect in methacrylamide. Dose rate 0.038 Mrad./hr., in air (1–4), *in vacuo* (5).

was followed with several samples, sealed with or without air, which had received doses of 13 and 3.75 Mrad. respectively at a dose rate of 0.04 Mrad./hr. (at 20 ± 3°C.). For reasons mentioned earlier no difference was observed between deaerated and aerated samples.

* The reference has suggested that this effect might be explained by the limitations of eq. (1) which does not take into account the decay in the rate of propagation of individual chains and that this becomes important in extended experiments.

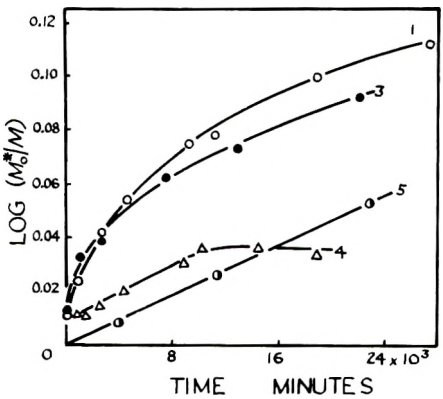

Fig. 5. Time dependence of the post-irradiation effect in methacrylamide; in air (1, 3, 4), *in vacuo* (5). For further details see Fig. 4.

Of two contradictory kinetic schemes proposed for this type of post-irradiation effect in acrylamide,[6–8,10] the second proposes a first-order reaction of radicals with monomer with no appreciable termination reaction.[8] Some electron spin resonance (ESR) measurements indicating constancy of the radical concentration over a long period support the validity of this scheme.

The authors' data (Fig. 4) confirm earlier results of experiments with acrylamide,[8] i.e., a reaction scheme involving a bimolecular termination step must be excluded. Curves 1, 3, and 4 in Figure 5 seem to be in even greater disagreement with the second scheme, but this may be due to the influence of air, admitted after irradiation, which decreases the number of growing chains. Curve 5, however, seems to suggest that *in vacuo* log-(M_0^*/M) increases linearly with time, as required by the expression[8]

$$\log(M_0^*/M) = k_p R_0 t/2.303 \tag{3}$$

Influence of Atmospheric Oxygen on the Post-Irradiation Effect

A comparison of the results in Table I shows that in the presence of air the rate of the post-irradiation polymerization decreases faster than *in vacuo*. Further evidence for the retarding influence of air may be seen by comparing experiments 4 and 5 (Fig. 5), the former being carried out in the presence of air, the latter *in vacuo*. Up to 200–250 hr. no retarding effect by air is noticeable, after this the rate of the post-irradiation polymerization in air decreases more rapidly than the corresponding rate *in vacuo*. Published results for acrylamide[10] do not appear to exclude a slow, diffusion-controlled, inhibition by atmospheric oxygen.

Influence of Secondary Factors on the Reproducibility of the Post-Irradiation Effect

Fadner and Morawetz[10] described the influence of sample preparation on the polymerization rate of methacrylamide, reporting the highest reac-

tion rates for shock-cooled samples, the lowest with large, slowly grown crystals. In the case of methacrylamide, something similar was noticed. Varying rates of sublimation gave different crystal sizes which gave rise to noticeably different polymerization rates. A dose of 13.9 Mrad. *in vacuo* (at 0.04 Mrad./hr.) gave a conversion of 11.9% in small crystals obtained by slow sublimation, but only 7.6% in large crystals obtained rapidly.

N-Arylmethacrylamides

The irradiated crystals were in many cases discolored, the color fading in the presence of air only after several weeks, but disappearing immediately on pouring the crystals into methanol. The infrared spectra (as KCl discs) of the solid, methanol-insoluble, irradiation products were found to be identical with the spectra of polymers obtained by peroxide initiation.

Some results on the conversion of *ortho*-substituted *N*-arylmethacrylamides are given in Table II. The corresponding *meta*- and *para*-isomers after identical irradiations (total dose, 24–25 Mrad.) gave clear solutions in methanol; that is, no polymer was detected.

TABLE II
Results on the Conversion of *ortho*-Substituted *N*-Arylmethacrylamides

	Monomer m.p., °C.	Dose, Mrad.	Conversion, %
Methacrylamide	108–109	13.9	9.4[a]
Methacrylanilide	84–85	24.2	—
N-(*o*-Chlorophenyl)methacrylamide	59–60	25.9	5.3
		40.7	11.9
N-(*o*-Bromophenyl)methacrylamide	47–48	15	4.1
		27.4	5.1
		40.7	9
N-(*o*-Ethoxyphenyl)methacrylamide	45–46	24	3
N-(*o*-Carboxyphenyl)methacrylamide	175–176	27.4	—

[a] Depends on crystal size, see text.

The conversion of *N*-(*o*-ethoxyphenyl)methacrylamide (Fig. 6) takes a similar course to that found for methacrylamide (Fig. 1) at a much lower dose rate. Owing to the extended irradiation time (220 hr.) the same complications arise in any detailed discussion as has been mentioned in dealing with the extended irradiations of methacrylamide. The presence of the aromatic ring in these *N*-substituted amides brings about a higher radiation resistance compared with methacrylamide, the doses given being not more than four times higher than in the irradiations described above but very much higher than in the previously reported work on acrylamide.[6–8,10] The higher reactivity of the *ortho*-isomers compared with *meta*- and *para*-isomers cannot be due to electronic effects of the substituents which should be similar for *ortho*- and *para*-isomers, but seems related to the absence of

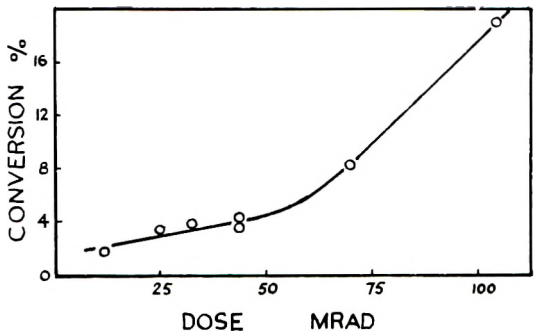

Fig. 6. In-source polymerization of *N*-(*o*-ethoxyphenyl)methacrylamide *in vacuo*. Dose rate, 0.5 Mrad./hr.

hydrogen bonding between neighboring amide groups in the crystal. Sokolova et al.[13–16] have also found that in the bulk polymerization of some *N*-arylmethacrylamides catalyzed by *tert*-butyl peroxide the *ortho*-isomers are more reactive than the *meta*- and *para*-isomers. They have also found that the *ortho*-isomers, such as *N*-(*o*-ethoxyphenyl) and *N*-(*o*-chlorophenyl)methacrylamide, show no or only weak hydrogen bonding in the crystalline or liquid states, whereas the *meta*- and *para*-isomers investigated all showed extensive intermolecular hydrogen bonding, even, in the case of *N*-(*p*-chlorophenyl)methacrylamide, m.p. 112–112.5°C., at temperatures as high as 120°C. This difference in molecular association, which also manifests itself in relatively lower melting points of the *ortho*-isomers, has been confirmed in the present investigation.

One of us (P. J.) thanks the Distillers Co. Ltd. for a maintenance award. The authors are indebted to Mr. G. R. Hall and Dr. A. J. Swallow, Department of Chemical Engineering and Nuclear Technology, Imperial College, for permission to use the kilocurie source.

References

1. Henglein, A., and R. Schultz, *Z. Naturforsch.*, **9b**, 617 (1954).
2. Schultz, R., A. Henglein, H. E. v. Steinwehr, and H. Bambauer, *Angew. Chem.*, **67**, 232 (1955).
3. Schultz, R., G. Renner, A. Henglein, and W. Kern, *Makromol. Chem.*, **12**, 20 (1954).
4. Mesrobian, R. B., P. Ander, D. S. Ballantine, and G. J. Dienes, *J. Chem. Phys.*, **22**, 565 (1954).
5. Restaino, A. J., R. B. Mesrobian, H. Morawetz, D. S. Ballantine, G. J. Dienes, and D. J. Metz, *J. Am. Chem. Soc.*, **78**, 2939 (1956).
6. Fadner, T. A., I. Rubin, and H. Morawetz, *J. Polymer Sci.*, **37**, 549 (1959).
7. Morawetz, H., and T. A. Fadner, *Makromol. Chem.*, **34**, 162 (1959).
8. Baysal, B., G. Adler, D. Ballantine, and P. Colombo, *J. Polymer Sci.*, **44**, 117 (1960).
9. Adler, G., and W. Reams, *J. Chem. Phys.*, **32**, 1698 (1960).
10. Fadner, T. A., and H. Morawetz, *J. Polymer Sci.*, **45**, 475 (1960).
11. Adler, G., *J. Chem. Phys.*, **31**, 848 (1959).
12. Patai, S., M. Bentov, and M. E. Reichmann, *J. Am. Chem. Soc.*, **74**, 845 (1952).

13. Sokolova, T. A., and V. N. Nikitin, *Izv. Akad. Nauk SSR, Otd. Khim. Nauk*, **1959**, 511.

14. Sokolova, T. A., L. A. Ovsyannikova, *Izv. Akad. Nauk SSR, Otd. Khim. Nauk*, **1959**, 1822.

15. Chetyrkina, G. H., T. A. Sokolova, and M. M. Koton, *Vysokomolekul. Soedin.*, **1**, 248 (1959).

16. Sokolova, T. A., G. H. Chetyrkina, and V. N. Nikitin, *Vysokomolekul. Soedin.*, **1**, 506, 1599 (1959).

17. *Organic Analysis*, J. Mitchell, Jr., et. al., Eds., Vol. III, Interscience, New York, 1956, p. 240.

Résumé

La polymérisation du méthacrylamide à l'état solide, induite par les rayons-γ a été décrite et discutée suivant des mécanismes réactionnels déjà appliqués à la polymérisation de l'acrylamide. Log (M_0/M) augmente linéairement avec (temps)^2 d'abord faiblement, puis rapidement à partir de 20% de conversion. Le taux de polymérisation (%/Mrad) augmente pour des intensités comprises entre 0.3 et 0.075 Mrad/hr. et diminue pour des intensités plus basses. Le méthacrylamide irradié montre un effet de post-polymérisation, dont le taux est influencé par la présence d'air, pour des périodes au delà de 200 h. Les méthacrylamides aryloiques solides substitués sont tous moins réactifs que le méthacrylamide. Seules quelques isomères substitués en position *ortho* (*o*-Cl, *o*-Br, *o*-éthoxy) montrent des réactivités remarquables. Ces résultats sont comparés avec les intensités des liaisons-hydrogène observées dans les spectres infra-rouges correspondants.

Zusammenfassung

Die durch γ-Strahlen induzierte Polymerisation von festem Methacrylamid wurd untersucht. Der zugehörige Reaktionsmechanismus wurde mit den für Acrylamid publizierten Ergebnissen verglichen. Log (M_0/M) nahm, nach einer kurzen Anlaufsperiode bis zu einem Umsatz von ca. 20% linear mit dem Quadrat der Reaktionsdauer zu. Anschliessend folgte, bei gleichen Koordinaten, eine zweite lineare Region mit stärkerem Anstieg. Die Umsatzgeschwindigkeit (%/Mrad) nahm für Strahlenintensitäten von 0.3–0.075 Mrad/Std. zu, doch fiel sie bei den kleinsten Strahlenintensitäten unerwarteterweise wieder ab. Bestrahltes Methacrylamid zeigte eine Nachpolymerisation, deren Geschwindigkeit für Reaktionszeiten über 200 Std. durch die Anwesenheit von Luft beeinflusst wurde. Von den untersuchten festen *N*-Arylmethacrylamiden, die alle weniger reaktiv waren als Methacrylamid, zeigten einzig einige *ortho*-substituierte Isomere (*o*-Cl, *o*-Br, *o*-Äthoxy) eine verhältnismässig hohe Reaktivität. Diese Resultate wurden mit Unterschieden in der Stärke der intermolekularen Wasserstoffbindungen, wie sie aus den IR-Spektren ersichtlich sind, in Verbindung gebracht.

Received October 2, 1961
Revised July 6, 1962

JOURNAL OF POLYMER SCIENCE: PART A VOL. 1, PP. 1919–1926 (1963)

Polymerization Studies on Allylic Compounds. I*

M. G. BALDWIN and SAMUEL F. REED, *Rohm & Haas Company, Redstone Arsenal Research Division, Huntsville, Alabama*

Synopsis

The polymerization of a series of α-(substituted methyl) acrylates was investigated. Polymerization rate measurements showed that each of the monomers, though containing allylic hydrogen atoms, polymerizes readily. Polymer viscosity data were obtained which indicate that appreciable nondegradative chain transfer occurs with several of the monomers. An explanation for the rapid polymerization of the monomers was proposed.

Introduction

Molecules derived from propene through replacement of one or more hydrogen atoms by other groups can undergo a variety of free radical reactions involving the basic propene structure. Among these are polymerization, displacement of substituents on the carbon atom adjacent to the double bond, and radical transfer reactions involving abstraction of allylic hydrogen atoms. The nature and position of the substituent groups determine the relative importance of the competing reactions. It is the purpose of this and subsequent papers to describe the free radical reactions of compounds of the type

$$CH_2=\underset{\displaystyle X}{\overset{|}{C}}-CH_2Y$$

where the groups X and Y will be varied. This paper deals with the results of polymerization studies on a series of α-(substituted methyl) acrylates, i.e., compounds of the above type for which

X is $-\overset{\displaystyle O}{\overset{\|}{C}}OCH_2CH_3$, and Y is —H, —OH, $-OCH_2CH_3$, $-O\overset{\displaystyle O}{\overset{\|}{C}}CH_3$, and $-\overset{\displaystyle O}{\overset{\|}{C}}OCH_2CH_3$

It has been clearly shown that monomers such as allyl acetate[1,2] and allyl alcohol[3] undergo free radical polymerization very slowly, yielding polymer of extremely low molecular weight. The explanation for this behavior is based on the occurrence of what is termed "degradative chain transfer" involving the allylic hydrogen atoms in the molecule. By degradative chain transfer is meant transfer between a growing polymer chain

* This work was performed under the sponsorship of the U. S. Army under Contract No. DA-01-021-ORD-11878.

radical and another molecule, in this case monomer, to form a radical which is not sufficiently reactive to initiate a chain. This results from the relatively high energy required for the formation of the normal chain propagating radical compared with that required for chain transfer at the allylic position. Other well-known allylic monomers, the methacrylates being the best examples, polymerize easily and cleanly with little chain transfer.[4] The compounds studied in this work are, in a sense, intermediate in structure between compounds such as allyl acetate and the methacrylates. From the data presented, conclusions can be drawn concerning the relative reactivity of the different radicals involved in the polymerization of allylic monomers.

Results

The rates of polymerization of the compounds studied in this work were measured in ethyl acetate solution, initiated by 2,2′-azobisisobutyronitrile (AIBN) at 60°C., by means of a dilatometric technique. The resulting polymers were obtained by precipitating the reaction mixtures in hexane, and the viscosities of solutions of the polymers in acetone were measured at 30°C. The data are summarized in Table I. The polymerization rates listed in Table I were obtained from the slopes of first-order plots for each monomer. These are shown in Figure 1. Close adherence to first-order kinetics with respect to monomer concentration was observed in all cases.

Several observations were made from the results shown in Table I. The most significant was that each of the compounds, although containing

TABLE I
Polymerization Data[a]

Monomer	Group Y in $\begin{array}{l} C\text{—}CH_2Y \\ \vert \\ C{=}O \\ \vert \\ OCH_2CH_3 \end{array}$	Monomer concn., moles/liter	Initial polymerization rate, % per min.	η_{sp}/c of polymer
I	—OH	3.86	0.516	0.18
II	$-OC(=O)CH_3$	3.01	0.390	0.59
III	$-OCH_2CH_3$	3.03	0.376	0.10
IV	$-COCH_2CH_3$	2.75	0.190	0.074
V	—H	4.03	0.190	0.56
Methyl methacrylate	—	4.47	0.152	0.56

[a] Polymerization rates were measured in ethyl acetate solution at 60°C. with (AIBN) = $6.17 \times 10^{-3}M$. Polymer viscosities were obtained from measurements on 1% solutions of the polymers in acetone at 30°C.

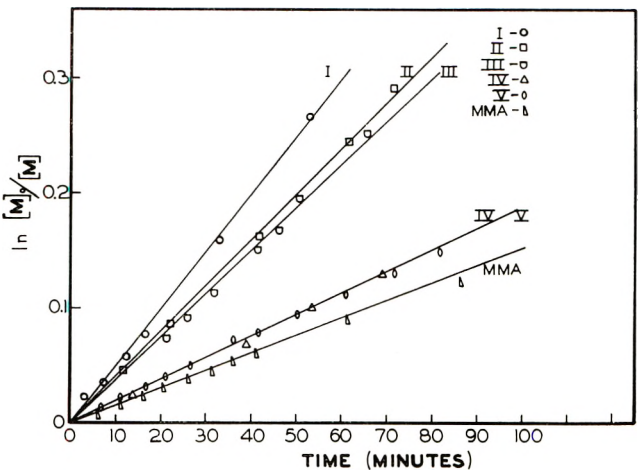

Fig. 1. First-order plots for monomers.

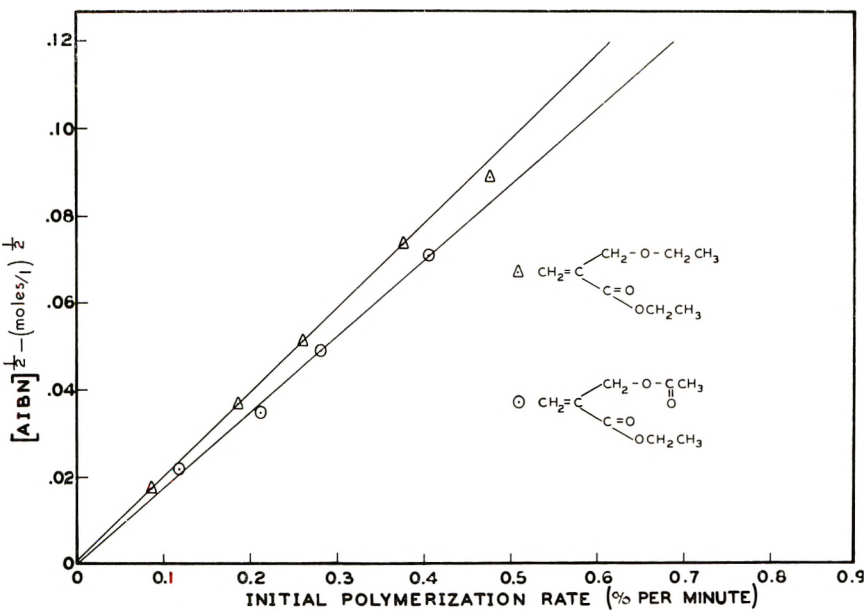

Fig. 2. Polymerization rates plotted against square roots of the initiator concentration.

allylic hydrogen atoms, polymerizes readily. Thus, degradative chain transfer can play at most only a very minor role in the polymerization of these compounds. However, it was noted that certain of the monomers apparently undergo considerable normal chain transfer, since the polymer viscosities are quite low. In fact, the data indicate that chain transfer occurs in the substituted monomers more readily than in the methacrylates.

Two of the monomers, II and III, thought to be representative of the group, were selected for more extensive study. Both were polymerized

in bulk at 60°C. with different AIBN concentrations, and the initial rates of polymerization measured. Figure 2 shows the polymerization rates plotted against the square roots of the initiator concentrations. Linear relationships were observed over a thirtyfold change in the initiator concentration for both monomers. These results indicate that bimolecular termination is operative in both cases, and support the conclusion that degradative transfer is not important in these systems, since degradative transfer leads to a first-order dependence of the polymerization rates on initiator concentration.[5]

The intrinsic viscosities of the polymers from II and III were obtained from measurements on acetone solutions of the polymers at 30°C. The data are given in Table II. The low, constant value of $[\eta]$ for polymer III substantiates the conclusion that considerable normal chain transfer has occurred with this monomer.

TABLE II
Polymer Intrinsic Viscosity as Function of Initiator Concentration

Monomer II 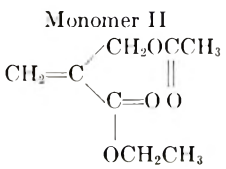		Monomer III 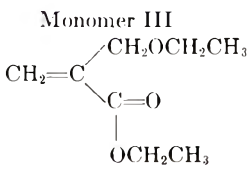	
[AIBN] × 10^3	$[\eta]$	[AIBN] × 10^3	$[\eta]$
9.45	0.63	7.93	0.27
6.30	0.75	5.28	0.31
3.15	0.86	2.64	0.29
1.58	0.88	1.32	0.30
0.315	1.00	0.264	0.31

The following conclusions can be drawn from the results of this study:

1. The monomers studied, although containing allylic hydrogen atoms, undergo rapid free radical polymerization. Thus degradative chain transfer is not important in the polymerization of any member of the series.

2. Normal chain transfer apparently does occur to an appreciable extent in some cases.

Discussion

In attempting to formulate a mechanism for the polymerization of the compounds studied here, the effects of the groups X and Y on the basic propene molecule were first considered. Addition of X ($-\overset{\overset{O}{\|}}{C}OCH_2CH_3$) to propene, i.e., changing from propene to the methacrylate, causes the polymerizability of the vinyl group under radical initiation to increase

enormously. This results from the appreciable decrease in the energy required to form the chain-carrying radical

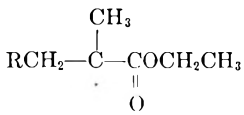

compared with that required to form the corresponding radical

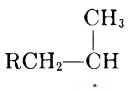

derived from the parent propene. The energy difference is due to the resonance stabilization of the methacrylate radical by the ester carbonyl group.

On the other hand, addition of Y (—$OCCH_3$, for example) to propene

has much less effect on the polymerizability of the vinyl group, since Y has relatively little effect on the stability of the chain-carrying radical

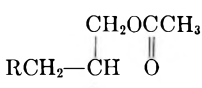

This radical, lacking resonance stability, is formed with difficulty and is highly reactive. Because of its high reactivity, chain transfer reactions to form the resonance stabilized radical

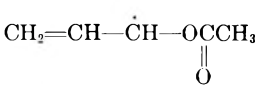

occur readily.

From these considerations it would be expected that the compounds studied here would be similar to the methacrylates in polymerization behavior. That is, they all polymerize rapidly because of the effect of resonance stabilization by the carboxylic ester group (X) on the chain-carrying radical. Group Y, which is separated by one carbon atom from the vinyl group, has little effect on the vinylic radical and thus has only secondary effects on the rates of initiation, propagation, and termination reactions involving this radical. Degradative chain transfer, which might normally be expected for allylic monomers, does not occur because: (*a*) the resonance stabilized normal propagating radical is not sufficiently reactive to undergo very frequent transfer and (*b*) when transfer does occur, the resulting radical is reactive enough to rapidly initiate a chain.

The differences in polymerization rate that were observed within the series are thought to be due to steric factors and/or to interactions of some kind between X and Y which indirectly affect the stability of the propagat-

ing radical. Likewise, the observed chain transfer activity of some of the monomers studied is probably due to electronic effects of the Y groups on the allylic hydrogen atoms of the monomer, together with steric effects which affect the lifetime of the propagating radical. It is felt that extension of this study to compounds having other X and Y groups might clarify these points.

Experimental*

Monomer Preparation

Ethyl α-(hydroxymethyl)acrylate (I) was purchased from the Koppers Co. and employed as an intermediate in the preparation of ethyl α-(acetoxymethyl)acrylate (II) and ethyl α-(ethoxymethyl)acrylate (III). The reaction of acetyl chloride with I in ether with pyridine employed as an acid acceptor gave II in 46% yield. For this study III was prepared by the reaction of I with ethanol in the presence of concentrated sulfuric acid. Its properties were similar to those reported by Ferris.[6] Ethyl methacrylate (V), was prepared from methacrylyl chloride and ethanol in the presence of pyridine. Diethyl itaconate (IV) and methyl methacrylate were obtained from Monomer-Polymer and Rohm and Haas Co. Each of the monomers was doubly distilled through an 18-in. semimicro spinning band column and checked for purity by vapor phase chromatography.† All compounds were considered to be at least 99.5% pure.

Preparation of Ethyl α-(Acetoxymethyl)Acrylate II

A solution of 20.4 g. (0.2 mole) of acetic anhydride in 50 ml. of anhydrous ether was added to a solution of 26 g. (0.2 mole) of ethyl α-(hydroxymethyl)acrylate and 15.8 g. (0.2 mole) of pyridine in 100 ml. of ether precooled to 0–5°C. The rate of addition was adjusted to maintain the temperature below 10°C. The reaction was continued for a period of two hours then washed with water and dried over anhydrous magnesium sulfate. The ether was removed by evaporation at reduced pressure leaving a clear liquid residue which on distillation through an 18-in. spinning band column yielded 16 g. (46%) of ethyl α-(acetoxymethyl)acrylate, b.p. 60°C. (1 mm.), n_D^{20} 1.4352 and 6.9 g. of a viscous residue. The residue, although not examined, likely represents polymer of the acrylate.

ANAL.: Calcd. for $C_8H_{12}O_4$: % C, 55.81; % H, 6.98. Found: % C, 55.80; % H, 6.97.

Preparation of Ethyl α-(Ethoxymethyl)Acrylate III

A mixture of 10.5 g. (0.08 mole) of ethyl α-(hydroxymethyl)acrylate, 10 g. of absolute ethanol, and 2 g. of concentrated sulfuric acid was heated to

* All boiling points uncorrected.

† An Aerograph gas chromatographic instrument, Model A-100-C, was used with a silicone Dow 11 on Fluoropak column.

95–100°C. for a period of twenty hours in the presence of 0.5 g. of hydroquinone. On cooling to room temperature the mixture was poured into 100 ml. of water and the organic layer extracted with ether. The combined ether extracts were washed with 5% sodium bicarbonate, with water, and dried over anhydrous magnesium sulfate. Removal of the ether by evaporation at reduced pressure left a clear liquid residue which was distilled through a spinning band column to give 4.19 g. (33%) of ethyl α-(ethoxymethyl)acrylate, b.p. 44–45°C. (0.9 mm.), n_D^{20} 1.4269.

ANAL.: Calcd. for $C_8H_{14}O_3$: % C, 60.76; % H, 8.86. Found: % C, 60.69; % H, 8.81.

Polymerization Studies

Materials

Ethyl acetate—reagent grade was distilled through a 45 plate column, the middle cut being retained.

Acetone—for viscosity determinations was commercial reagent grade, used without further purification.

AIBN—commercial material was recrystallized three times from absolute methanol (m.p. 102–103°C. with decomposition), and stored over Drierite at −20°C. in the dark until used.

Mercury—triply distilled mercury supplied by the Bethlehem Apparatus Co. was used in all experiments. It was taken from freshly opened containers and used without further purification.

Dilatometric Procedure

The dilatometer consisted of a Pyrex bulb and a section of calibrated 1 mm. diam. capillary tubing, which constituted the two arms of a U. The bulb was attached to the capillary through a ground glass joint. Above the capillary was a reservoir for holding and degassing mercury, and a ground glass joint through which the entire dilatometer could be attached, through a removable stopcock, to a high vacuum source.

The procedure used in making a polymerization rate determination involved the following steps. The sample bulb containing weighed amounts of monomer, solvent, and initiator was attached to the inverted dilatometer and held in place by means of metal springs. The contents of the bulb were then degassed at 10^{-5} mm. by three alternate freeze-thaw cycles. After degassing, the sample was frozen and the dilatometer inverted while still under high vacuum, causing mercury to flow from the reservoir, filling the capillary and trapping the frozen sample in the bulb. The dilatometer was removed from the vacuum line and placed in a constant temperature bath. After thermal equilibration had occurred, excess mercury was removed from the capillary and periodic readings of the height of the mercury level in the capillary were made with a cathetometer accurate to ±0.03 mm. The bath temperature was controlled to ±0.005°C.

In calculating rates of polymerization from the shrinkage rate data, it was assumed that the fraction of polymerization that had occurred at a given time was proportional to the fraction of the total polymerization shrinkage that had occurred at that time. The total shrinkage for each monomer was in turn calculated on the assumption that the change in volume on polymerization for each of the monomers is 22.9 cc./mole. This number was obtained experimentally for compound I from a dilatometric polymerization rate determination in ethyl acetate solution which was continued until no further shrinkage was observed. The value of 22.9 cc./mole is in good agreement with those reported for other methacrylates:[7] methyl methacrylate −22.6 cc./mole, ethyl methacrylate −22.3 cc./mole, and *n*-butyl methacrylate −22.7 cc./mole.

Viscosities of polymers were run in acetone solution at 30°C. in Ubbelohde-type viscometers.

References

1. Bartlett, P. D., and R. Altschul, *J. Am. Chem. Soc.*, **67**, 812, 816 (1945).
2. Bartlett, P. D., and F. A. Tate, *J. Am. Chem. Soc.*, **75**, 91 (1953).
3. Brown, A. C. R., and D. G. L. James, *Can. J. Chem.*, **40**, 796 (1962).
4. Baysal, B., and A. V. Tobolsky, *J. Polymer Sci.*, **8**, 529 (1952).
5. Flory, P. F., *Principles of Polymer Chemistry*, Cornell Univ. Press, Ithaca, N. Y., 1953, p. 172.
6. Ferris, A. F., *J. Org. Chem.*, **20**, 780 (1955).
7. Nichols, F. S., and R. G. Flowers, *Ind. Eng. Chem.*, **42**, 292 (1950).

Résumé

On a étudié la polymérisation d'une série d'acrylates ayant un groupement méthyle en position alpha. Les mesures de la vitesse de polymérisation indiquent que tous les monomères polymérisent rapidement quoique contenant desa tomes d'hydrogène allylique. On a obtenu des données de viscosité qui montrent que, dans le cas de beaucoup de monomères, il se fait un transfert de chaîne important sans dégradation. Une explication est proposée pour interprêter la polymérisation rapide des monomères.

Zusammenfassung

Die Polymerisation einer Reihe von α-substituierten Methylacrylaten wurde untersucht. Messung der Polymerisationsgeschwindigkeit zeigte, dass jedes von den Monomeren trotz des Gehaltes an Allylwasserstoffatomen leicht polymerisiert. Die gemessene Viskosität der Polymeren zeigte, dass bei einigen Monomeren in beträchtlichem Ausmass eine nicht-verzögernde Kettenübertragung stattfindet. Eine Erklärung für die rasche Polymerisation der Monomeren wird gegeben.

Received July 11, 1962

JOURNAL OF POLYMER SCIENCE: PART A VOL. 1, PP. 1927–1935 (1963)

Preparation and Properties of Some Poly-α-Methylstyrenes

DAVID E. BURGE* and DOUGLAS B. BRUSS, *Shell Development Company, Emeryville, California*

Synopsis

The preparation of 20–40 g. quantities of sharply defined fractions of poly-α-methylstyrene, for use as standards in the correlation of molecular weight methods, is described. The procedure involves a moderately careful synthesis and fractionation. Differences in the light-scattering second virial coefficient appear to be indicative of differences in the stereoregularity of the polymers prepared by different initiators. The intrinsic viscosities of all of the polymers studied are expressed by a Mark-Houwink equation that is the same in all cases.

Introduction

In any study of the properties of synthetic polymers, one of the most vexing problems is the distribution of molecular weights. Theoretical work is usually based on the behavior of a species of homogeneous molecular weight because in many cases the effect of polydispersity is difficult to assess. The general practice in experimental work is to use polymer fractions, but only rarely are these fractions examined to ensure that they have a narrow molecular weight distribution. The *a priori* assumption that such fractions have a narrow distribution is not necessarily valid. Our experience using conventional techniques on 20 to 50 g. quantities of polymer is that the fractions obtained can often have weight to number average molecular weight ratios as large as 1.5–2, which can hardly be considered as representative of a narrow distribution.

The recent development of anionic methods of polymerization[1,1] provides a new approach to the preparation of certain polymers with very narrow distributions, but the desired results can only be obtained by very careful experimental techniques. However, by a combination of only moderately careful synthetic methods with a simple fractionation procedure, large amounts of a series of poly-α-methylstyrenes have been prepared and studied by light scattering, osmometry, and viscometry. The results show that this procedure yields polymers with narrow distribution, and some interesting solution properties have been observed.

* Present address: Mechrolab, Inc., Mountain View, California.

Apparatus and Technique

Polymer Preparation

All polymers were synthesized in tetrahydrofuran (THF), which had been distilled from sodium naphthalene. The starting material, α-methylstyrene (Eastman, purified), was dried over porous barium oxide for several days before use. The butyllithium initiator (Foote Chemical Co.) was a commercial product obtained as a solution in heptane. The sodium naphthalene initiator was prepared by stirring a solution of naphthalene in THF with sodium metal overnight. The resulting deep green solution was then filtered.

Each polymer synthesis was carried out in a 1000-ml. round-bottomed flask which had been flushed with dry nitrogen and flamed several times. Approximately 500 ml. of THF were then distilled into the flask from a sodium naphthalene solution and the flask stoppered with a rubber serum cap. One-hundred milliliters of α-methylstyrene were added through the serum cap by means of a hypodermic syringe, and the initiator was added in the same manner in small increments until a faint red color persisted for about one hour. At this point, an additional amount of initiator was added, the quantity depending upon the final molecular weight desired. The solution was cooled rapidly with swirling in a slurry of Dry Ice-isopropanol and kept at this temperature for about one hour. The reaction was terminated by the addition of a small amount of methanol and the polymer recovered by precipitation in a large excess of methanol. This procedure was used in all of the preparations, the only variable being the amount and kind of initiator used.

Polymer Fractionation

Since the polymers prepared by this method did not have distributions as narrow as desired, a simple fractionation procedure was applied to each of them with the exception of those below a molecular weight of 5000. Fractionation was done by coacervation using toluene as the solvent and methanol as the nonsolvent. About 25 g. of polymer was dissolved in toluene, and the solution was poured into methanol contained in a $^1/_2$-gal. bottle. The total volume of toluene and methanol was one liter, the volume of methanol being sufficient to put essentially all of the polymer into the polymer-rich phase. This amount of methanol (34 to 40 vol.-%) depended on the molecular weight of the polymer. The mixture was shaken thoroughly and allowed to equilibrate at 30 ± 0.5°C. for 24 hr. The supernatant phase was drawn off, concentrated by evaporation, and the polymer recovered by precipitation with an excess of methanol. The process was repeated by adding successive liters of toluene-methanol mixtures, each containing one volume per cent less methanol than the preceding portion, until all of the polymer had been recovered.

This procedure is simply a systematic method of removing fractions of successively higher molecular weight. On the basis of literature data

and experience, several features of the fractionation are important. The temperature must be controlled to within 0.5 to 1°C., but closer regulation does not seem to be necessary. The polymer concentration in the supernatant phase must be kept small. This ultimately results in a compromise between the amount of polymer to be fractionated, the total amount of solvent-nonsolvent to be used, and the maximum concentration which will yield an adequate fractionation.

The authors have fractionated 20 g. of high molecular weight material and as much as 40 g. of low molecular weight material by using this method. These amounts do not represent the limit since a critical evaluation of the resulting concentrations was not made.

Light-Scattering Measurements

Light-scattering measurements were made with a dual phototube photometer; benzene was used as a reference standard for absolute scattering ratios. The solution was contained in a small conical cell similar to that described by Zimm.[13] The cell was suspended in a liquid bath of a design somewhat similar to that described by Baum and Billmeyer.[1] All measurements were made at 25 ± 0.2°C. in toluene at a wavelength of 546 mμ. A value of 16.3×10^{-6} cm.$^{-1}$ was used for the absolute scattering of benzene. The specific refractive index increment for poly-α-methylstyrene in toluene at 25°C. was measured with a Brice-Phoenix differential refractometer and was found to be 0.129 ml. g^{-1}. The values for molecular weights under 10,000 were somewhat lower.

Scattering measurements were carried out at 6 to 8 concentrations and at 9 angles from 20 to 135°. Reagent grade toluene was used, all solutions and the solvent being clarified by filtration through HA Millipore filters.

The second virial coefficient A_2, was determined from the concentration dependence of the scattering at zero angle by means of the usual equation:

$$Kc/R = 1/M_w + 2A_2c$$

For most of the polymers the angular dependence of the scattering was too small to obtain meaningful results for the size of the molecules.

Viscosity Measurements

Intrinsic viscosities were determined in toluene at 25°C. using small-volume cross-arm viscometers designed by H. W. Daeschner (private communication). These viscometers were designed so that the kinetic energy correction was negligible and a viscosity could be determined on about 0.5 ml. of solution. The maximum shear rate for these measurements was estimated to be about 500 sec.$^{-1}$.

Osmotic Pressure Measurements

Osmotic pressure measurements were made using the small volume osmometers described previously.[3] Dynamic measurements were made on

TABLE I
Properties of Some Poly-α-Methylstyrenes

Sample	Initiator	$\bar{M}_w \times 10^{-3}$	$A_2 \times 10^4$	$\bar{M}_n \times 10^{-3}$			$\bar{M}_w/\bar{M}_n$	Intrinsic visc.
				Osmotic[a]	Ebullioscopic	Vapor press.[b]		
1	BuLi	3.4	18.3	(2.2)	2.2		1.54	0.046
2	BuLi	4.5	14.7	(2.4)	2.4	2.4	1.87	0.049
3	BuLi	5.0	11.2	(3.7)	3.7	3.8	1.35	0.058
4	BuLi	7.7	15.7	(6.2)	6.2	5.8	1.24	0.064
5	Na naphthalene	25	8.3	(20),21			1.25	0.148
6	BuLi	53	6.7	(49),48			1.10	0.250
7	Na naphthalene	64	4.7	(57),62			1.03	0.295
8	BuLi	180	5.0	180			1.00	0.577
9	Na naphthalene	240	3.2	(240),250			0.96	0.750
10	BuLi	480	4.0	300			1.59	1.10
11	BuLi	500	3.0	450			1.11	1.15
12	BuLi	530	2.9	470			1.12	1.30
13	BuLi	640	3.0	560			1.14	1.30
14	Na biphenyl	840	2.8	450			1.87	1.80

[a] Dynamic osmotic pressure results are given in parentheses.
[b] Mechrolab Model 301 vapor pressure osmometer.

all of the lower molecular weight polymers to afford a measure of any membrane-permeating solute and thus establish a good criterion for polydispersity of the fraction. The technique was described in an earlier paper.[4] The validity of this technique is demonstrated by the close agreement between the results obtained by it, and the values obtained by ebulliometry and a differential vapor pressure technique (Mechrolab vapor pressure osmometer Model 301) on polymers in the 2,000- to 6,000-molecular weight range (see Table I). In this region, dynamic measurements were made using ultrafine filter membranes such as described by Vaughan.[12]

In the molecular weight range of 20,000 to 240,000, osmotic measurements were made by both the static and dynamic techniques using gel-cellophane membranes of grade No. 600. In each case the agreement was good, showing the absence of low molecular weight "tails" in the distribution curve. If membrane permeating solute were present in these samples, the dynamic results would be appreciably lower than the static results. In the molecular weight range above 240,000, only static determinations were made. All measurements were made in toluene at 30 ± 0.003°C.

Results and Discussion

All of the experimental results are summarized in Table I. The initiator used in each synthesis is given in column 2. Only the second virial coefficients obtained from the light-scattering measurements are reported since those obtained by osmometry were not as reproducible, probably because fewer concentrations were used in the osmotic work. The ratio of the weight to number average molecular weight is given as a criterion of polydispersity.

The validity of this criterion deserves some comment. Since we are dealing with just two averages or moments of the distribution function, this ratio is not completely definitive unless the form of the distribution function is known. However, regardless of the form of this function, the distribution must become narrower as the ratio of molecular weights approaches unity. When the ratio is unity, the molecular weight must have a unique value. If the experimental reliability of the two moments is good, the ratio will provide a fairly good index of the polydispersity.

The light-scattering results are repeatable to about 5%. The osmotic results are equally as repeatable in the range below 500,000, providing no solute permeates the membrane. As already mentioned, the close agreement between the values obtained by three distinct methods on samples of low molecular weight and the agreement between the static and dynamic results on polymers of higher molecular weight is convincing evidence that the membranes and measuring techniques are not subject to permeation errors on the samples considered.

By this criterion it can be seen that most of the polymers have a ratio below 1.25, the exceptions being samples number 1, 2, 3, 10, and 14. Samples 1, 2, and 3 were not fractionated and were not expected to be as

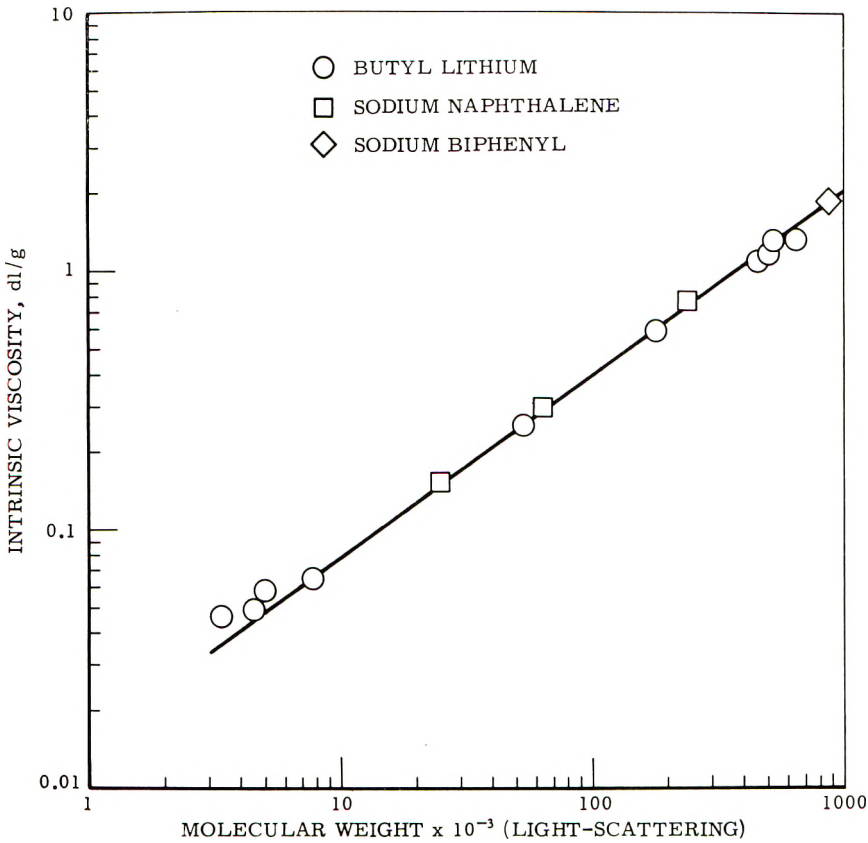

Fig. 1. Intrinsic viscosity-molecular weight correlation for poly-α-methylstyrene in toluene at 25°C.

narrow as the others. Sample 14 was an early preparation in which some of the techniques may not have been as good as in the latter preparations. Sample 10 was a fraction from the same original preparation as numbers 12 and 13. Though some low molecular weight material was removed before this cut, an appreciable amount evidently still remains in this fraction, giving it a higher weight to number average ratio than the succeeding cuts 12 and 13.

The intrinsic viscosity-molecular weight correlation is shown graphically in Figure 1. The Mark-Houwink equation derived from the graph is

$$[\eta] = 1.1 \times 10^{-4} M^{0.71}$$

which is in excellent agreement with the findings of Sirianni et al.[10] and McCormick.[9] The graph is presented here for two reasons. In the first place, it demonstrates that the equation is valid down to molecular weights of 10^4 and is not greatly in error below that, and secondly, that the correlation is valid for all polymers regardless of the initiator used to prepare them.

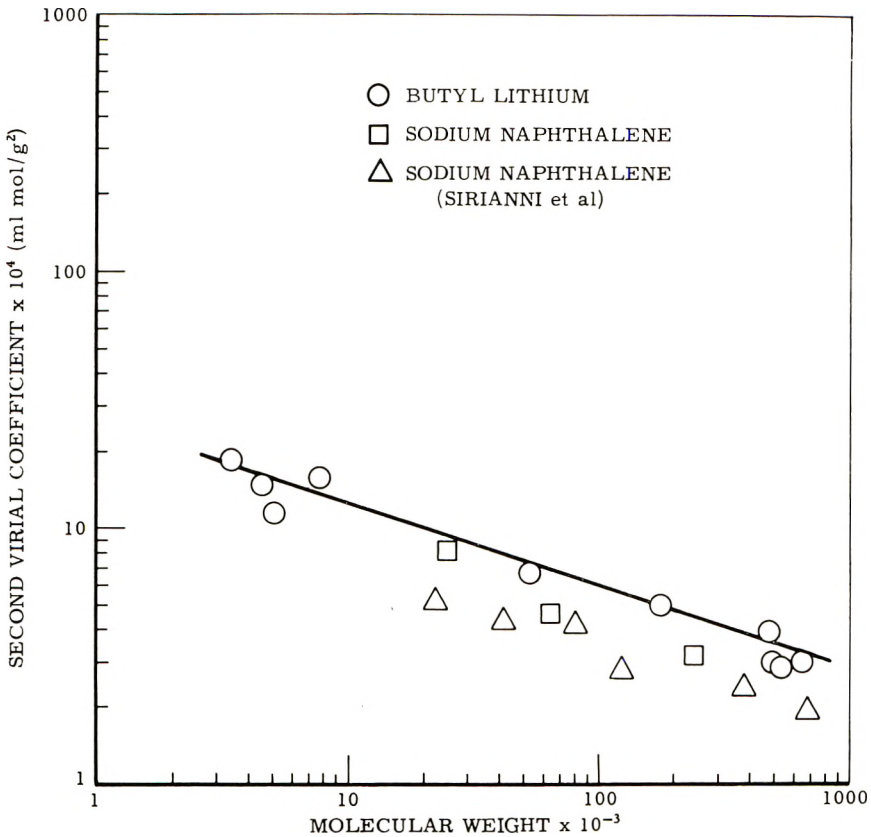

Fig. 2. Correlation between second virial coefficient and molecular weight from light-scattering studies.

This point will be discussed further along with the consideration of the second virial coefficient.

Figure 2 is a graph of the second virial coefficients versus molecular weight; both determined by light scattering. A least squares fit to a straight line has been drawn through the points for polymers prepared by butyllithium initiation, and this line can be represented by the equation:

$$A_2 = 2.45 \times 10^{-2} M^{-0.32}$$

Points are also shown for the sodium naphthalene initiated polymers as well as the results of Sirianni et al.[10] for polymers prepared by this initiator. It is obvious from the graph that these results tend to be lower than those for the butyllithium polymers, a difference which appears to be larger than the experimental error.

Possible reasons for this difference in second virial coefficients include polydispersity, chain branching, and chain microstructure. Since the polymers have all been shown to have rather narrow distributions, polydispersity does not appear to be a factor. Chain branching is not expected

in anionic polymerizations and, as far as is known, no evidence for it has been reported. Hence, chain microstructure is the most likely reason for the observed variations. A recent paper by Brownstein et al.[2] on the proton resonance spectra of poly-α-methylstyrenes indicated large differences in the stereoregularity of molecules prepared by different initiators. They found the sodium naphthalene preparation to be predominantly heterotactic and the butyl lithium preparations to be predominantly syndiotactic. Unfortunately, the polymerization was carried out in cyclohexane at 4°C. while the authors' was done in tetrahydrofuran so the results are not directly comparable. Nevertheless, there is good indication that the authors' polymers differ in stereoregularity as shown by the differences in the second virial coefficient.

This point is of particular interest since it has already been shown that the intrinsic viscosity is independent of the initiator used. Similar results have already been observed by others for polystyrene and polypropylene. Danusso and Moraglio[5] found a variation of second virial coefficient but not of viscosity between isotactic and atactic polystyrene. A further study of polystyrene led Krigbaum et al.[8] to the conclusion that under unperturbed or theta conditions the dimensions of isotactic polystyrene molecules were larger than of atactic molecules. However, their results for isotactic polymers were obtained under metastable conditions and must be viewed with some suspicion. Kinsinger and Hughes[6] have studied isotactic and atactic polypropylene and found no significant difference in the intrinsic viscosities. The experimental problems of high temperature measurement made it impossible to distinguish between the second virial coefficients. Another report by Kinsinger and Wessling[7] showed a difference in theta temperature for the two polypropylenes in phenyl ether.

The results reported in this work are in a good solvent far removed from theta conditions, but some preliminary experiments have been obtained in 1-chlorohexane at 25°C. The virial coefficients are an order of magnitude lower than in toluene, ranging from 0.2 to 0.7 $\times 10^{-4}$, and hence are much closer to theta conditions. From the few experiments made, the results indicate that again the second virial coefficient depends on the initiator used but the intrinsic viscosity does not. This effect should be studied further and preferably at exactly theta conditions.

The authors are indebted to Mr. H. McKerley for the ebullioscopic and vapor pressure measurements and to Mr. R. Dougherty for many of the light-scattering measurements.

References

1. Baum, F. J., and F. W. Billmeyer, *J. Opt. Soc. Am.*, **51**, 452 (1961).
2. Brownstein, S., S. Bywater, and D. J. Worsfold, *Makromol. Chem.*, **48**, 127 (1961).
3. Bruss, D. B., and F. H. Stross, *Anal. Chem.*, **32**, 1456 (1960).
4. Bruss, D. B., and F. H. Stross, *J. Polymer Sci.*, **55**, 381 (1961).
5. Danusso, F., and G. Moraglio, *J. Polymer Sci.*, **24**, 161 (1957).
6. Kinsinger, J. B., and R. E. Hughes, *J. Phys. Chem.*, **63**, 2002 (1959).
7. Kinsinger, J. B., and R. A. Wessling, *J. Am. Chem. Soc.*, **81**, 2908 (1959).

8. Krigbaum, W. R., D. K. Carpenter, and S. Newman, *J. Phys. Chem.*, **62**, 1586 (1958).
9. McCormick, H. W., *J. Polymer Sci.*, **41**, 327 (1959).
10. Sirianni, A. F., D. J. Worsfold, and S. Bywater, *Trans. Faraday Soc.*, 2124 (1959).
11. Szwarc, M., M. Levy, and R. Milkovich, *J. Am. Chem. Soc.*, **78**, 2656 (1956).
12. Vaughan, M. F., *J. Polymer Sci.*, **33**, 417 (1958).
13. Zimm, B. H., *J. Phys. Chem.*, **16**, 1099 (1948).

Résumé

On décrit la préparation de 20 à 40 g de fractions bien définies de poly-α-méthylstyrène, pour les utiliser comme étalons en vue d'établir une corrélation entre les méthodes de détermination du poids moléculaire. Le procédé implique la synthèse assez soignée et le fractionnement. Des différences dans le second coefficient viriel de la diffusion lumineuse indiquent des différences dans la stéréorégularité des polymères préparés par différents initiateurs. La viscosité intrinsèque de tous les polymères examinés sont exprimées par l'équation de Mark-Houwink, qui est la même dans tous les cas.

Zusammenfassung

Die Darstellung von scharf definierten Poly-α-methylstyrolfraktionen in 20–40 g-Mengen zum Gebrauch als Standards für die Korrelation von Molekulargewichtsbestimmungsmethoden wird beschrieben. Das Verfahren besteht in einer Synthese unter gut definierten Bedingungen und einer Fraktionierung. Unterschiede im zweiten Virialkoeffizienten bei Lichtstreuungsmessungen scheinen auf Unterschiede in der Stereoregularität von mit verschiedenen Startern hergestellten Polymeren hinzuweisen. Die Viskositätszahlen aller untersuchten Polymeren können durch die gleiche Mark-Houwink-Gleichung ausgedrückt werden.

Received July 10, 1962

JOURNAL OF POLYMER SCIENCE: PART A VOL. 1, PP. 1937–1946 (1963)

Polymerization of Vinyl Ethers with Magnesium Compounds. I. Catalytic Reactivity of Magnesium Halides

K. IWASAKI, H. FUKUTANI, and S. NAKANO, *Central Research Laboratory, Mitsubishi Chemical Industries Limited, Kawasaki, Japan*

Synopsis

An attempt was made to summarize the activity of magnesium halides in the polymerization of vinyl ethers. Bulk polymerization was carried out at temperatures of 0–80°C. Methyl, ethyl, isopropyl, and isobutyl vinyl ethers were used as monomers, and the relative reactivities of these monomers were compared. Except for the fluoride, magnesium halides had mild activity. Within a given group, the overall activation energies of polymerization decrease with increasing weight of halogen. On the other hand, the molecular weight of polyvinyl ethers obtained from this group of catalysts increases with decreasing weight of halogen. In addition, some differences were observed between the diethyl ether complex and the dioxane complex of magnesium bromide.

INTRODUCTION

It is well known that $BeCl_2$ and $ZnCl_2$ initiate cationic polymerization as Friedel-Crafts type catalysts, but catalysts from the other compounds, based on metals of group II of the periodic table have not been studied.

We have investigated the catalytic reactivity of these compounds and found that MgO, MgX_2, and RMgX were very active catalysts in the polymerization of vinyl ether. In this paper, we report the relative catalytic reactivity of magnesium halides.

It seemed very interesting that magnesium halides, including the complexes thereof, catalyzed polymerization of vinyl ether at a moderate rate, compared with catalysts such as $AlCl_3$, $TiCl_4$, and BF_3-etherate. The polymerization of vinyl ether with the last-named catalyst is violent, of the so-called "flash" type, but the polymerization with the former catalyst is so mild that relative reactivities among lower alkyl vinyl ethers have been clearly obtained.

EXPERIMENTAL

Materials

MgF_2. Hydrofluoric acid (40%) was reacted with commercial MgO at 100°C. in a polyethylene flask. The precipitate obtained was washed with

distilled water until the filtrate showed no acidity and heated at 400°C. in the air.

MgF_2–HF. Hydrofluoric acid (40%) was reacted with commercial MgO as described above. The precipitate obtained was filtered and charged into purified petroleum ether. It was filtered again and heated at 400°C. in air. The product was slightly soluble in water and showed acidity, but its composition was unknown.

$MgCl_2$. Reagent grade magnesium chloride hexahydrate was heated with a small amount of water in a porcelain dish, and an equimolar amount of ammonium chloride was added. The mixture was heated with stirring until it became solid and dehydrated at 110°C. after crushing. Just before use, the $MgCl \cdot NH_4Cl \cdot H_2O$ obtained above was powdered and heated to $MgCl_2$ *in vacuo* at 110°C. to constant weight.

$MgBr_2 \cdot 3C_4H_8O$. One mole of magnesium powder was suspended in dry diethyl ether under nitrogen, and then slightly less than one mole of bromine was added portionwise at 30°C. After the magnesium powder had almost disappeared, the unreacted magnesium was filtered out. An excess of anhydrous tetrahydrofuran was then added to the reaction mixture. The precipitate obtained was filtered and dried *in vacuo* at room temperature; purity, 90.5%

$MgBr_2 \cdot 2C_4H_8O_2$. $MgBr_2$ in ether solution was obtained by the same method mentioned above. An excess of anhydrous dioxane was added to the solution. Precipitate obtained was dried *in vacuo* at room temperature; purity, 96.6%

$MgI_2 \cdot 2(C_2H_5)_2O$. MgI_2 in ether solution was prepared by reacting magnesium powder with iodine in dry ether; the product was filtered and concentrated under reduced pressure; purity, 98.0%

Vinyl ethers according to Schildknecht's method, these were washed eight times with an equal volume of water made slightly alkaline with potassium hydroxide, dried with sodium metal, and distilled, the middle fraction being collected.

Procedure

The polymerization was carried out in bulk under stirring. In this experiment, polymerization with these catalysts was not accelerated by a polar medium, and reactions in solution diluted with inactive solvents were not induced. Because of their poor solubilities, it was necessary to disperse catalyst uniformly.

To obtain time–conversion curves, small portions of reaction mixture were sampled from time to time and poured into water–methanol mixtures. The polymer was precipitated, collected, washed several times with methanol, and dried *in vacuo* at 50°C. for one day.

The reduced viscosity η_{sp}/c was measured for 0.5 g. polymer in 100 ml. benzene solution at 25°C. in an Ostwald viscometer.

RESULTS

The results of the polymerization of vinyl ethers with magnesium halides and magnesium halide complexes at various catalyst concentrations [C] are summarized in Tables I–VII.

TABLE I
Bulk Polymerization of Isobutyl Vinyl Ether with $MgCl_2$, [C] = 8.22×10^{-2} mole/l.

50°C.			25°C.			0°C.		
Time, hr.	Conversion, %	η_{sp}/c	Time, hr.	Conversion, %	$\%_{sp}/c$	Time, hr.	Conversion, %	η_{sp}/c
1/2	92.5	0.58	1	0.4	0.38	2	0.1	—
1	97.5	0.57	3	3.5	0.40	7	0.1	—
2	97.4	0.55	5	6.7	0.46	14	0.15	—
			7	20.0	0.46			

From these results, overall activation energies of polymerization were calculated by use of the Arrhenius equation; these plots are shown in Figures 1 and 2.

In Table VIII, a comparison of the apparent catalytic reactivity of magnesium halides in the bulk polymerization of isobutyl vinyl ether is shown.

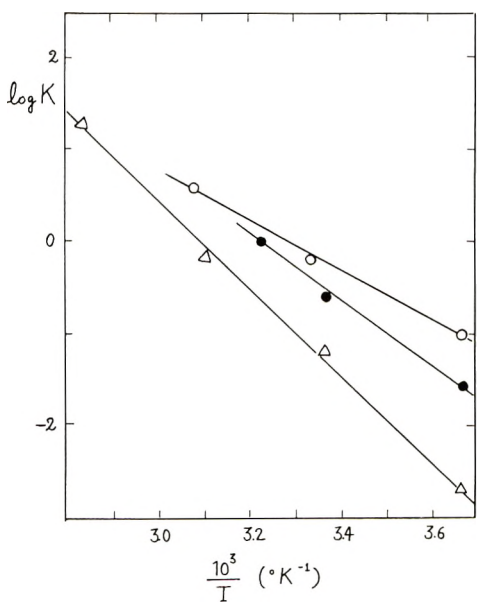

Fig. 1. Overall activation energy obtained with $MgBr_2 \cdot 3C_4H_8O$ in polymerization of (△) isobutyl vinyl ether; (●) ethyl vinyl ether; (○) isopropyl vinyl ether.

TABLE II

Bulk Polymerization of Isobutyl Vinyl Ether with $MgBr_2 \cdot 3C_4H_8O$, [C] = 1.58×10^{-2} mole/l.

80°C.			50°C.			25°C.			0°C.		
Time, hr.	Conversion, %	η_{sp}/c	Time, hr.	Conversion, %	η_{sp}/c	Time, hr.	Conversion, %	η_{sp}/c	Time, hr.	Conversion, %	η_{sp}/c
1/12	93.4	0.11	1	40.8	0.20	1.5	1.6	0.07	4	0.8	—
			2	69.0	0.22	5	10.2	0.09	8	1.2	—
			3.16	79.4	0.22	7	17.4	0.12	12	1.8	—
			4	86.4	0.24	9	24.5	0.14	16	2.0	—
						24	56.8		20	3.2	—

TABLE III

Bulk Polymerization of Ethyl Vinyl Ether with $MgBr_2 \cdot 3C_4H_8O$, [C] = 1.58×10^{-2} mole/l.

37°C.			25°C.			0°C.		
Time, hr.	Conversion, %	η_{sp}/c	Time, hr.	Conversion, %	η_{sp}/c	Time, hr.	Conversion, %	η_{sp}/c
1	55.6	0.30	2	31.8	0.32	4	12.1	0.12
2	81.6	0.35	4	49.6	0.39	8	23.6	.17
			6	65.0	0.42	12	36.0	0.20
			8	—	0.37	16	41.6	.21

TABLE IV

Bulk Polymerization of Isopropyl Vinyl Ether with $MgBr_2 \cdot 3C_4H_8O$, [C] = 0.57×10^{-2} mole/l.

52°C.			27°C.			0°C.		
Time, hr.	Conversion, %	η_{sp}/c	Time, hr.	Conversion, %	η_{sp}/c	Time, hr.	Conversion, %	η_{sp}/c
1/2	31.7	1.31	1	44.9	0.32	2	12.1	0.12
1	69.3	0.91	2	78.3	0.35	4	23.6	0.17
			3	81.0	0.35	8	36.0	0.20
						12	41.6	0.21

TABLE V

Bulk Polymerization of Isobutyl Vinyl Ether with $MgBr_2 \cdot 2C_4H_8O_2$, [C] = 1.58×10^{-2} mole/l.

82°C.			64°C.			50°C.		
Time, hr.	Conversion, %	η_{sp}/c	Time, hr.	Conversion, %	η_{sp}/c	Time, hr.	Conversion, %	η_{sp}/c
1	—	2.65	4	2.0	—	8	0.38	—
2	14.0	1.18	8	3.0	—	16	0.80	—
4	21.4	1.19	12	4.0	0.14	24	1.98	—
6	27.6	1.25	16	4.2	0.18			

TABLE VI

Bulk polymerization of Isobutyl Vinyl Ether with $MgI_2 \cdot 2(C_2H_5)_2O$, [C] = 1.56×10^{-2} mole/l.

50°C.			0°C.		
Time, hr.	Conversion, %	η_{sp}/c	Time, hr.	Conversion, %	η_{sp}/c
1.16	45.4	0.09	1	7.7	0.12
2	71.5	0.08	2	9.7	0.12
3	85.8	0.08	3	11.9	0.13
4	87.2	0.09	4	14.0	0.13
			5	21.2	0.15

TABLE VII

Bulk Polymerization of Isobutyl Vinyl Ether with MgF_2–HF Catalyst; 0.741 g. Catalyst Added to 100 ml. Monomer

80°C.			65°C.			50°C.		
Time, hr.	Conversion, %	η_{sp}/c	Time, hr.	Conversion, %	η_{sp}/c	hr.	Conversion, %	η_{sp}/c
1	12.6	1.48	2	16.7	0.81	2	7.1	0.76
2	17.6	1.42	4	40.8	1.13	4	10.9	1.04
4	23.6	1.14	6	54.6	1.03	6	17.5	1.08
6	27.6	0.89	8	62.0	0.92	8	25.1	1.37

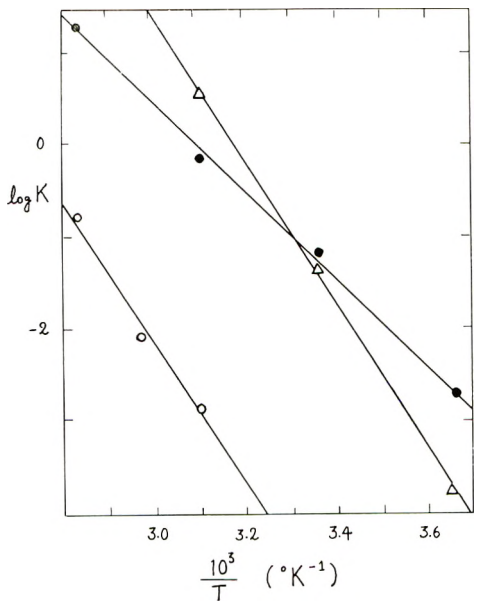

Fig. 2. Overall activation energy obtained in polymerization at isobutyl vinyl ether with MgX_2: (△) $MgCl_2$; (○) $MgBr_2 \cdot 2C_4H_8O_2$; (●) $MgBr_2 \cdot 3C_4H_8O$.

TABLE VIII

Comparison of Catalytic Reactivity of Magnesium Halides in the Bulk Polymerization of Isobutyl Vinyl Ether

Catalyst	Overall activation energy, kcal./mole	η_{sp}/c[a]	Reduced reaction velocity, %/min.[b]
MgF_2	—	—	0
MgCl	34.6	0.58	0.56
$MgBr_2 \cdot 3C_4H_8O$	22.0	0.24	0.68
$MgI_2 \cdot 2(C_2H_5)_2O$	6.9	0.15	0.65
$MgBr_2 \cdot 2C_4H_8O_2$	35.4	2.65	0.0008
MgF_2–HF	9.2	1.48	—

[a] The maximum value obtained from all reaction conditions.

[b] Arbitrary velocity of monomer consumption in per cent per minute at 50°C. reduced to the catalyst concentration of 1.58×10^{-2} mole/l. This comparison based on the estimation of the linear relationship between catalyst concentration and velocity.

Furthermore, in Table IX are listed the relative reactivities of lower alkyl vinyl ethers with $MgBr_2 . 3C_4H_8O$ at 0°C.

TABLE IX

Relative Reactivities of Lower Alkyl Vinyl Ethers with $MgBr_2 \cdot 3C_4H_8O$, [C] = 1.58 $\times 10^{-2}$ mole/l.

Vinyl ether	Initial reaction velocity, %/min.	Overall activation energy kcal./mole	η_{sp}/c[a]
Isopropyl vinyl ether	0.212	12.7	1.31
Ethyl vinyl ether	0.020	16.0	0.42
Isobutyl vinyl ether	0.0033	22.0	0.24
Methyl vinyl ether	0.00023	—	0.11

[a] The maximum value obtained for all reaction conditions.

DISCUSSION

To confirm the fact that magnesium halides have catalytic activity in vinyl ether polymerization, we wish to refer to the considerations of Emeleus and Anderson.[1] They suggest that the physical properties of metal halides are determined by the ionization potential of the metal atom. Properties of the halides are shown in Table X and may easily be divided into two classes, for example, by the difference of their electric conductivities Λ. Chlorides placed over the border-line seem to have an

TABLE X

Some Properties of Metal Chlorides

	HCl	LiCl	NaCl	KCl	RbCl	CaCl
m.p. °C.	−114	606	800	768	717	645
b.p. °C.	−85	1337	1442	1415	1388	1289
Λ	10	166	134	140	78	67
		$BeCl_2$	$MgCl_2$	$CaCl_2$	$SrCl_2$	$BaCl_2$
m.p., °C.		404	718	774	840	960
b.p., °C.		500	(1000)	(1100)	(1250)	(1350)
Λ		0.066	29	52	56	65
		BCl_3	$AlCl_3$	$GaCl_3$	$InCl_3$	$TlCl_3$
m.p. °C.		−017	—	75.5	586	25
b.p. °C.		12.6	183	205	(550)	(100)
Λ		0	15 10	10	14.7	10

ionic crystalline lattice; on the other hand chlorides under the line are thought to be molecular lattice compounds having a lower melting point. Compounds belonging to latter group are known as Lewis acid.

Magnesium chloride, in former group, exists so near the line that it has catalytic activity in vinyl ether polymerization.

Calcium chloride, placed far from the line, shows no activity. In this connection, the relative amounts of catalyst needed to complete polymerization at room temperature are shown in Table XI.

TABLE XI

Catalyst	Amount catalyst needed, mole/l.	Monomer reference	
$BF \cdot Et_2O$	10^{-1}	Methyl, ethyl, isopropyl, and isobutyl vinyl ether	Lewis acid
$TiCl_4$	10^{-3}	Isobutyl vinyl ether	Lewis acid
$AlCl_3 \cdot Et_2O$	10^{-3}	Isobutyl vinyl ether	Lewis acid
MgX_2	10^{-1}–10^{-2}	Ethyl, isopropyl, and isobutyl vinyl ether	?

As shown in Table XI, magnesium halides have lower activity than Lewis acid-type catalysts; therefore they failed to catalyze the polymerization of styrene and α-methylstyrene.

Table VIII shows the catalytic reactivities of magnesium halides. The overall activation energy of polymerization increases in the order: $MgBr_2 \cdot 2C_4H_8O_2 > MgCl_2 > MgBr_2 \cdot 3C_4H_8O > MgF_2$–$HF > MgI_2 \cdot 2(C_2H_5)_2O$. Though the reaction seems to be cationic, the overall activation energy is too high. The molecular weight of the product increases in the order: $MgBr_2.2C_4H_8O_2 > MgF_2$–$HF > MgCl_2 > MgBr_2.3C_4H_8O > MgI_2.2(C_2H_5)_2O$. As shown in Table IX, the relative reactivity of monomers in the polymerization with $MgBr_2 \cdot 3C_4H_8O$ as initiator is in the following order, isopropyl > ethyl > isobutyl > methyl vinyl ether.

This result agrees with the results of Eley[2] with I catalyst, rather than those of Schildknecht.[3]

Final considerations are given in Table XII. The ionic character of the bond between magnesium and halogen is calculated according to the equation of Hannay and Smyth[4] using the values of electronegativity of Pauling,[5] and compared with the results of experiments.

TABLE XII
Properties of Magnesium Halides

Property	MgF_2	$MgCl_2$	$MgBr_2$	MgI_2
Bond	Mg—F	Mg—Cl	Mg—Br	Mg—J
Ionic character, %	72.2	40.1	34.5	26.7
Crystalline lattice	ionic lattice	layer lattice	layer lattice	layer lattice
Type of crystal	Rutile	$CdCl_2$	CdI_2	CdJ_2
γ_{Mg}/γ_x	0.48	0.36	0.33	0.30
Lattice energy, kcal./mole	688∼ 708	593∼ 603	567∼ 591	540∼ 553
m.p. °C.	1270	716	695	650
Solubility in H_2O, g./100 g. H_2O (temp., °C.)	0.0008 (18)	54.5 (20)	101.5 (20)	139 (20)

The fact that the overall activation energy decreases with the lattice energy and increasing solubility of the halide will be explained by the following consideration. The rate-determining step of the polymerization depends chiefly on the initiation step comprising the solvation of catalyst, and the abnormally high value of activation energy obtained is due to large activation energy of initiation corresponding to poor solubility of catalyst in monomer.

As illustrated in Table XII, magnesium fluoride is highly ionic in nature. Therefore it is poorly soluble in monomer and does not show any activity. This is very analogous to the fact that aluminum fluoride, in the family of aluminum halides, has no catalytic action for polymerization of vinyl ethers.

The activity of the MgF_2–HF catalyst may be explained as follows. MgF_2–HF catalyst contains such a conjugated acid as the fluoromagnesium acid or a complex salt of hydrogen fluoride fixed on magnesium fluoride by fluorine bridge, and these are thought to be active species in the cationic polymerization.

The variation of molecular weight of the polymers obtained with these catalysts is closely related to the result of Fairbrother[6] with isobutene. The important mechanism of chain termination is still so obscure that we cannot clarify the relationship between molecular weight and catalyst.

At the end of this consideration, we must refer to the characterization of $MgBr_2.2C_4H_8O_2$. Being different from other $MgBr_2$–ether complexes, $MgBr_2.2C_4H_8O_2$ has higher melting point and poorer solubility. We speculate the possible structure of association as follows:

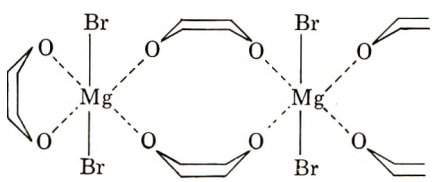

References

1. Emeleus, H. J., and J. S. Anderson, *Modern Aspects of Inorganic Chemistry*, Routledge, London, 1940, p. 14.
2. Eley, D. D., *J. Chem. Soc.*, **1954**, 1672.
3. Schildknecht, C. E., *Ind. Eng. Chem.*, **41**, 2891 (1949).
4. Hanay, N. B., and C. P. Smyth, *J. Am. Chem. Soc.*, **68**, 171 (1946).
5. Pauling, L., *The Nature of Chemical Bond*, Cornell Univ. Press, Ithaca, N. Y., 1940.
6. Plesch, P. H., *J. Chem. Soc.*, **1947**, 25.

Résumé

On a essayé de résumer l'activité des halogénures de magnésium dans la polymérisation d'éthers vinyliques. La polymérisation en "bloc" a été considérée à des températures variant de 0 à 80°C. On a utilisé comme monomères des méthyl–, éthyl–, isopropyl–, et isobutyl–vinyl–éthers et les réactivités relatives de ces monomères ont été comparées.

A l'exeption du fluorure, les halogénures de magnésium ont une faible activité. Pour un groupe donné, les énergies d'activation totales diminuent avec l'augmentation de poids de l'halogène. Au total certaines différences ont été observées entre les complexes de bromure de magnésium et d'éther diéthylique d'une part et de bromure de magnésium et de dioxanne d'autre part.

Zusammenfassung

Es wurde ein Versuch unternommen, einen Überblick über die katalytische Aktivität von Magnesiumhalogeniden bei der Polymerisation von Vinyläthern zu gewinnen. Die Polymerisation in Substanz wurdeb ei Temperaturen von 0–80 °C ausgeführt. Methyl–, Äthyl–, Isopropyl– und Isobutylvinyläther wurden als Monomeres verwendet und die relative Reaktivität dieser Monomeren verglichen. Mit Ausnahme des Fluorids besassen alle Magnesiumhalogenide eine schwache Aktivität. Innerhalb einer gegebenen Gruppe nimmt die Bruttoaktivierungsenergie der Polymerisation mit steigendem Atomgewicht des Halogens ab. Anderseits nimmt das Molekulargewicht der mit dieser Gruppe von Katalysatoren erhaltenen Polyvinyläther mit fallendem Atomgewicht des Halogens zu. Ausserdem wurden gewisse Unterschiede zwischen Diäthylätherkomplexen und Dioxankomplexen von Magnesiumbromid beobachtet.

Received February 2, 1961

JOURNAL OF POLYMER SCIENCE: PART A VOL. 1, PP. 1947–1954 (1963)

Specific Diluent Effects on Polymer Chain Dimensions

C. A. J. HOEVE* and M. K. O'BRIEN, *Mellon Institute, Pittsburgh, Pennsylvania*

Synopsis

Specific diluent effects on the unperturbed mean-square end-to-end distance $< r_0^2 >$ may be determined in dilute solutions at their Θ-points. Another method to determine these effects is described in this paper. It involves the measurement of the modulus of crosslinked polymers swollen with different diluents and interpretation of the results according to current rubber elasticity theory. As a result of the relatively high concentrations used in this method, combined with the introduction of crosslinks, specific diluent effects on chain dimensions are obtained, unobscured by excluded volume effects. The method is applied to polyethylene diluted with di-2-ethylhexyl azelate, α-chloronaphthalene, *n*-paraffin, tetralin, and *n*-hexadecane. Within 10% the value of $< r_0^2 >$ in *n*-hexadecane is equal to that in the other diluents used. In view of the similarity of the polyethylene molecule to those of *n*-hexadecane and *n*-paraffin this value must then also be equal to that for polyethylene in bulk. It may be concluded that, within experimental error, semi-ordering effects in the melt are absent and that no specific diluent effects exist.

Introduction

As insight in the physical properties of amorphous polymers grows, it becomes increasingly apparent that these properties are to a large extent determined by chain dimensions. It is then of primary importance to study factors influencing a suitable parameter indicative of chain dimensions, as for example, the mean-square end-to-end distance. In the absence of excluded volume effects the mean-square end-to-end distance $<r_0^2>$ is unperturbed,[1] as indicated by the subscript zero. Usually, the implicit assumption is made that it depends on temperature only. In order to investigate this assumption, let us consider more closely the factors which may influence $<r_0^2>$. At fixed bond lengths and bond angles the size of the random coil is determined by the minima in potential energy on rotation around chain bonds. Only for a few polymers are the potentials restricting rotation sufficiently known to permit analysis of the distribution of conformations and to calculate chain dimensions. The simplest polymer for which such an analysis has been carried out is polyethylene,[2] the chain bonds of which are distributed over trans and gauche conformations according to a Boltzmann distribution law. The question arises, however, to what extent intermolecular interactions may influence these potentials and

* Present address: National Bureau of Standards, Washington, D. C.

thereby chain dimensions. It is conceivable that interaction of solvent molecules with the trans conformation is energetically favored above that with the gauche conformation. This interaction, and therefore also $<r_0^2>$, would then depend on shape and size of solvent molecules. It is the object of this paper to investigate such specific diluent effects.

These specific interactions are to be distinguished from excluded volume effects, which are known[1] to occur in such dilute solutions that the chains do not overlap. In the latter case two groups, bonded through a large number of chain bonds, interact when in proximity. For a specified set of conformations of the intervening chain bonds, small deviations in rotational angles from their positions of minimum energy affect the potential energy of rotation only slightly. However, the distance between the two interacting groups, and therefore the potential energy, is sensitive to these deviations. If these groups are close together, the potential depends mainly on their relative position and not on the specific sequence of conformations of chain bonds connecting them. The interaction energy should then be essentially the same as for substituents belonging to different molecules.

Specific diluent effects may be measured in dilute solutions having nearly identical Θ-points. Such effects have been found[1,3,4] to be small with the exception of cellulose derivatives.[5] It is, however, not always possible to find a wide range of solvents with equal Θ-points, whereas corrections for excluded volume effects at ambient temperatures are often uncertain. In sufficiently concentrated solutions, in which chains overlap considerably, excluded volume effects are reduced as a result of a nearly uniform polymer segment density. Depending on molecular weight and solvent used, excluded volume effects may still persist[6] in the region, where some overlap occurs. Introduction of crosslinks between polymer chains before dilution and the relatively high polymer concentrations used in the method described below both contribute to reducing excluded volume effects. It may then be concluded that chain dimensions should be essentially unperturbed under these conditions. The results described in this paper are in agreement with this conclusion.

A convenient way to evaluate specific diluent effects is to perform stress-strain measurements on crosslinked polymers, swollen with a diluent, and to compare the results with those for the dry state. Flory[7] has given the following equation for a network in simple extension:

$$f = \nu kT \, (<\alpha>_0^2/L_{i0}) \, v_2^{-1/3} \, (\alpha - \alpha^{-2}) \qquad (1)$$

where f is the retractive force, ν is the number of chains in the sample, k is Boltzmann's constant, T the absolute temperature, L_{i0} is the length of the isotropic dry sample, and v_2 is the volume fraction of polymer in the sample. α is the extension ratio, defined by L/L_i, where L is the length of the sample at force f, and L_i is the length of the isotropic, diluted sample *at the volume corresponding to* v_2. In contradistinction, L_i', used below, is the length of the isotropic, diluted sample in swelling equilibrium with diluent. $<\alpha>_0^2 = <r_{i0}^2>/<r_0^2>$, where $<r_{i0}^2>$ is the mean-square end-to-end

distance of the polymer chains in the dry, isotropic sample, and $<r_0^2>$ is the mean-square end-to-end distance of free chains in the solution corresponding to v_2. It is to be noted that $<r_{i0}^2>$is proportional to $V_0^{2/3}$, where V_0 is the volume of the dry polymer sample; however, $<r_0^2>$ depends on potentials restricting rotation, on temperature, and possibly on the nature of diluents. With the aid of eq. (1) temperature coefficients of $<r_0^2>$ have previously[8] been deduced from the results of stress-temperature measurements. In analogy to this method, specific diluent effects on $<r_0^2>$ may be obtained by performing stress measurements on samples swollen with different diluents. It follows from eq. (1) that the ratio of the value of $fv_2^{1/3}$ for the dry state ($v_2 = 1$) to that for the diluted sample, measured at the same temperature and α, equals the ratio of $<r_0^2>$ of the polymer chain dissolved in the diluent to that in the bulk.

Unfortunately, several experimental difficulties prevent a successful application of this simple method. It is known that hysteresis loops occur in stress-strain measurements performed on amorphous polymers, indicating that thermodynamic equilibrium has not been attained.[9] However, equilibrium is approached more closely for diluted samples.[9] We have therefore compared stress-strain curves for samples diluted with different diluents. Another experimental difficulty is the accurate assessment of α and v_2. The volume fraction of polymer v_2 and α are given by $(L_{i0}/L_i)^3$ and L/L_i, respectively, and are easily measurable. However, during the stress-strain measurements an unknown quantity of diluent usually evaporates from the sample, thereby altering v_2 and L_i. In order to circumvent this difficulty we have kept the sample immersed in diluent during the stress-strain experiment and allowed swelling equilibrium to be established. Since v_2 then decreases on extension, correction for further dilution is necessary.

Procedure

The increase in degree of swelling may be obtained as follows. According to rubber elasticity theory,[7] we have the following equations for diluted samples in swelling equilibrium with diluent:

$$(\nu <\alpha>_0^2 V_1/N_a V_0) [v_2'^{1/3} - v_2'/2 <\alpha>_0^2] = - [\ln (1 - v_2') + v_2' + \chi_1 v_2'^2] \quad (2)$$

and

$$(\nu <\alpha>_0^2 V_1/N_a V_0) [L_{i0}/L - v_2/2 <\alpha>_0^2] = - [\ln (1 - v_2) + v_2 + \chi_1 v_2^2] \quad (3)$$

where V_1 is the molar volume of the diluent, N_a is Avogadro's number, L is the length of the strained sample, and χ_1 is the interaction parameter for solvent-polymer interaction. Here v_2' and v_2 are the volume fractions of polymer in swelling equilibrium with diluent at sample lengths L_i' and L, respectively. In order to obtain the value of v_2 at length L larger than L_i', the following procedure was applied. First the stress-strain curve for

the dry state was obtained. From this curve and the temperature, the value of $\nu <\alpha>_0^2$ was calculated according to eq. (1). Then the length L_i' was measured of the diluted, isotropic sample in swelling equilibrium with diluent at zero external force. We obtained χ_1 by substituting into eq. (2) v_2', given by $(L_{i0}/L_i')^3$, as well as values for $\nu <\alpha>_0^2$, V_1, and V_0. Strictly, the second terms on the left-hand sides of eqs. (2) and (3) cannot be evaluated, since the value of $<\alpha>_0^2$ is unknown. In order to permit calculation of χ_1 we have equated $<\alpha>_0^2$ to unity in these terms only. This procedure is a good approximation, if $<\alpha>_0^2$ is equal to, or larger than, unity. The samples of polyethylene crosslinked in the crystalline state meet this requirement since in this case $<\alpha>_0^2$ is probably somewhat larger than unity.[7] The value of v_2 may then be calculated at any length according to eq. (3). On using eq. (1) it is to be noted that α is not equal to L/L_i', since L_i' refers to v_2', instead of v_2. Correction for the volume change yields $\alpha = L/L_i = (L/L_i')(v_2'/v_2)^{1/3}$. We are now in a position to calculate the force on the diluted sample at any length L using the values of α, v_2, $\nu <\alpha>_0^2$, L_{i0}, and T. According to eq. (1) the ratio R between calculated and measured value of the force at specified L would equal the ratio of $<r_0^2>$ of the chain in diluent to that in bulk. However, since the value of $\nu<\alpha>_0^2$ has been calculated from measurements in the dry state for which equilibrium does not obtain, these R values do not represent the latter ratio. Nevertheless, the *relative* R values obtained for a polymer sample diluted with different diluents should be significant. We have therefore calculated the values of P, defined as the ratio of R for any diluent to that for the reference diluent, *n*-hexadecane. Then, P is equal to $(<r_0^2>_{\text{diluent}}/<r_0^2>_{\text{dry}})$ $(<r_0^2>_{\text{dry}}/<r_0^2>_{\text{hexadecane}}) = <r_0^2>_{\text{diluent}}/<r_0^2>_{\text{hexadecane}}$. In this procedure the measurements performed on the dry samples are used only to obtain the *corrections* resulting from volume increases on extension of the diluted sample. Under the conditions described in this paper these volume increases are about 10%. Of course, small deviations from equilibrium values may also obtain for the diluted samples. It is to be expected, however, that these deviations are approximately equal for the reference and other diluents and, therefore, they should not materially affect the results.

Experimental

Linear polyethylene (Super Dylan, low pressure polyethylene, obtained from the Koppers Co.) was chosen as the polymer. *n*-Paraffin, used as one of the diluents, melted from 65 to 70°C. Purification by urea adduct formation did not raise the melting point, nor did it change the infrared spectrum in the region of 1380 cm.$^{-1}$. It may then be concluded that these paraffins are practically linear and have an average chain length of at least 30 C atoms. *n*-Hexadecane, α-chloronaphthalene, di-2-ethylhexyl azelate (DEHA) and tetralin were reagent grade; no attempt was made to purify these diluents further. The molar volumes used in eqs. (2) and (3) for

paraffin, *n*-hexadecane, α-chloronaphthalene, DEHA, and tetralin are respectively 511, 322, 151, 514, and 150 cm.[3]

Polyethylene films of a uniform thickness of 1 to 2 mm. were pressed at about 150°C. and samples were cut at room temperature with a mold in the shape of a dumbbell. These samples were of uniform width of 3.1 mm. over a length of 25 mm. In order to crosslink them, they were irradiated at room temperature in evacuated glass containers by γ-radiation from a cylindrical Co^{60} source with a uniform dose rate of 0.61 Mrep/hr., or by the electron beam of a Van de Graaff accelerator. The samples marked *A* received a dose of approximately 40 Mrep of electron radiation. Those marked *B* and *C* received doses of 29.6 and 39.3 Mrep of γ-radiation. The dumbbell shape permitted the samples to be clamped in and stretched without breakage at the clamps. The clamps consisted of a pair of small metal plates, held together by screws. The lower clamp was fixed, while the upper clamp was suspended from a strain gage which could be adjusted vertically. The strain gage (Statham Instrument Co., transducer model G-1) had a capacity of 750 g. and a linear response of 0.05 mv./g. under a supplied e.m.f. of 12 v. The output of the strain gage was displayed on a Leeds & Northrup recorder, giving a full-scale deflection of 10 mv. The instrument was calibrated by addition of known weights before and after each experiment.

The length of the sample was measured with a cathetometer. Two thin metal pins, perforating the uniform section 20 mm. apart, served as markers. A stream of high purity nitrogen was passed through the sample chamber in order to prevent oxidative degradation. Samples were swollen in the sample chamber by diluent containing 0.5% of phenyl β-naphthylamine, used as an antioxidant. After the stress-strain experiment was completed the polyethylene sample was extracted with boiling xylene and evaporated to dryness at 150°C. in vacuum. The stress-strain curve for the dry sample was then usually identical, within experimental error, to that before swelling; otherwise the experiment was discarded. Stress-strain curves were obtained by stretching the sample at intervals to an extension ratio of about 1.3 and decreasing the length in similar intervals until the relaxed, isotropic state was reached. At each interval the length was kept constant for 20 min. before the force was read.

A liquid thermostat (containing silicone oil DC-550, Dow Corning Corp.) maintained a constant temperature of 150 ± 0.1°C.

Results and Discussion

Figure 1 illustrates some typical results obtained. It is seen that hysteresis is reduced on increasing the degree of swelling. This appears to be true for all cases investigated and is consistent with a closer approach to equilibrium in the swollen state.[9] The results for all diluents used are given in Table I. The volume fraction of polymer, given in the fourth column, is largest for DEHA, which is a poor solvent and smallest for tetralin, an excellent solvent. The ratio R between calculated and observed

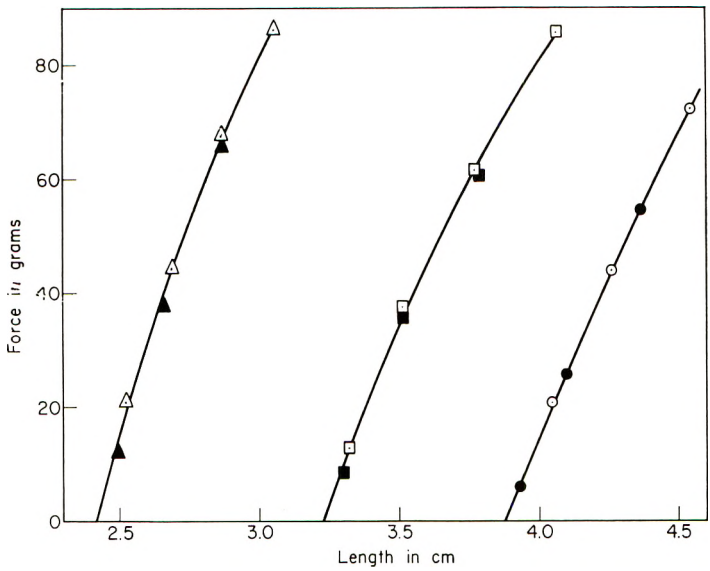

Fig. 1. Stress-strain curves for polyethylene samples. (△) Dry sample, (□) sample swollen with DEHA, and (○) sample swollen with *n*-hexadecane. Open and closed symbols denote force readings after increasing and decreasing the length, respectively.

force for the diluted state is given in the fifth column. As is observed, R deviates considerably from unity. Moreover, it is apparently strongly dependent on mode and degree of crosslinking. As noted in the introduction, failure to attain equilibrium for the dry samples is probably mainly responsible for these deviations. In general the R values should then be too high. This is observed for samples B and C, which are crosslinked by γ-irradiation. The low values for samples A, crosslinked by electron irradia-

TABLE I
Force Readings for Samples Diluted with Different Diluents

Sample	L/L_i'	Diluent	v_2	$R = f_{calc.}/f_{obs.}$	$P = \langle r_0^2\rangle_{diluent}/\langle r_0^2\rangle_{hexadecane}$
A	1.35	DEHA	0.386	0.97	1.13
A	1.275	α-Chloronaphthalene	0.218	0.86	1.01
A	1.15	Tetralin	0.194	0.76	0.89
A	1.31	*n*-Hexadecane	0.196	0.84	(1.00)
A	1.35	*n*-Hexadecane	0.221	0.87	(1.00)
B	1.24	DEHA	0.348	1.67	0.97
B	1.20	α-Chloronaphthalene	0.166	1.86	1.08
B	1.18	Paraffin	0.219	1.57	0.91
B	1.19	*n*-Hexadecane	0.176	1.72	(1.00)
C	1.20	DEHA	0.393	1.34	1.12
C	1.20	α-Chloronaphthalene	0.188	1.30	1.08
C	1.225	Paraffin	0.262	1.19	0.99
C	1.17	Tetralin	0.167	1.12	0.93
C	1.165	*n*-Hexadecane	0.228	1.20	(1.00)

0.855

tion, may be a result of the inhomogeneity of the high-energy electron beam. Equation (3), applicable to samples with uniform crosslinking density, could overestimate the increase in swelling on extension and thereby lead to too low values for the calculated force. Whatever the reasons are for the deviations, the P values given in the sixth column, denoting the ratio of the R values for several diluents to that for n-hexadecane, are close to unity. Moreover these values are independent of mode and degree of crosslinking. Since deviations from equilibrium should not be sensitive to the nature of the diluent, the values of P may be expected to equal $<r_0^2>_{\text{diluent}}/<r_0^2>_{\text{hexadecane}}$. The average values of P for the diluents DEHA, α-chloronaphthalene, paraffin, and tetralin are 1.07, 1.06, 0.95, and 0.91, respectively. The conclusion can therefore be drawn that the mean-square end-to-end distance of the polyethylene chain is independent of diluents to within experimental error, which is estimated to be ten per cent. Since diluents used range from poor (DEHA) to good (tetralin), excluded volume effects must be inappreciable, in accordance with expectation.

It is inconceivable that $<r_0^2>$ of polyethylene in bulk is appreciably different from that in n-paraffin and n-hexadecane, since the polyethylene molecule is identical to these molecules, except for chain length. It may therefore be concluded that, within experimental error, $<r_0^2>$ is unchanged on dilution of the dry sample. The absence of specific diluent effects is the more remarkable since detailed calculations[2] indicate chain dimensions to be sensitive to the distribution over trans and gauche states of chain bonds along the chain. Apparently this distribution is determined almost exclusively by intramolecular forces and is unaltered by large environmental changes from an aliphatic solvent (n-hexadecane) to a branched ester (DEHA), or to a polar (α-chloronaphthalene), or nonpolar (tetralin) aromatic compound. Furthermore, if polymer chains would tend to align locally, $<r_0^2>$ would be larger in n-hexadecane and paraffin than in the other diluents used. However, such increases are not observed. This is strong evidence against the often supposed semi-ordering effects in the melt, a conclusion in accordance with results[8] of previous stress-temperature measurements on diluted and undiluted samples. It may then be concluded that for nonpolar polymers the potential energy as function of rotational angle is virtually independent of intermolecular interaction and is determined by intramolecular interaction only. This independence of intermolecular interactions, implicitly assumed in most network theories and in polymer solution theory, constitutes gratifying justification for the basis of these theories.

On the other hand, it is known that the distribution over gauche and trans conformations of 1,2-dichloroethane is markedly changed[10,11] by environmental changes as a result of dipolar interaction. Therefore, larger effects may be expected for polar polymers. Measurements of the stress-strain relation of diluted networks offer an attractive method for investigating such effects.

The authors thank Prof. P. J. Flory for stimulating discussions pertaining to this paper. Financial support by the Wright Air Development Division, Air Research and

Development Command, U. S. Air Force, under Contract No. AF 33(616)-6968, is gratefully acknowledged.

References

1. Flory, P. J., *Principles of Polymer Chemistry*, Cornell Univ. Press, Ithaca, N. Y., 1953, ch. 14.
2. Hoeve, C. A. J., *J. Chem. Phys.*, **35**, 1266 (1961).
3. Flory, P. J., and J. E. Osterheld, *J. Phys. Chem.*, **58**, 653 (1956).
4. Orofino, T., to be published.
5. Flory, P. J., O. K. Spurr, and D. K. Carpenter, *J. Polymer Sci.*, **27**, 231 (1958).
6. Fixman, M., *Ann. N. Y. Acad. Sci.*, **89**, 657 (1961).
7. Flory, P. J., *J. Am. Chem. Soc.*, **78**, 5222 (1956).
8. Ciferri, A., C. A. J. Hoeve, and P. J. Flory, *J. Am. Chem. Soc.*, **83**, 1015 (1961).
9. Gee, G., *Trans. Faraday Soc.*, **42**, 585 (1946); Ciferri, A., and P. J. Flory, *J. Appl. Phys.*, **30**, 1498 (1959).
10. Mizushima, S. I., *Structure of Molecules and Internal Rotation*, Academic Press, New York, 1954, ch. 2.
11. Volkenstein, M. V., and V. I. Brevdo, *Zh. Fiz. Khim.*, **28**, 1313 (1954).

Résumé

On peut déterminer les effets spécifiques de dilution sur la distance moyenne carrée entre les extrémités $\langle r_0^2 \rangle$ dans des solutions diluées, à leur point Θ. Une autre méthode de détermination de ces effets se trouve décrite dans cet article. Celui-ci contient la mesure du module de polymères pontés gonflés par différents solvants et une interprétation des résultats en accord avec la théorie d'élasticité de caoutchoucs courants. Comme résultat des concentrations relativement élevées dans cette méthode, en plus de l'introduction de pontages, on obtient des effets de dilution spécifiques pour la dimension des chaînes, sans interférence des effets du volume exclu. On applique la méthode au polyéthylène dilué avec de l'azélate di-2-éthylhexylique, de l'alpha-chloronaphtalène, de la *n*-paraffine, de la tétraline et du *n*-hexadécane. À moins de dix pourcent près, la valeur de $\langle r_0^2 \rangle$ dans le *n*-hexadécane est égale à celle employée dans les autres diluants. Vu la similitude de la molécule du polyéthylène, celle du *n*-hexadécane et de la *n*-paraffine, cette valeur doit être égale à celle-là pour le polyéthylène pur. Nous pouvons conclure que dans les limites de l'erreur expérimentale, il n'y a pas d'effets semi-ordonnateurs dans la masse fondue et qu'il n'y a pas d'effets spécifiques du solvant.

Zusammenfassung

Spezifische Lösungsmitteleinflüsse auf das ungestörte mittlere End-zu-End-Abstands quadrat $\langle r_0^2 \rangle$ können beim Θ-Punkt in verdünnter Lösung bestimmt werden. Eine weitere Methode zur Bestimmung dieser Einflüsse wird in der vorliegenden Mitteilung beschrieben. Sie beruht auf der Messung des Elastizitätsmoduls vernetzter, in verscheidenen Lössungsmitteln gequollener Polymerer und Auswertung der Ergebnisse nach der bekannten Theorie der Kautschukelastizität. Als Folge der bei dieser Methode verwendeten, verhältnismässig hohen Konzentration im Verein mit der Einführung von Vernetzungsstellen werden spezifische Lösungsmitteleinflüsse auf die Kettendimensionen ohne Störung durch den Einfluss des ausgeschlossenen Volumens erhalten. Die Methode wird auf Polyäthylen, verdünnt mit Di-2-äthylhexylazelat, α-Chlornaphthalin, *n*-Paraffin, Tetralin und *n*-Hexadekan angewendet. Innerhalb von 10% kommt der Wert von $\langle r_0^2 \rangle$ in *n*-Hexadekan dem in den andern untersuchten Lösungsmitteln gleich. In Hinblick auf die Ähnlichkeit des Polyäthylenmoleküls mit dem *n*-Hexadekan- oder *n*-Paraffinmolekül muss dieser Wert dann auch dem für Polyäthylen in Substanz entsprechen. Man kann daraus schliessen, dass, innerhalb der Versuchsfehler, Semiordnungseffekte in der Schmelze fehlen und keine spezifischen Lösungsmitteleinflüsse bestehen.

Received July 10, 1962

JOURNAL OF POLYMER SCIENCE: PART A VOL. 1, PP. 1955-1961 (1963)

The Temperature Dependence of Magnesium Chloride Interaction with Polyacrylic Acid

ADA L. JACOBSON, *Department of Chemistry, University of Alberta, Calgary, Alberta, Canada*

Synopsis

The effect of temperature on a modified pH "titration" of polyacrylic acid is reported. The extent of acid ionization was varied by pretitration to various degrees with the strong base of a weak counterion binder, tetra-*n*-propyl ammonium hydroxide. The effect of subsequent additions of magnesium chloride to these pretitrated solutions at 15, 25, and 38°C. is reported. The release of hydrogen ions caused by this neutral salt addition varied with both degree of pretitration and temperature. The displacement caused by temperature on the maxima and minima behavior of hydrogen ions released as a function of degree of preionization can be explained by the effects of temperature on polymer configuration. The increased release of hydrogen ions at higher temperature can be explained by the combined effects of temperature on the polymer configuration and on the binding equilibria. The acid dissociation constants at 15, 25, and 38°C. have been obtained by titration with tetra-*n*-propyl ammonium hydroxide.

Introduction

As a result of a modified pH "titration" experiment, a model was presented in a previous paper[1] to account for the differences observed in this type of titration between polyacids and simpler monomeric acids. The essence of this model was the assumption that the accessibility of carboxyl groups (which depend on the polyacid configuration) would determine the cation binding. On the basis of this model an explanation was made for the maxima and minima which were observed only for the polyacid in a plot of the concentration of carboxyls ionized by the addition of the neutral salt of a strong binding agent as a function of degree of preionization. In this paper, the effect of temperature on the previously observed maxima and minima is reported. The effects produced by temperature variation are explicable on the basis of the model offered previously plus a consideration of the temperature effects on the equilibrium and binding constants.

Experimental

Equipment

A Leeds & Northrup pH meter was used for most of the 25 and 38°C. experiments. The 15°C. experiments and selected 25 and 38°C. check ex-

periments were made with a radiometer titrator with scale expander. Temperature control was ± 0.01 °C.

Technique

The experimental technique was similar to that previously reported[1] with the exception that in the radiometer titration experiments the radiometer syringe buret unit was used instead of a micropipette. The polyacrylic acid (PAA concentration 10^{-4} equivalents carboxyl/liter) was pretitrated to various extents with the strong base of the weak counterion binder, tetra-*n* propyl ammonium hydroxide (TNPAOH). The pH decrease caused by addition of aliquots of the strong counterion binder, magnesium chloride (10^{-5}–10^{-3} m./liter) was measured. Corrections for hydrolysis of magnesium chloride were applied in the high pH range.

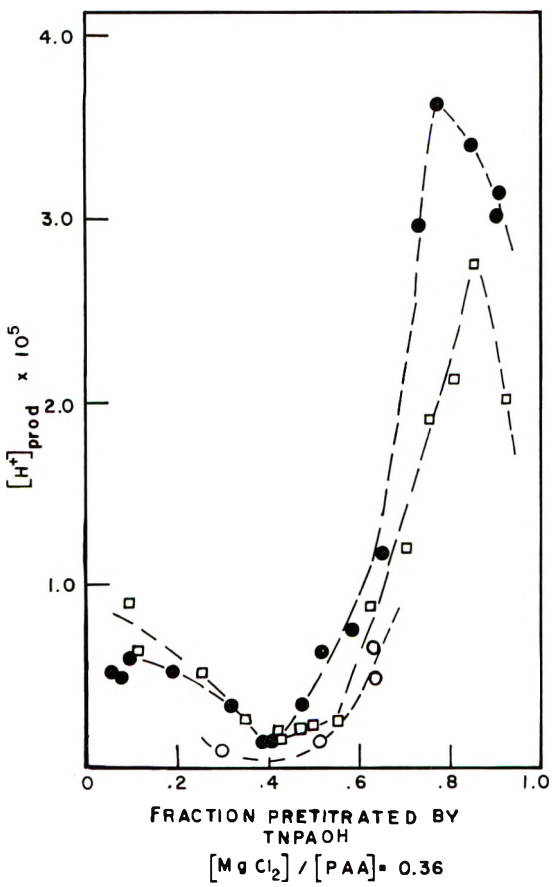

Fig. 1. Dependence of concentration of carboxyls ionized by $MgCl_2$ addition, $[H^+]_{prod.}$, on degree of preionization of the PAA at low concentration of added salt. (●) 38°C., (□) 25°C., (○) 15°C.

Results

The pH decrease observed on addition of $MgCl_2$ aliquots previously reported to be dependent on the degree of pretitration of the PAA[1] also varied with temperature. From this pH change, the total increase in concentration of hydrogen ions in solution, $[H^+]_{prod.}$ (including both hydrogen and hydroxyl ion concentration changes), was calculated. This value is

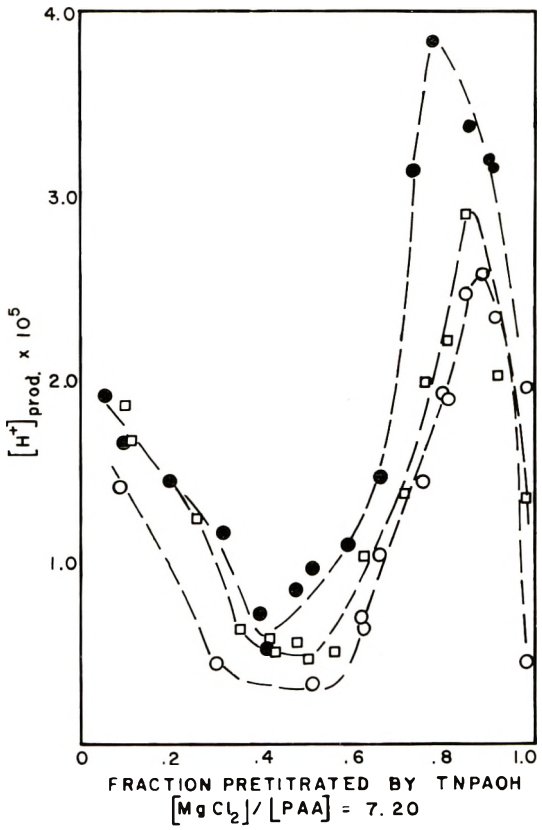

Fig. 2. Dependence of concentration of carboxyls ionized by $MgCl_2$ addition, $[H^+]_{prod.}$, on degree of preionization of the PAA with an excess of added salt. (●) 38°C., (□) 25°C., (○) 15°C.

equivalent to the concentration of carboxyl groups ionized by addition of the magnesium chloride aliquot. It is not equivalent to the total amount bound, however, as the binding to preionized carboxyl groups is not included. In Figure 1 the concentrations of carboxyl groups ionized by a relatively small concentration of magnesium chloride ($[MgCl_2]/[PAA] = 0.36$) at 15, 25, and 38°C. are plotted as a function of the degree of pretitration by the weak counterion binder TNPAOH. At all these temperatures both a maximum and minimum are observed. The shape of this type of curve is independent of the ratio of magnesium chloride to polyacid. In

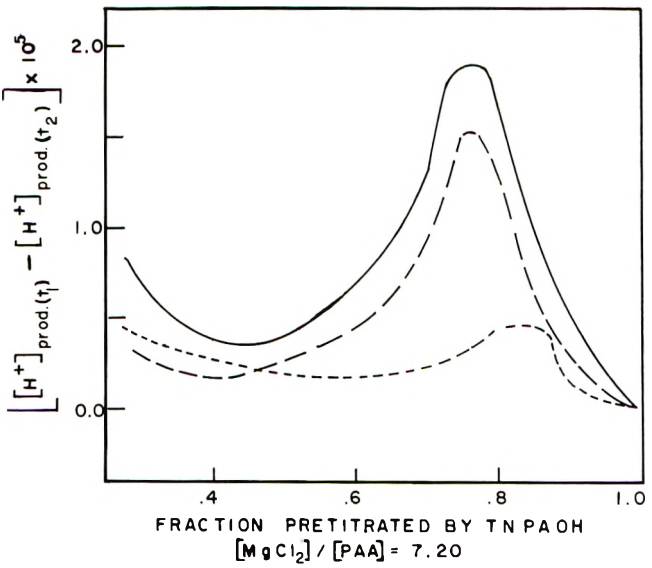

Fig. 3. Difference in concentration of carboxyls ionized by $MgCl_2$ addition with temperature with all other conditions constant as a function of degree of preionization of the PAA. (——) $t_2 = 38°C.$, $t_1 = 15°C.$; (– –) $t_2 = 38°C.$, $t_1 = 25°C.$; (- - - - -) $t_2 = 25°C.$, $t_1 = 15°C.$

Figure 2, the effect of the presence of an excess of magnesium chloride over polyacid ($[MgCl_2]/[PAA] = 7.2$) is shown. At higher magnesium chloride concentrations more carboxyl groups are ionized, but even with a very large excess of magnesium chloride the maximum and minimum still occur. The greatest temperature effect noted with a fixed magnesium chloride concentration is near the maximum for both the relatively small concentration of $MgCl_2$ (Fig. 1) and the large excess (Fig. 2). To illustrate this temperature effect in Figure 3 the differences in $[H^+]_{prod.}$ at two temperatures with all other conditions constant ($[MgCl_2]/[PAA] = 7.2$) are plotted as a function of degree of preionization by strong base.

Discussion

If the configurational change model is assumed, the changes caused by temperature variation can be predicted. Higher temperature should favor the transition from the spherical ball configuration of unionized PAA to the fully extended completely ionized configuration[2] at a lower degree of pretitration. As shown in Figures 1 and 2, at the higher temperature the displacement of the maxima and minima are to lower degrees of preionization. Initially at the low degrees of preionization where the configuration is not radically altered by addition of the strong base (since the "available" carboxyl groups are titrated by the initial additions of the strong base), the concentration of unionized available carboxyls decreases with increasing strong base titration. The small temperature effects produced near the

minima can be interpreted as indicating that the concentrations of available carboxyl groups are nearly equivalent at this point. This is consistent with the model that the outer sphere is in all cases nearly fully ionized at this degree of neutralization.

The very much larger temperature effect noted past the minima in Figures 1 and 2 indicates that the polyacid configuration only becomes temperature sensitive after it has started to unwind (by pretitration). At higher temperatures the unrolling to expose "buried" carboxyl groups which then become available is facilitated, and the winding chain form is easier to attain at the higher temperatures.

At the very high degrees of titration (>0.95), where essentially all the carboxyls are preionized and all remaining are available, the effect of temperature is less marked because of the very small concentration available. All curves must decrease to zero at full pretitration.

Though the configurational effects model can be used to explain the occurrence and displacement of these maxima and minima with fraction pretitrated, the marked increase in concentration of carboxyls ionized by magnesium chloride addition near the maximum at equivalent fractions pretitrated at the higher temperatures (Fig. 3) cannot be explained solely on this basis. This concentration increase can be understood with a consideration of the effects of increased temperature on the acid dissociation and binding constants. Prediction of the variation of these constants with temperature is difficult since even the values for the simplest acids such as formic and acetic pass through a maximum as a function of temperature.[3] To simplify the discussion only the average equilibrium constants

$$\text{—COOH} \overset{K_a}{\rightleftharpoons} \text{—COO}^- + \text{H}^+ \tag{1}$$

$$\text{M}^{2+} + \text{—COO}^- \overset{K_1}{\rightleftharpoons} \text{—COOM}^+ \tag{2}$$

$$\text{M}^{2+} + \text{—COOH} \overset{K_2}{\rightleftharpoons} \text{—COOM}^+ + \text{H}^+ \tag{3}$$

will be considered.

The acid dissociation constant, K_a, can be isolated from the pretitration data with TNPAOH. Since this titration is made with the strong base of a weak counterion binder, binding effects are minimal. The pK_a decreases from 8.18 to 8.10 to 8.06 for temperature changes 15 to 25 to 38°C. These values are in reasonable agreement with those obtained by Gregor[4] considering the concentration differences involved. However, variation in this equilibrium constant alone is not adequate to describe the temperature effect on hydrogen ion concentration since the $MgCl_2$ was added to solutions which were already pretitrated to the same degree at the three temperatures. A slight activity coefficient effect might occur on addition of $MgCl_2$, but at a concentration of added salt of 10^{-4} molar this should be inadequate to produce the large concentration changes of hydrogen ion observed. Consequently, the temperature effect on the binding equilibria (2) and (3) must also be considered to explain the increased ionization of carboxyls with $MgCl_2$ addition.

The equilibrium constant for binding of magnesium ions to ionized carboxyl groups (2) cannot be directly isolated from this experimental data. However, since dissociation is favored at higher temperature in equilibria (1), by analogy pK_1 would be expected to increase with temperature.

The equilibrium constant K_2 can be considered as determined by the competitive binding of hydrogen ions and magnesium ions. The change in K_2 with temperature will depend on the change in the stability of $-COOH$ compared to $-COOM^+$ with temperature. Binding of the divalent cation might be expected to be favored at higher temperature. Hence pK_2 would decrease at higher temperature. The concentration of hydrogen ion in solution after $MgCl_2$ addition can be expressed as

$$[H^+] = \frac{K_2\text{—(COOH)}}{K_1\text{—(COO}^-\text{)}}$$

Since K_2 is expected to increase and K_1 to decrease, at equivalent fractions pretitrated the concentration of hydrogen ions in solution will increase at higher temperatures.

With the configurational model the concentration of carboxyls expressed in these equilibria would be the "accessible" rather than the total concentration. At and near the maximum more carboxyls are accessible and thus involved in binding. Consequently, as illustrated in Figure 3, the effects produced by temperature variation in the equilibria are most pronounced at this point.

Support by Research Grant A-5271 from the U. S. Public Health Service is gratefully acknowledged. The work of Mrs. J. Maxwell in measuring some of these pH changes is greatly appreciated.

References

1. Jacobson, A. L., *J. Polymer Sci.*, **57**, 321 (1962).
2. Guinard, S., F. Boyer-Kawenoki, A. Dobry, and J. Tonnelat, *Compt. rend.*, **229**, 143 (1949).
3. *Handbook of Chemistry and Physics*, Chemical Rubber Publishing Co., Cleveland, 1961, p. 1758.
4. Gregor, H. P., and M. Frederick, *J. Polymer Sci.*, **23**, 451 (1957).

Résumé

On rapporte l'effet de la température sur une titration modifiée du pH dans le cas de l'acide polyacrylique. On fait varier le degré d'ionisation de l'acide par prétitration à divers degrés au moyen d'une base forte correspondant à un contre-ion liant faible, l'hydroxyde de tétra-*n*-propyl ammonium. On rapporte l'effet d'addition subséquentes de chlorure de magnésium à ces solutions prétitrées à 15, 25 et 38°C. Le départ d'ions hydrogènes causées par cette addition de sel neutre varie avec le degré de prétitration et avec la température. Le déplacement causé par la température, du comportement maximum et minimum des ions hydrogènes déchargés en fonction du degré de préionisation peut être expliqué par les effets de la température sur la configuration du polymère. L'augmentation de l'ionisation des ions hydrogènes à plus haute température peut être expliquée par les effets combinés de la température et sur la configuration du polymère et sur léquilibre de liaison. On a obtenu les valeurs de la con-

stante de dissociation de l'acide à 15, 25 et 38°C par titration au moyen d'hydroxyde de tétra-*n*-propyl ammonium.

Zusammenfassung

Der Temperatureinfluss auf eine modifizierte pH-"Titration" von Polyacrylsäure wird mitgeteilt. Das Ausmass der Ionisierung der Säure wurde durch verschieden starke Vortitration mit der starken Base eines schwachen Gegenionenbinder, Tetra-*n*-propylammoniumhydroxyd, variiert. Über den Einfluss eines Zusatzes von Magnesiumchlorid zu diesen vortitrierten Lösungen bei 15, 25, und 38°C wird berichtet. Die durch den Neutralsalzzusatz bewirkte Freisetzung von Wasserstoffionen hing von der Vortitration und von der Temperatur ab. Die temperaturbedingte Verschiebung der Maxima und Minima in Verhalten der freigesetzten Wasserstoffionen als Funktion des Vortitrationsgrades kann durch den Einfluss der Temperatur auf die Polymerkonfiguration erklärt werden. Die verstärkte Freisetzung von Wasserstoffionen bei höherer Temperatur kann durch den kombinierten Einfluss der Temperatur auf die Polymerkonfiguration und die Bindungsgleichgewichte erklärt werden. Die Säuredissoziationskonstanten wurden bei 15, 25, und 38°C durch Titration mit Tetra-*n*-propylammoniumhydroxyd erhalten.

Received May 18, 1962

JOURNAL OF POLYMER SCIENCE: PART A VOL. 1, PP. 1963–1970 (1963)

Bulk Copolymerization of Methyl Methacrylate with Phenyldichlorophosphine

ATANAZY BORYNIEC and BOGUMIŁ ŁASZKIEWICZ, *Department of Technology of Artificial Fibers, The Technical University of Łódź, Poland*

Synopsis

Copolymers of methyl methacrylate with phenyldichlorophosphine were isolated as compact, incombustible, and colorless thermoplastic resins. The copolymerization was carried out at 60°C. by the standard bulk method, azobisisobutyronitrile being used as catalyst. The experiments indicate that in the investigated reaction there are concurrent processes which lead to degradation. The effect of duration of the copolymerization process and the content of phenyldichlorophosphine in the methyl methacrylate copolymer on the extent of reaction and on the intrinsic viscosity of copolymer has been investigated.

Introduction

Among the great number of papers published in the chemical literature dealing with organophosphorus polymers there are only a few which are connected with copolymerization of vinyl monomers with organophosphorus compounds. First of all work of McCormack[1,2] on the copolymerization of alkyl- and aryldihalophosphines with some olefins and dienes should be considered. His investigations were carried out on the copolymerization of isoprene, methyl methacrylate, styrene, and acrylonitrile with phenyldichlorophosphine in cyclohexane and chloroform solution with 2,2′-azobisisobutyronitrile (AIBN) or benzoyl peroxide as initiator. With reference to McCormack's studies, Gefter[3] proposed the following scheme for reactions involved during the copolymerization of vinyl monomers with alkyl and aryldihalophosphines:

$$n\ \mathrm{CH_2{=}CH}(\mathrm{R}) + n\ \mathrm{PCl_2}(\mathrm{R}) \rightarrow \left(\mathrm{CH}(\mathrm{R})\text{–}\mathrm{CH_2}\text{–}\mathrm{P}(\mathrm{Cl_2})(\mathrm{R}) \right)_n$$

Stiles, Rust, and Vaughan[4] showed that phosphines add to olefins under conditions of free radical initiation according to the following scheme:

Initiation

$$\mathrm{R_2PH} + \mathrm{R}\cdot \rightarrow \mathrm{R_2P}\cdot + \mathrm{RH}$$

Addition:

$$\mathrm{R_2P}\cdot + \mathrm{RCH{=}CH_2} \rightarrow \mathrm{R_2PCH_2CHR}$$

Displacement:

$$R_2PCH_2CHR + R_2PH \rightarrow R_2PCH_2CH_2R + R_2P\cdot$$

A few years later Pellon[5] made chain transfer studies on reactions of copolymerization of olefins with phosphines. He accepted the following reaction scheme as a basis for interpretation of his results:

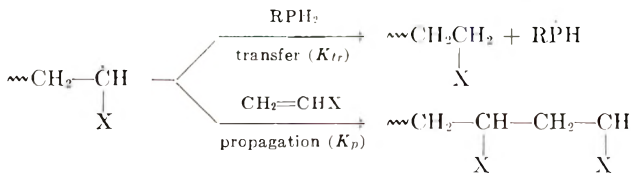

where K_{tr} and K_p are the velocity constants of chain transfer and propagation, respectively.

TABLE I

Effect of Reaction Time and the Content of Phenyldichlorophosphine (M′) in Methyl Methacrylate (M) Copolymer on the Extent of Reaction at 60°C.

Mole ratio of monomers (M/M′)	Time t, min.	Extent of reaction, %
1:0.000	10	3.1
	20	10.3
	30	18.3
	45	23.6
	60	51.2
	75	56.0
	105	97.3
	205	98.7
	360	99.1
	1200	99.4
1:0.025	10	5.5
	20	8.1
	30	10.3
	45	19.5
	60	33.9
	75	37.4
	105	63.7
	205	73.8
	360	76.2
	1200	76.4
1:0.050	10	4.0
	20	7.4
	30	10.4
	45	12.2
	60	14.4
	75	18.7
	105	43.2
	205	70.3
	360	71.5
	1200	73.9

The object of our investigations was to prepare copolymers of methyl methacrylate with phenyldichlorophosphine by bulk copolymerization using azobisisobutyronitrile as initiator.

The investigations were expected to supply some data regarding the copolymerization reaction of this system of monomers. The bulk copolymerization method was chosen especially to eliminate the influence of solvent on the reaction run.

Discussion of Experiments

All used reagents were purified carefully before each experiment. Methyl methacrylate and phenyldichlorophosphine were purified by vacuum distillation. The methyl methacrylate monomer was distilled in an apparatus

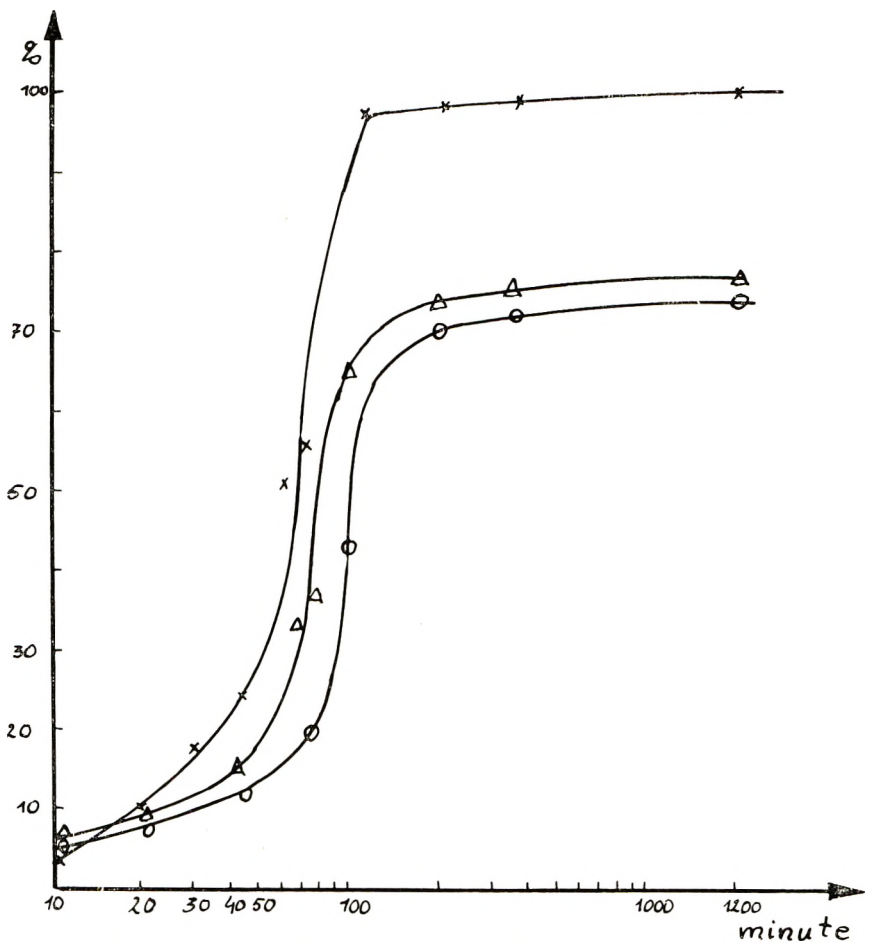

Fig. 1. The influence of the reaction duration and of the content of phenyldichlorophosphine (M′) in methyl methacrylate (M) copolymer on the extent of reaction at 60°C. at various mole ratio of monomers (M/M′): (×) 1:0.000; (△) 1:0.025; (○) 1:0.050.

equipped with a column filled up to 1 m. with copper rings. Azobisisobutyronitrile was purified by recrystallization from ethanol.

The copolymerization processes were carried out in the following manner. A mixture of monomers of known mole ratio was prepared in a conical flask and then 1% of initiator (relative to the weight of monomers) was added.

Glass ampules (10 cm. in length and 0.7 cm. in diameter) were filled with this mixture and sealed off. The ampules were deaerated by nitrogen free from oxygen. From the sample of copolymer an aliquot of about 0.3 g. was weighed out and put into a conical flask where it was dissolved in 20 ml. of acetone. After the dissolution, the copolymer was precipitated out with benzene. The precipitate was isolated and dried until constant weight had been achieved. The extent of reaction, expressed in per cent, was calculated from the difference of weights of the aliquot dissolved in acetone and the precipitate.

The experiments were carried out for methyl methacrylate homopolymer and also for copolymers of methyl methacrylate with phenyldichlorophosphine mixed at mole ratios 1:0.05 and 1:0.025.

TABLE II
Effect of the Content of Phenyldichlorophosphine (M′) in Copolymer and the Copolymerization Time on the Intrinsic Viscosity

Mole ratio of monomers (M/M′)	Time t, hr.	Intrinsic viscosity $([\eta])_{c\to 0}$
1:0.005	2	4.26
	5	3.12
	16	3.06
	26	3.02
	48	2.95
	96	2.94
1:0.010	2	4.18
	5	3.18
	16	2.97
	26	2.90
	48	2.88
	96	2.83
1:0.015	2	4.13
	5	2.94
	16	2.89
	26	2.63
	48	2.59
	96	2.23
1:0.025	2	3.59
	5	2.84
	16	2.69
	26	2.58
	48	2.49
	96	2.34

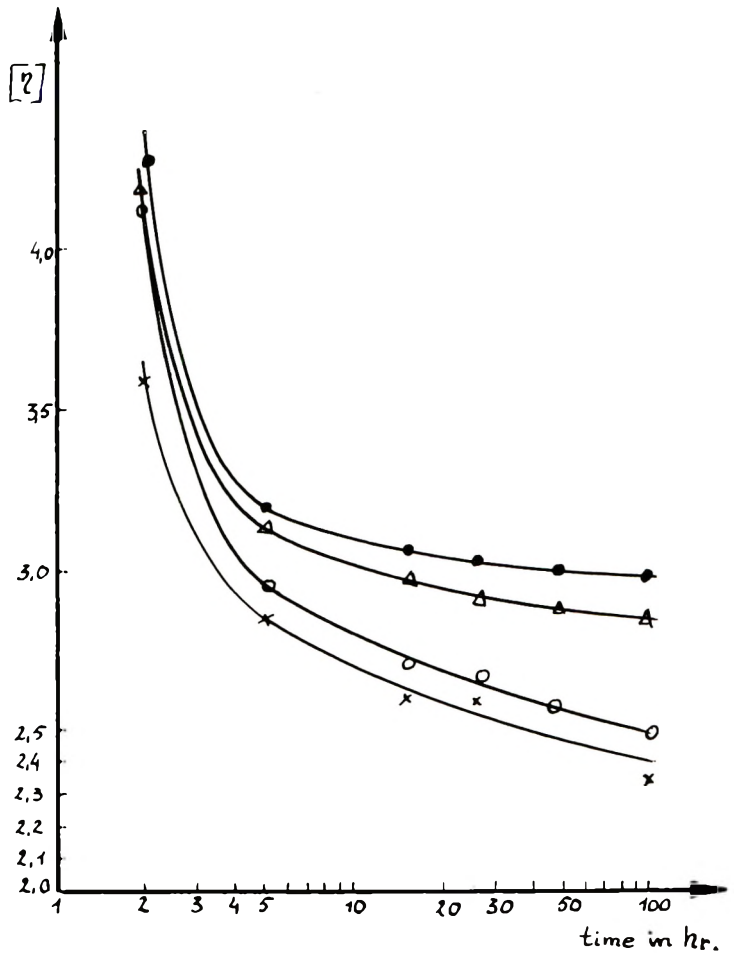

Fig. 2. The influence of the content of phenyldichlorophosphine (M′) in copolymer and of duration of the copolymerization process on the intrinsic viscosity at various mole ratios of monomers (M′/M): (●) 1:0.005; (△) 1:0.010; (○) 1:0.015; (×) 1:0.025.

The experimental results of this study are summarized in Table I and plotted in Figure 1.

On studying the extent of reaction of methyl methacrylate and phenyldichlorophosphine monomers some differences in solubility of various samples of copolymer were observed; it has been confirmed that this solubility depends on the duration of copolymerization process and on the mole ratio of monomers. Samples of copolymers which had been polymerized for periods longer than 5 hr. dissolved very slowly and without swelling in acetone or chloroform. Solutions of these samples had low viscosities. In connection with these observations it was decided to investigate the relation between intrinsic viscosity of the copolymers, the duration of the copolymerization, and the content of phenyldichlorophosphine in the copolymers.

The experimental results of these investigations are summarized in Table II and plotted in Figure 2.

Intrinsic viscosities $[\eta]$ were calculated from the relationship given by Thomas and Thomas:[6]

$$\eta = \eta_0 e^{c[\eta]}$$

where η and η_0 is the viscosity of solution and solvent, respectively, and c is concentration of solution given in grams/100 ml.

Applicability of this equation was confirmed for solutions at concentration limits from 0.13 g./100 ml. to 4 g./100 ml. by comparison with values calculated from extrapolation data. Viscosities were determined at 20 ± 0.5°C. in chloroform at a concentration of 0.5 g./100 ml.

The values in Tables I and II indicate that an increase of phenyldichlorophosphine content in the monomer mixture is connected with a decrease in the extent of reaction and the intrinsic viscosities of copolymers. Taking this into account it has been decided to investigate the possibility of obtaining copolymers of high content of phenyldichlorophosphine. Such copolymers were indeed obtained; all details connnected are presented in Table III. The copolymerization reaction was carried out in the same manner as previously, i.e., duration 2 hr. at 60°C.

TABLE III

Relation between Thermal Properties and Intrinsic Viscosity and the Content of Phosphorus in Copolymers of Methyl Methacrylate (M) with Phenyldichlorophosphine (M′)

M′ in monomer mixture, %	Phosphorus in copolymer, %	Melting of polymer, °C.	Softening temp. of polymer, °C.	Decomposition temp. of polymer, °C.	Intrinsic viscosity $[\eta]_{c\to 0}$
0.0	0.0	215–227	280–295	308	4.26
14.5	2.5	214–223	273–285	294	1.20
22.2	3.9	216–220	260–263	280	0.94
50.8	8.8	203–208	240–245	278	0.45
61.4	10.8	168–175	184–218	248	0.36

Properties of Copolymers

The copolymers of methyl methacrylate with phenyldichlorophosphine isolated were in the form of hard, colorless resins having some thermoplastic character.

It was also confirmed that combustibility of these copolymers decreases with increasing phosphorus content. For phosphorus contents higher than 1%, combustion of the copolymer held into a flame ceases as soon as it is taken away. Behavior of the copolymers at higher elevated temperatures is presented in Table III.

The copolymers dissolve in acetone and chloroform. It is possible to obtain transparent films from their solutions by the evaporation of solvent. The films have a great ability to accumulate electric charges.

Discussion of Results

Our previous studies[7] as well as the results presented in this paper support Gefter's scheme[3] for the copolymerization of olefins with phosphines. The reaction of vinyl monomers with phosphines is very similar to that one studied by Barb[8,9] on styrene and sulfur dioxide.

Bamford et al.[10] proposed the term "heteropolymerization" or "semi-vinyl copolymerization" for the reaction of vinyl monomers with sulfur dioxide, carbon monoxide, or oxygen. He proposed also the term "pseudo-monomer" for such nonolefin monomers as carbon oxide, oxygen, or sulfur dioxide. It seems that the term, semi-vinyl copolymerization, is more reasonable due to the fact that one of the reagents of monomer mixture used to the copolymerization process is usually a vinyl radical. By analogy the term semi-vinyl copolymerization ought to be used also for the polymerization of methyl methacrylate and other vinyl monomers with phosphines.

The results summarized in Table I indicate that the copolymerization of methyl methacrylate with phenyldichlorophosphine has a retarded period of initiation in comparison with that for the homopolymerization of methyl methacrylate alone. It is seen in Figure 1 that equilibrium of the investigated reaction is reached after about 2 hr., and the extent of reaction of methyl methacrylate and phenyldichlorophosphine monomers is lower than that achieved in homopolymerization of methyl methacrylate.

From the results presented in Table II it seems possible to deduce that some other processes occur together with the copolymerization of methyl methacrylate with phenyldichlorophosphine and they aim to produce degradation of the copolymer formed.

For the simplest copolymer, i.e., for copolymer having equal quantities of M and M′-mers set in alternate order, the following scheme of these processes may be given:

Initiation:

$$(MM')_n \begin{cases} \rightarrow \cdot(PM')_{n-1} + \cdot(P'M)_i \\ \rightarrow \cdot(P'M)_{n-i} + \cdot(PM')_i \end{cases}$$

Degradation:

$$\cdot(PM')_i \rightarrow \cdot P_{i-1}M'_i + M$$
$$\cdot(P'M)_i \rightarrow \cdot P'_{i-1}M_i + M$$

Transfer:

$$\cdot(PM)_i + (MM')_n \rightarrow \cdot(PM')_j + (MM')_i + (MM')_{n-j}$$
$$\cdot(P'M)_i + (MM')_n \rightarrow \cdot(P'M)_j + (M'M)_i + (MM')_{n-j}$$

Termination:

$$\left.\begin{matrix}\cdot(\mathrm{PM'})_i + \cdot(\mathrm{P'M})_j \\ \cdot(\mathrm{P'M})_i + \cdot(\mathrm{PM'})_j\end{matrix}\right\rbrace \rightarrow (\mathrm{MM'})_i + (\mathrm{MM'})_j$$

where M and M′ denote methyl methacrylate and phenyldichlorophosphine, respectively; i, j, and n indicate the degree of polymerization of copolymer or macroradicals, and ·P and ·P′ represent the active macroradical endgroup formed from the M- or M′-mer.

It is evident that for various quantities of M and M′-mers in copolymers in which they are not set in alternate order, the scheme would be more complicated, and the figures indicating degree of polymerization would be different for each mer.

References

1. McCormack, W. B., U. S. Pat. 2,671,077 (1954).
2. McCormack, W. B., U. S. Pat. 2,671,078 (1954).
3. Gefter, E. L., *Fosforørganicheskie Monomery i Polimery, Izdatelstwo Akademil Nauk SSSR*, Moscow, 1960, p. 207.
4. Stiles, A. R., F. F. Rust, and W. E. Vaughan, *J. Am. Chem. Soc.*, **74,** 3282 (1953).
5. Pellon, J., *J. Polymer Sci.*, **43,** 537 (1960).
6. Thomas, D. K., and T. A. J. Thomas, *J. Appl. Polymer Sci.*, **3,** 129 (1960).
7. Boryniec, A., and B. Łaszkiewicz, *Rocz. Chem.*, **36,** 365 (1962).
8. Barb, W. G., *Proc. Roy. Soc. (London)*, **A212,** 66, 177 (1952).
9. Barb, W. G., *J. Polymer Sci.*, **10,** 49 (1953).
10. Bamford, C. H., W. G. Barb, A. D. Jenkins, and P. F. Onyon, *The Kinetics of Vinyl Polymerization by Radical Mechanisms*, Butterworths London, 1958, p. 194.

Résumé

On a obtenu des copolymères de méthacrylate de méthyle avec la phényldichlorphosphine. Ils sont inflammables et sans couleur. La réaction de copolymérisation a été effectué par la methode en bloc avec le dinitrile de l'acide azoisobutyrique comme catalysateur, á une température de 60°C. Les expériences effectuées prouvent que dans la réaction examinée une degradation a lieu. On a déterminé l'influence de la durée de la réaction et de la teneur en phenyldichlorophosphine dans le copolymère sur le degré de transformation des monomères et la viscosité intrinsèque du copolymère.

Zusammenfassung

Es wurden Copolymere aus Methylmethacrylat und Phenyldichlorphosphin in Form unbrennbarer und farbloser thermoplastischer Harze dargestellt. Die Copolymerisation wurde in Substanz mit Azobisisobutyronitril als Starter bei 60°C. durchgeführt. Bei dieser Reaktion treten auch zum Abbau führende Prozesse auf. Der Einfluss der Reaktionsdauer und des Gehaltes an Phenyldichlorphosphin im Copolymeren mit Methylmethacrylat auf den Umsatz und die Viskositätszahl des Copolymeren wurde untersucht.

Received May 8, 1962

JOURNAL OF POLYMER SCIENCE: PART A VOL. 1, PP. 1971–1978 (1963)

Electron Exchange Polymers. XIX. Copolymerization Behavior of Vinylhydroquinone Dibenzoate

HIROYOSHI KAMOGAWA and HAROLD G. CASSIDY, *Department of Chemistry, Yale University, New Haven, Connecticut*

Synopsis

The copolymerization behavior of vinylhydroquinone dibenzoate monomer (VHDB), in solution under free radical initiator conditions, with styrene, α-methylstyrene, 4-vinylpyridine, methyl methacrylate, and methyl acrylate, to less than 10% conversion, showed good copolymerizabilities with these conventional monomers. Rates of polymerization are greater in VHDB-rich monomer compositions in spite of the bulky character of the benzoyl group. *Q-e* values (Alfrey and Price) are given. The resonance term (Q_1) for VHDB is near unity, which seems to indicate that the resonance effect in stabilizing the radical is almost as large as that of styrene The polarity term, e_1, is assigned a positive value for VHDB. Ultraviolet absorption spectra of the copolymers imply neighboring group interactions in the copolymer chains—interactions implied by the observed *Q-e* values, and implied in earlier work by electrometric titration behavior.

Vinylhydroquinone dibenzoate (VHDB) is the most convenient monomer for the synthesis of hydroquinone-type electron exchange polymers (redox polymers).[1] It polymerizes readily with free-radical initiators to yield polymers which, upon debenzoylation, show characteristic electron exchange behavior.[2,3]

The purpose of this study was to investigate the reactivity of VHDB monomer in its copolymerization behavior with free-radical initiators and to obtain information about the chemical structures of the various kinds of copolymers which may affect the electron exchange behavior of the hydrolyzed polymers.

EXPERIMENTAL

a. Materials

The preparation of vinylhydroquinone dibenzoate (VHDB) has been described elsewhere.[2] This monomer was recrystallized from 95% ethanol before use. All other (commercially obtained) monomers were purified by distillation from stabilizers just before use.

b. Copolymerization Procedures

VHDB, comonomer, and azobisisobutyronitrile as initiator in a proper solvent were put into a sealed tube. Solvents used were toluene for the

VHDB–styrene and VHDB–α-methylstyrene systems; chloroform for the VHDB–4-vinylpyridine system; and benzene for the VHDB–methyl methacrylate and VHDB–methyl acrylate systems. The tube was cooled with Dry Ice, evacuated, filled with nitrogen, and warmed to room temperature. This operation was repeated twice, after which the tube was flushed with purified nitrogen gas and then sealed.

Polymerizations were carried out in a constant temperature bath kept at 78°C. with boiling ethanol vapor. After 30 min., the tube was removed from the bath, cooled, and opened. Initial copolymer solutions thus produced (less than 10% conversion) were diluted with solvent and precipitated into hexane. The precipitated polymers were freeze-dried from benzene, except for the VHDB–4-vinylpyridine system. In the case of that system, benzene, glacial acetic acid, or *tert*-butyl alcohol was used as the freeze-drying solvent, depending upon the vinyl pyridine ratio in the copolymer.

c. Copolymer Compositions

Except for the VHDB–4-vinylpyridine system, all copolymer compositions were determined by acid hydrolysis of benzoate groups followed by redox titration with ceric sulfate,[3] with or without the addition of glacial acetic acid. A typical titration example is as follows.

About 0.05–0.1 g. of sample was weighed out, dissolved in 3 ml. of concentrated H_2SO_4, and allowed to stand for about 40 min. This solution was diluted to 220 ml. with distilled water to give ca. 0.5N H_2SO_4 solution. It was then titrated with 0.1N ceric sulfate with a Leeds and Northrup student potentiometer attached to a Speedomax recorder and employing a platinum wire and a calomel electrode. The stoichiometry of this method was checked by titrations of the VHDB homopolymer.

In the case of the VHDB–4-vinylpyridine system, this method was given up, since the acid-hydrolyzed and sulfonated polymers were neither soluble in water nor in glacial acetic acid. The method used was the potentiometric titration of the pyridine groups with perchloric acid.[4] Titrations were

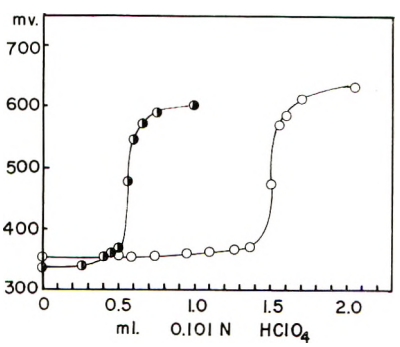

Fig. 1. Typical titration curves in the potentiometric titration of VHDB–4-VP copolymer: (○) mole fraction of VHDB in polymer 0.287; (◑) mole fraction of VHDB in polymer 0.647.

carried out with a Photovolt Model 110 pH meter. A combination of a glass electrode and a calomel electrode was used. Samples of copolymers were dissolved in about 50 ml. of glacial acetic acid and titrated with 0.1*N* $HClO_4$ in glacial acetic acid. The 0.1*N* $HClO_4$ was prepared by dissolving 10 ml. of 60% $HClO_4$ in 1 l. of glacial acetic acid. About 15 g. of acetic anhydride was added to remove water and the solution was allowed to stand overnight. It was then standardized against sodium carbonate in glacial acetic acid. Typical titration curves are shown in Figure 1.

d. Absorption Spectra

The measurements were carried out with a Bausch & Lomb recording spectrophotometer (Spectronic 505), chloroform being used as a solvent for VHDB copolymers.

RESULTS AND DISCUSSION

a. Monomer–Polymer Composition Curves and Monomer Reactivity Ratios

As indicated in Figures 2 and 3 and Tables I and II, VHDB shows good copolymerizabilities with conventional monomers, such as styrene (St). Figures showing similar data for 4-vinylpyridine (4-VP), methylmethacrylate (MMA), α-methylstyrene (α-MSt), and methylacrylate (MA) are not given because they were very like Figures 2 and 3, and the data could be summarized in the tables. It is surprising that, in general, rates of polymerization are greater in VHDB-rich monomer compositions, in spite of the bulky character of the group next to the vinyl group.

It is well known that the product of monomer reactivity ratios is a measure of the alternating tendency in copolymerization. These products

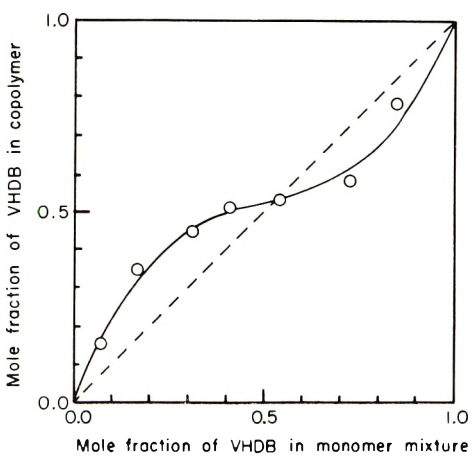

Fig. 2. Copolymer composition curves for VHDB–styrene copolymers. For reactivity ratios see Table I.

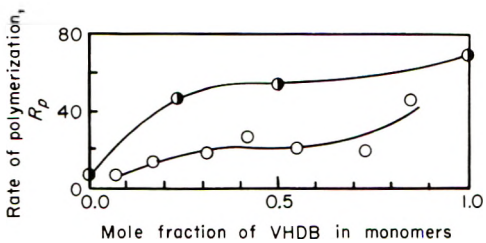

Fig. 3. Rate of polymerization R_p in VHDB–styrene copolymerization. (○) 0.2% azobisisobutyronitrile/monomers; (◑) 1.0% azobisisobutyronitrile/monomers.

TABLE I
Product of Reactivity Ratios ($\gamma_1\gamma_2$)

	Second monomer				
	α-Methyl-styrene	Styrene	4-Vinyl-pyridine	Methyl methacrylate	Methyl acrylate
$\gamma_1\gamma_2$	0.033	0.095	0.192	0.139	0.345
γ_1	0.30	0.43	0.40	0.41	0.75
γ_2	0.11	0.22	0.48	0.34	0.46

TABLE II
Q-e Values for Vinylhydroquinone Dibenzoate in Relation to Various Second Monomers

	Values for second monomer		Calculated values for VHDB	
Second monomer	Q_2	e_2	Q_1	e_1
Methyl acrylate	0.42	0.60	1.68	1.63
Methyl methacrylate	0.74	0.40	3.80	1.80
4-Vinyl-pyridine	0.82	−0.20	1.32	1.08
Styrene	(1.00)	(−0.80)	1.32	0.74
α-Methyl-styrene	0.98	−1.27	0.83	0.60

are shown in Table I, together with values of the reactivity ratios (γ_1,γ_2) calculated according to Mayo and Lewis' method.[5] It is worthy of note that this alternating tendency is greater in electronegative monomers, such as α-methylstyrene and styrene, in spite of the expected randomness of the polymer structures formed.

b. *Q-e* Values

At present, the best way to predict the monomer reactivity ratios in copolymerization with other monomers without too many experiments is to calculate the *Q-e* values proposed by Alfrey and Price.[6] Familiar equations are as follows.

$$\gamma_1 = (Q_1/Q_2) \exp \{-e_1(e_1 - e_2)\} \quad (1)$$

$$\gamma_2 = (Q_2/Q_1) \exp \{-e_2(e_2 - e_1)\} \quad (2)$$

In Table II are shown the Q-e values for VHDB calculated from the monomer reactivity ratios for the cited values of Q_2 and e_2 for each second monomer. The remarkable fact is that both values of Q_1 and e_1 are somewhat different from each other according to the kinds of second monomer used. Alfrey and Price's equations do not hold very well in this case. The fact that the values of Q_1, i.e., resonance term, are generally around unity seems to indicate that the resonance effect of this monomer is almost as large as that of styrene. Possible resonance forms are shown below.

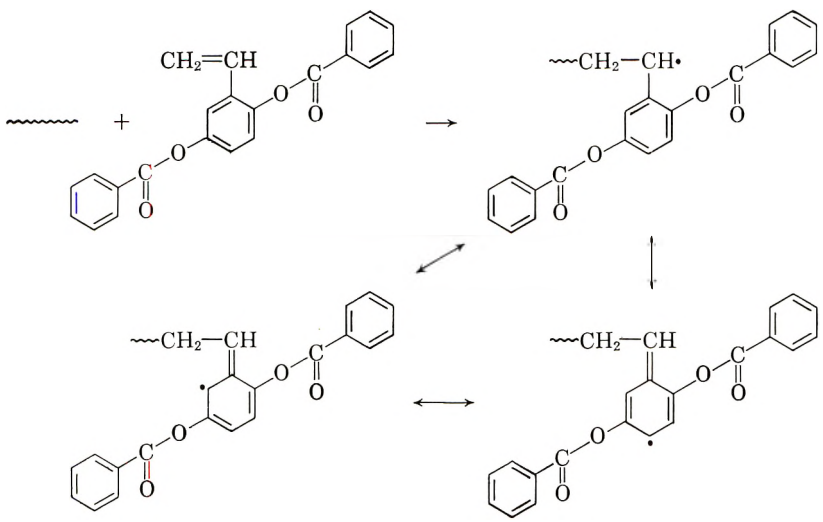

The polarity term, e_1, on the other hand, shows some peculiarity. It is generally accepted that styrene monomers substituted with an electron-donating group in the *para*-position, such as *p*-methoxystyrene and *p*-methylstyrene, have more negative e values than styrene itself.[7] The effect of the substituent is transmitted to the vinyl through the ring, and this can occur by conjugation only when it is in the *ortho*- or *para*-position. Hence one of the benzoate groups of VHDB, in the *meta*-position can exert an influence only via the inductive effect. An example of this kind is *m*-methylstyrene which has the e value of -0.72 (styrene, -0.80). With *ortho*-substituents, some anomalous behaviors have been observed, which are ascribed to *ortho*-effect[8] and which are considered to be due to steric hindrance and chelation. For example, 2-methylstyrene has a slightly more positive e-value (-0.78) than styrene. Since the steric effect of the benzoate group in the *ortho*-position must be much greater than that of methyl, it seems reasonable to assign a positive value of e for VHDB.

c. Ultraviolet Absorption Spectra of Copolymers

The spectra of VHDB homopolymer and its copolymers show a strong absorption at 244 mμ when measured in chloroform (Fig. 4). The acid-treated (hydrolyzed) polymer and copolymers also have a strong absorption at 303–306 mμ, which is characteristic of hydroquinone (Fig. 5). In Figure 4, the absorption of the second monomer, for example that of styrene, seems to disappear due to the extremely strong absorption of the

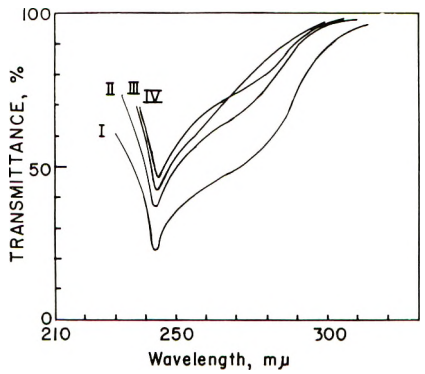

Fig. 4. Typical ultraviolet spectra of VHDB copolymers in chloroform: (*I*) VHDB homopolymer, 0.0154 g./l; (*II*) VHDB–St copolymer, 50.6% VHDB, 0.0155 g./l.; (*III*) VHDB–4-VP copolymer, 56.8% VHDB, 0.0115 g./l.; (*IV*) VHDB–MMA copolymer, 39.3% VHDB, 0.0115 g./l.

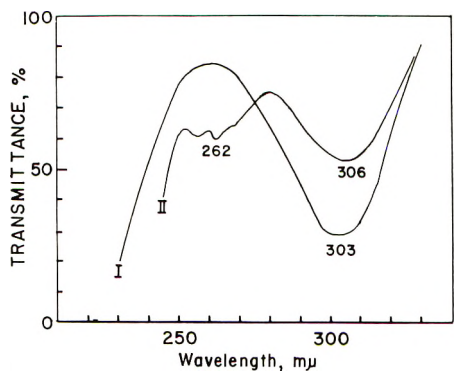

Fig. 5. Typical ultraviolet spectra of acid-treated copolymers in 0.5*N* sulfuric acid: (*I*) VHDB homopolymer, 0.0370 g./l.; (*II*) VHDB–St copolymer, VHDB mole fraction 0.0993, 0.103 g./l.

hydroquinone dibenzoate group, while, in Figure 5, the apparent separation of the absorption of the hydroquinone group and that of the second monomer can be observed. In order to examine the relationship between the absorption intensities of copolymers in chloroform and copolymer compositions, specific extinction coefficients calculated by Beer's Law were

plotted against the VHDB content in copolymers as determined by the titration method (Fig. 6). Large departures from linearity, the extents of which are dependent upon the copolymer system used, can be observed, although Beer's Law holds very well for homopolymer and mixtures of two homopolymers, as illustrated by the VHDB–styrene system. This large difference should mean some interaction between neighboring groups in the polymer chain, since the mixture of two homopolymers shows a normal additive effect. Such neighboring-group interaction has been implied by the electrometric titration behavior.[3] The greatest departures are shown by methyl acrylate and methyl methacrylate which do not contain any benzene or related rings. Here the maxima of E are observed at about 80%

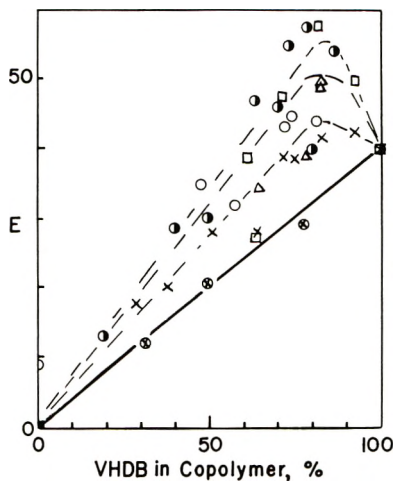

Fig. 6. Relationship between specific extinction coefficients E (in chloroform) and copolymer compositions. (⊗) mixture of homopolymers, VHDB and styrene; (×) VHDB–styrene copolymer; (○) VHDB–4-vinylpyridine; (◑) VHDB–methyl methacrylate; (□) VHDB–methyl acrylate; (△) VHDB–α-methylstyrene.

VHDB in copolymer, which corresponds to about 50 mole-%. This fact might possibly mean that two neighboring benzene or related groups, including those of the homopolymer, interact with each other, so that the absorption intensity at 244 mμ may be reduced without any visible shift of absorption. This corresponds with the fact that, in the estimation of e values of VHDB, a strong effect of the *ortho*-substituent which might be subject to steric hindrance was observed. It might also explain the cause of large differences between Q-e values, since both the resonance term and polarity term could be affected by the nature of the second monomer, due to the bulky character of VHDB.

We are pleased to acknowledge that this work was supported by a PHS research grant, A-3304, National Institute of Arthritis and Metabolic Diseases, Public Health Service.

References

1. Cassidy, H. G., *J. Am. Chem. Soc.*, **71**, 402 (1949).
2. Ezrin, M., I. H. Updegraff, and H. G. Cassidy, *J. Am. Chem. Soc.*, **75**, 1610 (1953).
3. Robinson, I. D., M. F. Refojo, and H. G. Cassidy, *J. Polymer Sci.*, **39**, 47 (1959).
4. Friz, J. S., *Anal. Chem.*, **22**, 1028 (1950).
5. Mayo, F. R., and F. M. Lewis, *J. Am. Chem. Soc.*, **66**, 1594 (1944).
6. Alfrey, T., Jr., and C. C. Price, *J. Polymer Sci.*, **2**, 101 (1947).
7. Young, L. J., *J. Polymer Sci.*, **54**, 411 (1961).
8. Remick, A. E., *Electronic Interpretations of Organic Chemistry*, Wiley, New York, 1949, p. 66.

Résumé

Il a été montré que le dibenzoate de vinylhydroquinone (VHDB) copolymérisait facilement en solution dans des conditions d'initiation radicalaire avec des monomères classiques tels que le styrène, l'α-méthylstyrène, la 4-vinylpyridine, le méthacrylate et l'acrylate de méthyle jusqu'à moins que 10% de conversion. Les vitesses de polymérisation sont plus élevées pour les compositions riches en monomères NHDB malgré le caractère volumineux du groupe benzoyle. On donne les valeurs de Q et e (Alfrey et Price). La réactivité Q_1 du VHDB s'approche de l'unité, ce qui semble indiquer que l'effet de résonance stabilisant le radical est semblable à celui du styrène. Le terme polarité e_1 est positif pour VHDB. Les spectres d'absorption dans l'ultra-violet des copolymères impliquent l'existence d'interactions entre groupes voisins dans les chaînes de copolymère; de telles interactions sont impliquées aussi par les valeurs de Q et e obtenues et, dans un travail plus ancien, par le comportement à la titration électrométrique.

Zusammenfassung

Das Copolymerisationsverhalten von monomerem Vinylhydrochinondibenzoat (VHDB) in Lösung bei radikalischem Start mit Styrol, α-Methylstyrol, 4-Vinylpyridin, Methylmethacrylat und Methylacrylat wurde bei Umsätzen kleiner als 10% untersucht; es zeigte mit diesen konventionallen Monomeren eine gute Copolymerisationsfähigkeit. Ungeachtet des sperrigen Charakters der Benzoylgruppe ist die Polymerisationsgeschwindigkeit bei VHDB-reichen Ansätzen grösser. Q- und e-Werte (Alfrey und Price) werden angegeben. Der Resonanzterm (Q_1) für VHDB ist nahe gleich eins, was dafür zu sprechen scheint, dass der Resonanzeffekt bei der Stabilisierung des Radikals fast so gross wie bei Styrol ist. Dem Polaritätsterm, e_1, wird für VHDB ein positiver Wert zugeschrieben. Ultraviolettabsorptionsspektren der Copolymeren lassen eine Wechselwirkung benachbarter Gruppen in den Polymerketten erkennen, wofür auch die beobachteten Q- und e-Werte sowie frühere Untersuchungen über das Verhalten bei der elektrometrischen Titration sprechen.

Received June 18, 1962

JOURNAL OF POLYMER SCIENCE: PART A VOL. 1, PP. 1979–1984 (1963)

Enthalpy and Free Energy Changes in Some Simple Polymerization Processes*

GEORGE S. PARKS and HELENE P. MOSHER, *Department of Chemistry, Stanford University, Stanford, California*

Synopsis

The heats of combustion of four polymers, viz., polyoxymethylene (Delrin), polymethylene, polyethylene (Marlex), and polypropylene, have been accurately measured. From these results the changes in enthalpy and free energy have been calculated for (*a*) the process of forming the respective polymer units from the elements and (*b*) the process of forming these polymers from their monomer building blocks.

INTRODUCTION

In an earlier study from this Laboratory highly accurate values for the heats of combustion of certain samples of polyethylene and polyisobutylene were reported.[1] The results for this high pressure polyethylene indicated that the material was about 50% crystalline at 25°C. On the other hand, the polyisobutylene was clearly amorphous and here the data showed that the heat of polymerization per isobutylene unit must be about 3000 cal. less than would be expected for a normal, unstrained product and thereby indicated the existence of appreciable steric repulsion effects in the polymer.

Recently, the authors have been fortunate in obtaining good samples of four new polymer products, viz., polyoxymethylene, polymethylene, "linear" polyethylene, and isotactic polypropylene. These have provided them with a basis for making new determinations of the heats of combustion of polymers, from which they have calculated values for the enthalpy and free energy changes in the corresponding polymerization processes.

EXPERIMENTAL

Apparatus and Method

The apparatus and general method for measuring the heats of combustion were essentially the same as those described previously by Parks and collaborators.[2,3] The energy equivalent of the system was checked at regular intervals by use of NBS benzoic acid, sample 39f. From previous experience the authors have found their method capable of yielding results precise to within 0.02%.

* This research was supported by a grant from the National Science Foundation.

The combustions were made with a Parr bomb (capacity 390 ml.) filled with oxygen to a pressure of 30 atm. at 24°C. and with 1 ml. of water initially in the bomb. In all cases most of the air originally in the bomb was washed out by two preliminary fillings with oxygen to a pressure of 5 atm. and thus the correction for nitric acid formation was kept down to less than 0.02% of the total heat involved. No tests for carbon monoxide were made in this work, but the high degree of concordance obtained in these and other sets of determinations really constitutes excellent evidence as to the completeness of the reported combustions.

Units

The unit of energy used throughout this paper is the *defined* conventional calorie, equal to 4.1840 absolute joules. The unit of mass is the gram true mass, which has been derived from the weight in air against brass weights by use of correction factors for buoyancy based on the polymer densities given in the next section. Atomic weights are the 1961 values[4] based on carbon-12.

Polymer Materials

In all cases the polymer materials were dried for periods of one to four weeks in a vacuum desiccator over anhydrous magnesium perchlorate, since water contributes nothing to the heat of combustion and thus constitutes the most objectionable impurity in work on organic compounds. All of these polymers contained small amounts of organic stabilizers, but the authors had definite information concerning the nature of the compound only in the case of the polymethylene.

Polyoxymethylene

This was a sample of Du Pont Delrin in the form of crystallized resin granules. It was about 99.3% pure. The remaining 0.7% represented small amounts of unspecified organic additives, which, however, the authors have reason to believe did not contribute any significant error to their results. They have taken 1.40 as the approximate density of this polymer.

Polymethylene

This was prepared from diazomethane by Dist Anal of Baton Rouge, La. It has been described as a linear polymer, without any branched components, of about 300,000 molecular weight.[5] The sample for which the present data are reported contained about 0.2% of 2,6-ditertiary-*p*-cresol as an oxidation inhibitor. Other samples without this inhibitor gave irregularly lower combustion values, indicative of some preliminary oxidation, perhaps within the bomb, prior to firing.

Polyethylene

This was Phillips Marlex linear polyethylene, resin No. 6002. It was in the form of small granules, with a reported density of 0.96, a value also

assumed for the preceding polymethylene sample. An analysis on this Marlex, made by Dist Anal, showed only about 4 methyl branches per 10,000 carbon atoms. Dole and Wunderlich,[6] in a study with presumably similar Marlex, have estimated the crystallinity as around 98% at room temperature.

Polypropylene

This was a stabilized material in nib form, which was given to the authors by the Shell Development Co. It was reported to be in the isotactic form with about 67% crystallinity. A subsequent analysis by the Dist Anal laboratory, using an infrared method, found it 64% crystalline. The authors have taken 0.91 for its density.

Combustion Results

The present experimental results for the combustions of these four polymers to yield liquid water and gaseous carbon dioxide are summarized in Table I. Here the second column records the number of combustions carried out on each sample. The resulting mean values for the energy evolved in the isothermal bomb process per gram at 25°C. represented by the term $-\Delta U_B/m$, and the mean deviations of the individual combustions from these mean values, represented by Δ, appear in the two succeeding columns.

TABLE I
Combustion Data for the Bomb Process at 25°C.

Polymer	No. of combustions	$-\Delta U_B/m$, cal./g.	Mean Δ, cal./g.
Polyoxymethylene	10	4,047.1	±0.8
Polymethylene	5	11,059.5	±0.8
Polyethylene	14	11,080.9	±2
Polypropylene	10	11,082.4	±2.2

In this connection it is interesting to note that the mean combustion value for polymethylene is 21.4 cal. lower than that for the Marlex polyethylene. Both materials are essentially similar linear hydrocarbon chains with negligible branching, although prepared in quite different ways. It is estimated that the value here for the authors' polymethylene with 0.2% stabilizer may be about 5 cal. lower than that corresponding to pure polymethylene, since 2,6-ditertiary-*p*-cresol should have a somewhat lower heat of combustion than a paraffin. The rest of this difference between the values for these two polymers may be ascribed to (*a*) somewhat incomplete crystallinity in the Marlex and (*b*) possibly a small amount of oxidation of this polymethylene sample prior to its treatment with stabilizer. The authors made five very concordant determinations on this polymethylene but were subsequently unsuccessful in obtaining similar material for a re-

checking of the latter possibility. On the other hand, if the hypothetical heat of fusion of a perfectly crystalline linear polymer of this type is taken as about 60 cal./g. at 25°C. and the value for polymethylene is valid, it might be concluded that the Marlex is only about 75% crystalline. In line with this argument, it is noted that Parks and Mosley[1] previously obtained 11,095 cal./g. for the combustion of Du Pont high-pressure polyethylene (polythene), which they thereby judged to be about 49% crystalline.

In the case of the isotactic polypropylene the heat of combustion per gram is only 1.5 cal. above that for the Marlex polyethylene. Previously, Parks and Mosley obtained a much higher value, i.e., a mean of 11,177 cal./g. for two samples of polyisobutylene. Apparently the steric repulsions which exist in the polyisobutylene are not here present in the polypropylene polymer.

DERIVED THERMAL DATA

Next, in part *A* of Table II, important thermal data have been assembled, computed per unit of polymer at 25°C. The values of $-\Delta U_c$ represent the combustion heat evolved in kilocalories per unit after correction to the standard constant-volume process, where the reactants and products are each at 1 atm., by means of the equations of Washburn.[7] From this quantity $-\Delta H_c$, the heat evolved in the isobaric process at 1 atm. was obtained by addition of the proper work term. Then the enthalpy change for the formation of a polymer unit from the elements ΔH^0_f was calculated from this $-\Delta H_c$ by use of -68.3174 and -94.0518 kcal.[8] for the ΔH^0_f of H_2O (*l*) and CO_2 (*g*), respectively.

TABLE II
Thermal Data for Polymer and Monomer Units at 25°C.

Function	(CH_2O)	(CH_2)	(C_2H_4)	(C_3H_6)
	Part *A*—for Polymer Forms			
$-\Delta U_c$, kcal.	121.44	155.08	310.76	466.21
$-\Delta H^0_c$, kcal.	121.44	155.38	311.36	467.10
ΔH^0_f, kcal.	−40.93	−6.99	−13.38	−20.01
S^0, cal.-deg.$^{-1}$	11	6	12	17
ΔF^0_f, kcal.	−27.20	0.93	2.46	4.05
	Part *B*—for Monomer Forms			
ΔH^0_f, kcal.	−27.70	66	12.50	4.88
ΔF^0_f, kcal.	−26.27	62.83	16.28	14.99

The last line in this part of Table II then contains the free energy changes in the hypothetical formation of the several polymer units from the elements, computed by the fundamental thermodynamic equation, $\Delta F = \Delta H - T\Delta S$. For these computations the authors have employed their estimates,

as given in the preceding line, for S^0_{298} for the four polymer units. These estimates were made primarily in the light of the empirical generalizations of Parks and Huffman[9] and with some allowance for small zero-point entropies, arising from the inevitable randomness in a polymer. In spite of their rather arbitrary character, it is believed that they are probably good to about 5%. The ΔS was then evaluated by taking the basic entropies of the elements as 1.36 cal.-deg.$^{-1}$ for graphitic C, 31.21 for gaseous H_2, and 49.03 for gaseous O_2.[8]

Part *B* of Table II contains the values of the enthalpies and free energies of formation of the four gaseous monomer units, which may be considered as the essential building blocks for these polymers. Here the data for formaldehyde and methylene have been obtained from the recent compilations of the "JANAF Thermochemical Tables."[10] Those for ethylene and propylene are the results recorded in the tables of API project 44.[11]

By subtraction of the monomer values from the corresponding polymer data in Table II, the following results are derived for the four polymerization processes:

$$CH_2O(g) \rightarrow \frac{1}{n}(CH_2O)_n;\ \Delta H^0_{298} = -13.23 \text{ kcal. and } \Delta F^0_{298} = -0.93 \text{ kcal.}$$

$$CH_2(g) \rightarrow \frac{1}{n}(CH_2)_n;\ \Delta H^0_{298} = -72.99 \text{ kcal. and } \Delta F^0_{298} = -61.90 \text{ kcal.}$$

$$C_2H_4(g) \rightarrow \frac{1}{n}(C_2H_4)_n;\ \Delta H^0_{298} = -25.88 \text{ kcal. and } \Delta F^0_{298} = -13.82 \text{ kcal.}$$

$$C_3H_6(g) \rightarrow \frac{1}{n}(C_3H_6)_n;\ \Delta H^0_{298} = -24.89 \text{ kcal. and } \Delta F^0_{298} = -10.94 \text{ kcal.}$$

While all these free energy changes are negative, indicative of the stability of the polymers with reference to the particular polymerizations at 25°C., the numerical value of ΔF^0 in the production of Delrin is surprisingly small. Here it is doubted that the authors' estimate of S^{298} for the polymer unit is seriously in error and one is inclined to suggest that the enthalpy and free energy values for formaldehyde itself are too low because of an error in the determination of the heat of combustion of this gas. For this polymerization a free energy decrease of at least 2 kcal. greater than the present result would be expected.

On the other hand, the free energy decrease for the polymerization of the energy-rich methylene free radical to polymethylene is strikingly large. It should be emphasized, however, that this value refers to the hypothetical process in which methylene is present at one atmosphere. In the actual process, methylene is produced from the decomposition of diazomethane and then goes over rapidly to the polymer so that its actual concentration is never more than a very small fraction of one atmosphere. Under such conditions the decrease in free energy is undoubtedly more nearly comparable to that for the other reactions.

In addition to the foregoing polymerization data and in this connection,

some corresponding figures are given for the production of polyisobutylene from its monomer:

$$\text{isoC}_4\text{H}_8 \rightarrow \frac{1}{n}(\text{isoC}_4\text{H}_8)_n;\quad \Delta H^0_{298} = -17.20 \text{ kcal. and } \Delta F^0_{298} = -3.88 \text{ kcal.}$$

These results come from an earlier, unpublished study, which the senior author based on the combustion data reviewed by Parks and Mosley.[1] The smaller decreases in ΔH^0 and ΔF^0, as compared with the production of polyethylene and polypropylene, are undoubtedly attributable to the steric repulsion effects of the two methyl branches attached on alternating carbon atoms in the polymer chain.

References

1. Parks, G. S., and J. R. Mosley, *J. Chem. Phys.*, **17**, 691 (1949).
2. Richardson, J. W., and G. S. Parks, *J. Am. Chem. Soc.*, **61**, 3543 (1939).
3. Moore, G. E., M. L. Renquist, and G. S. Parks, *J. Am. Chem. Soc.*, **62**, 1505 (1940).
4. *J. Chem. Educ.*, **38**, 625 (1961).
5. *Chem. Eng. News*, No. 20, 69 (1960).
6. Dole, M., and B. Wunderlich, *Makromol. Chem.*, **34**, 29 (1959).
7. Washburn, E. W., *J. Res. Natl. Bur. Std.*, **10**, 525 (1933).
8. Wagman, D. D., J. E. Kilpatrick, W. L. Taylor, K. S. Pitzer, and F. D. Rossini, *J. Res. Natl. Bur. Std.*, **34**, 143 (1945).
9. Parks, G. S., and H. M. Huffman, *The Free Energies of Some Organic Compounds*, Chemical Catalog Co., New York, 1932, p. 209.
10. Stull, D. R., Project Director, "JANAF Thermochemical Data," Dow Chemical Co., Midland, Mich., 1961.
11. Rossini, F. D., and co-workers, *Selected Values of Physical and Thermodynamic Properties of Hydrocarbons and Related Compounds*, Carnegie Press, Pittsburgh, Pa., 1953, p. 475.

Résumé

On a mesuré avec précision les chaleurs de combustion de quatre polymères qui sont: le polyoxyméthylène (Delrin), le polyméthylène, le polyéthylène (Marlex), et le polypropylène. A partir de ces résultats on a calculé les changements d'enthalpie et d'energie libre (*a*) pour la formation des unités polymériques à partir des élements, et (*b*) pour le formation de ces polymères à partir des monomères.

Zusammenfassung

Die Verbrennungswärmen von vier Polymeren, nämlich Polyoxymethylen (Delrin), Polymethylen, Polyäthylen (Marlex) und Polypropylen wurden genau gemessen. Aus den Ergebnissen wurden die Änderung der Enthalpie und freien Energie für den Bildungsvorgang (*a*) des betreffenden Polymerbausteins aus den Elementen und (*b*) der Polymeren aus den Monomerbausteinen berechnet.

Received July 30, 1962

JOURNAL OF POLYMER SCIENCE: PART A VOL. 1, PP. 1985–1993 (1963)

Thermodynamic Properties of Solutions of Cellulose Triacetate

W. R. MOORE and R. SHUTTLEWORTH, *Polymer Research Laboratories, Department of Chemical Technology, Bradford Institute of Technology, Bradford, Yorkshire, England*

Synopsis

The lowering of vapor pressures of solutions containing 10–50% by weight of cellulose triacetate in chloroform and methylene chloride have been measured at several temperatures. Attempts made to obtain similar data for solutions in *s*-tetrachlorethane failed apparently because of decomposition of solvent. Solvent activities, free energies, heats and entropies of dilution are obtained. Both systems become increasingly exothermal as the polymer concentration is increased. In the triacetate-chloroform system, $T\Delta\bar{S}_1$ decreases from relatively large values at low concentrations as the concentration is increased resembling comparable secondary cellulose acetate systems with acetone and dioxan as solvents. In the methylene chloride system, $T\Delta\bar{S}_1$ increases with concentration as in comparable cellulose nitrate-solvent systems. These results are interpreted in terms of solvation and chain stiffness. Values of the polymer-solvent interaction parameter χ_1 increase with concentration and values of the entropy contribution to χ_1 are greater than those suggested by lattice theories. Expression of volume fraction of polymer in terms of solvated rather than dry polymer should lead to values of χ_1 and the entropy contribution which are more in keeping with the predictions of lattice theories.

INTRODUCTION

Thermodynamic properties of solutions of cellulose triacetate do not seem to have been extensively studied. Free energies, heats, and entropies of dilution have been obtained for dilute solutions of cellulose triacetate in chloroform, methylene chloride, and *s*-tetrachlorethane.[1–3] Similar data for more concentrated solutions do not appear to have been obtained although they would be valuable both as an extension of results for dilute solutions and for comparison with results recently obtained using other cellulose derivatives.[4] The results of measurements of vapor pressure lowering for solutions of cellulose triacetate containing 10–50% of polymer by weight in chloroform and methylene chloride are given in this paper. For reasons to be given later similar measurements for solutions in *s*-tetrachlorethane could not be made. Thermodynamic data are obtained, discussed, and compared with those obtained for comparable solutions of secondary cellulose acetate and cellulose nitrate.

EXPERIMENTAL

The triacetate was obtained by nondegradative acetylation of a fraction of secondary acetate[4] of number average molecular weight 104,000. The number average molecular weight of the triacetate, obtained osmotically in chloroform at 25° was 157,000. The increase in molecular weight is more than can be accounted for by additional substitution and may be partly due to loss of low molecular weight material in acetylation. The acetic acid yield of the triacetate was 62.4 ± 0.1%.

It was intended to use chloroform, methylene chloride, and *s*-tetrachlorethane as solvents. Chloroform was purified by the method of Walden et al.[6] by drying over anhydrous calcium chloride for several days and then distilling and drying several times over anhydrous potassium carbonate and then fractionally distilling it after each drying. A middle fraction of the last distillate was cooled and degassed in vacuum, refractionated in vacuum, and a middle fraction collected for vapor pressure measurements. Vapor pressures between 15° and 40° agreed closely with those of Stull[7] and the density at 25° was in good agreement with published values.[8,9] Methylene chloride was washed with 5% sodium carbonate solution and water, dried over anhydrous calcium chloride, distilled, and again dried.[10] After three fractional distillations, a middle fraction was cooled and degassed in vacuum. After refractionation in vacuum, a middle fraction was collected for vapor pressure measurements. Vapor pressures between 15° and 40° and the density at 25° were in good agreement with published values.[8,11] *S*-tetrachlorethane was warmed, while stirring, with 8% of its volume of sulfuric acid for 30 min. The upper acid layer was separated and the process repeated until the upper layer was colorless. The *s*-tetrachlorethane was then steam distilled, dried with anhydrous potassium carbonate, and fractionally distilled.[10] After two further fractionations, a middle fraction was cooled and degassed in vacuum. It was refractionated in vacuum and a middle fraction collected for vapour pressure measurements. Vapor pressures between 15° and 40° were in good agreement with those of Stull[7] and the density at 25° agreed well with that given by Timmermans.[8]

Vapor pressures of the pure solvents and the lowering of vapor pressure of solutions were measured at four temperatures in the range 15–40° by the method previously described.[4] In spite of repeated attempts, it was not found possible to obtain vapor pressure lowerings for solutions in tetrachlorethane. The vapor pressure on the solution side was always considerably greater than that of the solvent and tended to increase with time. Evidence was obtained for the decomposition of *s*-tetrachlorethane and evolution of hydrogen chloride in the presence of polymer. It is perhaps significant that osmotic measurements indicate an apparently anomalous variation of molecular weight in *s*-tetrachlorethane with temperature.[1-3]

With the other solvents, measurements were first made at increasing concentrations of polymer and then at decreasing concentrations. Two

separate series of measurements were made in each case, fresh polymer and solvent being used for each. Activities, a_1, of the solvents were obtained from fugacity ratios as previously described;[4] values of the second virial coefficient of the vapor being obtained by the method of Lambert et al.[12]

RESULTS

Figures 1 and 2 show a_1 as a function of polymer weight fraction w_2 at each temperature. Hysteresis effects are absent and the two separate series of measurements on each system are in good agreement. Free ener-

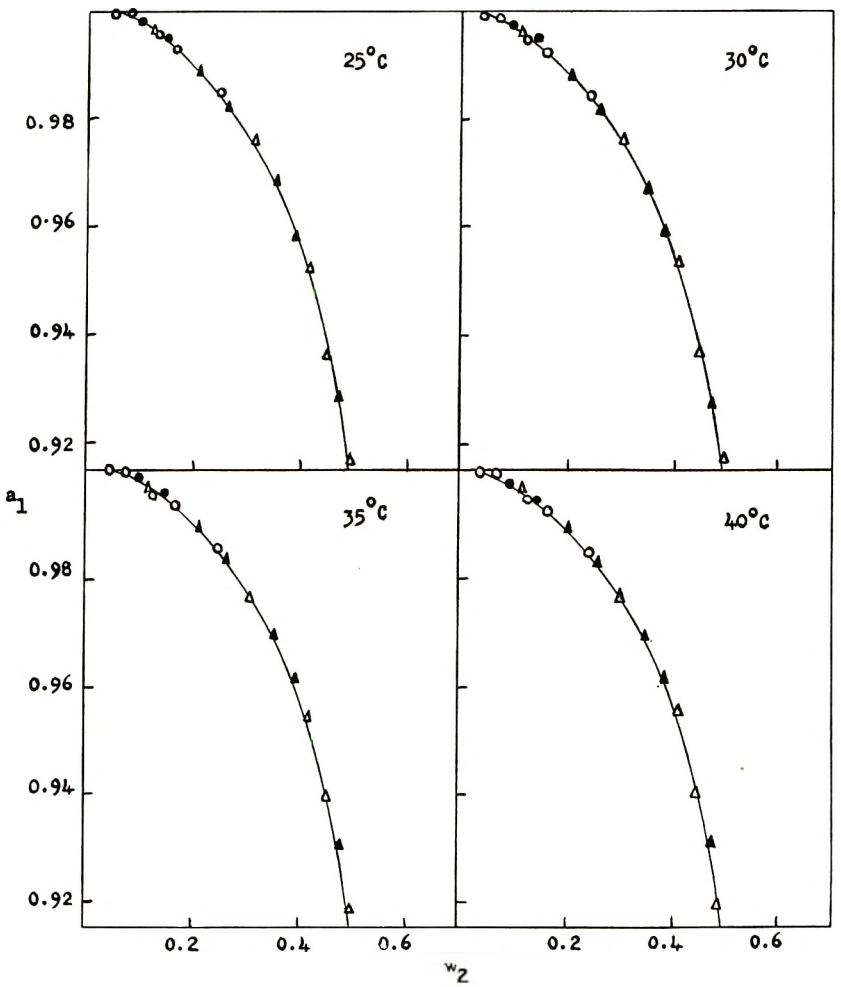

Fig. 1. (a_1) As a function of polymer weight fraction for the cellulose triacetate-chloroform system. (○) and (●) first series of measurements at increasing and decreasing concentration respectively; (△) and (▲) second series of measurements.

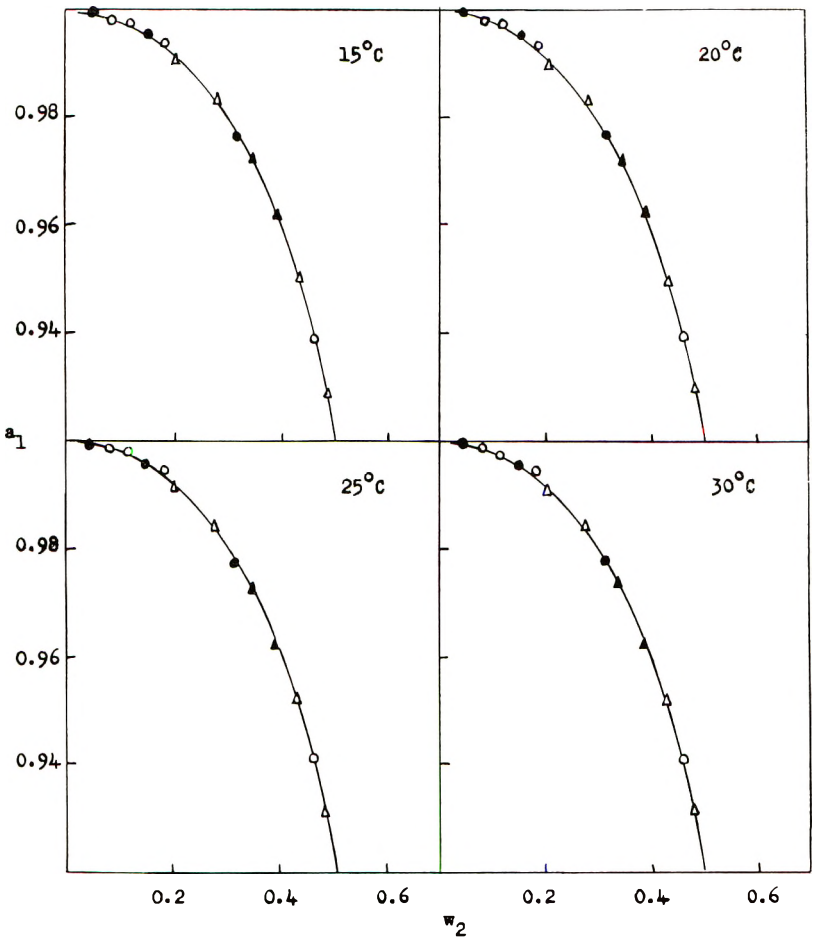

Fig. 2. (a_1) As a function of polymer weight fraction for the cellulose triacetate-methylene chloride system. Key symbols same as in Figure 1.

gies of dilution $\Delta\bar{F}_1$ at $w_2 = 0.1, 0.15, 0.2, 0.25, 0.3, 0.35, 0.4, 0.45$, and 0.5 were obtained from:

$$\Delta\bar{F}_1 = RT \ln a_1 \tag{1}$$

where R is the gas constant and T the absolute temperature. Values of a_1 were interpolated from the smooth curves in Figures 1 and 2. Heats $\Delta\bar{H}_1$ and entropies $\Delta\bar{S}_1$ of dilution were obtained from the relationships:

$$\Delta\bar{H}_1 = \delta(\Delta\bar{F}_1/T)/\delta(1/T) \tag{2}$$

and

$$-\Delta\bar{S}_1 = \delta\Delta F_1/\delta T \tag{3}$$

Values of $\Delta\bar{F}_1$, $\Delta\bar{H}_1$, and $T\Delta\bar{S}_1$ at 20° and 25° for methylene chloride and

30° and 35° for chloroform solutions are given in Table I which also includes "ideal" values of $T\Delta\bar{S}_1$ obtained from:

$$\Delta\bar{S}_{1(id)} = Rx_2 \tag{4}$$

TABLE I

Solvent	w_2	$-\Delta\bar{F}_1$	$\Delta\bar{H}_1$	$T\Delta\bar{S}_1$	$-\Delta\bar{F}_1$	$\Delta\bar{H}_1$	$T\Delta\bar{S}_1$	$T\Delta\bar{S}_{1(id)}$
		20° cal./mole			25° cal./mole			
	0.10	1.2	−0.4	0.8	1.2	−0.4	0.8	0.04
	0.15	2.5	−1.2	1.3	2.6	−1.2	1.4	0.06
	0.20	4.8	−2.0	2.8	4.8	−2.0	2.8	0.08
Methylene	0.25	7.6	−3.5	4.1	7.7	−3.7	4.0	0.11
chloride	0.30	11.3	−6.7	4.6	11.4	−6.9	4.5	0.14
	0.35	16.9	−11.4	5.5	17.0	−11.8	5.2	0.17
	0.40	23.4	−17.7	5.7	23.5	−17.3	6.2	0.21
	0.45	32.9	−27.1	5.8	33.0	−26.8	6.2	0.26
	0.50	45.5	−39.7	5.8	45.7	−39.2	6.5	0.32
		30° cal./mole			35° cal./mole			
	0.15	3.7	3.4	7.1	3.9	10.4	14.3	0.08
	0.20	6.7	−0.8	5.9	6.9	5.6	12.5	0.12
	0.25	10.2	−4.6	5.6	10.4	1.8	12.2	0.15
	0.30	13.9	−9.7	4.2	14.0	−2.6	11.4	0.20
Chloroform	0.35	18.8	−15.1	3.7	19.0	−8.9	10.1	0.25
	0.40	27.2	−23.9	3.3	27.3	−20.4	6.9	0.31
	0.45	38.4	−36.1	2.3	38.4	−34.3	4.1	0.38
	0.50	54.6	−53.8	0.8	54.7	−53.4	1.3	0.46

where x_2 is the mole fraction of polymer. Values of $\Delta\bar{H}_1$ and $T\Delta\bar{S}_1$ are estimated to be $\pm 10\%$ with probably greater uncertainty at lower concentrations.

Values of the polymer-solvent interaction parameter χ_1 obtained from

$$\ln a_1 = \ln (1 - \phi_2) + (1 - 1/x)\phi_2 + \chi_1\phi_2^2 \tag{5}$$

(where ϕ_2 is the volume fraction of polymer and x the number of segments in the polymer chain) are shown as a function of ϕ_2 in Figure 3. Additivity of volumes was assumed and the density of the dry polymer used to calculate ϕ_2. The use of this density and the significance of the broken lines in Figure 3 will be considered later.

DISCUSSION

The results are in general agreement with those obtained at lower concentrations[1,2] and are similar in character to those for comparable systems involving other cellulose derivatives.[4] The change from endothermal to increasingly exothermal character as w_2 increases in the triacetate-chloroform system is also shown by secondary acetate systems with acetone and dioxan as solvents.[4] The decrease of $T\Delta\bar{S}_1$ as w_2 increases in the chloroform system

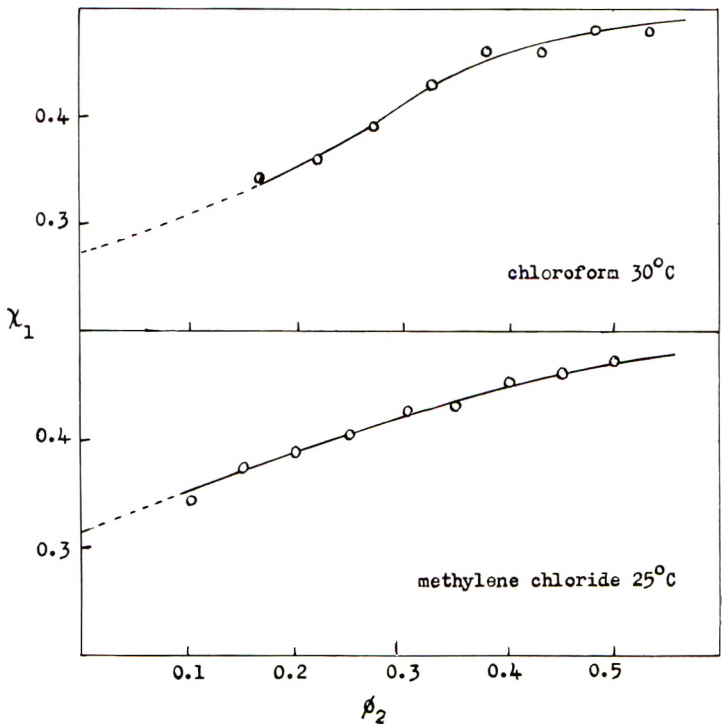

Fig. 3. (χ_1) As a function of polymer volume fraction.

is also shown by these secondary acetate systems. Negative values obtained with the secondary acetate systems are not reached with the chloroform system but these might be observed at values of w_2 greater than 0.5. At low concentrations values of $T\Delta\bar{S}_1$ approach those predicted by lattice theories[13] for flexible less polar polymers.

The triacetate-methylene chloride system, exothermal at all the concentrations studied, resembles comparable cellulose nitrate-solvent systems[4] both in negative values of $\Delta\bar{H}_1$ and positive values of $T\Delta\bar{S}_1$ both of which increase as w_2 increases. Thermodynamic quantities for the methylene chloride system seem to be little affected by small temperature changes but with the chloroform system, $\Delta\bar{H}_1$, tends to be less negative and $T\Delta\bar{S}_1$ to increase with an increase in temperature.

Negative values of $\Delta\bar{H}_1$ imply strong polymer-solvent interaction leading to solvation and orientation of solvent. Positive values at lower concentrations in the chloroform system might be due to endothermal dilution of solvated polymer. The variation of $T\Delta\bar{S}_1$ with w_2 for this system is in general agreement with these views, relatively large values at low concentrations being perhaps due to some chain flexibility. As in the case of comparable cellulose nitrate-solvent systems,[4] reasons for positive values of $T\Delta\bar{S}_1$ in the methylene chloride system are not clear. At low concentrations dilution may free solvent clusters blocking acetyl groups

permitting further solvation and orientation of solvent with a reduction of $T\Delta\bar{S}_1$ to near ideal values. This might also account for the exothermal character of this system at low concentrations.

It is also possible, at low concentrations in both systems, that exothermal solvation and endothermal dilution effects occur simultaneously. The sign and magnitude of $\Delta\bar{H}_1$ would then depend on the relative contributions of these two effects. The endothermal contribution should depend, at least in part, on the difference between the solubility parameters δ of solvated polymer and solvent. The value of δ for the solvated polymer may vary with the solvent but a value of 10 (cal./cc.)$^{1/2}$ at 25° has been suggested.[14] Chloroform, with $\delta = 9.3$ at 25° would be expected to lead to a greater endothermal effect than methylene chloride with $\delta = 9.85$ at 25° and this might account for positive values of ΔH_1 at low concentrations in the chloroform system.

Figure 3 shows the variation of χ_1 with ϕ_2 in each system. Presumably χ_1 decreases as ϕ_2 decreases below 0.15 in a manner similar to that indicated by the broken lines which cut the ordinates at values obtained for dilute solutions.[1,2] The variations of χ_1 with ϕ_2 differ from those for other cellulose derivative-solvent systems.[4] In secondary acetate-solvent systems, an initial fall in the value of χ_1 seems to be followed by increasingly positive values which may exceed 0.5 as ϕ_2 increases. In the cellulose nitrate-solvent systems χ_1 falls rapidly to large negative values as ϕ_2 is increased. Sharples and Swinton,[15] from studies of second order transitions in the cellulose triacetate-chloroform system, suggest that phase separation may occur, although this may not be readily apparent because of the similarity of the refractive indices of separated polymer and solvent. The values of χ_1 for this system do not suggest such phase separation.

According to simpler lattice theories,[13] χ_1 can be expressed as the sum of heat and entropy contributions χ_h and χ_s:

$$\chi_1 = \chi_h + \chi_s \tag{6}$$

with $\chi_h = \Delta\bar{H}_1/RT\phi_2^2$. Values of χ_1, χ_h, and χ_s are given in Table II. In each system χ_h becomes increasingly negative and χ_s increases as ϕ_2 is increased. Similar variations of χ_h and χ_s with concentration have been obtained for secondary cellulose acetate systems involving acetone and dioxan as solvents.[4] Values of χ_s in both triacetate systems, as in other cases involving cellulose derivatives,[1,2,4] are larger than would be expected from simpler lattice theories.

It has been pointed out that simpler lattice theories, without modification, are unlikely to apply to polar systems of the type studied.[1,2,4] Treatments suggested for polar interacting systems either involve empirical constants or equations not readily solved.[16,17] Values of ϕ_2 used in the calculation of χ_1 and χ_h were calculated assuming additivity of volumes and using the density of the dry polymer. The assumption, although not strictly true, should not greatly affect values of ϕ_2. Since the polymer will be fully or partially solvated at the concentrations used, ϕ_2 should more

TABLE II
Values of χ_1, χ_h, and χ_s

Solvent	ϕ_2	χ_1	χ_h	χ_s	Temp. °C.
	0.166	0.34	0.20	0.14	30
	0.220	0.36	−0.03	0.39	
	0.274	0.39	−0.10	0.49	
Chloroform	0.326	0.43	−0.15	0.58	
	0.378	0.46	−0.18	0.64	
	0.430	0.46	−0.22	0.68	
	0.481	0.48	−0.26	0.74	
	0.531	0.48	−0.32	0.80	
	0.101	0.34	−0.07	0.41	25
	0.151	0.37	−0.09	0.46	
	0.202	0.36	−0.08	0.44	
Methylene	0.252	0.40	−0.10	0.50	
chloride	0.302	0.42	−0.13	0.55	
	0.352	0.43	−0.16	0.59	
	0.402	0.45	−0.18	0.63	
	0.452	0.46	−0.22	0.68	
	0.502	0.47	−0.26	0.73	

logically be expressed in terms of solvated polymer. Since the degree of solvation and its variation with concentration is an unknown expression in such terms it is not possible although it is probable that expression in this way would lead to values of χ_1, χ_h, and χ_s more in keeping with those predicted by lattice theory.[18]

We are grateful for a Bradford City Research Scholarship held by R. S.

References

1. Tidswell, B. M., Ph.D. Thesis, London, 1958.
2. Moore, W. R., *Textile Res. J.*, **30**, 965 (1960).
3. Hagger, O., and A. J. A. van der Wyk, *Helv. Chim. Acta*, **23**, 484 (1940).
4. Moore, W. R., and R. Shuttleworth, *J. Polymer Sci.*, **A1**, 733 (1963).
5. Howlett, F., E. Minshull, and A. R. Urqhuart, *Shirley Inst. Mem.*, **18**, 241 (1941–3).
6. Walden, P., H. Ulich, and O. Werner, *Z. Physik. Chem., (Leipzig)*, **116**, 261 (1925).
7. Stull, D. R., *Ind. Eng. Chem.*, **39**, 517 (1947).
8. Timmermans, J., *Physical Constants of Organic Compounds*, Elsevier, Amsterdam, 1950.
9. Mumford, S. A., and J. W. C. Phillips, *J. Chem. Soc.*, **1950**, 75.
10. Vogel, A. J., *J. Chem. Soc.*, **1948**, 1833.
11. *International Critical Tables*, Vol. 3, McGraw-Hill, New York, p. 215.
12. Lambert, J. D., C. A. H. Roberts, J. S. Rowlinson, and J. T. Williamson, *Proc. Royal Soc. (London), Ser. A*, **196**, 113 (1949).
13. Flory, P. J., *Principles of Polymer Chemistry*, Cornell Univ. Press, Ithaca, N. Y., 1953 Chapter 12.
14. Magat, M., *Trans. Faraday Soc.*, **42**, 93 (1946).
15. Sharples, A., and F. L. Swinton, *Commun. Intern. Symp. Macromolecules, Weisbaden*, **1959**, V, B6.

16. Tompa, H., *J. Chem. Phys.*, **21**, 250 (1950).
17. Munster, A., *J. Chim. Phys.*, **49**, 128 (1952).
18. Moore, W. R., *Commun. Intern. Symp. Macromolecules, Weisbaden*, **1959**, *II*, B7.

Résumé

On a mesuré la diminution des tensions de vapeur de solutions contenant 10–50% en poids de triacétate de cellulose dans le chloroforme et le chlorure de méthylène. Des expériences tentées afin d'obtenir des données similaires pour des solutions dans le *s*-tétrachloroéthane, échouèrent apparemment à cause de la décomposition du solvant. On a obtenu les activités du solvant ainsi que les énergies libres, chaleurs et entropies de entropies de dilution. Les deux systèmes deviennent de plus en plus exothermiques au fur et à mesure qu'augmente la concentration en polymère. Dans le système triacétate-chloroforme, $T\Delta\bar{S}_1$ diminue depuis des valeurs relativement élevées pour des basses concentrations lorsque la concentration augmente et ce comportement ressemble à celui des systèmes constitués par l'acétate secondaire de cellulose en solution dans l'acétone ou le dioxanne. Dans le système avec le chlorure de méthylène, $R\Delta\bar{S}_1$ augmente avec la concentration de façon semblable au système nitrate de cellulose-solvant. On interprète les résultats en termes de solvatation et rigidité de chaîne. Les valeurs du paramètre χ_1 (interaction polymère-solvant) augmentent avec la concentration et les valeurs de la contribution de l'entropie à χ_1 sont plus grandes que celles suggérées par les théories à réseau. En exprimant la fraction de volume de polymère en termes de polymère-solvaté plutôt que polymère sec, on obtiendrait des valeurs de χ_1 et une contribution de l'entropie qui sont mieux en accord avec les prédictions de ces théories.

Zusammenfassung

Die Dampfdruckerniedrigung von Chloroform- und Methylenchloridlösungen mit einem Cellulosetriacetatgehalt von 10–50 Gew. % wurde bei mehreren Temperaturer gemessen. Versuche entsprechende Ergebnisse für *s*-Tetrachloräthanlösungen zu erhalten schlugen, offenbar wegen Zersetzung des Lösungsmittels, fehl. Die Lösungsmittelaktivität, freie Verdünnungsenergie, Verdünnungswärme und -entropie werden erhalten. Beide Systeme werden mit steigender Polymerkonzentration zunehmend exothermer. Im Triacetat-Chloroformsystem nimmt $T\Delta\bar{S}_1$ von verhältnismässig grossen Werten bei niedriger Konzentration mit steigender Konzentration in ähnlicher Weise ab, wie in vergleichbaren Systemen aus sekundärem Celluloseacetat und Aceton und Dioxan als Lösungsmitteln. Beim Methylenchloridsystem nimmt $T\Delta\bar{S}_1$ mit der Konzentration so wie in vergleichbaren Cellulosenitrat-Lösungsmittelsystemen zu. Diese Ergebnisse werden als Solvatisierungs- und Kettensteifigkeitseffekte gedeutet. Die Werte des Parameters χ_1 für die Polymer-Lösungsmittelwechselwirkung nehmen mit der Konzentration zu und der Entropiebeitrag zu χ_1 ist grösser als nach den Gittertheorien zu erwarten wäre. Die Angabe des Volumbruches des Polymeren als solvatisiertes und nicht als trockenes Polymeres sollte zu besser mit den Folgerungen aus der Gittertheorie stimmenden Werten für χ_1 und den Entropiebeitrag führen.

Received May 22, 1962

JOURNAL OF POLYMER SCIENCE: PART A VOL. 1, PP. 1995–2002 (1963)

Theory of the Modulus of Crystalline Polymers

LAWRENCE E. NIELSEN and FRED D. STOCKTON, *Monsanto Chemical Company, Plastics Division, Research Department, Springfield, Massachusetts*

Synopsis

A new theory for the elastic modulus of crystalline polymers has been developed for temperatures above the glass transition. The theory is based upon the assumption that crystallites behave as crosslinks and as a rigid filler. The shear modulus G is given by $G = (dRT/\bar{M}_c)F$, where F is a factor giving the relative increase in modulus due to the volume of the rigid crystallites. The number-average molecular weight $\bar{M}_c$ of the amorphous sequences is calculated as a function of degree of crystallinity from copolymer theory. The theoretical values of the modulus as a function of degree of crystallinity agree reasonably well with experimental values over a wide range.

Introduction

Numerous experimental data indicate that the elastic modulus of partially crystalline polymers is determined primarily by the degree of crystallinity.[1–3] For a given degree of crystallinity the modulus is nearly independent of the type of polymer or the temperature. Thermal history affects the modulus to some extent; the smaller the crystallite size, the higher the modulus at a constant degree of crystallinity.

A new theory is proposed which predicts the modulus as a function of the degree of crystallinity above the glass temperature. Within the limits of a proposed crystallization model, the crystallinity determines the modulus independent of adjustable constants. The theory postulates that crystallites act both as crosslinks and as a rigid filler. By exploiting the effects on the modulus of both the increase of the number of crosslinks and of the reinforcement of a rigid filler, this theory seems to give better agreement with experiment than theories presented heretofore.[4,5]

Theory

Crystallites tie molecules together like crosslinks. The effect of these crystalline crosslinks is estimated by the kinetic theory of rubber elasticity by:[6,7]

$$G = dRT/\bar{M}_c \tag{1}$$

in which G is the shear modulus, d the density of the rubber, R the gas constant, T the absolute temperature, and $\bar{M}_c$ the number-average mo-

lecular weight between crosslinks. In the case of crystalline polymers we assume that $\bar{M}_c$ is the number-average molecular weight of an amorphous sequence. Half of the problem of applying the present theory is the expression of $\bar{M}_c$ as a function of the crystallinity.

The effect of a rigid filler on the modulus of rubbers, on the other hand, can be estimated by theories of Guth and Smallwood,[8,9] Kerner,[10] Van der Poel,[11] and others.[12] The agreement between the various theories is not good. All agree, however, that the influence of the filler on the modulus of the matrix can be expressed as a multiplicative function, of the volume fraction, ϕ, of the filler. The theory proposed here becomes

$$G = (dRT/\bar{M}_c)F(\phi) \tag{2}$$

in which ϕ is the volume fraction of crystallites. The second half of the problem of applying the present theory is the expression of $F(\phi)$ as a function of crystallinity.

It is not the purpose of this paper to derive the functional form of F. Comparison of the various theories shows that for the ranges of crystallinity involved, they do not differ radically. The principal influence of the filler is due to ϕ itself. Here the Guth-Smallwood theory is assumed as typical:

$$F(\phi) = 1 + 2.5\phi + 14.1\phi^2 \tag{3}$$

Then the modulus of a crystalline rubber becomes:

$$G = (dRT/\bar{M}_c)(1 + 2.5\phi + 14.1\phi^2) \tag{4}$$

A calculation of the modulus of a partially crystalline rubber is carried out for the case of a copolymer in which the crystallizable sequences of (A) monomeric units are broken up by noncrystallizable (B) monomeric sequences. Individual polymer molecules are assumed to have infinite length. For simplicity it is assumed also that during the formation of the copolymer the probability that an A (or B) unit be added to the growing chain was constant and equal to the mole fraction of component A (or B respectively) in the copolymer. Stated otherwise, given any unit of a copolymer chain, the probability that the next unit be an A unit is constant and equal to X_A, in which X_A is the mole fraction of component A. Similarly the probability that the next unit be a B unit is X_B, the mole fraction of component B.

For such a random copolymer the fraction, $n_A(m)$, of material A contained in sequences m units long is:[13,14]

$$n_A(m) = (1 - X_A)X_A^{m-1} \tag{5}$$

The weight fraction of material A contained in sequences exactly m units long is:

$$w_A(m) = m(1 - X_A)^2X_A^{m-1} \tag{6}$$

Analogous equations hold for the B sequences.

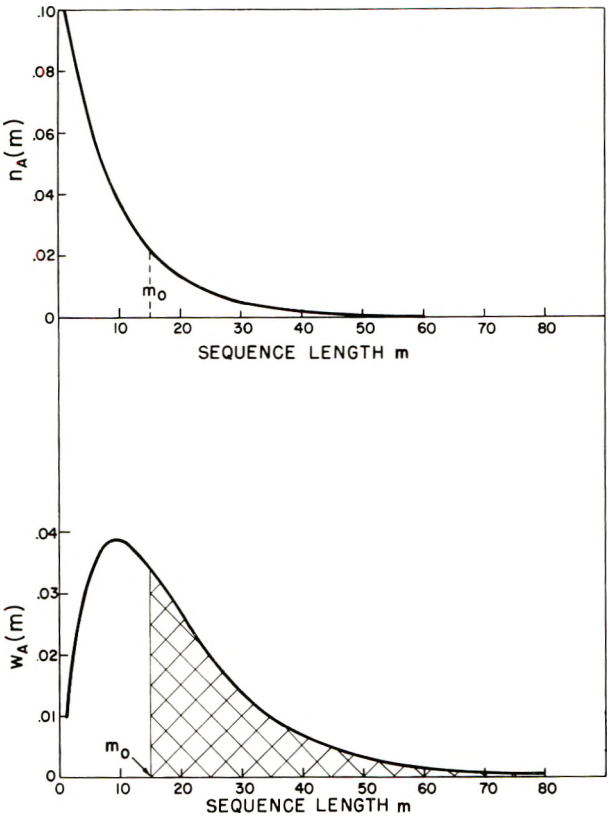

Fig. 1. The distribution of A sequence lengths in a copolymer containing 90 mole-% of a crystallizable comonomer A: (top) the number distribution of sequences, $n_A(m)$; (bottom) the weight distribution of sequences, $w_A(m)$.

Long sequences of A units crystallize at higher temperatures than shorter sequences of A units. Under the assumption that at a given temperature all but only A sequences of length m_0 units or longer are contained in crystallites, the weight fraction of material A in crystallites is:

$$f_A(m_0) = m_0 X_A^{m_0-1} - (m_0 - 1) X_A^{m_0} \tag{7}$$

If W_A is the weight fraction of component A in the copolymer, the crystallinity, w_c, is:

$$w_c = W_A f_A(m_0) \tag{8}$$

The quantity m_0 is a function of the temperature which increases without bounds at the melting point of the polymer. The quantities $n_A(m)$ and $W_A(m)$ are illustrated in Figure 1 for a random copolymer containing 90 mole-% A and for which the molecular weight of A units and B units is equal. The shaded area represents $f_A(m_0)$ for $m_0 = 15$. The crystallinity in this case is 49.6%.

The amorphous phase consists of all of the sequences of B units together with those sequences of A units that are less than m_0 long. While each crystalline sequence contains only A units, amorphous sequences may consist of many subsequences alternately of A and of B units. However, the number of amorphous sequences is equal to the number of crystalline sequences. Hence the knowledge of the $n_B(m)$ and of the $n_A(m)$ curves is sufficient to determine the number-average amorphous sequence length and the relative number of amorphous crosslinks as a function of m.

For example, since the relative number of amorphous sequences is equal to the relative number of crystalline sequences, it is proportional to the area under the $n_A(m)$ curve to the right of the line $m = m_0$. The relative number of A sequences of length m_0 or over is

$$R = \sum_{m=m_0}^{\infty} X_B X_A{}^{m-1} / \sum_{n=1}^{\infty} X_B X_A{}^{n-1} = X_A{}^{m_0-1} \tag{9}$$

This quantity R is also the relative number of chains in the amorphous region. The total relative length L represented in the amorphous region by both A and B is

$$L = \sum_{m=1}^{m_0-1} m X_B X_A{}^{m-1} + \sum_{m=1}^{\infty} m X_A X_B{}^{m-1} \tag{10}$$

$$= \frac{(m_0 - 1)\, X_A{}^{m_0+1} - m_0 X_A{}^{m_0} + 1}{X_A(1 - X_A)}$$

The average amorphous sequence length l_a is

$$l_a = L/R = [(X_A{}^{m_0+1} - 1)/X_A{}^{m_0}(X_A - 1)] - m_0 \tag{11}$$

The number-average molecular weight $\bar{M}_c$ of an amorphous chain is

$$\bar{M}_c = \left\{ \frac{M_A[(m_0 - 1)\, X_A{}^{m_0} - m_0 X_A{}^{m_0-1} + 1]}{1 - X_A} + \frac{M_B}{1 - X_B} \right\} \Big/ R \tag{12}$$

$$\bar{M}_c = M_A \left[\frac{1 - X_A{}^{m_0+1}}{X_A{}^{m_0}(1 - X_A)} - m_0 - \frac{1 - r}{X_A{}^{m_0}} \right] \tag{13}$$

where $r = M_B/M_A$ and M_A is the molecular weight of an A unit and M_B is the molecular weight of a B monomeric unit.

The ratio of the weight of the amorphous material to the weight of the crystalline material is:

$$R = \left[\frac{M_A\,[1 - f_A(m_0)]}{1 - X_A} + \frac{M_B}{1 - X_B} \right] \Big/ \left[\frac{M_A f_A\,(m_0)}{1 - X_A} \right] \tag{14}$$

Hence

$$\phi = \frac{1}{1 + (d_c/d_a)R} \tag{15}$$

in which d_c is the density of the crystalline regions and d_a is the density of the amorphous regions.

The values of $\bar{M}_c$ from eq. (13) and the value of ϕ from eq. (15), when substituted in eq. (4), admits the calculation of G.

Discussion

The new idea presented here is that the modulus of a partially crystalline rubber is changed due to the cross-linking effect of the crystallites and due to the effect of the crystallites acting as rigid fillers. The application of the theory revolves about the computation of $\bar{M}_c$ and of $F(\phi)$. By assuming a particular type of copolymer and a particular crystallization model, a rather simple form was derived for the modulus that nevertheless predicted a remarkably improved fit to existing experimental data. Obviously other forms of the dependence of $\bar{M}_c$ and of $F(\phi)$ could similarly be used. However, the dependence used here has the desirable feature that if the crystallinity is known, then the modulus is uniquely determined.

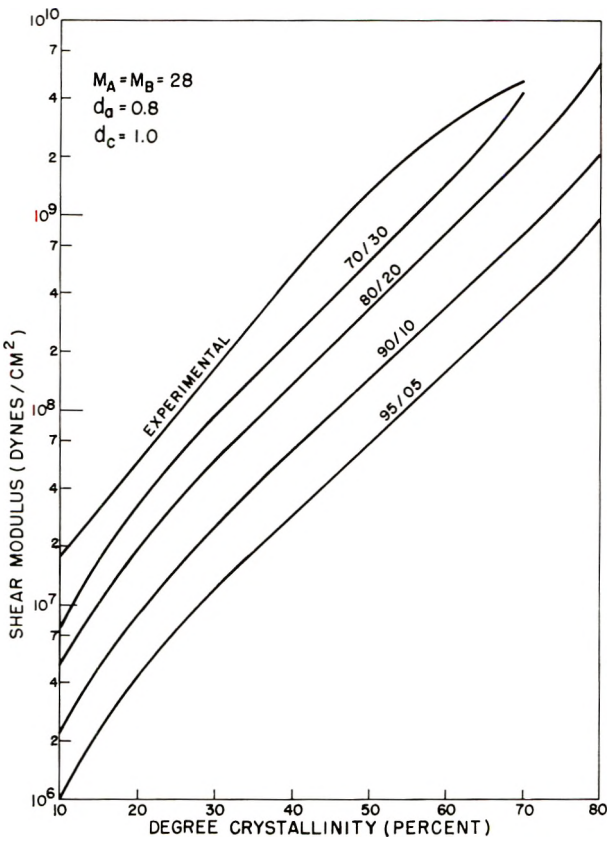

Fig. 2. Calculated values of shear modulus as a function of degree of crystallinity for copolymers of molar ratios indicated on the curves. The curve giving the maximum value of shear modulus as found experimentally is the upper curve.

The calculation of the modulus has been programmed for the IBM-650 computer. Typical results are given in Figure 2. The values used in the calculations were $M_A = M_B = 28$, density of the crystalline phase equals 1.00, and the density of the amorphous phase equals 0.80. These might be considered typical values for a polyethylene copolymer. Also shown in Figure 2 is the crude empirical relation found for ethylene copolymers and other polymers.[1] The numbers on the curves refer to the molar composition ratio X_A/X_B of the copolymers. The shapes of the theoretical curves are very similar to the shape of the empirical curve. Over a modulus range of a thousand to one, the theoretical values agree with the experimental values within a factor of five or ten. This agreement is considered quite good as the experimental curve is for the maximum values found for the modulus in most cases. In some cases the observed modulus values were as much as five times smaller than the maximum experimental values given in Figure 2. At high degrees of crystallinity the experimental curve is shown as having a curvature opposite to that of the theoretical curves. Actually it was found for polyethylenes which had moduli well below the maximum curve that the curvature was the same as the theoretical curves.

It seems appropriate at this point to ascertain the contribution to the obtained fit of the change in $\bar{M}_c$ as compared to the contribution of the reinforcement factor. To this end Table I was constructed. In Table I the ratio of $G_0 = RT\,d/\bar{M}_c$ at the indicated per cent crystallinity to the G_0 at a reference crystallinity (about 1%) was compared to the ratio of F at the indicated crystallinity to the F at the reference crystallinity.

TABLE I
Component Influence for Composition $X_A/X_B = 90/10$

Approx. crystallinity, %	$G_0/G_0(1\%)$	$F/F(1\%)$
1	1	1
10	1.705×10	1.272
20	5.0×10	1.823
30	9.63×10	2.74
40	1.715×10^2	3.54
50	2.77×10^2	4.71
60	4.72×10^2	6.29
70	8.70×10^2	8.37
80	1.78×10^3	1.075×10

The composition ratio was 90/10. The figures used were taken directly without interpolation from a table generated by a computer. The actual crystallinity was the value in the table nearest the crystallinity indicated in Table I. Although the figures in the second column vary with the composition, the orders of magnitude do not change. These may be taken as representative.

Experimentally also, the modulus decreases with temperature for crystalline polymers,[1] while the kinetic theory of rubber predicts the opposite effect.[6] In this theory part of the predicted increase in modulus with temperature is compensated for by the differences in coefficients of expansion of the crystalline and amorphous phases. Even at a constant degree of crystallinity the volume fraction of the crystalline phase decreases with an increase in temperature. Calculations show that in general this effect is not great enough to compensate for the increase in theoretical modulus predicted by the kinetic theory of rubber. However, it requires only a slight decrease in degree of crystallinity with an increase in temperature to have a negative temperature coefficient of the modulus.

In general our theory predicts a modulus less than the observed values. There are several reasons why this is to be expected. At crystallinities above about 40% the crystallites should impinge upon one another and form a continuous crystalline phase.[15] A continuous crystalline phase should produce a higher modulus than when the crystallites are only a dispersed phase.[10] Also, at the higher crystallinities many of the amorphous sequences are very short so that non-Gaussian behavior should become evident. Such non-Gaussian chains should be stiffer than those that rubber theory predicts. Finally, at low degrees of crystallinity the effects of chain entanglements are neglected in the theory. For many uncrosslinked amorphous rubbers the effect of chain entanglements is to give a shear modulus of the order of 3×10^6 dynes/cm.^{2} when measured by a dynamic mechanical test at 1 cycle/sec. If the effect of chain entanglements were added to the crosslinking effect of the crystallites, much better agreement would be found between the theory and experiment. However, to do this at present requires the addition of an arbitrary factor to the theory.

The theory has been developed for crystallizable copolymers. However, it should hold just as well for random (but not block) stereo-regular polymers where the mole fraction of component A is replaced by the tacticity of the polymer. Anything which breaks up the polymer chain to prevent crystallization (change in stereo configuration, chain entanglements, etc.) could be considered as a noncrystallizable B-unit.

The quantity m_0 is related to the temperature by an equation such as the one developed by Flory,[5] by a Garner-type equation,[16] or by a relation such as that used by Miller.[17] When the theoretical elastic modulus is plotted against temperature, curves similar in shape to the experimental curves are obtained. However, for a given value of the modulus, the theoretical value of m_0 is less than one would expect. This is in keeping with the fact that the theoretical modulus is less than the experimental modulus for a given crystallinity.

References

1. Nielsen, L. E., *J. Appl. Polymer Sci.*, **2**, 351 (1959).
2. McCrum, N. G., *ASTM Bull., No.* **242**, 80 (1959).
3. Riser, G. R., and L. P. Witnauer, *S.P.E. Trans.*, **2**, 7 (1962).

4. Bueche, F., *J. Polymer Sci.*, **22,** 113 (1956).
5. Flory, P. J., *Trans. Faraday Soc.*, **51,** 848 (1955).
6. Treloar, L. R. G., *The Physics of Rubber Elasticity*, 2nd Ed., Clarendon Press, Oxford, 1958, Chap. 4.
7. Flory, P. J., *Principles of Polymer Chemistry*, Cornell Univ. Press, Ithaca, N. Y., 1953, Chap. 11.
8. Smallwood, H. M., *J. Appl. Phys.*, **15,** 758 (1944).
9. Guth, E., *J. Appl. Phys.*, **16,** 20 (1945).
10. Kerner, E. H., *Proc. Phys. Soc. (London)*, **69B,** 808 (1956).
11. Van der Poel, C., *Rheol. Acta*, **1,** 198 (1958).
12. Bueche, A. M., *J. Polymer Sci.*, **25,** 139 (1957).
13. Alfrey, T., Jr., J. Bohrer, and H. Mark, *Copolymerization*, Interscience, New York, 1952.
14. Miller, R. L., and L. E. Nielsen, *J. Polymer Sci.*, **46,** 303 (1960).
15. Hoffman, J. D., J. J. Weeks, and W. M. Murphey, *J. Res. Natl. Bur. Std.*, **63A,** 67 (1959). Quotes unpublished calculations of J. I. Lauritzen, Jr.
16. Garner, W. E., K. van Bibber, and A. M. King, *J. Chem. Soc.*, **1931,** 1533.
17. Miller, R. L., *J. Polymer Sci.*, **57,** 975 (1962).

Résumé

On a développé une nouvelle théorie du module d'élasticité des polymères cristallins pour des températures supérieures à la transition vitreuse. Cette théorie se base sur la supposition que les cristallites se comportent comme des ponts et comme une charge rigide. Le module de cisaillement G est fourni par l'expression $G = (d\,RT/\bar{M}_c)F$, ou F est un facteur donnant l'augmentation relative du module au volume des cristallites rigides. Le poids moléculaire moyen en nombre $\bar{M}_c$ des séquences amorphes est calculé comme une fonction du degré de cristallinité suivant la théorie des polymères. Les valeurs théoriques du module en tant que fonction du degré de cristallinité sont en bon accord sur un large domaine avec les valeurs expérimentales.

Zusammenfassung

Eine neue Theorie des Elastizitätsmoduls kristalliner Polymerer bei Temperaturen oberhalb der Glasumwandlung wurde entwickelt. Die Theorie beruht auf der Annahme, dass sich die Kristallite wie Vernetzungsstellen und starre Füllstoffe verhalten. Der Schermodul G wird durch $G = (dRT/\bar{M}_c)F$ gegeben, wo F ein Faktor für die relative Zunahme des Moduls durch das Volumen der starren Kristallite ist. Das Zahlenmittel des Molekulargewichts $\bar{M}_c$ der amorphen Sequenzen wird als Funktion des Kristallinitätsgrades aus der Copolymerisationstheorie berechnet. Die theoretischen Werte des Moduls stimmen als Funktion des Kristallinitätsgrades mit den experimentellen Werten über einen weiten Bereich recht gut überein.

Received June 6, 1962

JOURNAL OF POLYMER SCIENCE: PART A VOL. 1, PP. 2003–2011 (1963)

Changes in the Stereospecificity of a Ziegler Catalyst Used in the Polymerization of Butadiene*

CHARLES R. McINTOSH, WILLIAM D. STEPHENS, and CURTIS O. TAYLOR, *Thiokol Chemical Corporation, Redstone Division, Huntsville, Alabama*

Synopsis

As a part of a program involving synthesis of various rubbers, the stereospecific polymerization of butadiene was studied. A Ziegler catalyst composed of cobaltous chloride, triethyl aluminum and aluminum chloride in benzene was used. The effect of catalyst age on stereospecificity of the polymers produced was observed over a period of nearly two years. Freshly prepared catalyst appears as a straw-yellow liquid over black insoluble solids. Within a few weeks a black separate liquid phase begins to form at the bottom of the catalyst. The amount of the dark lower layer increases on standing until all of the solids have been dissolved. Polymers prepared from the upper layer of catalyst showed decreasing percentages of *cis*-double bonds, an effect which was linear up to approximately one year. From one to two years, the upper layer produced polymers which were essentially constant at 70% *cis*-olefinic bonds. In contrast, the dark lower layer of catalyst yielded polymers which were high in *cis*-content (greater than 95% *cis*-bonds) over the entire period of the study.

INTRODUCTION

The synthesis of *cis*-polybutadiene was undertaken as a part of an overall program of polymer evaluation. The particular Ziegler catalyst chosen for this investigation is one which has not been extensively investigated. It is composed of cobaltous chloride, aluminum chloride, and triethyl aluminum. In general the catalysts were prepared in benzene in a dry box and were then transferred to the reaction flask. Highly purified butadiene was then bubbled into the flask until the benzene solution of the catalyst was saturated. The polymer was isolated by pouring the reaction mixture into isopropyl alcohol. It was noted during the synthesis of the polymer samples that if the catalyst was allowed to stand for several weeks, a dark insoluble liquid separated from the catalyst solution. The formation of the dark lower layer continued until all of the solids present in the catalyst system were dissolved. Usually the clear straw-yellow upper layer was used in polymerization of butadiene, and it was noted that the catalyst tended to lose stereospecificity after standing for a time. When a sample

* This work was supported by Army Ordnance Contract DA-01-021-ORD-11919 and was presented at the 81st Meeting of the American Chemical Society's Division of Rubber Chemistry, Boston, Mass., April 27, 1962.

of the dark lower catalyst layer was used in a polymerization reaction it was discovered that the percentage of *cis*-double bonds in the polymer was higher than the percentage of *cis*-bonds in polymer formed from the aged upper layer of catalyst. It was decided to study the effect of catalyst age on stereospecificity of both the upper and lower layers of catalyst.

EXPERIMENTAL

Preparation of the Catalyst

The Ziegler-Natta catalyst used in these studies was prepared from cobalt chloride, aluminum chloride, and triethyl aluminum. All transfers of the chemicals and reagents used in the preparation of this catalyst were done under conditions which exclude all moisture and oxygen. Where possible, all transfers, weighing, etc., were performed in a dry box which had been thoroughly purged and filled with prepurified nitrogen. The various reagents used and their subsequent purification are described below.

Cobalt chloride ($CoCl_2 \cdot 6H_2O$, Merck and Company, reagent grade) was heated at 130–140°C. under vacuum for 5–6 hr. on a rotary evaporator and stored in a closed container in a dry box.

Aluminum chloride (Matheson, Coleman, and Bell, anhydrous, purified powder) was used as received but, insofar as possible, a freshly opened bottle was used for each catalyst preparation.

Triethyl aluminum (Ethyl Corporation) was used as received. The triethyl aluminum was transferred from the 10 lb. shipping container through copper and stainless steel tubing, to a 250-ml. bottle fitted with a stopcock and serum cap.

Benzene (Baker and Adamson, reagent grade) was further purified by washing first with concentrated sulfuric acid, then with water to neutrality, and was then dried over anhydrous calcium chloride or "Drierite." The benzene was then distilled from calcium hydride under a blanket of dry nitrogen into a bottle containing calcium hydride and purged with dry nitrogen for 1–2 hr. The benzene was stored in 2-l. bottles, and each bottle was fitted with 24/40 stopper having an attached stopcock and serum cap to facilitate removal of the benzene without exposure to the atmosphere. All transfers of benzene from this bottle were done by exerting a positive nitrogen pressure in the bottle forcing the benzene through a length of stainless steel hypodermic tubing.

Nitrogen (Matheson Company, prepurified) was used in the dry box and as a protective blanket for all transfers and polymerizations.

In the dry box cobalt chloride (5 g., 38.5 mmoles) and aluminum chloride (5 g., 38.5 mmoles) were weighed into a dry 250 ml. bottle fitted with a stopcock and serum cap. A clean, dry, Teflon covered magnetic stirring bar was placed in the bottle at the same time. The tightly stoppered bottle was then removed from the dry box and purged with a stream of dry nitrogen for 1–2 hr. by inserting a 12-in., 20 gauge hypodermic needle through the serum cap to within 1 in. of the bottom of the bottle. Pre-

purified nitrogen was forced into the bottle through this needle and allowed to exhaust through a shorter needle placed in the same serum cap. By stirring and continued purging with nitrogen, dry benzene (100 ml.) was pumped into the catalyst bottle through hypodermic tubing. Triethyl aluminum (5 ml., 37 mmoles) was removed from the storage bottle by applying a slight positive nitrogen pressure on the bottle, forcing the aluminum alkyl into a hypodermic syringe. The alkyl was then transferred to the catalyst bottle with the syringe. When this operation was performed with caution, little alkyl was lost during the transfer and the fire hazard was minimized. The alkyl remaining in the syringe and needle was decomposed by rinsing with reagent grade benzene followed by benzene-isopropyl alcohol. All glassware and equipment were dried in a 130° oven for 24 hr. and then allowed to cool in a stream of dry nitrogen. Upon addition of the alkyl to the catalyst bottle, the mixture immediately turned black, but no exotherm was noted. Stirring and purging with nitrogen was continued for 30–45 min. When the stirring was discontinued, the black solids settled, leaving a straw-yellow liquid which is the active polymerization catalyst.

Stereospecific Polymerization of Butadiene

The polymerizations were usually performed in a 1-l., three-neck, round-bottom flask fitted with spherical ground-glass joints. The flask was also fitted with a mechanical stirrer, a glass dip tube extending nearly to the bottom of the flask, a gas entry tube for purging the surface of the liquid with nitrogen, and an outlet tube leading to a silicone oil bubbler trap. A catalyst addition tube fitted with a serum cap was incorporated in the exit tube system by means of a three-way stopcock. The flask and attached glassware were assembled hot (using a silicone stopcock grease) and allowed to cool while being purged with nitrogen. Approximately 500 ml. of dry benzene was pumped into the flask through the serum cap by means of hypodermic tubing, as described above. Since the addition of the catalyst to a saturated solution of butadiene in benzene resulted in extremely rapid and exothermic reactions, which were difficult to control (in less than 3 min. the polymer growth was so great that there was danger of rupturing the reaction vessel), a reverse addition technique was used. The catalyst (1–2 ml.) was added to the benzene in the reaction flask, and butadiene (Phillips Petroleum Company, special purity grade) was then passed through a purification train and then into the benzene solution of catalyst. The purification train contained two columns packed with indicating "Drierite," one column packed with Linde Molecular Sieves (Type 4A, 1/16-in. pellets) and a fritted glass bubble-type gas washing column containing 25 ml. of triethyl aluminum in 250 ml. of dry *n*-dodecane. The butadiene was added during 30–45 min., after which time the benzene was completely saturated. The polymerization was allowed to proceed until the viscosity of the reaction mixture was noticeably increased or until polymer collected around the stirrer shaft. Termination of the reaction was effected by the

addition of 25 ml. of a 20% solution of isopropyl alcohol in benzene. On addition of the quenching agent, the reaction mixture turned light blue-green in color. The polymer was isolated by pouring the reaction mixture into isopropyl alcohol containing 1–2% *N*-phenyl-β-naphthylamine. The precipitated polymer was removed by filtration and dried under vacuum at 35–40° during 24 hr. The percentages of *cis*-1,4-, *trans*-1,4-, and vinyl bonds were determined by infrared spectroscopy using a method which is essentially that of Silas, Yates, and Thornton[1] with the exception that the percentages are normalized to 100%. Thus 97% *cis*-1,4-poly-butadiene means that 97% of the olefinic bonds present are of the *cis*-configuration. The percentages of unsaturation were determined by the method of Lee, Kolthoff, and Mairs.[2] Intrinsic viscosity was measured in benzene solution at 30°.

Comparison of Catalyst Layers

Butadiene polymers were prepared using the clear upper layer of a cobalt chloride—aluminum chloride–triethyl aluminum catalyst which had been stored for periods ranging up to 2 yr. For periods up to 1 yr., the percentages of *cis*-1,4-, *trans*-1,4-, and vinyl double bonds were found to vary with the age of the catalyst with which the polymer was produced. Between 1–2 yr., the upper catalyst layer gave polymers with more or less constant composition (approximately 70% *cis*-1,4-bonds). Table I gives a summary of the properties of polymers prepared from the upper catalyst layer. The upper layer of catalyst may be used for any period of time up to about 2 mo., without any significant decrease in the stereospecificity, reactivity, or yield. The decrease in the percentage of *cis*-1,4-bonds with age is shown graphically in Figure 1.

The dark lower layer of the aged Ziegler catalyst was used to prepare butadiene polymers and the percentage of *cis*-1,4-, *trans*-1,4-, and vinyl

TABLE I
Properties of Polymers Prepared with the Upper Layer of an Aged Ziegler Catalyst

Catalyst age	Reaction time	Yield	(%) *cis*-1,4	(%) *trans*-1,4	(%) vinyl	$[\eta]$	(%) Ash	(%) Unsaturation
1 hr.	17 min.	8.1 g.	96	2	2	1.4	0.27	100
1 day	98 "	13.0 "	97	1	2	1.6	0.035	92
2 "	45 "	30.7 "	97	1	2	2.4	0.07	95
7 "	70 "	30.1 "	97	2	1	5.2	0.00	98
24 "	32 "	33.2 "	95	2	3	1.2	0.006	97
69 "	30 "	9.0 "	95	1	3	1.0	0.015	93
91 "	112 "	17.6 "	93	3	4	—	——	—
111 "	20 hrs.	2.7 "	91	5	5	—	0.17	—
228 "	19 hrs.	1.3 "	86	9	5	—	——	—
347 "	66 hrs.	3.0 "	70	25	4	1.5	0.25	63
669 "	26 hrs.	4.0 "	67	28	5	0.6	0.14	61

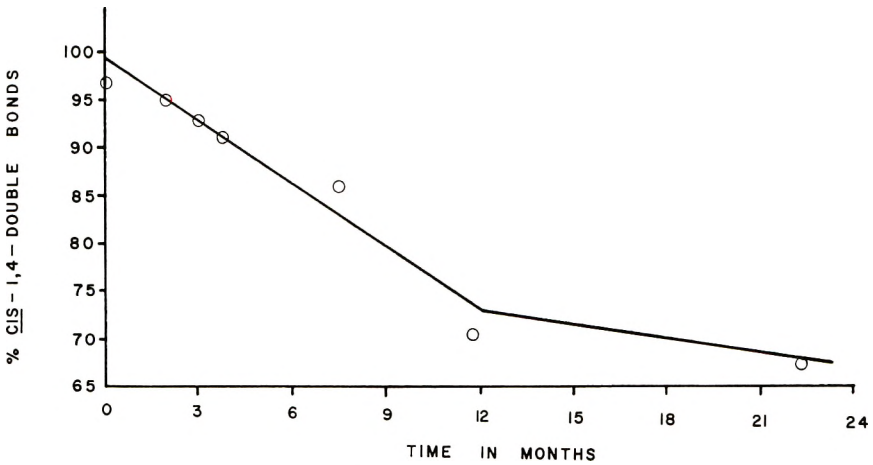

Fig. 1. Change in per cent of *cis*-1,4-double bonds in polybutadiene as a function of the age of the catalyst used in the polymerization. All polymerizations done using the upper layer of catalyst.

groups were determined on polymers made from catalysts of various ages. Table II gives a summary of the properties of various polymers formed from the bottom layer of these catalysts. That the reactivity of the lower layer is not drastically diminished with age is demonstrated by a comparison of the reaction times and yields shown in Table II.

The stereospecificity of the lower layer is unchanged over a long period of time as shown in Figure 2. This result was somewhat surprising in view of the behavior of the clear-yellow upper-layer catalyst. A comparison of Figure 1 and Figure 2 shows that while the percentage of *cis*-1,4 units for

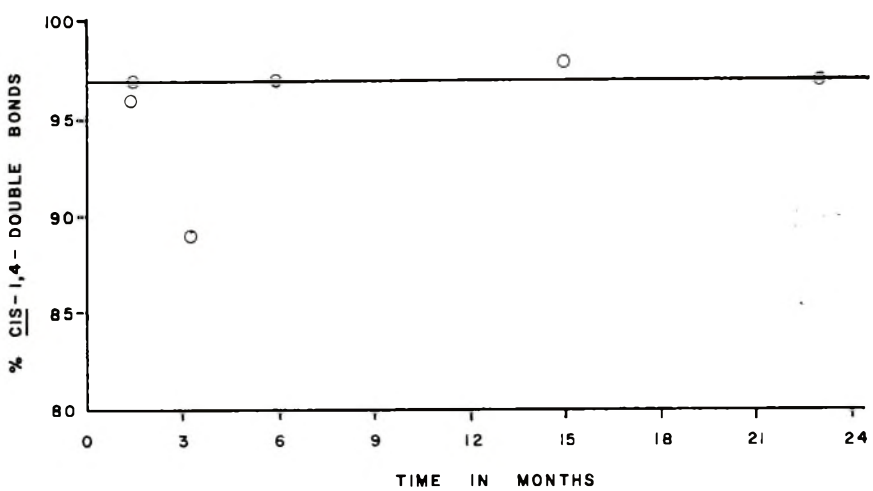

Fig. 2. Change in per cent of *cis*-1,4-double bonds in polybutadiene as a function of the age of the catalyst used in the polymerizations. All polymerizations done using the lower layer of catalyst.

TABLE II
Properties of Polymers Prepared with the Lower Layer of an Aged Ziegler Catalyst

Catalyst age	Reaction time	Yield	(%) *cis*-1,4	(%) *trans*-	(%) Vinyl	[η]	(%) Ash	Unsaturation (%)
42 days	9 min.	13.6 g.	96	2	2	——	——	—
43 "	14 "	—— "	97	1	2	1.5	0.24	92
103 "	95 "	1.7 "	89	2	9	0.94	0.3	88
179 "	35 "	5.1 "	97	1	2	——	——	—
450 "	35 "	4.4 "	98	1	1	0.62	0.065	80
696 "	22 "	6.0 "	97	2	1	——	0.53	—

the upper layer falls from 97 to 70 during 2 yr. the lower layer retains its ability to produce 97% *cis*-1,4 polymers during the entire period.

Studies on the Nature of the Lower Layer of Catalyst

In the freshly prepared catalyst, there remain fairly large quantities of undissolved solids (cobalt chloride along with some aluminum chloride). In order to determine if a lower layer would form in the absence of the undissolved solids a sample of the clear upper layer of a 3-week old catalyst was removed and stored in a sealed tube. After eleven months no lower layer was noted in the sample. This experiment indicates that the lower layer is formed only at the expense of the undissolved solids, primarily cobalt chloride, found in the fresh catalyst. The isolated upper layer was used to produce a sample of polybutadiene which proved to have 97% *cis*-1,4-olefinic bonds. Although in this experiment the reaction time was somewhat longer, several hours, no decrease in stereospecificity was noted.

After an attempt to distil the lower catalyst layer in the dry box had yielded only benzene, a two month old catalyst was filtered to give a filtrate composed of the upper and lower layers and an insoluble solid. The solid was washed several times with dry benzene in the absence of air and polymerization was attempted using the solid as the catalyst. The polymers formed from the solid, the upper and lower layers all proved to be high in *cis*-1,4 content (see Table III).

The results of cobalt and aluminum analyses on the upper and lower layers of catalysts of various ages are presented in Table IV. These data are rather inconsistent but do fit the general picture of what might be expected on the basis of results obtained on analysis of the microstructure of the polymers and on the yields of polymer obtained. There is a general decrease in the amount of cobalt and aluminum in the upper layer of catalyst on aging although the cobalt content of the lower liquid layer remains fairly constant and at a level considerably higher than that of fresh catalyst.

DISCUSSION OF RESULTS AND CONCLUSIONS

There have been few instances in the literature in which Ziegler catalysts prepared from these particular components have been discussed,[3-10] and

TABLE III
Properties of Polymers Prepared from Various Fractions of Aged Zielger Catalysts

Fraction	Catalyst age	Reaction time	Yield	(%) *cis*-1,4	(%) *trans*-1,4	(%) Vinyl	[η]	(%) Ash	(%) Unsaturation
Aged upper Layer isolated from solids	11 months	18 hrs.	3.8 g.	97	1	1	——	0.30	—
			Filtered catalyst						
Upper layer	2 months	1 hrs.	18.0 g.	96	1	3	2.92	0.65	96
Lower layer	2 "	0.5 "	8.0 "	97	1	2	——	0.12	—
Solids	2 "	1 "	8.0 "	98	2	1	——	0.37	92

very few references have been made to the effect of age on the stereospecificity of Ziegler catalysts. Generally, when using the "soluble" catalysts the clear supernate is used to the exclusion of the undissolved solid, and usually the batch of catalyst is consumed or discarded before the darkly colored lower layer has had time to develop.

TABLE IV
Cobalt and Aluminum Analysis of Aged Zielger Catalysts

Catalyst Age (days)	Upper layer (%) Co	Upper layer (%) Al	Lower layer (%) Co	Lower layer (%) Al
1	0.19	2.02	—	—
21	0.27	0.63	5.36	0.681
300	0.037	—	2.54	—
325	0.032	0.396	4.53	1.94

The effects of aging on the two phases of this catalyst system have been discussed above and the results of this work have indicated that selected portions of the catalyst can be used to produce stereoregular polymers after storing indefinitely. Attempts to discern the nature of the darkly colored lower layer of the catalyst have met with little success; however, limited evidence indicates that it is probably a complex with benzene. In addition, it was found that the clear upper layer of catalyst retained its stereospecificity with age if it was stored in the absence of undissolved solid components, which would indicate that different catalysts are involved.

Since many stereospecific catalysts are made *in situ* or a new catalyst is prepared for each batch of polymer, synthesis of small amounts of *cis*-1,4 polymers with such catalysts is troublesome. With a knowledge of the features of the cobalt chloride-aluminum chloride-triethyl aluminum system one can prepare a sample of catalyst and store it for future use. Stereospecific polymers may be obtained for many months by use of the lower catalyst layer.

References

1. Silas, R. S., J. Yates, and V. Thornton, *Anal. Chem.*, **31**, 529 (1959).
2. Lee, T. S., I. M. Kolthoff, and M. A. Mairs, *J. Polymer Sci.*, **3**, 66 (1948).
3. Brockway, C. E., and A. F. Ekar, to Goodrich-Gulf Chemicals, Inc., U. S. Patent 2,977,349 (Mar. 28, 1961).
4. Goodyear Tire and Rubber Company, British Patent 859,698 (Jan. 25, 1961).
5. Montecatini, Italian Patent 587,968 (Jan. 27, 1959).
6. Chemische Werke Huls, A. G., British Patent 779,111 (July 17, 1957).
7. Anderson, W. S., to Shell Oil Company, U. S. Patent 2,970,134 (Jan. 31, 1961).
8. Longiave, C., R. Castelli, and G. F. Croce, to Montecatini, Belgian Patent 573,680 (Dec. 1958).
9. Tucker, H., to Goodrich-Gulf Chemicals, Inc., Belgian Patent 575,671 (Feb. 13, 1959).
10. Gippin, M., *Ind. Eng. Chem., Prod. Res. and Develop.*, **1**, 32 (1962).

Résumé

On étudie la polymérisation stéréospécifique du butadiène dans un programme comprenant la synthèse des divers caoutchoucs. On utilise un catalyseur Ziegler composé de chlorure de cobalt, de triéthylaluminum et de chlorure d,aluminium dans le benzène. On a observè l'effet de vieillissement du catalyseur sur la stéréospécificité du polymère produit le long d'une période d'environ deux ans. Le catalyseur fraîchement préparé apparaît comme un liquide jaune pâle au-dessus d'un solide noir insoluble. Après quelques semaines une phase liquide noire séparable commence à se former au fond du catalyseur. La quantité de la couche noire inférieure augmente en laissant reposer jusqu'a ce que tout le solide soit dissous. Les polymères préparés à partir de la couche supèrieure de catalyseur montrent un pourcentage décroissant de doubles liaisons *cis*, effet qui est linéaire pendant approximativement un an. A partir d'un an ou deux ans, la couche supérieure produit des polymères qui sont essentiellement constants à 70% de liaison oléfiniques *cis*. Par contre, la couche inférieure noire de catalyseur donne des polymères qui sont riches en isomère *cis* (plus que 95% de liaison *cis*) le long de toute la pèriode étudiée.

Zusammenfassung

Als Teil eines Programmes zur Synthese verschiedener Kautschuksubstanzen wurde die stereospezifische Butadienpolymerisation untersucht. Es wurde ein Zieglerkatalysator aus Kobaltschlorid, Triäthylaluminium und Aluminumchlorid in Benzol verwendent. Der Einfluss des Alters des Katalysators auf die Stereospezifität der gebildeten Polymeren wurde über einen Zeitraum von fast zwei Jahren verfolgt. Frisch bereiteter Katalysator erscheint als eine strohgelbe Flüssigkeit über schwarzem, unlöslichen Festkörper. Innerhalb einiger Wochen beginnt sich eine getrannte schwarze flüssige Phase am Boden des Katalysators zu bilden. Die Menge der dunklen unteren Schichte nimmt beim Stehen zu, bis sich alles Festes gelöst hat. Mit der oberen Katalysatorschichte hergestellte Polymere ziegten einen abnehmenden Gehalt an *cis*-Doppelbindungen und zwar linear bis zu etwa einem Jahr. Zwischen ein und zwei Jahren führte die obere Schicht zur Bildung von Polymeren mit einem im wesentlichen konstanten Gehalt von 70% *cis*-Doppelbindungen. Im Gegensatz dazu lieferte die dunkle untere Schichte des Katalysators während des gesamten Zeitraymes der Untersuchung Polymere mit hohem *cis*-Gehalt (mehr als 95% *cis*-Bindungen).

Received May 21, 1962

JOURNAL OF POLYMER SCIENCE: PART A VOL. 1, PP. 2013–2020 (1963)

Nucleating Effect on the Kinetics of Crystallization and the Spherulites of Nylon 6

MASAKAZU INOUE, *Plastics Laboratory, Toyo Rayon Company, Ltd., Tokodori, Showaku, Nagoya, Japan*

Synopsis

The kinetics of isothermal crystallization and morphology of spherulites of nylon 6 nucleated by additives were discussed. Nylon 66, polyethylene terephthalate, and some inorganic phosphor compounds were used as nucleating agents. At crystallization temperatures in the range of 205 to 180°C., crystallization occurs through one- or two-dimensional growth and heterogeneous nucleation. The rate of crystallization increases by adding nucleating agents, followed by the decrease of the induction period of crystallization. Maximum crystallinity was not always obtained by the additives used for the present study. By adding nucleating agents, the size of spherulites decreases and the distribution becomes homogeneous, independent of the crystallization temperature.

Introduction

In a previous report,[1] the author stated that the mechanism of crystallization of nylon 6 depends on the crystallization temperature. In the present paper, a study is made of the nucleating effect on crystallization kinetics and morphology of spherulites of nylon 6.

It is well known that the physical, mechanical, and chemical properties of crystalline high polymers depend on the morphology of spherulites as well as the degree of crystallization. For example, the tensile properties of nylon 66 are improved with decreasing the size of spherulites[2] and the impact strength of polyoxymethylene depends remarkably on the size of spherulites.[3] The frictional properties of polyamides are improved by a high degree of crystallinity and the fine homogeneous spherulitic structure.[4]

The specimens having fine homogeneous spherulitic structure are obtained by adding a nucleating agent to the base polymers.[5] One of the favorable agents for nucleation is high polymer.[6] However, the mechanism of nucleating high melting polymer is not always obvious.

Experimental

Description of Specimens

As a base polymer, nylon 6 which has an average molecular weight of about 15,000 was used. And as nucleating agents nylon 66, polyethylene terephthalate, titanium dioxide, and some inorganic phosphor compounds

such as lead phosphate and sodium polyphosphate were employed. The homogeneous blending of nucleating agents into the base polymer was attained by melt mixing in the extruder.

Measurements of the Crystallization Rate and the Size of Spherulites

For the measurements of crystallization rate of solid plugs, a dilatometer of 10 mm. inner diameter, 2 mm. capillary diameter and a length of 50 mm. was used. The solid plugs of 9 mm. diam. and 40 to 50 mm. length were molded and inserted into the bulb, followed by the addition of purified mercury under vacuum.[1]

The rate constant of crystallization is calculated by using the Avrami equation:

$$a = a_\infty(1 - \exp\{-Kt^n\}) \tag{1}$$

where a and a_∞ are the degree of crystallinity at time t and infinity, respectively, K is a rate constant, and n is constant depending on the mechanism of nucleation and growth of the crystal.[7]

If half-time, $t_{1/2}$, is used, K is calculated by using eq. (2).

$$K = 2.3 \log 2/(t_{1/2})^n \tag{2}$$

The shape, size, and distribution of spherulites were studied by a polarizing microscope using thin film of the polymer.

Results and Discussions

Crystallization Kinetics

When additives are blended with nylon 6, the density of the mixture depends both on the density and content of additives and on the degree of crystallinity of the base polymer. Figure 1 shows the temperature dependence of the specific volumes of the base polymer and the mixtures. If the density of the base polymer is equal to that of the mixture in the melt state, the density of the mixture in the solid state may depend only on the degree of crystallinity of the base polymer. Figure 1 shows that the specific volume of the mixture is slightly smaller than that of the base polymer both in the solid state and melt state. It indicates that the density of the mixture is affected by that of the additive. Now, the value of density is compensated by assuming that the density of mixture is equal to that of the base polymer at a given temperature in the melt state.

The induction period of crystallization decreases by adding the nucleating agent. Figure 2 is obtained by a polarizing microscope using thin film. It can be seen that the effect of the nucleating agent on the induction period is fairly large at the higher crystallization temperatures.

The dilatometric crystallization of nylon 6 nucleated by nylon 66, polyethylene terephthalate, and lead phosphate is shown in Figures 3, 4, and 5, respectively. In all cases, the melt temperature was 260°C. The

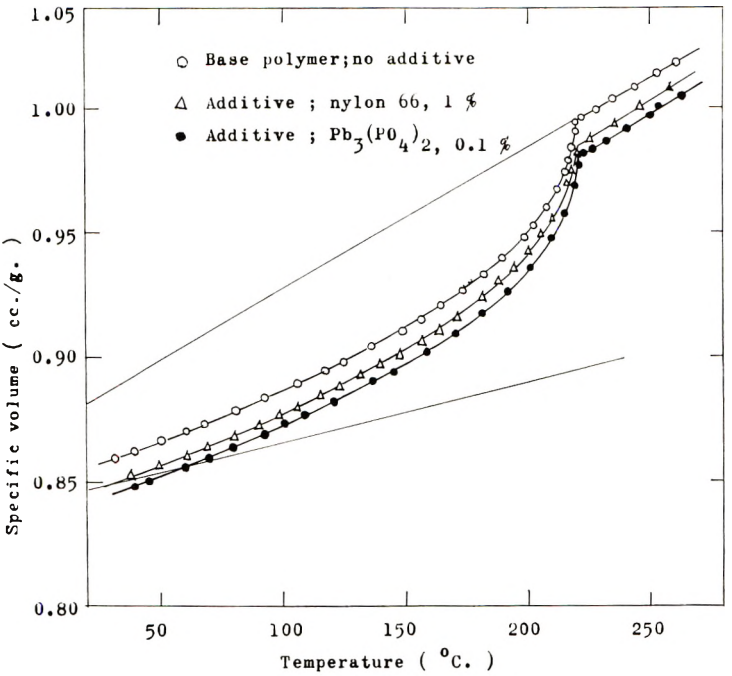

Fig. 1. Change of specific volume with temperature increase.

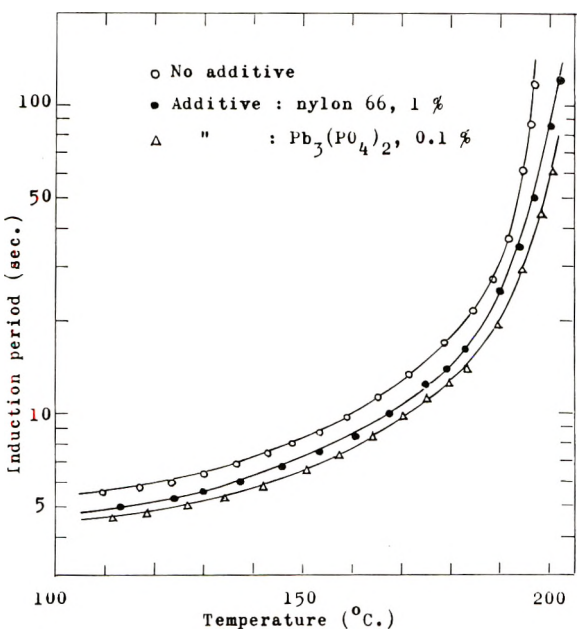

Fig. 2. Induction period of crystallization.

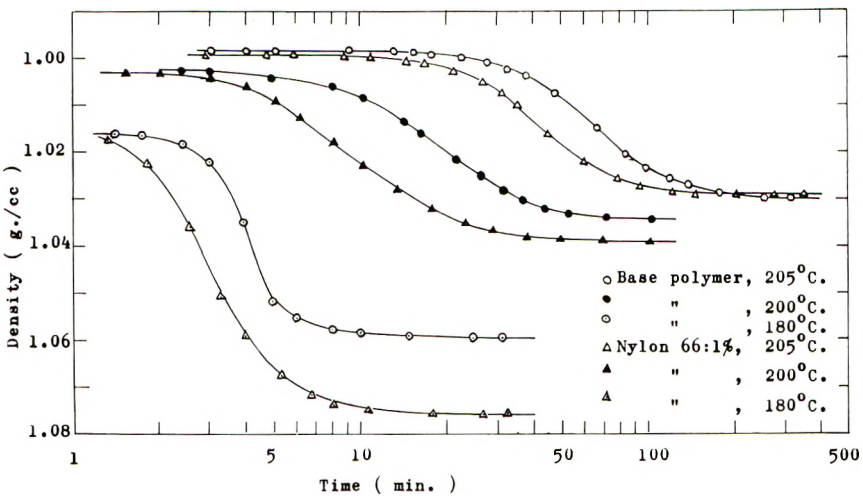

Fig. 3. Effect of nylon 66 as a nucleating agent on the crystallization isotherms of nylon 6.

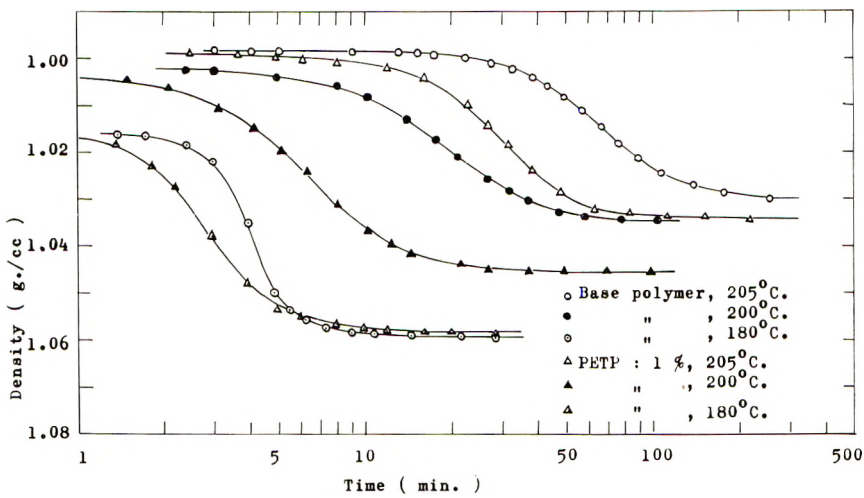

Fig. 4. Effect of polyethylene terephthalate (PETP) as a nucleating agent on the crystallization isotherms of nylon 6.

densities expressed in these figures are the compensated densities of the base polymer, which depend only on the degree of crystallinity. These figures indicate that crystallization is accelerated by adding additives. The crystallization kinetics are summarized in Table I.

The half-time, $t_{1/2}$ and rate constant K decrease owing to the nucleating crystallization by additives. The constant n, however, does not always change at various crystallization temperatures in the range of 205 to 180°C. In the previous paper,[1] it was reported that the value of n rapidly changes in the range of 207 to 210°C. Above 210°C. the value of n is 4 and below

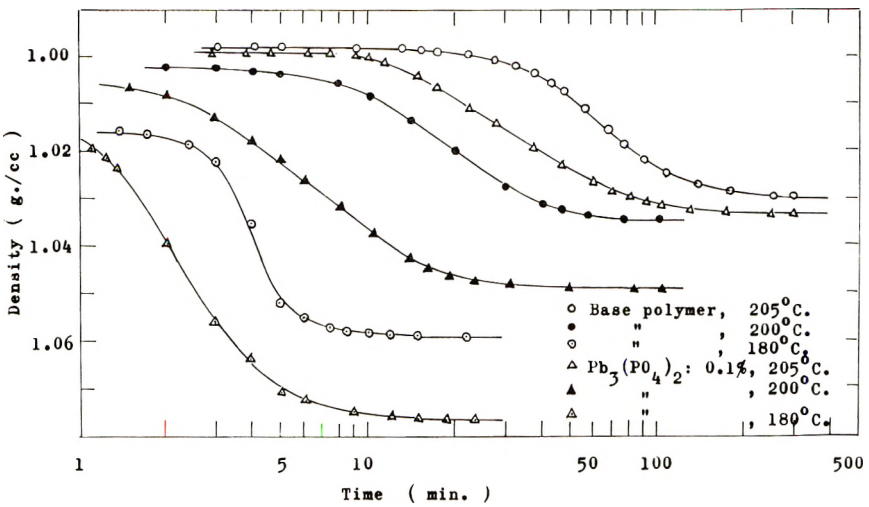

Fig. 5. Effect of $Pb_3(PO_4)_2$ as a nucleating agent on the crystallization isotherms of nylon 6.

TABLE I
Nucleating Effect on the Crystallization Kinetics and Crystallinity

Nucleating agent	%	Cryst. temp., °C.	$t_{1/2}$, min.	K, min.$^{-n}$	n	Density, g./cc.	Degree of crystn., %
Base polymer	—	205	70	1.68×10^{-5}	2.5	1.0310	28.9
		200	20	6.98×10^{-4}	2.3	1.0360	31.4
		180	4.1	3.58×10^{-2}	2.1	1.0590	30.5
Nylon 66	1	205	43	8.26×10^{-5}	2.4	1.0295	27.4
	1	200	10	3.49×10^{-2}	2.3	1.0400	35.3
	1	180	3.2	9.21×10^{-2}	2	1.0765	41.9
Polyethylene terephthalate	1	205	32	2.41×10^{-4}	2.3	1.0345	32.3
	1	200	6.5	1.37×10^{-2}	2.1	1.0460	35.1
	1	180	3	9.57×10^{-2}	1.8	1.0585	29.7
$Pb_3(PO_4)_2$	0.1	205	31	1.29×10^{-4}	2.5	1.0355	33.3
	0.1	200	6.5	1.14×10^{-2}	2.2	1.0460	35.1
	0.1	180	3.8	5.50×10^{-2}	1.9	1.0585	29.7

207°C. n is 2–2.5. It can be seen from Table I that the crystallization nucleated by additives is obviously heterogeneous nucleation; that is, the value of n is $2 \leqslant n \leqslant 3$ or $1 \leqslant n \leqslant 2$.

Table I gives the maximum density and the degree of crystallinity at each crystallization temperature. The relation of crystalline (V_c) and amorphous (V_a) specific volumes to temperature is given in eqs. (3) and (4), respectively.[8]

$$V_c = 0.8524 + 2.38 \times 10^{-4} \cdot T \tag{3}$$

$$V_a = 0.8816 + 5.64 \times 10^{-4} \cdot T \quad (4)$$

where T is the temperature (°C.).

The maximum crystallinities of nylon 6, nucleated by nylon 66, polyethylene terephthalate, and lead phosphate, are not always higher than those of the base polymer at the crystallization temperature in the range of 205 to 180°C. The additives used in this experiment give only the increasing effect on the crystallization rate.

Morphology of Spherulites

The spherulites of nylon 6 nucleated by additives at 150 and 5°C. were observed with thin film by a polarizing microscope. Figure 6 shows the photographs of spherulites. By adding the nucleating agent, the size of

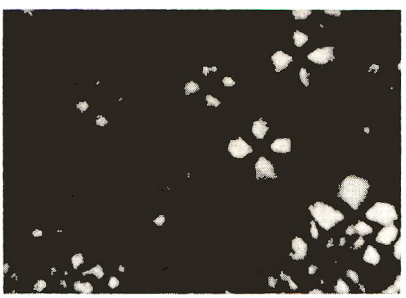

(*a*) Base polymer. 800×.

(*b*) Additive: nylon 66, 0.5%. 800×.

(*c*) Additive: $Pb_3(PO_4)_2$, 1%. 800×.

(*d*) Additive: polyethylene terephthalate, 1%. 800×.

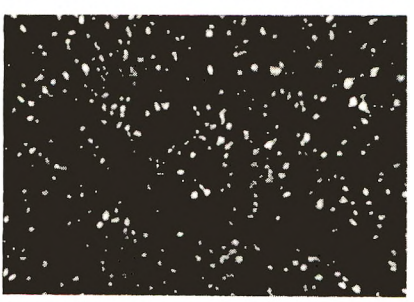

(*e*) Additive: $Pb_3(PO_4)_2$, 0.05%. 800×.

Fig. 6. Photographs of spherulites of nylon 6 nucleated by additives.

spherulites decreases and the distribution becomes homogeneous. The diameter of spherulites are given in Table II. In the base polymer, the size of spherulites varies depending on the crystallization temperature: crystallization at high temperature affords large spherulites, whereas at low temperature small spherulites are obtained. In the nucleated polymer, however, the size of the spherulite is almost independent of the crystallization temperature.

TABLE II
Nucleating Effect on the Size of Spherulites of Nylon 6

Nucleating agent	%	Diameter of spherulites, μ	
		Crystallized at 150°C.	Crystallized at 5°C.
Base polymer	—	50–60	15–20
Nylon 66	0.2	10–15	5–10
	1	4–5	4–5
Polyethylene terephthalate	0.2	10–15	5–10
	1	4–5	4–5
$Pb_3(PO_4)_2$	0.05	10–15	8–10
	0.1	4–5	4–5
	0.5	4–5	4–5
NaH_2PO_4	0.05	5–10	3–7
	0.1	3–7	3–5
	0.5	5–7	3–5
$Na_7P_5O_{16}$	0.05	5–6	4–6
	0.1	4–5	3–5
	0.5	6–9	5–8
TiO_2	0.05	20–25	5–10

The authors wish to thank Dr. M. Watanabe and Dr. N. Yoda for their helpful discussions and Mr. T. Suyama for his assistance in this work.

References

1. Inoue, M., *J. Polymer Sci.*, **55**, 753 (1961).
2. Starkweather, H. W., Jr., and R. E. Brooks, *J. Appl. Polymer Sci.*, **1**, 236 (1959).
3. Hammer, C. F., T. A. Koch, and J. F. Whitney, *J. Appl. Polymer Sci.*, **1**, 169 (1959).
4. Müller, A., and R. Pflüger, *Kunststoffe*, **50**, 203 (1960).
5. E. I. du Pont de Nemours, Brit. Pat., 798,038 (1958); Badische Anilin-u. Soda-Fabrik, Brit. Pat. 818,317 (1959); Imp. Chem. Ind., Brit Pat. 850,986 (1960).
6. Last, A. G. M., *J. Polymer Sci.*, **39**, 543 (1959).
7. Manderkern, L., *Chem. Rev.*, **56**, 903 (1956).
8. Čefelín, P., M. Chelír, and O. Wichterle, *Collection Czech. Chem. Commun.*, **25**, 1267 (1960).

Résumé

On discute la cinétique de la cristallisation isotherme et la morphologie de sphérulites de nylon 6, nucléés par des additifs. On a employé du nylon 66 du téréphtalate de polyéthylène et certains composés inorganiques phosphorés comme agents de nucléation. Dans le domaine des températures comprises entre 205° et 180°C, la cristallisation se

passe par croissance à une ou à deux dimensions et on a une nucléation hétérogène. Les agents de nucléation augmentent la vitesse de cristallisation et font diminuer la période d'induction de cristallisation. Le maximum de cristallinité n'augmente pas toujours quand on ajoute les additifs utilisés pour ces expériences. Par addition d'agents de nucléation, la taille des sphérulites diminue et la distribution devient homogène et indépendante de la température de cristallisation.

Zusammenfassung

Die Kinetik der isothermen Kristallisation und die Morphologie von Sphärolithen in Nylon 6 bei Keimbildung durch Zusätze wurde diskutiert. Nylon 66, Polyäthylenterephthalat und einige anorganische Phosphorverbindungen wurden als keimbildende Reagenzien verwendet. Bei einer Kristallisationstemperatur zwischen 205 und 180°C verläuft die Kristallisation in der Art eines ein- oder zweidimensionalen Wachstums und einer heterogenen Keimbildung. Die Kristallisationsgeschwindigkeit wird durch keimbildende Reagenzien erhöht und die Induktionsperiode der Kristallisation herabgesetzt. Die maximale Kristallinität nimmt durch die hier verwendeten Zusätze nicht immer zu. Durch Zusatz keimbildender Reagenzien nimmt die Grösse der Kristallite ab und die Verteilung wird, unabhängig von der Kristallisationstemperatur, homogen.

Received April 24, 1962
Revised May 27, 1962

JOURNAL OF POLYMER SCIENCE: PART A VOL. 1, PP. 2021–2029 (1963)

Copolymerization of Styrene and Aliphatic Olefins

C. G. OVERBERGER and KAZUO MIYAMICHI, *Department of Chemistry, Polytechnic Institute of Brooklyn, Brooklyn, New York*

Synopsis

An attempt has been made to study the composition of the products resulting from polymerization of equal molar amounts of styrene and 4-methyl-1-pentene and styrene and 3-methyl-1-butene with vanadium oxytrichloride and aluminum triisobutyl as the catalyst system. Fractionation of the products has revealed that some copolymers can be obtained with both olefins—a larger amount of copolymer being obtained with 4-methyl-1-pentene. Homopolymerization of both styrene and the α-olefin also occur. Qualitatively, in this catalyst system, the order of the polymerization rate is 4-methyl-1-pentene-1 > styrene > 3-methyl-1-butene. The results again collaborate the authors' early work that the copolymers obtained are not of uniform composition.

INTRODUCTION

Ziegler-Natta type of catalysts ordinarily are formed by combining a reactive organometallic compound such as an aluminum alkyl with a transition metal compound such as a titanium halide or vanadium halide. The function of the aluminum alkyl is in part to reduce the transition metal to a lower valence state and to provide an alkyl group for the transition metal. (The catalyst-forming reaction is complex, and attempts to define experimentally the precise nature of the active species generally have led to ambiguous results.) For example, there is no general agreement as to whether the polymer molecule grows from an aluminum center[1,2] or a transition metal center.[3–7]

The possible multiplicity of catalytic sites in these heterogeneous catalyst systems has been thought to lead to a broad molecular weight distribution in a homopolymerization[8] and to the formation of several different polymer species in a copolymerization.[9,10] If a catalyst having a single active site is used in a copolymerization, it may lead to the formation of copolymer having a uniform composition. This has recently been reported for homogeneous copolymerization of ethylene and propylene.[15]

Copolymerization experiments with a transition metal type of catalyst is expected to give not only a polymer of a new type but also some knowledge on the nature of the active site. The selection between two monomers at the growing polymer chain end is a sensitive measure of the structure and polarity of the active propagation site, and a change in this selectivity implies a change in the nature of the active sites.

In this paper, copolymerization of styrene with 4-methyl-1-pentene and 3-methyl-1-butene were investigated. Studies of the copolymerization of styrene and aliphatic olefins have not been published so far, although copolymerizations of styrene with styrene derivatives and copolymerization of two olefins have been investigated. Crystalline polyolefins are different from crystalline polystyrene in some properties, especially in solubility. If crystalline polymer would be formed, the experimental treatment and the interpretation of data would be difficult. Accordingly, it is preferable to use conditions leading to the formation of amorphous polymer. It has been found that increasing the size of the alkyl group in aluminum compounds results in the formation of catalytic complexes which form more amorphous polymer, and that transition metal compounds which are liquids and soluble in hydrocarbons tend as a rule to form more amorphous polymer.[11] Therefore, aluminum triisobutyl and vanadium oxytrichloride were chosen as the catalyst system.

EXPERIMENTAL

Purification of Materials

Styrene

Inhibitor was removed by washing with dilute sodium hydroxide solution followed by distilled water. After drying over "molecular sieves" styrene was distilled under nitrogen, b.p. 45°C. (15 mm.).

3-Methyl-1-butene and 4-Methyl-1-pentene

Both were research grades supplied by Phillips Petroleum Co. They were purified by distillation and flushed with prepurified nitrogen before use.

n-*Heptane*

n-Heptane was refluxed with concentrated sulfuric acid for approximately 10 hr., and then washed with water followed by dilute sodium hydroxide solution and distilled water. After drying over molecular sieves, the *n*-heptane was distilled, b.p. 98.4°C. The *n*-heptane was stored over molecular sieves and flushed with prepurified nitrogen before use.

Aluminum Triisobutyl

Aluminum triisobutyl was purified by distillation of a commercial product, b.p. 53°C./0.6 mm. under nitrogen, and stored in a glass-stoppered flask filled with nitrogen.

Vanadium Oxytrichloride

Vanadium oxytrichloride was purified by distillation of a commercial product, b.p. 54°C./59 mm. under nitrogen, and stored in a glass-stoppered flask filled with nitrogen.

Polymerization Technique

Polymerizations were carried out in sealed ampules. After an ampule had been heated in an oven at 110°C. overnight, it was stoppered with a self-sealing rubber cap while hot, and flushed with prepurified nitrogen through a hypodermic needle. Vanadium oxytrichloride, *n*-heptane, and aluminum triisobutyl were added by means of hypodermic syringes successively. The ampule was weighed after each addition. The ampule was immersed in a Dry Ice-trichloroethylene bath, and the monomer (or comonomer) was injected by means of hypodermic syringe. The syringe was weighed before and after addition. The ampule was sealed off, while being flushed with a slow stream of nitrogen through a hypodermic syringe. Polymerizations were carried out in a rotating oil bath. All polymerizations were carried to low conversions to insure constant monomer concentrations and to avoid diffusion-controlled processes.

The ampule's contents were cooled in a Dry Ice-trichloroethylene bath and then the ampule was opened. The contents were poured into about 5–10% hydrochloric acid in a methanol-isopropanol mixture (50/50) and stirred by means of a magnetic stirrer overnight. After digestion, the polymer was filtered, washed with methanol, and dried to constant weight under vacuum.

Fractionation

Fractionations were carried out at 40°C. by a precipitation method using carbon tetrachloride as the solvent and methanol as the nonsolvent. The concentration of the initial polymer solution was approximately 0.2 to 0.3%. The precipitant, after being separated from the solution phase, was dissolved again in carbon tetrachloride and then poured into a large volume of methanol. The precipitated polymers were then filtered, washed, and dried under vacuum at 40°C. to constant weight.

Viscosities were measured with a Ubbelohde-type viscometer at 30°C. in carbon tetrachloride.

Analysis of Copolymer Composition

Both infrared spectroscopy (solution method,[12] film method[13,14]) and radiochemical methods[9,10,12] have often been used for the analysis of copolymer composition. However, the potassium bromide pellet method of infrared spectroscopy has not been used since it has been said to be inaccurate. In this work the potassium bromide method was examined because of the difficulty of finding a suitable solvent for both polystyrene and the polyolefins.

Known mixtures of polystyrene and poly-4-methyl-1-pentene were prepared for the calibration. Five milligrams of the sample was mixed with 400 mg. of potassium bromide using a rotating vibrator to prepare a disc. The optical densities of the peak at 1603 $cm.^{-1}$ was calculated by a base-line method. Figure 1 shows the calibration curve. It was found

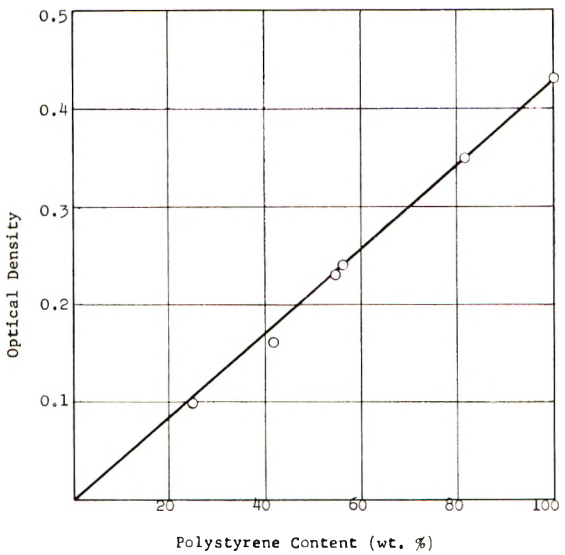

Fig. 1. Calibration curve.

that the optical density at 1603 cm.$^{-1}$ was proportional to the polystyrene content of the mixtures and the maximum deviation was $\pm 5\%$. This was considered to be good enough for the purpose of this experiment since even in the film method of infrared spectroscopy the average deviation is about $\pm 5\%$.

RESULTS

Copolymerization of Styrene and 4-Methyl-1-pentene with Various Ziegler-Type Catalysts

Copolymerizations of styrene (50 mole-%) and 4-methyl-1-pentene (50 mole-%) were carried out at 75°C. for the purpose of obtaining polymer for solubility tests. The following transition metal salts: VCl_3, $VOCl_3$, VCl_4, $TiCl_3$, and $TiCl_4$ were used with aluminum triisobutyl. These results will not be described here because of poor reproducibility of data. Moreover, the results of the solubility tests are meaningless since the copolymerization products have been found to be mixtures of copolymers and homopolymers.

Copolymerization of Styrene and Aliphatic Olefins with either Vanadium Oxytrichloride or Aluminum Triisobutyl

It has been found that at high or low mole ratios of aluminum alkyl to a transition metal compound polymerization proceeds by several different mechanisms and thus several different polymer species are being formed.

Styrene (St) and 4-methyl-1-pentene (4-Me-1-P) or 3-methyl-1-butene (3-Me-1-B) were copolymerized with vanadium oxytrichloride and with

aluminum triisobutyl alone. The results are shown in Tables I and II. As noted, vanadium oxytrichloride yielded almost pure polystyrene. On the other hand, aluminum triisobutyl was found to be a poor catalyst for any polymerization. The homopolymerizations of styrene, 4-methyl-1-pentene, and 3-methyl-1-butene were attempted with vanadium oxytrichloride. The results show that only styrene can be polymerized (Table III).

TABLE I
Copolymerization of Styrene Using Vanadium Oxytrichloride[a]

$VOCl_3$, g.	Heptane, g.	Comonomer, mole-%	Co-monomer, g.	Con-version, wt.-%	Product $[\eta]$ in CCl_4, 100 cc./g.	St content wt.-%
0.39	14.24	4-Me-1-P 30.5	2.85	56.5	0.37	95
0.61	14.65	3-Me-1-B 40.5	2.50	60.6	0.47	98

[a] 40°C., 5 hr.

TABLE II
Copolymerization of Styrene Using Aluminum Triisobutyl[a]

$Al(i\text{-}Bu)_3$, g.	Heptane, g.	Comonomer, mole-%	Co-monomer, g.	Con-version, wt.-%	Product	St con-tent, wt.-%
0.40	13.61	4-Me-1-P 40.5	2.81	Trace		—
0.60	14.69	3-Me-1-B 30.1	2.73	2–3		100

[a] 40°C., 5 hr.

These results indicate that the presence of excess unreacted vanadium oxytrichloride is not favorable because of the possibility of the formation of polystyrene, while with excess unreacted aluminum triisobutyl there is little possibility of the formation of homopolymers. Therefore, an excess of aluminum triisobutyl was used for succeeding experiments. There is a

TABLE III
Homopolymerizations with Vanadium Oxytrichloride[a]

$VOCl_3$, g.	Heptane, g.	Monomer	Monomer		Con-version, wt.-%
			g.	mole-%	
0.38	14.24	St	3.05	0.029	84
0.51	14.48	4-Me-1-P	2.51	0.030	0
0.40	13.99	3-Me-1-B	2.13	0.030	0

[a] 40°C., 5 hr.

minor possibility of the existence of cationic catalysts such as alkyl aluminum dichloride or dialkyl aluminum chloride.

Homopolymerization of Styrene, 4-Methyl-1-pentene and 3-Methyl-1-butene with Aluminum Triisobutyl-Vanadium Oxytrichloride

Styrene, 4-methyl-1-pentene, and 3-methyl-1-butene were homopolymerized with an aluminum triisobutyl-vanadium oxytrichloride catalyst using the same conditions. Qualitatively it was found that styrene was polymerized at a faster rate than 3-methyl-1-butene but less easily than 4-methyl-1-pentene (Table IV).

TABLE IV
Homopolymerizations with Aluminum Triisobutyl-Vanadium Oxytrichloride Catalyst[a]

$VOCl_3$, g.	Al-(i-Bu)$_3$, g.	Al/V, ratio	Heptane, g.	Monomer	Monomer g.	Monomer mole-%	Conversion, wt.-%
0.22	0.94	3.8	14.35	St	3.81	0.037	5.8
0.39	0.84	1.9	14.18	St	3.24	0.031	8
0.20	0.97	4.1	14.32	4-Me-1-P	3.05	0.036	15.4
0.18	0.82	4.1	14.38	3-Me-1-B	2.39	0.034	1.8
0.18	0.91	4.6	14.46	3-Me-1-B	2.43	0.035	2.6

[a] 40°C., 4.7 hr.

DISCUSSION

From the results of the homopolymerizations and copolymerizations, it is clear that styrene is more reactive than 3-methyl-1-butene but less reactive than 4-methyl-1-pentene (Table V).

TABLE V
Copolymerizations with Aluminum Triisobutyl-Vanadium Oxytrichloride Catalyst[a]

$VOCl_3$, g.	Al(i-Bu)$_3$, g.	Al/V, ratio	Heptane, g.	St content	Co-monomer, g.	Product Conversion, wt.-%	Product St content, wt.-%
				Styrene-4-Methyl-1-pentene			
2.5	9.4	3.3	140.6	(75 wt.-% 70 mole-%)	29.6	8.8	48
2.7	9.1	2.9	143	(75 wt.-% 70 mole-%)	32.8	8.9	47[b]
				Styrene-3-Methyl-1-butene			
2.6	9.4	3.2	139.4	(77 wt.-% 70 mole-%)	33	7.5	93[b]

[a] 40°C., 5 hr.
[b] Fractionated samples.

It has been suggested that a Ziegler-Natta catalyst consisting of an organometallic reducing agent and a transition metal compound forms bimolecular complexes having the halogen bridge structure.[10] Carrick[6] has proposed that propagation occurs at the transiton metal center based on the result that the relative monomer reactivities are altered by changes in the transition metal center but not by changes in the reducing agents. Steric effects are considered to play an important role in the initiation and propagation steps, although a polar effect should not be neglected. It has been reported[14] that propylene is generally less reactive than ethylene with heterogeneous Ziegler-Natta type of catalysts and this fact has been attributed to a steric factor. However, since these copolymers have been obtained at high conversion, the process may be diffusion controlled and the results may represent the difference in the rate of diffusion of ethylene and propylene.

In the present case reactivities of the monomers may also be explained by a steric effect. Since the bulky side group of 4-methyl-1-pentene is further from the polymerizing double bond than in the case of styrene and 3-methyl-1-butene, the degree of steric hindrance may be lower in 4-methyl-1-pentene.

The fractionation results reveal some interesting facts (Tables VI and VII). In both cases the copolymerization product was found to have fractionated in the order of decreasing molecular weights having increasing styrene contents. In the case of styrene and 4-methyl-1-pentene, the first two fractions, No. 1 and 2, are largely poly-4-methyl-1-pentene considering some errors in the fractionation and the anaylsis. Fraction No. 3 was soluble in boiling carbon tetrachloride but precipitated at 40°C.

TABLE VI
Fractionation of a Styrene-4-Methyl-1-pentene Copolymer

Fraction No.	Fraction, wt. g.	Fraction, wt.-%	$[\eta]$ in CCl_4, 100 cc./g.	St content of fraction wt.-%
1	0.092	4.1	Insol. in CCl_4	7 (5)[a]
2	0.350	15.4	Insol. in CCl_4	11 (5)[a]
3	0.248	10.9	Sol. in boiling CCl_4 but insol. in cold CCl_4	9
4	0.487	21.5	3.1	26
5	0.387	17	0.50	31
6	0.483	21.3	0.07	83
7	0.221	9.8	0.06	95
Total	2.268 (93% of the initial amount)	100		

[a] Calculated using the peak at 760 cm.$^{-1}$; since the absorption at 760 cm.$^{-1}$ was very strong compared to the absorption at 1603 cm.$^{-1}$, the latter peak was not useful for the sample having high styrene content.

TABLE VII
Fractionation of a Styrene-3-Methyl-1-butene Copolymer

Fraction No.	Fraction, wt.	Fraction, wt.-%	$[\eta]$ in CCl_4, 100 cc./g.	St content in fraction, wt.-%
1	0.0108	1	Insol. in CCl_4	75
2	0.1029	9	2.2	82
3	0.1174	10.3	1.2	86
4	0.1674	14.7	0.32	104
5	0.4022	35.2	0.20	100
6	0.3402	29.8	0.08	95
Total	1.1409 (92% of the initial amount)	100		

Both the solubility and the composition support the fact that this fraction is a copolymer. Fractions No. 4 and 5 may also be considered to be copolymers. Fractions No. 6 and 7 are largely polystyrene. In the case of styrene-3-methyl-1-butene, it is probable that fractions No. 1, 2, and 3 are copolymers, while fractions No. 4, 5, and 6 are polystyrene. The fact that more than 70% of the product is polystyrene shows the lower reactivity of 3-methyl-1-butene in the copolymerization. Although the reason why much low molecular weight polystyrene was formed is not clear, it may be due to the following causes: (*1*) soluble vanadium oxytrichloride which has not reacted to form complex (although excess aluminum triisobutyl has been used); (*2*) 3-methyl-1-butene acted as a degradative chain transfer agent; (*3*) impurities contained in the monomers; (*4*) water (since 3-methyl-1-butene was a liquid having a low boiling point it was used in a cooled state. During operation, water in the air was condensed on the hypodermic needle although it was wiped.)

From the fractionation data presented it is clear that the copolymerization product in both cases is a mixture of copolymers and homopolymers. The results may be explained by the assumption that there exists more than one active site on the catalyst.

A model for the existence of various active sites has been proposed by Overberger and Nozakura,[10] indicating that the polarity of the interstitial bond between a transition metal atom and an aluminum atom varies with different substituents of the aluminum compound. In the case of copolymerization of styrene and an olefin, selectivity of monomer by an active site may be more severe than in the cases of styrene and a styrene derivative and an olefin and another olefin.

The catalyst formed from aluminum triisobutyl and vanadium oxytrichloride is not soluble in hydrocarbon although both components are soluble. It would be interesting to use a soluble catalyst, such as a mixture of an aluminum halide, tetraphenyltin, and a vanadium halide, which is supposed to have a single active site.

References

1. Natta, G., P. Pino, G. Mazzanti, U. Gianini, E. Mantica, and M. Peraldo, *J. Polymer Sci.*, **26,** 120 (1957).
2. Natta, G., *J. Polymer Sci.*, **34,** 21, 88, (1959).
3. Friedlander, H. N., and K. Oita, *Ind. Eng. Chem.*, **49,** 1885 (1957).
4. Nenitzescu, C. D., and A. H. Ciresicahuch, *Angew. Chem.*, **68,** 438 (1956).
5. Ludlum, D. B., A. W. Anderson, and C. E. Ashby, *J. Am. Chem. Soc.*, **81,** 81 (1959).
6. Carrik, W. L., *J. Am. Chem. Soc.*, **80,** 6455 (1958).
7. Carrick, W. L., F. J. Karol, G. L. Karapinka, and J. J. Smith, *J. Am. Chem. Soc.*, **82,** 1502 (1960).
8. Carrick, W. L., R. W. Kluiber, E. F. Bonner, L. H. Wartman, F. M. Rugg, and J. J. Smith, *J. Am. Chem. Soc.*, **82,** 3883 (1960).
9. Overberger, C. G., and F. Ang, *J. Am. Chem. Soc.*, **82,** 929 (1960).
10. Overberger, C. G., and S. Nozakura, *J. Polymer Sci.*, **A1,** 1439 (1963).
11. Gaylord, N. G., and H. F. Mark, *Linear and Stereoregular Addition Polymers,* Interscience, New York–London, 1959, pp. 126, 129.
12. Natta, G., G. Mazzanti, A. Volvasson, and G. Pajaro, *Chim. Ind. (Milan),* **39,** 733 (1957).
13. Gossl, T., *Makromol. Chem.*, **42,** 1 (1960).
14. Karol, F. J., and W. L. Carrick, *J. Am. Chem. Soc.*, **83,** 2654 (1961).
15. Phillips, G. W., and W. L. Carrick, private communication.
16. Natta, G., *J. Polymer Sci.*, **34,** 88 (1959).

Résumé

On a essayé d'étudier la composition des produits résultant de la polymérisation de quantités équimoléculaires de styrène et de 4-méthyl-pentène-1, de styrène et de 3-méthyl-butène-1 avec de l'oxytrichlorure de vanadium et du triisobutyl-aluminium comme catalyseurs. Le fractionnement des produits montre que certains copolymères peuvent être obtenus avec les deux oléfines—une plus grande quantité de copolymère étant obtenue avec le 4-méthyl-pentène-1. Il y a également homopolymérisation de styrène et de l'alpha-oléfine. Qualitativement, avec ce système catalytique, l'ordre de la vitesse de polymérisation est 4-méthyl-pentène-1 > styrène > 3-méthyl-butène-1. Les résultats confirment à nouveau nos travaux antérieurs, à savoir que les copolymères obtenus ne sont pas de composition uniforme.

Zusammenfassung

Die Zusammensetzung der durch Polymerisation äquimolarer Mengen von Styrol und 4-Methylpenten-1, sowie von Styrol und 3-Methylbuten-1 mit Vanadinoxytrichlorid und Triisobutylaluminium als Katalysator erhaltenen Produkte wurde untersucht. Die Fraktionierung der Produkte zeigte, dass mit beiden Olefinen Copolymere erhalten werden können, wobei 4-Methylpenten-1 die grössere Copolymermenge bildet. Es tritt auch Homopolymerisation von Styrol und dem α-Olefin ein. Mit dem verwendeten Katalysator besteht qualitativ folgende Reinhenfolge der Polymerisationsgeschwindigkeit: 4-Methylpenten-1 > Styrol > 3-Methylbuten-1. Die Ergebnisse bestätigen unseren früheren Befund, dass die erhaltenen Copolymeren keine einheitliche Zusammensetzung besitzen.

Received May 7, 1962

JOURNAL OF POLYMER SCIENCE: PART A VOL. 1, PP. 2031–2038 (1963)

Mechanism of Secondary Crystallization in Polymers

F. RYBNIKÁŘ, *Research Institute for Rubber and Plastics Technology, Gottwaldov, Czechoslovakia*

Synopsis

In isothermal crystallization of polymers, where the fusion preceding the crystallization process is conducted at relative low temperatures or in samples subjected to γ-radiation, there is extensive secondary crystallization. Secondary crystallization, which has been found to start stepwise at a time equal to two half-times of primary crystallization, represents a new process of crystallization following the Avrami equation with $n = 1$. In addition to this crystallization process a further slow increase of crystallinity with time takes place.

The crystallization process of polymers is usually divided into two phases primary and secondary crystallization. During primary crystallization there arise and grow spherulitic crystalline formations which are characterized by a definite degree of organization, approaching more or less the ideal crystal structure. The course of the primary crystallization may be given by the Avrami equation in two ways. The first way is:

$$\alpha = 1 - \exp\{-Kt^n\} \tag{1}$$

In this case the growing crystalline aggregates have a degree of crystallinity $\alpha \cong 1$, i.e., their crystalline structure does not show any failures. However, at the end of primary crystallization the ideal crystalline state with $\alpha = 1$ is not attained throughout the whole sample because the process of crystallization in accordance with eq. (1) settles down due to kinetic reasons and proceeds only very slowly.

In the second case it is presumed that the growing morphological formations are distinguished by a fixed degree of crystallinity $\alpha_0 < 1$; thus

$$\alpha = \alpha_0(1 - \exp\{-Kt^n\}) \tag{2}$$

In eqs. (1) and (2) constants K and n are characteristic of a given type of nucleation and growth and t is the time of crystallization.

Supplementary crystallization changes, which cannot be characterized by eqs. (1) or (2) are usually termed secondary crystallization.

Secondary crystallization, therefore, represents a further increase in crystallinity consisting in additional crystallization of uncrystallized material or in further development of the already formed crystalline structure. Possibly, secondary crystallization may comprise both of these processes.

The mechanism of secondary crystallization in polymers has not yet been satisfactorily explained. The difficulties consist in the fact that the extent of secondary crystallization is, in comparison with primary crystallization, usually relatively small, and in most cases it is quite difficult to determine the onset of secondary crystallization. The described mechanisms of the secondary crystallization may be essentially divided into two groups. The proponents of the first group[1-3] characterize secondary crystallization as a reorganization of the remaining amorphous phase, where the variation of crystallinity or of other quantities proportional to the crystallinity (V_{sp}, density, etc.) is linearly related to the logarithm of time. The proponents of the second group[4,5] believe that the process of secondary crystallization is analogous to the relaxation process, where the logarithm of crystallinity change is linearly proportional to the time.

In a previous paper[6] we have shown that the process of primary and secondary crystallization, can be relatively easily distinguished, because the beginning of secondary crystallization is characterized by a sudden increase in crystallinity which appears at a time t of crystallization ($t \simeq 2r$, where r is the half-time of the primary crystallization). This fact makes possible a reliable determination of the beginning of secondary crystallization and permits the course of secondary crystallization, the rate and extent of which is highest just in the original period, to be followed. In those cases where the extent of the secondary crystallization in the time interval between $2r$ and $3r$ is only about 5–10% of the primary crystallization, it is not possible to study the mechanism of secondary crystallization in detail. However, the situation appeared to be very favorable in cases where the extent of secondary crystallization was of the same magnitude or even greater than the extent of the preceding primary crystallization.

Experimental

Measurements were made on commercial samples of polypropylene, i.e., Moplene (M) and Daplene (D), and poly-6-caproamide (6-PA). The samples of Daplene were subjected to radiation *in vacuo* from a Co^{60} source

TABLE I
Characteristic Values of Measured Samples of Moplene, Daplene, and Poly-6-caproamide

Sample	$[\eta]$, ml./g.	Extractable content, %	Ash content, %	Melt index at 190°C., g./10 min.
M	459[a]	6.2[b]	0.06	0.81
D[c]	357[a]	3.0[b]	0.06	4.56
6-PA	133[d]	2.2[e]		

[a] Inherent viscosity determined at c = 0.1 g./100 ml. in tetralin at 140°C.
[b] Extracted with cold n-heptane.
[c] Values of original sample.
[d] Determined at 25°C. in m-cresol.
[e] Extracted with boiling water.

having an activity of 250 C. The intensity of the γ-radiation was 14 rep/sec. The course of crystallization was followed by changes in density, as measured by density balance. The polypropylene samples were fused and crystallized in glycerol, those of poly-6-caproamide were treated in silicone oil. The equipment and the method of measurement were described previously.[7] The course of crystallization was characterized by the Avrami equation as a phase change of the amorphous fraction $\theta = 1$ at the beginning and $\theta = 0$ at the end of primary crystallization which was determined by the stepwise onset of the secondary crystallization. The density changes were followed with a sensibility better than ± 0.0005 g./cm.^{3}. Characteristic values for the samples studied are given in Table I.

Results and Discussion

In studies of the influence of the fusion conditions on crystallization kinetics of polypropylene and polyamides a marked increase was noted in the extent of secondary crystallization in place of the extent of the primary crystallization in cases where the fusion was conducted at relatively low temperatures. A similar effect was observed on the irradiated polypropylene samples. In contrast to normal samples, a low fusion temperature was not necessary to produce the increase in the extent of secondary crystallization. Some typical examples in which secondary crystallization reaches to a greater extent are given in Figures 1–3. These examples may be used for a detailed study of the mechanism of secondary crystallization. It can be seen that the secondary crystallization begins in all cases at $t \simeq 2r$. The rate of secondary crystallization is at first relatively high; later it becomes smaller and smaller. In cases where the sensitivity of the experimental procedures did not allow the end of the primary crystallization to be distinguished from the onset of secondary crystallization, the initial portion of the secondary crystallization was included with the primary crystallization.

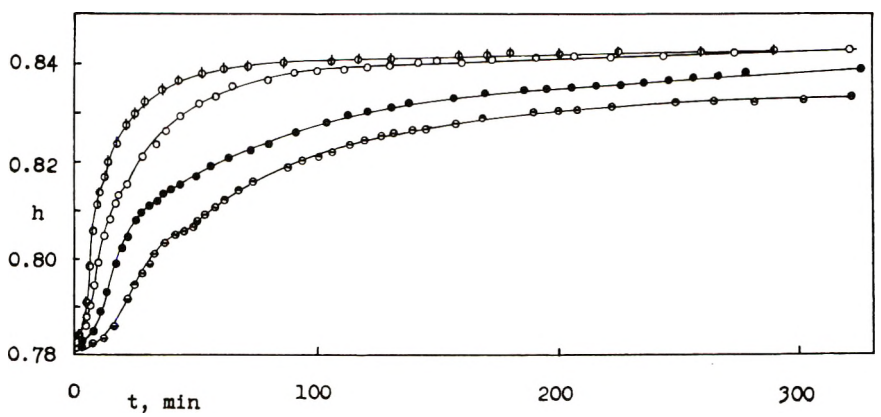

Fig. 1. Crystallization isotherms of Moplene samples at various crystallization temperatures T_c after fusion 15 min. at 170°C.: (⊕) 144°C.; (○) 146°C.; (●) 148°C.; (⊖) 150°C.

This caused the last 10–30% range of the "primary" crystallization to deviate systematically toward lower values as compared with the theoretical course according to the Avrami equation.[5,8–12]

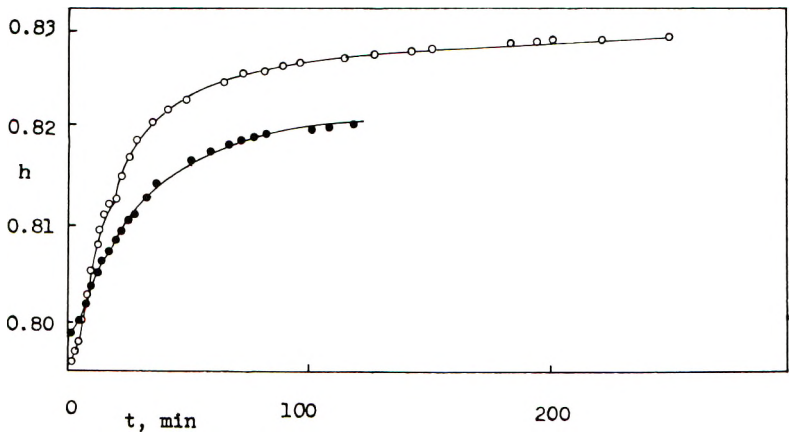

Fig. 2. Crystallization isotherms of γ-irradiated Daplene samples at various crystallization temperatures after fusion 15 min. at 190°C.: (●) 121.9°C.; 1.76×10^8 rep; (○) 123°C., 1.26×10^8 rep.

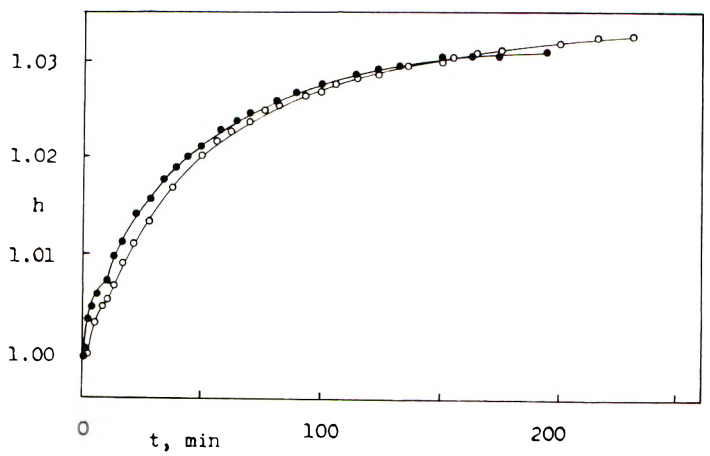

Fig. 3. Crystallization isotherms of poly-6-caproamide samples at various crystallization temperatures after fusion 15 min. at 225°C.: (●) 211.5°C.; (○) 212°C.

A comparison of the course of secondary crystallization in our samples with the two aforementioned types of mechanisms for secondary crystallization shows that neither the dependence of density on log t_2 nor the dependence of log of density on t_2 is in accord with the experimental values. A marked deviation exists in the early state of secondary crystallization, and only the terminating phase of density increase with time can be expressed as $\log h_2 = k_1 + k_2 t_2$, where h_2 is the density after secondary crystallization,

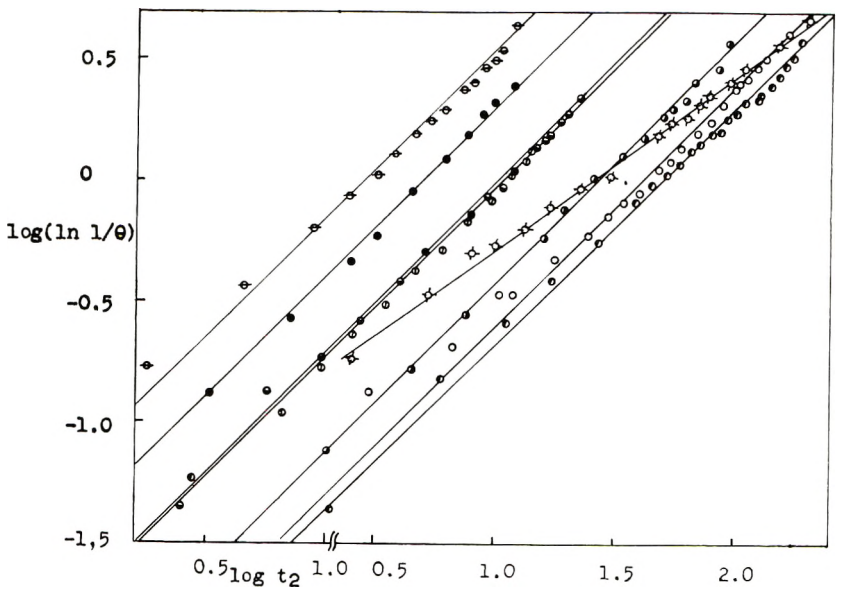

Fig. 4. Analysis of the course of secondary crystallization of polypropylene and poly-6-caproamide samples as a phase change according to the Avrami equation: (⊖) Moplene (M), 144°C.; (●) M, 146°C.; (⊙) M, 148°C.; (◒) M, 150°C.; (-☼-) Daplene (D), 123°C.; (◑) D, 121.9°C.; (○) 6-PA, 211.5°C.; (◐) 6-PA, 212°C.

$k_1 = h_1$ is the density at the end of primary crystallization, k_2 is a constant, and t_2 is the time of secondary crystallization.

The important inadequacy of the foregoing mechanisms for the course of secondary crystallization lies in the fact that they do not consider the possibility that the observed changes could be evoked by a further crystallization process. However the present results show that the initial portion of the secondary crystallization represents an independent crystallization process. If the analysis of the course of secondary crystallization is treated from this point of view, the secondary crystallization can be expressed by the Avrami equation with a value of $n = 1$. Figure 4 shows some typical examples which confirm this assumption. According to Morgan,[13] the value of $n = 1$ means that the growth of crystallites runs through predetermined nuclei either in fibrillar or laminar spherulitic form. Both growth mechanisms are typical where crystallites are grown under conditions of high supersaturation. Microscopic examination of the morphological structure in polarized light was not sufficient for objective discrimination of the growth mechanism occurring in the samples.

A comparison of the course of primary and secondary crystallization in the samples studied is shown in Table II. Secondary crystallization was analyzed as a phase change of the crystalline structure with a density h_1 into a more perfect crystalline structure with a density h_2. The exact determination of the end of secondary crystallization (that is, of the value h_2) is

TABLE II
Course of Primary and Secondary Crystallization[a]

Sample	T_c, °C.	Density, g./cc.			Half-time for primary crystallization	Time of onset of secondary crystallization	Half-time for secondary crystallization	Avrami constant for secondary crystallization
		Amorphous sample h_a	After primary crystallization h_1	After secondary crystallization h_2	r, min.	z, min.	r_2, min.	n_2
M[a]	144	0.786	0.817	0.840	6	12	10	1
M[a]	146	0.784	0.816	0.839	10	21	18	1
M[a]	148	0.783	0.812	0.833	16.5	33	40	1
M[a]	150	0.782	0.807	0.833	23.5	47.5	37.5	1
D[b,c]	123	0.798	0.815	0.829	9.5	20	15	0.8
D[b,d]	121.9	0.799	0.807	0.820	9	17.5	19	1
6-PA[e]	211.5	1.000	1.007	1.031	3	10	33	1
6-PA[e]	212	1.000	1.005	1.033	4.8	11	37	0.9

[a] Samples fused 15 min. at 170°C.
[b] Samples fused 15 min. at 190°C.
[c] Sample irradiated with a dose of 1.26×10^8 rep.
[d] Sample irradiated with a dose of 1.76×10^8 rep.
[e] Samples fused 15 min. at 225°C.

rather problematical, but it does not significantly affect the analysis of the course of secondary crystallization. The course of primary crystallization could not be analyzed in such detail as that of secondary crystallization, because the course of primary crystallization was rather fast. The values of the constant n for primary crystallization lie in the vicinity of 2 or 3. As far as the rate of secondary crystallization is concerned, it can be seen from the comparison of r and r_2 values that the rate of secondary crystallization reaches half that of primary crystallization with polypropylene samples and even a lower value with the poly-6-caproamide. However, even after the end of secondary crystallization, the slow increase of density with time does not stop. A reliable determination could not be made of the onset and course of the process characterized by a further slow increase of density with time, because this would necessitate more sensitive measurements and more prolonged times of crystallization than were used. However, it is very likely that this process will follow some of the previously suggested expressions.[1,5]

It may be concluded that the course of isothermal crystallization of polypropylene, poly-6-caproamide, and probably of other polymers can be divided into three distinct processes: the first, covering the time interval $t = 0$ to $t \simeq 2r$, is the primary crystallization characterized by the Avrami equation with the value of constant $n = 2$, 3, or 4; the second process is secondary crystallization beginning at time $z \simeq 2r$, representing a further process of crystallization whose value of $n = 1$, and the extent of which is closely related to the number of predetermined crystallization nuclei; the third process is a slow increase of crystallinity with time, which may be due to changes occurring in the remaining amorphous phase.

References

1. Kovacs, A. J., *Ric. Sci.*, **A25**, 668 (1955).
2. Collins, R. L., *J. Polymer Sci.*, **27**, 75 (1958).
3. Majer, J., *Collection Czech. Chem. Communs.*, **25**, 2454 (1960).
4. Buckser, S., and L. H. Tung, *J. Phys. Chem.*, **63**, 763 (1959).
5. Zachmann, H. G., and H. Stuart, *Makromol. Chem.*, **41**, 131, 148 (1960).
6. Rybnikář, F., *J. Polymer Sci.*, **44**, 517 (1960).
7. Rybnikář, F., *Chem. Průmysl*, **11**, 157 (1961).
8. Mandelkern, L., F. A. Quinn, and P. J. Flory, *J. Appl. Phys.*, **25**, 830 (1954).
9. Falkai, B., and H. A. Stuart, *Kolloid-Z.*, **162**, 138 (1959).
10. Buchdahl, R., R. L. Miller, and S. Newman, *J. Polymer Sci.*, **36**, 215 (1959).
11. Majer, J., et al., *Kunststoff-Rundschau*, **1**, 39 (1960).
12. Magill, J. H., *Polymer*, **2**, 221 (1961).
13. Morgan, L. B., *Phil. Trans. Roy. Soc. London*, **A247**, 13 (1954).

Résumé

Dans les cas de cristallisations isothermiques de polymères où la fusion précédant le processus de cristallisation a été menée à de températures relativement basses ou sur des échantillons obtenus par irradiation-γ, la seconde cristallisation couvre une grande étendue. Il a été constaté que la seconde cristallisation, procédant par étapes dans un temps égal à deux demi-temps de première cristallisation, représente un nouveau procédé

de cristallisation suivant l'équation de Avrami pour $n = 1$. De plus dans ce procédé de cristallisation il se produit une lente augmentation ultérieure de la cristallinité.

Zusammenfassung

Im Falle der isothermen Kristallisation von Polymeren, bei welcher das Schmelzen vor dem Kristallisationsprozess bei verhältnismässig tiefer Temperatur durchgeführt wurde oder bei γ-bestrahlten Proben, erreicht die Sekundärkristallisation ein grosses Ausmass. Es wurde sichergestellt, dass die in der doppelten Zeitdauer der Primärkristallisationshalbwertszeit stufenweise einsetzende Sekundärkristallisation einen neuen, der Avrami-Gleichung mit $n = 1$ gehorchenden Kristallisationsprozess darstellt. Zusätzlich zu diesem Kristallisationsprozess findet eine weitere langsame Zunahme der Kristallinität im Laufe der Zeit statt.

Received April 4, 1962
Revised May 29, 1962

JOURNAL OF POLYMER SCIENCE: PART A VOL. 1, PP. 2039–2047 (1963)

Maximum Relaxation Time on Polymers in the Vicinity of Critical Molecular Weight

HIROSHI SOBUE and KENKICHI MURAKAMI,
Department of Industrial Chemistry, Faculty of Engineering, University of Tokyo, Tokyo, Japan

Synopsis

It is a well-known fact that the relaxation spectra in the rubbery region of linear amorphous polymers show "box-type" functions which are characterized by three elements, τ_e, τ_m, and E_0, the minimum relaxation time, maximum relaxation time, and height of the curve, respectively. The equation $(\tau_m - \tau_e)/\log(\tau_m/\tau_e) = 2.303\,\alpha M_w^{\beta}/E_r(\tau_e)$ can be derived by a simple treatment described in this paper. Then $\log \tau_m = -\log E_0/\alpha(1 - 1/10^K) + \beta \log \bar{M}_w$ can be obtained from the above equation for the polymers synthesized by us. According to Fujita's results, however, τ_e is independent of molecular weight and τ_m becomes τ_3 when $\bar{M}_w$ conforms to M_c. For such a case the above equation is transformed into $\log(\tau_m/\tau_e - 1) - \log\log \tau_m/\tau_e = \beta \log \bar{M}_w/M_c$. On the other hand, $\log \tau_m$ experimentally obtained was plotted againt $\log \bar{M}_w$ for the same polymers and it was found that the results were raher on the straight line indicated by the former equation than on the curve shown by the latter. Also $\log(\tau_m + 0.234) = -5.87 + 1.65 \log \bar{M}_w$ was found to be suitable for the polymers in the vicinity of M_c.

It is a well-known fact that the relaxation spectra of the rubbery region of linear amorphous polymers show "box-type" functions with increasing sharpness of molecular weight distribution. Andrews and Tobolsky[1] and Ferry and co-workers[2] confirmed this fact with undiluted polyisobutylene and with concentrated solutions of the same polymer. It was also found that this box-type function depends strongly on molecular weight[1] and molecular weight distribution.[3,4] The above-mentioned results obtained experimentally, however, can be applied in the ranges of $M \gg M_c$ where M_c is the so-called critical molecular weight.

The purpose of this study is to find out whether there exists any kind of principles applicable to lower molecular weight polymers in the vicinity of M_c.

Fifteen samples of polystyrene were prepared by radical-initiated polymerization of styrene carried to low conversions.

It is shown by Baysal and Tobolsky[5] that the molecular weight distribution under these conditions is given by $X_n = np^{n-1}(1 - p)^2$ where X_n is the mole fraction of polymer whose degree of polymerization is n, and p is the conversion ratio. For this distribution the ratio of weight-average molecular weight to number-average molecular weight is $\bar{M}_w/\bar{M}_n = 1.5$.

TABLE I
Maximum Relaxation Time τ_m and Shear Viscosity η for Molecular Weights

Sample No.	$\bar{M}_{vt}$	$\bar{M}_w$	$\bar{M}_n$	τ_m at 115°C., min.	η_{shear} at 115°C.
1	1.78×10^4	1.86×10^4	1.24×10^4	5.80×10^{-2}	9.84×10^6
2	2.08×10^4	2.16×10^4	1.44×10^4	1.54×10^{-1}	1.45×10^7
3	2.51×10^4	2.61×10^4	1.74×10^4	3.30×10^{-1}	2.24×10^7
4	2.82×10^4	2.94×10^4	1.96×10^4	6.07×10^{-1}	2.46×10^7
5	3.47×10^4	3.62×10^4	2.41×10^4	6.30×10^{-1}	3.16×10^7
6	4.07×10^4	4.25×10^4	2.83×10^4	1.04	3.31×10^7
7	4.47×10^4	4.67×10^4	3.11×10^4	2.05	4.77×10^7
8	4.60×10^4	4.80×10^4	3.20×10^4	4.25	1.06×10^8
9	5.76×10^4	5.90×10^4	3.94×10^4	7.69	1.17×10^8
10	6.61×10^4	6.90×10^4	4.60×10^4	1.41×10	2.36×10^8
11	8.91×10^4	9.30×10^4	6.20×10^4	1.78×10	3.33×10^8
12	1.15×10^5	1.20×10^5	8.00×10^4	7.76×10	2.46×10^9
13	1.77×10^5	1.86×10^5	1.24×10^5	4.55×10^2	1.73×10^{10}
14	2.09×10^5	2.18×10^5	1.45×10^5	8.00×10^2	1.76×10^{10}
15	3.02×10^5	3.15×10^5	2.11×10^5	1.03×10^4	1.63×10^{11}

This is a fairly narrow distribution of molecular weight for a polydisperse polymer.

Table I shows the values obtained for fifteen polymers. The values of $\bar{M}_n$ were calculated from eq. (1) which was derived from the theory suggested by Baysal and Tobolsky:[5]

$$\bar{M}_n/\bar{M}_v = \sqrt[a]{2^{(a+1)}/\Gamma(a+3)} \tag{1}$$

The viscosity formula for polystyrene given by Zimm[9] was used in this work. The result obtained with eq. (1) was:

$$\bar{M}_n/\bar{M}_v = 0.697 \tag{2}$$

Equation (2) was calculated from eq. (1) using $a = 0.69$ which is a constant in Zimm's formula.[9]

The apparatus and procedures used for the measurements of relaxation were essentially the same as those employed in our previous study. Stress relaxation data for fifteen polymers at different temperatures were obtained. From these data master curves in the region of rubbery flow were constructed for these polymers at 115°C., using the time–temperature superposition principle. These master curves were shown in a previous paper.[4]

The steady-flow (tensile) viscosity η of typical monodisperse polymers that have relaxation spectra showing box distribution can be expressed by eq. (3):

$$\eta = E_0(\tau_m - \tau_e) \tag{3}$$

Here E_0, τ_m, and τ_e are the values characterizing such a box distribution function, E_0 being indicated by the height of the relaxation spectrum and τ_m and τ_e being the maximum and minimum relaxation time, respectively.

On the other hand,

$$\eta = \alpha \bar{M}_w^{\beta} \tag{4}$$

where $\bar{M}_w > M_c$.

Then from eqs. (3) and (4),

$$E_0(\tau_m - \tau_e) = \alpha \bar{M}_w^{\beta} \tag{5}$$

It is very probable that eq. (5) may be established very well in the region of $\bar{M}_w \gg M_c$.

According to Alfrey's approximation,[6]

$$\begin{aligned} E_r(t) &= \int_{-\infty}^{\infty} e^{-t/\tau} \bar{H}(\log \tau) d(\log \tau) \\ &= \int_{t}^{\infty} \bar{H}(\log \tau) d(\log \tau) \end{aligned} \tag{6}$$

Equation (6) may be modified to eq. (7) for monodisperse polymers:

$$\begin{aligned} E_r(\tau_e) &= \int_{\tau_e}^{\infty} \bar{H}(\log \tau) d(\log \tau) \\ &= 2.303\, E_0 \log (\tau_m/\tau_e) \end{aligned} \tag{7}$$

$E_r(\tau_e)$ is the relaxation modulus at a time scale corresponding to the initial zone of the rubbery region and is independent of both molecular weight and molecular weight distribution. Substituting eq. (7) into eq. (5), the following is obtained.

$$(\tau_m - \tau_e)/\log(\tau_m/\tau_e) = [2.303\alpha/E_r(\tau_e)]\bar{M}_w^{\beta} \tag{8}$$

Accordingly,

$$\log (\tau_m - \tau_e) - \log\log (\tau_m/\tau_e) = \log 2.303\alpha/E_r(\tau_e) + \beta \log \bar{M}_w \tag{9}$$

It was recently suggested by Tobolsky[3] according to their experimental results that E_0 is a parameter that depends only upon the molecular weight distribution. If this is so, eq. (10), in which $\bar{K}$ is a constant may be derived from eq. (7) for comparatively monodisperse polystyrenes having the index of $\bar{M}_w/\bar{M}_n = 1.5$.

$$\tau_m/\tau_e = \bar{K} \tag{10}$$

Here,

$$\bar{K} = E_r(\tau_e)/2.303E_0$$

Substituting eq. (10) into eq. (9), we have:

$$\log \tau_m = -\log (E_0/\alpha)(1 - 1/10^{\bar{K}}) + \beta \log \bar{M}_w \tag{11}$$

Then eq. (11) shows that the relationship between $\log \tau_m$ and $\log \bar{M}_w$ must be indicated as a straight line having the intercept $-\log(E_0/\alpha)$-$(1 - 1/10^{\bar{K}})$ and the slope β in the ranges where $\bar{M}_w \gg M_c$.

On the other hand, if the proposal of Fujita and his co-workers[6] is adopted, that τ_e is independent of molecular weight and that $\bar{M}_w$ becomes

M_c at the point $\tau_m \rightarrow \tau_e$, then eq. (8) may be treated in the following way:

$$\lim_{\tau_m \rightarrow \tau_e}(\tau_m - \tau_e)/\log(\tau_m/\tau_e) = \lim_{\bar{M}_w \rightarrow M_c}[2.303\alpha/E_r(\tau_e)]\bar{M}_w^{\beta}$$

$$\tau_e = [2.303\alpha/E_r(\tau_e)]M_c^{\beta} \tag{12}$$

If eq. (12) is substituted into eq. (9) it becomes

$$\log[(\tau_m/\tau_e) - 1] - \log\log(\tau_m/\tau_e) = \beta \log(\bar{M}_w/M_c) \tag{13}$$

The experimental values of $\log \tau_m$ plotted against $\log \bar{M}_w$ should fit the straight line indicated by eq. (13) when $\bar{M}_w \gg M_c$, if Fujita's proposal is right.

Now, from the data available for this kind of polystyrene polymer, and from our data, more values were selected as reasonable:

$$E_r(\tau_e) = 5.57 \times 10^6 \text{ dynes/cm.}^2$$

$$\beta = 3.4$$

$$E_0 = 1.58 \times 10^6$$

$$\tau_e = 0.564 \text{ (at } 115°\text{C.)}$$

The value of τ_e, given in minutes, is only applicable in equations based upon the Fujita proposal.

With the above data eq. (11) becomes:

$$\log \tau_m = -(6.19 - \log \alpha) + 3.4 \log \bar{M}_w \tag{A}$$

and eq. (13) becomes, assuming $M_c = 2.0 \times 10^4$,

$$\log(\tau_m - 0.56) - \log(\log \tau_m + 0.25) = -14.87 + 3.4 \log \bar{M}_w \tag{B}$$

The theoretical line A and the theoretical curve (B) are shown in Figure 1.

When the experimental values of $\log \tau_m$ (Table I) are plotted against $\log \bar{M}_w$ for the fifteen polymers, Figure 1, it is evident that the data conform approximately to the line A rather than the curve B. From this straight line A a slope of 3.4 (β) and intercept -15.10 were calculated; then $\log \alpha = -8.91$ was obtained from eq. (A), agreeing with the line A.

The values of η were computed for all fifteen polystyrene polymers from eq. (14):

$$\eta = 2.303 \int_{-\infty}^{\infty} tE_r(t)d(\log t) \tag{14}$$

The values of η computed by the above method were divided by 3 and so converted to those of η_{shear}, the shear viscosity; they are given in Table I. A plot of $\log \eta_{\text{shear}}$ versus $\log \bar{M}_w$ at 115°C. is given in Figure 2.

From the straight line in Figure 2 for the ranges of $\bar{M}_w \gg M_c$, the values $\log \alpha = -7.52$ and $\beta = 3.38$ of α and β were calculated from eq. (4). These values fit very well with those obtained by the other method described above.

As a matter of fact, it is very difficult to see any changes of τ_e in the relaxation spectra in our previous work.[4] So it is seen from these results that

the suggestion made by Tobolsky and his co-workers is preferable and it is concluded that τ_e is not a parameter independent of molecular weight but one dependent on it as well as on τ_m, while E_0 is dependent on molecular weight

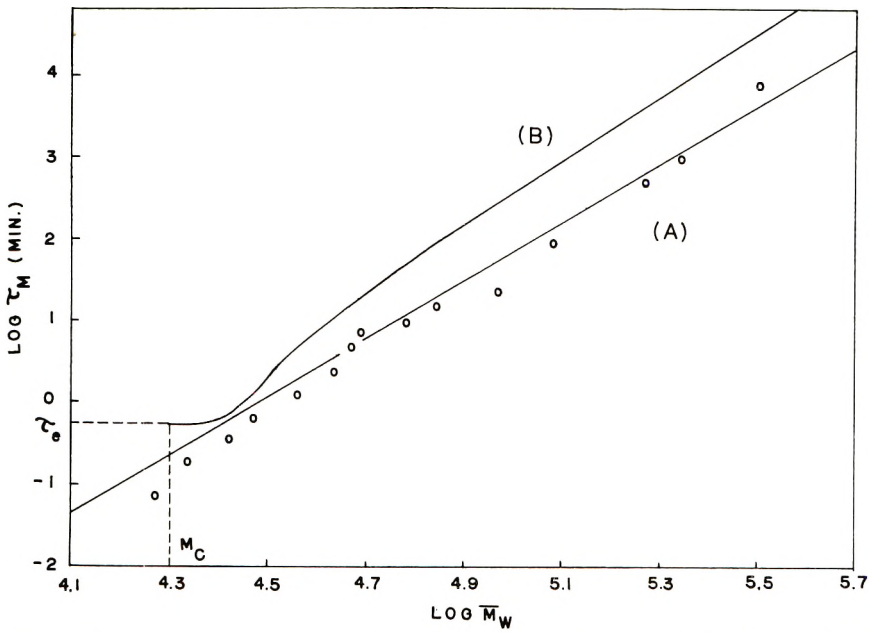

Fig. 1. Theoretical and experimental relationship between log τ_m and log $\bar{M}_w$, at 115°C

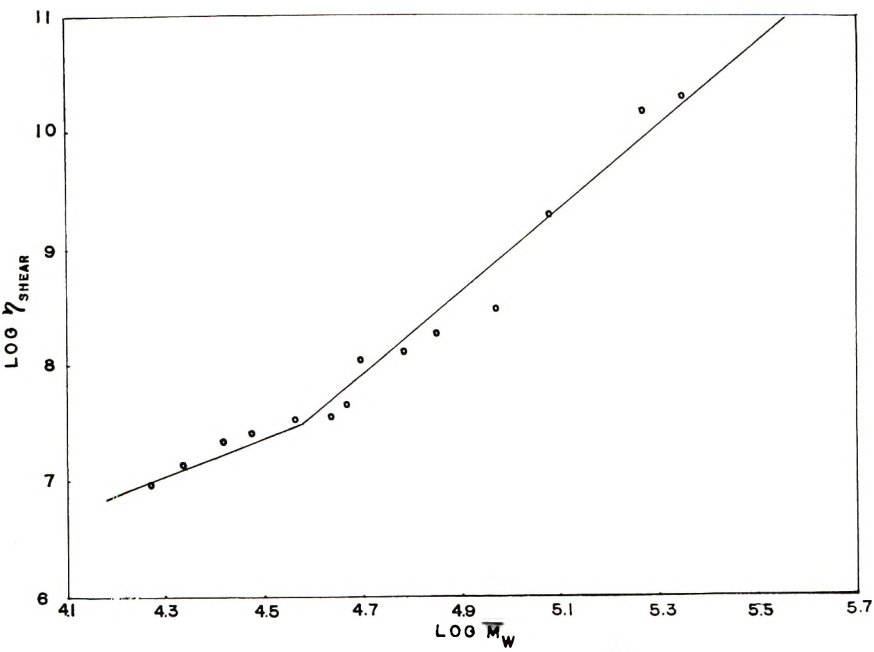

Fig. 2. Shear viscosity η vs. molecular weight $\bar{M}_w$ at 115°C.

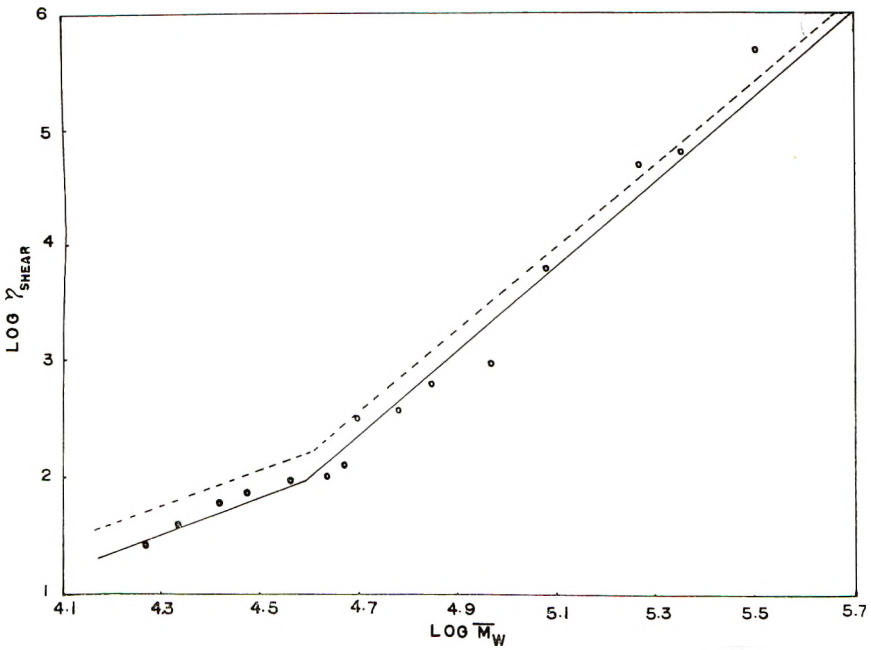

Fig. 3. Relationship between shear viscosity η and molecular weight $\bar{M}_w$ at 217°C: (- - -) data of Fox and Flory[7]; (—O—) data of Sobue and Murakami.

distribution. The solid line in Figure 3 is the relation between log η_{shear} and log $\bar{M}_w$ at 115°C. converted to that at 217°C. by using the following equation of Fox and Flory:[7]

$$\log (\eta_T/\eta_{217}) = 2.68 \times 10^{16} (1/T^6 - 1/490^6)e^{-1330/M} \qquad (15)$$

The experimental relation log η_{shear} versus log $\bar{M}_w$ at 217°C. taken from the viscosity measurements made by Fox and Flory are indicated by the dotted line in Figure 3. It is seen that both lines are situated very closely, and the experimental relation log τ_m versus log $\bar{M}_w$ for the samples which have molecular weights in the vicinity of M_c deviate more or less from the straight line expressed by eqs. (11) or (A). Then it is expected from the above-given facts that the samples having molecular weights in the vicinity of M_c would behave quite differently from those above M_c. It was obvious in the previous paper that the relaxation spectra of polymers in the vicinity of M_c could still be approximated by "box-type" functions. In calculating values of η for several samples in the vicinity of M_c, Y, which is given below, cannot be neglected when compared with the values of $E_0 (\tau_m - \tau_e)$:

$$\begin{aligned} Y &= 2.303 \int_{-\infty}^{\tau_e} \tau \bar{H} (\log \tau)\, d\,(\log \tau) \\ &= 2.303 \int_{-\infty}^{\tau_e} tE_r(t) d(\log t) \end{aligned} \qquad (16)$$

Accordingly, while eq. (5) can be established for the ranges of $\bar{M}_w \gg M_c$, eq. (17) may be established for the vicinity of M_c.

$$Y + E_0(\tau_m - \tau_e) = \alpha' \bar{M}_w^{\beta'} \qquad (17)$$

Here α' and β' are constants for polymers in the vicinity of M_c, as suggested by Fox and Flory. Nevertheless, when the suggestion of Tobolsky and co-workers is taken, and eq. (10) is substituted into eq. (17), we obtain:

$$(\tau_m + Y/k) = (\alpha'/k)\bar{M}_w^{\beta'} \tag{18}$$

Here $k = E_0(1 - 1/10^{\tilde{K}})$
Therefore:

$$\log (\tau_m + Y/k) = \log \alpha'/k + \beta' \log \bar{M}_w \tag{19}$$

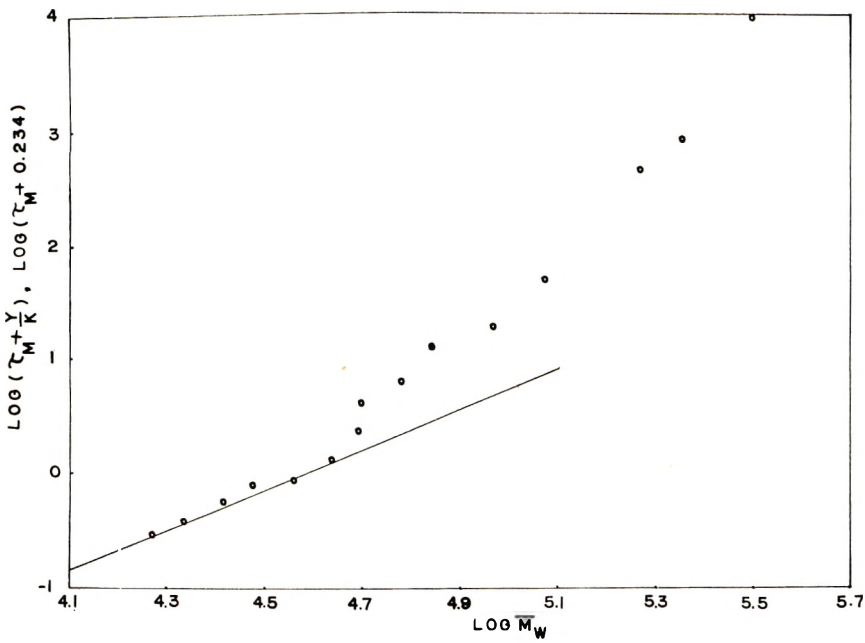

Fig. 4. Relationship between log $(\tau_m + Y/k)$ and molecular weight $\bar{M}_w$ at 115°C.

Since τ_e is found to be dependent on molecular weight, the values of Y also depend upon molecular weight, as is clearly seen from eq. (16). However, several samples of polymers in the vicinity of M_c used in our experiment (samples 1 to 5) have molecular weights which are closer to each other than those of the samples of higher molecular weight, as may be seen in Table I.

Accordingly, as the differences among the values of Y are so small, Y is regarded as the constant value for these polymers, which causes no inconvenience in the next calculation. The experimental data for these polymers in our experiment are as follows:

$$Y = 3.60 \times 10^5 \text{ min. at } 115°\text{C.}$$

$$K = E_0(1 - 1/10^{\tilde{K}}) = 1.54 \times 10^6$$

According to Fox and Flory,[7,8] the viscosity formula for polystyrene polymers in the vicinity of M_c is given by eq. (20):

$$\log \eta_{217} \cong 1.65 \log M - 5.38 \text{ at } 217°\text{C}. \tag{20}$$

The following values of α' and β' were obtained when the values of eq. (20) were converted to those at 115°C. by means of eq. (15): $\alpha' = -5.87$ and $\beta' = 1.65$.

By substituting Y, k, α', and β' into eq. (19), eq. (21) was obtained:

$$\log (\tau_m + 0.23) = -5.87 + 1.65 \log \bar{M}_w \tag{21}$$

Values of $\log (\tau_m + 0.23)$ were plotted against $\log \bar{M}_w$ for all fifteen polymers; see Figure 4. The polymers in the vicinity of M_c fit a straight line very well as seen in Figure 4. Since the straight line in Figure 4 was found to have a slope of 1.64 and an intercept of −7.22, it was regarded as the same as that expressed by eq. (19) or (21).

It is thus concluded that eq. (19) or (21) may be established for polydisperse polystyrene polymers which have molecular weights in the vicinity of M_c.

References

1. Andrews, R. D., and A. V. Tobolsky, *J. Polymer Sci.*, **7**, 221 (1951).
2. Ferry, J. D., I. Jordan, W. W. Evans, and M. F. Johnson, *J. Polymer Sci.*, **14**, 261 (1954).
3. Tobolsky, A. V., *J. Am. Chem. Soc.*, **74**, 3786 (1952); *J. Appl. Phys.*, **27**, 673 (1956).
4. Tobolsky, A. V., and K. Murakami, *J. Polymer Sci.*, **47**, 55 (1960).
5. Baysal, B., and A. V. Tobolsky, *J. Polymer Sci.*, **9**, 171 (1952).
6. Fujita, H., and K. Ninomiya, *J. Polymer Sci.*, **24**, 233 (1957).
7. Fox, T. G, and P. J. Flory, *J. Polymer Sci.*, **14**, 315 (1954).
8. Fox, T. G, and P. J. Flory, *J. Phys. Chem.*, **55**, 221 (1951).
9. Zimm, B. H., *J. Chem. Phys.*, **18**, 830 (1950).

Résumé

C'est un fait bien connu que l'image de la rélaxation de polymères linéaires amorphes dans la région caoutchouteuse peut être représentée par une fonction-type caractérisée par 3 éléments τ_e, τ_m et E_0. Dans ce cas-ci τ_e, τ_m et E_0 représentent respectivement le temps minimum de rélaxation, le temps maximum de rélaxation et la hauteur de la courbe. L'équation $(\tau_m - \tau_e)/\log (\tau_m/\tau_e) = 2{,}303\, \alpha \bar{M}_w^{\beta}/E_r(\tau_e)$ peut être déduite du simple traitement mentionné dans cet article. Nous pouvons ensuite déduire l'équation ci-dessus $\log \tau_m = -\log E_0/\alpha(1 - 1/10^K) + \beta \log M_w$ pour ce qui concerne les polymères synthétisés par nous. Cependant en comparant ces résultats à ceux de Fujita, τ_e est indépendant du poids moléculaire et τ_m devient τ_e lorsque $\bar{M}_w$ se confond à M_c. Dans ce cas, l'équation ci-dessus est transformée en $\log (\tau_m/\tau_e - 1) - \log \log \tau_m/\tau_e = \beta \log M_w/M_c$. D'autre part, $\log \tau_m$ obtenus expérimentalement ont été pontés en fonction de $\log \bar{M}_w$ pour les mêmes polymères et on a trouvé que de tels résultats expérimentaux étaient plutôt sur une ligne droite comme l'indique le première équation, que la courbe indiqué par la dernière. Pour les polymères au voisinage de M_c on trouve $\log (\tau_m + 0.234) = -5.87 + 1.65 \log \bar{M}_w$.

Zusammenfassung

Es ist wohl bekannt, dass die Relaxationsspektren im Kautschukbereich linearer amorpher Polymerer durch eine Rechteckverteilung dargestellt werden können, die durch drei Elemente, τ_e, τ_m und E_0 charakterisiert wird. Hier bedeutet τ_e die kleinste und τ_m die grösse Relaxationszeit und E_0 die Höhe der Kurve. Mit der in dieser Mitteilung angegebenen einfachen Behandlung kann die Gleichung $(\tau_m - \tau_e)/\log(\tau_m/\tau_e) = 2{,}303\ \alpha \bar{M}_w^{\beta}/E_r(\tau_e)$ abgeleitet werden. Soweit es die von uns synthetisierten Polymeren betrifft, kann dann aus obiger Gleichung $\log \tau_m = -\log E_0/\alpha(1 - 1/10^K) + \beta \log \bar{M}_w$ erhalten werden. Nach den Ergebnissen von Fujita ist aber τ_e unabhängig vom Molekulargewicht und τ_m wird gleich τ_e, wenn $\bar{M}_w$ dem M_c entspricht. In diesem Fall geht aber die obige Gleichung in $\log(\tau_m/\tau_e - 1) - \log\log \tau_m/\tau_e = \beta \log \bar{M}_w/M_c$ über. Andererseits wurden die experimentell erhaltenen $\log \tau_m$ – Werte für die gleichen Polymeren gegen $\log \bar{M}_w$ aufgetragen, wobei sich zeigte, dass die experimentellen Werte besser auf der durch die erste Gleichung geforderten geraden Linie lagen als auf der durch die zweite bedingten Kurve. Auch die Beziehung $\log(\tau_m + 0{,}234) = -5{,}87 + 1{,}65 \log \bar{M}_w$ erwies sich für die Polymeren in der Nachbarschaft von M_c als geeignet.

Received June 25, 1962

JOURNAL OF POLYMER SCIENCE: PART A VOL. 1, PP. 2049–2056 (1963)

A Thermodynamic Study of Viton Elastomer

RYONG-JOON ROE and WILLIAM R. KRIGBAUM, *Department of Chemistry, Duke University, Durham, North Carolina*

Synopsis

The temperature coefficients of the retractive force at successive fixed lengths were measured for a Viton fluoroelastomer sample. At each elongation the sample was held for at least 40 hr. before the tension measurement in order to minimize the relaxation effect. The range of elongations covered was confined to α values smaller than 1.65 because of the limited tensile strength of the sample. The results show departures from the predictions of simple gaussian theory of rubber elasticity in two respects. First, the tension f at 45°C. follows the Mooney equation with nonvanishing C_2 values ($2C_1$ = 3.324 kg./cm.^{2} and $2C_2$ = 2.865 kg./cm.^{2}). Secondly, the internal energy makes a negative contribution to the elastic force, and moreover the ratio of the internal energy component to the total tension f_e/f decreases with increasing α. The thermodynamic behavior of the Viton sample is thus qualitatively similar to that observed previously with a natural rubber network, except that the internal energy makes *positive* contribution in the latter. The experimental results were also compared with recent theories which purport to improve upon the simple Gaussian theory of rubber elasticity, but it is found that none of them can explain the results in satisfactory detail.

I. INTRODUCTION

According to the simple Gaussian theory of rubber elasticity (see Treloar[1]) the equilibrium tension f of a crosslinked polymer network, when stretched unidirectionally to relative elongation α, is given by

$$f = (\partial A/\partial L)_{T,V} = \nu kT[\alpha - (1/\alpha^2)] \tag{1}$$

where ν is the number of network chains per unit volume. Equation (1) implies that the energy component f_e of the total tension is equal to zero, *i.e.*,

$$f_e = (\partial E/\partial L)_{T,V} = f - T(\partial f/\partial T)_{V,L} = 0 \tag{2}$$

Experimental results show, in general, departures from the predictions of eqs. (1) and (2) in three important aspects. First, for large values of α the observed tension is much greater than that given by eq. (1). Secondly, for small values of α the experimental results are more accurately described by the Mooney equation[2]

$$f = 2C_1[\alpha - (1/\alpha^2)] + 2C_2[1 - (1/\alpha^3)] \tag{3}$$

where C_1 and C_2 are constants. Thirdly, the energy component f_e is nonvanishing and varies, moreover, with α. In this study we are concerned with the latter two behaviors occurring at small α values.

The value of the energy component f_e observed at small α may be either

positive or negative, depending on whether the average end-to-end dimension of the corresponding free chain decreases or increases with increasing temperature. Results of careful measurements of f and f_e for natural rubber crosslinked by radiation were presented in a previous paper.[3] Natural rubber networks exhibit positive values of f_e for small elongations. Measurements are presented here for a Viton fluoroelastomer network which exhibits negative values of f_e. Except that the sign of f_e is opposite, the thermodynamic behaviors of the Viton and rubber networks are qualitatively the same.

II. EXPERIMENTAL

The crosslinked sheet of Viton fluoroelastomer was kindly supplied by E. I. du Pont de Nemours and Co. A compounded stock consisting of Viton A, 100 parts, MgO, 5.0 parts, and hexamethylenediamine carbamate, 1.5 parts, was precured for 30 min. at 150°C. in a press, followed by a 24 hr. cure at 204°C. in an oven. A strip 1.6 mm. × 2.0 mm. × 15 cm. cut from the cured sheet was used for these measurements. The method of measurement has been described previously.[3] In the present work, however, the tension-temperature coefficient at a fixed length was first measured at the lowest elongation, and then the length was increased in successive steps until the sample strip broke at $\alpha \cong 1.65$. For each elongation the sample was held at 60°C. for at least 40 hr. before the tension measurement

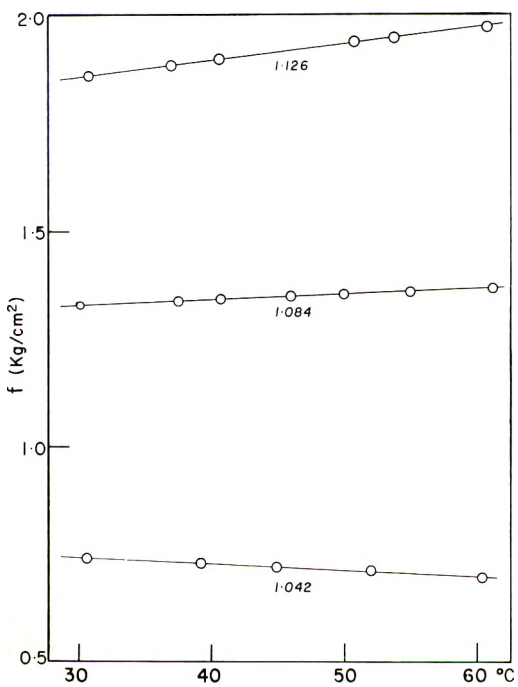

Fig. 1. Tension vs. temperature at constant length. The indicated relative elongations refer to 45°C.

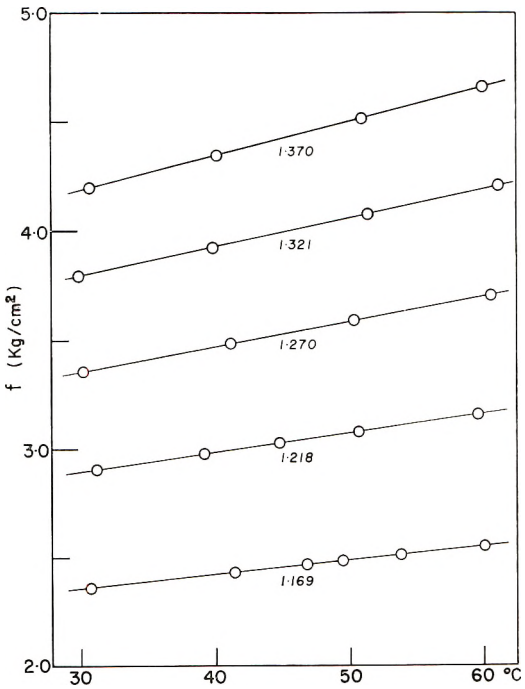

Fig. 2. Tension vs. temperature at constant length. The indicated relative elongations refer to 45°C.

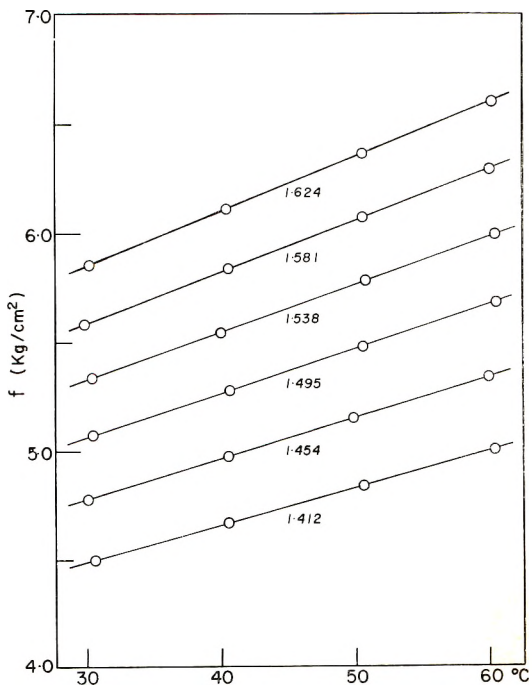

Fig. 3. Tension vs. temperature at constant length. The indicated relative elongations refer to 45°C.

in order to allow for relaxation. The results of the tension-temperature measurements are plotted in Figures 1–3. The α values shown refer to 45°C. (the average temperature). Table I lists the experimental values of the tension f at 45°C. and $(\partial f/\partial T)_{p,L}$. It is seen that the latter quantity is negative at the smallest elongation, the thermoelastic inversion[11] occurring at $\alpha \cong 1.07$.

TABLE I

α	f, kg./cm.^{2}	$\left(\frac{\partial f}{\partial T}\right)_{p,L} \times 10^2$, kg./cm.^{2}-deg.
1.042	0.719	−0.163
1.084	1.350	0.134
1.126	1.972	0.385
1.169	2.523	0.641
1.218	3.112	0.912
1.270	3.628	1.165
1.321	4.100	1.380
1.370	4.546	1.610
1.412	4.878	1.766
1.454	5.204	1.930
1.495	5.521	2.095
1.538	5.819	2.249
1.581	6.113	2.414
1.624	6.403	2.551

III. RESULTS AND DISCUSSION

A. The f_e/f Ratio

The fractional contribution of the internal energy to the total elastic tension f_e/f was calculated according to the relation

$$f_e/f = 1 - (T/f)(\partial f/\partial T)_{p,L} - [3T\lambda/(\alpha^3 - 1)] \quad (4)$$

where λ is the linear thermal expansion coefficient. Equation (4) was derived by Flory, Ciferri, and Hoeve[4] on the assumption that the rubber network obeys a modified Gaussian law,[5]

$$f = \nu kTG(T)[\alpha - (1/\alpha^2)] \quad (5)$$

where the temperature-dependent factor $G(T)$ takes into account the variation with temperature of the mean-square end-to-end distance, $\overline{r_0^2}$, of free chains. For our Viton sample λ was observed to be $2.3 \pm 0.1 \times 10^{-4}$ deg^{-1}. In Figure 4 values of f_e/f calculated from the experimental values of $(\partial f/\partial T)_{p,L}$ according to eq. (4) are plotted against α. It is seen that the f_e/f ratio at first decreases rapidly with increasing α, and then gradually levels off. A similar variation of f_e/f with α was observed for a natural rubber network at comparable α values, although f_e was positive in the latter case.

In Figure 4 the f_e/f ratio is apparently positive for $\alpha \cong 1$. It is, how-

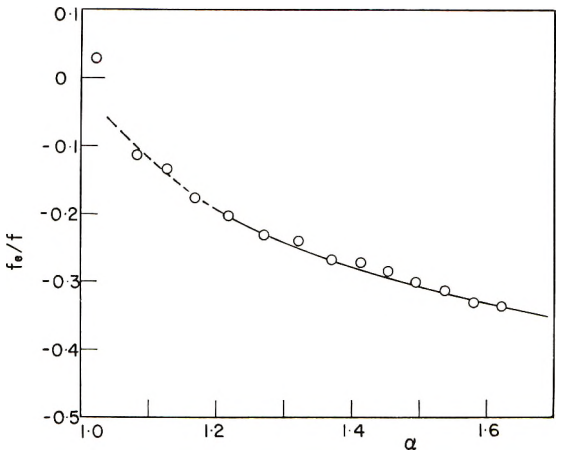

Fig. 4. Variation with elongation of the fractional contribution of internal energy to the total elastic tension, f_e/f.

ever, considered that a change in the sign of the f_e/f ratio at small α is unlikely, and the positive value may probably arise either from an experimental error or from some inadequacy in the Flory-Ciferri-Hoeve eq. (4). The third term on the right side of eq. (4) is sensitive to a small experimental error in α when α is near unity. One can also calculate f_e/f from the experimental data according to the approximate relation[12]

$$f_e/f \cong 1 - (T/f)(\partial f/\partial T)_{p,\alpha} \tag{4a}$$

which has been shown to hold for $\alpha \cong 1$. The values of f_e/f obtained by use of eq. (4a) are smaller than those given in Figure 4 by about 0.05, and therefore, negative in the whole range of α.

B. C_2 and f_s

According to the Mooney eq. (3), a plot of $f/[\alpha - (1/\alpha^2)]$ against $1/\alpha$ should yield a straight line. It is seen in Figure 5 that the experimental values of f_{45} conform to the Mooney equation. Values of the constants obtained from this line are:

$$2C_1 = 3.324 \text{ kg./cm.}^2$$

$$2C_2 = 2.865 \text{ kg./cm.}^2$$

Figure 6 represents a similar plot of the entropy component of the total elastic force, $f_s = f - f_e$. The linear relationship observed suggests that f_s also may be represented by a Mooney-type equation

$$f_s = 2C_{1s}[\alpha - (1/\alpha^2)] + 2C_{2s}[1 - (1/\alpha^3)] \tag{6}$$

In the plot, all points except the two at $\alpha \cong 1$ (where the experimental error is largest) lie nearly parallel to the abscissa, indicating that C_{2s} is nearly equal to zero. For natural rubber it was also found[3] that C_{2s} is much smaller than C_2.

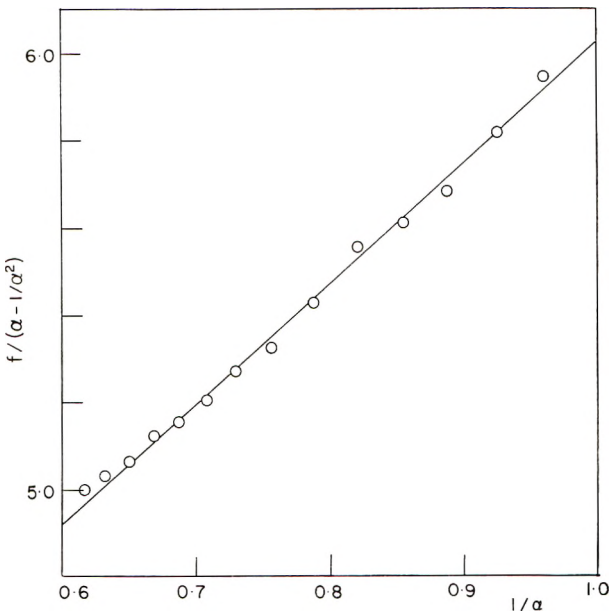

Fig. 5. Mooney equation plot of the total tension f at 45°C.

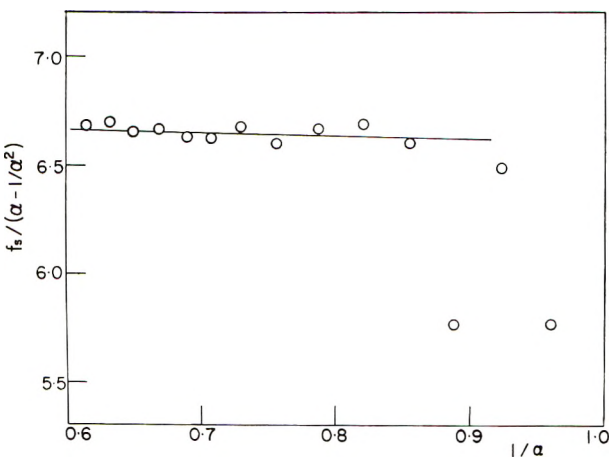

Fig. 6. Mooney equation plot of the entropy component f_s of the total tension at 45°C.

C. Comparison with Theories

The modified Gaussian theory [eq. (5)] leads to [5]

$$f_e/f = T(\partial \ln \overline{r_0^2}/\partial T)_p, \tag{9}$$

and thus predicts that the f_e/f ratio should be independent of α. However, the results shown in Figure 4 do not conform to this prediction. Moreover, f_e/f varies most rapidly as α approaches unity, whereas one would expect the gaussian theory to be obeyed more exactly in this region.

The cubic lattice theory of Krigbaum and Kaneko,[6] which takes into account the energy differences associated with different conformations of the network chains, shows that f_e/f can in fact vary with α, although the predicted variation may not be large enough to explain quantitatively the results appearing in Figure 4. The theory also predicts nonvanishing values of C_2. However, the predicted C_2 is negative when f_e is negative, whereas experimentally only positive C_2 values have been observed.

Ciferri and Flory[7] found that the magnitude of C_2 decreases as the time interval between measurements at successive elongations is made longer (from 3 min. to 30 min.), hence they conclude that C_2 should nearly vanish under equilibrium conditions. In this work a much longer interval of time (at least 40 hr.) was allowed between successive elongations. Krigbaum, Kaneko, and Roig,[8] working with a different Viton sample (crosslinked by radiation, and estimated to have a lower crosslink density than the present one), observed that most of the stress relaxation occurs soon after elongation, and that the stress reaches a nearly constant value after about an hour at 60°C. From these considerations it appears that, although some residual kinetic effects may still be present, the C_2 values observed must be very close to those obtained at thermodynamic equilibrium.

Vol'kenshteĭn et al.[9] and DiMarzio[10] proposed that the C_2 term can be accounted for through consideration of the entropy effects arising from the correlation between conformations of neighboring chains (as a result of the competition for space). However, it does not seem possible to explain the variation of f_e/f with α shown in Figure 2 from entropy effects alone.

IV. CONCLUSIONS

The internal energy makes a negative contribution to the elastic force of Viton fluoroelastomer on simple elongation. This may be contrasted with the positive contribution of the internal energy previously observed for a network of natural rubber. In other respects, both networks exhibit qualitatively similar deviations from the simple kinetic theory of rubber elasticity: C_2 in the Mooney equation is nonvanishing and positive, and f_e/f varies with α. None of the recent theories which purport to improve upon the simple kinetic theory were found to be able to explain these deviations in detail.

This work was supported by the U. S. Army Research Office (Durham).

References

1. Treloar, L. R. G., *The Physics of Rubber Elasticity*, 2nd ed., Oxford University Press, New York, 1958.
2. Mooney, M., *J. Appl. Phys.*, **11**, 582 (1940).
3. Roe, R-J., and W. R. Krigbaum, *J. Polymer Sci.*, **61**, 167 (1962).
4. Flory, P. J., A. Ciferri, and C. A. J. Hoeve, *J. Polymer Sci.*, **45**, 235 (1960).
5. Flory, P. J., *J. Am. Chem. Soc.*, **78**, 5222 (1956).
6. Krigbaum, W. R., and M. Kaneko, *J. Chem. Phys.*, **36**, 99 (1962).
7. Ciferri, A., and P. J. Flory, *J. Appl. Phys.*, **30**, 1498 (1959).

8. Krigbaum, W. R., M. Kaneko, and A. Roig, *J. Polymer Sci.*, **1**, 1 (1963).
9. Vol'kenshtein, M. V., Gotlib, Yu. Ya., and O. B. Ptitsyn, *Vysokomol. Soed.* **1**, 1056 (1959).
10. DiMarzio, E. A., *J. Chem. Phys.*, **36**, 1563 (1962).
11. Flory, P. J., *Principles of Polymer Chemistry*, Cornell University Press, Ithaca, N. Y., 1953, p. 446.
12. Elliott, D. R., and S. A. Lipmann, *J. Appl. Phys.*, **16**, 50 (1945); G. Gee, *Trans. Faraday Soc.*, **42**, 585 (1946).

Résumé

On mesure pour un échantillon de fluoroélastomère Viton les coefficients de température de la force de rétraction à des longueurs fixes successives. A chaque élongation, l'échantillon est maintenu pendant au moins 40 heures avant la mesure de la tension dans le but de minimiser les effets de rélaxation. Les domaines d'élongation étudiés sont limités à des valeurs de alpha inférieures à 1.65 par suite de la force de tension limitée de l'échantillon. Les résultats montrent des écarts par rapport aux prévisions de la théorie élémentaire gaussienne sur l'élasticité des caoutchoucs à deux points de vue. Premièrement, la tension f à 45°C suit l'équation de Mooney avec des valeurs de C_2, qui ne deviennent pas négligeables ($2C_1$ = 3.324 kg/cm² et $2C_2$ = 2.865 kg/cm²). En second lieu, l'énergie interne donne une contribution négative à la force d'élasticité et, de plus, le rapport de la composante énergétique interne à la tension totale f_e/f diminue avec l'augmentation de alpha. Le comportement thermodynamique de l'échantillon de Viton est donc qualitativement semblable à celui observé antérieurement avec un caoutchouc naturel réticulé compte tenu de ce que l'énergie interne donne une contribution positive dans ce dernier cas. Les résultats expérimentaux sont aussi comparés avec les théories récentes qui cherchent à se baser une théorie gausienne simple de l'élasticité des caoutchoucs mais on trouve qu'aucune de celles-ci ne peut expliquer les résultats avec les détails satisfaisants.

Zusammenfassung

Der Temperaturkoeffizient der rücktreibenden Kraft bei sukzessive festgelegten Längen wurde an einer Probe des Fluorelastomeren Viton gemessen. Die Probe wurde zur Ausschaltung des Relaxationseffektes mindestens 40 Stunden vor der Messung bei der betreffenden Elongation gehalten. Der Elongationsbereich wurde wegen der begrenzten Zugfestigkeit der Probe auf α-Werte kleiner als 1,65 beschränkt. Die Ergebnisse weichen in zweifacher Hinsicht von den Erwartungen der einfachen Gauss-Theorie der Kautschukelastizität ab. Erstens gehorcht die Spannung bei 45°C der Mooney-Gleichung mit nicht verschwindenden C_2-Werten ($2C_1$ = 3,324 kg./cm.² und $2C_2$ = 2,865 kg./cm.²). Zweitens liefert die innere Energie einen negativen Beitrag zur elastischen Kraft und ausserdem nimmt das Verhältnis der inneren Energie-Komponente zur Gesamtspannung, f_e/f, mit steigendem α ab. Das thermodynamische Verhalten der Viton-Probe ist also qualitativ dem früher bei einem Naturkautschuknetzwerk beobachteten ähnlich, ausgenommen, dass bei letzterem die innere Energie einen positiven Beitrag liefert. Die Versuchsergebnisse wurden auch mit neueren Theorien verglichen, welche eine Verbesserung der einfachen Gauss-Theorie der Kautschukelastizität liefern sollen; es zeigte sich aber, dass keine davon die Ergebnisse in allen Einzelheiten befriedigend erklären kann.

Received August 28, 1962

JOURNAL OF POLYMER SCIENCE: PART A VOL. 1, PP. 2057–2065 (1963)

Preparation and Aromatization of Poly-1,3-Cyclohexadiene. II*

D. A. FREY, MASAKI HASEGAWA, and C. S. MARVEL, *Department of Chemistry, University of Arizona, Tucson, Arizona,* and *Department of Chemistry and Chemical Engineering, University of Illinois, Urbana, Illinois*

Synopsis

Further work on the polymerization of 1,3-cyclohexadiene by the action of Ziegler-type catalysis and by cationic initiation has been carried out and polymers with an inherent viscosity of 0.1–0.19 have been obtained consistently. Dehydrogenation of the poly-1,3-cyclohexadiene by halogenation followed by pyrolysis has given good conversion to a polyphenyl which has some units which are incompletely aromatized. This polymer has very good heat stability but is not a useful polymer for plastic purposes.

In a previous communication[1] the properties of a poly-1,3-cyclohexadiene made by the action of a Ziegler-type catalyst on 1,3-cyclohexadiene and its subsequent dehydrogenation by treating with chloranil were described. This process resulted in a mixture of a black polyphenyl and carbon black which was completely intractable. The present paper describes further efforts to polymerize 1,3-cyclohexadiene with Ziegler-type catalysts and with cationic initiators and a new process for dehydrogenation of this polymer to yield a *p*-polyphenyl which appears to have approximately 100 recurring units.

In the current work, 1,3-cyclohexadiene, which has been shown by vapor-phase chromatography to be very pure with only traces of cyclohexene and benzene as impurities, has been polymerized with triisobutylaluminum in combination with titanium tetrachloride, vanadium trichloride, or tetrabutyl titanate[2] and by the cationic initiators, composed of boron trifluoride, phosphorus pentafluoride, and titanium tetrachloride under a variety of conditions of temperature, solvents, catalyst concentration, etc., as shown later in the experimental part. In all cases the poly-1,3-cyclohexadienes obtained had inherent viscosities in the range 0.04–0.19. The polymers made by Ziegler-type catalysts all seemed to have a regular 1,4 structure and those from cationic initiators were mixtures of

* The work discussed herein was supported by contracts AF 33(616)5486 and AF 33(616)7908 with the Materials Laboratory, Wright Air Development Division, Wright-Patterson Air Force Base, Ohio. Reproduction of this paper in whole or in part is permitted for any purpose of the United States Government.

1,2 and 1,4 units. In no case was a polymer with an inherent viscosity above 0.19 obtained. All the polymers had properties much like those recorded before.[1]

Some new procedures for dehydrogenation have been developed. One consists in adding bromine to the poly-1,3-cyclohexadiene and pyrolyzing the bromine addition product. The other involves chlorination of the polymer followed by pyrolysis. Both procedures give products which contain small amounts of residual halogen.

When bromination of poly-1,3-cyclohexadiene (inherent viscosity of 0.15) was done in refluxing *n*-butyl bromide solution, a tan powder containing 45.57% bromine (and having an inherent viscosity of 0.18) was obtained. Heating this product in a nitrogen atmosphere to 300°C. for 10 hr. and then an additional 8 hr. at 380°C. gave a dark brown product which contained only 2.4% bromine. This polymer had infrared aborption at 3100, 2980, 1605, 1480, 995, 795, 740, and 685 cm.$^{-1}$.

Another sample of brominated polymer was diluted with terphenyl and heated to 340–350°C. under nitrogen for 12 hr. The terphenyl was extracted with hot benzene, and the resulting dark polymer contained only 0.46% of bromine. This material was still soluble in 1-methylnaphthalene and had an inherent viscosity of 0.09 in this solvent. It is evidently a mixture of many *p*-phenylene units with some undehydrogenated units and a small amount of brominated units. If the assumption is made that each chain contains one bromine atom this polymer has about 100 C_6 recurring units.

More complete conversion to aromatic units was obtained by the chlorination and pyrolysis procedure. In general this procedure was used on poly-1,3-cyclohexadiene made by cationic initiation which consisted of a mixture of 1,2 and 1,4 structures. Chlorination was achieved by adding dry chlorine to a carbon tetrachloride solution of the poly-1,3-cyclohexadiene. The chlorinated polymer contained 50.58% of chlorine, which indicates some substitution as well as addition to the double bond. Pyrolysis of this chlorinated polymer by heating at 350–375°C. for 6 hr., cooling, grinding, and reheating to 400°C. under a pressure of 0.025 mm. for 22 hr. gave a shiny black polyphenyl insoluble in all solvents investigated. X-ray diffraction indicates it is amorphous. Analysis indicates a formula of $(C_6H_{3.78}Cl_{0.31})_n$. Infrared absorption at 3030 cm.$^{-1}$ indicates aromatic C—H; that at 2990, 2885, and 2840 cm.$^{-1}$ indicates aliphatic C—H; that at 1595 and 1460 cm.$^{-1}$ indicates sketal C=C; that at 1006 and 815 cm.$^{-1}$ indicates *p*-aromatic substitution; that at 885 and 760 cm.$^{-1}$ indicates *o*-aromatic substitution; and that at 695 cm.$^{-1}$ indicates C—Cl bonding. These data suggest that this material has some phenylene units (both 1,2 and 1,4), some chlorinated phenylene units and some partially hydrogenated phenylene units.

This black polymer was sulfonated by hot concentrated sulfuric acid to give a polymer soluble in methanol, concentrated sulfuric acid, and partially soluble in water. The sulfonated polymer contained 14.75%

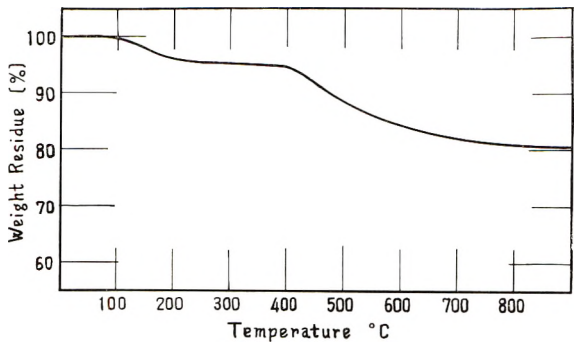

Fig. 1. Thermogravimetric analysis curve for dehydrogenated poly-1,3-cyclohexadiene.

sulfur, which indicates one sulfur for each twelve carbon atoms. On long heating at about 400°C. in the air this polymer was gradually oxidized. The thermogravimetric analysis curve determined for us at the Polymer Branch of the Nonmetallic Materials Laboratory, Directorate of Materials and Processes is shown in Figure 1.

EXPERIMENTAL

1,3-Cyclohexadiene boiling at 79–80°C., n_D^{25} 1.4715 was used. Gas chromatography indicated the presence of traces of cyclohexene and benzene. Addition of these materials in larger amounts did not affect polymerization results.

Poly-1,3-cyclohexadiene

a. From Ziegler-Type Catalysts

The conditions and general procedures described earlier[1] were used in some experiments. In other experiments the titanium tetrachloride was replaced by vanadium trichloride and by tetrabutyl titanate. A few typical runs are described in Table I.

When vanadium trichloride was substituted for titanium tetrachloride no polymer was obtained.

b. With Cationic Initiators

The general procedure for the polymerizations with boron fluoride or phosphorus pentafluoride initiation was as follows.

In a 100-ml. 3-necked round-bottomed flask, fitted with an inlet bubbler, drying tube, thermometer, mechanical stirrer, and serum cap, were placed 40 ml. of dry methylene chloride and 7.5 g. of 1,3-cyclohexadiene (freshly distilled, b.p. 76–77°C. uncorrected). The flask was immersed in a Dry Ice–acetone mixture, and after allowing the mixture to cool to −70°C., boron trifluoride was bubbled into the mixture for approximately 1 min. Within 30 sec. the mixture turned cloudy and solid polymer was visible.

TABLE I
Polymerization of 1,3-Cyclohexadiene with Ziegler-Type Catalysts

Solvent	Vol. solvent, ml.	Catalyst[a]	$Al(i\text{-}Bu)_3$[b] / catalyst	Wt. monomer, g.	Temp., °C.	Time, hr.	Conversion, %	Inherent viscosity[c]
Heptane	20	$TiCl_4$	2.88	7	−15	68	18.9	0.10
Heptane	30	$TiCl_4$	4.32	7	−15	68	2.9	0.11
Cyclohexane	8.75	$TiCl_4$	1.60	9.7	15	68	25.2	0.12
Cyclohexane	5.25	$TiCl_4$	0.96	9.7	15	68	54.8	0.14
Cyclohexane	8.75	$TiCl_4$	1.13	9.7	15	68	47.8	0.14
Heptane	100	$Ti(OBu)_4$	28.1	5	50	24	31.8	0.05
Methylene chloride	40	$Ti(OBu)_4$	0.22	3.5	−20	66.5	49	0.11

[a] The titanium tetrachloride was purified by the procedure of Clabaugh et al.[3]
[b] The triisobutylaluminum was obtained from the Texas Alkyls Corporation.
[c] Determined on a solution of 0.2 g. polymer in 100 ml. of benzene.

A temperature increase of approximately 20°C. took place during the addition of boron trifluoride. The polymerization mixture was stirred for $^1/_2$ hr., and the catalyst was decomposed by the addition of ethyl alcohol to the polymerization mixture at the temperature at which the polymerization was run. The polymerization mixture was poured into methyl alcohol, the polymer was removed by filtration and dried under reduced pressure (0.025 mm.) for 24 hr. The polymer was reprecipitated twice by addition of its benzene solution to methanol to yield 4.15 g. (55.4%). This benzene-soluble polymer had an inherent viscosity of 0.16 (0.200 g./100 ml. of benzene at 30°C.).

The benzene insoluble polymer was continuously extracted with refluxing xylene for 48 hr. This xylene solution was filtered, concentrated, and poured into a large excess of methyl alcohol. The polymer was filtered and dried under reduced pressure (0.025 mm.) for 18 hr. to yield 0.75 g. (10%). The polymer had an inherent viscosity of 0.19 (0.200 g./100 ml. of xylene at 30°C.).

ANAL. Calcd. for C_6H_8: C, 90.00%; H, 10.00%. Found: C, 89.59%; H, 10.32%.

When tetrahydrofuran was used as a solvent for the polymerization, only a trace amount of polymer was formed.

When phosphorus pentafluoride was used as the catalyst, the xylene-soluble polymer was produced in a yield of 86.6%. The inherent viscosity of the polymer was 0.10 (0.25 g./100 ml. of xylene at 30°C.).

Polymerization of 1,3-cyclohexadiene was effected with the use of titanium tetrachloride. The catalyst was prepared in a drybox under a nitrogen atmosphere by adding 0.22 ml. of a 10% solution of titanium tetrachloride (in methylene chloride) to 40 ml. of methylene chloride in a 4-oz. screw-cap bottle. The cap was placed on the bottle, removed from the drybox and placed in a Dry Ice–methanol bath. Freshly distilled 1,3-cyclohexadiene (3.0 g.) was added via a hypodermic syringe to the bottle. The polymerization bottle was placed in a bath at −20°C. for 66.5 hr. The catalyst was decomposed by the addition of 10 ml. of ethyl alcohol to the polymerization mixture at the temperature at which the reaction was carried out. The contents of the bottle were emptied into approximately 600 ml. of methanol. Poly-1,3-cyclohexadiene was removed by filtration, washed with methanol, and dried under reduced pressure (0.025 mm.) for 24 hr. The polymer was twice reprecipitated by addition of its benzene solution to methanol to yield 1.47 g. (49%). This poly-1,3-cyclohexadiene had an inherent viscosity of 0.11 (0.200 g./100 ml. of benzene at 30°C.). When benzene was used as a solvent only lower molecular weight polymers were obtained.

The polymers obtained by the above procedures melted in the range of 160–180°C., were white, and were oxidized slowly on exposure to air to give high melting, yellowish materials.

Bromination of Poly-1,3-cyclohexadiene

a. From Ziegler Catalysts

1. Attempted Preparation of *p*-Poly-2,3-dibromocyclohexane. A 2-g. portion of poly-1,3-cyclohexadiene (the inherent viscosities of the poly-1,3-cyclohexadiene used were 0.12–0.15 at 0.25 ml./100 ml. toluene, 25°C.) was dissolved in 30 g. of carbon tetrachloride, and 2 ml. of absolute ethanol was added to this solution. This solution was kept at 0–5°C., while a mixture of 7.0 g. of bromine and 5.0 g. of carbon tetrachloride were added. It took 2 hr. to complete the addition, and a tan precipitate was produced during this procedure.

After the reaction mixture was kept at 0–5°C. for an additional hour, the mixture was filtered, and the precipitated was washed with methanol; 3 g. of product was obtained after precipitation by adding methanol to a tetrahydrofuran solution of the product, inherent viscosity 0.25 (0.25 g./100 ml. tetrahydrofuran, 25°C.).

ANAL. Calcd. for $(C_6H_8Br_2)_x$: C, 30.00%; H, 3.33%; Br, 66.67%. Found: C, 37.69%; H, 4.09%; Br, 58.05%.

2. High Temperature Bromination of Poly-1,3-cyclohexadiene. A 5-g. portion of poly-1,3-cyclohexadiene (the inherent viscosities of the poly-1,3-cyclohexadiene used were 0.12–0.15 at 0.25 ml./100 ml. toluene, 25°C.) was dissolved in 200 ml. of *n*-butyl bromide. This solution was kept at reflux temperature, while a mixture of 32.0 g. of bromine and 50 ml. of *n*-butyl bromide was added during a 1-hr. interval. After the addition of bromine was completed, the solution was refluxed for 20 hr. A tan precipitate was obtained by adding methanol to the solution. A reprecipitation method by addition of water to the tetrahydrofuran solution was used. The product had inherent viscosity of 0.18 (0.25 g./100 ml. tetrahydrofuran, 25°C.).

ANAL. Found: C, 49.81%; H, 3.73%; Br, 45.59%.

b. From Cationic Catalysts

In a 1-l. three-necked round-bottomed flask fitted with a mechanical stirrer, dropping funnel, drying tube, and thermometer were placed 1.75 g. of poly-1,3-cyclohexadiene, 400 ml. of carbon tetrachloride, and 2.0 ml. of absolute ethyl alcohol. The mixture was cooled in an ice bath to 0–5°C. and 7.0 g. of bromine (excess) dissolved in 100 ml. of carbon tetrachloride was added dropwise over 2 hr. This mixture was stirred for 5 hr. at 0–5°C. and was then slowly allowed to warm to room temperature. The reaction mixture was stirred at room temperature for 14 hr. and then poured into approximately 1500 ml. of methanol. The polymer was filtered, washed with methanol, and dried under reduced pressure (0.025 mm.) for 12 hr. The polymer was twice reprecipitated from tetrahydrofuran with methanol to yield 3.63 g. (60.5% based on the addition of 1 mole of bromine to each recurring unit).

ANAL. Calcd. for $C_6H_8Br_2$: C, 30.00%; H, 3.33%; Br, 66.66%. Found: C, 37.08%; H, 3.99%; Br, 58.48%.

The bromination was also carried out in carbon disulfide; however, the polymer contained less bromine than when the bromination was carried out in carbon tetrachloride.

Pyrolysis of Brominated Polymer

a. Without Heat Transfer Agent

A sample of 0.20 g. of brominated poly-1,3-cyclohexadiene $(C_6H_{5.3}Br_{0.76})_x$ was put into a side-arm test tube which was equipped with a thermometer and nitrogen inlet and outlet tubes. While under a nitrogen atmosphere, the test tube was heated by a metal bath. A considerable amount of hydrogen bromide was obtained from the nitrogen which had been passed through the reaction tube. Shaking was needed occasionally to make the polymer powder heat uniformly. After heating at 300°C. for 10 hr., 0.118 g. of a dark brown powder was obtained.

ANAL. Calcd. for $(C_6H_4)_x$: C, 94.70%; H, 5.30%. Found: C, 84.13%; H, 5.11%; Br, 10.65%.

After heating at 380°C. for an additional 8 hr., 0.104 g. of the polymer was obtained.

ANAL. Calcd. for $(C_6H_4)_x$: C, 94.70%; H, 5.30%. Found: C, 91.92%; H, 5.39%; Br, 2.47%.

The infrared spectrum of this product, determined on a KBr disk, exhibited the following bands: 3100, 2980, 1605, 1480, 995, 795, 740, and 685 $cm.^{-1}$. An ultraviolet absorption spectrum determined on the polymer in concentrated sulfuric acid solution showed a λ_{max} at 325 mμ. The concentrated sulfuric acid solution was prepared as follows. The mixture of the sample and concentrated sulfuric acid was stirred by a magnetic stirrer at the room temperature for 2 hr. The mixture was filtered, and a filtrate was used as the sample of the ultraviolet absorption spectrum.

b. With Heat Transfer Agent

A 100-ml. three-necked flask was equipped with a thermometer, a nitrogen inlet tube, and a condenser which was connected with the nitrogen outlet tube. Brominated poly-1,3-cyclohexadiene (7.1 g.) and 90.0 g. of *p*-terphenyl were mixed thoroughly, placed in the flask and kept at 340–350°C. for 12 hr. under nitrogen. After the reaction was completed, the solid mixture was washed with hot benzene to remove a large part of *p*-terphenyl, then placed in a Soxhlet extractor and extracted with benzene for 24 hr. The polymer then obtained was reprecipitated by adding methanol to its 1-methylnaphthalene solution. The yield was 2.2 g. of *p*-polyphenyl; inherent viscosity, 0.09 (0.25 g./100 ml. 1-methylnaphthalene, 25°C.).

ANAL. Calcd. for $(C_6H_4)_x$: C, 94.70%; H, 5.30%. Found: C, 93.42%; H, 5.21%; Br, 0.46%.

Chlorination of Poly-1,3-cyclohexadiene

In a 500-ml. three-necked, round-bottomed flask fitted with a thermometer, inlet bubbler, mechanical stirrer, and drying tube were placed 2.0 g. of poly-1,3-cyclohexadiene and 250 ml. of carbon tetrachloride. This solution was cooled in an ice bath to 0–5°C. and dry chlorine was bubbled through the continuously stirred solution for 6 hr. As the chlorination progressed some of the halogenated polymer would precipitate out of the solution. The reaction mixture was allowed to stand overnight at room temperature, and the polymer was precipitated by adding the reaction mixture to a large excess of methyl alcohol. The polymer was removed by filtration, washed with methyl alcohol and dried under reduced pressure (0.025 mm.) for 24 hr. The polymer was twice reprecipitated from tetrahydrofuran with methanol to yield 3.53 g. (94.0% based on the addition of 1 mole of chlorine to each recurring unit).

ANAL. Calcd. for $C_6H_8Cl_2$: C, 47.72%; H, 5.34%; Cl, 46.94%. Found: C, 44.46%; H, 4.32%; Cl, 50.58%.

Dehydrogenation and Dehydrohalogenation of Polychlorocyclohexadiene

In a 50-ml. round-bottomed flask fitted with a stopcock was placed 0.75 g. of polychloro-1,3-cyclohexadiene. The flask was evacuated (0.025 mm.) five times, each time being filled with purified nitrogen. While under purified nitrogen the polymer was heated at 350–375°C. for 6 hr. Hydrogen chloride was evolved during the first 3 hr. of heating at 350–375°C. The reaction mixture was allowed to cool and the polymer was pulverized and heated at 400°C. under reduced pressure (0.025 mm.) for 22 hr.

ANAL. Calcd. for $(C_6H_4)_n$: C, 94.70%; H, 5.30%. Found: C, 82.94%; H, 4.49%; Cl, 12.50%.

Sulfonation of Polyphenyl

In a 100-ml., three-necked, round-bottomed flask fitted with an inlet nitrogen bubbler, condenser, thermometer, and magnetic stirrer were placed 0.5 g. of polyphenyl and 25 ml. of concentrated sulfuric acid. This mixture was heated at 250–280°C. for 116 hr. under a nitrogen atmosphere while being continuously stirred. The mixture was cooled, filtered and poured into 150 ml. of distilled water. The black precipitate was removed by centrifugation, washed with ethyl ether, and dried under reduced pressure (0.025 mm.) for 24 hr.

ANAL. Found: C, 39.75%; H, 3.20%; S, 14.75%; residue, 0.55%.

References

1. Marvel, C. S., and G. E. Hartzell, *J. Am. Chem. Soc.*, **81**, 448 (1959).
2. Imoto, M., and I. Soematsu, *Bull. Chem. Soc. Japan*, **34**, 26 (1961).
3. Clabaugh, W. S., R. T. Leslie, and R. Gilchrist, *J. Res. Natl. Bur. Std.*, **55**, 261 (1955).

Résumé

De récents travaux ont été réalisés sur la polymérisation du 1,3-cyclohexadiène par action du catalyseur du type Ziegler et par initiation cationique; on a obtenu des polymères ayant une viscosité inhérente de 0,1 à 0,19. Une déshydrogénation du poly-1,3-cyclohexadiène par halogénation suivie d'une pyrolyse a donné de bons rendements en polyphényle qui possède quelques unités non aromatisées. Ce polymère est thermiquement très stable, mais non utilisable comme plastique.

Zusammenfassung

Weitere Versuche über die Polymerisation von 1,3-Cyclohexadien durch Einwirkung von Ziegler-Katalysatoren und mit kationischem Start wurden ausgeführt und Polymere mit einer Viskositätszahl von 0,1 bis 0,19 erhalten. Dehydrierung des Poly-1,3-cyclohexadiens durch Halogenierung mit darauf folgender Pyrolyse führte zu einer befriedigenden Umwandlung zu einem Polyphenyl mit einigen unvollständig aromatisierten Bausteinen. Dieses Polymere besitzt eine sehr gute Wärmebeständigkeit, ist aber für die Verwendung als Kunststoff nicht brauchbar.

Received May 28, 1962

JOURNAL OF POLYMER SCIENCE: PART A VOL. 1, PP. 2067–2074 (1963)

Preparation and Polymerization of Vinyl 12-Hydroxystearate*

TOSHIYUKI SHONO and C. S. MARVEL, *Department of Chemistry, The University of Arizona, Tucson, Arizona*

Synopsis

Vinyl 12-hydroxystearate was prepared from 12-hydroxystearic acid by vinyl interchange procedure with vinyl acetate. In the reaction, no products having a free hydroxyl group were obtained. The main addition product had the 1-alkoxyethyl acetate structure. Vinyl 12-hydroxystearate was obtained by the treatment of this addition product with acid washed activated alumina in ether solution. Vinyl 12-hydroxystearate polymerized in an emulsion system at a pH of 7–8.5 with standard free radical initiation to give a colorless solid polymer (softening range was 71–75°C.). Vinyl 12-hydroxystearate was copolymerized with vinyl acetate, vinyl stearate and vinyl chloride and the copolymers thus obtained have been characterized.

Vinyl 12-hydroxystearate has been prepared from the acid by vinyl interchange with vinyl acetate in the presence of mercuric sulfate catalyst. Its homopolymer and a variety of copolymers have been prepared and their properties have been determined.

Vinylation of the hydroxy acid was carried out by the procedure of Adelman.[1] When an alcohol group as well as a carboxyl group is present in the acid molecule several reactions with vinyl acetate are possible. It has been observed that the addition of vinyl acetate to an excess of alcohol containing a small amount of mercury oxide and boron trifluoride results in the formation of an acetal and acetic acid in high yields. When the molar ratio of alcohol to vinyl acetate is less than two, 1-alkoxyethyl acetate occurs as one of the products. It has been suggested that the reaction proceeds as follows:[2]

$$CH_2{=}CHOCOCH_3 + ROH \rightarrow CH_3CH(OR)OCOCH_3 \quad (1)$$

$$CH_3CH(OR)OCOCH_3 + ROH \rightarrow CH_3CH(OR)_2 + CH_3COOH \quad (2)$$

In the preparation of vinyl pinolate

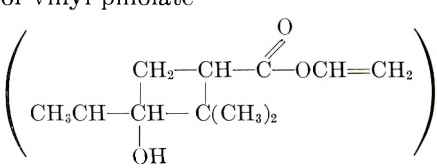

* This is a partial report of work done under contract with four Utilization Research and Development Divisions, Agricultural Research Service, U. S. Department of Agriculture, and authorized by the Research and Marketing Act. The contract was supervised by Dr. J. C. Cowan of the Northern Division.

by the exchange procedure, the reaction mixture was maintained at about 0°C. during and after the addition of the catalyst in order to avoid an undesirable reaction involving the hydroxyl group.[3]

In the reaction of vinyl acetate with 12-hydroxystearic acid, products having a free hydroxyl were not obtained. The main product seems to have the 1-alkoxyethyl acetate and vinyl ester structure. The product was a light yellow oil which hydrolyzed easily to give either vinyl 12-hydroxystearate or 12-hydroxystearic acid depending upon hydrolyzing conditions.

In the infrared spectrum, this compound showed two carbonyl absorption bands at approximately 1780 and 1755 cm.$^{-1}$, and a very strong C=C stretching band appeared at 1655 cm.$^{-1}$, but no hydroxyl bands were indicated.

TABLE I

Homopolymerization of Vinyl 12-Hydroxystearate (in Emulsion with Potassium Persulfate Initiation)

pH	Time, hr.	Conversion, %	Inherent viscosity	Softening range, °C.	Carbon found, %
7.00	17	0	—	—	—
7.00	25	33	0.459	72–75	—
7.00	39	72	0.174	71–74	73.61
7.00	41	64	0.153	71–75	—
5.58	39	4	—	71–73	73.47
No buffer	41	10	0.101	71–75	73.39
8.48	45	50	0.167	73–77	73.63
9.54	24	16	0.297	73–75	73.67

The crystalline material (m.p. 55–56°C.) obtained from the hydrolysis of this first compound using acid washed activated alumina (Merck) in ether solution proved to be the vinyl ester of 12-hydroxystearic acid. The structure was proved by reduction to ethyl 12-hydroxystearate which melted at 52–52.5°C. and gave no melting point depression after mixing with an authentic sample. The infrared spectrum of the crystalline vinyl ester showed OH stretching frequency at 3350 cm.$^{-1}$, vinyl ester absorption band at approximately 1765 cm.$^{-1}$, and C=C stretching frequency at 1655 cm^{-1}.

When the reaction mixture of the vinyl interchange reaction was distilled under vacuum, an unsaturated acid having a b.p. of 200–210°C. (0.4–0.7 mm.) and m.p. 47.5–48°C. was obtained. Titration indicated a molecular weight of 281.5 (calcd. 282). This unsaturated acid seems to be a mixture of 11- and 12-trans-octadecenoic acids (m.p. are 43.5–46.8 and 52.0–53.0°C., respectively).[4]

Vinyl 12-hydroxystearate polymerized in an emulsion system with standard free radical initiation to give colorless, solid polymers which were soluble in tetrahydrofuran. Vinyl 12-hydroxystearate was very sensitive to the

TABLE II
Copolymerization of Vinyl 12-Hydroxystearate

	Vinyl 12-hydroxystearate in monomer mixture		Other monomers	Polymerization methods	Polymerization condition		Conversion, %	Initiator	Inherent viscosity (0.24 g. 100 ml. solvent)	Softening range, °C.	Solubility		Vinyl-12-hydroxystearate in polymer (found by analysis), mole-%
	Mole-%	Wt.-%			Temp., °C.	Time, hr.					Soluble	Insoluble	
HSVA-1	10	27.5	Vinyl acetate	Bulk	70	15.5	Gel	AIBN	—	—	Insoluble gel		—
HSVA-2	10	27.5	Vinyl acetate	Solution	70	18.5	Gel	AIBN	—	—	Insoluble gel		—
HSVA-3	10	27.5	Vinyl acetate	Solution	70	8	33.3	AIBN	0.401	Rubber	Acetone, benzene	*n*-Hexane	9.5
HSVA-4	10	27.5	Vinyl acetate	Solution	70	17.5	60.3	AIBN	0.440	Rubber	Acetone, benzene	*n*-hexane	11.3
HSVS-50	48	50.0	Vinyl stearate	Emulsion	60	24	36.0	$K_2S_2O_8$	0.304	60–65	Benzene	Methanol	68.6
HSVS-20-1	20	17.4	Vinyl stearate	Solution	70	23	66.0	AIBN	0.180	45–46	Benzene	Methanol	30.8
HSVS-20-2	20	17.4	Vinyl stearate	Solution	70	41	74.2	AIBN	0.134	45–46	Benzene	Methanol	30.2
HSVS-10	10	9.5	Vinyl stearate	Solution	70	18.5	72.3	AIBN	0.247	48–50	Benzene	Methanol	16.6
HSVC-20	20	50.2	Vinyl chloride	Emulsion	55	17	62.2	$K_2S_2O_8$	1.562	80–90	Tetrahydrofuran	Methanol	13.8
HSVC-10	10	33.3	Vinyl chloride	Emulsion	55	16	69.5	$K_2S_2O_8$	1.597	85–95	Tetrahydrofuran	Methanol	7.9

pH of the polymerization system, but good results were obtained in the pH range of 7–8.5.

The results of the homopolymerization experiments by emulsion systems are collected in Table I.

Vinyl 12-hydroxystearate polymerized in *n*-hexane or benzene solution with α,α'-azobisisobutyronitrile (AIBN) initiation to give a solid colorless polymer with an inherent viscosity of about 0.1.

Vinyl 12-hydroxystearate was copolymerized with vinyl chloride, vinyl acetate, and vinyl stearate to yield fairly homogeneous copolymers. The polymerization experiments and the properties of the various copolymers obtained are described in Table II.

EXPERIMENTAL

Synthesis of Vinyl 12-Hydroxystearate

A 1-l., three-necked flask equipped with stirrer, reflux condenser with calcium chloride drying tube, and thermometer was charged with 25 g. of 12-hydroxystearic acid (recrystallized twice from acetone, having m.p. of 78–79°C.), 500 ml. of vinyl acetate (Eastern Organic Chemicals, stabilized), 0.1 g. of copper resinate, and 2 g. of mercuric acetate. The mixture was stirred vigorously, and 0.25 ml. of sulfuric acid was added at 10°C. After 2.5 hr. a homogeneous green solution resulted which was allowed to stand at room temperature (18–25°C.) for 4 days. Then 0.7 g. of sodium acetate was added with stirring and the mixture was filtered and then heated to 40°C. under water pump vacuum to remove most of the excess vinyl acetate. The residue was dissolved in 300 ml. of ether and was washed in a separatory funnel with two 500 ml. portions of dilute aqueous sodium chloride solution and then with 500 ml. of 1% sodium bicarbonate solution.

The unreacted acid and acetic acid were removed by repeated washing. The ether solution was decolorized by active charcoal and was stripped of solvent leaving a light yellow oil in almost quantitative yield.

The yellow oil was dissolved again in 300 ml. of ether and 100 g. of acid washed activated alumina (Merck) was added at room temperature. After 20 hr. the mixture was filtered and the activated alumina was washed well with ether. After being dried over anhydrous sodium sulfate, the ether was removed and 13.8 g. (51%) of crystalline substance was obtained. This substance was almost pure vinyl 12-hydroxystearate. It was recrystallized from *n*-hexane and ether yielding colorless crystals which were dried under vacuum, m.p. 55–56°C. 12-Hydroxystearic acid was removed from the vinyl ester by recrystallization from *n*-hexane.

ANAL. Calcd. for $C_{20}H_{38}O_3$: C, 73.61%; H, 11.65%. Found: C, 73.64%; H, 11.73%.

Vacuum Distillation of the Reaction Product of Vinyl Interchange Reaction

Fifty grams of light yellow oil which was obtained from vinyl interchange reaction was distilled under vacuum in the presence of clean copper wire

giving 22.6 g. of main fraction boiling 200–210°C. (0.4–0.7 mm.). This fraction solidified on standing. The solid was recrystallized from acetone and *n*-hexane yielding a colorless crystalline product which was dried under vacuum, m.p. 47.5–48°C.

ANAL. Calcd. for $C_{18}H_{34}O_2$ (octadecenoic acid): C, 76.59%; H, 12.05%. Found: C, 76.02%; H, 12.11%.

Catalytic Hydrogenation of Vinyl 12-Hydroxystearate

Vinyl 12-hydroxystearate (0.300 g.) was dissolved in 100 ml. of *n*-hexane and 0.5 g. of 5% palladium catalyst on charcoal was added to the solution. After hydrogenation under 20 psi pressure for about 12 hr. at room temperature the reaction mixture was filtered and the *n*-hexane was removed under reduced pressure. Colorless crystals which had a melting point of 52–52.5°C. were obtained in quantitative yield.

These crystals gave no melting point depression after mixing with an authentic sample of ethyl-12-hydroxystearate.

Homopolymerization of Vinyl 12-Hydroxystearate

1. *Emulsion Polymerization*

A 2-oz. polymerization bottle was charged with monomer, buffer solution, emulsifier and 2.5% aqueous solution of potassium persulfate in the following ratio: monomer, 1 g.; 2.5% aqueous solution of $K_2S_2O_8$, 0.5 ml.; emulsifier (Triton X-301), 0.2 g.; Buffer solution (standardized buffer solution from W. H. Curtin and Co.; pH 5.58, No. 33099C; pH 7.00, No. 33099; pH 8.48, No. 33098W; pH 9.54 No. 33098T4) 5 ml.

Polymerizations were carried out at 60°C. by tumbling the charges in a constant temperature bath for the times indicated in the tables. The polymers were isolated in the usual manner.

2. *Solution Polymerization*

Vinyl 12-hydroxystearate was dissolved in *n*-hexane or benzene and α,α'-azobisisobutyronitrile was added to the solution. The solution was heated (65°C.) in the sealed test tube under reduced pressure. The results of the homopolymerization experiments in solution are collected in Table III.

TABLE III
Homopolymerization of Vinyl 12-Hydroxystearate (in solution)

Vinyl 12-hydroxy-stearate, g.	Solvent	AIBN, mg.	Poly-meriza-tion time, hr.	Conver-sion, %	Inherent viscosity
0.5519	*n*-Hexane, 2 ml.	12.8	20	45.3	0.110
1.3450	Benzene, 5 ml.	24.3	40	28.2	0.114

Copolymerization of Vinyl 12-Hydroxystearate

1. *Bulk Copolymerization of Vinyl Acetate and Vinyl 12-Hydroxystearate*

HSVA-1. Vinyl acetate (2.9 g.), vinyl 12-hydroxystearate (1.1 g.) and α,α'-azo-bisisobutyronitrile (21.1 mg.) were heated at 70°C. in a sealed test tube under reduced pressure for 15.5 hr. The product is described in Table II.

2. *Solution Copolymerization of Vinyl Acetate and Vinyl 12-Hydroxystearate*

Vinyl acetate (2.9 g.) and vinyl 12-hydroxystearate (1.1 g.) were dissolved in benzene and α,α'-azobisisobutyronitrile was added to the solution. The solution was heated at 70°C. in a sealed test tube under reduced pressure. The polymer was precipitated by pouring the solution into *n*-hexane and purified by reprecipitation from a benzene-*n*-hexane system. Inherent viscosities were determined by means of an Ostwald viscosimeter using a solution of 0.06 g. of polymer in 25 ml. of benzene at 30°C.

The amounts of catalyst used were as listed in Table IV.

TABLE IV

	AIBN, mg.	Benzene, ml.
HSVA-2	22.9	5
HSVA-3	21.7	10
HSVA-4	24.3	10

The results are collected in Table II.

3. *Emulsion Copolymerization of Vinyl Stearate and Vinyl 12-Hydroxystearate*

HSVS-50. Vinyl 12-hydroxystearate (0.5 g.), 0.5 g. of vinyl stearate, 5 ml. of buffer solution (pH = 7), 0.2 g. of Triton X-301, and 0.5 ml. of 2.5% aqueous solution of potassium persulfate were placed into a 2-oz. polymerization bottle. The bottle was flushed with nitrogen and tumbled in a 60°C. bath for 24 hr. The polymer latex was coagulated with saturated sodium chloride solution.

The polymer was purified by reprecipitation with the benzene–methanol system. Inherent viscosity was determined as described above. The results are given in Table II.

4. *Solution Copolymerization of Vinyl Stearate and Vinyl 12-Hydroxystearate*

Vinyl stearate and vinyl 12-hydroxystearate were dissolved in benzene and α,α'-azobisisobutyronitrile was added to the solution. The solution was heated to 70°C. in the sealed test tube under reduced pressure. The

polymer was precipitated by pouring the solution into methanol and purified by reprecipitation using benzene–methanol system. The polymerization recipes are given in Table V. The products are described in Table II.

TABLE V

	Vinyl stearate, g.	Vinyl 12-hydroxy-stearate, g.	AIBN, mg.	Benzene, ml.
HSVS-10	5.0	0.53	28.9	5
HSVS-20-1	2.5	0.53	14.4	5
HSVS-20-2	25.0	5.3	144.1	50

5. *Emulsion Copolymerization of Vinyl Chloride and Vinyl 12-Hydroxystearate*

HSVC-10. The copolymerization procedure was to charge a 2-oz. polymerization bottle with 1.05 g. of vinyl 12-hydroxystearate, 6 ml. of buffer solution (pH = 7), 0.6 g. of Triton X-301, 1.3 ml. of 2.5% aqueous solution of potassium persulfate, and an excess of liquid vinyl chloride.

The vinyl chloride was allowed to evaporate until 2.1 g. remained. The bottle was capped and tumbled in a 55°C. bath for 16 hr. The resulting polymer latex was coagulated with saturated sodium chloride solution. The polymer was purified by reprecipitation using tetrahydrofuran-methanol system. Inherent viscosity was determined as described previously, tetrahydrofuran being used as solvent.

HSVC-20. Into a 2-oz. polymerization bottle were placed 2.1 g. of vinyl 12-hydroxystearate, 2.1 g. of vinyl chloride, 8.4 ml. of buffer solution (pH = 7), 0.8 g. of Triton X-301, and 1.7 ml. of 2.5% aqueous solution of potassium persulfate. The bottle was tumbled in a bath at 55°C. for 17 hr.

References

1. Adelman, R. L., *J. Org. Chem.*, **14**, 1057 (1949).
2. Croxall, W. J., F. J. Glavis, and H. T. Neher, *J. Am. Chem. Soc.*, **70**, 2805 (1948).
3. Parkin, B. A., Jr., and G. W. Hedrick, private communication.
4. Huber, W. F., *J. Am. Chem. Soc.*, **73**, 2730 (1951).

Résumé

On prépare le 12-hydroxystéarate de vinyle à partir de l'acide 12-hydroxystéarique par transvinylation avec l'acétate de vinyle. Dans cette réaction on n'obtient pas de produits contenant des groupes hydroxyles libres. Le produit principal de l'addition présente la structure de l'acétate 1-alkoxyéthylé. On obtint le 12-hydroxystéarate en traitant ce produit d'addition par de l'aluminum activé activé lavé á l'acide. Le 12-hydroxystéarate de vinyle polymérise en émulsion par initiation habituelle aux raddicaux libres, pour donner un polymére incolore solide (domaine de ramollissement 71 á 75°C) à pH 7 à 8.5. On a copolymérisé le 12-hydroxystéarate de vinyle avec l'acétate de vinyle le stéarate de vinyle et le chlorure de vinyle; les polymàres ainsi obtenus ont été caractérisés.

Zusammenfassung

Vinyl-12-hydroxystearat wurde aus 12-Hydroxystearinsäure durch Vinylaustausch mit Vinylacetate dargestellt. Bei dieser Reaktion wurden keine Produkte mit freier Hydroxylgruppe erhalten. Das Hauptadditionsprodukt besass 1-Alkoxyäthylacetatstruktur. Vinyl-12-hydroxystearat bildete sich bei Behandlung dieses Additionsproduktes mit säure-gewaschenem, aktivierten Aluminiumoxyd in Ätherlösung. Vinyl-12-hydroxystearat polymerisierte in einem Standardemulsionssystem mit Radikalstart bei pH 7 bis 8,5 zu einem farblosen, festen Polymeren (Erweichungsbereich 71-75°C). Die Copolymerisation mit Vinylacetat, Vinylstearat und Vinylchlorid wurde durchgeführt und die erhaltenen Polymeren charakterisiert.

Received August 28, 1962
Revised September 24, 1962

JOURNAL OF POLYMER SCIENCE: PART A VOL. 1, PP. 2075–2083 (1963)

Some Anomalous Brittleness Temperatures of Polyethylene

A. RUDIN and J. S. MACKIE, *Canadian Industries Limited, Central Research Laboratory, McMasterville, Quebec, Canada*

Synopsis

Rabesiaka and Kovacs have reported experiments in which the shapes of crystallization isotherms of several polyethylenes depended on the sample history as well as the intrinsic properties of the polymers. The suggestion was made that, in general, molten polyethylene is not in a true thermodynamic equilibrium and includes some quasi-indestructible clusters, which act as heterogeneous nuclei in the crystallization process. This paper reports anomalous brittleness temperature experiments on polyethylenes, the results of which are explainable in terms of quasi-indestructible clusters. The data are consistent with the supposition that the crystalline embryos responsible for the observed behavior result from strong entanglements or cross-linking in natural polyethylene and from binding to carbon black surfaces in black compounds. At the low, nonuniform shear rates in compression molding these clusters may survive relatively intact. If subsequent remelting is performed in the absence of shear, any ordered structure between entanglement points will expand but not break. Such configurations can contract to form crystalline embryos as the polymer is cooled.

INTRODUCTION

Rabesiaka and Kovacs[1] have recently reported experiments in which the shapes of crystallization isotherms of several polyethylenes depended on the sample history as well as the intrinsic properties of the polymers. The suggestion was made that, in general, molten polyethylene is not in a true thermodynamic equilibrium and includes some "quasi-indestructible" clusters, which act as heterogeneous nuclei in the crystallization process. These nuclei could be destroyed by heating only at high temperatures (>180°C.) for long periods. The present paper reports results of brittleness temperature experiments on polyethylenes which are explainable in terms of quasi-indestructible clusters, as suggested by Rabesiaka and Kovacs, and which provide some indication of the nature of these clusters.

EXPERIMENTAL TECHNIQUES

Brittleness temperatures were measured by the method of ASTM D-746,[2] modified to use of notched specimens.[3] In this procedure, compression-molded, rectangular polyethylene specimens are clamped as cantilevered bars, chilled to the required temperature, and struck by a

hammer moving at a specified, constant speed. The brittleness temperature reported is that at which 50% of the specimens tested failed. With proper control of the testing procedure, the standard deviation of distribution of failures is less than 2°C.[3] For the number of test specimens used, statistical analysis of the present data showed that 50% failure temperatures differing by 4°C. were significant at the 95% confidence level.

Specimens were prepared for this study by a compression-molding technique (ASTM D-1928-62T) described in detail elsewhere.[4] Polyethylene granules were homogenized by fluxing on a two-roll mill and then compression-molded in a picture frame chase, using heavy aluminum foil parting sheets. After molding, the polyethylene plaque, frame, and parting sheets could be handled as a unit. To impose a standardized thermal history on the polymer, this molding unit was heated to a temperature above the melting point of the polyethylene and then cooled to room temperature at a standard, controlled rate. Most of the specimens examined were quenched from the melt temperature, generally 130°C., by immersion in water at 18°C. In this case the center of the 0.19-cm. thick polyethylene molding cooled through the freezing range at a rate of about 400°C./min.

Low density polyethylenes were used in the present study. Molecular characteristics of the polyethylenes used are listed in Table I. Sample A contained only an antioxidant; samples B and C were commercial compounds containing 3% channel carbon black.

EXPERIMENTAL RESULTS

The brittleness temperatures of quenched specimens of these materials, listed in Table I, were found to reflect the temperature of the press used to compression-mold the samples. The warmer the press temperature, the colder was the observed brittleness temperature. Other aspects of the specimen preparation and testing procedures which were investigated were found to be without effect on the brittleness temperature. These experiments, which are not reported in detail here, for the sake of brevity, included variation of temperature and duration of roll mill fluxing before molding, variation of dwell time at full pressure and cooling rate during molding, and variation of the remelting temperature, before quenching, between 120°C. and 180°C. Brittleness temperature was also independent of the thermal history of the molded specimens before the final melting and quenching steps of the conditioning process. For example, when polymer A moldings were remelted, cooled to room temperature at 5°C./hr. and then melted again and quenched, the subsequent brittleness temperature reflected the original molding temperature, and corresponded to the figure given in Table I for specimens melted and quenched immediately after molding.

The phenomenon described here was confined to specimens remelted and quenched after molding. Test pieces remelted and cooled slowly to room temperature and as-pressed samples, which were not remelted, had

TABLE I
Brittleness Temperature as a Function of Molding Temperature

Sample	Melt index[a]	$\bar{M}_w$[b]	CH_3/1000 CH_2	Filler	Brittleness temperature, °C. Quenched specimens molded at 126°C.	Brittleness temperature, °C. Quenched specimens molded at 170°C.
A	0.3	7.6×10^5	24	None	−33	−42
B	0.4	6.5×10^5	24	Channel black (3%)	−29	−35
C	2.0	1.2×10^5	—	Channel black (3%)	−21	−28

[a] A.S.T.M. D-1238-57T, Condition E.
[b] $\bar{M}_w$ from light scattering in α-chloronaphthalene at 140°C.

brittleness temperatures which were independent of the original molding temperature. Not all low density polyethylenes tested exhibited this effect. The number of samples examined was not sufficiently large to permit broad conclusions to be drawn, but there seemed to be an indication that the sensitivity of brittleness temperatures of remelted, quenched specimens to molding temperature was promoted by the presence of carbon black.

Pseudohomogeneous Nucleation

The observed differences in brittleness temperatures are suspected to be due to differences in solid texture resulting from differences in crystallite nucleation during quenching. During the quenching process the midplane of the molded plate cools from 130°C. to 18°C. in about 15 sec. Under these conditions, the presence or absence of a crystallization promoter in the melt is likely to result in a noticeable change in the texture of quenched samples. When this is present, pseudohomogeneous nucleation will give rise to fewer crystalline regions, but these will be large and well developed. At slower cooling rates, the crystalline texture should be similar to that produced by homogeneous crystallization because, in this case, it matters less whether embryonic crystals are present at the beginning or are born continuously at later times during the process. On the other hand, density measurements indicated that the overall crystallinity was not significantly different in the two cases. Therefore homogeneous nucleation must give rise to smaller crystallites which should result in a stronger structure, characterized by cooler brittleness temperatures.

Electron micrographs of etched polyethylene surfaces showed that different solid structures were indeed involved. The etching process, described in an earlier article,[5] removes uncrystallized polymer and reveals the underlying spherulitic structure. Etched surfaces of quenched specimens of

black compound B, which is sensitive to molding temperature, are shown in Figure 1. The sample molded at the lower temperature (Fig. 1*a*) has a more fully developed spherulitic structure than its counterpart which was molded hot (Fig. 1*b*). (The latter micrograph is marred by fibers, which are redeposited polyethylene, and have no bearing on this discussion.[5]) Qualitatively, the difference in solid structure parallels the brittleness temperatures of the specimens. For contrast, electron micrographs

Fig. 1. Etched surface of polyethylene B: (*a*) compression-molded at 126°C., brittleness temperature −29°C.; (*b*) compression-molded at 171°C., brittleness temperature −35°C. ×12,150.

of etched surfaces of another black polyethylene compound are shown in Figure 2. This compound is less sensitive to compression-molding temperature, and there is much less difference in the structure revealed by etching.

Postulate of Quasi-Indestructible Clusters

If the observed differences are indeed due to pseudohomogeneous nucleation, the nature of these nuclei remains to be explained. Turnbull[6]

Fig. 2. Etched surface of polyethylene B*: (*a*) compression-molded at 126°C., brittleness temperature −36°C.; (*b*) compression-molded at 171°C., brittleness temperature −39°C. × 12,160.

has shown that if a substance contains a normally stable and wettable impurity possessing pores or cavities on its surface, crystalline embryos can persist in these on an equilibrium basis at temperatures well above the ordinary melting point. Such a body can act as a crystallization growth centre as soon as the polymer is supercooled. By sufficient superheating, the embryos in the cavities can be melted out, thus rendering them inactive as nucleation centers.[7] If this is the cause of the present observations, molding at 170°C. apparently melts the embryos. In that case remelting at the same temperature should have the same effect. It does not, however, so that this explanation must be discarded. Another possibility is the existence of a few, very large, perfect crystals which survive in the melt and serve as nucleating centers. This hypothesis is not consistent with the fact that remelting at temperatures as high as 180°C. and milling at temperatures as high as 160°C. were without effect.

It is suggested that the embryos responsible for pseudohomogeneous nucleation are quasi-indestructible clusters of the type postulated by Rabesiaka and Kovacs[1] and that these clusters can sometimes survive at the low, nonuniform shear rates prevailing in compression molding. Physically, these clusters could result from strong entanglements or cross-linking in natural polyethylene and binding to carbon black surface in black compounds. Nonuniform breakdown of structure has been observed in the flow of gels and elastomers. According to Mooney,[8] when a material containing a three-dimensional thixotropic structure is deformed this structure must be broken up. At first, the broken units may be large in comparison with molecular dimensions and may contain many molecules still held together by forces of appreciable strength. If the shear strength of such units is greater than the shear stress developed between the units as they roll and slide over each other they may persist indefinitely while the material is being sheared. It seems reasonable, furthermore, to assume that the shear stress–shear rate relationship is not uniform throughout the whole sample during compression molding, particularly when this is a flash-type operation, as was the case in the present work and in that of Rabesiaka and Kovacs.[1] Thus the polymer with the lowest shear strength will undergo the most shear strain during this process, and elements with a stronger structure can remain undamaged. If there are crystalline elements in such a flow unit or molecular cluster (i.e., between points of high shear strength) the polymer chains comprising them may survive compression molding in a relatively ordered configuration. (The weakest regions, which undergo the most shear strain, will become more oriented but there is probably ample time for this order to relax during the press hold time at maximum temperature.) During remelting prior to quenching, the crystalline structure in the postulated molecular clusters will expand, but it will not break because it is not being sheared. These configurations can contract to form crystalline embryos as soon as the polymer is cooled. It is suggested that where these clusters exist, they are broken down more thoroughly at higher molding temperatures, so that the

solid structures of the quenched specimens and their brittleness temperatures can vary with molding temperature.

A recent study of the crystallization of polycaproamide[9] has indicated that molecular configurations in the solid are not greatly extended in the unsheared melt, similar to the conclusions from the present work on polyethylene.

Within our limited experience, sensitivity of solid texture to molding temperature seems to be more marked with carbon black compounds than with natural polyethylene. Bondi[10] has suggested that the shear stresses at very low shear rates (in a parallel plate plastometer) may be of the same order of magnitude as the yield strength of carbon black–polystyrene structures. The same author[10] observed that yielding and flow of oil–acetylene black gels took place in restricted locations rather than uniformly through the mass. In studying the flow behavior of rubbers, Mullins and Whorlow[11] noted that the thixotropy was very much more pronounced in black stock than in masticated smoked sheet and that the structure-forming ability decreased as a result of exposure to elevated temperatures. These observations parallel the present ones with natural and black polyethylene.

The foregoing considerations suggest that the rate of shearing should influence the extent to which thixotropic structure is broken. The shear strength of the postulated quasi-indestructible clusters should be higher, the greater the shearing rate. If an increase in press closing speed has any effect, therefore, it should favor retention of structure and should result in quenched specimens with correspondingly warmer brittleness temperatures. Experimentally, this was found to be true in a qualitative sense. (There appeared to be little point in attempting to measure press closing speeds or shear rates quantitatively, because of the nonuniformity of shear rates in compression molding and the fact that press platen speeds were not uniform throughout the whole stroke.) The data in Table II show that the brittleness temperature of quenched specimens of polyethylene A is sensitive to press temperature and shear rate during molding. There is presumably considerable thixotropic structure (or quasi-indestruct-

TABLE II
Effect of Mold Closing Speed and Mold Temperature

Polyethylene	Press temperature, °C.	Brittleness temperature of quenched specimens, °C.		
		Fast press speed	Intermediate press speed	Slow press speed
A	168–170	−35	−42	−49
A	126	—	−33	—
C	170–171	−27	−28	—
C	126	—	−21	—
C*	170–171	−29	−28	—
C*	126	—	−25	—

ible clusters) in this material. The brittleness temperature of carbon black compound C is sensitive only to temperature in this range of molding conditions, while compound C*, which is a variant of C, apparently has no pronounced structure, since its quenched brittleness temperature was not affected by press temperature or molding shear rate.

The experiments of Rabesiaki and Kovacs were performed at considerably slower cooling rates than the quenching studies reported here. It seems likely that the polyethylenes examined in the present study would not exhibit anomalous brittleness temperatures at the cooling rates used in the former authors' dilatometry experiments.[1] If this were so, the difference could be due to the relative insensitivity of the brittleness temperature test, and to the fact that the polyethylenes used by Rabesiaka and Kovacs were high density materials, which presumably did not have any significant long branching and would therefore be more prone to develop thixotropic structure because of molecular entanglements.[12,13]

In summary, although alternative explanations for the present results are certainly possible, the postulate of quasi-indestructible clusters is attractive, particularly since it does not seem to be inconsistent with experience with other thermoplastics and rubber.

The authors are grateful to M. H. Waldman for molecular weight measurements.

References

1. Rabesiaka, J., and A. J. Kovacs, *J. Appl. Phys.*, **32**, 2314 (1961).
2. *A.S.T.M. Standards on Plastics*, Am. Soc. Testing Materials, Philadelphia, 1961.
3. Birks, A. M., and A. Rudin, *A.S.T.M. Bull.*, No. **246**, 49 (1960).
4. Birks, A. M., and A. Rudin, *A.S.T.M. Bull.*, No. **242**, 63 (1959).
5. Mackie, J. S., and A. Rudin, *J. Polymer Sci.*, **44**, 407 (1961).
6. Turnbull, D., *J. Chem. Phys.*, **18**, 198 (1950).
7. Hoffman, J. D., J. J. Weeks, and W. M. Murphey, *J. Res. Natl. Bur. Stds.*, **63A**, 67 (1959).
8. Mooney, M., in *Rheology, Vol. 2*, F. R. Eirich, Ed., Academic Press, New York, 1958, p. 218.
9. Magill, J. H., *Polymer*, **3**, 43 (1962).
10. Bondi, A., *Proc. 2nd Intern. Congr. of Rheology*, V. G. W. Harrison, Ed., Butterworths, London, 1954.
11. Mullins, L., and L. Whorlow, *Trans. Inst. Rubber Ind.*, **27**, 55 (1951).
12. Moore, L. D., Jr., *J. Polymer Sci.*, **36**, 155 (1959).
13. Schreiber, H. P., and E. Bagley, *J. Polymer Sci.*, **58**, 29 (1962).

Résumé

Rabesiaka et Kovacs ont décrit des expériences dans lesquelles les formes des isothermes de cristallisation de plusieurs polyéthylènes dépendaient aussi bien de la préparation de l'échantillon que des propriétés intrinsèques des polymères. On a suggéré qu' en général le polyéthylène fondu n'est pas en équilibre thermodynamique véritable et qu'il contient certains amas quasi indestructibles qui agissent comme noyaux hétérogènes dans le processus de cristallisation. Cette communication rapporte des expériences sur la température anormale de décomposition des polyéthylènes; les résultats de cellesci peuvent être expliqués en tenant compte des aggrégats quasi indestructibles. Les résultats sont en accord avec la supposition que l'embryon cristallin responsable du

comportement observé résulte de gros enchevêtrements ou de pontage dans le polyéthylène naturel et de liens avec les surfaces de noir animal dans les composés contenant ce dernier. À des vitesses de cisaillement basses et non-uniformes dans des moules de compression, ces aggrégats peuvent rester relativement intacts. Si une refonte ultérieure est effectuée en absence de cisaillement, toute structure ordonnée entre les points d'enchevêtrement s'étirera mais ne cassera pas. De telles configurations peuvent donner lieu à la formation d'embryons cristallins quand on refroidit le polymère.

Zusammenfassung

Rabesiaka und Kovacs haben über Versuche berichtet, bei welchen die Gestalt der Kristallisationsisothermen verschiedener Polyäthylene von der Vorgeschichte der Proben und den spezifischen Eigenschaften der Polymeren abhängig waren. Es wurde angenommen, dass sich geschmolzenes Polyäthylen im allgemeinen nicht in einem wahren thermodynamischen Gleichgewicht befindet und gewisse "quasi-beständige" Cluster enthält, die als heterogene Keime beim Kristallisationsprozess wirksam sind. In der vorliegenden Arbeit wird über Versuche zur anomalen Sprödigkeitstemperatur von Polyäthylenen berichtet, deren Ergebnisse auf Grund der Annahme quasi-beständiger Cluster verständlich sind. Die Annahme erscheint gerechtfertigt, dass die für das beobachtete Verhalten verantwortlichen Kristallembryos bei reinem Polyäthylen durch starke Verschlingungen oder durch Vernetzung und bei russhältigen Mischungen durch Bindung an die Russoberfläche entstehen. Bei der niedrigen, uneinheitlichen Schergeschwindigkeit beim Pressguss können diese Cluster verhältnissmässig intakt erhalten bleiben. Bei einem darauf folgenden neuerlichen Schmelzen ohne Scherung wird eine geordnete Struktur zwischen Verschlingungspunkten zwar gedehnt aber nicht zerstört. Solche Konfigurationen können sich beim Abkühlen des Polymeren unter Bildung von Kristollembryos zusammenziehen.

Received May 1, 1962
Revised May 30, 1962

JOURNAL OF POLYMER SCIENCE: PART A VOL. 1, PP. 2085–2092 (1963)

Examination of Kinetics of Graft Copolymerization on Preirradiated Polymethyl Methacrylate

E. TURSKA and S. POŁOWIŃSKI, *Polish Academy of Science, Department of Physical Chemistry of Polymers, Politechnika Łódzka, Łódź, Poland*

Synopsis

The kinetics of graft copolymerization of vinyl acetate on polymethyl methacrylate has been investigated. Polymethyl methacrylate was preirradiated in the presence of air by γ-rays, the polymer being used as the initiator of the polymerization in the one-phase system. The rate of reaction for low conversion is proportional to the concentration of monomer raised to the power of $^3/_2$ and to the concentration of initiator to the $^1/_2$ power. The reaction satisfied the kinetic equation for ordinary addition polymerization if the decrease of the amount of the initiator during the process is taken into consideration. The activation energy of this process has been found. The quantity of the homopolymers produced in this reaction is negligible and need not be taken into account in rough calculations as far as kinetics are concerned.

INTRODUCTION

Graft polymers are usually obtained by the method of preirradiation in a two-phase system.[1] Because of this it is difficult to examine the kinetics of this process, whereas the kinetics of the graft copolymerization carried out in a one-phase system by a chemical method were discussed previously.[2,3]

In this paper we consider the kinetics of the formation of the graft copolymers by preirradiation, when the reaction is carried out in a one-phase system.

The object of our investigation is preirradiated polymethyl methacrylate (PMMA), grafted with vinyl acetate. Both PMMA and the grafted copolymers formed in the process are soluble in the monomer.

As the polymerization was carried out by means of a macroinitiator and a monomer, the process may be supposed to follow the kinetic law governing ordinary addition polymerization.

It has been stated[4] that the rate of polymerization of vinyl acetate initiated by benzoyl peroxide is given by

$$-dM/dt = K_p I^{1/2} M^{3/2} \tag{1}$$

where M is monomer concentration at time t, I is initiator concentration, and K_p is the overall rate constant for polymerization.

In our previous work we proved[5] that thermal decomposition of hydro-

peroxide groups in PMMA subjected to γ-irradiation in air is a first-order reaction, its rate constant being expressed by eq. (2):

$$k_1 = 3.61 \times 10^5 \exp \{-15{,}000/RT\} \quad (2)$$

The rate of the thermal decomposition is high and that is why the decrease of the concentration of the initiator in the course of time should be taken into consideration.

When we substitute in eq. (1) the expression $I = I_0 \exp \{-k_1/t\}$ we get, after integration eq. (3):

$$1/M^{1/2} - 1/M_0^{1/2} = 2K_p I^{1/2}(1 - \exp \{k_1 t/2\})(1/k_1) \quad (3)$$

where M = concentration of the monomer after time t, M_0 = original concentration of the monomer, I_0 = original concentration of the initiator, k_1 = rate constant for the decomposition of the initiator, and K_p = overall rate constant of polymerization.

EXPERIMENTAL AND RESULTS

1. Materials

PMMA was prepared by the polymerization of the monomer in benzene solution, the polymerization being initiated by benzoyl peroxide at 80°C. The polymer was twice precipitated from benzene solution with ethanol, and then dissolved in toluene and heated at 110°C. for 12 hr., so as to decompose trace quantities of initiator remaining. Then the dried and precipitated polymer was ground and sieved, to obtain a powder about 0.2–0.3 mm. in grain diameter. The powdered polymer was irradiated in the presence of air by γ-rays of 0.37 Mr/hr. intensity. The total dose was 6 Mr.

The content of hydroperoxide groups was determined by an amperometric method[6] to be 3.8×10^{-5} mole/g. The molecular weight, as measured by a viscometric method, was 5.38×10^4.

Vinyl acetate was purified by shaking it with $NaHCO_3$ solution, and then dried and distilled under nitrogen, the fraction boiling at 72.2–72.3°C. at 750 mm. Hg being collected.

2. Graft Copolymerization

Irradiated PMMA (0.33 g.) was put in 5-ml. ampules. The samples were degassed under vacuum (10^{-4} mm. Hg) and flushed with nitrogen. Then 4.5 g. of vinyl acetate was added to each ampule and the system was degassed at −72°C. and flushed several times with nitrogen.

The ampules were then sealed and heated at 100, 90, 80, or 70°C., for various lengths of time, constant temperature being maintained within ±0.1°C. After cooling the ampules the quantity of reacted vinyl acetate was determined by weight by evaporating the monomer under vacuum and weighing the samples.

The results of the four series of experiments carried out at various temperatures are given in the Tables I–IV.

To verify whether the results obtained are in good agreement with the equation derived, the value of $[(1 - \exp\{k_i t/2\})(1/k_1)]$ was calculated for each measurement and plotted in Figure 1 against $(1/M^{1/2}) - (1/M_0^{1/2})$.

TABLE I
Graft Copolymerization at 100°C.

Heating time, min.	Amt. vinyl acetate reacted, g.	$1/M^{1/2} - 1/M_0^{1/2}$
3	0.0140	0.0008
8	0.4453	0.016
10	0.4575	0.017
20	0.9351	0.039
47	1.6206	0.080
90	1.6830	0.084

TABLE II
Graft Copolymerization at 90°C.

Heating time, min.	Amt. vinyl acetate reacted, g.	$1/M^{1/2} - 1/M_0^{1/2}$
13	0.5431	0.021
20	0.7908	0.032
25	0.8868	0.037
37	1.1410	0.050
50	1.2789	0.058
82	1.5997	0.078

TABLE III
Graft Copolymerization at 80°C.

Heating time, min.	Amt. vinyl acetate reacted, g.	$1/M^{1/2} - 1/M_0^{1/2}$
10	0.1424	0.006
20	0.3707	0.014
35	0.5787	0.024
57	0.8448	0.036
90	1.1858	0.054
150	1.4707	0.070

TABLE IV
Graft Copolymerization at 70°C.

Heating time, min.	Amt. vinyl acetate reacted, g.	$1/M^{1/2} - 1/M_0^{1/2}$
10	0.0218	0.001
20	0.2014	0.008
30	0.2999	0.011
60	0.5261	0.021
120	0.7180	0.029
180	1.0709	0.046

TABLE V
Dependence of the Rate Constant of Polymerization on Temperature T

Temperature T, °C.	$(1/T) \times 10^3$	$K_p \times 10^5$	-10 g. K_p
100	2.681	157	2.8125
90	2.755	78.3	3.1062
80	2.833	52.4	3.2807
70	2.915	30.2	3.5200

As shown in Figure 1, eq. 3 is satisfied within the limits of experimental error, and thus the overall rate constant K_p may be calculated. In Table V the obtained values of K_p and the corresponding values of $1/T$ are given.

As shown in Figure 2 the Arrhenius equation is satisfied; owing to this, the coefficients of the equation can be calculated.

The dependence of the overall rate constant on temperature may be expressed by the formula:

$$K_p = 8.66 \times 10^{10} \exp \{-14{,}000/RT\}$$

To prove that the rate of the reaction is dependent on the concentration of the initiator, a series of experiments with various quantities of irradiated PMMA was carried out. The experiments were carried out in the same way as previous ones, but the amount of irradiated PMMA used varied in the range 0.1–0.6 g. All the samples were heated at 80°C. for 15 minutes.

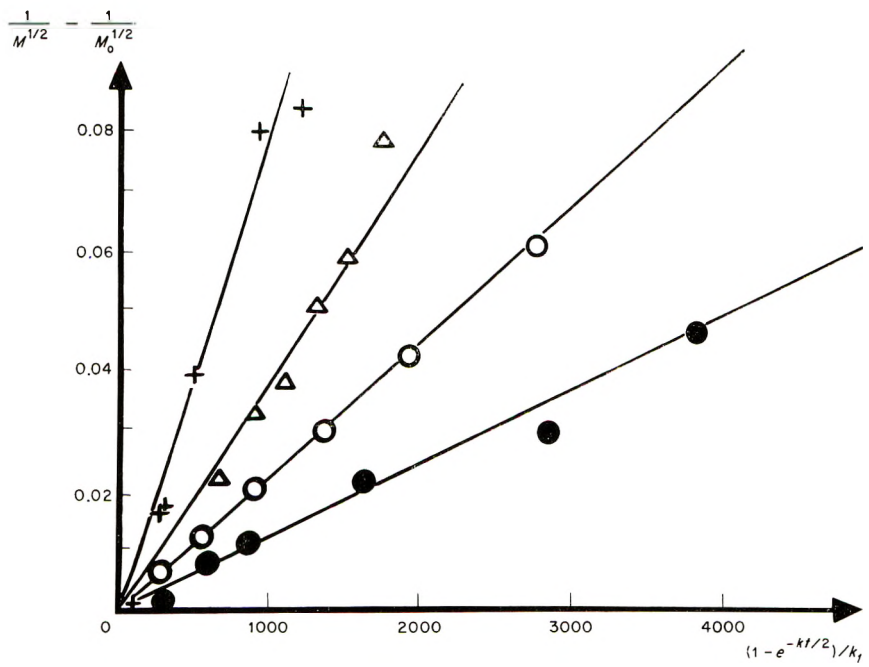

Fig. 1. Plot of $(1/M^{1/2}) - (1/M_0{}^{1/2})$ vs. $[1 - \exp\{-k_1 t/2\}](1/k_1)$ for polymerization at (+) 100°C.; (△) 90°C.; (○) 80°C.; (●) 70°C.

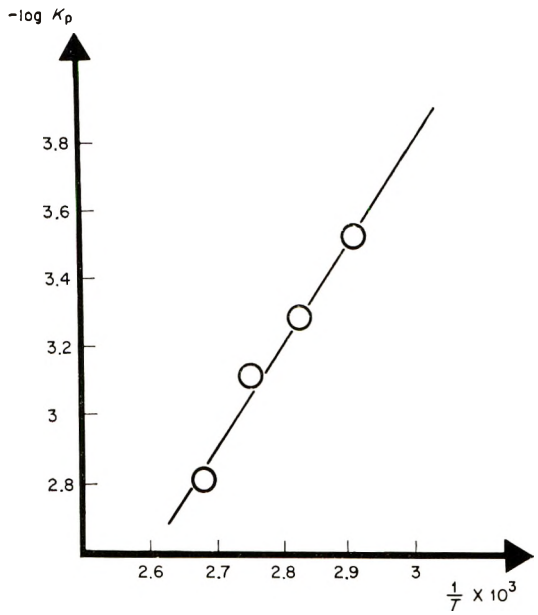

Fig. 2. Dependence of the rate constant of the polymerization on temperature.

As the time of the reaction is short, the quantity of the reacted vinyl acetate ought to be proportional to $I^{1/2}$, according to eq. (1).

The results of the experiments are given in Table VI.

A plot of the amount of reacted vinyl acetate ΔM against the quantity of the irradiated PMMA is given in Figure 3.

TABLE VI
Influence of the Initiator Concentration on the Rate of Polymerization

Amt. of irradiated PMMA, g.	Amt. vinyl acetate reacted, g.	$I^{1/2} \times 10^2$
0.1042	0.1587	3.23
0.2098	0.2128	4.58
0.3300	0.2500	5.74
0.4395	0.3076	6.63
0.6454	0.4313	8.03

3. Graft Copolymerization in Solution

In solution, the rate of reaction for low conversion should be, according to eq. (1), proportional to the concentration of the monomer, raised to the power of $^3/_2$. To verify this relation graft copolymerization was carried out in benzene solutions of monomer.

Samples of irradiated PMMA containing about 0.33 g. each were placed in ampules; after degassing, to each of them was added 5 ml. of mixed

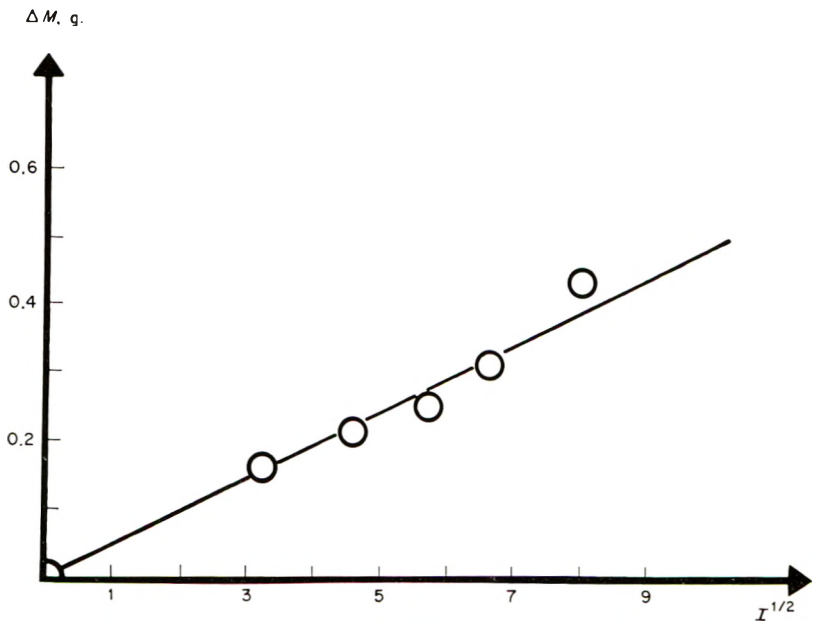

Fig. 3. Plot of the amount of reacted vinyl acetate ΔM against the amount of irradiated PMMA.

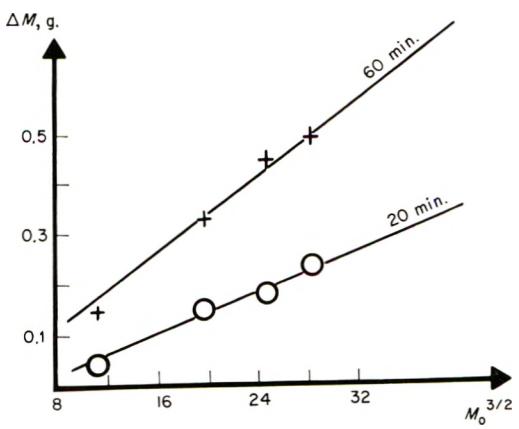

Fig. 4. Relation between the quantity of the reacted monomer ΔM and the original concentration: (×) after 60 min.; (○) after 20 min.

vinyl acetate and benzene. After being degassed again at −72°C. the samples were heated at 80°C.

The quantity of the reacted vinyl acetate was determined by weight. Two series of the experiments were carried out, the samples being heated for 20 min. in the first series and for 60 min. in the second series. The results of the two series of experiments were given in Table VII and Figure 4.

TABLE VII
Dependence of the Rate of Polymerization on the Monomer Concentration M

$M^{3/2}$, mole/l.	Amt. vinyl acetate reacted, g.	
	After 20 min.	After 60 min.
11.52	0.0388	0.1442
19.72	0.1460	0.3258
24.82	0.1791	0.4445
28.27	0.2390	0.4929

4. Determination of Homopolymers

The determination of homopolymers in the product obtained was carried out by the method of Smets and Cleasen[7] based on the difference of the solubility of homopolymers and graft copolymers in ethanol.

All the samples obtained were examined, and it was found that the content of homopolymer did not exceed, in any sample, 1% of the total quantity of the product. In Table VIII are given some typical results of the determination of the homopolymers in one copolymerization series carried out without a solvent at 90°C.

TABLE VIII
Determination of Homopolymers Formed in Grafting at 90°C.

Heating time, min.	Amt. product obtained, g.	Amt. homopolymers, g.
20	1.1246	0.0067
25	1.2219	0.0069
37	1.4710	0.0069
50	1.6108	0.0073

DISCUSSION

When copolymerization is carried out in a one-phase system and preirradiated polymer is used as an initiator, the usual equations for addition polymerization may be used to examine the kinetics of the process.

In our system the polymerization of the monomer initiated by the macroinitiator satisfies the kinetic equation for ordinary addition polymerization, if the decrease of the amount of the initiator during the process is taken into consideration.

The results obtained agree with those of the examination of the kinetics of the polymerization of the vinyl monomers initiated by peresters produced chemically.[2,3] The polymer formed in the reaction may link to the backbones of the preirradiated polymer, producing graft copolymers as well as separate chains of homopolymers.

The quantity of the homopolymers produced is negligible and need not be taken into account in rough calculations as far as kinetics are concerned.

In this case, the rate of the formation of the branches of the graft copolymer is in good agreement with the kinetic formula, eq. (3), for ordinary addition polymerization.

The mechanism of the reaction may be complicated, and it is possible that chain transfer both to the backbone and to the branches of the graft copolymers takes place. Because of this, the number of branches ought to be higher than the number of hydroperoxide groups in the preirradiated polymer.

The examination of the kinetics of the graft copolymerization by the method described above in different systems will be the object of future investigations.

References

1. Chapiro, A., *J. Polymer Sci.*, **48**, 109 (1960).
2. Smets, G., and A. Poot, *J. Polymer Sci.*, **34**, 287 (1959).
3. Smets, G., A. Poot, and L. Duncan, *J. Polymer Sci.*, **54**, 65 (1961).
4. Conix, A., and G. Smets, *J. Polymer Sci.*, **10**, 525 (1953).
5. Turska, E., and S. Polowinski, *J. Polymer Sci.*, **58**, 839 (1962).
6. Abrahamson, E. W., and H. Linschiz, *Anal. Chem.*, **24**, 1355 (1952).
7. Smets, G., and M. Cleasen, *J. Polymer Sci.*, **8**, 289 (1952).

Résumé

On a étudié la cinétique de la copolymérisation greffée de l'acétate de vinyle sur le polyméthacrylate de méthyle. Le polyméthacrylate de méthyle a été irradié par les rayons-γ en présence d'air, et ce polymère a été employé comme initiateur de polymérisation dans un système à une seule phase. On a constaté que la vitesse initiale de la polymérisation est proportionnelle à la concentration de l'initiateur à l'exposant $^1/_2$ et de la concentration du monomère à l'exposant $^3/_2$. On a constaté que la réaction de la formation du copolymère greffé est conforme à l'équation cinétique déduite du principe classique de la cinétique de la polymérisation par addition en admettent le changement de concentration de l'initiateur avec le temps. On a déterminé l'énergie d'activation du processus étudié. On a constaté que la quantité des homopolymères qui se produisent dans la réaction est minime et négligeable.

Zusammenfassung

Die Kinetik der Pfropfcopolymerisation von Polymethylmethacrylat mit Vinylazetat wurde untersucht. Polymethylmethacrylat wurde in Anwesenheit von Luft mit γ-Strahlen bestrahlt und dann als Polymerisationsstarter im Einphasensystem verwendet. Es wurde festgestellt, dass die Anfangsgeschwindigkeit der Polymerisation der Wurzel aus der Starterkonzentration und der $^3/_2$-Potenz der Monomerkonzentration proportional ist. Weiters wurde festgestellt, dass die Reaktion, welche zur Bildung des Pfropfcopolymeren führt, bei Berücksichtigung der zeitlichen Änderung der Starterkonzentration, durch die Gleichungen der klassischen Polymerisationskinetik dargestellt werden kann. Die Aktivierungsenergie der untersuchten Reaktion wurde berechnet. Die Menge des bei dieser Reaktion entstehenden Homopolymernen ist sehr klein und kann bei den kinetischen Betrachtungen vernachlässigt werden.

Received July 31, 1962

JOURNAL OF POLYMER SCIENCE: PART A VOL. 1, PP. 2093–2099 (1963)

On the Additivity of Osmotic Properties of Polyelectrolyte–Salt Solutions

A. KATCHALSKY and Z. ALEXANDROWICZ, *Polymer Department, Weizmann Institute of Science, Rehovot, Israel*

Synopsis

The simple additivity of osmotic pressure and ionic activity observed in polyelectrolyte–salt solutions is derived from a straightforward thermodynamic consideration. The basic assumption of this work is that the activity coefficient of the coions is practically uneffected by the presence of the largely screened polymeric ions.

Recent investigations have shown that the osmotic pressure of mixtures of ionized polyelectrolyte and low molecular salt obey a particularly simple empirical rule. It was found that if the osmotic pressure of the salt-free polyelectrolyte solution be denoted by π_p and the corresponding osmotic pressure of the polyelectrolyte–free salt solution be denoted by π_s, then the osmotic pressure of the mixture π is given by the sum of the individual contributions:

$$\pi = \pi_p + \pi_s \tag{1}$$

This rule was found to hold for various polyelectrolytes in a very wide range of concentrations of the salt and of the polymer.[1] Similar rules were found for the activity of the counterion and of the salt.[1–5]

Such a simple additivity of osmotic activities is, of course, expected for dilute solutions of noninteracting species. Since a strong electrostatic interaction exists, however, between the ions of the neutral salt and of the polyelectrolyte, this behavior is rather unexpected. The aim of this communication is to show that eq. (1) and the related equations—which should hold for any highly charged polyelectrolyte independent of its structure, molecular weight, and degree of ionization—can be derived thermodynamically from the equation of Gibbs-Duhem on the basis of the sole assumption that the osmotic activity of the coions is not significantly influenced by the presence of the polyion.

Consider a solution containing n_p polyelectrolyte and n_s neutral salt molecules per unit volume. Let us assume for the sake of simplicity that the counterion of the polyelectrolyte be the cation of a mono-monovalent salt. The polymer molecules are assumed to be evenly charged and carry ν charges per macromolecule. Thus the solution contains $n_p\nu + n_s$ counterions and n_s coions.

In accord with the usual treatment of polyelectrolyte solutions we subdivide the unit volume under consideration into n_p subvolumes assigned to each polymolecule

$$V = 1/n_p \tag{2}$$

This procedure regards the polyelectrolyte molecules as the central ions in the subvolumes, which establish an electrostatic field in which the small ions are symmetrically distributed around the polyion. On the basis of symmetry considerations it is assumed that the electrostatic potential ψ attains its maximum absolute value in the central region of V and passes through a minimum on the border between neighboring subvolumes. Denoting the border surface by R the electrostatic symmetry requirement states that

$$(\nabla\psi)_R = 0 \tag{3}$$

The absolute magnitude of the potential ψ depends on the point of reference at which the potential is taken to be zero. The common procedure is to consider a polyelectrolyte solution maintaining a Donnan equilibrium with an external salt solution and to take the zero point of potential in the external solution. For our purpose it is more convenient to assume $\psi_R = 0$ at the boundary surface between neighboring subvolumes. This choice leads to simpler equations and is particularly useful for the treatment of salt-free solutions to which no Donnan equilibrium can be assigned.

The small ions in V are subjected to the action of a central potential. If their instantaneous mutual interactions are disregarded,[6] the distribution is adequately represented by Boltzmann's equation, and the number concentration of the ith ion at point $\vec{r}$ is given by

$$\vec{n_i^r} = n_i^\circ \exp\left(-\epsilon_i\psi_r/kT\right) \tag{4}$$

where n_i° is the number of ions of ith type per unit volume in the region where $\psi = 0$, and since in our choice $\psi_R = 0$, we write

$$n_i^\circ = n_i^R \tag{5}$$

A local electrochemical potential $\vec{\tilde{\mu}_i^r}$ may be attributed to each ion at every point $\vec{r}$ of the solution

$$\vec{\tilde{\mu}_i^r} = \mu_i^\circ + kT \ln \vec{n_i^r} + \epsilon_i\psi_r$$

with eqs. (4) and (5) this gives

$$\begin{aligned}\vec{\tilde{\mu}_i^r} &= \mu_i^\circ + kT \ln n_i^\circ - \epsilon_i\psi_r + \epsilon_i\psi_r = \mu_i^\circ + kT \ln n_i^\circ \\ &= \mu_i^\circ + kT \ln n_i^R\end{aligned} \tag{6}$$

In other words, the electrochemical potential throughout the solution is equal to the chemical potential at the boundary of the subvolume.

On the other hand, the chemical potential given by eq. (6) may be compared with the average macroscopic expression

$$\mu_i = \mu_i^\circ + kT \ln f_i n_i \tag{7}$$

based on the known average number concentration n_i and the empirical activity coefficient f_i. The activity coefficient f_i is referred to an ideal solution of small ions without polyelectrolyte. From eqs. (6) and (7) we find that the activity coefficient of the ith ion is given by the ratio of the surface and average number concentrations, i.e.,

$$f_i = n_i^R / n_i \tag{8}$$

Following the treatment of Langmuir[7] and of Verwey and Overbeek[8] for colloidal solutions, Marcus[6] has shown that for polyelectrolyte solutions the osmotic pressure of the system is fully determined by the concentration of the small ions in the boundary surface between neighboring subvolumes, or that

$$\pi = kT \sum_i n_i^R \tag{9}$$

This result is to be ascribed to the fact that at R the polyelectrolytic field is zero, so that the solution at R may be regarded as ideal in the sense of eq. (7). Denoting the activity coefficient of the $(n_p\nu + n_s)$ positive counterions by f_+ and that of the n_s negative coions by f_- we may write, combining eqs. (8) and (9), that

$$\pi = kT[(n_p\nu + n_s)f_+ + n_s f_-] \tag{10}$$

It is generally more convenient to express the observable data in terms of osmotic coefficients instead of osmotic pressures. The practical osmotic coefficient of Bjerrum may be written as the ratio of the observed osmotic pressure to the ideal pressure, given by van't Hoff's law

$$\varphi = \pi/\pi_{\text{ideal}} = \sum n_i^R / \sum n_i = [(n_p\nu + n_s)f_+ + n_s f_-]/(n_p\nu + 2n_s) \tag{11}$$

It is worth noticing that for salt-free polyelectrolyte solutions, for which $n_s \to 0$, the activity coefficient of the counterions equals the osmotic coefficient of the salt-free solution, which we shall designate φ_p, or

$$\lim_{n_s \to 0} f_+ = \varphi_p \tag{12}$$

From both theoretical considerations[9] and experimental analysis,[1,2,10] it is known that φ_p of chain polyelectrolytes is only slightly dependent on polymer concentration, does not depend on the molecular weight, and is mainly determined by the charge density of the polyion.

An alternative definition of the osmotic coefficient is in terms of the activity coefficient of water f_w.

$$\begin{aligned} \varphi(\textstyle\sum n_i/n_w) &= -\ln a_w \\ &= -\ln[f_w n_w/(n_w + \textstyle\sum n_i)] \simeq \textstyle\sum n_i/n_w - \ln f_w \end{aligned} \tag{13}$$

or

$$n_w \ln f_w = \sum n_i(1 - \varphi) \tag{14}$$

Comparing eqs. (11) and (14) we find that

$$n_w \ln f_w = (n_p\nu + n_s)(1 - f_+) + n_s(1 - f_-) \tag{15}$$

The main assumption of this note is that the activity coefficient of the coions is close to unity in the whole range of concentrations and ionizations investigated, i.e.,

$$f_- = 1 \tag{16}$$

The reasoning underlying this assumption is well known: it is realized that it is only the counterions which are strongly attracted by the polymeric ion, and their activity coefficient undergoes a drastic decrease. The coions are slightly repelled by the screened polyion and are moreover attracted by the counterion atmosphere; both effects cancel each other and leave f_- largely unchanged. Indeed, a detailed calculation of the electrostatic potential and of the ionic distributions for cylindrical macroions[11]—which demonstrated the approximate validity of the additivity rules—also led to the result that f_- is not very different from unity for a wide range of salt concentrations. The experimental study of the single ionic activity coefficients in various polyelectrolyte solutions[2,12] likewise shows that in all cases f_- is rather close to unity.

Introducing this assumption into eq. (15) we get

$$n_w \ln f_w = (n_p\nu + n_s)(1 - f_+) \tag{17}$$

The activity coefficient of the low molecular salt is given by the product of f_+ and f_-, or

$$f_s = f_+f_- \tag{18}$$

In view of the requirement $f_- = 1$ we find for the salt component in polyelectrolyte systems

$$f_s = f_+ \tag{19}$$

It is now possible to apply the Gibbs-Duhem equation to our three-component solution, comprising polymer (p), salt (s) and water (w):

$$n_p(\partial \ln f_p/\partial n_s) + n_s(\partial \ln f_s/\partial n_s) + n_w(\partial \ln f_w/\partial n_s) = 0 \tag{20}$$

which is readily shown to follow immediately from the expression for activities.

Introducing the well-known cross relations

$$\partial \ln f_p/\partial n_s = \partial \ln f_s/\partial n_p \tag{21}$$

and f_s and $\ln f_w$ from eqs. (19) and (17), we get from eqs. (20) and (21)

$$n_p(\partial \ln f_+/\partial n_p) + n_s(\partial \ln f_+/\partial n_s) + (1 - f_+) - (\partial f_+/\partial n_s)(n_p\nu + n_s) = 0$$

or

$$(n_p/f_+)(\partial f_+/\partial n_p) + (\partial f_+/\partial n_s)[(n_s/f_+) - (n_p\nu + n_s)] = (f_+ - 1) \quad (22)$$

Equation (22) is a differential equation for f_+ as function of n_p and n_s which may be solved for suitable boundary conditions. According to the standard procedure we have to solve first the characteristic ordinary differential equations

$$dn_p/(n_p/f_+) = dn_s/[(n_s/f_+) - (n_p\nu + n_s)] = df_+/(f_+ - 1) \quad (23)$$

Solving first the relation of n_p and f_+

$$dn_p/(n_p/f_+) = df_+/(f_+ - 1)$$

we get

$$\frac{n_p f_+}{f_+ - 1} = a$$

or

$$f_+ = a/(a - n_p) \quad (24)$$

The second relation between n_p and n_s which is

$$dn_p/n_p = dn_s/[n_s - (n_p\nu + n_s)f_+]$$
$$= dn_s/[n_s - a(n_p\nu + n_s)/(a - n_p)]$$

is integrated at constant a to give

$$(n_p - a)/(n_s + \nu a) = b \quad (25)$$

Upon introducing a from eq. (24) we get

$$b = -n_p/[f_+(n_p\nu + n_s) - n_s] \quad (26)$$

Now by the general theory of partial differential equations any function χ of a and b, say $\chi(a,b) = 0$ or $b = \chi'(a)$ solves eq. (22).

Introducing the values of a and b into the general solution we get

$$n_p/[f_+(n_p\nu + n_s) - n_s] = \chi'[(n_p - f_+)/(f_+ - 1)] \quad (27)$$

We shall now apply the boundary condition eq. (12) that $f_+ \to \varphi_p$ when $n_s \to 0$. The left-hand side of eq. (27) gives in this limiting case $1/\nu\varphi_p$ which is evidently independent of n_s and, as pointed out above, practically independent of n_p too. Thus, χ' is a constant, the value of which is given by $1/\nu\varphi_p$, and we may write eq. (27) in the form

$$n_p/[f_+(n_p\nu + n_s) - n_s] = 1/\nu\varphi_p$$

In other words, the activity coefficient of the counterions is

$$f_+ = (n_p\nu\varphi_p + n_s)/(n_p\nu + n_s) \quad (28)$$

This remarkably simple expression for the activity coefficient f_+ may be made clearer by considering the activity of the mono-monovalent salt in a polyelectrolyte solution

$$a_s = a_+a_- = f_+(n_p\nu + n_s)f_-n_s$$

Use of eq. (16) for f_- and eq. (28) for f_+ gives

$$a_s = n_s(n_p\nu\varphi_p + n_s) \tag{29}$$

We readily recognize that the activity of the coions is equal to their number concentration, since f_- was assumed to be unity. On the other hand, the activity of the counterions $a_+ = n_p\nu\varphi_p + n_s$ is composed of the counterions contributed by the salt n_s and unaffected by the presence of the polyelectrolyte, plus the effective number of counterions $n_p\nu\varphi_p$ contributed by the polyelectrolyte and unaffected by the presence of salt. This rather astounding additivity of ionic activities is confirmed by the experimental results.[1-4] A similar behavior is shown by the osmotic pressure. When f_+ from eq. (28) is introduced into eq. (10) we obtain

$$\pi = kT(n_p\nu\varphi_p + 2n_s) = \pi_p + \pi_s \tag{30}$$

where $\pi_s = 2kTn_s$ is the ideal osmotic pressure of the salt, while $\pi_p = kTn_p\nu\varphi_p$ is the osmotic pressure of salt free polyelectrolyte solution.

For many purposes it is convenient to regard the fraction φ_p of counterions as "free" and the fraction $1 - \varphi_p$ as "bound" to the polyelectrolyte. The result of the present calculation is then that the degree of binding is practically independent of the ionic strength and is determined only by the charge density of the polymolecules.

It should be realized, however, that the assumed invariability of f_- and of φ_p with respect to the polymer concentration and the consequently derived additivity of the colligative properties should not be taken too literally. Although the result constitutes a very useful approximation it cannot be used for the derivation of all the solution properties. A better approximation is required for the exact treatment of Donnan equilibria in a large excess of added salt, which will be the subject of a following communication.[13]

We are indebted to Prof. J. Gillis of the Weizmann Institute for his helpful suggestions.

References

1. Alexandrowicz, Z., *J. Polymer Sci.*, **43**, 337 (1960) and **56**, 115 (1962).
2. Nagasawa, M., M. Izumi, and I. Kagawa, *J. Polymer Sci.*, **37**, 375 (1959) and **38**, 213 (1959).
3. Mock, R. A., and C. A. Marshall, *J. Polymer Sci.*, **13**, 263 (1954).
4. Katchalsky, A., R. Cooper, J. Upadhyay, and A. Wasserman, *J. Chem. Soc.*, **1961**, 5198.
5. Wall, F. T., and M. I. Eitel, *J. Am. Chem. Soc.*, **79**, 1556 (1957).
6. Marcus, R. A., *J. Chem. Phys.*, **23**, 1057 (1955).
7. Langmuir, I., *J. Chem. Phys.*, **6**, 893 (1938).

8. Verwey, E. J. W., and J. Th. G. Overbeek, *Theory of the Stability of Lyophobic Colloids*, Elsevier, Amsterdam, 1948, p. 92.
9. Lifson, S., and A. Katchalsky, *J. Polymer Sci.*, **13**, 43 (1954).
10. Kern, W., *Z. Physik. Chem. (Leipzig)*, **A184**, 197 (1937).
11. Alexandrowicz, Z., *J. Polymer Sci.*, **56**, 97 (1962).
12. Kagawa, I., and K. Katsuura, *J. Polymer Sci.*, **9**, 405 (1952).
13. Alexandrowicz, Z., and A. Katchalsky, in preparation.

Résumé

L'additivité simple de la pression osmotique et de l'activité ionique observée dans les solutions de sels de polyélectrolytes est dérivée d'un raisonnement thermodynamique direct. L'hypothèse de base de ce travail est que le coefficient d'activité des co-ions n'est pratiquement pas affecté par la présence d'ions polymériques fortement entourés par un écran d'ions.

Zusammenfassung

Die in Polyelektrolytlösungen beobachtete einfache Additivität von osmotischem Druck und Ionenaktivität wird auf Grund einer elementaren thermodynamischen Betrachtung abgeleitet. Die Grundannahme dabei ist, dass der Aktivitätskoeffizient der Nebenionen durch die Gegenwart der weitgehend abgeschirmten Polymerionen praktisch nicht beeinflusst wird.

Received July 18, 1962

JOURNAL OF POLYMER SCIENCE: PART A VOL. 1, PP. 2101–2107 (1963)

Polycondensation of Xylylene Dibromides by Transition Metals in Water Suspension

KEIITI SISIDO, NOBUO KUSANO, RYÔZI NOYORI, YÔKO NOZAKI, MASATOSI SIMOSAKA, and HITOSI NOZAKI,
Department of Industrial Chemistry, Faculty of Engineering, Kyoto University, Kyoto, Japan

Synopsis

Treatment of benzyl chloride with iron powder in water suspension results in the formation of benzyl radicals, which are subsequently dimerized into bibenzyl. This reaction has now been extended to *p*-xylylene dibromide under a set of conditions as summarized in Table I. High yields (70–80%) of poly-*p*-xylylene, which was identified by infrared spectrum, x-ray diffraction pattern, and other properties, were obtained with reduced iron suspended in a mixture of xylene and water (50:50) or in dimethylformamide. Zinc powder coated with nickel (Urushibara nickel CB) gave comparable yields of poly-*p*-xylylene, while cobalt powder or zinc-cobalt couple afforded inferior yields. Similar reaction of *o*- and *m*-xylylene dibromides gave soluble polymers. The presence of *o*-xylylene as an unstable intermediate of the polymerization of *o*-xylylene dibromide has been indicated by trapping this transitory hydrocarbon with acrylonitrile and with methyl acrylate as diene adducts.

A recent publication of Alder and Fremery[1] concerned with the formation of intermediary *o*-xylylene in the reaction of *o*-xylylene dibromide with zinc in acetic acid or in dimethylformamide has prompted the authors to record similar observations in the reaction of xylylene dibromides with fine powders of transition metals in water suspension.

A previous paper from this laboratory[2] has dealt with the reaction of benzyl chloride under analogous conditions to afford bibenzyl *via* benzyl radicals. A similar reaction of benzyl chloride with other metals including nickel, cobalt, and zinc has been recorded.[3,4] The reaction of *p*-xylylene dibromide (I) has now been examined and the results are summarized in Table I. The main product was found to be poly-*p*-xylylene

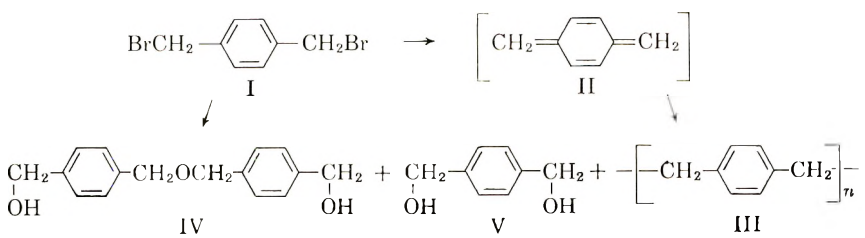

(III) which showed an infrared spectrum, x-ray diffraction pattern, and other properties essentially identical with those of samples prepared by the recorded method.[5] Minor products were 4,4′-bis(hydroxymethyl)dibenzyl ether (IV) and *p*-xylylene glycol (V).

High yields (70–80%) of poly-*p*-xylylene were obtained with reduced iron suspended in a mixture of xylene and water or in dimethylformamide. Nickel and cobalt powders gave inferior yields. Zinc–nickel and zinc–cobalt couples which are called Urushibara nickel CB and Urushibara cobalt B, respectively, and contain about 10% of the transition metals, have been prepared by the method of Taira.[6] The nickel–zinc couple gave high yields of poly-*p*-xylylene in a mixture of xylene and water as a dis-

TABLE I

Preparation of Poly-*p*-xylylene from *p*-Xylylene Dibromide and Finely Divided Transition Metals[a]

Metal	Dispersion medium (and vol., ml.)	Reaction temp., °C.	Reaction time, hr.	Yield of poly-*p*-xylylene	
				g.	%
Fe[b,c]	Water (120)	100	5	3.6	69
Fe[b]	Water (50) and xylene (50)[d]	95	20	3.6	69
Fe[b]	DMF (100)[e]	140	15	4.2	81
Ni[f]	Water (50) and xylene (50)[d]	95	15	2.7	52
Ni–Zn[g]	Water (100)	100	15	3.4	65
Ni–Zn[g]	Water (50) and xylene[d] (50)	95	20	4.2	81
Co[h]	Water (50) and xylene[d] (50)	95	15	2.1	40
Co–Zn[g]	Water (100)	100	15	1.0	19
Co–Zn[g]	Water (50) and xylene[d] (50)	95	20	3.0	58
Zn[i]	Water (100)	100	15	2.7	52
Zn[i]	Water (50) and xylene[d] (50)	95	20	4.1	79
Zn[i]	Xylene[d] (100)	135–140	15	1.1	21
Zn[i]	DMF[e] (100)	140	15	2.0	38

[a] For a standard procedure see Experimental. Unless otherwise stated, 13.2 g. (0.05 mole) of *p*-xylylene dibromide and 20.0 g. of metal powder were used.

[b] Commercially available reduced iron of 150 mesh particle size.

[c] Details are given in Experimental. The reaction was carried out with 12.0 g. of reduced iron.

[d] Commercial mixture.

[e] Dimethylformamide. Attempted condensation of *p*-xylylene dibromide in this medium by means of nickel-zinc or cobalt-zinc couple gave much inferior yields of poly-*p*-xylylene.

[f] Commercially available powder of 300 mesh particle size.

[g] See Taira.[6]

[h] Commercial powder of 1–2 μ particle diameter.

[i] Commercial zinc dust of 200 mesh particle size was used after washing with 10% ammonium chloride solution and water.

persion medium. The aqueous layer of this reaction mixture contained nickel ions and zinc ions in a ratio of approximately 1:3, while in the original couple the content of nickel was 10%. Clearly, nickel was consumed in preference to zinc in the dehalogenation condensation, however, neat zinc dust gave fair to good yields of poly-*p*-xylylene in water suspension.

When alcohol, such as methanol, ethylene glycol, or aqueous ethanol, was used as a dispersion medium, yields of poly-*p*-xylylene were less than 10%; these data were not included in Table I.

Similar treatment of *o*-xylylene dibromide with reduced iron afforded an amorphous polymer whose analyses were close to poly-*o*-xylylene. *m*-Xylylene dibromide also gave a soluble polymer, besides a small amount of [2.2]metacyclophane.[7]

Supposedly, the polymerization of *p*- and *o*-xylylene dibromides would proceed via *p*-xylylene (II) and its *ortho* isomer, respectively, as transitory intermediates, while that of *m*-xylylene dibromide through step-by-step dehalogenation. This is because no resonance-stabilized pseudobiradicals can be expected from the last halide. Attempted demonstration of the intermediary *o*-xylylene by adduct formation with anthracene,[8] maleic acid, or with *p*-benzoquinone failed, poly-*o*-xylylene being the only product isolated. However, when the reaction of *o*-xylylene dibromide with reduced iron suspended in water was carried out in the presence of a large excess of acrylonitrile or of methyl acrylate, the formation of poly-*o*-xylylene was completely suppressed and 2-cyano- and 2-methoxycarbonyl-1,2,3,4-tetrahydronaphthalenes were obtained in 64 and 58% yields, respectively. The acrylonitrile adduct could also be isolated in the presence of nickel or cobalt powder in 18 and 20% yields, respectively. These observations are analogous to those of Alder and Fremery[1] and clearly point to the transitory formation of *o*-xylylene in the reaction of *o*-xylylene dibromide with metal powders. The failure of obtaining the anthracene adduct of *o*-xylylene, which has actually been prepared by the pyrolysis of 1,3-dihydroisothianaphthene-2,2-dioxide in the presence of anthracene at about 290°C.[8] might be ascribed to the difference in reaction temperatures. Presumably, the formation of the anthracene adduct predominates at the higher temperature, while the polymerization of *o*-xylylene is favored near the boiling point of water but is slower than formation of the Diels-Alder adduct. Isolation of *p*-xylylene (II) has not succeeded as yet; however, we would be safe to assume that the pseudobiradical (II) is a reactive intermediate in the polymerization of *p*-xylylene dibromide. The lower molecular weight of poly-*o*-xylylene than that of *m*-isomer, as described below, is still an open question.

EXPERIMENTAL

Reaction of *p*-Xylylene Dibromide with Transition Metals

A typical run is described below. All temperatures were uncorrected. For other experiments carried out with changes in dispersion media and metal powders, see Table I.

A solution of 13.2 g. (0.05 mole) of *p*-xylylene dibromide[9] in 50 ml. of commercial xylene mixture was added all at once to a suspension of 20.0 g. of reduced iron powder in 50 ml. of water. This mixture was heated under refluxing and vigorous stirring for 20 hr. After cooling to room temperature, the reaction mixture was centrifuged. The solids were dried and extracted thoroughly with benzene in a Soxhlet apparatus. The insoluble residue, which was a mixture of poly-*p*-xylylene and inorganic substances, was treated with 100 ml. of boiling 6*N* hydrochloric acid and filtered. This treatment was repeated until the filtrate became completely free from iron ions. The remaining solid was washed with water and dried. Yield 3.6 g. (69%).

Poly-*p*-xylylene thus obtained did not melt below 350°C., and its solubility characteristics agreed with those reported.[5] The Beilstein test was slightly positive, and the low carbon content might be ascribed to the presence of a small amount of oxygen or bromine as terminal groups.

ANAL. Calcd. for $(C_8H_8)_n$: C, 92.26%; H, 7.74%. Found: C, 91.55%; H, 7.69%.

Infrared absorptions (potassium bromide disk): 1905 (w), 1786 (w), 1460 (m), 821 (vs) cm.$^{-1}$. X-ray crystallographic data (CuKα) are given in order of (*hkl*), *d*, A. (intensity), and 2θ: (110), 5.37 (s), 16.5; (011), 5.06 (m), 17.6; (111), 4.55 (w), 19.5; (21$\bar{1}$), 3.98 (s), 22.3; (20$\bar{2}$), 3.95 (s), 22.5; (020), 3.23 (vw), 27.6. These data are in good agreement with those recorded for α-poly-*p*-xylylene.[10]

When the reaction was carried out with 13.2 g. (0.05 mole) of the halide and 12.0 g. of reduced iron suspended in 100 ml. of neat water two minor products were isolated along with poly-*p*-xylylene (69% yield). 4,4′-Bis-(hydroxymethyl)dibenzyl ether, m.p. 96.7°C., was obtained in a 5% yield as colorless leaflets upon careful recrystallizations of soluble fractions from benzene. The same compound was obtained in low yield by the reaction of *p*-xylylene dibromide with *p*-xylylene glycol in the presence of sodium in dioxane followed by hydrolysis. Infrared absorptions (Nujol): 3200 (vs), 1090 (vs), 1028 (vs), 1014 (vs), 824 (vs) cm.$^{-1}$.

ANAL. Calcd. for $C_{16}H_{18}O_3$: C, 74.39%; H, 7.02%. Found: C, 74.58%; H, 7.13%.

Extraction of the aqueous layer of the reaction mixture with ether gave *p*-xylylene glycol (4% yield), m.p. and mixed m.p. 115–116°C. (reported[11] 115–116°C.).

When nickel or cobalt powder was used as a condensation agent, the excess of these metals was removed by dissolving in 3*N* nitric acid at room temperature.

Analysis of the aqueous layer formed in the reaction of *p*-xylylene dibromide with nickel–zinc couple,[6] which contained 9.9% of nickel and 90.0% of zinc, was carried out as follows according to the A.S.T.M. method.[12] After refluxing a mixture of 20.0 g. of the nickel–zinc couple, 13.2 g. (0.05 mole) of *o*-xylylene dibromide, 50 ml. of water, and 50 ml. of

xylene for 20 hr., the aqueous layer was separated and the upper layer was extracted with two 10 ml. portions of water. The combined water layer was diluted to 100 ml., and 2 ml. of the aqueous solution was pipetted. After buffering the sample with tartaric acid and ammonium chloride solutions, the nickel ions were precipitated as nickel dimethylglyoxime (60.6 mg.), and the filtrate was treated with hydrogen sulfide. The precipitating zinc sulfide was converted into zinc oxide, which weighed 54.4 mg. These data indicated the aqueous layer contained nickel and zinc ions in a ratio of 1:3.2.

Reaction of *o*-Xylylene Dibromide with Reduced Iron

A mixture of 13.2 g. (0.05 mole) of *o*-xylylene dibromide (prepared from *o*-xylene by the method described in the literature[9]), 12.0 g. of reduced iron, and 120 ml. of water was refluxed for 5 hr. under vigorous stirring. After cooling, the reaction mixture was treated with 100 ml. of benzene and filtered. From this benzene solution 4.5 g. (87%, calculated as pure xylylene polymer) of brownish gray gum was obtained. The product solidified upon treatment with petroleum ether (b.p. 30–50°C.) and this solid showed a wide melting point range (89–170°C.). The analytical data were as good as those for the *p*-isomer.

ANAL. Calcd. for $(C_8H_8)_n$: C, 92.26%; H, 7.74%. Found: C, 91.48%; H, 7.68%.

The observed molecular weight (cryoscopic method in benzene) was about 1100. Infrared absorptions (potassium bromide disk): 1953 (w), 1923 (w), 1805 (w), 1451 (s), 749 (vs) cm.$^{-1}$. Attempted purification of this polymer by recrystallization or chromatography did not give a pure hydrocarbon.

Reaction of *m*-Xylylene Dibromide with Reduced Iron

To a suspension of 24.0 g. of reduced iron in 240 ml. of boiling water a solution of 26.4 g. (0.1 mole) of *m*-xylylene dibromide (prepared from *m*-xylene by the method described in the literature[9]) in 100 ml. of xylene was added dropwise during 15 min. under vigorous stirring and refluxing. Heating and stirring were continued for an additional 5 hr. After distilling off of xylene, the reaction mixture was subjected to steam distillation under reduced pressure. The volatile solids were collected and recrystallized from ethanol to afford 0.1 g. (1%) of colorless crystals, m.p. 132–133°C. The recorded[7a] melting point of [2.2]metacyclophane is 132.5–133°C. The product gave correct analyses and the constitution was further confirmed by infrared spectrum and molecular weight.

The nonvolatile residue was treated with benzene and the inorganic substances which remained undissolved were removed by centrifuging. Concentration of the benzene solution gave 10.0 g. of a yellow gum. The presence of bromine was indicated by the Beilstein test and also by the low carbon content.

ANAL. Calcd. for $(C_8H_8)_n$: C, 92.26%; H, 7.74%. Found: C, 90.62%; H, 7.53%.

Infrared absorptions (Nujol): 1940 (w), 1960 (w), 1770 (w), 1695 (w), 795 (vs), 710 (vs) cm.$^{-1}$. The polymer was soluble in benzene or in dioxane but was either insoluble or very sparingly soluble in ethanol, *n*-butanol, ether, or in petroleum ether (b.p. 30–50°C.). Attempted purification of this polymer by reprecipitation from a mixture of benzene and methanol or by chromatography on alumina failed to afford poly-*m*-xylylene with improved analytical figures. The chromatographic fractions had molecular weights ranging between 1800 and 3700 (cryoscopic method in camphor).

Reaction of *o*-Xylylene Dibromide in the Presence of Dienophiles

(*a*) *2-Cyano-1,2,3,4-tetrahydronaphthalene.* To a mixture of 15.0 g. (0.28 mole) of acrylonitrile, 10.0 g. of reduced iron, 200 ml. of water, and 100 ml. of xylene, a solution of 13.2 g. (0.05 mole) of *o*-xylylene dibromide in 100 ml. of xylene was added during 3 hr. under refluxing and vigorous stirring. After completion of the addition, 5.0 g. of reduced iron was added and heating and stirring were continued for an additional 7 hr. Working up the organic layer, followed by chromatography of the evaporation residue on an alumina column, gave 5.0 g. (64%) of a solid, m.p. 48–52°C. Two recrystallizations from ethyl acetate–ligroin (b.p. 80–100°C.) gave an analytically pure sample, m.p. 54–55°C. (recorded[1] m.p. 55°C.). Infrared absorptions (Nujol): 2240 (m), 748 (vs) cm.$^{-1}$.

When 13.2 g. of *o*-xylylene dibromide was treated similarly as above with 15.0 g. of nickel or cobalt powder (see Table I), the same adduct was obtained in yields of 1.4 g. (18%) and 1.6 g. (20%), respectively.

(*b*) *2-Methoxycarbonyl-1,2,3,4-tetrahydronaphthalene.* To a refluxing mixture of 15.0 g. (0.12 mole) of methyl acrylate, 10.0 g. of reduced iron, 200 ml. of water, and 100 ml. of xylene, a solution of 13.2 g. (0.05 mole) of *o*-xylylene dibromide in 100 ml. of xylene was added dropwise during 3 hr. with vigorous stirring. Then 5.0 g. of reduced iron was added and the whole mixture was stirred under refluxing (88–95°C.) for an additional 7 hr. Distillation of the organic layer gave 5.5 g. (58%) of an oily product, b.p. 103–105°C. at 3 mm. (recorded[1] b.p. 70°C. at 0.03 mm.), n_D^{20} 1.5330. Infrared absorptions (neat): 1742 (vs), 744 (vs) cm.$^{-1}$. The liquid sample gave correct analyses for carbon and hydrogen.

Analyses were performed by Miss Kenko Ogawa. The authors are indebted to Mr. M. Asano for x-ray diffraction measurements.

References

1. Alder, K., and M. Fremery, *Tetrahedron*, **14**, 190 (1961).

2. Sisido, K., Y. Udô, and H. Nozaki, *J. Am. Chem. Soc.*, **82**, 434 (1960). See also earlier papers cited there.

3. (a) Ng. Ph. Buu-Hoï, and Ng. Hoán, *J. Org. Chem.*, **14**, 1023 (1949); (b) W.

Kawai, and S. Tsutsumi, *J. Chem. Soc. Japan, Ind. Chem. Sect.*, **62**, 1469 (1959); (c) K. Isogai, *J. Chem. Soc. Japan, Pure Chem. Sect.*, **80**, 1028 (1959).

4. For reactions with tin powder see (a) K. Sisido, Y. Takeda, and Z. Kinugawa, *J. Am. Chem. Soc.*, **83**, 538 (1961); (b) K. Sisido, and Y. Takeda, *J. Org. Chem.*, **26**, 2301 (1961); (c) K. Sisido, Y. Takeda, and H. Nozaki, *J. Org. Chem.*, **27**, 2411 (1962).

5. For a review see (a) L. A. Errede and M. Szwarc, *Quart. Revs.* **12**, 301 (1958); cf. (b) J. H. Golden, *J. Chem. Soc.*, **1961**, 1604; (c) H. E. Winberg, F. S. Fawcett, W. E. Mochel, and C. W. Theobald, *J. Am. Chem. Soc.*, **82**, 1428 (1960).

6. Taira, S., *Bull. Chem. Soc. Japan*, **34**, 261 (1961).

7. (a) W. S. Lindsay, P. Stokes, L. G. Humber, and V. Boekelheide, *J. Am. Chem. Soc.*, **83**, 943 (1961); (b) N. L. Allinger, M. A. Da Rooge, and R. B. Hermann, *J. Am. Chem. Soc.*, **83**, 1974 (1961).

8. (a) K. Sisido, Y. Udô, and H. Nozaki, *J. Org. Chem.*, **26**, 584 (1961); (b) K. Sisido, R. Noyori, and H. Nozaki, *J. Am. Chem. Soc.*, **84**, 3562 (1962).

9. Snell, J. M., and A. Weissberger, *Organic Syntheses*, **3**, 788 (1955).

10. Brown, C. J., and A. C. Farthing, *J. Chem. Soc.*, **1953**, 3270.

11. Bourquelot, E., and A. Ludwig, *Compt. rend.*, **159**, 2213 (1914).

12. *ASTM Methods for Chemical Analysis of Metals*, American Society for Testing Materials, Philadelphia, 1956, p. 225.

Résumé

En traitant le chlorure de benzyle par la poudre de fer en suspension aqueuse, on obtient des radicaux benzyles qui sont ultérieurement dimérisés en dibenzyles. On applique à présent cette réaction au dibromure de *p*-xylylène suivant une série de conditions, résumées dans le Tableau I. Avec le fer réduit en suspension dans un mélange de xylène et d'eau (50:50) ou dans le diméthylformamide, on obtient des pourcentages élevés (70–80%) de poly-*p*-xylylène, qui est identifié par spectre infra-rouge, par film de diffraction de rayons-x, et par d'autres propriétés. La poudre de zinc, couverte de nickel (Hrushibara nickel CB) donne des pourcentages identiques de poly-*p*-xylylène, tandis que la poudre de cobalt ou le couple zinc-cobalt donnent des rendements inférieurs. On obtient des polymères solubles par une réaction similaire des dibromures de *ortho* et *m*-xylylène. La présence d'*o*-xylylène, comme intermédiaire instable de la polymérisation du dibromure d'*o*-xylylène, a été mise en évidence en piégeant cet hydrocarbure intermédiaire avec l'acrylonitrile et l'acrylate de méthyle comme produits d'addition au diène.

Zusammenfassung

Behandlung von Benzylchlorid mit Eisenpulver in wässriger Suspension führt zur Bildung von Benzylradikalen, die sich dann zu Bibenzyl dimerisieren. Diese Reaktion wurde nun unter verschiedenen Bedingungen (Tabelle I.) auf *p*-Xylylendibromid ausgedehnt. Hohe Ausbeuten (70–80%) an Poly-*p*-xylylen, das durch das Infrarotspektrum, Röntgenbeugungsdiagramm und andere Eigenschaften identifiziert wurde, konnten mit reduziertem, in einer Xylol-Wassermischung (50:50) oder in Dimethylformamid suspendierten Eisen erhalten werden. Mit Nickel überzogenes Zinkpulver (Urushibara-Nickel CB) ergab ähnliche Ausbeuten an Poly-*p*-xylylen, während Kobaltpulver oder die Zink-Kobalt-Kombination geringere Ausbeuten lieferte. Die analoge Reaktion mit *o*- und *m*-Xylylendibromid führte zu löslichen Polymeren. Die Anwesenheit von *o*-Xylylen als instabiles Zwischenprodukt bei der Polymerisation von *o*-Xylylendibromid wurde durch Abfangen mit Acrylnitril und mit Methylacrylat als Dienaddukt nachgewiesen.

Received July 17, 1962

JOURNAL OF POLYMER SCIENCE: PART A VOL. 1, PP. 2109–2117 (1963)

Elektronenspinresonanz-Untersuchungen an Peroxydradikalen in bestrahltem Polypropylen

H. FISCHER, K.-H. HELLWEGE, und P. NEUDÖRFL, *Deutsches Kunststoff-Institut, Darmstadt, Germany*

Synopsis

Peroxide radicals are formed by oxidation of carbon radicals in irradiated isotactic polypropylene. An interpretation of their ESR-spectra is given. The recombination of the peroxide radicals follows a chain reaction mechanism, which is derived from the reversibility of formation of peroxide radicals, the time dependence of their concentration, and from the oxygen consumption of samples containing peroxide radicals. The reactions are discussed in view of the radiation induced oxidative degradation of polypropylene.

I. Einleitung

In vorausgehenden Arbeiten[1,2] wurde die Interpretation der Elektronenspinresonanz-(ESR)-Spektren von langlebigen Radikalen in unter Vakuum bestrahltem isotaktischem Polypropylen dargelegt. Es konnte dabei gezeigt werden, dass insbesondere die Analyse der Spektren gestreckter, d.h. orientierter Proben zur relativ sicheren Identifizierung der gebildeten Makroradikale führt. Nach unseren Vorschlägen, die sich zum Teil von den Deutungen anderer Autoren unterscheiden,[3–6] treten im wesentlichen folgende Kohlenstoffradikale auf, die in verschiedenen Temperaturbereichen beobachtet werden können: (*1*) Alkylradikale (R_1) der Struktur

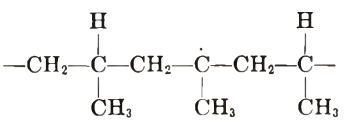

die bei einer Bestrahlung bei 77°K vorwiegend gebildet werden, (*2*) Allylradikale (R_2) der Struktur

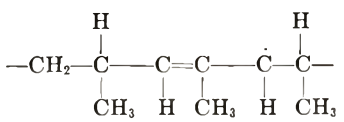

denen das Spektrum einer bei 77°K bestrahlten und auf Zimmertemperatur erwärmten Probe oder auch das Spektrum einer direkt bei Zimmertemperatur bestrahlten Probe zugeordnet wird (Abb. 3*a*).

Weiterhin wurde ein Spektrum angegeben (vgl. Ref. 2, Abb. 4), das bei Zimmertemperatur bestrahltem und anschliessend bei 370°K getempertem isotaktischem Polypropylen entspricht (Abb. 3*b*). Es konnte nicht schlüssig einer bestimmten Radikalsorte zugeordnet werden, da es zu wenig in Einzellinien aufgelöst ist. Jedoch erscheint es plausibel,[7] das Spektrum durch Radikale (R_3) zu interpretieren, deren unpaariges Elektron über eine Kette konjugierter Doppelbindungen delokalisiert ist.

In der vorliegenden Arbeit wird nun die Bildung von Peroxydradikalen aus den Kohlenstoffradikalen (R_1–R_3) behandelt. Ihre Spektren werden diskutiert. Weiterhin werden Untersuchungen zur Rekombination der Peroxydradikale beschrieben, deren Ergebnisse zu Vorschlägen für den Mechanismus der ablaufenden Reaktionen führen. Die bei der Durchführung der Arbeit angewandte experimentelle Technik sowie die untersuchten Substanzen sind mit den früher angegebenen[1,2] identisch.

II. Bildung der Peroxydradikale und Deutung ihrer ESR-Spektren

Bricht man bei Zimmertemperatur das Vakuum über bestrahlten Polypropylenproben auf, die Radikale vom Typ R_2 enthalten, so wandelt sich das ESR-Spektrum, wie auch bereits früher beschrieben, in die in Abbildung 1*a* dargestellte Kurve um (Abb. 1).

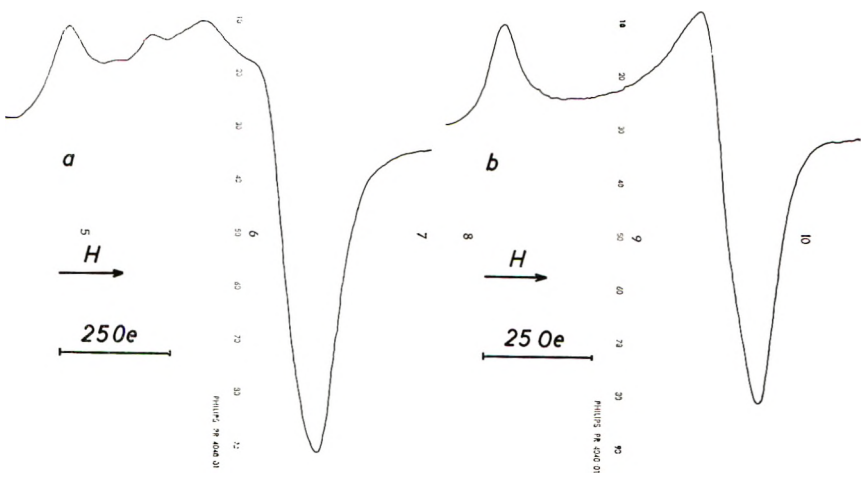

Abb. 1. ESR-Spektren von Peroxydradikalen in unter Vakuum bestrahltem Polypropylen: (*a*) Aufnahme des Spektrums unmittelbar nach dem Aufbrechen des Vakuums; (*b*) Aufnahme des Spektrums nach einstündiger Temperung der Probe unter Luftzutritt bei 70°C.

Die Geschwindigkeit dieser Umwandlung ist abhängig vom Oberflächen–Volumen-Verhältnis Φ der Proben. Solche Erscheinungen sind bei bestrahlten Polymeren geläufig. Sie werden durch eine Oxydation der Kohlenstoffradikale zu Peroxydradikalen erklärt.[8–10] Spektren, die mit der in Abbildung 1*a* wiedergegebenen Kurve völlig identisch sind, erhält

man auch, wenn man Polypropylen direkt in Luft bestrahlt oder wenn man Sauerstoff bei Zimmertemperatur auf Proben einwirken lässt, die Radikale vom Typ $R_3^{\cdot}$ enthalten (Abb. 3*c*). Dagegen ändert sich das Spektrum des Radikals $R_1^{\cdot}$ (Ref. 2, Abb. 1), beobachtbar im Temperaturbereich von 100–200°K, nach einem Aufbrechen des Vakuums nicht. Dies ist vermutlich auf die bei tieferen Temperaturen geringere Diffusionsgeschwindigkeit des Sauerstoffs zurückzuführen. Die in den Abbildungen 1*a* und 3*c* dargestellten, in ihrer Form identischen Spektren der durch Oxydation von $R_2^{\cdot}$-und von $R_3^{\cdot}$-haltigen Proben erzeugten Radikale gehen bei einer Erhöhung der Messtemperatur irreversibel und wiederum in völlig gleicher Weise unter einem Absinken der Intensität auf etwa 50% der Ausgangswerte in das in Abbildung 1*b* wiedergegebene Spektrum über. Dieses Spektrum ändert seine Form bei weiterer Erhöhung der Messtemperatur nicht mehr. Die Abbildungen 1*a* und 3*c* können nicht durch Superposition der Spektren der Radikale $R_2^{\cdot}$ und $R_3^{\cdot}$ (Abb. 3*a*, 3*b*) und des nach der Temperung der Probe gefundenen Spektrums (Abb. 1*b*) erzeugt werden. Es entstehen also offensichtlich bei der Oxydation der Kohlenstoffradikale $R_2^{\cdot}$ und $R_3^{\cdot}$ jeweils mehrere Radikalsorten, die verschieden stabil sind. Ihre ESR-Spektren zeigen keine Hyperfeinstruktur; das unpaarige Elektron ist offenbar bei allen entstehenden Radikalen nur mit der Sauerstoffgruppe verknüpft. Daher kann man ihre Kettenstruktur nicht mit Sicherheit festlegen. Wir nehmen jedoch an, dass das Spektrum der Abbildung 1*b* Radikalen $R_2OO\cdot$ und $R_3OO\cdot$ der Form

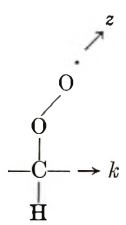

zuzuordnen ist, wobei die Kette der Struktur der Radikale $R_2^{\cdot}$ und $R_3^{\cdot}$ entspricht. Mit dieser Annahme lässt sich Abbildung 1*b* in Analogie zu Ergebnissen anderer Autoren an bestrahlten Polymeren und niedermolekularen Substanzen[11–13] unter Zugrundelegung eines achsialsymmetrischen *g*-Tensors der Radikale deuten, dessen Symmetrieachse vermutlich die Verbindungslinie (*z*) der Sauerstoffatome ist. Über die Struktur der instabilen Oxydationsprodukte lässt sichdagegen keine Aussage aus dem Spektrum gewinnen.

Werten wir das Spektrum der Abbildung 1*b*, das den stabilen Peroxydradikalen $R_2OO\cdot$ bzw. $R_3OO\cdot$ zugeschrieben wird, unter Zugrundelegung von Searl und Mitarbeiter[11] angegebener Relationen aus, so erhalten wir als Werte der Komponenten des achsialsymmetrischen *g*-Tensors

$$g_{\parallel} = 2.034 \pm 0.001$$

$$g_{\perp} = 2.004 \pm 0.001$$

Schliesslich zeigt der Vergleich der Abbildung 1*b* mit von diesen Autoren[11] berechneten Kurven, dass die Absorptionskurve eines einzelnen Radikals $R_2OO\cdot$ oder $R_3OO\cdot$ Lorentzform hat. Die Spektren von Peroxydradikalen in orientierten Proben hängen vom Winkel θ zwischen der Richtung des Magnetfelds und der Streckrichtung ab. Die bereits früher angegebenen Spektren (Ref. 2, Abb. 7) entsprechen den Radikalen, die in nicht orientierten Proben das Spektrum der Abbildung 1*a* hervorrufen. Orientierte und getemperte Proben, die, wie oben beschrieben, nur Radikale vom Typ $R_2OO\cdot$ oder $R_3OO\cdot$ enthalten, zeigen dagegen die in Abbildung 2 wiedergegebenen Spektren, die mit von Lebedev u. Mitarbeiter[13] gefundenen Kurven übereinstimmen (Abb. 2).

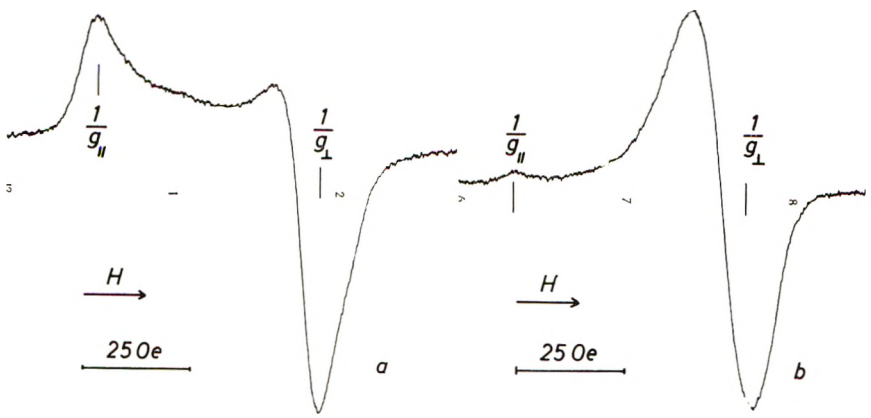

Abb. 2. Richtungsabhängigkeit des ESR-Spektrums von Peroxydradikalen in bestrahltem Polypropylen: (*a*) $\theta = 90°$; (*b*) $\theta = 0°$.

Die Abweichungen der beobachteten von berechneten Resonanzkurven[13] sind sicher, wie auch Lebedev u. Mitarbeiter annehmen, zum Teil auf die nicht vollständige Ausrichtung der Ketten bei der Streckung zurückzuführen. Es ist jedoch auch möglich, diese Abweichungen durch eine sterische Konfiguration der Radikale zu deuten, in der die Verbindungslinie der Sauerstoffatome (z) mit der Kettenrichtung (k) einen bestimmten Winkel α einschliesst. Nimmt man dies als gegeben an, so erhält man aus den von anderen Autoren[11] berechneten Formeln für die Form der Resonanzkurve für $\theta = 0°$ eine zu

$$g = (g_\parallel{}^2 \cos^2 \alpha + g_\perp{}^2 \sin^2 \alpha)^{1/2}$$

symmetrische Kurve. Dagegen ergibt sich in gleicher Weise für $\theta = 90°$ eine unsymmetrische Kurve, die der beobachteten nahezu entspricht. Aus dem Messwert für die Lage des Nulldurchganges des für $\theta = 0°$ aufgenommenen Spektrums (Abb. 2*b*)

$$g = 2.0085 \pm 0.0010,$$

der sich deutlich von dem für $\alpha = 90°$ zu erwartenden Wert $g = g_\perp$ unterscheidet, berechnet man den Winkel α zu $\alpha = 67° \pm 5°$.

III. Reaktionen der Peroxydradikale

Die in Teil II dieser Arbeit beschriebene Oxydation der Kohlenstoffradikale zu Peroxydradikalen ist teilweise reversibel, wie in Abbildung 3 dargestellt wird.

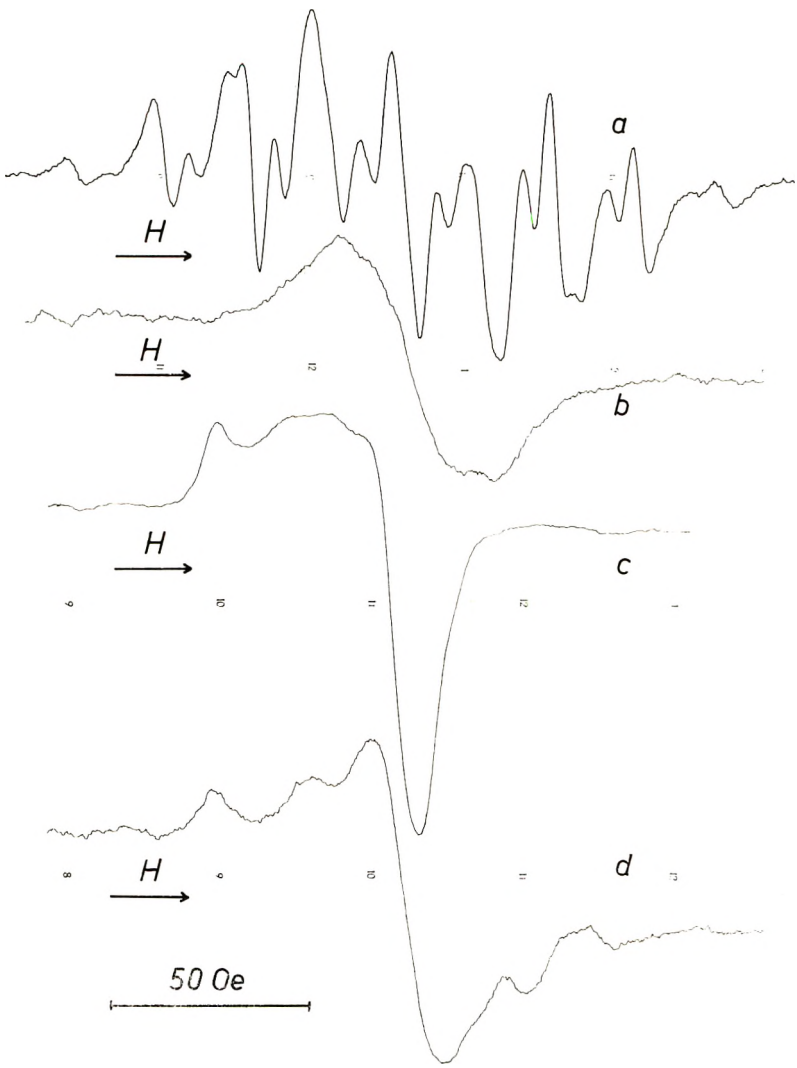

Abb. 3. Reversibilität der Bildung der Peroxydradikale: (*a*) ESR-Spektrum einer bei 20°C unter Vakuum bestrahlten Polypropylenprobe; (*b*) Spektrum der Polypropylenprobe nach einstündiger Temperung unter Vakuum bei 70°C; (*c*) Spektrum der getemperten Probe nach dem Aufbrechen des Vakuums; (*d*) Spektrum der Probe nach einer anschliessend durchgeführten zwanzigstündigen Temperung unter Vakuum bei 40°C.

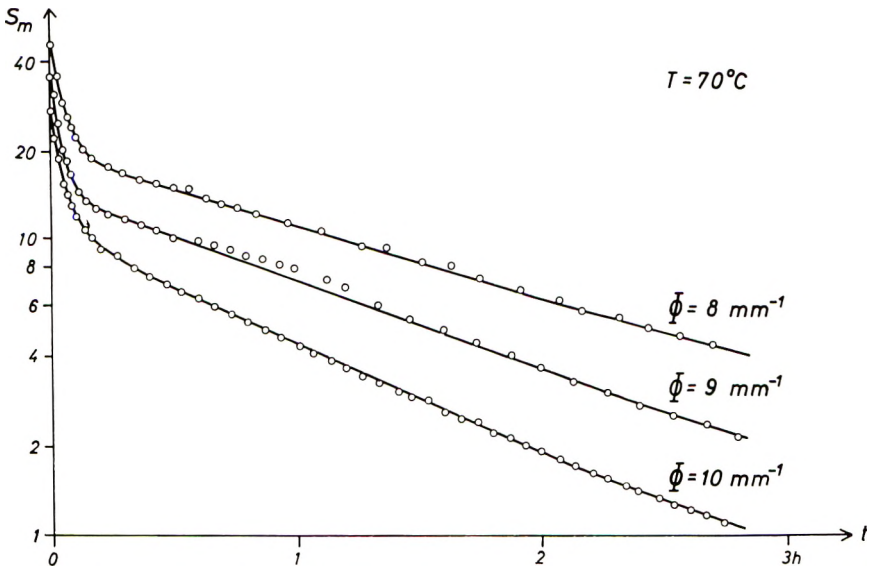

Abb. 4. Zeitlicher Abfall der Konzentration der Peroxydradikale in bestrahltem Polypropylen bei Proben mit verschiedenem Oberflächen–Volumen-Verhältnis Φ (Konzentrationseinheit willkürlich).

Abbildung 3*a* zeigt das ESR-Spektrum der Allylradikale $R_2^{\cdot}$, das während einer Temperung der Probe unter Vakuum bei 70°C in die Resonanzkurve der Radikale $R_3^{\cdot}$ übergeht (Abb. 3*b*). Nach anschliessendem Aufbrechen des Vakuums erscheint das den Peroxydradikalen zugeordnete Spektrum (Abb. 3*c*). Eine weitere Temperung der Probe unter Vakuum bei 40°C führt schliesslich zu einem Spektrum (Abb. 3*d*), das als Überlagerung der Spektren der Kohlenstoffradikale $R_3^{\cdot}$ und $R_2^{\cdot}$ dargestellt werden kann. Dies bedeutet, dass an Stelle der Peroxydradikale nach der Temperung wieder Kohlenstoffradikale vorhanden sind. Insbesondere ist erstaunlich, dass bei dem beschriebenen Versuch Radikale vom Typ $R_2^{\cdot}$ in einer Probe erscheinen, die vor dem Sauerstoffzutritt nur Radikale vom Typ $R_3^{\cdot}$ enthielt. Diese Tatsache ist sicher nicht durch die Annahme zu erklären, dass die beobachtete Reversibilität der Bildung der Peroxydradikale auf einfache Umkehrung der Oxydation unter Sauerstoffabspaltung zurückzuführen ist. Es scheinen vielmehr weitaus kompliziertere Reaktionen abzulaufen.

Die im folgenden beschriebenen Experimente sind nun durchgeführt worden, um Einblick in die Art dieser Prozesse zu gewinnen. Ihre Ergebnisse sind von Loy[10] berichteten, für Peroxydradikale in bestrahltem PVC geltenden Resultaten ähnlich. Trägt man die Konzentration der Peroxydradikale in bei Zimmertemperatur bestrahltem isotaktischem Polypropylen während einer Temperung oberhalb Zimmertemperatur halblogarithmisch über der Zeit auf, so erhält man Abklingkurven, für die Abbildung 4 typische Beispiele zeigt.

Nach anfänglich steilerem Verlauf gehen die Kurven in Geraden über. Die Steigung dieser Geraden hängt ausser vom Oberflächen–Volumen-Verhältnis der Proben, worauf später noch eingegangen wird, auch von der Temperatur ab, bei der die Abklingkurven aufgenommen werden. Trägt man die Steigung über der reziproken Temperatur wiederum halblogarithmisch auf, so ergibt sich ebenfalls eine Gerade. Die Temperaturabhängigkeit der Steigung des geradlinigen Teils der Abklingkurven lässt sich also durch eine Aktivierungsenergie beschreiben. Ihr Wert, $\Delta E \approx 14$ kcal/mol, hat die gleiche Grössenordnung wie die für PVC angegebene[10] Aktivierungsenergie ($\Delta E \approx 12$ kcal/mol).

Eine Aufnahme von ESR-Spektren der Proben während der Temperung liefert, dass dem Abfall am Anfang der Abklingkurven die Änderung des Spektrums von Abbildung 1*a* zu Abbildung 1*b* parallel läuft. Dieser Abfall beschreibt also die Rekombination der instabilen Oxydationsprodukte. Dagegen entspricht der gerad-linige Verlauf den Reaktionen der stabileren Radikaltypen $R_2OO\cdot$ und $R_3OO\cdot$.

Aus Abbildung 4 geht hervor, dass die Steigung der Geraden bei einer bestimmten Temperatur vom Verhältnis der Oberfläche der Proben zu ihrem Volumen abhängt. Dies deutet, wie auch bereits der exponentielle Abfall der Radikalkonzentration, auf den Ablauf diffusionsabhängiger Prozesse während der Radikalrekombination hin.

Da bekannt ist,[14] dass bei der Rekombination von Radikalen in bestrahltem Polyäthylen Sauerstoff verbraucht wird, liegt die Vermutung nahe, dass auch im vorliegenden Fall während der Temperung Sauerstoff von den Proben aufgenommen wird.

Zur experimentellen Klärung dieser Frage wurde die Sauerstoffaufnahme während der Radikalrekombination unter Anwendung einer von anderen Autoren[14] angegebenen Technik verfolgt. Wir fanden, dass pro verschwundenes Sauerstoffradikal bei Zimmertemperatur etwa 5–6, bei 70°C etwa 3–4 Moleküle Sauerstoff verbraucht werden. Eine Sauerstoffaufnahme der Proben während des Abbaues der Peroxydradikale ist aber nur durch Annahme eines Kettenreaktionsmechanismus zu erklären, der, in Erweiterung des von B. R. Loy[10] für PVC vorgeschlagenen Prozesses, etwa in den folgenden Stufen ablaufen könnte:

$$\left.\begin{array}{ll} R_{2/3}OO\cdot + R_1H \rightarrow R_{2/3}OOH + R_i & (1) \\ R_i \rightarrow R_2 \rightarrow R_3 & (2) \\ R_2 + O_2 \rightarrow R_2OO\cdot & (3a) \\ R_3 + O_2 \rightarrow R_3OO\cdot & (3b) \end{array}\right\}$$

und der durch die Rekombination zweier Radikale abgeschlossen wird. In der ersten Stufe (1) des Prozesses wird durch die Übertragung eines tertiären Wasserstoffatoms von einer Nachbarkette aus dem Peroxydradikal eine Hydroperoxydgruppe und ein Alkylradikal R_i gebildet. Die zweite Stufe (2) beschreibt die Umwandlung des Alkylradikals R_i in ein Allylradikal, das sich seinerseits weiter in ein Radikal R_3 umsetzen kann. Diese Umwandlungen kommen durch inter- oder intramolekulare

Wanderung[15] der Radikalstelle zu während der Bestrahlung gebildeten Doppelbindungen[16] zustande. Schliesslich wird durch die dritte Stufe, die die Oxydation der Kohlenstoffradikale $R_2^{\cdot}$ und $R_3^{\cdot}$ zu Peroxydradikalen wiedergibt, der Kreis geschlossen.

An Hand des angegebenen Reaktionsschemas können nun folgende einfache Schlüsse gezogen werden.

(*1*) Die beobachtete Reversibilität der Oxydation der Kohlenstoffradikale zu Peroxydradikalen ist nicht auf eine einfache Umkehrreaktion zurückzuführen. Vielmehr wird der nach der Sauerstoffzufuhr in der Probe ablaufende Kreisprozess bei erneuter Evakuierung nach Stufe (2) unterbrochen. Daher entstehen Kohlenstoffradikale, und zwar wird das beobachtete ESR-Spektrum je nach der Vorgeschichte der Probe eine Superposition von Spektren der Radikale $R_2^{\cdot}$ und $R_3^{\cdot}$ darstellen.

(*2*) Der Rekombinationsprozess der Radikale wird durch die Diffusion des Sauerstoffs in die Probe gesteuert. Er stellt sich dadurch scheinbar als Prozess erster Ordnung dar, obwohl die endgültige Rekombination zweier Radikale ein Prozess zweiter Ordnung ist.

(*3*) Während des Ablaufs des Kreisprozesses wird mit jedem Umlauf pro Radikal eine Sauerstoffmolekel in die Probe eingebaut. Die niedrigere Sauerstoffaufnahme bei höheren Temperaturen kann durch eine Erhöhung der Wanderungsgeschwindigkeit der Radikalstellen und damit der Rekombinationsrate der Kohlenstoffradikale erklärt werden.

Weiterhin liegt es nahe, den angegebenen Kreisprozess mit dem strahlenchemischen Abbau von Polypropylen unter Einfluss von Sauerstoff in Verbindung zu bringen. In Stufe (1) des Reaktionsmechanismus werden Hydroperoxydgruppen gebildet, die gemäss der Struktur der Radikale $R_2^{\cdot}$ und $R_3^{\cdot}$ einer oder mehreren Kohlenstoffdoppelbindungen benachbart sind. Solche Verbindungen können nun nach[17]

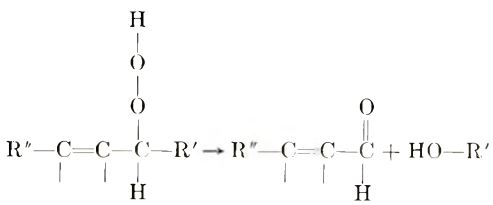

unter Ausbildung eines Kettenbruchs disproportionieren. Dabei treten Carbonyl- und Hydroxylgruppen auf, die auch UR-spektroskopisch beobachtbar sind.[18,19]

Obwohl die angegebenen Mechanismen die bei der Rekombination der Radikale in bestrahltem Polypropylen unter dem Einfluss von Sauerstoff ablaufenden Reaktionen sicher nur sehr grob beschreiben—z.B. wird der anfänglich steile Abfall der Abklingkurven nicht berücksichtigt—liefern sie doch die Deutung aller wesentlichen Messergebnisse. Darüber hinaus erlauben sie die Aufstellung eines Vorschlags zur Erklärung des unter Einfluss von Sauerstoff auftretenden Strahlungsabbaus von Polypropylen.

Wir danken Herrn Dr. U. Johnsen für wertvolle Diskussionen.

Literatur

1. Fischer, H., und K.-H. Hellwege, *V. Proc. Intern. Symp. Free Radicals, Uppsala* (1961).
2. Fischer, H., und K.-H. Hellwege, *J. Polymer Sci.*, **56**, 33 (1962).
3. Libby, D., M. G. Ormerod, und A. Charlesby, *Polymer*, **1**, 212 (1960).
4. Charlesby, A., and M. G. Ormerod, *Proc. Intern. Symp. Free Radicals, Uppsala* (1961).
5. Onishi, S., Y. Ikeda, M. Kashiwagi, und J. Nitta, *Polymer*, **2**, 119 (1961).
6. Lebedev, Yu. S., und Yu. D. Tsvetkov, *Zh. Strukt. Khim.*, **2**, 607 (1961).
7. Onishi, S., Y. Ikeda, I. Sugimoto, und J. Nitta, *J. Polymer Sci.*, **47**, 503 (1960).
8. Abraham, R. J., und D. H. Whiffen, *Trans. Faraday Soc.*, **54**, 1291 (1958).
9. Onishi, S., M. Kashiwagi, Y. Ikeda, und J. Nitta, *Proc. Intern. At. Energy Conf., Warsaw* (1959).
10. Loy, B. R., *J. Phys. Chem.*, **65**, 58 (1961).
11. Searl, J. W., R. C. Smith, und S. J. Wyard, *Bull. Amp.*, **9**, 236 (1960).
12. Lebedev, Yu. S., *Zh. Strukt. Khim.*, **3**, 151 (1962).
13. Lebedev, Yu. S., Yu. D. Tsvetkov, und G. M. Shidomirov, *Zh. Strukt. Khim.*, **3**, 21 (1962).
14. Lawton, E. J., R. S. Powell, und J. S. Balwit, *J. Polymer Sci.*, **32**, 277 (1958).
15. Koritskii, A. T., Yu. N. Molin, W. N. Shamshev, N. Y. Buben, und V. V. Voevodskiĭ, *Vysokomolekul. Soedin.*, **1**, 1182 (1959).
16. Black, R. M., und R. J. Lyons, *Proc. Roy. Soc. (London)*, **A253**, 322 (1959).
17. Grassie, N., *High Polymer Degradation Processes*, Butterworths, London, 1956, p. 212.
18. Hirt, R. C., N. Z. Searle, und R. G. Schmitt, *SPE Trans.*, **1**, 21 (1961).
19. Germar, H., unveröffentlichte Ergebnisse.

Résumé

On a formé des radicaux peroxydiques par oxydation des radicaux hydrocarbonés présents dans le polypropylène isotactique irradié. Leurs spectres E S R ont été éclaircis en admettant une structure stérique déterminée des radicaux. Par ailleurs, au départ de la dépendance de la concentration des radicaux peroxydiques en fonction du temps, aux dépens de la réversibilité de leur formation, de même qu'aux dépens de l'absorption d'oxygène des échantillons, qui contiennent des radicaux peroxydiques, on a pu déduire un mécanisme de réactions en chaîne, qui décrit leur recombinaison. On discute également la relation existant entre ces réactions et la dégradation du polypropylène observée sous l'influence de l'oxygène.

Zusammenfassung

Die Bildung von Peroxydradikalen durch Oxydation der Kohlenstoffradikale in bestrahltem isotaktischem Polypropylen wird dargelegt. Ihre ESR-Spektren werden unter Annahme einer bestimmten sterischen Struktur der Radikale gedeutet. Weiterhin kann aus dem zeitlichen Verlauf der Konzentration der Peroxydradikale, der Reversibilität ihrer Bildung, sowie aus der Sauerstoffaufnahme von Proben, die Peroxydradikale enthalten, ein Kettenreaktionsmechanismus abgeleitet werden, der ihre Rekombination beschreibt. Der Zusammenhang der angegebenen Reaktionen mit dem unter dem Einfluss von Sauerstoff beobachteten Strahlungsabbau von Polypropylen wird diskutiert.

Received July 17, 1962

JOURNAL OF POLYMER SCIENCE: PART A VOL. 1, PP. 2119–2126 (1963)

Crystallinity in Ethylene–Propylene Copolymers

J. F. JACKSON,* *Physical Research Laboratory, The Dow Chemical Company, Midland, Michigan*

Synopsis

A mathematical expression has been developed which treats crystalline content of ethylene–propylene copolymers as a function of monomer sequence length distribution in the copolymer chains. The model is based on the Goldfinger-Kane mathematical relationship for sequence length distributions derived from the conventional copolymer equation. Use of the general Flory theory for depression of the crystalline melting point by copolymerization provides independent evidence in substantiation of the model.

INTRODUCTION

Copolymerization of ethylene with α-olefins and α-olefins with each other by means of the so-called Ziegler-Natta catalysts (transition metal halide–aluminum alkyl) has received increasing attention in recent years. Unusual properties of the copolymers so formed have been described in papers by Natta[1,2] and by others.[3] The former treat specifically of the crystalline morphology of styrene-substituted styrene copolymers, indicating the phenomena of isomorphism of chains and isomorphism and isodimorphism of monomeric units.

In a recent paper on measurement of the dimensions of the polyethylene unit cell, Swan discusses similar phenomena in ethylene–propylene copolymers.[3]

The present study of copolymerization of ethylene with propylene also has indicated the presence of such phenomena and has allowed their interpretation in a specific sense. Several sets of data are shown to fit this interpretation.

EXPERIMENTAL

Ethylene–propylene copolymers have been prepared using various metal halide catalysts in conjunction with aluminum alkyls and alkyl aluminum halides as cocatalysts. All polymerizations were carried out under identical conditions, and polymers obtained were treated and analyzed in an identical manner (exceptions: A, C, and I, Figs. 1 and 2).

Conventional copolymerization constants, r_1 and r_2,[4] were obtained for each system by the Fineman-Ross diagram technique.

* Present address: Chemistry Department, University of Colorado, Boulder, Colorado.

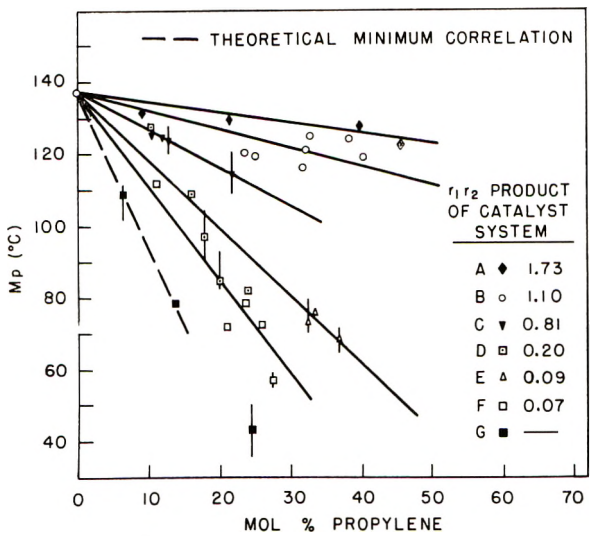

Fig. 1. Crystalline melting point as a function of copolymer composition.

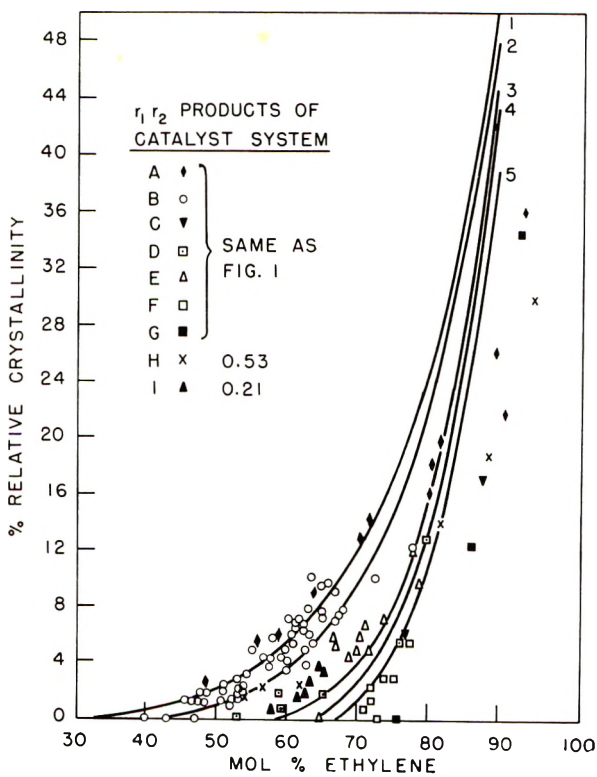

Fig. 2. Relative crystallinity determined by x-ray as a function of copolymer composition [% crystallinity $= \sum_{8}^{\infty} P_A(8)$]. Curves calculated for the following r_1r_2 products: (*1*) 1.73, (*2*) 1.17, (*3*) 0.20, (*4*) 0.01, (*5*) 0.00.

Relative crystalline content was determined by x-ray diffraction techniques, and reference made to infrared absorption spectra. Polymers ranged from highly crystalline plastics to amorphous rubbers.

Melting points of the crystallites were determined by observation of birefringence patterns under crossed polaroids. Temperature was programmed at 1°C./min. Determinations made at temperature programs less than 0.1°C./min. showed no substantial difference in melting point.

RESULTS

Correlations of per cent relative crystallinity with mole-per cent ethylene in the copolymer were dependent upon the catalyst–cocatalyst system used. Table I shows some of the effects of this dependency. (Per cent relative crystallinity is the ratio of the area of crystalline peaks to area of the amorphous portion in the x-ray diffraction pattern.)

TABLE I
Effect of Catalyst System on the Crystallinity of Ethylene–Propylene Copolymers

Polymer	r_1r_2 Product of catalyst system	Composition, mole-% ethylene	% Relative crystalline content, %	Unit cell	Appearance of 13.7μ band in infrared	M.P. (disappearance of crystals), °C.	Approximate ethylene sequence length, s
1	1.10	59.5	5.0	Normal PE	Definite	119	29
2	1.10	67.5	10.5	Normal PE	Definite	121	31
3	0.09	67.5	4.4	Distorted PE	None	73–77	8
4	0.09	66.5	5.7	Distorted PE	None	75–77	8
5	0.09	59.5	0.0	—	—	—	<8

Correlations of mole-per cent propylene versus melting point (determined by disappearance of birefringence in the polymer) are presented in Figure 1. The spherulite structure was not particularly well developed in any of the samples. Wide melting point ranges were observed.

DISCUSSION

I. Variation of Crystalline Content with Composition

In no case examined in this study did the crystalline diffraction pattern show evidence of polypropylene crystallinity. It was postulated that diffraction patterns arose from fringed micelles consisting solely of methylene sequences greater than a certain minimal length.

Calculation of the distribution of ethylene sequences as a function of r_1 and r_2 values[5] for the polymers obtained allowed correlation for low crystalline content (0–10%) according to eqs. (1) and (2):

$$(\% \text{ relative crystallinity}) = \sum_{s}^{\infty} P_A(s) \tag{1}$$

$$\sum_{s}^{\infty} P_A(s) = (x + r_1/x + y - r_1)^{s-1}(y - 2r_1/x + y - r_1)(1 - x + r_1/x + y - r_1)^{-1} \tag{2}$$

where

$$x = 2Fr_1r_2 - r_1F - r_1Q$$

$$y = 1 - F + Q$$

$$Q = (F^2 - 2F + 4Fr_1r_2 + 1)^{1/2}$$

and where $\sum_{s}^{\infty} P_A(s)$ is the probability of occurrence of ethylene sequences s units and greater, and F is the molar ratio of ethylene to propylene in the copolymer.

Graphically, these equations indicate that total probability of sequence formation is a strict function of F, s, and r_1r_2 product only. Further, they predict that probability (and therefore crystallinity) will increase with increasing r_1r_2 product at constant F and s.

Several critical assumptions are included in this correlation: (*1*) unique propagating sites (see addendum A); (*2*) concentration at the site is equivalent to bulk monomer concentration; (*3*) no effect of the penultimate monomer on the probabilities of alternative propagation reactions as calculated; (*4*) crystalline content directly proportional to probability of methylene sequence formation.

The fit of data achieved as shown in Figure 2 required that s equal 8 ethylene units. (A similar treatment has been published recently by Natta,[11] leading to a different conclusion.)

II. Melting Point Variation

The data of Table I appear superficially to be inconsistent with the Flory melting point depression theory for random copolymers. However, the inconsistency may be reconciled by use of the more general Flory equation[6] for melting point depression:

$$1/T_m - 1/T_m^\circ = R/h_u[1/x + (1/x - L_e + 1)] \tag{3}$$

where R is the gas constant, h_u is enthalpy of fusion per crystalline methylene unit (taken as 940 cal./unit),[7] x the number of methylene units in sequence, L_e the equilibrium crystallite length, and T_m° the unit ratio of enthalpy to entropy of polymethylene (taken as 140°C.).

The relationship of x to L_e is derived by Flory:

$$-\ln D = (1/x) + (1/2)(L_e/x)^2 + (2/3)(L_e/x)^3 + \ldots \quad (4)$$

where D is the Flory nucleation parameter (see addendum B).

Use of eq. (3) requires empirical determination of the x, L_e relationship. This was accomplished by reference to the data of Reding[8] for various homopolymers of the alkene-1 homologous series (see Table II).

TABLE II
Melting Points for Various Homopolymers of the Alkene-1 Homologous Series

	Melting point, °C.	Second-order transition, °C.
Polyethylene	137	—
Polypropylene	167	−18
Polybutene-1	120	−25
Polypentene-1	70	−24
Polyhexene-1	−55	—
Polyheptene-1	−40	—
Polyoctene-1	−38	—
Polydodecene-1	+45	−25
Polyoctadecene-1	+70	—

Reding proposed side chain crystallization to explain the observed increase in melting point for the higher homologs. If this is the case, the

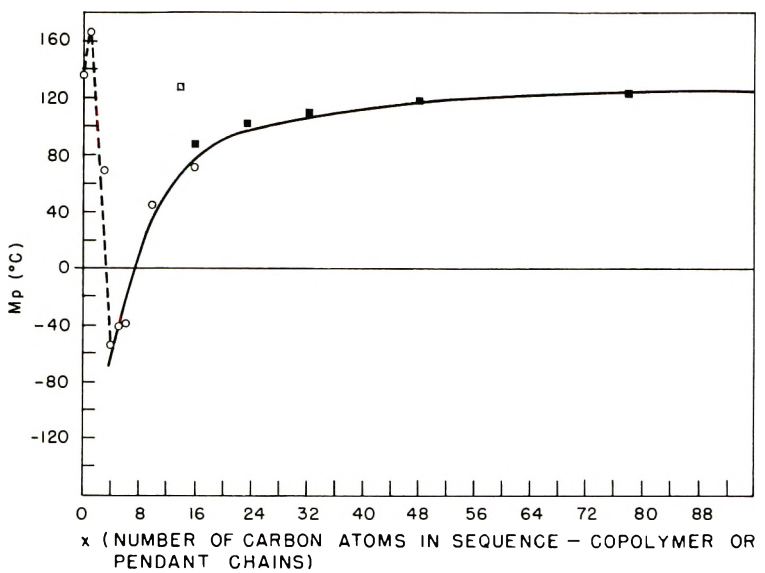

Fig. 3. Effect of methylene sequence length on crystalline melting point: (——) calculated from melting point depression theory; (○) melting point data for poly-1-olefins;[8] (■) melting point data for ethylene–propylene copolymers according to Swan;[3] (□) block copolymer.[3]

data should correlate approximately with pendant chain length according to the Flory theory.

The fit of eq. (3) as shown in Figure 3 requires that L_e/x approach a value ca. 0.5 for pendant chain lengths greater than 20 carbon atoms. (Methyl groups and carbon atoms alpha to tertiary carbons are assumed to be excluded from crystallites.)

Considering the methylene sequences within polymer chains to be analogous to the pendant chains, one may estimate the sequence lengths for the polymers of Table I.

The limiting value of sequence length found by this method is of the same order of magnitude as that found by the first method. In addition, the value of sequence length for low density polyethylene is of the order of magnitude measured by infrared techniques.[9,10]

III. Disposition of Melting Point, Crystallite Volume Data

In his treatment of the distortion of cell parameters by branches on the polyethylene backbone, Swan[3] correlates the variation of a and b parameters with mole-per cent propylene in a so-called uniformly random ethylene–propylene copolymer. He also notes a linear relationship between "relative volume" and melting point of these polymers as well as for a polymer suspected of being a block copolymer.

On the assumption that the uniformly random copolymer is, in fact, a copolymer with a high degree of alternation of the monomers, one may calculate average sequence lengths of the ethylene units (Table III). The value $\bar{s}_a$ is the mole ratio of ethylene to propylene in the copolymer.

TABLE III
Average Ethylene Sequence Length Assumed from Data of Swan[3]

Propylene, mole-%	$\bar{s}_a$ (assumed avg. sequence length of ethylene units)	Melting point, °C.
1	99	132
2	49	127
4	24	118
6	16	110
8	12	102
12	8	84
4.3 (block copolymer)	13.3	128

Transposing Swan's correlation in this manner, one may compare it with the correlation of Figure 3. The close correspondence shown provides further evidence of the applicability of the present treatment.

CONCLUSIONS

The concurrence of results for the two methods of estimating limiting sequence length in the polymers studied suggests that the nature and amount of the crystallite portion in branched polyethylene depend to a large

extent upon the spacing of branched units along the polymethylene backbone. In this light, the findings of Swan[3] are not surprising, i.e., one would expect various correlations of copolymer composition with unit cell size but a unique correlation between unit cell size and crystalline melting point (see Fig. 1). Furthermore, this model does not presuppose a single crystal model. (The applicability of the Flory theory is based upon exclusion of branched units of the chain from crystallites.)

The extension of the present model to other systems might provide explanation for certain phenomena of isomorphism of monomeric units discussed by Natta.[1,2]

In addition the concurrence provides evidence that under certain conditions of polymerization, copolymer formed from ethylene and propylene consists of ordered alternating monomer sequences, i.e., r_1r_2 product approaches zero.

ADDENDA

A. Other authors have considered the possibility that differences in crystallinity as treated in the present discussion may arise from diversity of polymerizing sites inherent in Ziegler-Natta catalyst systems. In such a viewpoint these sites are considered to be polymerizing ethylene and propylene "randomly" (i.e., r_1r_2 product near unity for all sites). Differences observed would then be due to differences in the monomer-polymer composition curves for such sites. (In terms of conventional copolymerization theory, individual r_1 and r_2 values would be different for different sites, but the product r_1r_2 would be similar for all sites.) Observations of effects in the present study (under certain polymerization conditions) indicate that such interpretation may have validity. However, such effects differ in magnitude and regularity from the effects considered in this paper.

B. The Flory nucleation constant provides a repository for a certain degree of ignorance of the relative entropies of amorphous and crystalline regions. Flory uses it to account for entropy of nucleation and for the end effect (ordering of molecules extending out of the crystal lattice). In the present interpretation, this parameter must also account for the reverse of the end effect, i.e., distortion of the crystal lattice. (An enthalpy effect would also be present.) The latter effects would be great for short sequence lengths, D increasing rapidly toward a constant or unity for infinitely long sequences, L_e/x approaching a constant or zero and h_u approaching a constant value.

C. The term "random" in reference to ethylene–propylene copolymers has been greatly misused in the literature due to lack of understanding. In this paper it is used to designate the fact that the product of the reactivity ratios defined by the copolymerization equation is unity.

The author expresses gratitude to the following for their help and advice: D. R. Peterson and Ann L. Johnson, Chemical Physics Research Laboratory; L. H. Tung and W. C. Taylor, Petrochemical Research Laboratory; E. D. Holly and H. W. McCormick, Physical Research Laboratory.

References

1. Natta, G., *Makromol. Chem.*, **35,** 94 (1960).
2. Natta, G., et al., *J. Polymer Sci.*, **51,** 527 (1961).
3. Swan, P. R., *J. Polymer Sci.*, **56,** 409 (1962).
4. Alfrey, T., Jr., and G. Goldfinger, *J. Chem. Phys.*, **12,** 205 (1944).
5. Goldfinger, G., and T. Kane, *J. Polymer Sci.*, **3,** 462 (1948).
6. Flory, P. J., *J. Chem. Phys.*, **17,** 223 (1949).
7. Quinn, F. A., and L. Mandelkern, *J. Am. Chem. Soc.*, **80,** 3178 (1958).
8. Reding, F. P., *J. Polymer Sci.*, **21,** 547 (1956).
9. Bryant, W. M. D., *J. Polymer Sci.*, **2,** 547 (1947).
10. Sporati, C. A., W. A. Franta, and H. W. Starkweather, Jr., *J. Am. Chem. Soc.*, **75,** 6110 (1953).
11. Natta, G., et al., *Chim. Ind. (Milan)*, **42,** 125 (1960).

Résumé

On a développé une expression mathématique traitant du degré de cristallinité des copolymères éthylène–polypropylène comme fonction de la distribution de la longueur des séquences de monomère dans les chaînes de copolymères. Le modèle est basé sur la relation mathématique de Goldfinger-Kane pour des distributions de longueur des séquences dérivées de l'équation conventionnelle des copolymères. En employant la théorie générale de Flory pour la diminution du point de fusion cristallin par copolymérisation, on donne une preuve indépendante de la validité du modèle.

Zusammenfassung

Ein mathematischer Ausdruck zur Darstellung des Gehalts von Äthylen–Propylencopolymeren an kristallinen Bereichen als Funktion der Monomersequenzlängenverteilung in den Copolymerketten wurde entwickelt. Das Modell beruht auf der mathematischen, aus der üblichen Copolymergleichung abgeleiteten Beziehung von Goldfinger-Kane für Sequenzlängenverteilungen. Die allgemeine Theorie von Flory für die Herabsetzung des kristallinen Schmelzpunktes durch Copolymerisation liefert eine unabhängige Bestätigung des Modells.

Received September 13, 1962

JOURNAL OF POLYMER SCIENCE: PART A VOL. 1, PP. 2127–2133 (1963)

Counterion Binding in Partially Neutralized Copolymers of Crotonic Acid and Vinyl Alcohol

S. SUGAI and A. E. WOODWARD, *College of Chemistry and Physics, The Pennsylvania State University, University Park, Pennsylvania*

Synopsis

A series of copolymers of partially neutralized crotonic acid and vinyl alcohol have been prepared with acid monomer contents ranging from 4 to 43 mole-%. The extent of binding of sodium counterions was studied by a transference method employing radiotracers. Comparison of these data with those obtained previously by Nagasawa and Rice for maleic acid copolymers and Wall and co-workers for poly(acrylic acid) gives further support to the contention that the overall charge density on a polyion governs the total counterion binding. Results of potentiometric titrations and viscosity measurements are also reported.

I. Introduction

A number of investigations[1–5] have been carried out which demonstrate that monovalent counterions to a polyanion are closely associated with the latter, a large proportion of them moving with the polyion upon application of a force. To date only one such study has been reported[4] which deals with copolymers; in that investigation, polymers with a local nonuniformity of charge density, prepared from a dibasic monomer, maleic acid, and a neutral monomer in varying ratios, were studied. Comparison of counterion binding results of the copolymers at high degrees of neutralization with NaOH with data obtained[1] for poly(acrylic acid) at varying degrees of neutralization led to the conclusion that total counterion binding depends principally on the overall charge distribution rather than the local charge distribution.

To investigate this effect further, a series of copolymers of a monobasic acid, crotonic acid, and a neutral monomer, vinyl alcohol, has been prepared and counterion binding studies made. In addition, potentiometric titrations and viscosity measurements were also carried out on copolymer solutions. These data are presented and discussed herein.

II. Experimental

A. Reagents

Crotonic acid (Eastman) was recrystallized from water. Vinyl acetate (Monomer-Polymer) was vacuum-distilled at 35°C. just prior to use.

Benzoyl peroxide (Eastman) and all organic solvents (reagent grade) were used as received.

B. Apparatus and Procedures

The general polymerization techniques, the conductance apparatus, the conductiometric titration procedure and the measurement of solution viscosity (in an Ubbelohde dilution viscometer) were described previously.[6]

Potentiometric titrations, performed with a Beckman pH meter, Model G, were carried out in distilled water at 25 ± 1.5°C. under a nitrogen atmosphere with the use of standard NaOH solutions (5×10^{-2}–$5 \times 10^{-3} M$).

For the transference measurements a glass cell fitted with a fritted disk in the center and with a round platinum electrode at each end was used. After filling the cell with polymer solution it was suspended in a water bath at 25.0 ± 1.0°C., nitrogen gas was passed through the solution, and after 30 min. electrolysis was commenced. Electric fields of 0.5–3.0 v./cm. with currents of 0.1–2 ma. were employed, the duration of electrolysis being adjusted in order to keep the total number of equivalents of electricity passed small [$(0.6–9) \times 10^{-5}$ eq.]. The amounts of polymer in the anode and cathode compartments after electrolysis were obtained by weighing the residue following vaporization of the solvent with an infrared lamp. The change in sodium ion concentration in the two compartments was measured by the Na^{24} tracer method used by Huizenga, Grieger, and Wall.[1] This radioisotope was prepared by irradiation of aqueous NaOH solutions in the Penn State reactor facility. The γ-ray decay of Na^{24} was followed by use of a liquid cell and a scintillation counter. Values for the equivalent conductance of Na^+ were obtained by a method given previously.[1,7]

C. Polymer Preparations

Copolymerization of Crotonic Acid and Vinyl Acetate. All polymerizations were performed at 75°C. in the absence of solvent with the use of benzoyl peroxide (Bz_2O_2) as initiator. Under these conditions crotonic acid does not polymerize in the absence of a comonomer. The amounts of vinyl acetate (VA), crotonic acid (CA), and Bz_2O_2 used, the time of polymerization t, the yield, and mole percentage of acid monomer in the copolymer, CA/(CA + VA), are given in Table I. The polymer was precipitated from the reaction solution by pouring the latter in *n*-heptane or *n*-hexane at ~60°C. accompanied by vigorous stirring; the precipitated polymer was dissolved in methyl ethyl ketone, reprecipitated, and dried in a vacuum oven to constant weight. Analysis for acid units was carried out conductiometrically under a nitrogen atmosphere in a 1:1 mixture of methanol and water; the results were found to agree closely with those obtained by use of phenolphthalein indicator.

Hydrolysis of Vinyl Acetate–Crotonic Acid Copolymers. To a ~5 wt.-% solution of the copolymer in methanol a 10 wt.-% solution of NaOH in methanol was slowly added while the mixture was vigorously stirred, a large excess of NaOH being used. Copolymers 1 and 2 were found to

TABLE I
Vinyl Acetate–Crotonic Acid Copolymerizations

Co-polymer no.	CA, g.	VA, g.	Bz_2O_2, g.	Time t, hr.	Yield, %	[CA/(CA + VA)] × 100, mole-%
1	0.6	19.5	0.05	0.75	?	4.0 ± 1.0
2	1.3	18.7	0.1	1.50	12	14.0 ± 1.5
3	3.0	17.0	0.1	4.00	15	21.1 ± 2.0
4	7.4	12.6	0.05	6.75	15	32.0 ± 2.0
4′	7.4	13.0	0.05	11.00	9	31.0 ± 1.5
5	10.0	4.0	0.1	18.00	15	43.0 ± 2.0

precipitate from this mixture. After 24 hr. standing, absolute ethanol was added and the precipitated polymer collected. This procedure was found from infrared analysis to lead to a 100% conversion of poly(vinyl acetate) to poly(vinyl alcohol). Aqueous solutions of the hydrolyzed copolymers were dialyzed first against distilled water and then HCl solution (0.01–0.1M). Complete exchange of all sodium ions with hydrogen ions was found to lead to precipitation, and therefore the dialysis versus acid was stopped just prior to that occurrence. Following a final dialysis against distilled water, the copolymers were freeze-dried.

D. Solution Viscosity Measurements

Solution viscosities at four concentrations from 0.02 to 0.6 g./100 cc. were carried out at 25°C. for the vinyl alcohol-neutralized crotonic acid copolymers with degree of neutralization $\alpha = 1$ for copolymers 1, 3, and 4′ and $\alpha = 0.72$ for copolymer 2; dilutions were made with distilled water. The data were found to give linear $(\eta_{sp}/c)^{-1}$ versus $c^{1/2}$ plots. From these, intrinsic viscosities of 1.69, 1.59, 8.3, and 9.1 dl./g. were obtained for copolymers 1, 2, 3, and 4′, respectively. Increases in the specific viscosity from 0.145 at $\alpha = 0.60$ to 0.33 at $\alpha = 0.95$ for copolymer 3 ($c = 0.077$ g./100 cc.) and from 0.093 at $\alpha = 0.81$ to 0.19 at $\alpha = 0.89$ ($c = 0.44$ g./100 cc.) were found. This behavior is typical of polyelectrolytes in general.

E. Potentiometric Titrations

Potentiometric titrations were carried out on solutions of polymers 1, 2, 3, 4, and 4′ from degree of neutralizations of 0.8, 0.8, 0.6, 0.6, and 0.6 respectively, to 1.2, quantities of polymer of 12.5, 16.5, 17.5, 3.0, and 132.0 mg. respectively, being used. Due to insolubility of the copolymers, α values lower than 0.6–0.8 could not be attained in aqueous solution. The pH versus α plots were of a type usually found for a weak acid, being similar to those given by Nagasawa and Rice[4] for maleic acid–vinyl alcohol copolymers with mole ratios of 1:4.84 to 1:16.3.

TABLE II

Co-polymer no.	CA / CA + VA, mole-%	[Polymer], g./100 cc.	α	r, eq./l. $\times 10^3$	k, mho/cm. $\times 10^4$	V_A, cc.	W_A, mg.	V_C, cc.	W_C, mg.	N_0, counts/min. cc.	N_C counts/min. cc.
1	4	0.1	0.72	0.630	0.31	36.5	34.8	39.0	29.0	4924	6544
2	14	0.1	0.72	2.024	0.65	38.0	34.0	38.9	26.0	6358	8802
3	21	0.1	0.72	2.863	1.08	35.3	34.5	35.7	26.0	10048	11438
1	4	0.1	0.88	0.770	0.41	35.8	29.5	27.5	20.0	4256	5792
2	14	0.1	0.88	2.494	1.34	34.0	34.5	36.5	26.0	6396	7708
3	21	0.1	0.88	3.500	2.05	34.7	34.0	36.5	24.0	4560	4818
5	43	0.1	0.88	6.097	2.82	34.8	38.2	36.0	34.5	6136	6538
1	4	0.1	1.0	0.875	0.53	38.0	37.0	35.2	25.0	7188	12200
2	14	0.1	1.0	2.811	2.20	37.5	34.5	38.0	25.5	8980	11142
3	21	0.1	1.0	3.977	2.31	39.0	33.5	38.2	28.7	10884	11882
4′	32	0.1	1.0	4.385	2.89	34.2	31.3	33.2	24.0	1845	3809
5	43	0.1	1.0	6.928	3.05	38.0	39.9	37.2	36.9	8390	9036
1	4	0.2	1.0	1.750	1.08	33.8	63.8	34.1	61.0	2407	3328
3	21	0.2	1.0	7.954	4.21	38.2	69.5	39.0	65.5	11102	10200

The data obtained for copolymers 1, 2, and 3 are given in Figure 1 in the form of pK versus pH plots. K is the apparent dissociation constant

$$K = a_{H^+}[COO^-]/[COOH] \approx (a_{H^+})\alpha/(1 - \alpha) \quad (1)$$

where $[COO^-]$ is the concentration of free carboxyl ions, [COOH] is the concentration of acid groups, and α is the degree of neutralization.

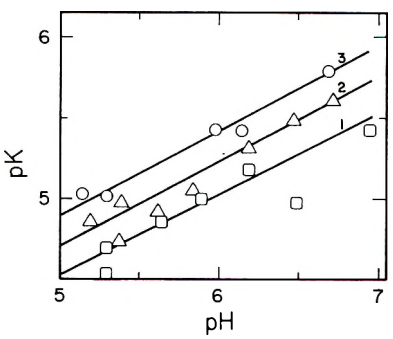

Fig. 1. Plot of pK vs. pH for crotonic acid–vinyl alcohol copolymers 1, 2, and 3.

In order to obtain α values from values for the amount of NaOH added in the titrations, the point where $\alpha = 1$ was taken as the point of maximum slope of the plot of pH versus amount NaOH added. The rest of the scale was determined by assuming the CA content of the copolymers was the same before and after hydrolysis and thereby employing the results of the titrations before hydrolysis. Over the pH range traversed the present data appear to obey the empirical relationship given by Kern:[8]

$$pK = pK_0 + B\text{pH} \quad (2)$$

Transference Measurements

N_A, counts min. cc.	p, moles $\times 10^{+5}$	I, ma.	t, hr.	N_e, eq. $\times 10^{+5}$	q, eq./l., $\times 10^{+5}$	Δ_{Na}, mho/ cm. eq.	t_p	Δ_p, mho/eq. cm.	f
3312	1.064	0.085	2.00	0.63	11.93	49.94	—	—	0.62
3574	4.044	0.475	1.85	3.28	11.54	49.83	0.19	12	0.53
7214	2.602	0.850	1.00	3.17	11.00	49.82	0.27	12	0.51
2490	1.604	0.140	2.00	1.04	5.42	49.90	0.17	10	0.88
4144	3.359	0.520	1.45	2.81	14.07	49.81	—	—	0.64
2574	4.529	1.780	1.00	6.64	14.90	49.75	0.34	25	0.79
5534	2.446	1.650	0.50	3.08	5.61	49.68	0.37	30	0.56
1594	3.075	0.350	3.75	4.90	13.84	49.88	0.12	7	1.07
7308	2.763	0.670	1.50	3.75	11.74	49.75	—	—	0.94
10042	1.514	1.200	1.17	5.24	6.21	49.70	0.23	15	0.91
3547	2.819	1.000	1.13	4.21	8.35	49.64	0.45	40	0.72
7624	2.695	1.946	1.23	8.90	3.26	49.63	—	—	0.78
1546	4.618	0.395	1.80	2.65	7.63	49.83	0.12	8	1.04
10140	0.095	1.640	0.67	4.07	6.14	49.60	0.24	16	0.80

From this plot values of 2.4 ± 0.1 for pK_0 and 0.45–0.50 for B were found. It was ascertained that these data are not adequately represented by either the equation given by Kagawa and Tsumura[9] or by Katchalsky and Spitnik[10] in agreement with the results of Nagasawa and Rice.[4]

III. RESULTS AND DISCUSSION

The results of the transference measurements are recorded in Table II, where r is the stoichiometric concentration of Na^+; k the conductivity of the solution; V_A and V_C the volume of solution in the anode and cathode compartments, respectively; W_A and W_C the weight of polymer in the anode and cathode compartments, respectively; N_0, N_C, and N_A the activity of Na^{24} in the original solution, the cathode compartment after electrolysis, and the anode compartment after electrolysis, respectively; p the equivalents of Na^+ passed from anode to cathode compartments; I the total current; t the time of electrolysis; N_e the equivalents of electricity passed; q the equivalents/liter of carboxylate ions passed; Δ_{Na^+} the specific conductance of Na^+; t_p the fraction of current carried by polymer ions; Δ_p the equivalent conductance of the polymer ions; and f the fraction of unbound counterions. The background activity count was 1012 counts/min. in all cases. Equation (2) of Wall and Hill[11] was used for calculation of f, the concentration of polymer being given in terms of the total number of monomer units in the copolymer.

The data in Table II show that for any given copolymer the fraction of free Na^+ increases with increasing degree of neutralization, an effect not heretofore reported for polyelectrolytes. This apparent increase is no doubt a consequence of the change in solubility that these copolymers undergo upon a change in α, with precipitation taking place when the degree of neutralization is reduced to values in the 0.6–0.8 range. Copolymers 1 and 5 were found to show the lowest solubility.

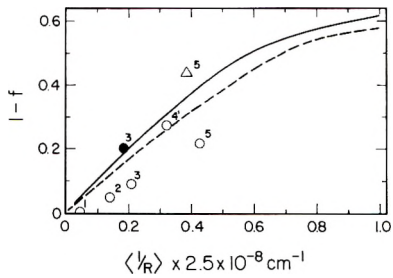

Fig. 2. Fraction of bound sodium counter ions as a function of the reciprocal average distance between two neighboring charges on a polyelectrolyte: (——) partially neutralized poly(acrylic acid),[2,4] (- -) maleic acid copolymers at $\alpha = 0.95$;[4] and crotonic acid–vinyl alcohol copolymers 1, 2, 3, 4, and 5: (○) $\alpha = 1.0$, $c = 0.10$ g./100 cc.; (●) $\alpha = 1.0$, $c = 0.20$ g./100 cc.; (△) $\alpha = 0.88$, $c = 0.10$ g./100 cc.

A second effect which is observed in the data is that at constant α a decrease in f occurs as the amount of acidic monomer is increased in the copolymer. A comparison of the data for samples 1, 2, 3, 4, and 5 at $\alpha = 1$ and for sample 5 $\alpha = 0.89$ with that obtained for partially neutralized poly(acrylic acid)[1] and that for completely neutralized copolymers of maleic acid and vinyl alcohol[4] is given in Figure 2, where the fraction of counter ions bound $(1 - f)$ is plotted versus the reciprocal average distance between charges on the polyion. Although considerable scatter does occur in the present data, reasonable agreement with previous results is found.

By the method of Wall et al.[12] a measurement of the rate of Na^+ exchange for copolymer 4 at a polymer concentration of 0.1 g./100 cc. with $\alpha = 1$ and $N_e = 3.75 \times 10^{-5}$ eq. was made and a value for k in l./eq. min. of 6 was obtained, a value of the same order of magnitude as that found by Wall et al.[12] for partially neutralized poly(acrylic acid).

We wish to express our thanks to Professor S. A. Rice of the University of Chicago for helpful discussions concerning this work, to Dr. W. D. Taylor for aid in the polymer preparation, and to Professor W. W. Miller of The Pennsylvania State University for his help in the radiotracer studies. This investigation was supported in part by research grant A2704 from the National Institute of Arthritis and Metabolic Diseases, Public Health Service.

References

1. Huizenga, J. R., P. F. Grieger, and F. T. Wall, *J. Am. Chem. Soc.*, **72**, 2636 (1950).
2. Huizenga, J. R., P. F. Grieger, and F. T. Wall, *J. Am. Chem. Soc.*, **72**, 4228 (1950).
3. Wall, F. T., H. Terayama, and S. Techakumpuch, *J. Polymer Sci.*, **20**, 477 (1956).
4. Nagasawa, M., and S. A. Rice, *J. Am. Chem. Soc.*, **82**, 5070 (1960).
5. Ferry, G. V., and S. J. Gill, *J. Phys. Chem.*, **66**, 999 (1962).
6. Taylor, W. D., and A. E. Woodward, *J. Polymer Sci.*, **A1**, 1473 (1963).
7. Longsworth, L. G., *J. Am. Chem. Soc.*, **54**, 2741 (1932).
8. Kern, W., *Z. Physik. Chem. (Leipzig)*, **A181**, 269 (1938).
9. Kagawa, I., and K. Tsumara, *J. Chem. Soc. Japan. Ind. Chem. Sect.*, **67**, 437 (1946).
10. Katchalsky, A., and P. Spitnik, *J. Polymer Sci.*, **2**, 432 (1947).

11. Wall, F. T., and W. B. Hill, *J. Am. Chem. Soc.*, **82,** 5599 (1960).
12. Wall, F. T., P. F. Grieger, J. R. Huizenga, and R. H. Doremus, *J. Chem. Phys.*, **20,** 1206 (1952).

Résumé

On a préparé une série de copolymères d'acide crotonique partiellement neutralisé et d'alcool vinylique contenant de 4 à 43% de môles d'acide monomère. L'importance de la liaison des contre-ions sodiques est étudiée par une méthode de transfert utilisant des radiotraceurs. La comparaison de ces résultats avec ceux obtenus précédemment par Nagasawa et Rice pour des copolymères d'acide maléique et par Wall et ses collaborateurs pour l'acide polyacrylique, soutient la thèse selon laquelle la densité globale de charge du polyion détermine la liaison totale du contre-ion. On a effectué des titrations potentiométriques et les résultats obtenus peuvent être exprimés de façon adéquate par l'équation de Kern.

Zusammenfassung

Eine Reihe von Copolymeren aus teilweise neutralisierter Crotonsäure und Vinylalkohol mit Gehalten an Säuremonomerem von 4 bis 43 Mol-% wurden hergestellt. Das Ausmass der Natriumgegenionen-Bindung wurde nach einer Überführungsmethode mit Radiospurenelementen untersucht. Ein Vergleich der Ergebnisse mit den früher von Nagasawa und Rice für Maleinsäurecopolymere und von Wall und Mitarbeitern für Polyacrylsäure erhaltenen liefert eine weitere Stütze für die Behauptung, dass die Bruttoladungsdichte an einem Polyion für die Gesamtgegenionen-Bindung ausschlaggebend ist. Schliesslich wurden auch potentiometrische Titrationen ausgeführt, wobei eine adäquate Darstellung der Ergebnisse durch die Gleichung von Kern möglich war.

Received September 5, 1962

JOURNAL OF POLYMER SCIENCE: PART A VOL. 1, PP. 2135-2143 (1963)

Photosensitivity of Dry-Heated Polyacrylonitrile*

TSUNEO YOSHINO and YASUO MANABE, *Basic Research Laboratory, Toyo Rayon Company, Ltd., Kamakura, Kanagawa, Japan*

Synopsis

Polyacrylonitrile heated under appropriate conditions (time and temperature) in nitrogen or *in vacuo* was found to be photosensitive. On exposure to visible light, the visible light absorption of a heat-treated polyacrylonitrile film shifts to longer wavelength, and an ESR absorption is detected in heat-treated powder. Solubility to acids changes on exposure to light, and acids of appropriate concentrations dissolve only the unexposed portion of a polyacrylonitrile film and leave the exposed portion. The relation between these effects of light on dry-heated polyacrylonitrile is discussed.

Polyacrylonitrile can be produced in practically colorless form, but dry-heating causes color development in the polymer substance from yellow to black. The black polymer, after prolonged heat treatments at high temperature, develops stability to flame,[1] semiconductivity,[2] and other remarkable physical properties. The dry-heating of polyacrylonitrile is, therefore, of interest and has been subject to many investigations.[1-4]

This paper gives the results of an investigation of photosensitivity of polyacrylonitrile dry-heated in nitrogen or *in vacuo*.

Photosensitivity Manifested in Visible Light Absorption

A polyacrylonitrile film dry-heated for an appropriate time and temperature in the darkness in a nitrogen atmosphere, when exposed to light, was found to change color from yellow to dark orange at room temperature. The color change of the film was found not to be due to contact with oxygen, nitrogen, carbon dioxide, air, or water, but to take place even *in vacuo* when exposed to light. (It is reported by Vosburgh[5] that polyacrylonitrile fabric heated in the absence of oxygen (for example, in nitrogen) to reddish-yellow discoloration gradually darkens if allowed to stand at room temperature in air.) The color change is due to a shift to longer wavelength of the visible absorption caused by the heat treatment as shown in Figure 1. The heating period and temperature suitable for the appearance of the photosensitivity are limited to fairly narrow ranges, as shown in Table I. A polyacrylonitrile film heat-treated in an oxidizing atmosphere, e.g., oxygen, air, or chlorine, does not become photosensitive.

Copolymerization of a small amount of acrylamide or acrylic acid with

* Presented at the 15th meeting of the Chemical Society of Japan, Kyoto, April 1962.

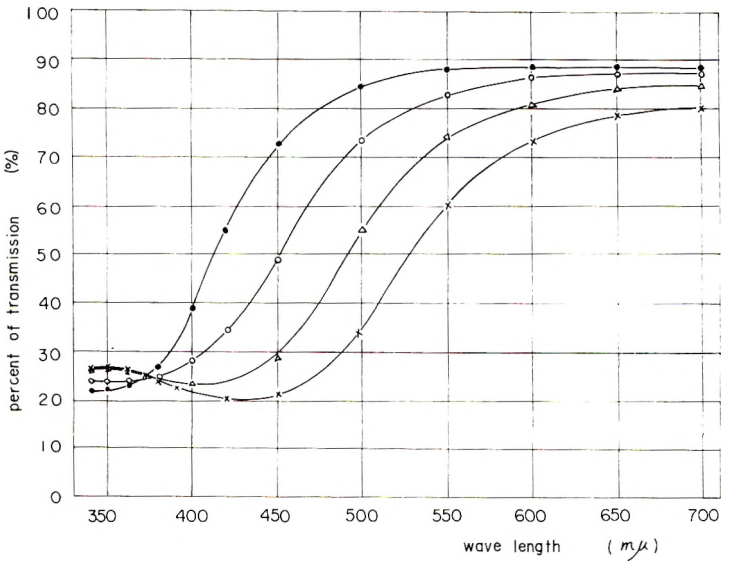

Fig. 1. Shift of light absorption curve of a dry-heated polyacrylonitrile film by exposure to light: (●) unexposed film; (○) 3 min.; (△) 60 min.; (×) 300 min.

acrylonitrile, markedly accelerates discoloration of the copolymer; this is considered to be the result of fused ring formation. Acrylonitrile copolymer with a few per cent of acrylamide or acrylic acid shows nearly the same photosensitivity as polyacrylonitrile, when heated at temperatures about 20°C. lower than those for polyacrylonitrile listed in Table I.

The maximum shift of light absorption by exposure to light was found to be about 120 mμ. The shift depends on the thickness of polymer films. On exposure of film to light from a 100-w. ultrahigh-pressure mercury lamp or to a 1500-w. xenon lamp at a distance of 7 cm., the shift reaches half the maximum value in several minutes, and after a long exposure (about 10

TABLE I

Absorption Shift on Exposure to Light in Relation to Heating Temperature and Time[a]

Time, min.	Absorption shift, mμ								
	220°C.	230°C.	240°C.	260°C.	280°C.	300°C.	320°C.	340°C.	360°C.
2.5									42
10	0	5	7	58	57	54	46	27	36
15	9	4	18	59	50	60	44	15	0
30	5	22	56	50	42	40	41	0	
45	37	57	61						
60	34	60	66						
75	52	67	50						
90		68							
120		52	54						
180		56	40						

[a] Films were exposed for 60 minutes.

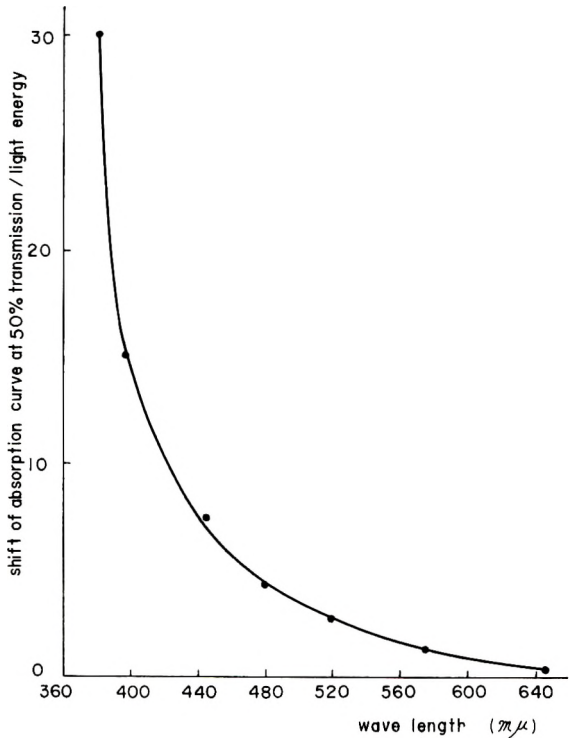

Fig. 2. Spectral photosensitivity of a dry-heated polyacrylonitrile film.

hr.) the shift tends to decrease from the maximum. The sensitivity is higher for incident light of shorter wavelength, as shown in Figure 2.

The visible absorption of a heat-treated polyacrylonitrile film shifts to longer wavelength when allowed to stand in a dark place for a long time. The amount of the shift is same in air and *in vacuo*. The velocity of the shift decreases markedly with time, and the shift seems to reach a limiting value after about 100 hr. at room temperature. The higher the temperature, the larger the apparent saturation value is. However the shift obtained by annealing in nitrogen for 30 min. at 110°C. in the dark is only a few millimicrons.

When a heat-treated polyacrylonitrile film is exposed to light after annealing and/or storage in the darkness, the absorption curve shifts to longer wavelength at the time of exposure. As seen in Table II, the total shift is nearly equal to the shift of a film exposed in the same condition immediately after the heat treatment, if the time of exposure is not too short. That the total shift is equal is also seen in that the absorption curve of a light-exposed film does not move to longer wavelength when the film is allowed to stand in the darkness for a long time. These facts seem to show that incident light not only causes a chemical change which actually does not take place in the darkness but also accelerates the change of labile chemical structures which requires a long time in the dark.

TABLE II
Shifts of Light Absorption after Light Exposure, Annealing, and Storage[a]

Treatment of films	Absorption shift, mμ			
	Annealing[b]	Storage[c]	Exposure for 5 min.	Exposure for 60 min.
Exposure			61	75
Annealing and exposure	2		68	88
Storage and exposure		31	32	50
Annealing, storage and exposure	3	29	37	55

[a] Films were dry-heated at 260°C. for 10 min. in nitrogen.
[b] At 110°C. for 30 min. in nitrogen.
[c] Allowed to stand in the dark in air for 120 hr. at room temperature.

Photosensitivity Revealed in the Change of Solubility

The infrared spectrum of a portion of polyacrylonitrile film exposed to light does not differ from that of the portion of film not exposed to light. The change of the chemical structures responsible for the visible absorption shift is, therefore, considered to take place only in a very small frac-

TABLE III
Acid Solubility of Light-Exposed and Unexposed Portions of Dry-Heated Films[a]

Acid	Acid concn., wt.-%	Solubility[b]	
		Unexposed	Exposed
HCl	35.4	S	I*
	33.8	S	I
	30.8	S	I
	29.2	S*	I
	27.6	S*	I
	27.2	I*	I
HCOOH	42.2	S	S*
	38.4	S	I*
	33.7	S*	I
	29.2	I*	I
H_2SO_4	60.0	S	S*
	51.0	S	I*
	40.8	S	I*
	35.2	S*	I
	31.6	I*	I
HNO_3	49.4	S	S*
	47.8	S	I
	46.8	S*	I
	41.4	S*	I
	29.4	I*	I

[a] Films about 1μ in thickness heated at 260°C. for 5 min. and exposed to light for 60 min.
[b] Solubility: S = soluble; S* = almost completely soluble; I* slightly soluble; I = insoluble.

tion of the polymer. However solubility to some liquids is different in these portions. Acids of appropriate concentration dissolve the unexposed portion and leave only the exposed portion, as seen in Table III. Polyacrylonitrile of low molecular weight (about 30,000) was found to be less sensitive to light with respect to its solubility as well as to the shift of light absorption, and the unexposed portion was not preferentially dissolved by acids.

The difference in solubility between the light-exposed and the unexposed portion of a dry-heated polymer film does not change appreciably if the film is allowed to stand over a week in the dark before or after exposure to light. On annealing for 30 min. at 110°C. *in vacuo*, however, the light-exposed portion becomes more insoluble to acids while the solubility of the unexposed portion remains almost unchanged, as shown in Table IV.

TABLE IV
Effect of Annealing on the Lowest Concentrations of Formic Acid Dissolving the Light-Exposed or Unexposed Portions of Polyacrylonitrile Films[a]

Sample[c]	Treatment	Lowest acid concentration, vol.-%[b]	
		Unexposed portion	Exposed portion
1	Annealed	32	58
1	Not annealed	30	50
2	Annealed	30	62
2	Not annealed	32	56
3	Annealed	34	52
3	Not annealed	34	46

[a] Films about 2μ in thickness heated at 260°C. for 5 min. *in vacuo*, exposed for 30 min. in air.

[b] Concentrations of formic acid in the aqueous solutions used ranged from 12–62 vol.-% at 2% intervals.

[c] Each polymer film was cut into two pieces, each with exposed and unexposed portions, and one of them was annealed for 30 min. at 110°C. *in vacuo*.

Heat- and Light-Induced ESR Absorption

An ESR absorption of about 10^{17} spins/g. with a width of about 20 gauss occurs in polyacrylonitrile, when powder of the polymer is dry-heated for an appropriate time and temperature. There are two time–temperature regions suitable for producing the appearance of the ESR absorption, as shown in Table V.

When heat-treated polyacrylonitrile powder is exposed to light, the heat-induced ESR absorption increases, and an ESR absorption occurs if the sample is heat-treated in the intermediate condition between those mentioned above. The light-induced ESR absorption takes place both in nitrogen and in air and does not decrease over a month. The lower limit of the time–temperature region for the appearance of the light-induced ESR absorption, including the one increased by light, is the same as the ower limit of the region for the photosensitivity in light absorption. The

TABLE V
ESR Absorption of Heat-Treated Powder in Relation to Heating Temperature and Time[a]

		ESR absorption, 10^{17} spins/g.									
	Time, min.	210°C.	220°C.	230°C.	240°C.	250°C.	260°C.	270°C.	280°C.	290°C.	300°C.
Before exposure	10				0.57	1.12	0.21	weak	weak	weak	0.21
	15			0.72	1.68	0.32	weak	weak	weak	weak	weak
	30		1.14	1.37	0.21	weak	weak	weak	weak	0.36	0.55
After exposure	10				0.67	1.41	0.81	0.67	0.81	0.54	0.67
	15			0.92	2.98	1.13	0.56	0.56	0.71	0.56	0.74
	30	weak	1.53	2.40	1.27	1.18	0.90	0.71	0.78	0.97	1.99

[a] Heat-treated *in vacuo* and exposed to light for 120 min. *in vacuo*.

light-induced ESR absorption decreases, however, to about half when the polymer powder is annealed for 30 min. at 110°C. or dipped in dioxane, whereas the light absorption of a polymer film subjected to these treatments never shifts to shorter wavelength. The unpaired electrons produced by light are, therefore, not responsible for the shift of the light absorption to longer wavelength and rather seem to be connected with the photosensitivity revealed in the change of solubility to acids.

It seems probable that the incident light produces unpaired electrons in the dry-heated polymer which accelerate formation of network structures by extinguishing themselves, and that some of the electrons remain unpaired and join in the formation of network structures at the elevated temperature of annealing.

The decrease of the ESR absorption when the film is dipped in dioxane seems not to be related with the formation of network structures, since the absorption recovers its intensity when dioxane is removed.

Experimental

Purified acrylonitrile was dissolved in dimethyl sulfoxide to form a 20% solution. To one part of this solution was added 0.0032 part of azobisisobutyronitrile recrystallized three times from methanol. Nitrogen was introduced into the solution to remove oxygen, and the polymerization reaction was continued for 16 hr. at 40 ± 1°C. in a nitrogen atmosphere. The polymer solution was diluted with dimethylsulfoxide and poured into water. Impurities were extracted from the precipitated polymer by water and methanol at their boiling temperatures, and the purified polymer was dried in vacuum at 50°C. The molecular weight of the polymer obtained by viscosity measurement and Onyon's equation[6] was 370,000 except for the low molecular weight polymer used in investigating the dependency of the photosensitivity on the molecular weight. This polymer was prepared in the same way except for the addition of dodecyl mercaptan, 0.4 wt.-%, to the dimethyl sulfoxide solution of acrylonitrile. Copolymers were also prepared in the same way, and the compositions were determined by measurement of infrared absorption.

The dried polymer was dissolved in dimethyl sulfoxide and poured on clean level glass plates, the solvent being evaporated *in vacuo* for 24 hr. The polymer films were separated from the glass plates in water. A single polymer film thus prepared was cut into pieces, and comparisons of photosensitivity under different conditions of treatment were made only between these small films from a single film.

In the dry heat treatment, a polymer film was affixed to a mica or a glass plate and inserted in a box at distances of 5 mm. from both the top and the bottom of the box. An aqueous solution of polyvinyl alcohol was used to affix the film, but this was found to have no influence on the photosensitivity of the polymer film. The top and the bottom of the box consist of mica plates wound with Nichrome ribbons. The box was inserted in a glass tube with a cover, and air in the tube was evacuated or replaced by purified

nitrogen after the evacuation. The electric current through the Nichrome ribbons was regulated so as to prevent visible radiation from the ribbons. The temperature of the polymer film was recorded by the use of a thermocouple inserted in the heating box.

In the annealing, a dry-heated polymer film on a mica or a glass plate was put in a glass tube, air in the tube was evacuated or replaced by purified nitrogen, and the tube was dipped in a salt bath. Both the heat treatment and the annealing were carried out in a dark room.

The polymer film or powder was exposed to light from a 100-w. ultrahigh pressure mercury lamp at a distance of 7 cm. The shift of light absorption curve was measured at 50% transmission.

Infrared absorption was measured by means of a Nippon Bunko model DS-402G grating spectrophotometer, and visible and ultraviolet spectra by a Shimazu model QR-50 spectrophotometer. The latter was also used to obtain monochromatic light from a 1-kw. tungsten lamp for the purpose of measuring the spectral photosensitivity of heat-treated polymer films. Films for visible absorption measurement were 0.5–3μ in thickness.

Samples for ESR absorption measurement were prepared as follows. Purified polyacrylonitrile was powdered in an agate mortar and a glass tube for ESR absorption measurement was stuffed with the powder. After air in the tube was evacuated, the tube was heated in the dark. In exposing to light, the sample tube was shaken continuously in order to expose the major part of the powder to light, since only the peripheral layer of the powder receives full intensity of light. The ESR absorption was measured by a Japan Electron Optics JES-1 type ESR spectrometer.

References

1. Houtz, R. C., *Textile Res. J.*, **20**, 786 (1950).
2. Topchiev, A. V., et al., *Dokl. Akad. Nauk SSSR*, **128**, 312 (1959); *Chem. Ind.*, **1960**, 184.
3. Burlant, W. T., and J. L. Parson, *J. Polymer Sci.*, **22**, 249 (1956).
4. Kennedy, J. P., and C. M. Fontana, *J. Polymer Sci.*, **39**, 501 (1959).
5. Vosburgh, W. G., *Textile Res. J.*, **30**, 882 (1960).
6. Onyon, P. F., *J. Polymer Sci.*, **22**, 13 (1956).

Résumé

Le polyacrylonitrile, chauffé à l'état sec durant un temps approprié sous atmosphère d'azote ou sous vide, devient photosensible. Lors de l'exposition à la lumière visible, l'absorption de cette dernière par un film de polyacrylonitrile préchauffé subit un déplacement bathochrone; une absorption ESR apparaît dans la poudre préchauffée. La solubilité dans les acides est modifiée par exposition à la lumière. Les acides de concentration appropriée ne dissolvent que les parties nonexposées d'un film de polyacrylonitrile, laissant intactes les parties exposées. La relation entre ces effets de la lumière sur le polyacrylonitrile chauffé à l'état sec est discutée.

Zusammenfassung

Durch bestimmte Zeit auf geeignete Temperatur unter Stickstoff oder im Vakuum trocken erhitztes Polyacrylnitril erwies sich als lichtempfindlich. Unter Einwirkung

von sichtbarem Licht verschob sich die Lichtabsorption von wärmebehandelten Polyacrylnitrilfolien im Sichtbaren nach grösseren Wellenlängen und im wärmebehandelten Pulver wird eine ESR-Absorption hervorgerufen. Die Säurelöslichkeit ändert sich durch Einwirking von Licht und Säuren von geeigneter Konzentration lösen nur den nichtexponierten Teil einer Polyacrylnitrilfolie unter Zurücklassung des exponierten Teiles. Die Beziehung zwischen diesen Lichteffekten bei trocken erhitztem Polyacrylnitril wird diskutiert.

Received July 17, 1962

JOURNAL OF POLYMER SCIENCE: PART A VOL. 1, PP. 2145–2154 (1963)

Radiation Dosimetry in Polyethylene with Silicon Solar Cells

R. SALOVEY and W. ROSENZWEIG, *Bell Telephone Laboratories, Murray Hill, New Jersey*

Synopsis

Irradiation dose rates and complete depth–dose curves in polyethylene have been directly determined with a silicon solar cell. In this manner, an average dose rate of 0.297 Mrad/sec. per incident μamp./cm.^{2} for 1 m.e.v. electrons in 120-mil thick Marlex polyethylene was measured. The corresponding dose rate ascertained by ferrous sulfate dosimetry is 0.260 Mrad/sec. This difference is in the expected direction and may arise from differences in backscatter between polyethylene and silicon. The facility of the solar cell measurement and the complete definition of irradiation dose as a function of absorber thickness commend the device for general application in irradiation dosimetry.

INTRODUCTION

Attempts to measure and elucidate the effects of ionizing radiation are contingent on an accurate knowledge of the absorbed dose. The diverse methods of radiation dosimetry reflect the importance and difficulty of determining the irradiation dose.[1–3] The standard unit of absorbed dose for ionizing radiation is the rad, which corresponds to an energy absorption of 100 ergs/g. of any given material. The megarad (Mrad) or 10^6 rads is a convenient unit in studies of the electron irradiation of polymers.

Irradiation doses may be directly determined by precision calorimetry or in an ionization chamber combined with a known value of the average energy to form an ion pair. Neither method is sufficiently convenient or unambiguous for routine dosimetry. Therefore, a variety of dosimeters have been suggested and devised for establishing irradiation dose. These include measuring the oxidation of ferrous ions, the evolution of hydrogen from irradiated organic materials, the bleaching of blue cellophane, the coloration of glass and polymers, and the physical changes in plastics.[1] The most satisfactory and extensively studied secondary standard is the ferrous sulfate dosimeter.[3b] However, measurement of the oxidation of ferrous ions is limited to absorbed doses of about 10^4 rads—well below the doses ordinarily encountered in polymer studies. Moreover, this chemical dosimeter is very sensitive to organic impurities and requires careful purification of reactants. Silicon solar cells, as solid-state ionization chambers, have been suggested as versatile radiation dosimeters.[4] In this communication, we examine their applicability to the irradiation of polymers

and determine irradiation dose as a function of polyethylene absorber thickness using a silicon solar cell. The absorbed dose, measured in this manner, is then compared with the dose ascertained from ferrous sulfate dosimetry (the oxidation of ferrous ions in aqueous solution by absorption of radiation). Finally, to gain further insight into electron penetration, we studied the attenuation in current on interposing polyethylene absorbers in the electron beam.

EXPERIMENTAL DETAILS AND RESULTS

A. Solar Cell Measurements

The irradiation source was a beam of monoenergetic 1 m.e.v. electrons (slightly modified by subsequent scattering) from a High Voltage Engineering Company Van de Graaff generator. The incident electron flux was determined by absorbing a defined portion of the beam onto a Faraday cup (a total absorber) and measuring the resultant current. In performing the depth–dose study, a Faraday cup and a silicon solar cell were mounted side by side under identical defining apertures and situated at equal beam intensities in an electron beam (so that interchanging the positions of cup and solar cell produces no change in a given measurement). The ratio of solar cell current to Faraday cup current (J_{sc}/J_e) was measured on irradiation. Polyethylene (Marlex, 6000 Series, Type 50, density 0.96 g./ml.) absorbers of known thickness were interposed additively in the beam on top of the solar cell and the current ratio repeatedly determined as a function of polyethylene thickness (Fig. 1). The initial point (at 4.2 mils) is an equivalent thickness of polyethylene corresponding to a thin aluminum sheet necessary

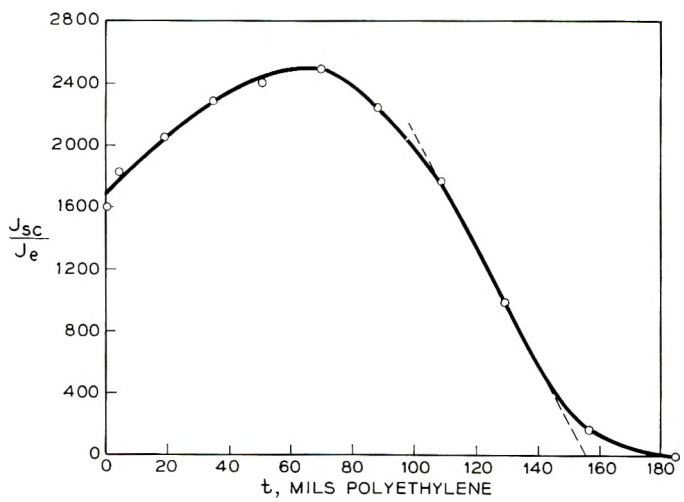

Fig. 1. Depth–dose curve, 1 m.e.v. electrons in polyethylene determined with silicon solar cell (11.1 micron diffusion length). Electrons scattered by $5^1/_2$ mils of aluminum and $4^1/_2$ in. of air prior to absorption.

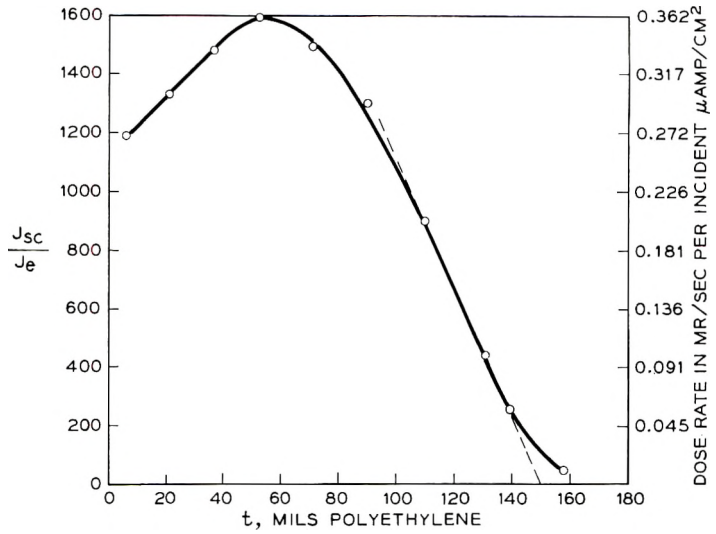

Fig. 2. Depth–dose curve, 1 m.e.v. electrons in polyethylene determined with silicon solar cell (8.8 micron diffusion length). Electrons scattered by 7 mils of aluminum and 10 in. of air prior to absorption.

to provide electrical contact. In this case, a monoenergetic 1 m.e.v. electron beam traverses $5^1/_2$ mils of aluminum and $4^1/_2$ in. of air before striking the Faraday cup and solar cell cover. The depth–dose behavior with polyethylene absorbers was also investigated with a slightly different geometrical arrangement which was carefully reproduced for all subsequent dosimetric studies reported here. In this case, the electron beam traverses 7 mils of aluminum and 10 in. of air before striking the cup and solar cell. The effect of adding polyethylene absorbers under these conditions is shown in Figure 2. This depth–dose curve differs from that in Figure 1 because the apparently minor geometrical changes in scattering conditions produce different electron energy spectra. This point will be discussed subsequently.

Our calculations will concern Figure 2, as this represents the experimental arrangement comparable to subsequent studies. The ratio of currents J_{sc}/J_e measures the number of electrons generated per incident electron in a slab of silicon defined by the diffusion length L of the minority carriers and the surface area of the solar cell. The average energy to produce a hole-electron pair in silicon is 3.6 e.v.[5] Therefore, for 1 electron incident on 1 cm.^{2} area, the energy per unit volume deposited in silicon is $(J_{sc}/J_e)(3.6/L)$e.v./cm.^{3}. To get the corresponding energy absorbed per unit volume in polyethylene, we correct for the relative linear stopping powers of polyethylene to silicon; this yields $(J_{sc}/J_e)(3.6/L)(0.96/2.33) \times (1.29)$ e.v./cm.^{3}. The first correction term corresponds to the ratio of mass densities, the second to the ratio of relative mass stopping powers.[6] For a measured diffusion length of 8.8 microns for the solar cell of Figure 2 (see Appendix) and an average value for the absorbed dose in a sample of poly-

ethylene 120 mil thick (corresponding to the depth of aqueous solutions used for subsequent dosimetry) the derived dose rate in megarads is calculated as *0.297 Mrad/sec.* per incident μamp./cm.^{2}, where 1 rad = 6.24×10^{13} e.v./g. The dose rates corresponding to values of J_{sc}/J_e are shown in Figure 2.

B. Ferrous Sulfate Oxidation

The ferrous sulfate dosimeter consists of a $10^{-3}M$ solution of ferrous ammonium sulfate in $0.1N$ aqueous sulfuric acid. A 5-ml. portion of this solution was placed in a 5-cm. diameter petri dish centered in the electron beam and exposed in air for 10–40 seconds to a total dose of about 10^4 rads. The concentration of the resultant ferric ions was measured by scanning the irradiated solution in a Beckmann DK-2 spectrophotometer at 350–290 mμ and determining the absorption maximum at 304 mμ.[3b,c] The incident electron flux was ascertained by measuring the electron beam current on a shutter interposed momentarily in the beam prior to irradiation and applying a previously determined and repeatedly checked relation between shutter current and incident electrons/cm.^{2} sec.

The average of many determinations of the dose rate with the ferrous sulfate dosimeter is 0.272 ± 0.016 Mrad/sec. per incident μamp./cm.^{2}. This dose rate was obtained irrespective of whether ordinary distilled water or such water redistilled from potassium permanganate was used to prepare the solution. However, if the ferrous sulfate dosimeter was prepared with water successively redistilled from alkaline permanganate and sulfuric acid, the corresponding dose rate is reduced to 0.243 ± 0.008 Mrad/sec.

Similar ferrous ammonium sulfate solutions in sulfuric acid were prepared containing, in addition, $10^{-3}M$ sodium chloride. For this dosimeter, the average of repeated determinations is 0.224 ± 0.005 Mrad/sec. per incident μamp./cm.^{2} (regardless of whether distilled water was used or the water was redistilled from potassium permanganate or successively redistilled from alkaline permanganate and sulfuric acid and whether or not the sodium chloride was washed and recrystallized).

C. Current Attenuation by Polyethylene Absorbers

An aluminum Faraday cup with a $^1/_2$-in. diameter and $^1/_8$-in. thick defining aperture was employed to study the penetration of 1 m.e.v. electrons into polyethylene. Current readings were taken, as usual, with the electron beam traversing 7 mils of an aluminium scatterer and 10 in. of air. Polyethylene absorbers of known thickness were placed on top of the cup and the residual current measured as a function of absorber thickness (Fig. 3). We repeatedly interposed a shutter in the beam immediately prior to each irradiation and normalized the cup currents to unit shutter current. Corresponding results were also obtained in an identical arrangement in which $^1/_{32}$-in. thick copper replaced the $^1/_8$-in. thick aluminum defining aperture (Fig. 3). Since the deposition of energy in the polymer is more closely defined with the use of the thin aperture (as will be subsequently

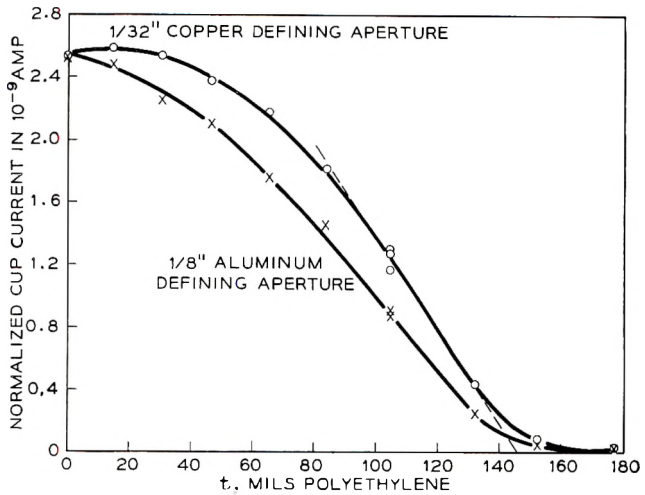

Fig. 3. Absorption of 1 m.e.v. electrons by polyethylene.

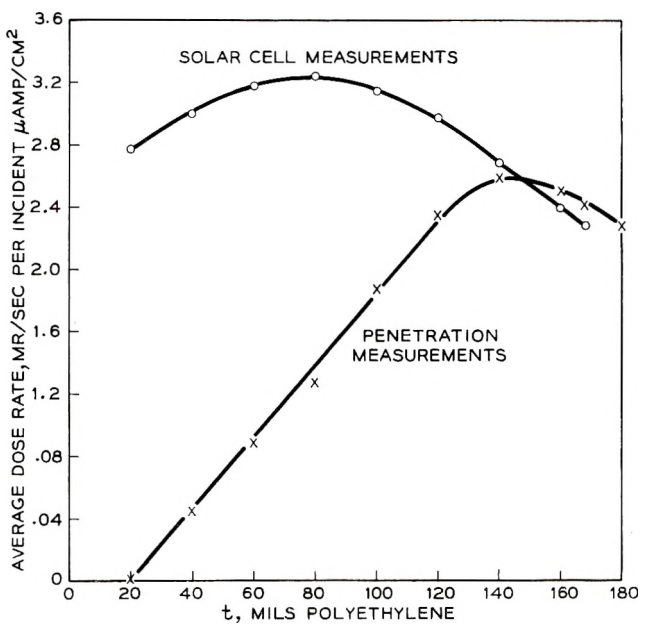

Fig. 4. Average dose rate as a function of polyethylene thickness.

discussed), we will examine the data obtained with the thin aperture and calculate dose rates. If we consider (incorrectly) that the rate of energy deposition in a given thickness of polyethylene is the product of incident electron energy (1 m.e.v.) and the attenuation in current produced by that thickness, we may calculate the dose rate as a function of polyethylene thickness. These results are compared with the actual dose rate, calculated

from the depth–dose study with a silicon solar cell, as a function of polyethylene absorber thickness in Figure 4.

DISCUSSION

The difference in the depth–dose curves determined by solar cell measurements and shown in Figures 1 and 2 reflect the ionization in polyethylene by energetic electrons of slightly different energy spectra. Since the scattering path traversed by the originally monoenergetic 1 m.e.v. electrons (before striking the absorber) is greater in Figure 2 than Figure 1, the average energy per incident electron is correspondingly slightly lower in Figure 2. The extrapolated range in both cases is about 150 mils of polyethylene, referring to the penetration of the most energetic electrons (1 m.e.v.) which are of identical energy in each case. However, the earlier maximum in Figure 2 corresponds to a larger proportion of low energy electrons which are less penetrating, producing enhanced ionization at smaller depths.

Assuming a 120-mil thick sample of polyethylene (corresponding to the depth of aqueous solutions used in ferrous sulfate dosimetry), we recall that the average dose rate from the solar cell dosimetry is 0.297 Mrad/sec. per incident μamp./cm.^{2}. The derivation of this figure has been indicated above. Experimentally, we measured the ionization in silicon and converted to ionization in polyethylene. The effect on ionization in a layer at a given depth by lower lying layers (backscatter) is not corrected for. This is an experimental limitation and the solar cell measurement is in error to the extent that backscatter is not the same for polyethylene and silicon. Since there is more backscatter from silicon (higher atomic number), we would expect the solar cell reading to be somewhat high.

The incident electron flux at which ionization in the solar cell was measured could be varied widely and the same values of J_{sc}/J_e determined. However, since the solar cell diffusion length is degraded on bombardment,[4] it is preferable to use low electron fluxes so that the diffusion length is essentially constant throughout a series of measurements. Since a ratio is measured in the solar cell experiments, the constancy of incident electron flux is inconsequential.

A variety of dose rates have been determined by ferrous sulfate dosimetry. The presence of organic impurities has been shown to enhance the absolute dose rate.[3c,7] Thus, the observed dose rate is reduced from 0.272 to 0.243 Mrad/sec. per incident μamp./cm.^{2} on very careful purification of reagents. The experiments with added $10^{-3}M$ salt were performed to test reagent purity. In the presence of added sodium chloride, the effect of organic inpurities is supposed to be totally suppressed.[7] Therefore, the appropriate dose rate is 0.224 Mrad/sec. per incident μamp./cm.^{2}. The reproducibility of this value and the approach to it on purification perhaps indicate the total suppression of trace (and variable) amounts of impurities.

In order to compare this dose rate with that obtained from solar cell dosimetry, we must first apply several corrections. The ferrous sulfate

dose rate, measured in aqueous solutions, must be corrected for the relative mass stopping powers of polyethylene as compared to water. Since the stopping power of polyethylene is 1.06 times that of water,[6] the actual dose rate is 6% higher in polyethylene. Moreover, the ferrous sulfate dosimetry is measured over a 5-cm. diameter petri dish (using less than 0.3 cm. depth of solution) while a 1.27-cm. diameter Faraday cup was used to measure the corresponding incident current per unit area. A study of the electron beam intensity profile by means of a solar cell, for the scattering condition under consideration, indicates that the average ionization over a 5-cm. circle is about 6.5% lower than over the smaller area. Thus, the ferrous sulfate oxidation dose rate must be corrected to the actual incident electron intensity by increasing the measured dose rate by 6.5%. A further correction may arise in the spectrophotometric analysis for resultant ferric ion concentration. The temperature dependence of the extinction coefficient for the optical absorption of ferric ions was considered by measuring the temperature in the spectrophotometer sample holder (~35°C.). However, the actual temperature of the dosimeter solutions may well have been at least 5°C. lower. This would lead to a 3.5% underestimate in dose rate. Applying these corrections, the actual dose rate from ferrous sulfate dosimetry is about 0.260 Mrad/sec. per incident μamp./cm.^{2}. Since we are assuming a simple impurity suppression by the added sodium chloride and, therefore, our lowest value from the ferrous sulfate dosimetry, it is possible that the true dose rate may be higher. In any case, the agreement with the solar cell dosimetry is within 13%, and in a direction which is reasonable from differences in backscatter.

The time requirements and uncertainties arising from the preparation and purification of dosimeter solutions, the necessity to ensure complete penetration by the energetic electrons of the ferrous sulfate dosimeter and to assess their uniformity over an extended surface, and the temperature dependence of spectrophotometry introduce a complexity in marked contrast to the simple and relatively unequivocal solar cell measurements. Moreover, the solar cell dosimetry defines a complete depth–dose relation and indicates the ionization as a function of depth in an absorber.

The attenuation in current recorded by a Faraday cup on interposing polyethylene absorbers is shown in Figure 3 for two defining aperture thicknesses with otherwise identical cups. The minimum thickness of a defining aperture is determined by the penetration of the incident electrons. That is, the material out of which the defining aperture is cut and which surrounds it in use must be sufficiently thick to stop the incident electron beam. Since copper has a higher density than aluminum, it is possible to replace the aluminum defining aperture by a thinner copper one. In the absence of polyethylene absorber, the current registered on the cup is identical for either aperture (of equal area). However, the current readings upon adding polyethylene absorbers are higher for the $^1/_{32}$-in. thick copper than for the $^1/_8$-in. thick aluminum defining aperture. This difference may be attributed to the fact that electrons scattered through wide angles by the

polyethylene absorbers strike the vertical walls around the defining aperture and do not enter the Faraday cup to be counted. In order to minimize the "loss" of electrons scattered through wide angles, it is necessary to use as thin a wall as possible. The $^1/_{32}$-in. copper aperture is quite adequate for these measurements, as shown by the initial horizontal points in the penetration curve and the initial coincidence of the two sets of data (Fig. 3). The extrapolated range for 1 m.e.v. electrons obtained from these measurements is about 150 mils in polyethylene, in fairly good agreement with the previous solar cell measurements.

In Figure 4 we have plotted the average dose rate as a function of polyethylene absorber thickness determined from the solar cell depth–dose curve in Figure 2. That is, if $D(x)$ is the dose rate as a function of the depth x, then by determining $1/t\int_0^t D(x)dx$ we calculate the average dose rate for a given thickness t. The corresponding dose rates as a function of thickness determined by the current attenuation study in Figure 3 (upper curve) are also shown in Figure 4. For this calculation, we make the artificial assumption that the rate of energy deposition in a given thickness of polyethylene is the product of incident electron energy (1 m.e.v.) and current attenuation produced by that thickness. Actually, this considers only that part of the energy deposition due to electrons stopped by a given thickness of absorber. However, some energy is certainly deposited by electrons that traverse the absorber and lose energy but are not stopped by the given thickness. It also ignores the contribution of the backscattered electrons. The importance of these energy deposition terms can be seen by the deviation between the curves in Figure 4. The curves coincide, as they must, at maximum penetrations when it is valid to neglect both the electrons that traverse but do *not* stop in the absorber and the backscatter component.

For 1 m.e.v. electrons and polyethylene thicknesses greater than 140 mils, almost all the electrons are stopped, and the average dose can be calculated on this basis.

CONCLUSIONS

Irradiation dose as a function of absorber thickness may be simply and directly measured with a silicon solar cell. In this manner, we determined an average dose rate of 0.297 Mrad/sec. per incident μamp./cm.^{2} for 1 m.e.v. electrons in Marlex polyethylene 120 mils thick. This compares to a corrected value of 0.260 Mrad/sec. ascertained by relatively tedious ferrous sulfate dosimetry. This difference is in the expected direction and may arise from backscatter differences between polyethylene and silicon. The comparative simplicity of the solar cell measurements commend the device for general application in irradiation dosimetry.

For 1 m.e.v. electrons and polyethylene thicknesses in excess of 140 mils, almost all the incident electrons are stopped and the average dose rate may be calculated from the incident current. The importance of minimizing

the wall height of the Faraday cup defining aperture for penetration measurements is demonstrated.

APPENDIX

The silicon solar cell is, in essence, a solid-state ionization chamber whose sensitive volume extends from the upper surface to a depth L, where L is the bulk minority carrier diffusion length. For a given cell the unknown value L may be determined by measuring J_{sc}/J_e as a function of depth in silicon for a monoenergetic beam of electrons of known energy. In such a measurement J_{sc}/J_eL represents the average specific ionization at a given depth for an incident electron so that the integral of this quantity over all depths must equal the total ionization which the incident electron is able to produce. The latter is equal to the electron energy divided by the average energy to produce a hole-electron pair, 3.6 e.v. in silicon. In terms of symbols:

$$1/L\int_0^\infty (J_{sc}/J_e)\,dx = E/3.6 \qquad (1)$$

where E is the incident electron energy in electron-volts. Equation (1) has one unknown, L, for which it can be solved.

We sincerely thank F. R. Dammont, J. A. O'Sullivan, and J. V. Pascale for their assistance in experimental aspects of this work and W. M. Augustyniak for suggesting the single aperture Faraday cup design employed in this study.

References

1. Charlesby, A., *Atomic Radiation and Polymers*, Pergamon Press, New York, 1960, Chapter 6.
2. Bovey, F. A., *The Effects of Ionizing Radiation on Natural and Synthetic High Polymers*, Interscience, New York, 1958, p. 32.
3. Swallow, A. J., *Radiation Chemistry of Organic Compounds*, Pergamon Press, New York, 1960, (a) p. 36; (b) *ibid.*, p. 42; (c) *ibid.*, p. 51.
4. Rosenzweig, W., *Rev. Sci. Instr.*, **33,** 379 (1962).
5. Chynoweth, A. G., private communication.
6. Nelms, A. T., *Natl. Bur. Std. Circ.*, No. **577,** 15, 21 (1956); *ibid.*, 19, 21 (1958).
7. Dewhurst, H. A., *J. Chem. Phys.*, **19,** 1329 (1951).

Résumé

Les doses d'irradiation et les courbes complètes de profondeur-dose ont été déterminées pour le polyéthylène avec une cellule solaire en silicone. De cette façon, on a mesuré une dose moyenne de 0.297 Mrad/sec/μamp/cm^2 introduit pour des électrons de 1 m.e.v. au sein de polyéthylène Marlex d'une largeur de 120 mm. La dose correspondante vérifiée par dosage au sulfate ferreux est 0.260 Mrad/sec. Cette différence répond à ce qu'on attendait et peut résulter de différences en diffusion réfléchie entre le polyéthylène et la silicone. La facilité de mesure et la définition complète de la dose d'irradiation, comme fonction de l'épaisseur de l'absorbeur, recommendent une application générale de ce procédé dans la dosimétrie des irradiations.

Zusammenfassung

Bestrahlungsdosisleistung und vollständige Dosis–Tiefenkurven in Polyäthylen wurden direkt mit einer Silicium–Solarzelle bestimmt. Auf diese Weise wurde eine mittlere

Dosisleistung von 0,297 Mrad/sek pro einfallendes μamp./cm.^{2} für 1 m.e.v.-Elektronen in 120-mil dickem Marlex–Polyäthylen gemessen. Durch Ferrosulfat–Dosimetrie wurde für die entsprechende Dosisleistung 0,260 Mrad/sek erhalten. Der Unterschied liegt in der erwarteten Richtung und ist möglicherweise durch Unterschiede in der Rückwärtsstreuung zwischen Polyäthylen und Silicium bedingt. Die Einfachheit der Messung mit der Solarzelle und die vollständige Bestimmung der Bestrahlungsdosis als Funktion der Absorberdicke empfehlen diese Methode für eine allgemeine Anwendung bei der Bestrahlungsdosimetrie.

Received May 5, 1962

JOURNAL OF POLYMER SCIENCE: PART A VOL. 1, PP. 2155–2162 (1963)

Irradiation of Polyethylene Oxide and Polypropylene*

R. SALOVEY and F. R. DAMMONT, *Bell Telephone Laboratories, Incorporated, Murray Hill, New Jersey*

Synopsis

The solubility behavior of electron-irradiated (*in vacuo*) polyethylene oxide indicates a ratio of main-chain scission density to the density of crosslinked units of 0.6, independent of molecular weight. This value, derived from measurements at high doses, correlates well with the observed increase in intrinsic viscosity and invariance of number-average molecular weight at low irradiation doses. Analogous measurements on polypropylene indicate a linear dependence of $S + S^{1/2}$ (where S is the sol fraction of the irradiated polymer) on the reciprocal irradiation dose. This treatment leads to a ratio of scission-to-crosslinking of 0.8. Increased scission in polypropylene as compared to polyethylene oxide is evidenced by a gradual decrease in the intrinsic viscosity as a function of dose. This decrease is not indicative of an initial irradiation degradation of the polymer, because the number-average molecular weight is relatively unaffected by irradiation until quite close to the gel point. The intrinsic viscosity of the progressively crosslinked polymer is apparently depressed by branching. Direct comparison of the results on polypropylene with theory is uncertain because of a nonrandom initial molecular weight distribution. It is reemphasized that the intrinsic viscosity is not a simple indication of molecular weight changes in crosslinking polymers.

INTRODUCTION

Two classes of polymeric materials may be distinguished on the basis of irradiation behavior; polymers that crosslink and polymers that degrade. Materials in the "crosslinking" category evidence an increasing weight-average molecular weight and ultimately gel on irradiation. Simultaneous radiation-induced crosslinking and main-chain scission often occur in such polymers. Assuming random scission and crosslinking, proportional to dose, the relative importance of these reactions may be derived by analyzing the solubility behavior of the polymer on irradiation.[1] The ratio of scission to crosslinking defines the effect of irradiation and is an important radiation characteristic of a polymer.

Often, changes in intrinsic viscosity have been measured in order to ascertain the effect of irradiation on polymer molecular weight.[2,3] However, the intrinsic viscosity of an irradiated crosslinking polymer indicates changes in branching and molecular weight distribution as well as an in-

* Presented at the 142nd meeting of the American Chemical Society, Atlantic City, New Jersey, September 1962.

creasing weight-average molecular weight.[4,5] On crosslinking the intrinic viscosity is simultaneously depressed by branching, altered by distribution changes, and increased as molecules are joined. Therefore, changes in the intrinsic viscosity of crosslinking polymers do not simply indicate variations in molecular weight. The intrinsic viscosity of such polymers at doses below that necessary for gelation was shown to be severely depressed because of branching.[5] Recently, it was indicated that the effect of branching on the instrinsic viscosity had been previously overestimated,[6] and the intrinsic viscosity of irradiated polymers was reconsidered.[7]

We have measured the number-average molecular weight and intrinsic viscosity as a function of irradiation dose for polyethylene oxide and polypropylene homopolymers. Corresponding scission-to-crosslinking ratios were derived from the irradiation-solubility behavior. These data are compared in the light of current theories.

EXPERIMENTAL DETAILS

1. Materials

Samples of Carbowax, commercially available polyethylene oxides in a variety of molecular weights, were obtained from Union Carbide Chemicals Company. Specifically, Carbowax 1540, a white waxy material, and Carbowax 4000 and 6000, white crystalline solids, were studied.

The sample of atactic polypropylene, Epolene, was made by Tennessee Eastman Company.

Molecular weights of these materials are listed in Table I.

TABLE I
Molecular Weights of the Unirradiated Polymers

Material	$\bar{M}_n$	$[\eta]$, dl./g.	$\bar{M}_v$
Carbowax 1540	1,300	0.054	2,400
Carbowax 4000	2,840	0.107	5,900
Carbowax 6000	7,000	0.209	13,500
Epolene	11,000	0.430	40,000

Number-average molecular weights were derived from vapor pressure depression measurements (described below) and are in fairly good agreement with the manufacturer's values from endgroup titrations. Viscosity-average molecular weights were calculated from intrinsic viscosity measurements in dilute benzene solution at 30°C. For the Carbowaxes, we used an empirical expression relating intrinsic viscosity and molecular weight strictly applicable for water solutions of higher molecular weight polyethylene oxides.[8] However, measurements of the instrinsic viscosity of Carbowax 4000 and 6000 in benzene agree within 10% to those determined in aqueous solution.[9] A corresponding expression relating the intrinsic vis-

cosity of polypropylene in benzene solution to molecular weight[10] was applied.

2. Irradiation

Polymers were evacuated and sealed under high vacuum (10^{-6} mm. Hg) in thin-walled Pyrex tubes and irradiated in a beam of 1 m.e.v. electrons from a Van de Graaff generator. We measured the absorbed dose using silicon solar cells[11] and the ferrous sulfate dosimeter.[12] Following irradiation, the polymers were annealed at 150°C. or at 100°C. *in vacuo* to minimize the concentration of trapped radicals. Such heat treatment did not effect major changes in the molecular weight of the unirradiated polymers. Specimens were stored *in vacuo* until immediately prior to any given measurement, as all the materials, particularly the polypropylene, were sensitive to air exposure.

3. Solubility

The insoluble fraction of irradiated polymers was determined by placing a weighed sample in an extracted and weighed thimble under a stream of refluxing benzene in a Soxhlet extractor for 6 hr. The thimble containing the swollen extracted gel was removed, dried overnight *in vacuo* at 120°C., and weighed.

4. Intrinsic Viscosity

We measured the viscosity as a function of concentration of dilute benzene solution of polyethylene oxide and polypropylene at 30°C. in Cannon-Ubbelohde semimicro dilution viscometers and derived therefrom the corresponding intrinsic viscosity.[13]

5. Vapor Pressure Osmometry

The number-average molecular weight of all polymers was obtained by measuring the vapor pressure depression by the polymer in dilute benzene solution at different concentrations in a Mechrolab vapor pressure osmometer.[14] In this instrument, a drop of solution and of solvent are placed on each of two thermistors suspended in a thermostat saturated with solvent vapor. Since the vapor pressure of the solvent above the solution drop is lower than that of pure solvent, solvent vapor condenses on the drop and its temperature rises. Calibration with materials of known molecular weight in the same solvent, permits quantitative correlation of the steady-state temperature differential with solute molecular weight. We have found the instrument to be most useful up to molecular weights of about 10,000.

RESULTS AND DISCUSSION

In Figure 1, the gel fraction as a function of irradiation dose is shown for several polyethylene oxides differing in molecular weight. For comparison

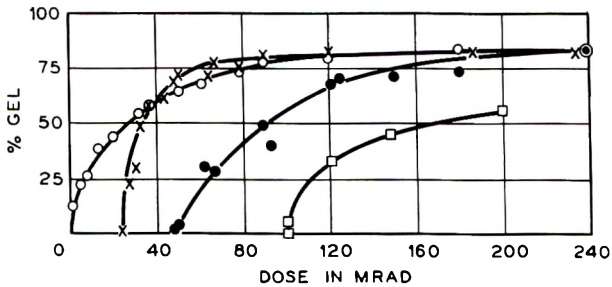

Fig. 1. Gel fraction of irradiated polyethylene oxide: (O) Polyox WSR 35; (×) Carbowax 6000; (●) Carbowax 4000; (□) Carbowax 1540.

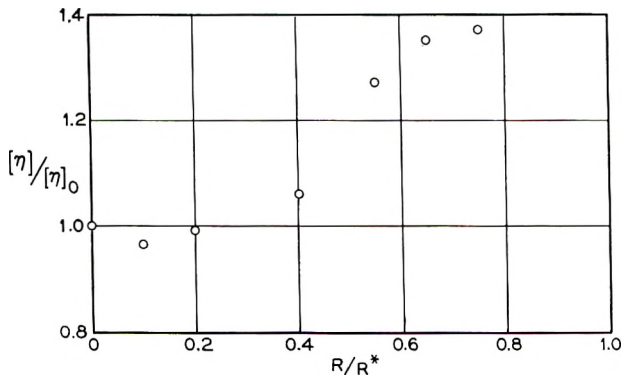

Fig. 2. Intrinsic viscosity of irradiated Carbowax 4000; $[\eta]_0 = 0.107$ dl./g. at 30°C. in benzene, $R^* = 48$ Mrad.

we have included Polyox WSR 35, a very high molecular weight polyethylene oxide also available from Union Carbide Chemicals Company. The gel fractions are rapidly increasing functions of dose, with the gel point, the dose at the onset of gelation, characteristic of molecular weight. In fact, the gel dose is considered to be proportional to the reciprocal of the weight-average molecular weight.[15] Moreover, regardless of the initial molecular weight, the polyethylene oxides attain a limiting gel content of 82.5% at high doses. (Presumably, at sufficiently high doses, the low molecular weight Carbowax 1540 will exhibit a similar gel fraction.) The relative incidence of scission to crosslinking corresponding to this limiting gel fraction is 0.6.[1] The relative change in intrinsic viscosity of irradiated Carbowax 4000 is indicated at increasing fractions of the gel dose, R^*, in Figure 2. Similar results were obtained for Carbowax 1540 and 6000. The Carbowaxes are characterized by approximately random molecular weight distributions. That is, since weight and viscosity averages are quite close,[16] the ratio of weight-average and number-average molecular weights is near two (Table I). Therefore, it is possible to compare these results with theories assuming random initial molecular weight distributions. Considering the ratio of scission to crosslinking (0.6), the change in intrinsic

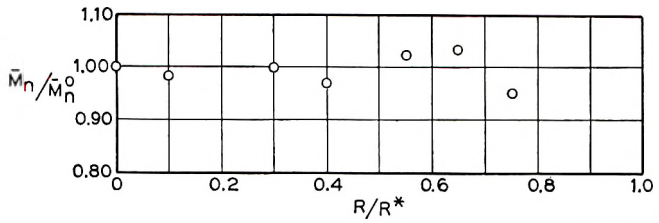

Fig. 3. Number-average molecular weight of irradiated Carbowax 4000; $\bar{M}_n^\circ$ = 2840, R^* = 48 Mrad.

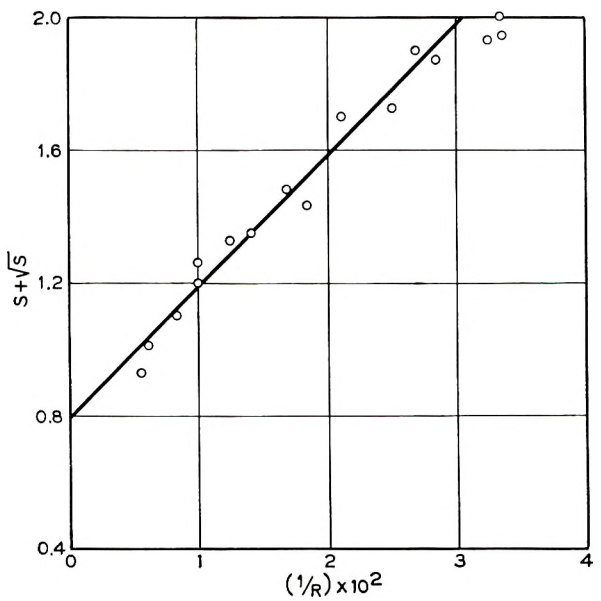

Fig. 4. Gel fraction of irradiated polypropylene.

viscosity is quite large (~40%) and is in fair agreement with calculations by Kilb.[7] However, these results cannot unequivocally distinguish between alternate theories[5,7] because the theoretical intrinsic viscosity of branched polymers is quite sensitive to the exponent in the relation between intrinsic viscosity and molecular weight. Moreover, solution measurements at doses approaching the gel point may be inaccurate if there are any traces of gel in the irradiated polymer.

Analogously, fractional increments in the number-average molecular weight of Carbowax 4000 were determined as a function of irradiation dose (Fig. 3). Again, similar results were ascertained for Carbowaxes 1540 and 6000. As predicted[7] for initially "random" polymers evidencing scission-to-crosslinking ratios of about 0.5, the number-average molecular weight is independent of dose.

For the polypropylene sample it was found that a treatment due to Charlesby[1] was applicable in that $(S + S^{1/2})$ (where S is the sol fraction of

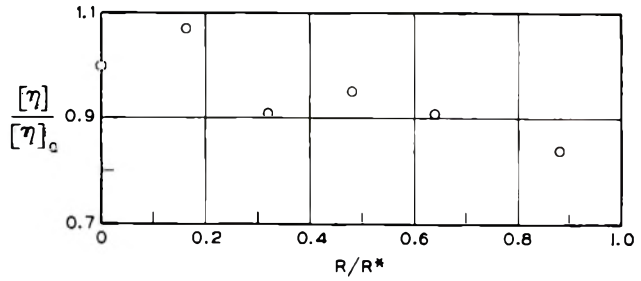

Fig. 5. Intrinsic viscosity of irradiated polypropylene; $[\eta]_0$ = 0.43 dl./g. at 30°C. in benzene, R^* = 30 Mrad.

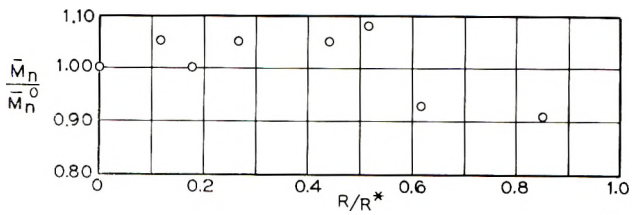

Fig. 6. Number-average molecular weight of irradiated polypropylene; $\bar{M}_n^\circ$ = 11,000, R^* = 30 Mrad.

the irradiated polymer) was directly proportional to the reciprocal irradiation dose (Fig. 4). Although this relation was developed for initially random polymers, it did not obtain for the Carbowaxes. It has been suggested[1] that even small deviations from a random distribution may lead to nonlinearity. That the treatment applies to the polypropylene, which is certainly not initially random (Table I), perhaps results from the higher incidence of scission in this polymer. The extrapolated value of $S + S^{1/2}$ to infinite dose corresponds to a scission-to-crosslinking ratio of 0.8 for polypropylene. In this treatment, all the gel fraction data were equally weighted to obtain the limiting gel fraction and the corresponding ratio of scission-to-crosslinking. However, in ordinary plots of the gel fraction versus dose (Fig. 1), the limiting gel fraction is preferentially influenced by the solubility behavior at high doses. The value of 0.8 for polypropylene is in good agreement with previous results derived from solubility measurements.[2]

The intrinsic viscosity of irradiated polypropylene is a gradually decreasing function of dose (Fig. 5) and has been previously observed.[2] This result is surprising in view of the scission-to-crosslinking ratio[7] of 0.8 and may reflect the nonrandom initial molecular weight distribution. This decrease in intrinsic viscosity was taken to indicate an initial degradation of the polymer.[2] However, measurements of the number-average molecular weight of the irradiated polymer at various doses (Fig. 6) evidence no initial degradation. We observe that, within experimental error, the number-average molecular weight is invariant with increasing dose, at least until quite close to the gel point.

It has been suggested that ratios of scission-to-crosslinking derived from gel fraction measurements are overestimates and may not correlate well with studies at low irradiation doses,[15] that is, studies of solubility behavior at high doses involve highly crosslinked polymers. Since branched materials evidence enhanced scission as compared to linear alkanes, then perhaps the relative importance of the scission reaction would be overemphasized by studies of highly crosslinked or branched materials. However, at least for polyethylene oxides, scission-to-crosslinking ratios derived at high doses correlate well with intrinsic viscosity and number-average molecular weight changes at low radiation doses.

CONCLUSIONS

The solubility behavior of electron-irradiated (*in vacuo*) polyethylene oxide indicates a ratio of main chain scission density to the density of crosslinked units of 0.6, indepedent of molecular weight. This value, derived from measurements at high doses, correlates well with the observed increase in intrinsic viscosity and invariance of number-average molecular weight at low irradiation doses.

Analogous measurements on polypropylene indicate a linear dependence of $S + S^{1/2}$ (where S is the sol fraction of the irradiated polymer) on the reciprocal irradiation dose. This treatment[1] leads to a ratio of scission-to-crosslinking of 0.8. Increased scission in polypropylene as compared to polyethylene oxide is evidenced by a gradual decrease in the intrinsic viscosity as a function of dose. This decrease is not indicative of an initial irradiation degradation of the polymer, because the number-average molecular weight is relatively unaffected by irradiation until quite close to the gel point. The intrinsic viscosity of the progressively crosslinked polymer is apparently depressed by branching. Direct comparison of the results on polypropylene with theory is uncertain because of a nonrandom initial molecular weight distribution.

It is reemphasized that the intrinsic viscosity is not a simple indication of molecular weight changes in crosslinking polymers.

The authors acknowledge with thanks the experimental assistance of J. V. Pascale in irradiation.

References

1. Charlesby, A., and S. H. Pinner, *Proc. Roy. Soc. (London)*, **A249,** 367 (1959).
2. Black, R. M., and B. J. Lyons, *Nature*, **180,** 1346 (1957); *Proc. Roy. Soc. (London)*, **A253,** 322 (1959).
3. Pearson, R. W., in *Radioisotopes in Scientific Research, Proc. 1st (UNESCO) Intern. Conf. Paris*, **1,** 151 (1957).
4. Dole, M., *J. Phys. Chem.*, **65,** 700 (1961).
5. Shultz, A. R., P. I. Roth, and G. B. Rathmann, *J. Polymer Sci.*, **22,** 495 (1956).
6. Zimm, B. H., and R. W. Kilb, *J. Polymer Sci.*, **37,** 19 (1959).
7. Kilb, R. W., *J. Phys. Chem.*, **63,** 1838 (1959).
8. Bailey, F. E., Jr., J. L. Kucera, and L. G. Imhof, *J. Polymer Sci.*, **32,** 517 (1958).
9. Barnes, W. J., W. G. Luetzel, and F. P. Price, *J. Phys. Chem.*, **65,** 1742 (1961).

10. Kinsinger, J. B., and R. E. Hughes, *J. Phys. Chem.*, **63**, 2002 (1959).
11. Salovey, R., and W. Rosenzweig, *J. Polymer Sci.*, **A1**, 2145 (1963).
12. Swallow, A. J., *Radiation Chemistry of Organic Compounds*, Pergamon Press, New York, 1960, p. 42.
13. Onyon, P. F., in *Techniques of Polymer Characterization*, Butterworths, London, 1959, p. 171.
14. Brady, A. P., H. Huff, and J. W. McBain, *J. Phys. Colloid Chem.*, **55**, 304 (1951).
15. Chapiro, A., *Radiation Chemistry of Polymeric Systems*, Interscience, New York–London, 1962.
16. Flory, P. J., *Principles of Polymer Chemistry*, Cornell Univ. Press, Ithaca, N. Y., 1953, p. 313.

Résumé

Le comportement de la solubilité de l'oxyde de polyéthylène irradié par des électrons (sous vide) indique un rapport de densité de scission de chaîne principale par rapport à la densité d'unités pontées de 0.6, indépendant du poids moléculaire. Cette valeur, dérivée de mesures à des doses élevées, correspond bien à l'augmentation observée de la viscosité intrinsèque et à l'invariance du poids moléculaire moyen en nombre aux doses d'irradiation basses. Des measures analogues sur le polypropylène indiquent une dépendance linéaire de $S + \alpha S^{1/2}$ (où S est la fraction sol du polymère irradié) sur l'inverse de la dose d'irradiation. Cette manière d'agir mène à un rapport de scission pour le pontage à 0.8. L'augmentation de la scission dans le polypropylène comparée à l'oxyde de polyéthylène est mise en évidence par une décroissance graduelle de la viscosité intrinsèque en fonction de la dose. Cette décroissance n'indique pas une dégradation initiale par irradiation du polymère parce que le poids moléculaire moyen en nombre n'est relativement pas affecté par l'irradiation jusqu'au point de gel. La viscosité intrinsèque du polymère progressivement ponté est apparement abaissée par ramification. Une comparaison directe des résultats avec la théorie est incertaine à cause de la distribution non-statistique du poids moléculaire initial. On réinsiste encore sur le fait que la viscosité intrinsèque ne constitute pas une mesure simple du changement du poids moléculaire dans les polymères pontés.

Zusammenfassung

Das Löslichkeitsverhalten von elektronen-bestrahltem Polyäthylenoxyd (im Vakuum) führt zu einem molekulargewichts-unabhängigen Verhältnis von Hauptkettenspaltungsdichte zu Vernetzungsdichte von 0,6. Dieser, aus Messungen bei hoher Dosis abgeleitete Wert stimmt gut mit der beobachteten Viskositätszunahme und der Invarianz des Zahlenmittels des Molekulargewichts bei niedriger Bestrahlungsdosis überein. Analoge Messungen an Polypropylen zeigen eine lineare Abhängigkeit von $S + S^{1/2}$ (wo S der Solanteil des bestrahlten Polymeren ist) vom Reziprokwert der Bestrahlungsdosis. Die Berechnung ergibt ein Spaltungs-Vernetzungsverhältnis von 0,8. Die Zunahme der Spaltung bei Polypropylen im Vergleich zu Polyäthylenoxyd wird durch eine stetige Abnahme der Viskositätszahl als Funktion der Dosis bestätigt. Diese Abnahme ist nicht auf einen anfänglichen Strahlungsabbau des Polymeren zurückzuführen, da der Zahlenmittelwert des Molekulargewichts durch die Bestrahlung bis ganz nahe zum Gelpunkt verhältnismässig wenig beeinflusst wird. Die Viskositätszahl des zunehmend vernetzten Polymeren wird offenbar durch Verzweigung herabgesetzt. Ein direkter Vergleich der Ergebnisse am Polypropylen mit der Theorie ist wegen der nichtstatistischen Natur der Ausgangsmolekulargewichtsverteilung schwierig. Es wird erneut betont, dass die Viskositätszahl kein einfaches Mass für Molekulargewichtsänderungen in vernetzungsfähigen Polymeren bildet.

Received October 2, 1962

JOURNAL OF POLYMER SCIENCE: PART A VOL. 1, PP. 2163–2169 (1963)

Relative Reactivity Ratios for Two New 2-Chloro-1,3-Butadiene Systems

G. S. WICH and N. BRODOWAY, *E. I. du Pont de Nemours and Company, Inc., Elastomer Chemicals Department, Wilmington, Delaware*

Synopsis

The relative reactivity ratios in free-radical, emulsion copolymerizations for the systems 2-chloro-1,3-butadiene/methyl isopropenyl ketone and 2-chloro-1,3-butadiene/methacrylic acid were found to be 3.6 and 0.1 and 2.68 and 0.15, respectively. Consequently, copolymers are formed substantially richer in 2-chloro-1,3-butadiene units than the comonomer feed, have little alternation tendency, and do not form azeotropes. Distributions of monomer units in the copolymers are described.

INTRODUCTION

The high relative reactivity of 2-chloro-1,3-butadiene in free-radical copolymerization with other dienes or activated olefins has been reported in both oil phase and emulsion systems.[1,2] This paper describes the measurement of the relative reactivity ratios of 2-chloro-1,3-butadiene/methyl isopropenyl ketone and 2-chloro-1,3-butadiene/methacrylic acid monomer mixtures.

EXPERIMENTAL MATERIALS AND METHODS

Monomers

The 2-chloro-1,3-butadiene (chloroprene) was distilled from a 50% mixture with xylene (b.p. 59°C., n_D^{20} 1.4578) and stored under nitrogen below −20°C. without stabilization. The active oxygen content at reaction time was 10–20 ppm. The methyl isopropenyl ketone (MIPK) was freed from stabilizer and dimer by distillation. The fraction boiling at 29°C. (50 mm. Hg) was collected and stored below −20°C. Glacial methacrylic acid stabilized with 0.025% of *p*-methoxyphenol was employed without distillation. Analyses for carboxyl groups and unsaturation were made by titrating with standard solutions of base and bromine.

Apparatus

Polymerizations were carried out in four-necked round-bottomed flasks fitted with agitators, thermometers, nitrogen inlets, burets, and hydrometer holders. The conversions were followed by measuring the changes in specific gravities with hydrometers calibrated in thousandths of a point.

Polymerizations

All operations were carried out under nitrogen and the distilled water was purged with nitrogen before emulsification. Emulsion recipes employed are given in Table I. Since the methacrylate anion has been shown to be much less reactive in polymerization than the undissociated methacrylic acid,[3] the emulsion system for copolymerization of methacrylic acid was maintained at a pH of 2.5 or lower to keep the acid undissociated.

TABLE I
Emulsion Recipes

Material	Parts per hundred of monomer	
	A	B
2-Chloro-1,3-butadiene	$100 - x$	$100 - x$
Methyl isopropenyl ketone	x	—
Methacrylic acid	—	x
tert-Dodecyl mercaptan	1.5	—
Oleic acid	4.0	—
Distilled water	150	150
Lomar PW[a]	4.0	—
Sodium hydroxide	1.076	—
Ultrawet K[b]	—	2.0

[a] Sodium sulfonate of a naphthalene–formaldehyde condensation product supplied by Jacques Wolf.

[b] An alkylbenzene sodium sulfonate supplied by the Atlantic Refining Company.

Polymerizations were initiated at 40°C. by careful addition of a 5% solution of potassium persulfate. The internal temperature was maintained at 40 ± 0.5°C. by external cooling. As soon as the specific gravity rose at least 0.003 point, the copolymerizations were arrested by pouring the entire emulsion into methanol containing a trace of a polymerization inhibitor such as phenothiazine.

Purification of Analytical Samples

Copolymers of 2-chloro-1,3-butadiene and methyl isopropenyl ketone were purified by repeated extractions with acetone. Similar treatment of a polychloroprene control yielded a reference value of 39.4% chlorine. Copolymers of 2-chloro-1,3-butadiene and methacrylic acid were purified by double precipitation from tetrahydrofuran solutions, water being used as the nonsolvent. The copolymers were dried at room temperature *in vacuo*.

DISCUSSION OF RESULTS

Determination of Relative Reactivity Ratios

The usual assumptions have been employed concerning the kinetic chain length, the existence of a steady state, and the constancy of monomer feed

composition at low conversion.[4] Furthermore, the presence of mercaptan modifier was assumed not to affect the relative reactivities.

Fineman and Ross[5] have derived the following expression which permits straightforward calculation of relative reactivity ratios r_1 and r_2 from copolymerization data:

$$\frac{f_1(1 - 2F_1)}{(1 - f_1)F_1} = r_2 + \left[\frac{f_1^2(F_1 - 1)}{(1 - f_1)^2F_1}\right] r_1 \qquad (1)$$

where f_1 denotes the mole fraction of unreacted monomer M_1 in the feed and F_1 denotes the mole fraction of M_1 monomer units in the increment of copolymer formed at the initial stage of copolymerization.

Each value of f_1 was taken to be the mole fraction of 2-chloro-1,3-butadiene in the initial monomer feed mixture. Each value of F_1 was obtained by analysis of the copolymer for chlorine. The copolymer composition data for emulsion-copolymerized 2-chloro-1,3-butadiene and methyl isopropenyl ketone are given in Table II. These data employed in eq. (1) yielded the straight line plot in Figure 1. The slope of the line is 3.6 and represents r_1 (M_1 = 2-chloro-1,3-butadiene). The intercept at the y axis gives r_2 (M_2 = methyl isopropenyl ketone) = 0.1.

The corresponding copolymer composition data for the emulsion copolymerization of 2-chloro-1,3-butadiene and methacrylic acid are contained in

TABLE II

Dependence of Copolymer Composition on Monomer Feed for the 2-Chloro-1,3-Butadiene/Methyl Isopropenyl Ketone System

Conversion, %	Chlorine in copolymer, %	Mole fraction of 2-chloro-1,3-butadiene	
		Feed (f_1)	Copolymer (F_1)
—	39.4	1.00	1.00
5.3	36.2	0.74	0.92
7.9	35.7	0.69	0.90
4.7	34.3	0.59	0.86
9.2	31.9	0.49	0.80
8.5	29.9	0.39	0.75
13.3	20.5	0.19	0.51

TABLE III

Dependence of Copolymer Composition on Monomer Feed for the 2-Chloro-1,3-Butadiene Methacrylic Acid System

Conversion, %	Chlorine in copolymer, %	Mole fraction of 2-chloro-1,3-butadiene	
		Feed (f_1)	Copolymer (F_1)
5.07	38.4	0.898	0.958
3.48	36.8	0.795	0.918
1.21	34.7	0.694	0.865
3.25	33.2	0.587	0.826
3.72	27.4	0.393	0.681

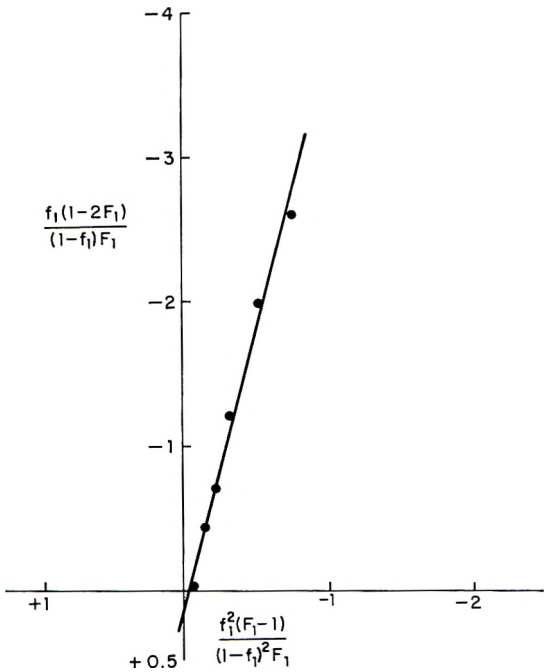

Fig. 1. Relative reactivity plot for 2-chloro-1,3-butadiene/methyl isopropeny. ketone copolymerization. Slope = r_1 = 3.6 ± 0.2, y axis intercept = r_2 = 0.1 ± 0.05

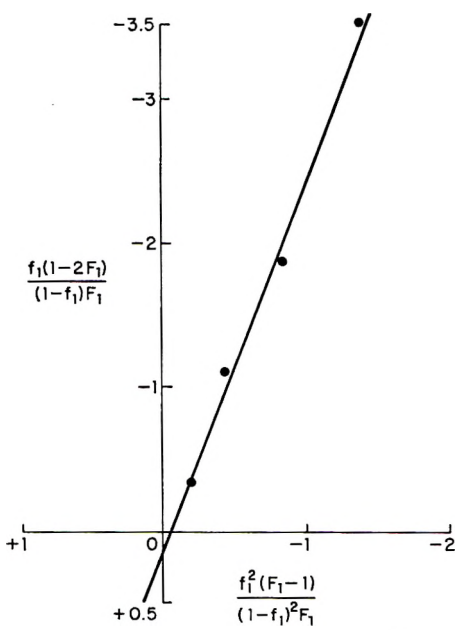

Fig. 2. Relative reactivity plot for 2-chloro-1,3-butadiene/methacrylic acid copolymerization. Slope = r_1 = 2.7 ± 0.2, y axis intercept = r_2 = 0.15 ± 0.05.

Table III. When employed in eq. 1, the above data yielded the straight line plot shown in Figure 2. From the slope r_1 is 2.7 (2-chloro-1,3-butadiene) and from the intercept at the y axis r_2 is 0.15 (methacrylic acid).

Detailed Structure of Copolymer Chains

In both cases the copolymers were formed relatively richer in 2-chloro-1,3-butadiene than the comonomer feed. This is a consequence of the preference of both 2-chloro-1,3-butadiene radical ($m_1\cdot$) and methyl isopropenyl ketone or methacrylic acid radical ($m_2\cdot$) for 2-chloro-1,3-butadiene (M_1) monomer. The arrangements of the monomer units in the copolymers are also similar. Copolymerization azeotropes are unlikely since both r_1 and r_2 are not greater than unity or less than unity. The alternation tendency is small since r_1 and r_2 are not simultaneously close to zero.

The distributions of the sequence lengths of 2-chloro-1,3-butadiene and methyl isopropenyl ketone or methacrylic acid units were calculated by known methods[6] for copolymers prepared from equimolar monomer mixtures. These are shown in Tables IV and V.

TABLE IV
Distribution of Sequence Lengths in Copolymer From Equimolar Monomer Mixture (2-Chloro-1,3-Butadiene/Methyl Isopropenyl Ketone)

Units per sequence	% of 2-Chloro-1,3-butadiene sequences	% of MIPK sequences
1	21.8	90.9
2	17.1	8.26
3	13.3	0.75
4	10.4	0.068
5	8.2	0.0962
>5	29.2	0.0158

TABLE V
Distribution of Sequence Lengths in Copolymer From Equimolar Monomer Mixture (2-Chloro-1,3-Butadiene/Methacrylic Acid)

Units per sequence	% of 2-chloro-1,3-butadiene sequences	% of methacrylic acid sequences
1	27.2	87.0
2	19.8	11.3
3	14.4	1.48
4	10.5	0.19
5	7.6	0.025
>5	20.5	0.005

Less than 1% of the methyl isopropenyl ketone sequences contain more than two monomer units, whereas over 60% of the 2-chloro-1,3-butadiene sequences contain more than two monomer units. Similarly, only 1.7% of the methacrylic acid sequences contain more than two monomer units,

whereas 53% of the 2-chloro-1,3-butadiene sequences contain more than two monomer units. Thus both copolymers are elastomers resembling in properties the homopolymer of 2-chloro-1,3-butadiene.

Infrared spectra confirm that 2-chloro-1,3-butadiene units in the copolymers are present in all possible modes of addition, and that these structures are present in the same ratio as in the homopolymer prepared at the same temperature.

Comparison with Other 2-Chloro-1,3-butadiene Copolymerizations

The relative reactivities obtained show the same high reactivity for 2-chloro-1,3-butadiene as do previously reported copolymerizations shown in Table VI. Alternation is reported only with the highly polar vinylidene cyanide.[11]

TABLE VI
Relative Reactivity Ratios with 2-Chloro-1,3-butadiene (M_1)

Comonomer (M_2)	r_1	r_2	Reference
Styrene	6.3 ± 0.1	0.00	1
Styrene	7 ± 2	0.05 ± 0.02	7
Styrene	8.11 ± 0.34	0.053 ± 0.005	8
Butadiene	3.41 ± 0.07	0.059 ± 0.015	1
Isoprene	3.65 ± 0.11	0.133 ± 0.025	1
Acrylonitrile	6.07 ± 0.53	0.01 ± 0.1	1
Acrylonitrile	5.35 ± 0.2	0.045 ± 0.004	8
Methyl methacrylate	6.12 ± 0.2	0.08 ± 0.007	8
Methyl acrylate	11.1 ± 1.5	0.078 ± 0.01	8
1,1-Diphenylethylene	3.2 ± 0.2	0.0 ± 0.05	8
Isopropyl vinyl ether	11.45	0.164	9
Vinylpyridine	5.195	0.064	10
Vinylquinoline	2.1	0.38	10
Diethyl fumarate	6.65 ± 0.37	0.027 ± 0.009	8
Vinylidene cyanide	0.016	0.0048	11
Vinyl formate	30	0.01	13

The Q and e values for 2-chloro-1,3-butadiene, based on its copolymerization with butadiene,[1] are calculated to be 8.07 and 0.46, respectively. The reported Q and e values for methacrylic acid[12] are 2.0 and 0.7, respectively. Based on the copolymerization of vinylidene chloride and methyl isopropenyl ketone,[12] the Q and e values for methyl isopropenyl ketone are 1.95 and 1.23, respectively. Thus, the calculated relative reactivities for 2-chloro-1,3-butadiene/methacrylic acid are 4.5 and 0.21, and for 2-chloro-1,3-butadiene/methyl isopropenyl ketone are 5.9 and 0.094, in fair agreement with the experimental values.

The high Q value of 2-chloro-1,3-butadiene indicates the strong tendency of the monomer to add to radicals. The relatively neutral e value permits the radical to react with only small alternating tendencies with both electron-releasing and electron-attracting substituents in the comonomer.

References

1. Simha, R., and L. A. Wall, *J. Res. Natl. Bur. Std.*, **41**, 521 (1948).
2. Mayo, F. R., and C. Walling, *Chem. Revs.*, **46**, 191 (1950).
3. Katchalsky, A., and G. Blauer, *Trans. Faraday Soc.*, **47**, 1360 (1951).
4. Flory, P. J., *Principles of Polymer Chemistry*, Cornell Univ. Press, Ithaca, N. Y., 1953, pp. 178–199.
5. Fineman, M., and S. D. Ross, *J. Polymer Sci.*, **5**, 259 (1950).
6. Alfrey, T., Jr., J. J. Bohrer, and H. Mark, *Copolymerization*, Interscience, New York, 1952, pp. 133–145.
7. Alfrey, T., Jr., A. I. Goldberg, and W. P. Hohenstein, *J. Am. Chem. Soc.*, **68**, 2464 (1946).
8. Doak, K. W., and D. L. Dineen, *J. Am. Chem. Soc.*, **73**, 1084 (1951).
9. Mitsengendler, S. P., V. N. Krasulina, and L. B. Trukhmanova, *Izv. Akad. Nauk SSSR, Otdel. Khim. Nauk*, **1956**, 1120.
10. Koton, M. M., and O. K. Surnina, *Dokl. Akad. Nauk SSSR*, **113**, 1063 (1957); also M. M. Koton, *J. Polymer Sci.*, **30**, 331 (1958).
11. Gilbert, H., F. F. Miller, S. J. Averill, E. J. Carlson, V. L. Folt, H. J. Heller, F. D. Stewart, R. F. Schmidt, and H. L. Trumbull, *J. Am. Chem. Soc.*, **78**, 1669 (1956).
12. Chapin, E. C., G. E. Ham, and C. L. Mills, *J. Polymer Sci.*, **4**, 597 (1949).
13. Ushako, S. N., and L. B. Trukhmanova, *Izv. Akad. Nauk SSSR, Otdel. Khim. Nauk*, **1957**, 980.

Résumé

On a étudié les rapports de réactivité relative des systèmes 2-chloro-1,3-butadiène-méthylisopropénylcétone et 2-chloro-1,3-butadiène acide méthacrylique au cours de leur copolymérisation en émulsion en présence de radicaux libres. Ces valeurs s'élèvent respectivement á 3.6 et 0.1, et 2.7 et 0.15. Par conséquent, les copolymères formés sont considérablement enrichis en unités de 2-chloro-1,3-butadiène comparés au mélange des comonomères de départ. Il y a peu de tendance á l'alternance et aucun azéotrope n'est formé. On a donné des détails sur la distribution des unités de monomères au sein des copolymères.

Zusammenfassung

Die relativen Reaktivitätsverhältnisse für die radikalische Emulsionscopolymerisation der Paare 2-Chlor-1,3-butadiene-Methylisopropenylketon und 2-Chlor-1,3-butadien-Methacrylsäure wurden zu 3,6 und 0,1 bzw. 2,7 und 0,15 bestimmt. Demzufolge enthalten die Copolymeren wesentlich mehr 2-Chlor-1,3-butadien-Einheiten als die vorgegebene Monomermischung, zeigen geringe Alternationstendenz und bilden kein Azeotrop. Die Verteilung der Monomereinheiten in den Copolymeren wird beschrieben.

Received July 30, 1962
Revised November 30, 1962

JOURNAL OF POLYMER SCIENCE: PART A VOL. 1, PP. 2171–2178 (1963)

Anionic Block Polymerization. I. Block Polymerization of Styrene on Polystyrene

M. BAER, *Monsanto Chemical Company, Plastics Division, Springfield, Massachusetts*

Synopsis

Anionic block polymerization of styrene onto polystyrene anions was found to be a useful diagnostic method which can readily reveal when the chosen polymerization conditions are conducive to complete catalyst consumption and quantitative block polymerization. With Na-naphthalene as initiator, it was shown that under the proper polymerization conditions (*a*) the initiator is essentially completely consumed in the first polymerization step, thus avoiding initiation of new chains in the following polymerization steps, (*b*) in each block polymerization step, styrene adds quantitatively to the preformed live anions, and (c) essentially no termination is observed throughout the successive block polymerization steps. The ratio of monomer to initiator greatly affects the efficiency of initiator consumption. The rate of agitation is also considered to play a dominant role.

INTRODUCTION

In very recent years, several publications[1–6] have appeared dealing with the preparation of block copolymers by means of anionic polymerization initiated by Na-naphthalene. The block copolymers, as prepared, are in many cases contaminated by large amounts of homopolymers and are far from homogeneous in composition.

The purpose of the present work was to find polymerization conditions which would result in block copolymers of sufficient purity to justify their use for mechanical properties studies. Block polymers of known composition, molecular weight, and essentially free from contaminating homopolymers were desired.

Repeated block polymerization of styrene onto polystyrene was chosen as the diagnostic method to define polymerization conditions conducive to complete initiator consumption and quantitative block polymerization. Graham et al.[3,4] have recently demonstrated that styrene can be quantitatively block polymerized with only moderate termination.

RESULTS AND DISCUSSION

In order to prepare pure block copolymers the following two requirements must be met: (*1*) the polymeric dianions must not be destroyed to any large extent during the course of block polymerization, (*2*) essentially no residual

initiator must contaminate the preformed polymeric dianion; this guarantees that on addition of the second monomer, growth takes place only on the preformed polymeric dianions without contamination by homopolymers arising through initiation of new chains by residual initiator.

To prove that new polymer chains are not initiated during block polymerization, the following conditions (similarly treated by Graham et al. [3,4]) must be satisfied. First we define $W_{(n)}$ = the total weight in grams of polymer n prior to monomer addition $(n + 1)$; $W_{(n+1)}$ = the total weight in grams of polymer following addition and polymerization of monomer $(n + 1)$; $\bar{M}_{n_{(n)}}$ = number-average molecular weight of polymer n prior to monomer addition $(n + 1)$; $\bar{M}_{n_{(n+1)}}$ = number-average molecular weight of polymer following addition and polymerization of the monomer $(n + 1)$. Then, if new chains are not formed during polymerization of the subsequent monomer:

$$W_{(n+1)}/W_{(n)} = \bar{M}_{n_{(n+1)}}/\bar{M}_{n_{(n)}} \tag{1}$$

but if new chains are formed,

$$W_{(n+1)}/W_{(n)} > \bar{M}_{n_{(n+1)}}/\bar{M}_{n_{(n)}} \tag{2}$$

Equation (1) holds true independently of the number of chains terminated in the preformed polymer or during block polymerization of the subsequent monomer as long as some "live" chains remain present and are available for polymerization at all times. Information on the degree of termination and degree of polydispersity was gained in our work by taking advantage of the fact that $\bar{M}_v$ magnifies the effect of the higher molecular weight fractions. The relation,

$$W_{(n+1)}/W_{(n)} < \bar{M}_{v_{(n+1)}}/\bar{M}_{v_{(n)}} \tag{3}$$

occurs in cases where some of the chains grow to proportionately greater size either because of poor uniformity of mixing during the addition of monomer to the preformed polymer, or because of termination of a fraction of the live chains. The relation,

$$W_{(n+1)}/W_{(n)} > \bar{M}_{v_{(n+1)}}/\bar{M}_{v_{(n)}} \tag{4}$$

is expected because of formation of new chains, due to unconsumed initiator, or because the preformed polymer is of poor molecular weight uniformity and contains a large fraction of live low molecular weight polymer.

In Table I it is shown that for each styrene block polymerization step, the $\bar{M}_v$ ratios are very close to the polymer weight ratios (W). In addition, since the ratio $\bar{M}_v/\bar{M}_n$ also remains constant throughout the various block polymerization steps, it follows that $\bar{M}_n$ ratios must also be equal to the W ratios, thus fulfilling the requirements of eq. (1) for proof that new chains are not formed during polymerization.

TABLE I

Block Polymerization of Styrene Monomer on Polystyrene Anions at Initial [M]/[I] = 230; $\bar{M}_{nk} = 4.8 \times 10^4$ with Na-Naphthalene as Initiator

Styrene addition step	Temp., °C.	Conversion, %	$\bar{M}_v \times 10^{-5}$	$\bar{M}_n \times 10^{-5}$	$W_{(n+1)}/W_{(n)}$	$\bar{M}_{v(n+1)}/\bar{M}_{v(n)}$	$\bar{M}_v/\bar{M}_n$
1	−60	100	0.86	0.68			1.26
2	−56	100.1	1.8		2.03	2.09	
3	−50	100.3	2.8	2.22	1.56	1.55	1.26
4	−35	100.3	3.7		1.36	1.32	
5	−5	98	4.5	3.5	1.27	1.22	1.28

The fact that the $\bar{M}_v$ ratios remain close to the W ratios throughout the various steps also suggests that extensive termination of live chains at any particular step has not occurred.

The same results are observed in Table II except for the fact that a very small amount of water was introduced just prior to styrene addition step 3. This, as contemplated under eq. (3), resulted in a drastic increase of the $\bar{M}_v$ ratio over the W ratio.

TABLE II

Block Polymerization of Styrene Monomer on Polystyrene Anions at Initial [M]/[I] = 264; $\bar{M}_{nk} = 5.5 \times 10^4$; with Na-Naphthalene as Initiator

Styrene addition step	Temp., °C.	Conversion, %	$\bar{M}_v \times 10^{-5}$	$W_{(n+1)}/W_{(n)}$	$\bar{M}_{v(n+1)}/\bar{M}_{v(n)}$
1	−59	100	0.68		
2	−60	98	1.37	2.06	2.02
3[a]	−55	96	2.65	1.54	1.90[a]
4	−20	105	3.6	1.36	1.38
5	+3	98	4.5	1.22	1.25

[a] Small amount of water added during monomer addition.

The effect of the monomer/initiator ([M]/[I]) ratio on the completeness of initiator consumption can be established by comparing Table III with Tables I and II, where the polymerization conditions and intensity of agitation used were identical. While essentially complete consumption of initiator, as shown by W ratios being equal to $\bar{M}_v$ ratios, is obtained with [M]/[I] values of 230–264, [M]/[I] values of around 100 result in $\bar{M}_v$ ratios considerably lower than the W ratios. As discussed under eq. (4), this shows incomplete consumption of initiator or formation of a large fraction of live low molecular weight polymer. At the lower [M]/[I] ratios the intensity of agitation used is no longer sufficient to give adequate mixing and to produce pure block polymers.

TABLE III
Block Polymerization of Styrene Monomer on Polystyrene Anions with Na-Naphthalene as Initiator

Run no.	Styrene addition step	Temp., °C.	[M]/[I]	Conversion, %	$\bar{M}_{nk} \times 10^{-4}$	$\bar{M}_v \times 10^{-4}$	$W_{(n+1)}/W_{(n)}$	$\bar{M}_{v(n+1)}/\bar{M}_{v(n)}$
6	1	−60	99	98.5	2.05	5.4		
	2	−55		105		9.8	2.06	1.81
	3	−40		98		11	1.51	1.12
	4	−30		98		15	1.29	1.36
3	1	−65	101	96	2.10	6.8		
	2	−65		98		10.0	2.08	1.47
	3	−65		98		13.5	1.56	1.35

The fraction f of initiator consumed was shown by Levy and Szwarc[7] to be always less than one and was calculated to decrease with decreasing ratio of [M]/[I] and increasing k_p/k_i ratio. Their calculated values for f are only valid, however, if one assumes instantaneous mixing with resulting homogeneous concentration of the monomer in the batch throughout the course of monomer addition to the initiator solution. In practice, where the time required for mixing is considerably greater than the half-lifetime of the reaction, the rate of monomer addition, and the rate of mixing play a dominant role.

The discrepancy between the kinetic number-average molecular weight, $\bar{M}_{nk}$, and $\bar{M}_n$ of Table I, which was also observed by other authors[8-10] in their work, cannot be easily explained. Data of Table I show that it cannot be attributed to unconsumed initiator. The discrepancy may be due to the fact that the Na-naphthalene titer, based on total basicity, titrates other soluble basic impurities in addition to Na-naphthalene. During the preparation of the initiator, in fact, some dihydronaphthalene is undoubtedly formed through reaction with impurities or by proton abstraction from the solvent. Reaction of dihydronaphthalene with the Na-naphthalene adduct during catalyst preparation would result in a dihydronaphthalene anion which may not be sufficiently basic to initiate styrene polymerization. Its presence would not be distinguished from Na-naphthalene by titration of total basicity, nor by any titrations with alkyl halides. Its red or brown color becomes apparent only when Na-naphthalene is stored at room temperature for a prolonged period of time.

EXPERIMENTAL

Materials

Styrene and α-methylstyrene were stored over calcium hydride, fractionally distilled under nitrogen at reduced pressure, and redistilled twice at 10^{-4} cm. Hg, first from calcium hydride and sodium wire, and second,

from a sodium mirror. The monomers were collected into calibrated ampules constructed with a side arm sealed by a glass break-off tip. After distilling in an equal volume of solvent, the ampules were sealed, stored at −60°C., and used within two days.

Nitrogen (Air Reduction Co., prepurified) was purified by passing through successive columns containing reduced copper and molecular sieves and finally by scrubbing through a solution of disodium benzophenone ketyl in a high boiling ether (tetraethylene glycol dimethyl ether).

1,2-Dimethoxyethane (Ansul Chemical Co., Ether 121), after drying over calcium sulfate was refluxed in the presence of benzophenone and a large excess of sodium ribbon until the characteristic blue color of the monosodium ketyl persisted. The solvent was distilled twice (the second time from the purple disodium benzophenone ketyl) and stored under nitrogen. The solvent was finally distilled *in vacuo*, from a flask attached to the vacuum manifold, directly into the desired receivers.

The apparatus for catalyst preparation was connected to the vacuum manifold and consisted of two 300-ml. flasks interconnected by means of a fine fritted glass filter. The equipment was carefully flamed under vacuum and cooled under nitrogen before use.

Na-naphthalene was prepared by distilling into the apparatus dimethoxyethane (100 ml.), dissolving recrystallized naphthalene (1.0 g.) in the solvent, and adding an excess of clean sodium under a nitrogen atmosphere. The green color of Na-naphthalene formed immediately on agitation with a magnetic bar. After 1–2 hr. of agitation at about 5°C., the solution reached the theoretical titer of 0.078 mole/l. and was filtered into the receiving flask under nitrogen pressure.

Freshly prepared catalyst, stored at 5°C., was used in this work. If the catalyst solution is stored for hours at room temperature, one observes a change in color from deep green to a brown-green which must result from attack on the solvent by the initiator. If excess sodium is not removed by filtration, the titer of the solution increases with time to a value considerably larger than the theoretical value for the mono-sodium adduct. Reactions of Na-naphthalene with solvent or proton donating impurities result in the formation of sodium salts, dihydronaphthalene, and regenerated naphthalene,[11,12] which in turn reacts further with the excess sodium to give a high titer for total basicity.

In this work the amount of base in an aliquot, determined by titration with 0.1*N* H_2SO_4, was assumed to be a direct measure of its Na-naphthalene content.

Polymerization

Equipment. The equipment used in polymerization is shown in Figure 1. Flask 1, a one-liter flask, is used for solvent distillation. Flask 2 is a graduated one-liter flask. Flask 3, the reactor, has a one-liter capacity and is connected to a thermowell, to the vacuum manifold, to the syphon extend-

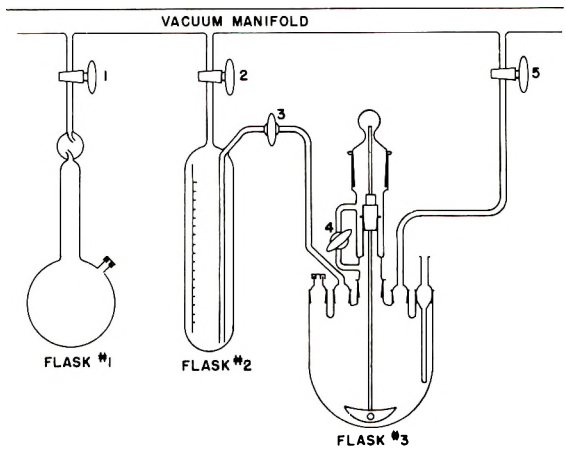

Fig. 1. Distillation flasks and polymerization equipment.

ing from flask 2, and to an adapter sealed with a serum stopper (tightly compressed inside the adapter). The center neck is connected with a stirrer assembly which is capped with a glass stopper; this permits drying and evacuation of the reactor without danger of leaks through the stirrer gland and without need for stirrer shaft removal. The stirrer, furnished with a $2^1/_2$-in. blade, was rotated at the measured speed of 1500 rpm.

Hypodermic syringes were used for charging monomers, initiator, and for withdrawing samples through the serum stopper. The syringes and needles were carefully dried at 150°C. and nitrogen-purged before use.

Procedure. All parts of the equipment were thoroughly dried by flaming and by maintaining a vacuum of 10^{-4} cm. Hg, or better, for several hours.

The degassed pure solvent was distilled under vacuum into flask 2 and syphoned into the evacuated reactor. The vacuum was released with pure nitrogen and a constant nitrogen pressure of 1 cm. Hg was maintained on the reactor. The solvent in the reactor was titrated by dropwise addition of the initiator solution (normally less than 0.1 ml. of a 0.08*M* catalyst solution was consumed) and the desired amount of initiator was introduced.

The monomer solution was injected into the batch agitated at a set speed of 1500 rpm. After 10–15 min. an aliquot of the polymer solution was withdrawn. The same operation was performed at each successive monomer addition. At the completion of the run, the "live" polymer anions were terminated by syringing in 1.0 ml. of degassed methanol followed by 1.0 ml. of glacial acetic acid.

Aliquots of the polymerization batch were withdrawn with a syringe and discharged through a serum stopper into a preweighed flask containing 1.0 ml. of methanol. The amount of polymer in the weighed aliquot was obtained by diluting the sample with solvent, precipitating in methanol, filtering, and weighing the polymer dried to constant weight.

Molecular Weights

Number-average molecular weights were obtained at 30°C. in toluene with a modified Fuoss-Mead osmometer. A No. 600 gel cellophane membrane was used.

Viscosity-average molecular weights of polystyrene were obtained in toluene at 25°C. by using the relation:[13]

$$[\eta] = 5.74 \times 10^{-5} M^{0.78}$$

The writer wishes to thank Dr. M. Ezrin for osmotic molecular weight determinations, and Dr. R. Buchdahl, Dr. J. D. Cotman, Jr., and Dr. M. J. Vignale for helpful discussions and suggestions.

References

1. Champetier, G., M. Fontanille, and P. Sigwalt, *Compt. rend.*, **250**, 3653 (1960).
2. Leng, M., and P. Rempp, *Compt. rend.*, **250**, 2720 (1960).
3. Graham, R. K., D. L. Dunkelberger, and E. S. Cohn, *J. Polymer Sci.*, **42**, 501 (1960).
4. Graham, R. K., J. R. Panchak, and M. J. Kampf, *J. Polymer Sci.*, **44**, 411 (1960).
5. Szwarc, M., M. Levy, and R. Milkovich, *J. Am. Chem. Soc.*, **78**, 2656 (1956).
6. Szwarc, M., and A. Rembaum, *J. Polymer Sci.*, **22**, 189 (1956).
7. Levy, M., and M. Szwarc, *J. Am. Chem. Soc.*, **82**, 521 (1960).
8. Wenger, F., paper presented at the 138th Meeting of the American Chemical Society, New York, September 1960; *Meeting Abstracts*, p. 22T.
9. Wenger, F., *Makromol. Chem.*, **36**, 200 (1960).
10. Lyssy, T., *Helv. Chim. Acta*, **42**, 2245 (1959).
11. Scott, N. D., J. F. Walker, and V. L. Hansley, *J. Am. Chem. Soc.*, **58**, 2442 (1936).
12. Paul, D. E., D. Lipkin, and S. I. Weissman, *J. Am. Chem. Soc.*, **78**, 116 (1956).
13. Trementozzi, Q. A., *J. Phys. Colloid Chem.*, **54**, 1227 (1950).

Résumé

On a trouvé que la polymérisation anionique séquencée du styrène, sur des anions de polystyrène est une méthode utile d'investigation qui est à même de révéler immédiatement si les conditions de polymérisation choisies peuvent mener à une consommation entière du catalyseur et une polymérisation séquencée quantitative. On a démontré que dans les conditions caractéristiques de la polymérisation par initiation au sodium-naphtalène (*a*) l'initiateur est entièrement consommé, essentiellement dans la première étape de la polymérisation, évitant ainsi l'initiation de chaînes nouvelles dans les étapes suivantes. (*b*) Dans chaque étape de la polymérisation séquencée le styrène est fixé quantitativement aux anions formés antérieurement, et (*c*) partiquement aucune terminaison n'est observée pendant les étapes successives de la polymérisation séquencée. Le rapport du monomère à l'initiateur affecte grandement l'efficacité de la consommation de l'initiateur. On estime que la vitesse de l'agitation joue également un rôle prépondérant.

Zusammenfassung

Anionische Blockpolymerisation von Styrol auf Polystyrolanionen erwies sich als diagnostische Methode zur einfachen Feststellung, ob bestimmte Polymerisationsbedingungen zum vollständigen Katalystatorverbrauch und zur quantitativen Blockpolymerisation führen, als brauchbar. Mit Na-Naphthalin als Starter liess sich zeigen, dass unter geeigneten Polymerisationsbedingungen (*a*) der Starter in der ersten Poly-

merisationsstufe vollständig verbraucht und daher der Start neuer Ketten in den folgenden Polymerisationsstufen vermieden wird, (*b*) in jeder Blockpolymerisationsstufe Styrol sich quantitativ an die vorgebildeten "lebenden" Anionen addiert und (c) im wesentlichen in den sämtlichen aufeinanderfolgenden Blockpolymerisationsstufen kein Abbruch auftritt. Das Verhältnis von Monomerem zu Starter hat grossen Einfluss auf die Ausbeute beim Starterumsatz. Ebenso wird der Vermischungsgeschwindigkeit eine beherrschende Rolle zugeschrieben.

Received March 17, 1962
Revised November 6, 1962

JOURNAL OF POLYMER SCIENCE: PART A VOL. 1, PP. 2179–2184 (1963)

The Role of Metal Chelates in Polymerization Initiation. I. Chromous Chelates

JOAN BOND and D. B. HOBSON, *The Royal College of Advanced Technology, Salford, Lancashire, England*

Synopsis

The polyaminocarboxylic acids, ethylenediaminetetraacetic acid (EDTA), cyclohexanediaminetetraacetic acid (CDTA), and diethylenetriaminepentaacetic acid (DTPA) have been used to chelate the chromous and chromic ions when the system chromous ion–hydrogen peroxide is being used as an initiator for the emulsion polymerization of styrene. With CDTA and DTPA the zero-order rates of polymerization increase continuously with increasing pH but with EDTA the zero-order rate is constant over the range pH 5–7 and increases rapidly above pH 7. These results are to be anticipated from the variation of the redox potential of the chromous ion–chromic ion–chelating agent system with pH, since with CDTA and DTPA the redox potential decreases continuously with pH while with EDTA the redox potential varies only slightly over the range pH 5–7.

INTRODUCTION

The system, chromous ion–polyaminocarboxylic acids–hydrogen peroxide, has been studied as an initiator for the emulsion polymerization of styrene. The relative zero-order rates of polymerization, over the pH range 2–7, have been compared with the reducing power of the chromous chelates as indicated by the variation of redox potential of the chromous ion–chromic ion–polyaminocarboxylic acid system with pH. The polyaminocarboxylic acids which have been studied are, ethylenediaminetetraacetic acid (EDTA), diethylenetriaminepentaacetic acid (DTPA), and cyclohexanediaminetetraacetic acid (CDTA).

EXPERIMENTAL

A. Preparation and Purification of Materials

Styrene, the polyaminocarboxylic acids, nitrogen, the emulsifying agent which was prepared by sulfating the condensation product of capryl alcohol with 21 molecules of ethylene oxide, and hydrogen peroxide were purified as described by Bond and Jones.[1,2]

In preparation of chromous sulfate, the apparatus (Fig. 1) was freed from oxygen by passing purified nitrogen through for 30 min. and a slow stream was maintained throughout the preparation. A 72 g. portion of analytical

reagent grade potassium chromium sulfate was dissolved in 35 ml. distilled water and placed with 50 g. granulated zinc in the bulb B and 70 ml. concentrated hydrochloric acid was added slowly from a tap funnel. The chromic sulfate was reduced to a bright blue solution of chromous sulfate in two hours. When the evolution of hydrogen had stopped, the tap T was opened to allow the solution to pass through the glass wool filter into the reservoir of an automatic buret R, which contained a filtered solution of 84 g. sodium acetate in 100 ml. distilled water. The dark red precipitate of chromous acetate was washed repeatedly with distilled water, the filtrate being removed through the glass wool plug attached to the filter pump.

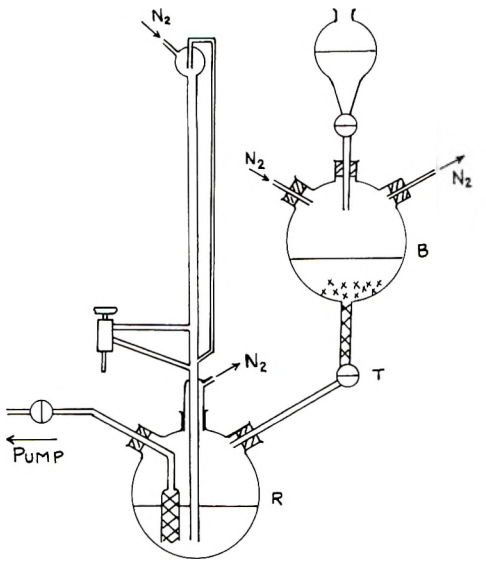

Fig. 1. The apparatus for the preparation and storage of chromous sulfate.

Dilute sulfuric acid was added dropwise with shaking until the chromous acetate had all dissolved to form a blue solution of chromous sulfate. Care was taken to add just sufficient acid as oxidation of chromous ions to chromic ions is rapid in the presence of hydrogen ions.[3] Nitrogen was bubbled continuously through the solution to prevent oxidation and pressure of nitrogen was used to fill the buret.

B. Estimation of the Concentration of the Chromous Sulfate Solution

To a five-necked, round-bottomed flask fitted with platinum and calomel electrodes, a nitrogen inlet tube, a glass stirrer and stirrer guide which incorporated a nitrogen outlet tube and a fifth neck covered by a self-sealing cap were added 50 ml. 0.1*M* copper sulfate solution and 50 ml. concentrated hydrochloric acid. The flask was placed in a consant temperature bath at 25°C. and nitrogen was bubbled through the solution for 1 hr. Chromous sulfate solution was added from the automatic buret, the tip of which

passed through the self-sealing cap, in milliliter aliquots and the EMF of the cell,

$$Hg \mid Hg_2Cl_2(s)\ KCl(\text{saturated solution}) \parallel [CuCl_4]^{=}[CuCl_2]^{-}Pt$$

was measured after each addition. At the end point of the titration there was a sudden large decrease in the EMF, the concentration of the chromous sulfate solution being accurately determined from a graph of EMF against milliliters of chromous sulfate solution.

C. Polymerization Technique

The emulsion polymerization of styrene was carried out as outlined previously,[2] the composition of the reaction mixture being as follows: 50 g. styrene monomer, 140 g. distilled water, 0.2 g. hydrogen peroxide, 0.04 g. chromous ion added as chromous sulfate, 2.5 g. emulsifying agent, and the equivalent amount of polyaminocarboxylic acid to complex the metal ion. Due to the exceptional ease of oxidation of the chromous ion it was important to remove completely all traces of oxygen from the reaction mixture and vessel before the addition of the chromous sulfate solution. The rate of polymerization was determined by the weight conversion method.[4]

RESULTS

The results are presented in Table I and Figure 2.

TABLE I
To Show the Variation of Zero-Order Rates of Polymerization and Redox Potentials with pH

Complexing agent	pH	Zero-order rate of polymerization % conversion/hr.	Redox potential, m.v.
EDTA	3.0	34	−360
	3.5	43	−365
	4.0	47	−375
	4.5	49	−395
	5.0	50	−415
	6.0	52	−435
	6.5	53	−445
	7.0	77	−455
CDTA	2.5	10	−434
	3.0	17	−442
	4.0	28	−461
	5.0	39	−480
	6.0	50	−498
	7.0	62	−516
DTPA	2.5	29	−400
	3.0	32	−414
	4.0	39	−442
	5.0	45	−472
	6.0	52	−500
	7.0	59	−526

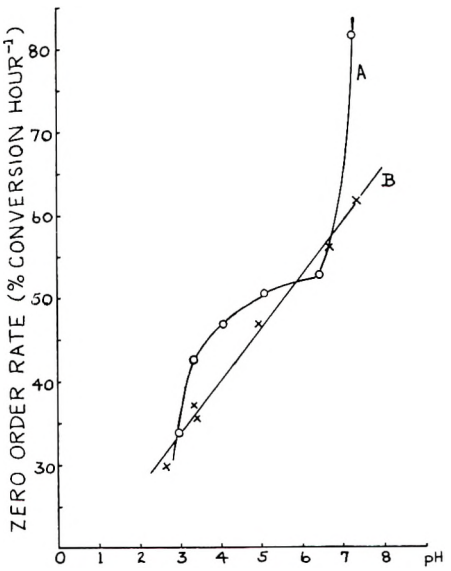

Fig. 2. The variation of the zero-order rate of polymerization of styrene with pH in the presence of (*A*) chromous ion–EDTA–hydrogen peroxide and (*B*) chromous ion–CDTA–hydrogen peroxide.

DISCUSSION

Redox potential measurements on the chromous ion–chromic ion system both in the absence and presence of chelating agents, were made by the method of Bond and Jones,[5] the platinum electrode which would catalyze the oxidation of chromous ions to chromic ions in the presence of hydrogen

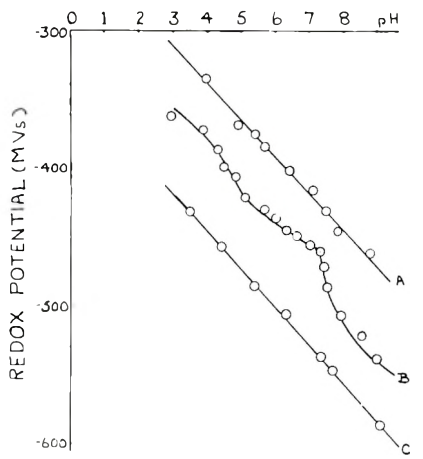

Fig. 3. The variation of the redox potential with pH of (*A*) the chromous ion–chromic ion systems, (*B*) the chromous ion–chromic ion–EDTA system, and (*C*) the chromous ion–chromic ion–DTPA system.

ions, being replaced by a tin electrode and the results are shown graphically (Fig. 3). The value for the unchelated system is quoted in the literature[6] as −0.42 v. in sulfate solution but no mention is made of the pH of the solution. However, there is good agreement between this value and that of −0.417 v. which we obtained at pH 7, the results being reproducible to 1 mv.

When EDTA is used to complex the chromous and chromic ions there is a decrease in the rate of change of redox potential with pH over the range pH 5–7 and the redox potential–pH curve is similar to that of the ferrous ion–ferric ion–EDTA system discussed by Schwarzenbach.[7] The corresponding graphs for the chromous ion–chromic ion–CDTA and chromous ion–chromic ion–DTPA systems do not show any point of inflection, so it must be assumed that over the entire pH range either a proton or a hydroxyl ion is attached to the chelate, whereas in the case of the chromous ion–chromic ion–EDTA system the reducing power of the chromous chelate is virtually independent of pH in the region of the point of inflection where the chelate will be neither protonated nor hydroxylated.

There is good correlation between the rate of polymerization and the variation of redox potential with pH of the various systems investigated. With EDTA, the zero-order rate of polymerization is constant over the range pH 5–7 as anticipated from the redox potential graph and when hydroxylation of the chelate commences at about pH 7, the rate of polymerization increases rapidly in a similar manner to that of the ferrous ion–EDTA–hydrogen peroxide initiated polymerization. When CDTA and DTPA are used as chelating agents, the rate of polymerization increases continuously with increasing pH, and this can be predicted from the redox potential measurements which show that the reducing power of the chelated chromous ion increases with increasing pH. In the absence of chelating agents it was found to be impossible to reproduce the zero order rate of polymerization, but the tendency was for the rate to be higher than that in the presence of chelating agent. This initiator could not be used above pH 7 due to the precipitation of chromic hydroxide.

The authors wish to thank the Governors of the Royal College of Advanced Technology, Salford, England, for a grant to one of us (D.B.H.) which allowed this work to be carried out.

References

1. Bond, J., and T. I. Jones, *J. Polymer Sci.*, **42**, 67 (1960).
2. Bond, J., and T. I. Jones, *J. Polymer Sci.*, **42**, 75 (1960).
3. Knapp, B. B., and J. H. Walton, *J. Phys. Chem.*, **14**, 679 (1937).
4. Bovey, F. A., J. M. Kolthoff, J. A. Medalia, and E. J. Meehan, *Emulsion Polymerization*, Interscience, New York-London, 1955, p. 284.
5. Bond, J., and T. I. Jones, *Trans. Faraday Soc.*, **55**, 1310 (1959).
6. Grube, G., and G. Breitinger, *Z. Elektrochem.*, **33**, 112 (1927).
7. Schwarzenbach, G., and J. Heller, *Helv. Chim. Acta*, **34**, 576 (1951).

Résumé

On a employé les acides polyaminocarboxyliques, l'acide éthylènediaminetétraacétique (EDTA), l'acide cyclohexanediaminetétraacétique (CDTA), et l'acide diéthylènetraminepentaacétique (DTPA) pour réaliser la chélation des ions chromeux et chromiques dans le système d'initiation ion chromeux–peroxyde d'hydrogène en vue de la polymérisation en émulsion du styrène. Avec CDTA et DTPA les vitesses d'ordre zéro de polymérisation augmentent continuellement par augmentation du pH mais avec EDTA la vitesse d'ordre zéro est constante dans le domaine de pH 5–7 et augmente rapidement au-dessus de pH 7. Ces résultats découlent de la variation de potentiel de réduction avec le pH du système de chélation ion chromeux–ion chromique, ainsi avec CDTA et DTPA le potential de réduction décroît continuellement avec le pH tandis qu'avec EDTA le potentiel de réduction ne varie que légèrement dans le domaine de pH 5–7.

Zusammenfassung

Die Polyaminokarboxylsäuren, Äthylendiamintetraessigsäure (EDTA), Cyclohexandiamintetraessigsäure (CDTA), und Diäthylentriaminpentaessigsäure (DTPA) wurden zur Chelatbildung mit Chrom-II- und Chrom-III-ionen im Startersystem Chrom-II-ion–Wasserstoffperoxyd bei der Emulsionspolymerisation von Styrol verwendet. Mit CDTA und DTPA nimmt die Polymerisationsgeschwindigkeit nullter Ordnung mit steigendem pH kontinuierlich zu, hingegen ist die Geschwindigkeit nullter Ordnung mit EDTA über den pH-Bereich 5–7 konstant und nimmt oberhalb pH 7 rasch zu. Diese Ergebnisse entsprechen dem, was man nach der pH-Abhängigkeit des Redoxpotentials des Systems Chrom-II-ion–Chrom-III-ion-Chelatbildner erwarten würde, da mit CDTA und DTPA das Redox-potential mit dem pH kontinuierlich abnimmt, während mit EDTA das Redoxpotential sich im pH-Bereich 5–7 nur schwach ändert.

Received August 10, 1962

JOURNAL OF POLYMER SCIENCE: PART A VOL. 1, PP. 2185–2188 (1963)

The Role of Metal Chelates in Polymerization Initiation. II. Cupric Chelates

JOAN BOND and D. B. HOBSON, *The Royal College of Advanced Technology, Salford, Lancashire, England*

Synopsis

The polyaminocarboxylic acids, nitrilotriacetic acid (NTA), ethylenediaminetetraacetic acid (EDTA), cyclohexanediaminetetraacetic acid (CDTA), and diethylenetriaminepentaacetic acid (DTPA) have been used to chelate the cupric ion when the system cupric ion–hydrogen peroxide is used as an initiator for the emulsion polymerization of styrene. The same maximum zero order rate of polymerization of approximately 60% conversion/hr. is obtained in all cases, although with NTA this occurs from pH 3–6 while with EDTA, CDTA, and DTPA the maximum occurs in the regions pH 4–7, pH 3–7, and pH 6.5–9.5, respectively.

INTRODUCTION

The polyaminocarboxylic acids, nitrilotriacetic acid (NTA), ethylenediaminetetraacetic acid (EDTA), cyclohexanediaminetetraacetic acid (CDTA), and diethylenetriaminepentaacetic acid (DTPA) have been used as chelating agents for the metal ion when the system cupric ion–hydrogen peroxide is used as an initiator for the emulsion polymerization of styrene. The zero-order rate of polymerization has been measured over the pH range 2–10.

EXPERIMENTAL

The procedure used was identical to that reported in Part I of this series,[1] the composition of the reaction mixture being 50 g. styrene monomer, 150 g. distilled water, 0.07 g. copper (added as copper sulfate solution previously purified to remove all traces of iron), 0.2 g. hydrogen peroxide, 2.5 g. emulsifying agent and the equivalent amount of polyaminocarboxylic acid to complex the cupric ion. The zero-order rate of polymerization was determined by the weight conversion method.

RESULTS

The results are presented graphically in Figure 1 and tabulated in Table I.

TABLE I

Complexing agent	pH	Zero-order rate of polymerization % conversion/ hr.
None	2.0	57
NTA	2.0	27
	3.0	62
	4.0	66
	5.0	63
	6.0	58
	7.0	Nil
EDTA	2.0	24
	2.5	39
	3.0	45
	3.5	48
	5.0	62
	6.0	66
	7.0	59
	8.5	11
CDTA	2.0	23
	3.0	38
	4.0	53
	5.0	58
	6.0	62
	7.0	63
	8.0	Nil
	9.5	Nil
DTPA	2–5.0	Nil
	6.0	58
	7.0	72
	9.0	70
	9.6	70
	10.0	7

DISCUSSION

The measurements of the zero-order rate of polymerization show that both unchelated and chelated cupric ions with hydrogen peroxide form a good initiating system for emulsion polymerization. The addition of a polyaminocarboxylic acid to the cupric ion solution extends the pH range over which polymerization can be carried out since above pH 2 erratic results were obtained in the absence of chelating agent. The zero-order rate of polymerization against pH curves are all of the same form, each having a plateau corresponding to a zero-order rate of about 60% conversion/hr.

When NTA is used to complex the cupric ions the plateau extends from pH 3 to 6 and the rate of polymerization is reduced to zero between pH 6 and 7. The variation of zero-order rate of polymerization with pH when CDTA is used as chelating agent is almost identical to that obtained in

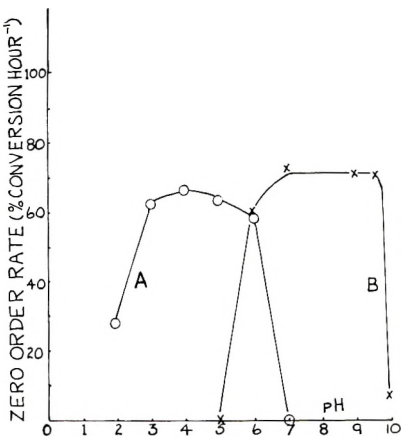

Fig. 1. The variation of the zero-order rate of polymerization with pH when NTA (curve *A*) and DTPA (curve *B*) are used to chelate the cupric ions.

the presence of EDTA; with EDTA the rate rapidly diminishes to zero between pH 8 and 9 while with CDTA the change occurs in the region pH 7–8. When DTPA is used no polymerization is observed at pH values less than 5, and the plateau extends from pH 6 to 9.5. The following reaction scheme is suggested for the initiation of polymerization:

$$H_2O_2 + CuY^{2-} \rightarrow HO_2^{\cdot} + H^+ + CuY^{3-}$$
$$H_2O_2 + CuY^{3-} \rightarrow HO\cdot + OH^- + CuY^{2-}$$

where H_4Y = EDTA.

Since the copper ion is held to the polyaminocarboxylic acids by electrostatic forces, the larger the negative charge on the acid ion, the more stable will be the binding to the copper ion.[2] Therefore, since in alkaline solution DTPA forms a pentavalent ion, EDTA and CDTA form tetravalent ions and NTA a trivalent ion, it is to be expected that the copper chelate of DTPA will be more stable than those of EDTA and CDTA which in turn will be more stable than that of NTA. This is borne out by the stability constants of the copper chelates[3,4] and their behavior in alkaline solution in promoting polymerization with hydrogen peroxide.

It was observed that, above pH 7, the solution of cupric ion–NTA becomes dark green and this can be explained as being due to the formation of an unreactive dihydroxylated complex in alkaline solution because of the ease of access of hydroxyl ions to the copper in this chelate. This access is impeded in the EDTA and CDTA complexes because of the chelate structure and consequently hydroxylation commences at a higher pH than with NTA. Addition of alkali to a copper–DTPA solution causes a deepening of the blue color, and this is probably due to the formation of a stable monohydroxylated complex which is reactive to hydrogen peroxide in the pH region 6–10. This complex is extremely stable in the acid region and does not promote any polymerization with hydrogen peroxide.

The authors wish to thank the Governors of the Royal College of Advanced Technology, Salford, England for a grant to one of us (D. B. H.) which allowed this work to be carried out.

References

1. Bond, J., and D. B. Hobson, *J. Polymer Sci.*, **A1**, 2179 (1963).
2. Kroll, H., *Symposium on the Use of Metal Chelates in Plant Nutrition*, Wallace, Ed., National Press, California, 1956, 28 p.
3. Holloway, J. H., and C. N. Reilley, *Anal. Chem.*, **32**, 249 (1960).
4. Schwarzenbach, G., and E. Freitag, *Helv. Chim. Acta*, **34**, 1503 (1951).

Résumé

En vue de polymériser en émulsion le styrène, initié par le système ions cuivrique-peroxyde d'hydrogène, on a chelaté les ions cuivriques avec les acides polyaminocarboxyliques suivants: l'acide nitrilo-triacètique (NTA), l'acide éthylènediaminotétraacétique (EDTA), l'acide cyclohexanediamino-tétraacétique (CDTA), et l'acide diéthylènetriamino-pentaacétique (DTPA). On obtient le même maximum de vitesse de polymérisation d'ordre zéro soit environ 60% de conversion par heure dans tous les cas. Avec la NTA ce maximum est obtenu entre pH 3 et 6, tandis qu'avec l'EDTA, la CDTA et la DTPA le maximum est obtenu respectivement dans les régions de pH de 4 à 7, de 3 à 7, et de 6.5 à 9.5.

Zusammenfassung

Die Polyaminokarboxylsäuren, Nitrilotriessigsäure (NTA), Äthylendiamintetraessigsäure (EDTA), Cyclohexandiamintetraessigsäure (CDTA), und Diäthylentriaminpentaessigsäure (CTPA) wurden zur Chelatbildung mit Kupfer-II-ionen im Startersystem Kupfer-II-ion–Wasserstoffperoxyd bei der Emulsionspolymerisation von Styrol verwendet. In allen Fällen wird die gleiche maximale Polymerisationsgeschwindigkeit nullter Ordnung von etwa 60% Umsatz pro Stunde erhalten; allerdings liegt diese maximale Geschwindigkeit mit NTA bei einem pH von 3–6, während sie mit EDTA, CDTA und DTPA in den pH-Bereichen 4–7, bzw. 3–7 bzw. 6,5–9,5 auftritt.

Received August 10, 1962

JOURNAL OF POLYMER SCIENCE: PART A VOL. 1, PP. 2189–2191 (1963)

Polymerization of Acrylonitrile in Dimethylsulfoxide

E. F. T. WHITE* and M. J. ZISSELL,† *Courtaulds Limited, Research Laboratory, Maidenhead, Berks, England*

Synopsis

Kinetic constants for the polymerization of acrylonitrile in dimethylsulfoxide have been measured and compared with those for dimethylformamide solution.

N,N-Dimethylformamide (DMF) has been used as the solvent in many kinetic studies of the polymerization of acrylonitrile and other vinyl monomers in solution.[1] However, chain transfer,[2] retardation,[3] and induced catalyst decomposition,[4] due to facile hydrogen abstraction from the amide by radicals, may complicate the interpretation of the kinetics. Dimethylsulfoxide (DMS), also a powerful solvent for polyacrylonitrile, appears to be much less active in transfer reactions with polyacrylonitrile radicals[5] and we have therefore used this solvent in a further study of acrylonitrile polymerization.

For the polymerization of acrylonitrile in solution, the molecular weight of the resulting polymer is given by the equation

$$\frac{1}{P} = \frac{k_3}{k_2} + \frac{(Ik_4)^{1/2}}{2k_2[\mathrm{M}]} + \frac{k_3'[\mathrm{S}]}{k_2[\mathrm{M}]} \tag{1}$$

where, k_2, k_3, k'_3, and k_4 are the velocity coefficients for propagation, transfer to monomer (M) and solvent (S), and termination by combination, respectively.[2] For solvents of low transfer activity, the transfer constant k'_3/k_2 may best be estimated from the intercept of a plot of $1/P$ against $I^{1/2}$ or $[\text{initiator}]^{1/2}$. This has been done in Figure 1 for the polymerization of acrylonitrile in dimethylsulfoxide and in ethylene carbonate at 50°C; results for dimethylformamide at 40 and 60°C.[6] are shown for comparison. Values of $k'_3/k_2 = 1.1 \times 10^{-5}$ and 5×10^{-5} were found for dimethylsulfoxide and ethylene carbonate, respectively (if transfer to monomer k_3/k_2 is neglected), compared with 2.3×10^{-4} and 4.6×10^{-4} at 40 and 60°C., respectively, for dimethylformamide. Ulbricht[5] gives $k'_3/k_2 = 7.9 \times 10^{-5}$, 4.7×10^{-5} and 2.8×10^{-4} for dimethylsulfoxide, ethylene carbonate, and dimethylformamide, respectively, at 50°C. Prevot-Bernas and Sebban-Danon[7] find that for transfer to monomeric acrylo-

* Present address: AMF British Research Laboratory, Blounts Court, Sonning Common, Reading, Berks, England.

† Present address: Coates Bros., Resin Division, St. Mary Cray, Kent, England.

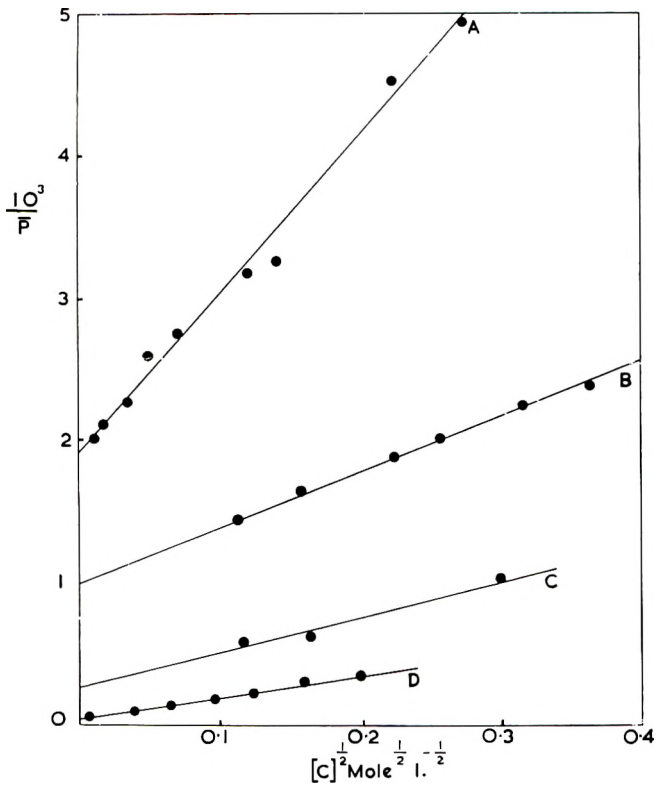

Fig. 1. Polymerization of acrylonitrile at different initiator concentrations: (*A*) in DMF at 60°C.; (*B*) in DMF at 40°C.; (*C*) in ethylene carbonate at 50°C.; (*D*) in DMS at 50°C.

nitrile at 60°C., $k_3/k_2 = 2 \times 10^{-5}$; clearly when allowance is made for monomer transfer in the above result for DMS, transfer to the solvent is extremely low.

In addition to the low transfer activity of dimethylsulfoxide, rates of polymerization and molecular weights of polyacrylonitrile are higher than in dimethylformamide. At 60°C., acrylonitrile polymerizes 50% faster in dimethylsulfoxide than in dimethylformamide, at 50°C. the difference in rates is even more marked. Assuming that the rate of initiation (I) is the same in each solvent and for azobisisobutyronitrile has the value[6] $I = 1.54 \times 10^{-5}$ [initiator] mole l.$^{-1}$ sec.$^{-1}$, we find $k_2k_4^{-1/2} = 0.15$ mole$^{-1/2}$l.$^{1/2}$ sec.$^{-1/2}$ in DMS, $k_2k_4^{-1/2} = 0.078$ mole $^{-1/2}$l.$^{1/2}$sec$^{-1/2}$ in DMF. Similarly, at 50°C. $I = 1.39 \times 10^{-6}$ [initiator] mole l.$^{-1}$ sec.$^{-1}$, and $k_2k_4^{-1/2} = 0.16$ mole$^{-1/2}$l.$^{1/2}$sec.$^{-1/2}$ in DMS, $k_2k_4^{-1/2} = 0.082$ mole$^{-1/2}$l.$^{1/2}$sec.$^{-1/2}$ in DMF.

The chain transfer constants for triethylamine and carbon tetrabromide towards the polyacrylonitrile radical at 60°C., were found to be the same in dimethylformamide and in dimethylsulfoxide solution. This suggests that k_2 is the same in both solvents, and hence that k_4 is approximately four times larger in dimethylformamide than in dimethylsulfoxide. Measure-

ments of lifetimes of polyacrylonitrile radicals in dimethylsulfoxide solution by a conventional rotating sector technique using di-*tert* butyl peroxide as the photoinitiator have shown that the rate coefficients for propagation and termination are k_2 = 1910, 11,600 mole^{-1}l.sec.$^{-1}$ and $k_4 = 2.9 \times 10^8$, 1.9×10^{10} mole^{-1}l.sec.$^{-1}$ at 25 and 60°C., respectively.

We thank Miss P. A. Smith for experimental assistance.

References

1. Bamford, C. H., A. D. Jenkins, and R. Johnston, *Proc. Roy. Soc.*, **241A**, 364 (1957).
2. Bamford, C. H., A. D. Jenkins, R. Johnston, and E. F. T. White, *Trans. Faraday Soc.*, **55**, 168 (1959).
3. Onyon, P. F., *Trans. Faraday Soc.*, **52**, 80 (1956).
4. Bamford, C. H., and E. F. T. White, *J. Chem. Soc.*, **1959**, 1860.
5. Ulbricht, J., *Faserforsch. Textiltech.*, **11**, 62 (1960).
6. Bamford, C. H., A. D. Jenkins, and R. Johnston, *Trans. Faraday Soc.*, **55**, 179 (1959).
7. Prevot-Bernas, A., and J. Sebban-Danon, *J. Chim. Phys.*, **53**, 418 (1956).

Résumé

On a mesuré les constantes cinétiques de la polymérisation de l'acrylonitrile dans le diméthylsulfoxide et ces valeurs ont été comparées avec celles obtenues en solution dans le diméthylformamide.

Zusammenfassung

Die kinetischen Konstanten der Polymerisation von Acrylnitril in Dimethylsulfoxyd wurden gemessen und mit denjenigen für Dimethylformamidlösung verglichen.

Received August 10, 1962

JOURNAL OF POLYMER SCIENCE: PART A VOL. 1, PP. 2193–2205 (1963)

Optical Rotatory Properties of Polyaldehydes *

AKIHIRO ABE and MURRAY GOODMAN, *Department of Chemistry, Institute for Polymer Research, Polytechnic Institute of Brooklyn, Brooklyn, New York*

Synopsis

We have studied the optical rotatory properties of several polyaldehydes possessing optically active side chains, such as poly-(*R*)(+)-citronellal, poly-(*R*)(+)-6-methoxy-4-methylhexanal, and poly-(*S*)(+)-2-methylbutanal. An enhancement is observed for the optical activity of the polymers compared to their model compounds. The magnitude of the enhancement depends on the separation between the asymmetric site and the main chain. Specific rotation values are independent of intrinsic viscosity and crystallinity of the polymers over the range measured. It was shown that the rotatory dispersion and the temperature dependence of the rotatory dispersion are essentially the same both for the polymers and their model compounds. We conclude from these data that the enhancements of the optical activity arise from a conformational rigidity around the asymmetric center in the side chain of the polymer.

INTRODUCTION

Polymers from optically active α-olefins have been prepared independently by Bailey and Yates,[1] by Pino and his group,[2–4] and by Murahashi, Nozakura and their co-workers.[5] The properties of these polymers have been studied extensively in Pino's laboratory.

As reported in our previous paper,[6] we have prepared a series of partially crystalline optically active polyaldehydes. With reference to the optical activity, these polyaldehydes exhibited the same behavior as that found in the hydrocarbon polymers. We made the following observations: (*a*) the optical activity enhancement for the polymers is large when compared with the optical activities of the corresponding model compounds and monomers; (*b*) the closer the asymmetric center is to the main chain, the higher is the optical activity of the polymer; (*c*) the rotatory dispersions of these polymers fit simple Drude plots.

We have investigated the optical activity of these polyaldehydes in relation to their viscosity and crystallinity, and also the temperature dependence of their optical rotations.

* From a thesis submitted by A. Abe in partial fulfillment of the requirements for the degree of Doctor of Philosophy in Chemistry at the Polytechnic Institute of Brooklyn.
Supported by the United Carbon Fellowship in Chemistry at the Polytechnic Institute of Brooklyn.

EXPERIMENTAL

Synthesis of the Monomers and Model Compounds

(R)(S)-2-Methylbutanal. (*R*)(*S*)-2-Methylbutanol was prepared from 2-bromobutane by a standard Grignard reaction using formaldehyde (yield 33%), or alternatively by reduction of (*R*)(*S*)-2-methylbutyric acid with lithium aluminum hydride (yield 55%). This alcohol (40 g.; 0.45 mole) was oxidized by a mixture of sodium dichromate dihydrate (49.4 g.; 0.17 mole), 30 ml. of 98% sulfuric acid and 90 ml. of water under a nitrogen atmosphere.[7a] The aldehyde was removed by distillation as formed and was collected at Dry Ice–acetone temperatures. The organic layer was separated, dried by molecular sieves, and distilled under nitrogen to give 12 g. of crude 2-methylbutanal (b.p. 90–100°C.) and 15 g. of recovered 2-methylbutanol (b.p. 125–129°C.). The aldehyde fraction was again dried by molecular sieves for 5 hr. and a fraction boiling between 92–95°C. at atmospheric pressure was collected (9 g., yield 23%).

(S)(+)-2-Methylbutanal. Active primary amyl alcohol (98% optical purity) was oxidized by the dichromate–acid mixture as described above. Pure (*S*)(+)-2-methylbutanal was obtained which gave $[\alpha]_D^{25.5}$ = +30.7° (*C* = 0.0654, benzene) and showed one peak on analysis by gas chromatography (yield 28%).

(R)(+)-Citronellal. Commercial (R)(+)-citronellal was distilled under reduced pressure using a Heligrid-packed column, and the fraction boiling at 60–62°C. at 2 mm. Hg was collected. Examination by gas chromatography showed that the aldehyde was pure. The content of the α- and β-forms could not be detected by a polyglycol gas chromatographic column. The optical activity of pure (*R*)(+)-citronellal was observed to be $[\alpha]_D^{26}$ = +12.9° (*C* = 0.0558, benzene).

(R)(+)-6-Methoxy-4-methylhexanal. Purified (*R*)(+)-citronellal was reduced to (*R*)(+)-citronellol in ether with lithium aluminum hydride [yield 91.4% of pure alcohol, $[\alpha]_D^{23}$ = +4.53° (*C* = 0.0367, benzene)]. The (*R*)(+)-citronellol thus obtained was converted to the methyl ether by a Williamson synthesis using sodium and methyl iodide [b.p. 58–60°C./1 mm. Hg, 90.0% of pure ether, $[\alpha]_D^{23}$ = + 5.59° (*C* = 0.0838, benzene)]. The double bond of this (*R*)(+)-citronellyl methyl ether was cleaved by ozonolysis and the resulting ozonide was reduced with a zinc-acetic acid mixture to give (*R*)(+)-6-methoxy-4-methylhexanal [b.p. 45°C. 2 mm. Hg, yield 60% of pure aldehyde, $[\alpha]_D^{25}$ = + 2.47° (C = 0.0263, benzene)], n_D^{23} = 1.4301, d_4^{23} 0.907.

ANAL. Calcd. for $C_8H_{16}O_2$: C, 66.7%; H, 11.1%. Found: C, 66.9%; H, 11.2%.

Diethyl Acetal of (R)(+)-citronellal. Ammonium nitrate (1 g.) in 15 ml. of absolute ethanol was added to a mixture of (*R*)(+)-citronellal (24 g., 0.16 mole) and triethyl orthoformate (28.5 g., 0.19 mole).[7b] This mixture was refluxed for 15 min. on a water bath and gave a yellowish-brown solution. The solution was cooled quickly by using a Dry Ice–ace-

tone bath and alcoholic potassium hydroxide solution was added to make the mixture slightly alkaline. Immediate fractionation gave 22.8 g. of crude acetal (b.p. 75–95°C. 1 mm. Hg). Redistillation yielded pure diethyl acetal of (*R*)(+)-citronellal (19.3 g.) boiling at 88–90°C./1 mm. Hg); yield 54%, $[\alpha]_D^{25} = +4.91°$ ($C = 0.1168$, chloroform), $n_D^{25} = 1.4380$, $d_4^{25} = 0.853$.

ANAL. Calcd. for $C_{14}H_{28}O_2$: C, 73.7%; H, 12.3%. Found: C, 73.6%; H, 12.5%.

Diethyl Acetal of (R)(+)-6-Methoxy-4-methylhexanal. (*R*)(+)-6-Methoxy-4-methylhexanal was treated with triethyl orthoformate and ammonium nitrate as described above and a fraction boiling at 70–72°C./1 mm. Hg was collected. Yield 41% of pure diethyl acetal, $[\alpha]_D^{25} = +3.78°$ ($C = 0.0962$, chloroform), n_D^{25} 1.4240, d_4^{25} 0.878.

ANAL. Calcd. for $C_{12}H_{26}O_3$: C, 66.1%; H, 11.9%. Found: C, 66.1%; H, 21.1%.

Polymerization

Polymerization was carried out in diethyl ether or *n*-hexane as a solvent in a sealed glass tube at the temperature of Dry Ice–acetone. Various types of catalysts listed in Table I were employed to obtain polymers with different properties.

TABLE I

10%	Triisobutylaluminum in toluene
20%	Butyllithium in *n*-heptane
25%	Diethylzinc in *n*-heptane
16%	*sec*-Butyl Grignard reagent in diethyl ether.
	Boron trifluoride etherate (commercial)
	Aluminum trichloride

The results of the polymerizations are summarized in Tables II–V. The chemical analyses were carried out by Schwarzkopf Microanalytical Laboratory.

TABLE II
Polymerization of (*R*)(*S*)-2-Methylbutanal[a]

Catalyst used	Monomer, g.	Solvent	Monomer concn., %	Catalyst, g.	Polymer yield, %	Reaction time, hr.
Al(*i*-Bu)$_3$	5.0	Ether	30	0.04	40.0	17
Al(*i*-Bu)$_3$	1.6	*n*-Hexane	40	0.04	44.0	48
$ZnEt_2$	1.6	Ether	53	<0.25	0.3	24
$CH_3CH_2CHMgBr$ (with CH_3 branch)	1.6	Ether	53	<0.32	3.1	20
$BF_3 \cdot Et_2O$	1.6	Ether	53	<1 ml.	0.3	22

[a] The microchemical analyses gave erratic results because of entrapped methanol.

TABLE III
Polymerization of (*S*)(+)-2-Methylbutanal[a]

Catalyst used	Monomer, g.	Solvent	Monomer concn., %	Catalyst, g.	Polymer yield, %	Reaction time, hr.
Al(*i*-Bu)$_3$	1.6	Ether	40	0.016	6.3	120
Al(*i*-Bu)$_3$	1.6	*n*-Hexane	40	0.016	7.5	192

[a] The microchemical analyses gave erratic results because of entrapped methanol.

TABLE IV
Polymerization of (*R*)(+)-Citronellal

Catalyst used	Monomer, g.	Solvent	Monomer concn., %	Catalyst, g.	Polymer yield, %	Reaction time, hr.
Al(*i*-Bu)$_3$	4.0	Ether	30	0.016	13.0[a]	17
Al(*i*-Bu)$_3$	4.0	Ether	57	0.08	15.0	24
BuLi	4.0	*n*-Hexane	57	0.08	13.0	24
$ZnEt_2$	4.0	*n*-Hexane	57	0.1	7.5	31
$ZnEt_2$	4.0	Ether	57	<0.25	30.0[b]	48
$CH_3CH_2CHMgBr$ (CH$_3$)	4.0	Ether	57	0.32	5.0[c]	24
$BF_3 \cdot Et_2O$	4.0	Ether	57	1 ml.	10.0	23
$AlCl_3$	4.0	*n*-Hexane	57	0.5	0.1	408

[a] Calcd. for $(C_{10}H_{18}O)_n$: C, 77.9%; H, 11.7%. Found: C, 77.8%; H, 11.6%.
[b] Found: C, 77.6%; H, 11.6%.
[c] Found: C, 74.3%; H, 11.3%.

TABLE V
Polymerization of (*R*)(+)-6-Methoxy-4-methylhexanal

Catalyst used	Monomer, g.	Solvent	Monomer concn., %	Catalyst, g.	Polymer yield, %	Reaction time, hr.
Al(*i*Bu)$_3$	1.6	Ether	40	0.04	31.0[a]	24
Al(*i*-Bu)$_3$	1.6	*n*-Hexane	40	0.04	31.0	30
Al(*i*-Bu)$_3$	3.2	—	Bulk	0.032	47.0	24
Al(*i*-Bu)$_3$	2.4	Ether	48	0.03	46.0[b]	72
BuLi	1.6	Ether	40	0.04	0.8	72
$ZnEt_2$	2.4	*n*-Hexane	40	0.125	2.1	72

[a] Calcd. for $(C_8H_{16}O_2)_n$: C, 66.6%; H, 11.1%. Found: C, 65.4%; H, 11.1%.
[b] Found: C, 66.4%; H, 11.2%.

The polymerization systems were added to a large volume of methanol with vigorous stirring. After a few hours, the precipitates were filtered and washed several times with methanol. These crude polymers were then treated in different ways, depending upon the solubility of the individual polymer.

(*a*) The poly-2-methylbutanals were dried at 60°C. under reduced pressure (1–2 mm. Hg) overnight. The polymers were obtained as white powders.

(*b*) Poly-(*R*)(+)-citronellal samples were dissolved in chloroform. After filtration, addition of methanol gave a white polymer in fibrous or powdered form. These polymers were dried in the same manner as above.

(*c*) Poly-(*R*)(+)-6-methoxy-4-methylhexanal obtained by using a triisobutylaluminum catalyst was soluble in chloroform at extremely low concentrations. At higher concentrations, the polymer swelled but did not dissolve. After filtration, most of the chloroform was removed by distillation under reduced pressure. Addition of methanol gave a transparent gel, which was dried at 60°C. under reduced pressure (1–2 mm. Hg) overnight. A translucent elastomerlike polymer was obtained. On the other hand, the low molecular weight polymer formed by diethylzinc was soluble in almost all organic solvents. Addition of water to the methanol solution was the only possible way to precipitate the purified polymer. This polymer was washed with a small amount of methanol and dried overnight at 60°C. under 0.5 mm. Hg pressure to yield a soft white powder.

RESULTS

All the polymers prepared showed a large infrared absorption band attributable to acetal linkages in their main chains.

These uncapped higher polyaldehydes were found to be fairly unstable even at room temperature, and, as expected, decomposed to the respective monomers at elevated temperatures. As shown in Table VII, the de-

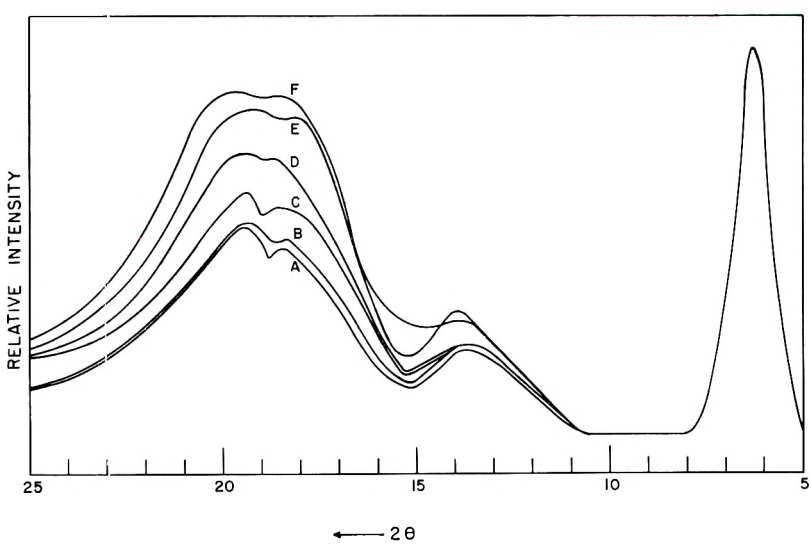

Fig. 1. X-ray diffraction pattern of poly-(*R*)(+)-citronellal. The initiators and solvents used in the polymerizations were: (*A*) BuLi, *n*-hexane; (*B*) Al(*i*-Bu)$_3$, ether; (*C*) $ZnEt_2$, ether; (*D*) $CH_3CH_2CH(CH_3)MgBr$, ether; (*E*) $BF_3 \cdot Et_2O$, ether; (*F*) $ZnEt_2$, *n*-hexane.

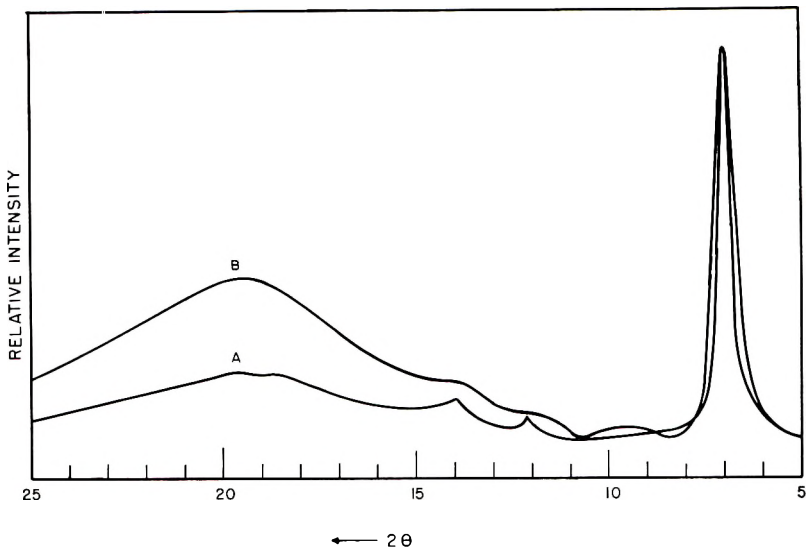

Fig. 2. X-ray diffraction pattern of poly-(*R*)(+)-6-methoxy-4-methylhexanal. The initiators and solvents used in the polymerizations were: (*A*) Al(*i*-Bu)$_3$, ether; (*B*) $ZnEt_2$, *n*-hexane.

composition temperature decreases as intrinsic viscosity and crystallinity decrease.

X-ray examination was carried out using a Norelco diffractometer. The position of the characteristic crystalline peaks in the powder diagrams are listed in Tables VI–VIII. The results for poly-(*S*)(+)-2-methylbutanal and poly-(*R*)(*S*)-2-methylbutanal have been discussed in our previous paper.[6] The powder diagrams of poly-(*R*)(+)-citronellal and poly-(*R*)(+)-6-methoxy-4-methylhexanal are shown in Figures 1 and 2, respectively. As can be seen, the crystallinity is drastically altered by changing the catalyst.

Viscosity measurements were carried out at 26.7°C. by using an Ubbelohde-type viscometer. Poly-(*S*)(+)-2-methylbutanal was insoluble in all solvents tried. Poly-(*R*)(+)-citronellal and poly-(*R*)(+)-6-methoxy-4-methylhexanal were found to be soluble to varying extents in such solvents as chloroform, benzene, toluene and dioxane at room temperature except when the molecular weight was extremely high. As shown in Tables VII and VIII, the crystallinity and the decomposition temperature decrease, maintaining similar relative orders as the molecular weight (intrinsic viscosity) decreases.

The optical activities of the soluble polymers were measured by using a Rudolph-type spectropolarimeter. As shown in Table VII, all of the poly-(*R*)(+)-citronellals have almost the same optical rotatory power irrespective of their polymerization systems. The optical rotations, therefore, are essentially independent of the intrinsic viscosity and the crystallinity. Table IX shows a comparison of the optical activity of the polymers and

TABLE VI
Properties of Poly-2-methylbutanal

Polymer	Polymerization system: Catalyst	Polymerization system: Solvent	Decomposition temp., °C.	Crystalline peak, A.
Poly-(*R*)(*S*)-2-methylbutanal	Al(*i*-Bu)$_3$	Ether	195–197	9.9
	Al(*i*-Bu)$_3$	*n*-Hexane	195–197	10.0
	$ZnEt_2$	Ether	125–130	—
	$CH_3CH_2CHMgBr$ (with CH_3 branch)	Ether	125–130	—
	$BF_3 \cdot Et_2O$	Ether	110–115	—
Poly-(*S*)(+)-2-methylbutanal	Al(*i*-Bu)$_3$	Ether	195–197	10.0
	Al(*i*-Bu)$_3$	Ether	195–197	—

TABLE VII
Properties of Poly-(*R*)(+)-citronellal

Polymerization system: Catalyst	Polymerization system: Solvent	Decomposition temp., °C.	Viscosity [η], 100 ml./g.[a]	Optical activity[b]: [α]$_D$	[*M*]$_D$	[*M'*]$_D$[c]
Al(*i*-Bu)$_3$[d]	Ether	165–170	3.25	−90.1	−139	−101.8
Al(*i*-Bu)$_3$	Ether	175–185	3.70	−82.7	−127	−93.5
BuLi	*n*-Hexane	160–165	4.45	−91.1	−140	−102.9
$ZnEt_2$	*n*-Hexane	—	0.355	−80.5	−124	−91.0
$ZnEt_2$	Ether	115–120	1.34	−85.4	−132	−96.5
$CH_3CH_2CHMgBr$ (with CH_3 branch)	Ether	120–130	1.31	−83.8	−129	−94.7
$BF_3 \cdot Et_2O$	Ether	90–92	0.345	−89.5	−138	−101.1
				−93.6[e]	−144[e]	−102.0[e]
$AlCl_3$	*n*-Hexane	120–125	—	−84.5	−130	−95.5

[a] In chloroform at 26.7°C.
[b] In chloroform.
[c] In benzene.
[d] Crystalline peak 13.6 A.
[e] Corrected for index of refraction of the solvent.

the corresponding model compounds. There is a large enhancement of optical activity in the polymer when compared with the optical activity of the corresponding model compound.

A study of the temperature dependence of the optical activities shows that the absolute rotations of both soluble polymers and model compounds decreased with increasing temperature. All samples of the poly-(*R*)(+)-citronellal investigated showed essentially the same magnitude of temperature dependence (Table X). In other words, the temperature dependence is independent of the values of intrinsic viscosity which, in turn, are related to the type of the catalyst employed in the polymeriza-

TABLE VIII
Properties of Poly-(*R*)(+)-6-methoxy-4-methylhexanal

Polymerization system		Decomposition temp., °C.	Viscosity $[\eta]$, 100 ml./g.[a]	Optical activity		
Catalyst	Solvent			$[\alpha]_D$	$[M]_D$	$[M']_D$[e]
$Al(i\text{-}Bu)_3$[d]	Ether	170–175	—	—	—	—
$Al(i\text{-}Bu)_3$	Ether	165–175	10.0	—	—	—
$ZnEt_2$	*n*-Hexane	105–108	0.787	+36.7[b]	+52.8[b]	+38.5[b]
				+36.9[c]	+53.1[c]	+39.5[c]

[a] In chloroform at 26.7°C.
[b] In chloroform.
[c] In dioxane.
[d] Crystalline peak 12.5 A.
[e] Corrected for the index of refraction of the solvent.

TABLE IX
Molar Rotations of Polymers and Model Compounds

(*R*)(+)-Citronellal series	(*R*)(+)-6-Methoxy-4-methylhexanal series
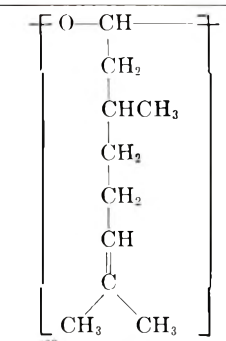	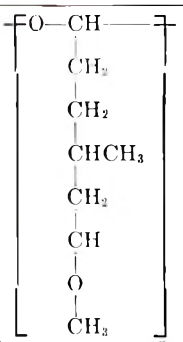
$[M]_D^{28} = -140.3$ $[M']_D^{28} = -102.9$ $CHCl_3$	$[M]_D^{26} = +52.8$ $[M']_D^{26} = +38.5$ $CHCl_3$
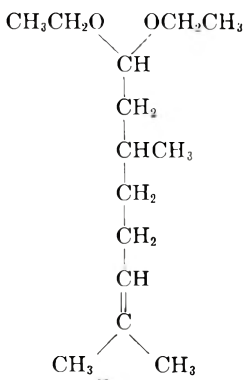	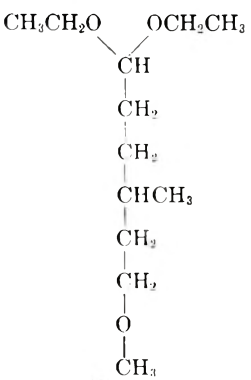
$[M]_D^{25} = +11.2$ $[M']_D^{25} = +8.25$ $CHCl_3$	$[M]_D^{25} = +8.24$ $[M']_D^{25} = +6.01$ $CHCl_3$

TABLE X
Temperature Dependence of Optical Activity of Poly-(*R*)(+)-citronellal and That of the Model Compound in Chloroform[a]

	Wavelength, mμ	$\frac{\Delta[\alpha]}{\Delta T}$ (corr.)[b]	$\frac{\Delta[\alpha]}{[\alpha]\Delta T}$ (corr.)[b]
Model compound	589	−0.036	−0.0073
	500	−0.052	−0.0070
	400	−0.089	−0.0067
	365	−0.122	−0.0070
Polymer initiated by $Al(i\text{-}Bu)_3$	589	0.10	−0.0011
	546	0.17	−0.0016
	508.6	0.11	−0.0009
	435	0.25	−0.0014
	405	0.31	−0.0015
	365	0.36	−0.0013
Polymer initiated by $BF_3.Et_2O$	589	0.13	−0.0014
	500	0.20	−0.0015
	400	0.30	−0.0014
	365	0.38	−0.0014

[a] Temperature interval 22–50°C.
[b] Corrected for the thermal expansion coefficient and the refractive index change with temperature.

TABLE XI
Temperature Dependence of Optical Activity of Poly-(*R*)(+)-6-methoxy-4-methylhexanal and That of the Model Compound in Chloroform[a]

	Wavelength, mμ	$\frac{\Delta[\alpha]}{\Delta T}$ (corr.)[b]	$\frac{\Delta[\alpha]}{[\alpha]\Delta T}$ (corr.)[b]
Model compound	589	−0.0033	−0.00089
	500	−0.0044	−0.00084
	400	−0.0070	−0.00079
	365	−0.0078	−0.00071
Polymer initiated by $ZnEt_2$	589	−0.075	−0.0020
	500	−0.110	−0.0020
	400	−0.118	−0.0013
	365	−0.169	−0.0015

[a] Temperature interval 22–50°C.
[b] Corrected for the thermal expansion coefficient and the refractive index change with temperature.

tions. As shown in Tables X and XI, the polymers and the model compounds differ considerably in the temperature coefficients of their absolute rotations at a given wavelength. The values of the rotations were corrected for changes in volume and refractive index with temperature. While $\Delta[\alpha]/\Delta T$ largely depends on the wavelength, the ratio of $\Delta[\alpha]/\Delta T$ to $[\alpha]$ is found to be almost independent of wavelength. For poly-(*R*)-

TABLE XII
Constants for the Simple Drude Plot for Poly-(*R*)(+)-citronellal and Its Model Compound in Chloroform Solution

	Temperature, °C.	λ_c, mμ[a]	$K \times 10^{-7}$[a]
Model compound	25.0	219	0.148
	51.5	226	0.118[b]
Polymer initiated by $Al(i\text{-}Bu)_3$	27.0	166	−2.88
	50.0	163	−2.81[b]
Polymer initiated by BuLi	22.0	150	−2.96
	50.0	153	−2.83[b]
Polymer initiated by $ZnEt_2$	25.0	152	−2.77
Polymer initiated by $CH_3CH_2CH(CH_3)$-MgBr	27.0	158	−2.70
Polymer initiated by $BF_3 \cdot Et_2O$	22.0	158	−2.88
	50.0	157	−2.77[b]
Polymer initiated by $AlCl_3$	26.0	155	−2.73

[a] The ranges of the errors in measurements for λ_c's and K's are the order of ±5% and ±0.5%, respectively.

[b] Corrected for the thermal expansion coefficient and the refractive index change with temperature.

TABLE XIII
Constants for the Simple Drude Plot for Poly-(*R*)(+)-6-methoxy-4-methylhexanal and Its Model Compound in Chloroform Solution

	Temperature, °C.	λ_c, mμ[a]	$K \times 10^{-7}$[a]
Model compound	25.0	143	0.123
	52.0	151	0.118[b]
Polymer initiated by $ZnEt_2$	26.0	190	1.14
	51.5	188	1.09[b]

[a] The ranges of the errors in measurements for λ_c's and K's are the order of ±5% and ±0.5%, respectively.

[b] Corrected for the thermal expansion coefficient and the refractive index change with temperature.

(+)-citronellal this ratio* is much greater for the model compound than for the polymer. In the (*R*)(+)-6-methoxyhexanal series, on the other hand, both $\Delta[\alpha]/\Delta T$ and $\Delta[\alpha]/[\alpha]\Delta T$ ratios* are greater for the polymer than for the model compound. Optical rotatory dispersions of these soluble polymers and model compounds were found to fit the simple Drude plot.[8]

$$[\alpha] = \frac{K}{\lambda^2 - \lambda_c^2} \tag{1}$$

The constants K and λ_c obtained are summarized in Tables XII and XIII.

* This discussion is based on the absolute values of the temperature coefficients.

With increasing temperature, the absolute values of K decrease while λ_c values remain constant within experimental error.

Storage of the polymer solutions caused no change in their optical activities. Addition of *n*-butanol (a very poor solvent) to a benzene solution of poly-(*R*)(+)-citronellal did not affect the optical activity until the polymer precipitated. Chloroform solutions of poly-(*R*)(+)-citronellal exhibited no concentration effect on the specific rotation in a range between 0.5% and 2% solute.

DISCUSSION

The effect of temperature upon optical rotation consists mainly of changes in the solvent–solute interactions and in the equilibrium of all conformations. For the sake of simplicity, we may assume that only two forms[9,10] contribute to the optical activity, that is, a high temperature form A and a low temperature form B, which have values of a and b for their optical rotations, respectively. Equation (2) therefore follows:

$$(\alpha - b)/(a - \alpha) = e^{\Delta s/R} \times e^{-\Delta H/RT} = K_{eq} \tag{2}$$

where α is the optical activity observed at a given temperature T and K_{eq} is the equilibrium constant.

Rewriting this equation gives:

$$\alpha = (b + aK_{eq})/(1 + K_{eq}) \tag{3}$$

By differentiating eq. (3), eq. (4) is obtained.

$$d\alpha/dT = [(a - b)/(1 + K_{eq})^2](dK_{eq}/dT) \tag{4}$$

Dividing eq. (4) by eq. (3) we obtain:

$$\frac{1}{\alpha}\left(\frac{d\alpha}{dT}\right) = \frac{[(a/b) - 1](dK_{eq}/dT)}{(1 + K_{eq})[1 + (a/b)K_{eq}]} \tag{5}$$

It should be noted that $d\alpha/dT$ contains an $(a - b)$ term while $(1/\alpha)$, $(d\alpha/dT)$ involves only the ratio of a and b. The experimental fact that $(1/\alpha)(\Delta\alpha/\Delta T)$ remains almost constant over a relatively wide range of wavelengths implies that the ratio a/b is independent of wavelength since a and b are the only wavelength-dependent terms in eq. (5). In other words, a and b have similar wavelength dependences which fit simple Drude equations having the same λ_c and different constants K. This explains the experimental fact that by raising the temperature the absolute values of K decrease while λ_c values remain constant. In this respect, both the polymers and the model compounds examined show the same behavior (Tables X and XI). Poly-(*R*)(−)-3,7-dimethyloctene-1 was also found to behave in a similar manner with temperature.[11] The fact that $\Delta\alpha/\Delta T$* of the model compound of poly-(*R*)(+)-citronellal is smaller than that of the corresponding polymer at a given wavelength while $(1/\alpha)(\Delta\alpha/\Delta T)$* is much greater for the model compound can be explained in terms of the

* See footnote p. 2202.

relative magnitudes of $(a - b)$ and a/b terms of the polymer and model compound in the above equations. As pointed out by Pino et al.,[3,4] $d\alpha/dT$ values* for the polymers are much greater than those of the model compounds. It should, however, be recalled that the value of $d\alpha/dT$ depends not only on the ΔH and ΔS terms but also on the magnitude of the $(a - b)$ term. Unfortunately the variation in values for the optical activities of the polymers and the model compounds over the temperature range studied is too small to calculate reliable values of a, b, ΔH, and ΔS. Mathematical considerations of equilibria consisting of more than two conformational forms[12] lead to the same conclusions as described above.

In summary, we consider that changes in temperature alter the equilibria among conformational forms which, in turn, are responsible for the optical rotatory properties of the aldehyde and hydrocarbon polymers. We do not consider that changes in solvent–solute interactions with temperature alter significantly the rotatory properties of these polymers.

The origin of the optical activity enhancements observed for the polymers over the model compounds can arise from conformational rigidity around the asymmetric centers.[13] We wish to emphasize that the optical rotatory phenomena of these polymers are not comparable to those encountered with many polypeptides,[14] in which an intramolecularly hydrogen bonded structure, the α-helix, may contribute a special helical rotation since the α-helix itself is asymmetric. Thus, in addition to the optical activity derived from the asymmetric carbon atoms, polypeptides can have contributions to their rotations which are clearly assignable to the helix. In this respect, many polypeptides behave quite differently from their low molecular weight analogs. In optically active aldehyde and hydrocarbon polymers all activity arises from the asymmetric side chains and their stereochemical arrangements.[15] While we do not exclude the explanation that short-range excesses of one helical form over the other contribute to optical activity enhancements as suggested by Pino,[16] we do not feel that this is the major factor involved.

We wish to thank Dr. William Houlihan of the Trubek Laboratories for the generous supply of citronella and Dr. A. Maggiolo of the Welsbach Corporation for the ozonolysis of the citronellyl methyl ether.

References

1. Bailey, W. J., and E. T. Yates, *J. Org. Chem.*, **25**, 1800 (1960).
2. Pino, P., D. P. Lorenzi, and L. Lardicci, *Chim. Ind. (Milan)*, **42**, 712 (1960).
3. Pino, P., and D. P. Lorenzi, *J. Am. Chem. Soc.*, **82**, 4745 (1960).
4. Pino, P., D. P. Lorenzi, L. Lardicci, and F. Ciardelli, *Vysokomol. Soedin.*, **3**, 1597 (1961).
5. Nozakura, S., S. Takeuchi, H. Yuki, and S. Murahashi, *Bull. Chem. Soc. Japan*, **34**, 1673 (1961).
6. Goodman, M., and A. Abe, *J. Polymer Sci.*, **59**, S37 (1962).

* See footnote p. 2202.

7. Weygand, C., *Organic Preparations*, Interscience, New York, 1945, (a) p. 143; (b) *ibid.*, p. 187.

8. Djerassi, C., *Optical Rotatory Dispersion*, McGraw-Hill, New York, 1960.

9. Kauzmann, W. J., J. E. Walter, and H. Eyring, *Chem. Revs.*, **26**, 339 (1940).

10. Foss, J. G., and J. A. Schellman, *J. Phys. Chem.*, **63**, 2007 (1959).

11. Goodman, M., M. A. Stake, A. Abe, and E. S. Clark, to be published.

12. Bernstein, H. J., *J. Chem. Phys.*, **17**, 885 (1949).

13. Liquori, A., et al., reported similar conclusions based on polyvinyl-L-menthyl ethers at the International Symposium on Macromolecular Chemistry, Montreal, Canada, 1961.

14. Stahmann, M., *Polyamino Acids, Polypeptides and Proteins*, Univ. of Wisconsin Press, Madison, 1962.

15. Brewster, J. H., *J. Am. Chem. Soc.*, **81**, 5475 (1959).

16. Pino, P., Paper presented at the Polymer Section of the Gordon Research Conferences, New London, N.H., July 3, 1962.

Résumé

Nous avons étudié les propriétés de rotation optique de différentes polyaldéhydes qui possèdent des chaînes latérales optiquement actives, comme le poly-(*R*)(+)-citronellal, poly-(*R*)(+)-6-méthoxy-4-méthylhexanal et le poly-(*S*)(+)-2-méthylbutanal. On a observé une augmentation en ce qui concerne l'activité optique des polymères, en comparaison avec leurs composés modèles. La grandeur de cette augmentation dépend de la séparation entre le centre d'assymétrie et la chaîne principale. Les valeurs spécifiques de rotations sont indépendantes de la viscosité intrinsèque et de la cristallinité des polymères, dans le domaine examiné. On a montré que la dispersion de rotation et la dépendance de la température de la dispersion de rotation sont essentiellement les mêmes pour les polymères comme pour leurs mélanges modèles. De ces données nous pouvons conclure que les augmentations de l'activité optique proviennent de la rigidité conformationnelle autour du centre asymétrique dans la chaîne latérale du polymère.

Zusammenfassung

Wir haben die optische Drehung einiger Polyaldehyde mit optisch aktiven Seitenketten, wie Poly-(*R*)(+)-citronellal, Poly-(*R*)(+)-methoxy-4-methylhexanal und Poly-(*S*)(+)-2-methylbutanal untersucht. Eine Erhöhung der optischen Aktivität der Polymeren gegenüber ihren Modellverbindungen wird beobachtet. Die Grösse der Erhöhung hängt von der Entfernung zwischen Asymmetriezentrum und Polymerhauptkette ab. Die spezifischen Drehungswerte sind im untersuchten Bereich von der Viskositätszahl und der Kristallinität der Polymeren unabhängig. Die Rotationsdispersion und ihre Temperaturabhängigkeit sind im wesentlichen für Polymere und ihre Modellverbindungen die gleichen. Aus diesen Ergebnissen wird der Schluss gezogen, dass die Erhöhung der optischen Aktivität durch eine Konformationsstarrheit um das aktive Zentrum in der Polymerseitenkette zustande kommt.

Received October 4, 1962

JOURNAL OF POLYMER SCIENCE: PART A VOL. 1, PP. 2207–2212 (1963)

Resistivity Studies on Polymer Semiconductors

H. A. POHL, C. G. GOGOS, and C. CAPPAS, *Plastics Laboratory, School of Engineering, Princeton University, Princeton, New Jersey*

Synopsis

Eighteen polyacene polymers were synthesized, and their resistivities were found to be of the order of 10^4–10^5 ohm-cm. The resistivity of these polymer semiconductors was found to be sensitive to changes in the conditions of synthesis, changes in the structure of the polymers, and variations of pressure and temperature during experimentation. The forbidden energy gap for these polymers was about 0.5 e.v. Although the formalism of the simple intrinsic semiconductor band model was not strictly applicable to the data on these polymers, such a treatment was found instructive.

Introduction

Semiconduction in a number of polyacene quinone radical polymers was demonstrated a few years ago by Itoh and Pohl.[1–3] These materials exhibited a specific conductivity in the range of 10^{-4}–10^{-12} mho/cm., a negative temperature coefficient of resistance, a high thermoelectric power, a measurable Hall coefficient, and non-ohmic behavior at junctions. The conductivity was sensitive to presence of impurities and changes in molecular structure. This work is a continuation of the investigations of this laboratory into the basic nature of organic semiconductors.

An important factor in producing intrinsic organic semiconductors with low resistivity appears to be an extensive conjugation through π-bonded electrons. Both experiment and theory support this view.[4–6] However, recent work in this laboratory has shown that although this may be a necessary condition, it is by no means a sufficient one.

Phenolphthalein is formed when two moles of phenol are reacted with one mole of phthalic anhydride in the presence of $ZnCl_2$. Continued condensation on the phenyl ring leads to a semiconductive polymer. Substitution appears to occur at the *ortho* position. Analogous and highly conjugated polymers can be prepared by replacing the phenol and phthalic anhydride molecules with complex ones. For example 1,8-dihydroxyanthraquinone reacted with naphthalic anhydride in the presence of $ZnCl_2$ forms such a conjugated polymer. Eighteen such polymers were synthesized, very careful attention being paid to purity of reactants and conditions of preparation. The polymers were condensation products of naphthalic anhydride (NA); pyromellitic anhydride (PMA); and various hydroxyanthraquinones: 1-monohydroxyanthraquinone (ANQN-1), 1,8-dihy-

TABLE I

Compound	ANQN derivative (1 mole)	NA, moles	PMA, moles	$ZnCl_2$, moles	Temp., °C.	Time, hr.	$\rho_{50°C.}$, ohm-cm.	E_g, e.v.	n_i, cm.$^{-3}$	μ_{mean}, cm.^{2}/v.-sec.
A_1	1,8-Dihydroxy	0.5	—	8	306	24	1.63×10^5	0.51	3.15×10^{15}	1.22×10^{-2}
A_2	"	"	0.25	8	306	24	8.0×10^4	0.49	4.73×10^{15}	1.65×10^{-2}
B_1	"	"	—	8	256	24	3.5×10^5	0.56	1.39×10^{15}	1.29×10^{-2}
B_2	"	"	0.25	8	256	24	3.0×10^6	0.57	1.12×10^{15}	1.86×10^{-2}
C_1	"	"	—	4	256	24	8.6×10^4	0.61	5.49×10^{14}	1.32×10^{-1}
C_2	"	"	0.25	4	256	24	1.5×10^4	0.68	1.58×10^{14}	2.64
D_1	"	"	—	4	306	24	4.6×10^4	0.44	1.16×10^{16}	1.17×10^{-2}
E_1	"	"	0.25	2	306	24	1.8×10^4	0.63	3.8×10^{14}	9.14×10^{-1}
F_1	"	"	0.25	8	306	12	1.1×10^5	0.49	4.73×10^{15}	1.2×10^{-2}
F_2	"	"	"	8	306	30	5.6×10^4	0.50	4.1×10^{15}	2.72×10^{-2}
G_1	"	"	"	8	306	6	1.5×10^6	0.47	6.9×10^{15}	6.04×10^{-3}
G_2	"	"	"	8	256	6	1.6×10^4	0.43	1.39×10^{16}	2.81×10^{-2}
H_1	1-Mono-hydroxy-	"	"	8	306	24	1.5×10^4	0.54	2.90×10^{15}	1.43×10^{-1}
H_2		"	"	8	256	24	1.6×10^4	0.40	2.36×10^{16}	1.66×10^{-2}
J_1	1,2,4-Tri-hydroxy-	"	"	8	306	24	9.2×10^4	0.59	5.99×10^{15}	1.14×10^{-2}
J_2		"	"	8	256	24	3.2×10^6	1.4	4.95×10^8	39.5
K_1	1,2,5,8-Tetra-hydroxy	"	"	8	306	24	1.4×10^6	0.50	4.73×10^{15}	9.44×10^{-3}
K_2		"	"	8	256	24	3.5×10^9	—	—	—

droxyanthraquinone (ANQN-2), 1,2,4-trihydroxyanthraquinone (ANQN-3), or 1,2,5,8-tetrahydroxyanthraquinone (ANQN-4). $ZnCl_2$ was used as catalyst.

The effect of substituent groups on anthraquinone, of mole ratio, and of temperature on the physical properties of the resultant polymers was studied in the manner of Latin square variations.

Experimental

The reacting monomers were carefully purified until the melting point range was within 0.5°C. They were then mixed by grinding thoroughly with catalyst, placed in a test tube and reacted at 256°C. (biphenyl bath) or 306°C. (benzophenone bath) for a specified number of hours. In some cases the reaction was carried out under a blanket of nitrogen, in an attempt to exclude oxygen. All reactions yielded black, hard polymers. The crude product was again finely ground and leached with 10% hydrochloric acid solution for about 24 hr. to extract the catalyst and anhydrides. It was then exhaustively extracted with boiling distilled water, ethyl alcohol, and benzene, successively, for 24 hr. each, in a Soxhlet extraction apparatus. The polymer, insoluble in the above solvents, was dried at 60°C. in air and stored in a desiccator. The appropiate data on the eighteen polymers appear in Table I. Samples of four of these polymers were analyzed for carbon, oxygen, and hydrogen, and the results are shown in Table II. Radioactivation analyses for Zn showed less than 5 ppm of Zn remaining.

TABLE II

Compound	C, %	H, %	O, %
A_2	79.29	3.10	15.23
B_2	75.09	2.75	19.53
H_1	82.85	3.53	10.59
J_1	71.03	2.76	23.91

Resistivity measurements on the polymers were made by placing the sample between two finely polished stainless-steel electrodes with a phenolic resin tube as a retaining ring. The electrodes had an area of 0.318 cm.^{2}, and the resistance R of the phenolic tube was about 10^{15} ohms. The resistivity cell was placed between two blocks of aluminum, heated with a single insulated coil which had equal lengths of thermal contact with each of the aluminum blocks. The outer surfaces of the aluminum blocks were insulated with thin sheets of phenolic resin (R about 10^{13} ohms) and the whole system was placed in a hydraulic press. The resistance of the sample was measured under pressures of 5700 and 7200 kg./cm.^{2}. Temperature measurements were made with a copper–constantan thermocouple inserted in the cell. Measurements were taken at each temperature after thermal equilibrium had been established in the sample. This required allowing

the sample to remain under a given thermal input for 3–5 hr., so that temperature gradients were essentially eliminated.

Results and Discussion

The resistivities were calculated from the area of the electrodes, the thickness of the sample, and the resistance of the sample. The results appear in Table I. The measured resistivities were observed to obey the empirical relationship of eq. (1):

$$\rho = \rho_0 e^{E_g/2kT} \tag{1}$$

A typical plot of log ρ versus $1/T$ is shown in Figure 1 for samples A_2 and K_1. Both sets of results were taken by gradually increasing the temperature and allowing about two hours for thermal equilibrium. The experimental quantity E_g was obtained from the slopes of these lines. The E_g values thus calculated are given in Table I. It is referred to as the energy interval and was found to be the same for the polymers under consideration at about 0.5 e.v.

The following conclusions were drawn from an examination of the experimental results.

(*1*) The resistivity decreases on increasing the aromatic hydrocarbon to catalyst ratio.

(*2*) The resistivities of the synthesized semiconductors are of the order of 10^4–10^9 ohm-cm.

(*3*) The resistivity also decreases on increasing the reaction time, but changes little after about 30–40 hr.

(*4*) The resistivity increases with increasing the number of substituent groups on the anthraquinone molecule.

(*5*) Homopolymers have higher resistivities than copolymers.

(*6*) The change of resistivity with respect to pressure, at constant temperature, is constant and reversible.

(*7*) No definite relation was found for the effect of polymerization temperature on the polymer resistivity.

The $ZnCl_2$ serves both as a catalyst and solvent in the system investigated here. It is to be expected that dilution of the reactants will decrease the extent of condensation reaction, other factors being held constant. It is then logical to observe as we do that the resistivity is lower, i.e., the extent of the condensation reaction to form conductive polymeric structures is higher, in these polymers prepared either at low dilution in $ZnCl_2$ or for longer reaction times. A plot of the conductivity against catalyst concentration must then be expected to show a maximum at some optimum $ZnCl_2$ concentration.

A similar conclusion may be drawn about the relative conductivities of the variously substituted anthraquinone polymers. Decreasing the number of remaining reactivities on the aromatic portion of the anthraquinone molecule in the progression mono- through tetrahydroxy-sub-

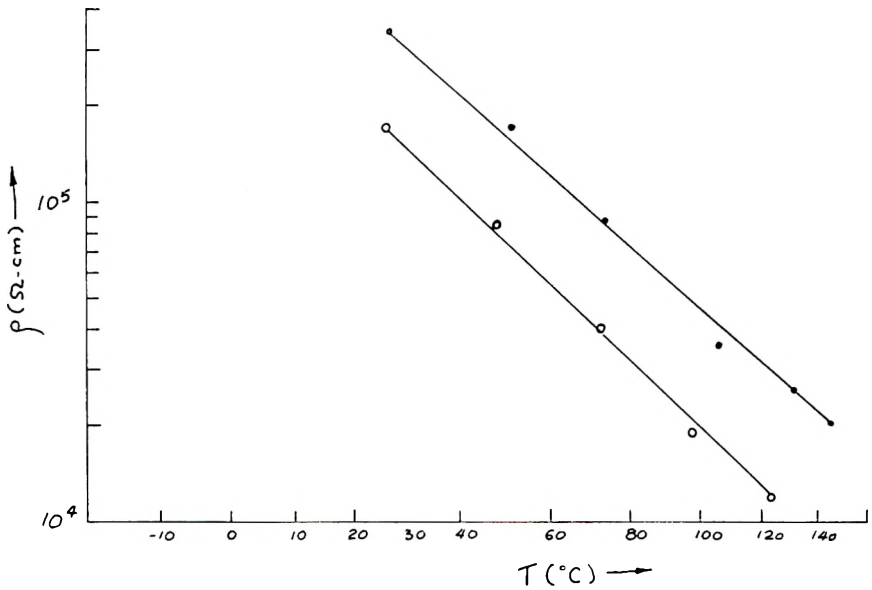

Fig. 1. (O) A_2, copolymer of 1,8-dihydroxyanthraquinone, naphthalic anhydride, and pyromellitic dianhydride. (●) K_1, copolymer of 1,2,5,8-tetrahydroxyanthraquinone, naphthalic anhydride, and pyromellitic dianhydride.

stituted anthraquinone might be expected to interfere increasingly with the condensation reactions leading to the formation of the conductive polymeric structures. It is not surprising, therefore, to observe that the relative resistivities of the polymers increase in that order.

It is also understandable that the increased probability for ether-link formation by hydroxyl-hydroxyl condensation in the presence of the $ZnCl_2$, in the order mono- through tetrahydroxy-derivatives will compete with and diminish the extent of conductive conjugated polymeric structures.[5] There is considerable evidence that the presence of two single bonds in series between conjugated portions of the polymer greatly reduces the electron transport abilities, by reducing the extent of π-electron conjugation between the conjugated portions (compare, for example, polystyrene with polyphenylene). For these reasons, then, it is reasonable to expect that the relative resistivities of the polymers increase in the order mono-, di-, tri-, tetrahydroxyanthraquinone, which is what was observed.

If one uses the formalism of the simple intrinsic semiconductor band model, assuming that mobility is governed by lattice scattering and obeys a three-halves power in its temperature variation, one can calculate the carrier concentrations and mobilities. By use of eqs. (2)-(4)[7]

$$n_i = n_0 e^{-E_g/2kT} \tag{2}$$

$$\sigma = |e| \mu_{\text{mean}} n_i \tag{3}$$

$$\mu_{\text{mean}} = (\mu_e + \mu_h)/2 \tag{4}$$

one arrives at the values shown in Table I. The carrier concentrations so inferred are in the order of 10^{15} cm.$^{-3}$ and the mobilities in the order of 0.01–1 cm.^{2}/v.-sec. The latter result already indicates that the calculations are made in a region where the lattice scattering model does not apply well (i.e., $\mu < 10$ cm.^{2}/v.-sec.), so that one cannot interpret rigorously the data on these materials using the mathematical formalism implying long scattering mean free paths. The implication that these materials have low carrier mobilities and moderate levels of carrier concentrations does, however, remain and is therefore instructive.

References

1. Pohl, H. A., J. A. Bornman, and W. Itoh, Plastics Laboratory Technical Report No. 60C (Princeton University, 1960).
2. Itoh, W., Master's Thesis, Princeton University, Princeton, N.J., 1960.
3. Pohl, H. A., in *Modern Aspects of the Vitreous State*, J. B. Mackenzie, Ed., Butterworths, London, 1962.
4. Eley, D. D., *Research (London)*, **13**, 293 (1960).
5. Pohl, H. A., *Chem. Eng.*, **68**, 104 (1961).
6. Pohl, H. A., Ed., *Semiconduction in Molecular Solids*, Proc. Princeton University Conference, Ivy-Curtis Press, 1960.
7. Blakemore, J. S., *Elect. Commun.*, **29**, 131, June 1952.

Résumé

Dix-huit polymères polyacènes ont été synthétisés et leurs résistivités ont été trouvées être de l'ordre de 10^4–10^5 ohm-cm. On a trouvé que la résistivité de ces polymères semiconducteurs est sensible à des changements dans les conditions de synthèse, à de changements dans la structure des polymères et à des variations de pression et de température durant l'expérimentation. L'intervalle défendu d'énergie pour ces polymères est d'environ 0.5 eV. Quoique le formalisme du modèle de bande sémi-conductrice intrinsèque ne soit pas strictement applicable aux données pour ces polymères, on a trouvé que pareil traitement était cependant instructif.

Zusammenfassung

Achtzehn Polyacenpolymere wurden synthetisiert und ihr spezifischer Widerstand grössenordnungsmässig zu 10^4–10^5 Ohm-cm bestimmt. Der spezifische Widerstand dieser Polymerhalbleiter war von den Synthesebedingungen, von Veränderungen in der Struktur der Polymeren und von Druck und Temperaturänderungen während der Versuche abhängig. Die verbotene Energielücke betrug bei diesen Polymeren etwa 0,5 eV. Obwohl der Formalismus des einfachen Bandmodells des eigentlichen Halbleiters auf die Ergebnisse an den Polymeren nicht streng angewendet werden konnte, erwies sich eine solche Behandlung doch als recht instruktiv.

Received September 19, 1962

JOURNAL OF POLYMER SCIENCE: PART A VOL. 1, PP. 2213–2218 (1963)

Ebulliometric and Endgroup Molecular Weights of Polyoxypropylene and Polyoxyethylene Glycols*

A. J. HAVLIK, J. MOACANIN, and I. OTTERNESS,† *Jet Propulsion Laboratory, California Institute of Technology, Pasadena, California*

Synopsis

A study was made of the number-average molecular weights of a series of preparations of polyoxypropylene glycol (POPG) and polyoxyethylene glycol (POEG). The number average molecular weights of the POPG and POEG samples were determined by ebulliometry and compared to molecular weights estimated from functional endgroup analyses. Differences in results obtained with the two methods were noted and discussed in terms of the foreign functional group contents of the samples.

I. INTRODUCTION

The number-average molecular weights of polyoxypropylene glycols (POPG) have been estimated from the concentration of hydroxyl groups present in these materials.[1] Additional studies showed that other functional groups such as carbon-carbon double bonds and carbonyl groups[2–4] are also present. Studies of diisocyanate-linked elastomers[5] suggested that the carbon-carbon double bonds replaced some of the terminal hydroxyl groups, and chemical studies[6] indicated that the carbon-carbon double bonds are located at the chain ends. If this is true, the number-average molecular weight as determined from hydroxyl group analysis is in error.

To establish the presence of end groups other than hydroxyls, there is need for fractionation studies and direct molecular weight determinations of POPG's.[7] In the present study, number-average molecular weights ($\bar{M}_n$) were determined on a series of samples of POPG and polyoxyethylene glycols (POEG) by the ebulliometric method. The $\bar{M}_n$ obtained from these measurements were compared to the molecular weight values calculated from the hydroxyl and total functional group contents, respectively. These comparisons showed that other functional groups in addition to the hydroxyls must be considered as chain ends in the POPG materials.

* This paper presents results of work carried out at Jet Propulsion Laboratory, sponsored by the National Aeronautics and Space Administration, Contract No. NAS 7-100.

† Present address: Department of Chemistry, University of Southern California, Los Angeles, California.

II. EXPERIMENTAL

A. Materials

Benzene, Baker's Reagent Grade, was distilled and contained less than 0.01% water (Karl Fischer method).

Biphenyl, obtained from A. Daigger and Co., Los Angeles, California, was recrystallized twice from benzene, dried, and then sublimed under vacuum.

Naphthalene, obtained from Eastman Organic Chemicals, Rochester, New York, was used as received.

The polyoxypropylene glycols, P-400 and P-750, and the polyoxyethylene glycol, E-600, were obtained from the Dow Chemical Co., Midland, Michigan; PPG-2025 was obtained from the Union Carbide Chemicals Co., New York, N. Y. The POPG fraction of molecular weight ca. 5000 was obtained by fractional precipitation of a sample of POPG[8] prepared by the potassium hydroxide-catalyzed polymerization of propylene oxide.[2]

B. Chemical Group Analysis

An estimate of the functional group content was obtained by either chemical or spectral methods for each sample of the polyether glycols. The analyses for the hydroxyl groups were carried out by either acetylation or infrared techniques,[1] and the unsaturation content was obtained by the mercuric acetate procedure.[3] As part of the determination of unsaturation, the acidity contents or carboxyl groups were determined. Analyses for carbonyl groups were made by both infrared and oximation techniques.[7] The infrared procedure for the carbonyl groups was based on the assumption that all such groups show the same extinction coefficient at 5.75 μ.

C. Viscometry

Kinematic viscosities were determined in Cannon-Ubbelhode suspended-level capillary viscometers. The two viscometers used were calibrated with viscosity standard oil K (National Bureau of Standards), and had efflux times of 128.9 and 332.5 sec., respectively, at 25.00 ± 0.02°C. The efflux times for the POPG and POEG were from 80 to 800 sec.

D. Ebulliometry

The boiling-point-elevation measurements were made in a differential ebulliometer (manufactured by Hallikainen Instruments, Berkeley, California) which was a less sensitive version of the instrument described by Dimbat and Stross.[9] Solutions of biphenyl in benzene were used to calibrate the instrument. Additional calibration values obtained on naphthalene solutions checked the biphenyl values within ±1%. Reliable measurements of temperature differences ΔT could be made 0.001 to 0.0005°C. Inasmuch as a 1% solution of a substance of molecular weight 4000 in benzene gives a ΔT of about 0.007°C., a precision of ±8% should be ex-

TABLE I
Molecular Weights and Functional Group Analyses of POPG's

Preparation	Analyses				Molecular weight		
					Endgroups		Boiling point
	Hydroxyl, meq./g.	Unsaturation, meq./g. × 10^2	Carbonyl meq./g. × 10^2	Acidity meq./g. × 10^2	M_{OH}	M_{total}	M_{eb}
P-400 (VII-D-39)	4.53; 4.59	0.27; 0.27	<1.0	0.38	442; 436	438	425; 425; 423
P-750 (VII-D-X)	2.94; 2.94; 2.93; 2.93	0.54; 0.54	3.8	0.21	681; 681; 683; 683	671	666; 670; 665; 665
PPG 2025 (VII-D-45)	0.94; 0.94	7.08; 7.08	<1.0	0.12	2125; 2125	1960	2000; 1960; 1900; 1900
POPG Fraction 11[a] (IV-D-56-13B)	0.31	(16)	2.0	(0.25)	6540	(4100)	5000; 5300; 5200; 4400

[a] Molecular weight by light scattering M_w 5900, molecular weight from intrinsic viscosity in methanol M_v 5400. Unsaturation and acidity analyse not available; values shown are for the unfractionated polymer. Hydroxyl for this sample by *IR;* for others, by acetylation.

pected for this range. For lower molecular weights the precision is proportionately better.

To evaluate the apparatus for polyether type materials, measurements were made on four POPG preparations; the results are given in Table I. For P-400 and P-750, molecular weights agreed to better than ±0.5% (i.e., 423–425, and 665–670) and for PPG-2025, ±2.5% (1900–2000). For the POPG fraction 11, molecular weights agreed to ±8% (4400–5300). These results show that precise molecular weight measurements can be made below 1000, although useful results are obtained up to 5000. For high molecular weights the response could not be increased by going to higher concentrations because of foaming. For PPG-2025 the slope of $\Delta T/c$ vs. concentration gave a second virial coefficient of 20×10^{-4}; for the fraction, the scatter was too high to get a significant slope estimate. For P-400 and P-750 the slope was zero over the concentration range studied.

III. DISCUSSION

Number-average molecular weights from ebulliometry (M_{eb}) and functional group contents for four samples of POPG are given in Table I. Molecular weights were calculated from both the hydroxyl and total functional group contents, assuming every molecule to be difunctional. The total group content is the sum of the hydroxyls, carbon-carbon double bonds, carboxyls, and carbonyls. As can be seen the major contribution to the total number of functional groups is given by the hydroxyls. The other groups are present in smaller but significant amounts. For all the samples, the total-functional-group molecular weights are in good agreement with M_{eb}, while the hydroxyl molecular weights (M_{OH}) are significantly larger than those obtained from ebulliometry. This shows that, in the bulk samples of the POPG's studied, other endgroups are present in addition to hydroxyls, and it is very likely that these are made up of the total of the other functional groups found by chemical analysis.

Further studies were made of the M_{eb} and M_{OH} for fractions of POPG obtained by molecular distillation of P-750.[7] Table II gives both molecular weight values, together with values for the bulk viscosities of the fractions. The progressive increase in M_{eb} is paralleled by an increase in ν, showing that separation on the basis of molecular weight was achieved by distillation. Excepting fraction 10 and the residue, the M_{OH} values are consistently higher. by about 30 units, than M_{eb}, again indicating that not all chain ends are hydroxyl terminated. The results given in Table II are internally consistent, since M_{eb} for unfractionated polymer and the weighted average of the fractions are the same (665). Similar agreement is obtained from the M_{OH} values.

The results of a similar study carried out on polyoxyethylene glycol are given in Table III. Again, there is a progressive increase for ν, M_n and M_{OH}. The weighted M_{eb} for the fractions is 630, in excellent agreement with 625 for the unfractionated polymer; the weighted M_{OH} is 633, again

TABLE II
Molecular Weights and Bulk Viscosities of POPG Fractions

Fraction	Hydroxyl, meq./g.	Viscosity at 25.00°C., cstokes	Molecular weight[a]	
			M_{OH}	M_{eb}
1	3.69	62.3	542	489; 498
2	3.33	81.2	600	564; 498
3	3.07	88.3	652	612; 615
4	2.96	93.0	676	644; 654
5	2.81	98.0	712	679; 686
6	2.73	102.8	733	702; 713
7	2.62	108.0	764	726; 733
8	2.48	114.3	807	779; 761
9	2.34	121.7	856	815; 828
10	2.24	133.8	893	899; 912
Still residue	1.95	242.3	1025	1230; 1200

[a] Fractions (VI-D-22) obtained by molecular distillation of P-750. $M_n = [\Sigma(w_i/M_i)]^{-1} = 712$; including the contents of the cold trap (1.35% of total) and assuming it to be dipropylene glycol, then $M_n = 665$ in agreement with the unfractionated polymer. Similarly, $[OH] = \Sigma w_i[OH]_i = 2.70$ meq./g. giving $M_n = 739$; again, by estimating a correction for the cold trap content one gets agreement with the unfractionated polymers.

in agreement with 630 for the unfractionated polymer. For this material, in contrast to POPG, there is no systematic deviation between M_{eb} and M_{OH}. This shows that POEG is virtually all hydroxyl-terminated and that the deviations between M_{eb} and M_{OH} observed for POPG's are not an artifact.

TABLE III
Molecular Weights and Bulk Viscosities of POEG Fractions

Fraction	Hydroxyl, meq./g.[b]	Viscosity at 60.0°C., cstokes	Molecular weight[a]	
			M_{OH}	M_{eb}
1	5.06; 5.07	18.3	395; 394	393; 391
2	4.13; 4.17	21.8	484; 480	478; 486
3	3.80; 3.76	23.0	526; 532	523; 515
4	3.61; 3.62	24.5	554; 553	556; 562
5	3.29; 3.23	26.1	608; 620	585; 595
6	3.12; 3.15	27.7	641; 635	624; 614
7	3.02; 3.01	28.9	662; 665	650; 657
8	2.92; 2.91	31.2	685; 688	696; 694
9	2.79; 2.72	32.7	717; 736	717; 740
10	2.59; 2.62	34.9	772; 764	796; 782
Still residue	2.18; 2.15	41.9	917; 930	918; 930

[a] Acetylation carried out in sealed tubes. This modification of the standard procedure[1] was carried out by S. Vango, JPL.

[b] Fractions (VII-D-40) obtained by molecular distillation of E-600 (IV-O-64). $M_{eb} = 625 \pm 8$, [OH] = 3.17 and 3.18 by acetylation, unsaturation $< 10^{-3}$ meq./g., $M_{OH} = 630$. For combined fractions $M_n = [\Sigma(w_i/M_i)]^{-1} = 630$. Similarly $[OH] = \Sigma w_i[OH]_i = 3.16$ meq./g., giving $M_n = 633$.

IV. CONCLUSIONS

The results of the present study definitely establish the presence of end groups other than terminal hydroxyls in POPG, for molecular weights up to 5000. It follows, therefore, that the hydroxyl group content provides an upper limit for the number-average molecular weight of the POPG's. The difference between M_{OH} and M_{eb} can be quantitatively accounted for by the other functional groups present. In contrast, the low molecular weight POEG's are completely hydroxyl-terminated. These conclusions, of course, are of importance to the characterization of POPG's and POEG's used in the study of diisocyanate-linked elastomers and foams.

References

1. Burns, E. A., and R. F. Muraca, *Anal. Chem.*, **31**, 397 (1959).
2. St. Pierre, L. E., and C. C. Price, *J. Am. Chem. Soc.*, **78**, 3432 (1956).
3. Burns, E. A., R. F. Muraca, and F. Chang, Progr. Rept. No. 20-345, Jet Propulsion Laboratory, Pasadena, California, January 1, 1958.
4. Havlik, A. J., and A. F. Hildebrandt, Paper 34, Division of Polymer Chemistry, presented to the 134th Meeting of the American Chemical Society, September 1958.
5. Smith, T. L., and A. B. Magnusson, *J. Polymer Sci.*, **42**, 391 (1960).
6. Dege, G. J., R. L. Harris, and J. S. MacKenzie, *J. Am. Chem. Soc.*, **81**, 3374 (1959).
7. Havlik, A. J., "Chemical Structure and Molecular Weight Distribution of Polyoxypropylene glycol," in preparation.
8. Moacanin, J., and A. J. Havlik, Paper 47, Division of Polymer Chemistry, presented to the 135th Meeting of the American Chemical Society, April 1959.
9. Dimbat, M., and F. H. Stross, *Anal. Chem.*, **29**, 1517 (1957).

Résumé

On a étudié les poids moléculaires moyens en nombre de séries de polyoxypropylène glycol (POPG) et de polyoxyéthylène glycol (POEG). Les poids moléculaires moyens en nombre ont été déterminés par ébullioscopie et comparés aux poids moléculaires estimés au départ d'analyses de fonctions terminales. On a noté les différences des résultats obtenus par les deux méthodes et celles-ci sont discutées en termes de concentration de groupements fonctionnels voisins des échantillons.

Zusammenfassung

Das Zahlenmittel des Molekulargewichts einer Reihe von Polyoxypropylenglykol-(POPG)- und Polyoxyäthylenglykol-(POEG)-präparaten wurde untersucht. Die Zahlenmittelwerte des Molekulargewichts der POPG- und POEG-Proben wurden ebullioskopisch bestimmt und mit den aus der Endgruppenanalyse erhaltenen Werten verglichen. Unterschiede zwischen den Ergebnissen der beiden Methoden wurden festgestellt und auf Grundlage der Annahme eines Gehaltes der Proben an funktionellen Fremdgruppen diskutiert.

Received August 21, 1962

JOURNAL OF POLYMER SCIENCE: PART A VOL. 1, PP. 2219–2224 (1963)

Poly(4-methyl Pentene): X-Ray Measurement of Crystalline Density and Observation of a Structural Anomaly

MORTON LITT, *Central Research Laboratory, Allied Chemical Corporation, Morristown, New Jersey*

Synopsis

The unit cell of annealed poly(4-methyl pentene) was measured by x-rays; the unit cell is tetragonal with $a = b = 18.50 \pm 0.03$ A. and $c = 13.76 \pm 0.07$ A., which leads to a crystalline density of 0.832. This is lower than the density of the quenched polymers. Previous workers have postulated a 7_2 helix for the polymer. A reflection of 001 was observed consistently, which is forbidden for this helix. A superficial investigation indicates that the polymer crystallizes in a helical form but probably the side groups are displaced from a helical arrangement because of interference by neighboring side groups.

Introduction

The unit cell of poly(4-methyl pentene) has been determined recently[1] and a crystalline density of 0.813 was obtained. Since the polymer density is in the range of 0.831 to 0.838, it was thought worth while to redetermine the unit cell dimensions to see whether this very strange result was really correct. Other workers[2] have commented on it and have given a figure of 0.828 for the crystalline density, which is still below that of the polymer. In the present work, while the unit cell measurements were being made, some new information was found which will be discussed in relation to the conformation of the polymer chain.

Experimental

Extruded fibers of polymer were slowly drawn in an environmental chamber at 120°C. to a 10:1 draw ratio. When a large length of fiber was needed, ordinary fiber with a 10:1 draw ratio was used. Fiber photographs were taken on a Unicam flat plate camera at 4 and 5 cm.

For the unit cell determination, $hk0$ spacings were found by wrapping oriented annealed fiber around the sample holder of the Norelco wide-angle goniometer at right angles to the x-ray beam and scanning the reflections. X-ray photographs of such fibers show essentially complete orientation, all reflections on all layers being elliptical spots rather than arcs.

The layer line spacings were determined by placing an oriented fiber in a

5.74 cm. radius powder camera with its axis perpendicular to the x-ray beam and parallel to the flat sides of the camera. Angular measurements were taken at the meridian and d spacings calculated[3] according to the formula $\lambda = d \sin 2\theta$.

Results and Discussion

Table I lists the d spacings found for the layer lines. A value was found for c equal to 13.76 ± 0.07 A. for two standard deviations of the mean.

TABLE I
Layer Line Spacings of Oriented Fiber

l index	Obsd. d, A.	d (calcd.), A.[a]
1	13.77	13.76
2	6.90	6.88
3	4.57	4.59
4	3.44	3.44
5	2.76_1	2.75_2
6	2.92_2	2.29_4

[a] c = 13.76 ± 0.07 A.

Observations of the reflections were made as far as 53.4° of 2θ in the $hk0$ plane and are listed in Table II along with calculated d spacings based on $a = b = 18.50$ A. Relative structure factors corrected for single-crystal Lorentz and polarization factors are given too, since these were obtained

TABLE II
$hk0$ Reflections of Poly(4-methyl Pentene)

Index	Obsd. d, A.	Calcd. d, A.[a]	F, obsd.
200	9.25	9.25	95
220	6.50	6.54	33
400	4.60	4.63	12
420	4.15	4.14	26
340	3.71_0	3.70_0	3
440	3.28_7	3.27_0	8
600	3.08_4	3.08_3	6
620	2.92_3	2.92_6	(b)
640	2.57_0	2.56_6	(b)
800	2.31_0	2.31_3	5
820	2.25_0	2.24_2	6
660	2.17_6	2.18_0	4
840	2.07_8	2.06_8	4
670	1.99_9	2.00_7	3
860	1.84_6	1.85_0	3
1000	1.84_6	1.85_0	3
1020	1.82_4	1.81_4	3
1040	1.71_6	1.71_6	3

[a] $a = b = 18.50 \pm 0.03$ A.
[b] Too small to be measured.

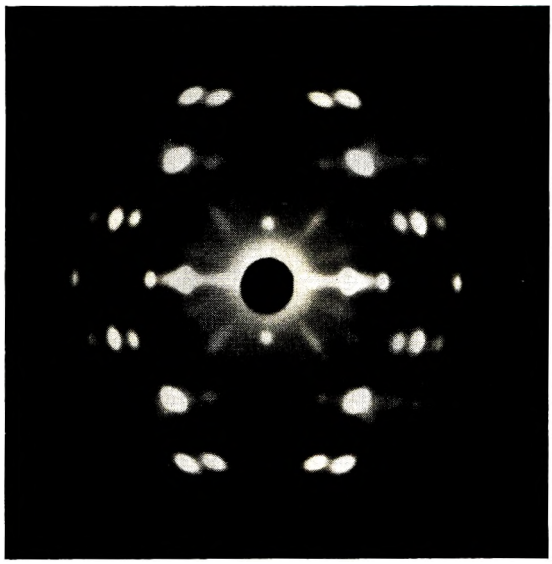

Fig. 1. Flat plate photograph of oriented fiber of poly(4-methyl pentene) with filtered Cu$K\alpha$ radiation; fiber normal to x-ray beam.

easily from the goniometer tracings. The only reflections with h or k odd that could be observed are shown in Table II; the others, listed by Frank et al.,[1] such as 210 and 320, were unobservable.

The density of the unit cell is 0.382 ± 0.007 at room temperature, which is still below most of the experimental values but checks well with the 0.828 of Griffith et al.[2] Since the density of a quenched and therefore amorphous sample was found[2] to be 0.838, the strange fact still remains that the crystalline polymer is of lower density than a quenched or amorphous polymer.

Annealed polymer samples have the crystalline density and must therefore be almost wholly crystalline. This is borne out by the almost complete lack of amorphous scattering in the fiber photographs.

During this investigation an interesting observation was made. The fiber photographs showed a weak but consistent 001 reflection. The only other meridional reflection that could be observed was the expected 007. This is illustrated in Figures 1 and 2 which show the photographs of a fiber normal to the x-ray beam and with the fiber at an angle of 3.4° to the normal, which would cause the reflection to split if it were not truly 001. If the molecule crystallizes in a perfect 7_2 helix, the 001 reflection is precluded.[4] The polymer therefore cannot be a perfect helix in the crystallite of oriented fiber.

An attempt was then made to determine whether the molecule was an irregular helix or had a nonhelical structure. This was done by assuming the molecule was a regular helix—for example, as described by Corradini and Pasquon.[5] The structure factors signs were then fixed for the $hk0$ projections with the use of Keller's postulate[1] that the space group was $P\bar{4}$,

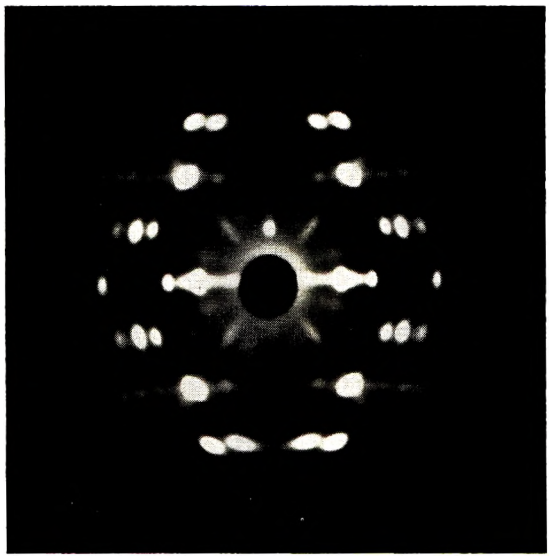

Fig. 2. Flat plate photograph of oriented fiber of poly(4-methyl pentene) with filtered Cu$K\alpha$ radiation; fiber tilted 3.4° from normal.

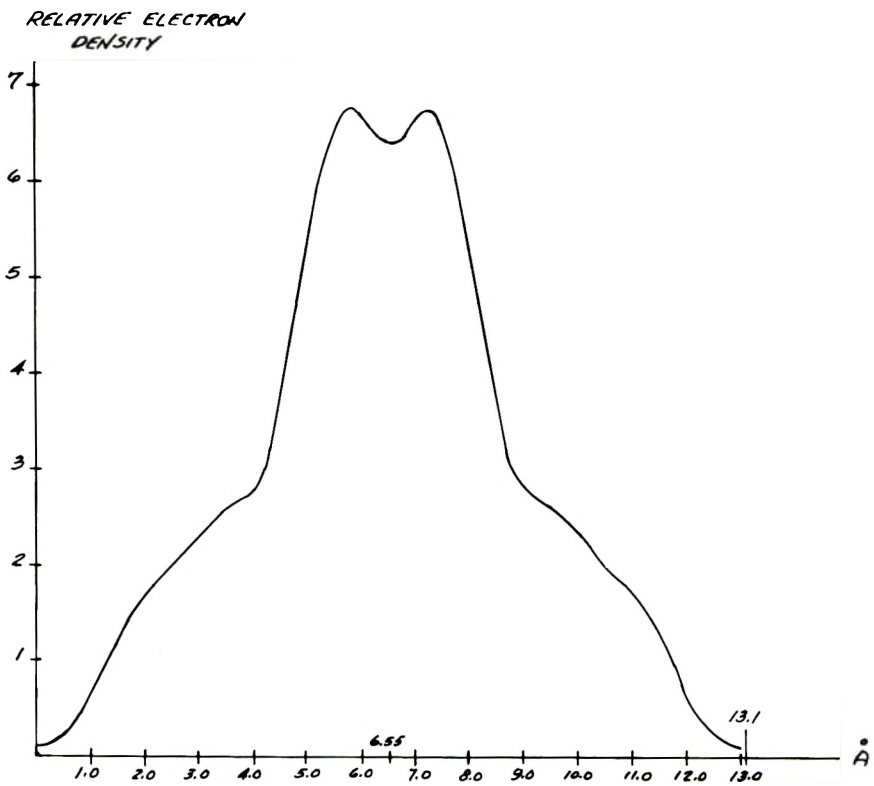

Fig. 3. Cross section of poly(4-methyl pentene) helix along diagonal for one half of unit cell. Projected on x-y plane.

and the chain axes were projected on the points $^1/_4$, $^1/_4$; $^1/_4$, $^3/_4$; etc., of the x-y plane. Three possible helices were considered: first, that postulated by Corradini and Pasquon,[5] where the Bessel function summation is positive to index 600 and negative afterward; second, when the summation is positive to 220 and negative afterward; and third, where the summation is positive to 220, negative to 600, and positive afterward. The last two hypothetical Bessel function summations are based on the work of Frank et al.,[1] who thought that the intensity of the reflections went through 0 at about d = 3.5 A., between indices 220 and 400.

It was felt that if the molecule were an irregular helix, one of these summations would give a projection which made sense from a chemical standpoint. If the molecule were not helical, then an attempt to force it into that shape by picking the Fourier signs as above would lead to a projection which would make chemical nonsense. In fact, the first summation, based on the postulation of Corradini and Pasquon,[4] gave a perfect projection though no atoms or groups were resolved, so that poly(4-methyl pentene) is probably very much like their postulated structure. A cross section through the diagonal, where there is no overlap with other molecules, is shown in Figure 3.

One can tentatively conclude that the molecule is an irregular helix in the crystallite. The lack of symmetry is probably caused by a combination of interference between isobutyl side chain groups on adjacent turns of the helix and the necessity of fitting into the neighboring molecules. The diameter of the helix is about 10.5 A. and, as the center-to-center distance is only 9.25 A., there is considerable overlap between chains.

I should like to thank Mr. Forrest Rahl for his interest and cooperation with the experimental work. The gift of the monomer, 4-methyl pentene, by the California Chemical Company, is greatly appreciated.

References

1. Frank, F. C., A. Keller, and A. O'Connor, *Phil. Mag.*, **8**, (4), 200 (1959).
2. Griffith, J. H., and B. Ranby, *J. Polymer Sci.*, **44**, 369 (1960).
3. *International Tables for X-ray Crystallography*, The Kynoch Press, Birmingham, England, 1959, Vol. 2, p. 178, Eq. (25) Modified.
4. Cochran, W., F. H. C. Crick, and V. Vand, *Acta Cryst.*, **5**, 581 (1952).
5. Corradini, P., and I. Pasquon, *R. C. Accad. Lincei*, **19**, 453 (1956).

Résumé

On a mesuré par rayons-X la cellule unitaire du poly(4-méthyl pentène) recuit; la cellule unitaire est tétragonale et $a = b = 18.50 \pm 0.03$ A. et $c = 13.76 \pm 0.07$ A. ce qui donne une densité à l'état cristallin de 0.832. Ceci est plus faible que la densité des polymères refroidis brutalement. Des chercheurs ont postulé antérieurement une configuration hélicoïdale 7_2 pour le polymère. On a toutefois observé une réflection, 001, interdite pour cette hélice. Un examen superficiel indique que le polymère cristallise sous forme hélicoïdale mais que des groupements latéraux sont probablement déplacés de cet arrangement hélicoïdal à cause d'une interférence avec les groupements voisins.

Zusammenfassung

Die Elementarzelle von getemperten Poly(4-methylpenten) wurde mit Röntgenstrahlen gemessen; die Elementarzelle ist tetragonal mit $a = b = 18{,}50 \pm 0{,}03$ A. und $c = 13{,}76 \pm 0{,}07$ A.; daraus ergibt sich die kristalline Dichte zu 0,832. Sie ist kleiner als die Dichte des abgeschreckten Polymeren. Frühere Autoren haben für das Polymere eine 7_2-Helix angenommen. Ein für diese Helix verbotener Reflex, 001, wurde durchwegs beobachtet. Eine vorläufige Untersuchung zeigt, dass das Polymere in einer Helix kristallisiert, dass aber die Seitengruppen, wahrscheinlich wegen der gegenseitigen Beeinflussung benachbarter Gruppen, aus der Helixanordnung verschoben sind.

Received June 29, 1962

JOURNAL OF POLYMER SCIENCE: PART A VOL. 1, PP. 2225–2230 (1963)

The Chemical Structure of Polyisobutylene Obtained by Ziegler Catalysis

R. BACSKAI and S. J. LAPPORTE, *California Research Corporation, Richmond, California*

Synopsis

The chemical structure of polyisobutylene prepared with different catalysts was studied by independent physicochemical methods. No significant difference has been found in the infrared spectra, proton magnetic resonance spectra, and viscosity behavior of polymers prepared with Ziegler catalysts compared to a sample of polyisobutylene obtained with BF_3 catalyst. The methyl–methylene proton ratio in the polymers was determined from their proton magnetic resonance spectra. Based on these results, the normal polyisobutylene structure was assigned to the polymers. The rearranged structure as suggested by Topchiev and coworkers was ruled out. Alkylation studies with liquid isobutylene polymers substantiated this finding.

The polymerization of isobutylene with Ziegler catalysts was first reported by A. V. Topchiev and co-workers.[1a,b] The Soviet workers found that the addition of relatively small amounts of $TiCl_4$ to $AlEt_3$ forms an active catalyst capable of polymerizing isobutylene at 0°C. to a product having a molecular weight of 5000–6000. It was also reported that the molecular weight of the polymer could be varied by changing the polymerization temperature; and polyisobutylene with a molecular weight of 12,000 was obtained at −50°C.

Topchiev and co-workers made the observation that polyisobutylene, synthesized with a Ziegler catalyst, has a considerably flatter viscosity curve than the products obtained with conventional acid catalysts. Since the infrared spectra of the polymers were also different, they concluded that the organometallic catalyst leads to macromolecules of a different type than that found in polyisobutylenes previously known.[1a]

In a subsequent publication, it was tentatively proposed that the differences arise due to the rearranged polymer structure (I) formed in the presence of the Ziegler catalyst compared to the normal polymer (II) obtained with conventional acidic catalysts.[1b] No analogous reaction has

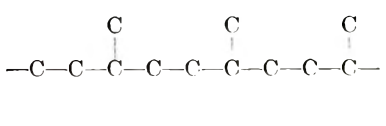

(I)

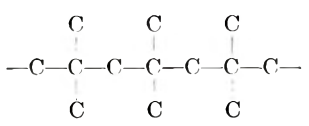

(II)

been reported in the polymerization of other alpha olefins with Ziegler catalysts.[2] Since the polymer represented by (I) would be of theoretical and possibly of commercial interest and is not available by a direct, unequivocal synthesis, we tried to confirm the structural assignment of the Soviet authors by both physical and chemical methods.

Isobutylene was polymerized with Ziegler catalysts following the experimental procedure outlined by Topchiev and co-workers. For comparison, a BF_3-catalyzed polyisobutylene was also prepared. The results are summarized in Table I.

TABLE I
Polymerization of Isobutylene

Catalyst system	[Al]/[Ti]	Solvent	Temp., °C.	Molecular weight[a]	Physical appearance of polymer
$(C_2H_5)_3Al + TiCl_4$	2	*n*-Heptane	−30	21,000	Tacky rubber
$(C_2H_5)_3Al + TiCl_4$	0.5	*n*-Heptane	−30	29,000	Tacky rubber
BF_3	—	CH_2Cl_2	−78	19,000	Tacky rubber
$(iso—C_4H_9)_3Al + TiCl_4$	0.5	Hexane	50	—	Viscous oil[b]
$(iso—C_4H_9)_3Al + TiCl_4$	24	Hexane	50	—	[c]
$(C_2H_5)_3Al + TiCl_3$[d]	2	*n*-Heptane	−30	—	[c]

[a] Calculated from viscosity measurements.
[b] 92% conversion of isobutylene, 36% dimers and trimers.
[c] No polymer formation.
[d] Stauffer Chemical Company, $TiCl_3AA$.

Infrared Spectra

The infrared spectra of the rubbery polymers prepared with either Ziegler catalysts or BF_3 were identical with each other. A typical spectrum

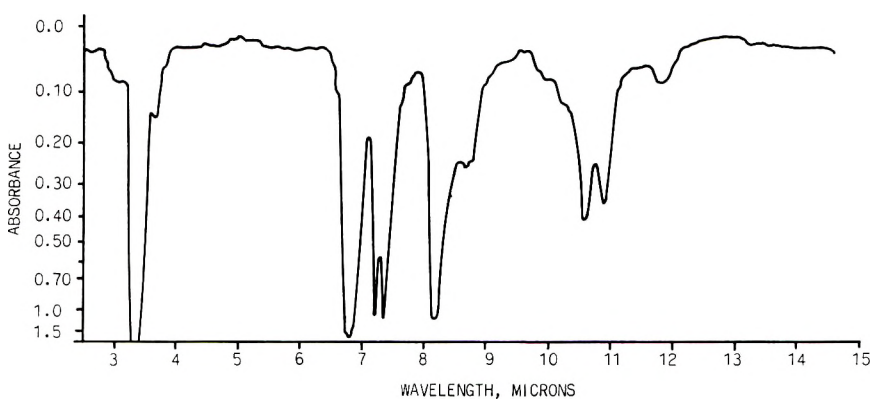

Fig. 1. The infrared spectrum of polyisobutylene prepared with different catalysts.

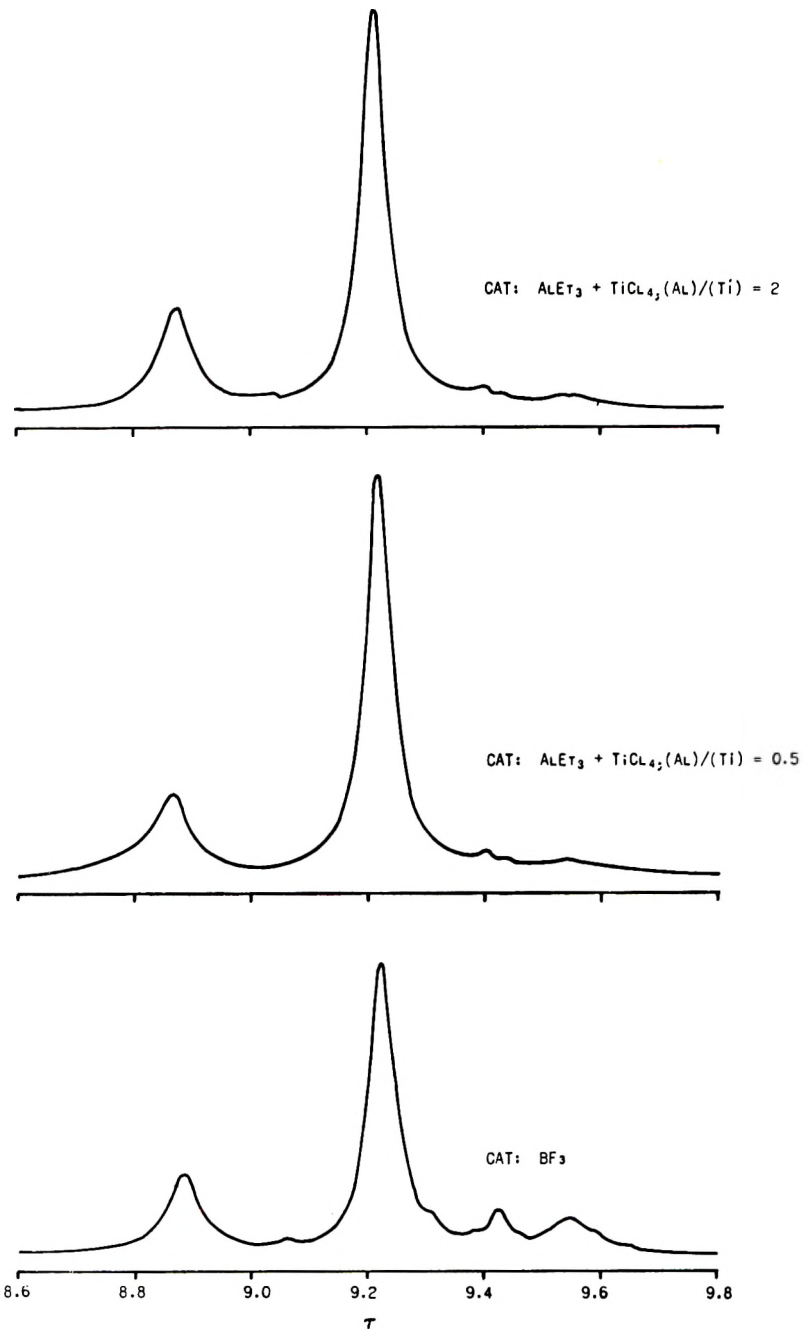

Fig. 2. The proton magnetic resonance spectra of polyisobutylenes prepared with different catalysts.

is indicated in Figure 1. Most revealing are the split methyl absorptions at 7.2 and 7.3 μ characteristic of *gem*-dimethyl groups.[3a] The infrared spectrum of the lower molecular weight polymer prepared at 50°C. was essentially the same as that shown in Figure 1 except for new absorptions at 11.2 and 11.8 μ, characteristic of unsymmetrically-disubstituted and trisubstituted double bonds expected as end groups in a polymer of structure (II).[3b]

Proton Magnetic Resonance Spectra

Most definitive in elucidating the structures of the polyisobutylenes are the proton magnetic resonance spectra. These are shown in Figure 2 and tabulated in Table II. The high molecular weight polymers prepared by the different catalysts each contain methyl and methylene protons, in a ratio close to 3, at τ[4] values of 8.88–8.89 and 9.22–9.24, respectively. This CH_3/CH_2-proton ratio is inconsistent with the rearranged structure (I) and can best be accommodated by the normal structure (II). The slight deviation from the theoretical CH_3/CH_2-proton ratio and the appearance of weak absorptions at higher fields point to the presence of some other structure in the polymers. The nature of this additional minor structure is not known, but it is evident that it is present to a larger extent in the BF_3-catalyzed polymers.

TABLE II
Proton Magnetic Resonance Spectra of Polyisobutylenes[a]

Catalyst	[Al]/[Ti]	τ	Relative intensity
$AlEt_3 + TiCl_4$	2	8.89	1.0
		9.22	2.7
		9.43, 9.58	0.15
$AlEt_3 + TiCl_4$	0.5	8.88	1.0
		9.24	2.9
		9.42	0.14
		9.58	0.09
BF_3	—	8.89	1.0
		9.22	2.7
		9.43	0.29
		9.55	0.43

[a] Spectra run on Varian A-60 NMR spectrometer as 20% solutions in benzene at room temperature under standard operating conditions.

Viscosity Behavior

It is expected that any major difference in the chain structure of the different polyisobutylenes should also be reflected in the viscosity behavior of their solutions. Figure 3 indicates the concentration dependence of the reduced specific viscosity for dilute solutions of the high polymers. The

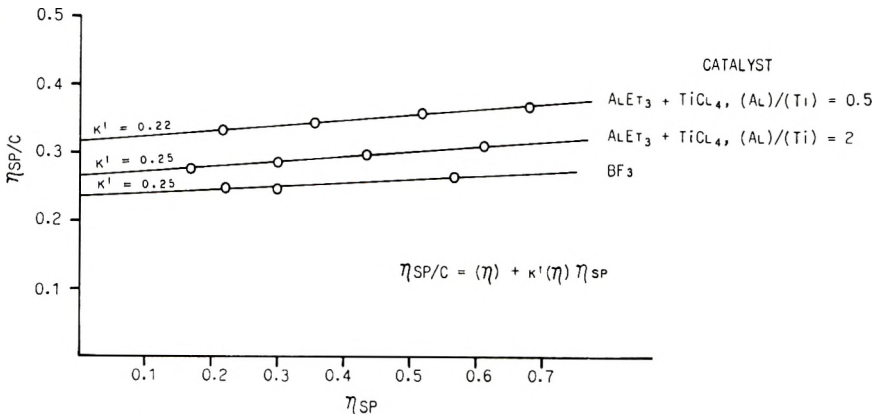

Fig. 3. The change of reduced specific viscosity with specific viscosity for polyisobutylenes obtained with different catalysts.

Huggins constants[5] of the polymers do not vary considerably, indicating that there exists no fundamental difference in the skeletal structure of the polyisobutylenes studied.

Alkylation Stability of Polymers

The stability of the lower molecular weight polyisobutylenes to HF catalyzed alkylation of aromatics may also be utilized as a criterion of structure. Thus, diisobutylene and toluene give no octyltoluenes on alkylation with HF at 3–6°C. but rather a mixture of *t*-butyl and di-*t*-butyltoluenes, products of olefin fragmentation.[6] On the other hand, straight chain alkenes are stable to HF alkylation, undergoing no fragmentation.[7]

The HF catalyzed alkylation of benzene at 15°C. with a C_8–C_{12} fraction of isobutylene polymer prepared with triisobutyl aluminum-$TiCl_4$ (Al:Ti = 0.5) gave upon distillation, 25% *t*-butylbenzene, 48% dialkylbenzenes containing C_4 and C_8 side chains, and a higher molecular weight residue. This fragmentation is more likely to occur with a compound having structure (II) than structure (I).

Conclusions

There seems to be no significant difference in the chemical structure of polyisobutylenes prepared with either BF_3 or trialkylaluminum-$TiCl_4$ catalysts. All available evidence indicates that normal structural units (II) are dominant in the polyisobutylenes studied in this work; and the rearranged structure (I), proposed by Topchiev and co-workers, must be ruled out.

The structural identity of the polymers suggests that certain Ziegler catalyst systems contain cationic species capable of initiating the polymerization of isobutylene. Our results indicate that at high [Al]/[Ti] ratios the reduction of $TiCl_4$ by aluminum trialkyl compounds is complete enough to destroy the cationic character of the catalyst. This is also borne

out by the fact that $TiCl_3$ (prepared from $TiCl_4$ by Al reduction) in combination with aluminum trialkyl, normally an excellent Ziegler catalyst, is inactive in isobutylene polymerization.

References

1(a) Topchiev, A. V., and B. A. Krentsel, paper given at International Symposium on Macromolecular Chemistry, Prague, 1957, abstract, pp. 42–43. (b) A. V. Topchiev, B. A. Krentsel, N. F. Bogomolova, and Yu. Ya. Goldfarb, *Proc. Acad. Sci. USSR, Chem. Technol. Sect.* (*English Transl.*), **3**, 659–662 (1957).

2. Gaylord, N. G., and H. F. Mark, *Linear and Stereoregular Addition Polymers*, Interscience, New York, 1959, p. 133.

3(a) Bellamy, L. J., *The Infrared Spectra of Complex Molecules*, 2nd ed., Wiley, New York, 1958, p. 24. (b) *Ibid.*, p. 39.

4. Jackman, L. M., *Applications of Nuclear Magnetic Resonance Spectroscopy in Organic Chemistry*, Pergamon Press, London, 1959, p. 47.

5. Huggins, M. L., *J. Am. Chem. Soc.*, **64**, 2716 (1942).

6. Calcott, W. S., J. M. Tinker, and V. Weinmayr, *J. Am. Chem. Soc.*, **61**, 1010 (1939).

7. Olson, A. C., *Ind. and Eng. Chem.*, **52**, 833 (1960).

Résumé

On étudie par différentes méthodes physico-chimique la structure chimique du polyisobutylène préparé avec divers catalyseurs. On ne trouve pas de différences fondamentales dans les spectres infrarouges, dans les spectres de résonance magnétique du proton et dans le comportement viscosimétrique des polymères préparés avec un catalyseur Ziegler, si on les compare à un échantillon de polyisobutyléne obtenu avec le catalyseur BF_3. On détermine le rapport protonique méthyl/méthylène dans les polymères par les spectres de résonance protonique. On donne à ces polymères la structure des polyisobutylène normal sur la base de ces résultats. On exclut la structure réarrangée suggérée par Topchiev et collaborateurs. Les études d'alkylation faites avec les polyméres d'isobutylène liquide soutiennent cette constatation.

Zusammenfassung

Die chemische Struktur des mit verschiedenen Katalysatoren hergestellten Polyisobutylens wurde mit unabhängigen, physikalisch-chemischen Methoden untersucht. Kein charakteristischer Unterschied wurde in den Infrarotspektren, protonmagnetischen Resonanzspektren und im Viskositätsverhalten zwischen Polymeren, die mit Ziegler-Katalysatoren hergestellt wurden, und einer mit BF_3 als Katalysator erhaltenen Polyisobutylenprobe gefunden. Das Methyl-Methylenprotonenverhältnis in den Polymeren wurde aus ihren protonmagnetischen Resonanzspektren bestimmt. Auf Grund dieser Ergebnisse wurde den Polymeren die normale Polyisobutylenstruktur zugeordnet. Die von Topchiev und Mitarbeitern vorgeschlagene Umlagerungsstruktur konnte ausgeschlossen werden. Alkylierungsversuche an flüssigen Isobutylenpolymeren bestätigten diese Befunde.

Received May 18, 1962

JOURNAL OF POLYMER SCIENCE: PART A VOL. 1, PP. 2231–2236 (1963)

Copolymerization Studies. IV. Transannular Copolymerization of Bicyclo[2.2.1]hepta-2,5-diene*

N. L. ZUTTY, *Research and Development Department, Union Carbide Chemicals Company, South Charleston, West Virginia*

Synopsis

Bicyclo[2.2.1]hepta-2,5-diene, in the presence of free-radical initiators, homopolymerizes to a low molecular weight, soluble polymer containing both 3,5-disubstituted nortricyclene and 5,6-disubstituted bicyclo[2.2.1]hept-2-ene units in the polymer backbone. When the bicycloheptadiene (M_2) is copolymerized with vinyl chloride, vinylidene chloride, acrylonitrile, ethyl acrylate, and methyl methacrylate, only the transannular product, 3,5-disubstituted nortricyclene, is found in the high molecular weight copolymers. Reactivity ratios for the above mentioned copolymerizations at 50°C. are: $r_1 = 0.74$, $r_2 = 0.35$; $r_1 = 1.41$, $r_2 = 0.08$; $r_1 = 0.67$, $r_2 = 0.08$; $r_1 = 3.05$, $r_2 = 0.01$; $r_1 = 10.0$, $r_2 = 0$; respectively. From these data, the Q and e values for bicyclo[2.2.1]hepta-2,5-diene average 0.09 and -1.04, respectively.

These investigations stem from two observations. The first was by Schmerling,[2] who noticed that small yields of low molecular weight, soluble, polymers were formed when bicyclo[2.2.1]hepta-2,5-diene (I) was warmed with a radical source. The second was in these laboratories when it was observed that under the mild homopolymerization conditions for bicycloheptadiene, bicyclo[2.2.1]hept-2-ene (II), was almost inert to reaction.

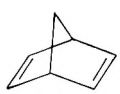

I

II

Since sterically there could not be enough difference between the monoolefin and the diolefin to allow facile polymerization through one double bond in the latter and not the former case, another propagation mechanism must have been in operation.

By analogy with free-radical reactions of bicycloheptadiene[3] it was thought that the homopolymerization could involve an intramolecular addition followed by an intermolecular addition, thus:

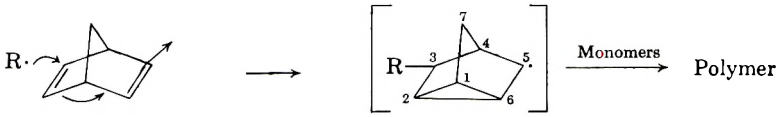

* For Part III of this series, see Burkhart and Zutty.[1]

That just such a mechanism was in operation was easily seen from the infrared spectrum.

The appearance of a strong band at 12.4 μ in the homopolymer absent in both bicycloheptene and bicycloheptadiene was indicative of the 3,5-disubstituted nortricyclene structure (III) in the polymer.[4,5] (The 3,6-disubstituted nortricyclene absorbs at 11.7 μ.[6]) However, the strong band in the homopolymer at 14.1 μ coupled with a band at 6.4 μ also showed the presence of a cis-strained double bond. From such data poly(bicyclo[2.2.1]hepta-2,5-diene) is thought to be a more or less alternating copolymer containing both 3,5-disubstituted nortricyclene (III) and 5,6-disubstituted bicyclo[2.2.1]hept-2-ene (IV) (the structure obtained via addition through only one double bond in its backbone).

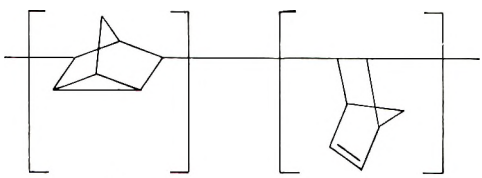

III IV

These data, along with the copolymerization data presented below, make it suspect that the formation of the nortricyclene structure is energetically more favorable than reaction through only one double bond but that steric requirements make it improbable for two nortricyclene units to be adjacent to each other.

It is interesting to note that the distance between the 2-6 and 3-5 carbon atoms in bicyclo[2.2.1]hepta-2,5-diene has been calculated[7] from electron diffraction data and found to be 2.37 A., or about 1.6 times the normal carbon-carbon single bond distance in 1,3-butadiene.

Kargin[8] and co-workers have also studied this reaction, although at somewhat higher temperatures, and have indicated the structure of the resulting polymer to be solely that which is formed via polymerization through only one double bond of the bicyclohepta-2,5-diene (IV). Quite recently, however, Graham, Buhle, and Pappas[9] have noted that 2-carboxyethylbicyclo[2.2.1]hepta-2,5-diene homopolymerizes to a polymer containing structures due both to transannular addition, and reaction through only one double bond of the molecule.

Once the mechanism of the free radical-initiated homopolymerization of bicycloheptadiene became evident, attention was turned to copolymerization reactions. It was found that bicycloheptadiene copolymerized well, leading to high molecular weight, soluble polymers with acrylonitrile, ethyl acrylate, vinylidene chloride, vinyl chloride, and methyl methacrylate. Quite surprising was the fact that these copolymers contained very little, if any, unsaturation and had evidently formed via reaction of the bicycloheptadiene almost solely through the nortricyclene route. These data were again based upon infrared spectra which in all cases studied

showed almost the complete absence of the double bond bands at 6.4 and 14.1 μ and the appearance, when not masked by bands due to comonomer, of a strong band at 12.4 μ due to the 3,5-disubstituted nortricyclene. This was the case in all the copolymers reported below in the monomer-polymer composition curves in Figures 1–5. Thus it can be said that relatively easily attacked vinyl monomers and bicyclo[2.2.1]hepta-2,5-diene copolymerize to polymers having the following schematic structure:

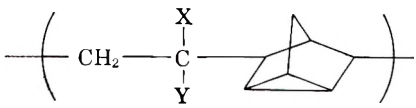

The monomer–polymer composition curves for the above mentioned copolymerizations may be found in Figures 1–5. The monomer reactivity ratios (r_1 and r_2), calculated by the method of Fineman and Ross[10] from these data are shown in Table I. The Q and e values (based on styrene: $Q = 1.0$, $e = -0.8$) for bicyclo[2.2.1]hepta-2,5-diene calculated from these monomer reactivity ratios utilizing the best Q and e data available for vinyl chloride, vinylidene chloride, and acrylonitrile copolymerizations[11] are also shown.

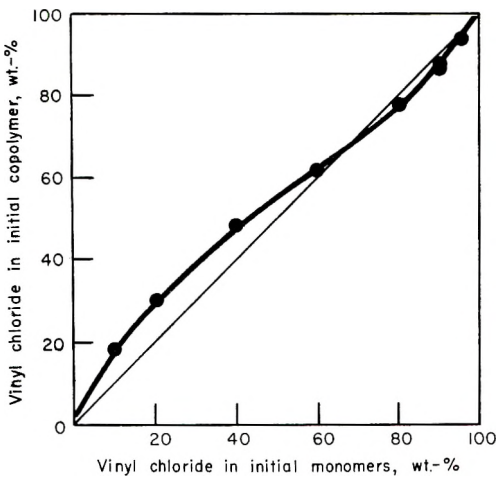

Fig. 1. Vinyl chloride–bicyclo[2.2.1]hepta-2,5-diene.

TABLE I
Monomer Reactivity Ratios and Q and e Values for Bicyclo[2.2.1]hepta-2,5-diene Copolymerizations at 50°C.

M_1	r_1	r_2	Q_2	e_2
Vinyl chloride	0.74	0.35	0.06	−1.33
Vinylidene chloride	1.41	0.08	0.09	−1.19
Acrylonitrile	0.67	0.08	0.13	−0.60
Ethyl acrylate	3.05	0.01	—	—
Metnyl methacrylate	10.0	~0.00	—	—

The r_1r_2 product in all cases is considerably less than unity showing these copolymers to be quite alternating in nature, perhaps due, in part, to the steric requirements of the nortricyclene group. The low Q value for bicycloheptadiene shows bicycloheptadiene or intermediates to have

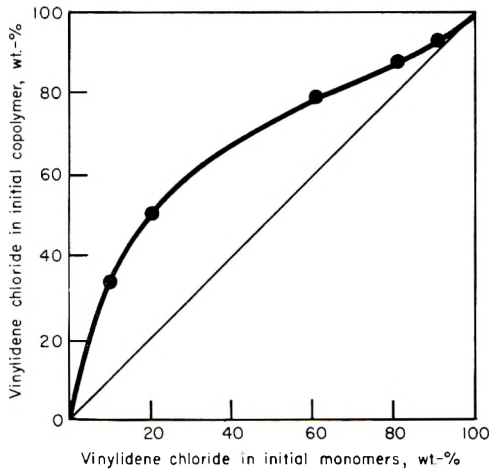

Fig. 2. Vinylidene chloride–bicyclo[2.2.1]hepta-2,5-diene.

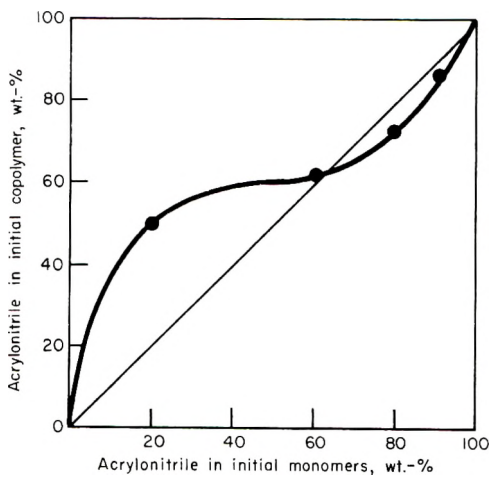

Fig. 3. Acrylonitrile–bicyclo[2.2.1]hepta-2,5-diene.

a fairly low degree of resonance stabilization while the high negative e value shows negative polarization of the radicals involved. These Q, e values are similar to those for isobutylene ($Q = 0.02$, $e = -1.1$),[12] perhaps giving a clearer picture of the relative degrees of resonance stabilization and polarities encountered in the polymerization of bicycloheptadiene.

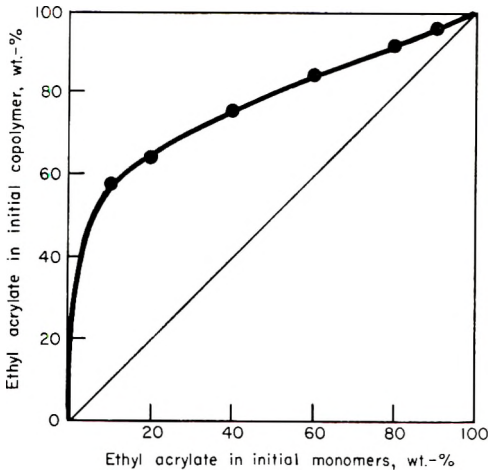

Fig. 4. Ethyl acrylate–bicyclo[2.2.1]hepta-2,5-diene.

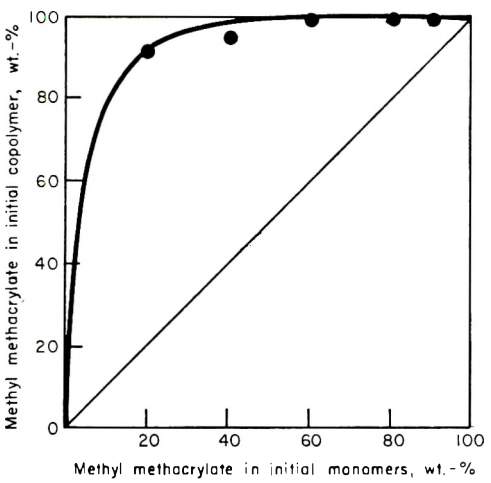

Fig. 5. Methyl methacrylate–bicyclo[2.2.1]hepta-2,5-diene.

Experimental

All copolymerizations were run in crown-capped tubes rotating in a water–glycol bath at 50 ± 2°C. The initiator was 0.2 wt.-% azobisisobutyronitrile. Most of the reactions were run in bulk, although several copolymerizations were carried out in 50% (v/v) benzene solution. Conversions were held to less than 10%. The copolymers formed were all of high molecular weight. Their reduced viscosities, measured at 0.2 wt.-% concentration in an appropriate solvent at 30°C., were greater than 0.3. Copolymer compositions were determined by the appropriate elemental analyses. The bicyclo[2.2.1]hepta-2,5-diene (Shell Chemical Company) was carefully fractionated under pure nitrogen before use. Other monomers were freed from inhibitor by flash vacuum distillation and

center cuts retained for use. Polymerization rates varied depending on the comonomer pairs and their composition but usually were in the 0.5 to 5%/hr. range. Polymers were isolated by precipitation in methanol, washing with methanol and drying *in vacuo* at 55°C. Infrared spectra were run on either Baird or Perkin-Elmer double-beam instruments using a sodium chloride prism.

The author is indebted to Mr. D. M. Harmon for carrying out many of these experiments.

References

1. Burkhart, R. D., and N. L. Zutty, *J. Polymer Sci.*, **A1**, 1137(1963).
2. Schmerling, L., U. S. Pat. 2,930,781 to Universal Oil Products (1960).
3. See, for example, S. J. Cristol, G. D. Brindell, and J. A. Reeder, *J. Am. Chem. Soc.*, **80**, 635 (1958).
4. Schmerling, L., *J. Am. Chem. Soc.*, **78**, 2819 (1956).
5. Roberts, J. D., *J. Am. Chem. Soc.*, **72**, 3116 (1950).
6. Kaplan, L., H. Kwart, and P. R. Schleyer, *J. Am. Chem. Soc.*, **82**, 2342 (1960).
7. Wilcox, C. F., Jr., S. Winstein, and W. C. McMillan, *J. Am. Chem. Soc.*, **82**, 5450 (1960).
8. Kargin, V. A., N. A. Plate, and L. A. Dudnik, *Vysokomol. Soedin.*, **1**, 420 (1959).
9. Graham, P. J., E. L. Buhle, and N. Pappas, *J. Org. Chem.*, **26**, 4658 (1961).
10. Fineman, M., and S. D. Ross, *J. Polymer Sci.*, **5**, 259 (1950).
11. Thompson, B. R., and R. H. Raines, *J. Polymer Sci.*, **41**, 265 (1959).
12. Price, C. C., *J. Polymer Sci.*, **44**, 288 (1960).

Résumé

Le bicyclo[2.2.1]hepta-2,5-diène homopolymérise en présence d'initiateurs par radicaux libres pour donner un polymère soluble de bas poids moléculaire qui contient dans la chaîne principale des unités de nortricyclène-3,5-disubstitué et de bicyclo[2.2.1]-hept-2-ène-5,6-disubstitué. Lorsque le bicycloheptadiène (M_2) est copolymérisé avec le chlorure de vinyle, le chlorure de vinylidène, l'acrylonitrile, l'acrylate d'éthyle et le méthacrylate de méthyle, on ne trouve, dans les copolymères de hauts poids moléculaire, que le produit transannulaire, le nortricyclène-3,5-disubstitué. Les rapports de réactivité des copolymérisations mentionnées ci-dessus, à 50°C. sont respectivement $r_1 = 0.74$, $r_2 = 0.35$; $r_1 = 1.41$, $r_2 = 0.08$; $r_1 = 0.67$, $r_2 = 0.08$; $r_1 = 3.05$, $r_2 = 0.01$; $r_1 = 10.0$, $r_2 = 0$. En utilisant ces données et les valeurs de Q et de e, on obtient pour le bicyclo-[2.2.1]hepta-2,5-diène respectivement 0.09 et -1.04.

Zusammenfassung

Bicyclo[2.2.1]hepta-2,5-dien polymerisiert in Gegenwart radikalischer Starter zu einem niedermolekularen, löslichen Polymeren, das in der Hauptkette 3,5-disubstituierte Nortricyclen- und 5,6-disubstituierte Bicyclo[2.2.1]hept-2-en-einheiten enthält. Bei Copolymerisation des Bicycloheptadiens (M_2) mit Vinylchlorid, Vinylidenchlorid, Acrylnitril, Äthylacrylat und Methylmethacrylat tritt in den hochmolekularen Copolymeren nur das transannulare Produkt, 3,5-disubstituiertes Nortricyclen, auf. Die Reaktivitätsverhältnisse für die Copolymerisationen in der oben angegebenen Reihenfolge sind bei 50°C.: $r_1 = 0.74$, $r_2 = 0.35$; $r_1 = 1.41$, $r_2 = 0.08$; $r_1 = 0.67$, $r_2 = 0.08$; $r_1 = 3.05$, $r_2 = 0.01$; $r_1 = 10.0$, $r_2 = 0$. Aus diesen Zahlen ergeben sich die Q- und e-Werte für Bicyclo-[2.2.1]hepta-2,5-dien in Mittel zu 0.09 bzw. -1.04.

Received March 19, 1962
Revised May 4, 1962

BOOK REVIEWS

N. G. GAYLORD, Editor

Radiation Chemistry of Polymeric Systems High Polymers, A. CHAPIRO, Ed., Interscience, New York, 1962, xvi + 712 pp. $21.00.

Understandably enough, a great number of papers dealing with radiation chemistry have appeared in recent years. For various reasons, a large fraction of the research work represented by these has dealt with polymers and polymerization. This has had the beneficial effect of increasing both our knowledge of radiation effects and of polymeric systems.

Recently, several books and a number of review articles have dealt with radiation and polymers. The volume under review is an excellent one of this genre. It starts by surveying in elementary fashion what is known of radiochemical processes and what is known of the interaction of ionizing radiation with matter. Then there is a chapter on the radiation chemistry of hydrocarbons. This is followed by a generalized kinetic treatment of radiation-induced polymerization. Then comes the essential core of the book. Radiation polymerization in homogeneous and heterogeneous media is covered by going through an analysis of the data available on several monomer systems. Radiation effects on formed polymer, both in the solid state and in solution are also covered. The book closes with a chapter on radiation-induced graft copolymerization.

The treatment of the subject matter is lucid, logical, and easy to understand. There are apparently few errors. A few points should be mentioned, however.

Several workers in the field might take issue with the author's interpretation of their data. At times the personal bias of the author becomes apparent. For example, in several instances he makes the evidence for ionic mechanisms seem stronger than the data warrants. These defects, however, merely reflect the fact that there is still room for a good deal of controversy in this field. At any rate, the author is honest enough to admit in the introduction that in many things the treatment of the data just reflects the author's personal thinking on the subject. On the whole, this may be considered an excellent book. Anyone interested either in radiation effects or polymers will find the time reading this book well spent.

G. Adler

Brookhaven National Laboratory
Upton, Long Island, New York

Introduction to Polymer Chemistry, J. K. STILLE, Wiley, New York, 1962, xi + 248 pp. $6.95.

Of the many books published over the past 10 years in the field of polymer science, none has been concerned in depth and breadth with the organic chemistry of polymerization processes. This book was intended to help fill that void and was written as a textbook for a one semester course in polymer chemistry for organic chemists. The avowed goal of the book is "to help prepare organic chemists for the polymer chemistry that most of them face at one time or another during their careers." While this book is the only reasonably lengthy treatment of this subject since Ritchie's, *A Chemistry of Plastics and High Polymers* published in 1949, it unfortunately falls short of these intentions and goals.

As a textbook, the treatment of the subject matter leaves much to be desired. The author has placed an inordinate emphasis on areas of his own research interest. For example, there is more space devoted to the subject of Diels-Alder polymers, a highly

tenuous area of research, than to the chemistry of phenol-formaldehyde polymerization, a subject which a great many organic chemists have faced and will face "at one time or another during their careers." There is an entire chapter of eight pages on cyclopolymerization, another area of immediate interest to the author of the book, but only six pages devoted to the general subject of the mechanism and kinetics of radical polymerization. The introductory chapter on definitions and classifications is quite disappointing. Unfortunately, the largely meaningless classical demarcations of condensation and addition polymerization reactions are still used. Some of the discussions in this chapter are rather naive and misleading, such as the use of poly(ethylene adipate) and phenol-formaldehyde as typical examples of copolymers. The chapter on the physical chemistry of polymers suffers considerably when the subject of the glassy state is discussed, and the author continually confuses the meanings of the words conformation and configuration. The discussion on molecular weight determination in the chapter on characterization of polymers obviously was not critically reviewed before publication. The section on light scattering is hopelessly confusing. However, from this point on the book improves considerably in clarity and competence.

The descriptive sections of the book are handled satisfactorily and, except for a few minor errors, chapters 6 thru 10 (covering 110 pages) are well written and substantially complete for the purpose of this book. These chapters contain concise, qualitative discussions on the preparations and properties of essentially all important polymers. If there is any real criticism to be made of these discussions, considering their purpose, it is that they are not properly weighted and should have been more critical. It is the feeling of the reviewer that considerably more emphasis should have been placed on reaction mechanisms and physical-organic interpretations. However, not every instructor may wish to take such an approach in a one semester, first course in organic-polymer chemistry.

In spite of its shortcomings, the book remains the only available up-to-date treatment of the entire subject of organic-polymer chemistry and should serve satisfactorily as supplementary reading for a senior undergraduate or first-year graduate course on the subject. It could also serve well as a ready source to leading references, because the discussions are well documented. In fact, these descriptive discussions alone are well worth the modest price requested, for which the publishers are to be complimented.

Robert W. Lenz

Eastern Research Laboratory
The Dow Chemical Company
Framingham, Massachusetts

Soviet Research on Organo-Silicon Chemistry, 1959, Parts I and II, Consultants Bureau, New York, 1961, 528 pp. in 2 Vols. $40.

These two paper bound volumes continue the initial effort of the Consultants Bureau to bring to American readers a comprehensive collection of articles published in Soviet journals in the areas of organosilicon chemistry and silicone research. The general purposes remain the same as those described in my previous review (*J. Polymer Sci.*, **45,** 553 (1960)). The arrangement and format are the same as in the initial series, and the same comments apply here.

Volume I of the 1959 series comprises a section on the chemistry of silicon-functional compounds, with papers by A. D. Petrov, N. N. Sokolov, M. G. Voronkov, K. A. Andrianov, B. N. Dolgov, and many other famous names, and a section on organofunctional compounds such as chloroalkyl and cyanoethyl silanes. A final section on derivatives of orthosilicic acid is also very interesting, especially from the standpoint of the preparation of simple volatile compounds of silicon, even though it does not strictly

come under the heading of organosilicon chemistry because the subject compounds all have their organic groups attached to silicon through intermediate oxygen atoms.

Volume II is devoted to organosilicon polymers and their derivatives containing metals and metalloids. In it are papers describing siloxane liquid and solid polymers which contain boron, phosphorus, titanium, antimony, aluminum, or other metals or metalloids. This is an area of research in which Soviet chemists have been predominant, and the papers are extremely important for all those who are concerned with silicone polymers in this country. Such readers will also be interested in the dozen or so miscellaneous papers which treat such topics as the all-union conference on the chemistry and the practical uses of organosilicon compounds, the use of organosilicon compounds for paper sizing, the effects of organosilicon compounds on the acid resistance on ceramic materials, the water-repellent treatment of textiles, and the use of silicone coatings to prevent the adhesion of ice. The translating and editing are done with competence, and the collection is undoubtedly worth the purchase price several times over for those who deal constantly with silicone materials.

Harvard University
Cambridge, Massachusetts

Eugene G. Rochow

Unsolved Problems in Polymer Science, FRANK R. MAYO, Ed., National Academy of Sciences—National Research Council, Washington, D. C., 1962, 210 pp. $3.50.

Gaps in our knowledge of the basic principles of polymer formation, structure and behavior are pinpointed in 42 contributions prepared by some of the leading authorities in the polymer field.

Part A deals with the preparation and reactions of organic macromolecules, including polymerization mechanisms and kinetics, chemical transformations, graft and block copolymers, cross-linking, and degradation.

Part B covers the same field for the inorganic and mixed macromolecules; the need for positional synthesis and improved characterization techniques is emphasized.

Part C is concerned with the constitution of polymers. It contains chapters dealing with microstructure, e.g., valence bonds, geometrical configurations, and sequential arrangement of structural units, and with macrostructure, e.g., chain length, nonlinearity, and network systems.

Part D on macromolecular solutions highlights the need for more information on quantitative relationships involved in macromolecular conformation, thermodynamic properties, intramolecular and intermolecular forces, and polarity and charge of component groups.

Part E on solid polymer systems focuses attention on the problems relating to the conformation of macromolecules in the bulk state, including crystallization, morphology and semicrystalline polymers, the glass transition, melting, and crystalline-liquid phase equilibria.

Part F mechanical properties, and *Part G*, miscellaneous properties, deal with linear and nonlinear viscoelastic behavior of polymers, mechanochemistry, dielectric and spectral characteristics, interfacial and adsorption phenomena, and permeability and diffusion in condensed systems.

The literature references cited in the report provide a selective bibliography or recent books, reviews, and significant contributions to polymer science.

This excellent and highly stimulating review of some of the unsolved problems in polymer science should be of interest to everyone concerned with polymers. It is useful, for once, to hear not about the things we know but about the things we *don't* know.

Polytechnic Institute of Brooklyn
Brooklyn, New York

C. G. Overberger
E. H. Immergut

ERRATUM

Dynamic Bending Properties of Fibers: Effect of Temperature on Nylon 66, Terylene, Orlon, and Viscose Rayon

(article in *J. Polymer Sci.*, **61**, 271–292, 1962)

By R. MEREDITH and BAY-SUNG HSU
Royal College of Science and Technology, Glasgow, Scotland

On p. 275 in column one of Table I, under Fiber, the units are μg./cm.

On p. 285 the line following eq. (2) should be deleted.

The last line on the page should read:

$$(1/u)\,(d^4u/dx^4) = \rho A(d^2v/dt^2)/[-\eta I(dv/dt) - E'Iv]$$

On p. 286 eq. (5) should read:

$$(d^2v/dt^2) + b(dv/dt) + a^2v = 0$$

The 11th line should read:

$$= 0 \text{ and at } x = 1,\ d^2u/dx^2 = d^3u/dx^3 = 0. \text{ etc.}$$

Eq. (7) should read:

$$(d^2v/dt^2) + b(dv/dt) + a^2v = (F/\rho A)\sin \omega t$$

Eq. (8) should read:

$$f(\omega) = (F/\rho A)/\sqrt{(a^2 - \omega^2)^2 + b^2\omega^2}$$

On p. 287 line 4 should read:

$$\Delta\omega = b[1 + {}^1/_4(b/a)^2 + {}^7/_{32}(b/a)^4 + \ldots]$$

Line 30 should read: If $\eta\omega$, and . . . etc.

On p. 288 eqs. (18) should read:

$$m^2(k - 1) = (\pi/4)/[L^2 + (\pi/4)^2]$$

$$m^2k' = -L/[L^2 + (\pi/4)^2]$$

On p. 289 eq. (20) should read:

$$(1 + \rho_a k/\rho)\,(d^2v/dt^2) + (b + \rho_a k'\omega/\rho)\,(dv/dt) + a^2v = (F/\rho A)\sin \omega t$$

Eq. (21) should read:

$$f(\omega) = (F/\rho A)\left\{[a^2 - (1 + \rho_a k/\rho)\omega^2]^2 + (b + \rho_a k'\omega/\rho)^2\omega^2\right\}^{-1/2}$$

In line 12 replace reference 3 by reference 6.

In line 14 replace reference 4 by reference 7.